UNITED STATES OF AMERICA

WEATHER ANALYSIS AND FORECASTING

When you can measure what you are speaking about and express it in numbers, you know something about it; but when you cannot measure it, when you cannot express it in numbers, your knowledge is of a meager, unsatisfactory kind.

—LORD KELVIN.

WEATHER ANALYSIS
AND FORECASTING

A Textbook on Synoptic Meteorology

BY

SVERRE PETTERSSEN, Ph. D.

Meteorological Institute
Blindern, Norway

To

LIEUT.-COL. E. GOLD, D.S.O., M.A., F.R.S.

In recognition of his distinguished service
as President of the Commission for
Synoptic Weather Information

PREFACE

The recent advances of meteorological science have aroused widespread attention throughout the world, all the more because they have led to actual application of the principles of physics and mathematics in the forecasting of the weather. As a result, the weather forecasts have become factors of considerable economic importance, superseding even the most optimistic expectations of twenty years ago.

The results of the recent researches will be found in a multitude of papers and journals dealing with special problems, and most textbooks on meteorology deal with the science in a general way that is not specifically adapted to practical use. The author therefore believed that it would meet a widespread demand to present in a comprehensive form the principles and theories underlying the modern methods of weather analysis and forecasting in such a manner that their application to actual forecasting is facilitated.

The material is presented in eleven chapters, each of which is more or less independent of the others. Only the last three chapters are interdependent. The book is written mainly for teaching purposes, but it is hoped that it will be of considerable use also to professional forecasters

The book makes no pretense of covering the entire field of meteorology; it deals only with those aspects of the subject which experience has shown to be directly applicable to actual forecasting. Although it is desirable that the reader should possess knowledge of the general principles of meteorology, the book is intended to be, as far as possible, independent of general textbooks.

This book originated from a series of lectures on synoptic meteorology delivered during the years 1935 to 1940 at the following institutions: U.S. Navy Department (1935), California Institute of Technology (1935), U.S. Weather Bureau (1936 and 1939), the Meteorological Service of Canada (1936), the Meteorological Service of Norway (1938), Oslo University (1939), and the Massachusetts Institute of Technology (1939 1940). In publishing the lectures in this revised form the author wishes to acknowledge his great indebtedness to the above institutions and their chiefs and staffs for the encouragement and assistance received. Special thanks are due to Dr. Th. Hesselberg, Director of the Norwegian Meteorological Service, for his unfailing support, and to Messrs. O. A. Eide, L. Naess, S. Naess, and F. Pedersen of Vervarslinga på Vestlandet for

their assistance in preparing the statistical data in Chap. III. Thanks are also due to Dr. Bleeker of the Dutch Meteorological Service, to Commander Trendell of the Royal Navy, to Messrs. Grytöyr and Thrane of the Norwegian Weather Service for having critically read the first three chapters, to Miss Whitcomb and Messrs. Austin and Garstens of the Massachusetts Institute of Technology for their help in preparing the indexes and checking the formulae. Finally, the author's warm thanks go to Mr. Jerome Namias for his assistance in writing the chapter on isentropic analysis and to Dr. J. Bjerknes for his permission to reproduce Figs. 125, 127, 153, 154, 173 and 174 from "Physikalische Hydrodynamik."

<div align="right">SVERRE PETTERSSEN.</div>

CONTENTS

v_{gs}	geostrophic wind.
x	mixing ratio of aqueous vapor.
x, y, z	space coordinates.
α	specific volume of air.
γ	actual lapse rate of temperature.
γ_d, γ_m	dry- and moist-adiabatic lapse rate.
Δ	difference.
λ	Coriolis parameter, *i.e.*, $2\omega \sin \varphi$
ρ	density of air.
θ	potential temperature.
θ_w	potential wet-bulb temperature
θ_{sw}	potential pseudo-wet-bulb temperature.
θ_e	potential equivalent temperature.
θ_{se}	potential pseudo-equivalent temperature.
θ_d	inclination of a surface of discontinuity.
θ_p	inclination of an isobaric surface.
Φ	geopotential.
φ	latitude.
ψ	stream function; angle indicating the direction of motion; angle between the axis of dilatation and the isotherm.
ν	frequency of oscillation.
Σ	area.
σ	curvature.
Ω	angular velocity.
ω	angular velocity of the earth.

2. *Vectors*

A	acceleration.
c	velocity of pressure systems; velocity of propagation.
D	displacement.
F	frictional force.
$-I$	isallobaric gradient.
i, j, k	unit vectors of the coordinate axes.
n, t	unit vectors along a normal and a tangent, respectively.
v	wind velocity.
v_{gr}	gradient wind.
v_{gs}	geostrophic wind.
∇	the Hamilton operator: $\nabla = (\partial/\partial x)i + (\partial/\partial y)j + (\partial/\partial z)k$; usually applied only in the horizontal plane; then $\nabla = (\partial/\partial x)i + (\partial/\partial y)j$.

3. *Clouds*

Ci	cirrus.	Sc	strato-cumulus
Cs	cirro-stratus.	Ns	nimbo-stratus
Cc	cirro-cumulus.	Cu	cumulus.
As	alto-stratus.	Cb	cumulo-nimbus.
Ac	alto-cumulus.	St	stratus.

4. *Air Masses*

A	arctic air.	E	equatorial air.
Pc	polar continental air.	M	monsoon air.
Pm	polar maritime air.	S	*supérieure* air.
Tc	tropical continental air.	t	transitional.
Tm	tropical maritime air.	r	returning.

WEATHER ANALYSIS AND FORECASTING

AIR-MASS CHARACTERISTICS

The principles of the modern methods of air mass analysis are based on the fact that the tropospherical circulation has a tendency to produce vast bodies of air whose physical properties vary but slightly within each body, while abrupt and rapid changes usually occur along the border between adjacent air masses.

In studying the production and the transformation of air masses by means of synoptic charts and aerological ascents, we find that the physical properties of an air mass depend solely upon its life history. We notice, also, that some of the physical properties are apt to change rapidly and frequently according to the dynamical, kinematic, and physical state of the air, whereas other properties will remain almost constant for long periods of time. We may therefore speak of *conservative* and *nonconservative properties* of the air masses.

In the study of synoptic weather charts we are mainly interested in four aspects of the air-mass theory, *viz.*:

1. The production of air masses.
2. The transformation of air masses.
3. The conservative properties of the air masses which may serve as an aid in identifying the air masses from one chart to the next.
4. The average or typical weather conditions in the various types of air mass.

Before we proceed to discuss these four points, we must consider the air-mass characteristics as such, especially with regard to conservatism.

1. Conservatism.—No physical property of the air is strictly conservative. Radiation, mixing, conduction, etc., will invariably cause changes in space and time. Nevertheless, when we say that an air-mass property is conservative (or quasi-conservative), we do so with a treble reservation, *viz.*, that the changes in the property in question within a certain *interval of time* are *not appreciably greater than the inaccuracy of the observation* when the air is subject to a *specified process*.

1

Only with these reservations is it reasonable to speak of conservatism of meteorological elements; for all elements will vary, the changes depend on the process in operation, and the amount of change may assume any possible value with increasing time.

As regards time interval, it suffices that the conditional conservatism is maintained from one map to another; *i.e.*, the property must remain conservative for at least 12 hr. as far as the surface observations are concerned and for about 24 hr. with regard to the upper-air observations.

As regards process, the term conservatism usually refers to approximate isobaric conditions when we are concerned with the surface observations but to approximate adiabatic conditions when we discuss the conditions in the upper atmosphere. Though within moderate intervals of time adiabatic processes are responsible for the major changes in the traveling air masses in the upper atmosphere, nonadiabatic quasi-isobaric processes are predominant near the surface of the earth.

2. Air-mass Characteristics.—The most important air-mass characteristics are

1. The temperature of the free atmosphere.
2. The potential temperature.
3. The surface-air temperature.
4. The maximum temperature.
5. The lapse rate of temperature.
6. The diurnal amplitude of temperature.
7. The horizontal temperature gradient.
8. Specific humidity or ratio of mixing.
9. Dew-point temperature.
10. Wet-bulb temperature.
11. Wet-bulb potential temperature.
12. Equivalent potential temperature.
13. Forms of clouds.
14. Hydrometeors and impurities of the air.
15. Diurnal variation in clouds and hydrometeors.
16. Visibility.
17. Wind structure.

In this chapter, the most important of these elements will be discussed in order to demonstrate under which circumstances they may be regarded as true air-mass characteristics. Other elements, mostly of secondary importance as air-mass characteristics, will be treated in due course in later sections.

In order to make adequate use of the various characteristics, it is necessary to ascertain that the observations which we make use of are *representative*. By this we mean that the observed quantity should be representative of the value characteristic of the entire air mass or a

large portion thereof. This is the same as saying that the observations should not be influenced locally. The representativeness of the observations will be discussed in connection with each particular element.

3. The Temperature of the Free Atmosphere.—Temperature observations from balloons, airplanes, and kites are representative but not conservative. The temperature changes in the free atmosphere are mainly due to absorption of heat, eddy transfer of heat, and dry-adiabatic and moist-adiabatic processes. From the first theorem of thermodynamics we obtain

$$(1) \qquad \frac{dT}{dt} = \frac{1}{c_p}\frac{dQ}{dt} + \frac{R}{c_p}\frac{T}{p}\frac{dp}{dt}$$

where dQ/dt is the heat added to, or withdrawn from, a unit mass of air per unit time, R is the gas constant, T the temperature and p the pressure of the air, and c_p is the specific heat of air at constant pressure. In a dry-adiabatic process (*i.e.*, $dQ = 0$), we obtain

$$(2) \qquad T = T_0 \left(\frac{p}{p_0}\right)^{\frac{c_p - c_v}{c_p}}$$

The rate of change in temperature is then about 1°C. per 100 meters ascent or descent.

When condensation occurs, the latent heat of vaporization is made free and is mostly used to heat the air. In such a process, the rate of cooling of ascending air is less than in a dry-adiabatic process, the rate of cooling varying from 0.4°C./100 m. ascent when the water-vapor content is high to almost the dry-adiabatic rate when the water-vapor content is excessively low.

Let v_h, $-\nabla_h p$, and $-\nabla_h T$ denote the horizontal wind vector and the horizontal gradients of pressure and temperature, respectively, and let v_z denote the vertical velocity. Substituting from the equation of static equilibrium,

$$\frac{1}{\rho}\frac{\partial p}{\partial z} = -g$$

we obtain from Eq. (1)

$$(3) \qquad \frac{dT}{dt} = \frac{1}{c_p}\frac{dQ}{dt} + \frac{RT}{c_p p}\frac{\partial p}{\partial t} + \frac{RT}{c_p p} v_h \cdot \nabla_h p - v_z \gamma_d$$

where γ_d is the dry-adiabatic lapse rate of temperature.

The terms containing $\partial p/\partial t$ and $\nabla_h p$ are always exceedingly small and may be neglected in comparison with the other terms. We then obtain

$$(4) \qquad \frac{dT}{dt} = \frac{1}{c_p}\frac{dQ}{dt} - v_z \gamma_d$$

or

$$(5) \qquad \frac{\partial T}{\partial t} = \frac{1}{c_p} \frac{dQ}{dt} - \nabla_h T \cdot v_h - v_z(\gamma_d - \gamma)$$

where γ is the actual lapse rate of temperature. The variation in temperature of the individual parcels (*i.e.*, dT/dt) depends on the absorption of heat (dQ/dt) and the vertical velocity (v_z). The variation in temperature in a fixed point (*i.e.*, $\partial T/\partial t$) depends on the absorption of heat, the horizontal advection ($\nabla_h T \cdot v_h$), the vertical velocity, and the stability of the air ($\gamma_d - \gamma$).

Assuming horizontal homogeneity (*i.e.*, $\nabla_h T = 0$) and adiabatic conditions ($dQ = 0$), we obtain from Eq. (5)

$$(6) \qquad \frac{\partial T}{\partial t} = -v_z(\gamma_d - \gamma)$$

If the air is saturated,

$$(7) \qquad \frac{\partial T}{\partial t} = -v_z(\gamma_m - \gamma)$$

where γ_m indicates the moist-adiabatic rate.

Thus, when $\gamma_d > \gamma$, an ascending current causes a local decrease in temperature, and a descending current (subsidence) causes a local increase. When $\gamma_d < \gamma$, the reverse is true. Similar rules hold for saturated air when γ_m is substituted for γ_d.

When $\gamma = \gamma_d$ (or, in saturated air, $\gamma = \gamma_m$), the vertical velocities have no influence on the local temperature variations. As the lapse rate in the free atmosphere does not normally exceed the adiabatic rate, it follows that the effect of vertical velocity on the temperature changes in the free atmosphere increases with the stability of the air. This is the same as saying that *the temperature in any isobaric level is the more conservative for adiabatic changes the smaller the stability of the air.*

Though we may put $\nabla_h T = 0$ within the quasi-homogeneous air masses, it is not permissible to do so in the zone of transition between adjacent air masses or in air masses where the horizontal temperature gradient is appreciable. In such cases, the term $-\nabla_h T \cdot v_h$ may be important; this happens when the wind has a large component normal to the isotherms. In fact, the most rapid and pronounced temperature changes in the free atmosphere are due to this term (*i.e.*, *advection*).

Absorption of heat (*i.e.*, dQ/dt) is the major cause of temperature variations near the earth's surface. It is convenient to distinguish between absorption of radiation and absorption of heat from the underlying surface. Concerning absorption of radiation, it suffices here to remark that the fact that the diurnal variation in temperature in the free

atmosphere is small shows that the effect of radiation on the temperature variations in the free atmosphere is but slight as far as temperature changes during short intervals of time are concerned. Local and individual temperature changes caused by radiation alone are not likely to exceed 1 or 2°C. in 24 hr. Thus, the temperature variations in the free atmosphere caused by radiation are less than the changes that would occur if the air ascended or descended 200 m. in 24 hr. The effect of radiation is, therefore, negligible when the problem is to identify air masses in the free atmosphere from one map to the next. But radiation will be of considerable importance for the slow transformation of air masses when they stream for long intervals of time from one latitude to another (see Chap. III).

Mixing between horizontally and vertically adjacent air masses or stirring of a uniform air mass may under certain circumstances have a considerable influence on the temperature of the free air. The effect of horizontal mixing on temperature is but slight as far as changes within the air masses from one map to the next are concerned. Its influence is appreciable only near the zones of transition between adjacent air masses. When the horizontal mixing (lateral mixing) has occasion to persist over long periods, its effect on the distribution of temperature becomes important inasmuch as it tends to destroy fronts (frontolysis) and to create horizontal homogeneity within the air masses. These processes are, however, so slow that they are of minor importance for the identification of the air masses from one map to another.

Vertical mixing may under certain circumstances have a considerable influence on the distribution of temperature. The eddy flux of heat in nonsaturated air across a horizontal unit area per unit time may be expressed by[1]

$$F = -Kc_p\rho(\gamma_d - \gamma)$$

where K is the coefficient of eddy transfer of heat and ρ is the density of the air. If the air were saturated, γ_m should be substituted for γ_d. Through vertical mixing, heat is transported downward when the stratification is stable and upward when the stratification is unstable. Vertical mixing will therefore always have a tendency to establish an adiabatic lapse rate; and when this state is reached, vertical mixing has no influence on the temperature distribution along the vertical.

If no heat is supplied to, or withdrawn from, the air from some external source, it follows that *the air temperature in any level is the more conservative for vertical mixing the closer the lapse rate is to the adiabatic rate.*

When the air absorbs heat from the underlying surface or gives off heat to it, the conditions are somewhat different. The heating from

[1] See BRUNT [19].

below (*i.e.*, $dQ/dt > 0$) steepens the lapse rate; and as soon as a super-adiabatic state is reached, convective currents set in, and the heat absorbed from below is carried upward, where, in addition, the latent heat of vaporization will be made available to increase the air temperature still further. The heat gained from the underlying surface will be distributed over a deep air column; and as the air streams toward warmer regions, it will be capable of absorbing more heat. This will result in a profound change in temperature at all levels (see Chap. II).

The reverse condition, when the air gives off heat to the underlying surface (*e.g.*, by streaming toward colder regions), has no such far-reaching and quickly acting effect on the temperature conditions in the free atmosphere above the layer influenced by surface friction. The air in contact with the colder surface will be cooled from below; great stability will develop which hinders convection and damps the mechanical turbulence set up along the surface of the earth. As a result, the cooling from below affects chiefly the friction layer, above which inversions easily develop (see Par. 54); the exchange of heat between the surface layer and the free atmosphere is thus hindered. As the gain of heat from the underlying surface or the loss of heat to it is proportional to the difference between the temperature of the surface and that of the air, we may say that *the temperature at any level is the more conservative the closer the air temperature is to the temperature of the underlying surface.* Furthermore, *the temperature in the free atmosphere is more conservative when the surface air is warmer than the underlying surface, than it is when it is colder than the underlying surface.* Finally, as the intensity of the eddy transfer of heat along the vertical increases with the wind velocity, it follows that, other conditions being equal, *the temperature of the free atmosphere is the more conservative the smaller the wind velocity.*

4. The Potential Temperature.—Let dQ denote the amount of heat given to or withdrawn from an air particle. The dry-adiabatic process is realized when

(1) $$dQ = 0$$

in which case Eq. 3(1) holds. Putting $p_0 = 1000$ mb., we may write

(2) $$\theta = T \left(\frac{1000}{p} \right)^{\frac{c_p - c_v}{c_p}}$$

where θ denotes the *potential temperature* of the air whose temperature is T and pressure is p.

The potential temperature is conservative with respect to dry-adiabatic processes. It is therefore a valuable means of identifying air masses where condensation phenomena do not occur. It has a wide range of applicability in air-mass analysis in typically continental

climates where condensation phenomena are infrequent; but, in regions with a pronounced maritime circulation, it is less useful owing to frequent liberations of the latent heat of vaporization.

In recent years, mostly through the work of Rossby, potential temperature has enjoyed a position of renewed interest in air-mass analysis on account of its relation to entropy. If S denotes entropy, the following relation holds:

$$(3) \qquad S = \int \frac{dQ}{T} + \text{constant}$$

From Eqs. (1) and (2) it follows that a surface of constant potential temperature is also a surface of constant entropy (isentropic surface). The use of isentropic surfaces and potential temperature will be described in Chap. VIII.

5. The Surface-air Temperature.—In order to distinguish between the temperature of the free air and the temperature observed close to the surface of the earth, we shall call the latter the "surface-air temperature." The temperature observed near the surface of the earth is often neither representative nor conservative. It is not representative because of many local or orographical influences, and it is not conservative on account of the preponderance of nonadiabatic irreversible processes in the air close to the earth's surface. Of such influences we mention insolation, outgoing nocturnal radiation, conduction of heat from and to the surface of the earth, evaporation and condensation, etc.

Although insolation during the day tends to produce a steep lapse rate and increased mixing with the air above, thereby causing the surface-air temperature to become more representative, the cooling by night will cause the formation of inversion layers close to the surface of the earth and so make the observed temperature less representative.

The surface-air temperature is representative when the lapse rate of the surface layer conforms to that of the free air above (Fig. 1a). When there is an inversion close to the surface, the representative temperature T_r at the surface may be determined by continuing the temperature-height curve from the inversion point downward as shown in Fig. 1b.

On account of the diurnal insolation, the lapse rate in the surface layer will steepen during the forenoon and approach or slightly supersede the dry-adiabatic rate. The surface-air temperature T_s may then become higher than the representative temperature T_r. Usually $T_s = T_r$ at about noon. It is therefore easily understood that the midday temperatures are far more representative than are the morning and night temperatures (Fig. 1b). In summer, the evening temperatures are fairly representative, whereas, in the colder seasons, they are often nonrepresentative owing to the development of ground inversions.

Figure 1c shows a case where there is no ground inversion but a frontal surface near the ground. In this case, too, we may determine the representative surface temperature T_r of the air above the frontal surface. Figure 1d shows a case with a frontal surface above a ground inversion. Such cases occur frequently over land in northern latitudes in winter. In such cases, one should determine the representative temperature T_r in both masses.
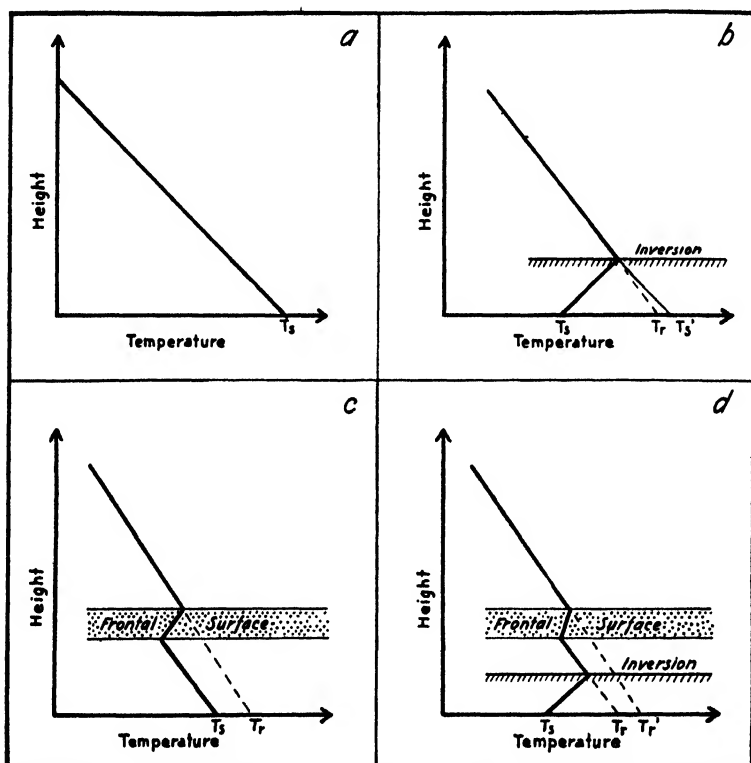
FIG. 1.—Showing how to determine the representative surface-air temperature from temperature-height curves.

At sea, the diurnal influences are negligible, and the temperature observations are always representative provided that thermometers were well exposed. A cursory inspection of the synoptic charts of today will suffice to convince the reader that the quality of the ship reports is far from satisfactory.

Well-exposed coastal or island stations are usually representative. As a general rule, we may say that the temperature observations are most representative when the wind velocity is high and the sky is cloudy or overcast. This is particularly true in the colder part of the day and in

winter.   In summer, strong wind and sunshine render the midday temperatures the most representative.

6. The Maximum Temperature.—The diurnal maximum temperature over land on sunny days is fairly representative, for it depends largely on the temperature conditions in the air above the ground layer.   A typical example is shown in Fig. 2.   The heavy line represents the temperature-height curve, say at sunrise when a pronounced inversion has developed over night.   As the sun rises, the surface layer of air is heated rapidly because the heat gained is distributed in a shallow layer of air.   After some hours of sunshine, the surface layer is heated to such an extent that the inversion is dissipated, the lapse rate under the inversion point having become dry-adiabatic. From now on, the heat transferred to the air from the surface of the earth is spread in a deep layer of air, and the temperature near the surface of the earth will not rise appreciably beyond the point determined by the adiabatic through the inversion point as shown in Fig. 2.
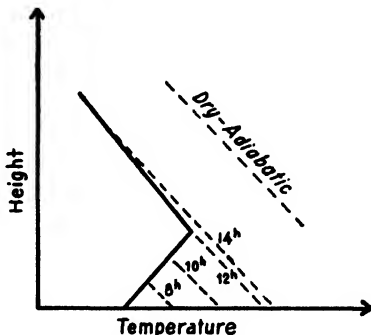
Fig. 2.—Showing the relation between the maximum temperature and the temperature above the ground inversion. Dashed lines indicate dry-adiabatics

In many cases where the lapse rate above the inversion is steep, the diurnal increase in temperature stops suddenly when the inversion is nullified; a "flat" diurnal maximum is then recorded by the thermograph in the screen (Fig. 3).   If the air above the inversion is pronouncedly stable, the temperature at the surface will continue to rise and a "rounded" maximum is recorded.   The above-described condition is typical in stagnant air in the warm season.   If the wind velocity is high, turbulent mixing will destroy the inversion. The example shown in Fig. 2 illustrates
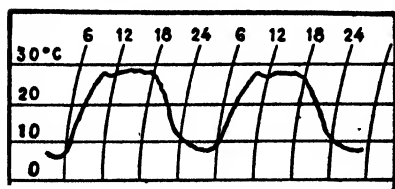
Fig. 3.—Examples of "flat" maxima of temperature which develop when the ground inversion is destroyed by diurnal heating.   Compare Fig. 2.

a method of predicting the approximate maximum temperature from the early morning ascents.

What has been said above applies when a ground inversion has developed overnight.   Inversions of more permanent nature (as may often occur over continents in winter) will usually not be nullified by the diurnal insolation alone.   In such cases, the maximum temperature will

not attain so high a value as shown in the diagram, except when the wind velocity increases sufficiently to destroy the inversion completely.

7. The Lapse Rate of Temperature.—The rate of decrease in temperature along the vertical is called the lapse rate. As will be shown in Chap. II, the lapse rate is expressive of the stability conditions of the air; and since stability conditions depend on the life history of the air mass, it becomes an important air-mass characteristic. From the observed distribution of temperature and humidity along the vertical, important conclusions may be drawn with regard to the development of clouds and hydrometeors. Conversely, from cloud and hydrometeor observations and also from the general life history of the air mass, conclusions
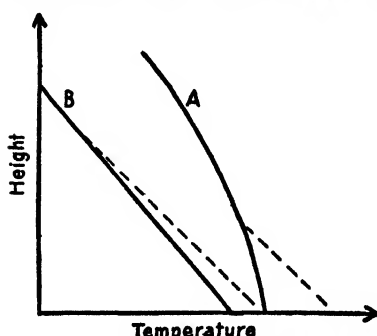
Fig. 4.—Connection between lapse rate and diurnal amplitude of temperature. Broken lines indicate dry-adiabatics.

may be drawn with regard to the lapse rate and its variations. It is convenient to leave detailed discussion to the sections dealing with stability, clouds, hydrometeors, and kindred phenomena.

8. The Diurnal Amplitude of Temperature.—There is a relation between the lapse rate and the amount of diurnal variation in temperature that is useful in the analysis of weather maps. In the temperature-height curves in Fig. 4, curve A represents a highly stable air mass and curve B one that is only slightly stable. We assume that both ascent curves refer to the conditions at sunrise. As the sun rises, heat is transferred from the surface to the air. In the case represented by curve A, the heat will be accumulated in a shallow layer of air, whereas, in the case represented by curve B, the heat will be distributed in a deep layer of air. The midday temperatures are indicated by the broken lines. We thus see that, other conditions being equal, the air mass which has the greatest lapse rate (curve B) has the smallest diurnal variation in temperature, and vice versa.

Let us now imagine that curve A represents the conditions in an air mass adjacent to the mass whose conditions are indicated by curve B. From the diagram, we see that the true or representative difference in air temperature between the two masses near the ground is clearly shown at midday, whereas it is indistinct in the early morning. Fronts between air masses of different stability may often be difficult to detect on the morning maps, whereas they show up clearly on the midday map. Thus, a front that is indistinct on the evening map and completely masked on the morning map may be quite pronounced on the following midday map.

The effect of stability on the diurnal variation in temperature is most clearly shown in cases where a well-developed inversion is present near the ground. The following table shows this for San Diego, Calif., where a pronounced inversion is present near the ground throughout the foggy season. When the inversion is close to the ground, the heat absorbed from the ground is distributed in a shallow layer of air, and a large diurnal variation results. When the inversion is high, the layer to be heated is deep, and the diurnal amplitude decreases accordingly.

RELATION BETWEEN THE DIURNAL AMPLITUDE OF TEMPERATURE AND THE HEIGHT OF THE INVERSION *

Height of Base of Inversion, M.	Diurnal Amplitude of Temp., °F.
0–50	23
0–100	17
100–200	14
200–300	10
300–400	9
400–500	7

* Petterssen [54].

Referring again to Fig. 4, it is of interest to note that the colder of the two adjacent air masses will normally be less stable than the warmer mass. But the least stable mass will usually be more turbulent than the more stable one, the turbulence will tend to prevent the formation of ground inversion in the colder mass, and the lack of turbulence in the more stable mass will favor the formation of such inversion.

The intensity of turbulence does not depend alone on the degree of thermal stability of the air. Particularly near the ground, the mechanical turbulence will be strong when the wind velocity is high. Moreover, the amount of insolation received by the underlying surface depends on the cloudiness. Thus, thermal stability, wind velocity, and amount of clouds should be taken into consideration in the analysis.

The conditions that are favourable for large diurnal variation of the difference in temperature between adjacent air masses are:

In the Warm Mass	In the Cold Mass
Great stability	Instability or slight stability
Slight wind velocity	High wind velocity
Cloudless	Cloudy or overcast

Figure 5 shows a typical example of the conditions described above. From Oct. 4 to Oct. 6, 1938, there was a stagnant mass of tropical air over southeast Russia, separated by a front from air of maritime polar origin farther to the west. The temperatures for seven stations on each side of the front are plotted in the diagram where small crosses indicate the morning temperatures and small circles the midday temperatures.

The diagram shows the following features:

1. The morning temperatures in the warm mass are nonrepresentative; they vary considerably from day to day and from one station to another. As is to be expected, they were highest and most uniform on Oct. 4 when the wind velocity was highest.

2. The morning temperatures in the cold mass are fairly representative; they are lowest on Oct. 4 when there was rain and strong wind.

3. The midday temperatures in the warm mass are representative because the dispersion is slight and there is but little variation from

OCTOBER 1938					
4 th		**5 th**		**6 th**	
Cold air	Warm air	Cold air	Warm air	Cold air	Warm air

Temperature °C axis: 22, 20, 18, 16, 14, 12, 10, 8, 6, 4, 2

Bottom remarks					
Rain. Overcast. Strong wind.	Cloudy. Moderate breeze.	Cloudy. Moderate breeze.	Fair. Light wind. Morning mist.	Mist. Mostly calm.	Fair. Calm in the morning. Light breeze at mid-day.
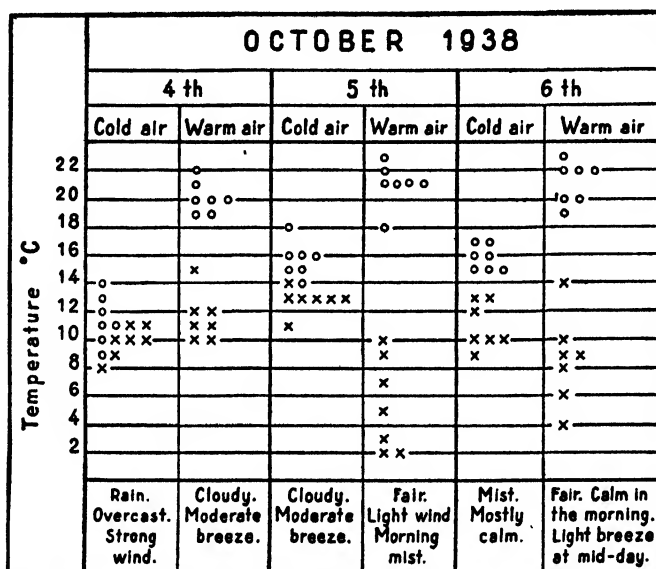
FIG. 5.—Crosses indicate morning temperatures; circles indicate midday temperatures. Note the large amplitude in the warm and stable mass as compared with the small amplitude in the colder and less stable mass.

one day to the next. They are on the whole slightly lower on Oct. 4 than on Oct. 5 and 6, on account of the greater cloudiness and the higher wind velocity.

4. The diurnal amplitude is large in the warm and stable mass and slight in the cold and less stable mass. The diurnal variation is least when the sky is cloudy and the wind is high.

5. On Oct. 5 and 6, the morning temperatures are lower in the warm and stable mass than in the cold and less stable mass. On Oct. 4, the morning temperatures are about equal in both masses. Thus, on the three morning maps under discussion, it would not be possible to locate the front by means of temperatures only, whereas the front is perfectly distinct on the midday maps.

Figure 6 shows another example which illustrates the same principles. A front separating continental tropical air from maritime polar air remained quasi-stationary over Germany from Aug. 12 to 15, 1938. The upper curve in Fig. 6 shows the mean temperature for 10 stations in the warm and stable air, and the lower curve the mean temperature for 10 stations in the colder and less stable air. Again, we notice the great difference in the surface-air temperature at midday and the small difference in the morning and the evening.
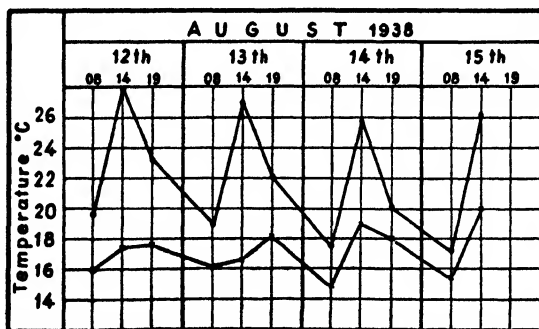
FIG. 6.—Illustrating the dependence of diurnal amplitude on stability.

9. The Horizontal Temperature Gradient.—It will be shown in Chap. III that an essential feature in the production of air masses is the tendency to produce homogeneity. This is particularly true of the air masses produced in well-defined anticyclones in southern latitudes where the surface properties are homogeneous and where the anticyclonic divergence tends to frustrate temperature gradients. When such an air mass moves out of its source regions, it will usually preserve its original homogeneity. Slight horizontal temperature gradients are therefore characteristic of air masses not only in their sources, but also while they move toward colder regions.

Figure 7 shows an example. The entire mass of tropical air coming from a southern anticyclone is extremely homogeneous. The slight temperature differences that occur are easily explained as the effect of land and sea. The example is particularly interesting because it shows that under uniform sky conditions and sufficient wind velocity the surface air temperatures are fairly homogeneous when the air mass comes from a well-defined source.

In the polar air to the north of the front, the temperatures are far more variable, which is characteristic of polar air. Often, when the temperature contrasts along the fronts are indistinct, the front may be located as the limit between the quasi-homogeneous and the heterogeneous air.

10. Further Remarks on Temperature Analysis.—The fact that the surface-air temperatures are often nonrepresentative has led to the undesirable development in air-mass and frontal analysis of considering them as useless or even misleading. From the foregoing paragraphs, it appears that the temperature observations are of inestimable value in identifying air masses and locating fronts when they are used correctly. It is true that temperature observations when used uncritically may be misleading, but the skilled analyst will always be able to draw useful
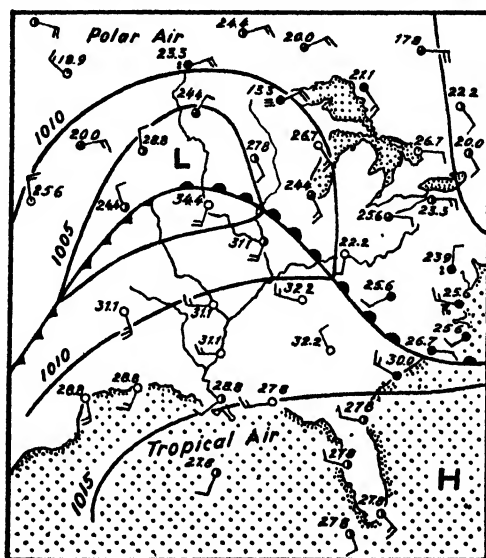
Fig. 7.—Weather chart July 14, 1937, 00ʰ30 GMT. The tropical air is not only characterized by its high temperature, but also by its homogeneity. The symbols are explained in Par. 176.

conclusions from them by considering the nature and temperature of the surface, the cloudiness, the wind velocity, and other factors. It should also be borne in mind by the analyst that the processes which render the temperature observations nonrepresentative and nonconservative are in themselves interesting and require analysis and explanation.

Full use of the temperature observations in air-mass analysis cannot be obtained unless they are studied in relation to the trajectories of the air. Figure 8 shows the trajectories of two different parcels of air belonging to a maritime tropical air mass.

Curve *A* represents the trajectory of air that moved up from the Gulf of Mexico across the United States toward the North Atlantic. On the Gulf Coast, the air temperature was 29°C., which is only slightly higher than the normal temperature of the sea surface in July. While the air mass moved across the continent, the temperature rose to 32°C.

on July 15; during the following 2 days, it decreased to 30°C. Twenty-four hours later, the temperature in the moving mass had dropped to 20°C. The development is altogether as one would expect when considering the influence of the surface over which the air has traveled.
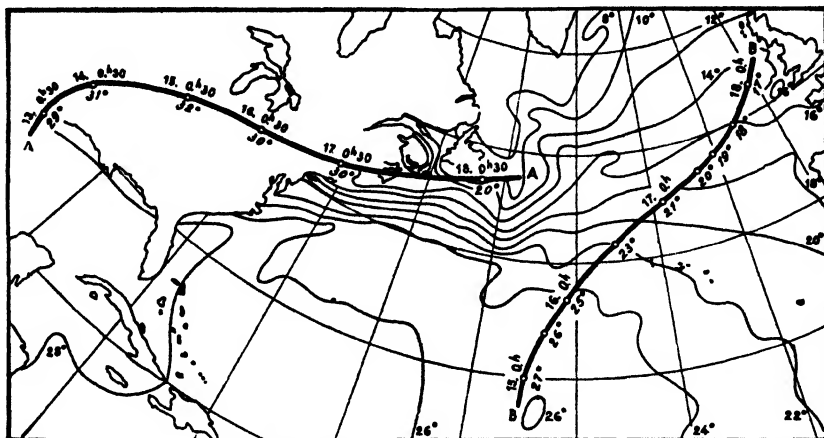
Fig. 8.—Trajectories and air temperatures compared with the temperature of the surface of the sea.

The trajectory shows that the wind velocity was moderate to high, which indicates that the temperatures are representative.

Curve *B* shows the trajectory of a parcel of air that moved from the southwest of the Azores toward Ireland. The air temperature changed
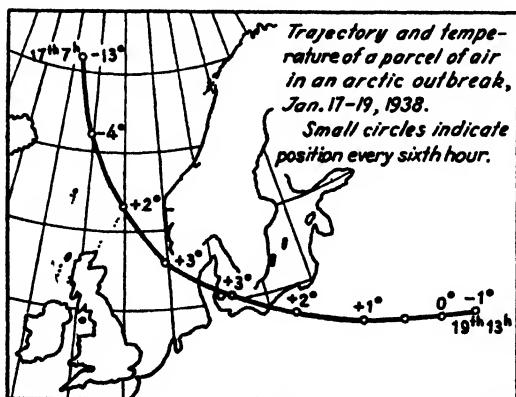
Fig. 9.

gradually from 27 to 17°C. The changes are quite in agreement with what one would expect from the temperature of the sea surface.

Figure 9 shows the trajectory of a parcel of air belonging to an outbreak of an arctic air mass. The air, coming directly from the arctic snow

fields, has a temperature which is considerably lower than that of the surface of the sea. On its way from Jan Mayen to the Shetland Isles, the temperature of the moving parcel of air changes from -13 to $+2°C$. because it moves perpendicularly to the sea-surface isotherms. In the southeast part of the North Sea, the air moves along the sea-surface isotherms, and there are but slight temperature changes. As the air enters the continent of Europe, its temperature begins to decrease because the air is streaming over a surface that presumably is colder than the air. The consequences of such temperature variations on the stability conditions in the moving air masses will be discussed in later sections.

The examples above suffice to show that the surface air temperature is not a conservative property. However, the changes in temperature that occur in the moving masses are easily understood and may be predicted with reasonable accuracy by considering the distribution of the temperature of the surface of the earth, the wind velocity, and the cloudiness of the air. The forecaster must not overlook these details, for great developments may result from the humblest facts.

11. Humidity.—Let e denote the partial pressure, and E the saturation pressure of the aqueous vapor. The *relative humidity* of the air is then defined as

$$R = 100 \frac{e}{E} \qquad \text{(per cent)}$$

The relative humidity, which expresses the degree of saturation, is nonconservative with respect to both isobaric and adiabatic temperature changes. In the vicinity of the surface of the earth, it is representative under the same condition as renders the surface air temperature representative.

Absolute humidity (a) is the mass of aqueous vapor, expressed in grams per cubic meter of air. It is obtained from the formula

$$a = f_0 \frac{T_0}{p_0} \frac{e}{T}$$

where f_0 is the density of aqueous vapor under standard pressure p_0 and temperature T_0, whence

$$a = 217 \frac{e}{T} \qquad \text{(grams per cubic meter)}$$

Absolute humidity is nonconservative with respect to isobaric as well as adiabatic temperature variations; and as it does not readily express the degree of saturation, it is even less suitable than relative humidity for air-mass analysis. This applies to the air near the surface of the earth as well as to the free atmosphere.

Specific humidity (*q*) is the mass of aqueous vapor, expressed in grams per kilogram of humid air. It is obtained from the formula

$$q = \frac{623e}{p - 0.377e} \quad \text{(grams per kilogram)}$$

or

$$q = \frac{0.623e}{p - 0.377e} \quad \text{(grams per gram)}$$

where *p* denotes the pressure of the humid air.

The ratio of mixing (*x*) is the mass of aqueous vapor, expressed in grams per kilogram of dry air. It is related to *e* and *p* as follows:

$$x = \frac{623e}{p - e} \quad \text{(grams per kilogram)}$$

or

$$x = \frac{0.623e}{p - e} \quad \text{(grams per gram)}$$

From the foregoing definitions, it follows that the ratio of mixing and the specific humidity are both conservative with respect to isobaric and dry-adiabatic temperature variations. They are therefore both suitable for application in the analysis of weather charts and aerological ascents. When condensation occurs or when water vapor is transferred to the mass either through evaporation or mixing, the specific humidity and ratio of mixing become nonconservative. The application of specific humidity or ratio of mixing to air-mass analysis will be explained in a later section in connection with isentropic analysis.

12. Dew-point Temperature.—The temperature to which humid air can be cooled at constant pressure without causing condensation is called the dew-point temperature, or dew point.

The dew point is conservative with respect to isobaric temperature variations. However, when the underlying surface is heated (*e.g.*, diurnally), the vapor-pressure gradient between the surface and the air increases, with the result that evaporation is accelerated, and the dew-point temperature rises. Conversely, when the underlying surface is cooled, the vapor-pressure gradient decreases and may become reversed so that dew is deposited on the ground. The dew-point temperature is then lowered. In humid regions the dew point has a maximum during the day, and a minimum during the night, with a diurnal amplitude of about one-fifth to one-sixth of the diurnal variation in temperature (see Fig. 68). In arid regions, such as deserts and steppes, the diurnal variation is reversed, on account of dryness of the ground and the intense eddy transfer of humidity along the vertical during the day.

When the air temperature varies dry-adiabatically, the corresponding dew point will vary; but this variation is so slight that it is often negligible. Figure 10 shows an extreme case of such variation. Consider a parcel of air at pressure 1000 mb., temperature 20°C., and relative humidity 40 per cent, which corresponds to a dew point of 6.2°C. If the parcel rises dry-adiabatically, it will become saturated at 815 mb. and 3°C. While the air temperature thus varied 17°C., the corresponding dew point varied only about 3°C. From Fig. 10, it is seen that the dew point below the condensation level varies along the constant-humidity line and the temperature varies along the dry-adiabatic line.
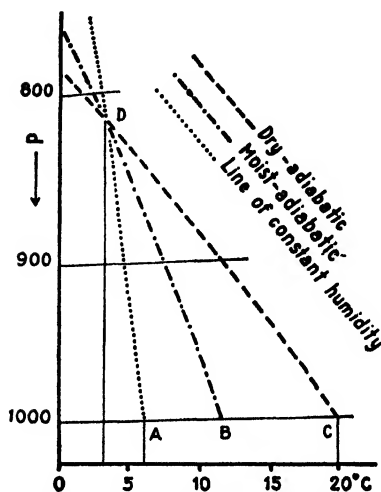
Fig. 10.—Adiabatic variation of dew point. When the air temperature decreases dry-adiabatically from *C* to *D*, the corresponding dew point decreases only the small amount as indicated by the line *AD*. Above the condensation level *D*, the dew point follows the moist-adiabatic.

In dry-adiabatic processes the variation in dew point is only one-fifth to one-sixth of the dry-adiabatic rate of change in temperature. Above the condensation level, both the dew point and the air temperature vary along the moist-adiabatic line.

With respect to air-mass analysis, the dew point has the following advantages:

1. Together with the air temperature, it shows the degree of saturation of the air.

2. It is conservative with respect to isobaric temperature variations.

3. It is quasi-conservative with respect to dry-adiabatic variations.

4. Its diurnal variation is considerably smaller than that of the air temperature.

5. It is often representative when the air temperature is locally influenced.

The last point requires explanation: Say that the representative air temperature is 20°C. but, for some reason, it is influenced locally (*e.g.*, because of a low inversion which has formed overnight) so that the thermometer shows only 15°C. While the air near the surface cools from 20 to 15°C., the relative humidity would rise accordingly so that both air temperature and relative humidity become nonrepresentative, but the dew point would not be affected by this change unless evaporation or condensation occurred.

The dew point is of inestimable value in the analysis of weather charts for the purpose of predicting the formation of fog and frost. If the air

temperature falls below the dew point, fog will form.   This applies both
to radiation fog and advection fog.   If the air temperature falls below
0°C., frost will occur if the dew point is below freezing; but if the dew
point is above zero, fog will form which will hinder further appreciable
cooling.

13. Wet-bulb Temperature.—The temperature recorded by a well-
ventilated wet-bulb thermometer is called the wet-bulb temperature of
the air.   The wet-bulb temperature may be defined more precisely as
the lowest temperature to which the air can be cooled at constant pres-
sure by evaporating water into the air.   As the wet-bulb temperature
is of considerable interest in connection with the analysis of aerological
ascents, its thermodynamic properties will be discussed in detail.

When the ventilation has continued for some time, the wet-bulb
thermometer assumes a constant temperature, indicating that there is no
net gain or loss of heat.   The heat gained from the air is then expended
in evaporating water from the wet bulb.

Following Normand [49], we assume that the air which is in contact
with the wet bulb assumes the temperature of the wet bulb and becomes
saturated at that temperature.   This assumption involves the fact that
the heat contained in a parcel of air equals the heat which it contains
when it becomes saturated at its wet-bulb temperature, minus the content
of heat of the water which must be supplied to the parcel of air in order
to render it saturated.

The symbols are used in the following discussion:
T = temperature of the air.
x = ratio of mixing (grams per gram).
T_w = wet-bulb temperature.
x' = ratio of mixing of saturated air whose temperature is T_w.
L = latent heat of vaporization at the temperature T_w.
c_p = specific heat of dry air at constant pressure.
c_p' = specific heat of aqueous vapor at constant pressure.

The process at the wet-bulb thermometer may be described as follows:
$(1 + x)$ grams of humid air is cooled from T to T_w and thus expends
enough heat to evaporate $(x' - x)$ grams of water.   The result of this
process is that $(1 + x')$ grams of air becomes saturated at the tempera-
ture T_w at which the evaporation is supposed to take place.   The follow-
ing equation then holds:

$$(c_p + xc_p')(T - T_w) = L(x' - x)$$

or

(1) $$c_pT + Lx + xc_p'(T - T_w) = c_pT_w + Lx'$$

Disregarding the small term $xc_p'(T - T_w)$, we obtain

$$(2) \qquad\qquad T_w = T - \frac{L}{c_p}(x' - x)$$

As x' is the ratio of mixing when the air is saturated at the temperature T_w, it follows that T_w is uniquely determined by T and x.

It is readily seen that the wet-bulb temperature is conservative with respect to evaporation from, and condensation on, rain falling through the air. From Eq. (2) it follows that the air may be cooled by the amount $T - T_w$ if $x' - x$ grams of water is evaporated into it. Suppose a smaller amount of water is evaporated into the air. The temperature would then drop from T to T_1, where $T_1 > T_w$. The wet-bulb temperature, which is the lowest temperature to which the air can be cooled by evaporating water into it, would remain unchanged. If another portion of the water were evaporated into the air, the wet-bulb temperature would remain unaltered; and when the amount $x' - x$ grams has been evaporated, $T = T_w$, the air has become saturated, and no further evaporation is possible. Thus, *the wet-bulb temperature is conservative with respect to evaporation from falling rain when the heat of vaporization is supplied by the air.*

Similarly, if part of the moisture content of the air (*i.e.*, x) is condensed at constant pressure and the latent heat used to heat the air, the wet-bulb temperature would remain unchanged.

The foregoing applies when the heat of vaporization (or condensation) is supplied by the air. If evaporation takes place from terrestrial sources of water, the heat of vaporization is not supplied by the air. In such cases, the wet-bulb temperature is not conservative.

Following Normand, we assume that the process which takes place at the wet bulb is isentropic. This involves that the entropy of a parcel of air equals the entropy of the same parcel of air when it is saturated at the wet-bulb temperature, minus the entropy of the water which must be supplied to it in order to render it saturated. The actual increase in entropy is the difference between the entropy that the water has received at the temperature T_w and the entropy that the air has lost by being cooled from T to T_w, or

$$\Delta S = (c_p + xc_p')\frac{T - T_w}{T_w} - (c_p + xc_p')\int_{T_w}^{T}\frac{dT}{T}$$
$$= (c_p + xc_p')\left(\frac{T - T_w}{T_w} - \ln\frac{T}{T_w}\right)$$

Expanding the expression for $\ln(T/T_w)$, we obtain

$$\Delta S = (c_p + xc_p')\frac{1}{2}\left(\frac{T - T_w}{T_w}\right)^2$$

Having regard to the smallness of the last factor, we see that ΔS amounts to only a small fraction of the entropy received by the water. The process may therefore be regarded as an isentropic one.

It will be seen from a humidity table that the depression of the wet-bulb thermometer is always small when the air temperature is low. In such cases, the process may be regarded as isentropic even when the air is relatively dry. However, when the air temperature is high and the relative humidity is low, the depression of the wet-bulb thermometer is considerable. In such cases, the assumption of isentropic conditions may introduce a noticeable error. This point will be discussed in Par. 16.

We consider next the behavior of the wet-bulb temperature relative to adiabatic variations. The physical conditions of a parcel of air are represented by a point in Fig. 11. We shall now show that the dry-adiabatic through such a point, the moist-adiabatic through the point which represents its wet-bulb temperature, and the dew-point line intersect one another at the point which represents the condensation level of the parcel in question.

We consider a parcel of air at A whose temperature is T and dew point is T_d. The line CD is the line of constant mixing ratio x. In a dry-adiabatic process, A will

FIG. 11.—Showing the relation between temperature T, wet-bulb temperature T_w, and dew-point temperature in an adiabatic process.

move along the line AD in the diagram, and the corresponding dew point will be found on the line CD, which is called the dew-point line of the parcel at A. As the parcel A arrives at D, it becomes saturated, its temperature equaling the dew-point temperature. The point D, then, represents the condensation level of the parcel at A.

Let us next consider a parcel of saturated air at B determined by the moist-adiabatic through D. Its temperature is then equal to the wet-bulb temperature T_w, and its mixing ratio is x'. We let this parcel of air ascend; as it arrives at D, it is still saturated, and it contains x grams aqueous vapor plus $(x' - x)$ grams liquid water. In the point D, the parcel that ascended from B has the same mixing ratio and the same temperature as has the parcel that ascended from A to D. We remove the liquid water at D and let the parcel descend dry-adiabatically; it

must then arrive at the point A where its temperature and mixing ratio will be the same as those of the parcel A. The entropy of the parcel at B is, therefore, equal to the entropy of the parcel at A plus the entropy of the water removed at D. It follows, then, that the wet-bulb temperature must be the same at the beginning and at the end of the process. Consequently, the wet-bulb temperature of the parcel A is the temperature of the saturated parcel at B. It thus follows from Fig. 11 that the dry-adiabatic through A, the moist-adiabatic through B, and the dew-point line (the line of constant mixing ratio) through C intersect one another in the point D.

If the parcel at A ascends dry-adiabatically to an arbitrary level, say E, the wet-bulb temperature would vary moist-adiabatically from B to F, and the dew-point would move along the dew-point line from C to G. Thus, in a dry-adiabatic process, the wet-bulb temperature is determined by the moist-adiabatic running through the point that represents the wet-bulb temperatures. As the parcel ascends above the condensation level, $T = T_w$, and the wet-bulb temperature is determined by the same moist-adiabatic as below the condensation level.

If the parcel A descends to the 1000-mb. level, its temperature becomes equal to its potential temperature (*i.e.*, θ). During this process, the wet-bulb temperature varies moist-adiabatically and becomes equal to the potential wet-bulb temperature (*i.e.*, θ_w). Simultaneously, the dew point assumes the value indicated by θ_d (*i.e.*, the potential dew-point temperature).

The foregoing deductions are based on the assumption that the process at the wet bulb is isentropic. This assumption holds with satisfactory accuracy when the depression of the wet-bulb temperature is not excessively large. If the air temperature is high and the relative humidity (or x) is low, there is a noticeable increase in entropy. In such cases, the potential wet-bulb temperature is not strictly conservative with respect to dry-adiabatic changes.

From the foregoing, it follows that *the potential wet-bulb temperature* θ_w *is conservative with respect to evaporation from falling rain and quasi-conservative with respect to dry-adiabatic and moist-adiabatic changes.*

It is readily seen from Fig. 11 that the wet-bulb temperature is non-conservative with respect to nonadiabatic variations. Thus, if the air temperature of the parcel A is increased from A to A', the condensation level would rise from D to D', and the wet-bulb temperature would increase from B to B'; a corresponding increase of the potential wet-bulb temperature would result.

14. Equivalent Temperature.—Let T_e denote the temperature of perfectly dry air, the wet-bulb temperature of which is T_w. In this case $x = 0$, which substituted into Eq. *13*(1) gives

(1) $$T_e = T_w + \frac{L}{c_p} x'$$

From this and from Eq. *13*(2), we obtain

(2) $$T_e = T + \frac{L}{c_p} x$$

This shows that T_e may be interpreted as the temperature which the air would assume if all aqueous vapor were condensed at constant pressure and the latent heat thereby liberated used to increase the air temperature. Similarly, $(T_e - T)$ may be interpreted as the increase in temperature that would result if such condensation were to take place. $(T_e - T)$ is called the *equivalent-temperature difference*, and T_e is called the *equivalent temperature* of the air.

Equation (2) corresponds to the original definition of equivalent temperature as given by Robitsch [62]. As x' indicates the ratio of mixing of saturated air at the temperature T_w, it follows from Eq. (1) that *the equivalent temperature is uniquely determined by the wet-bulb temperature, and vice versa.*

The potential equivalent temperature is defined in the same way as potential temperature, *viz.*,

$$\theta_e = T_e \left(\frac{1000}{p}\right)^{\frac{c_p - c_s}{c_p}}$$

Both θ_e and θ_w are strictly conservative with respect to evaporation from falling rain and quasi-conservative with respect to dry-adiabatic and moist-adiabatic changes.

The wet-bulb temperature has the advantage over the equivalent temperature that it is directly observable; and, when it is not directly observed, it is more easily evaluated. Moreover, the wet-bulb temperature, together with the air temperature, indicates the degree of saturation.

15. Pseudo-equivalent Temperature.—The definition of equivalent temperature given above is based on the assumption that the moisture content of the air is condensed at constant pressure. Stüve [79] and Rossby [63] have introduced a new definition which is more logical inasmuch as it provides a function of T and x that is strictly conservative with regard to all adiabatic changes and closely related to the stability criteria of the air.

A parcel of humid air at A (see Fig. 12), whose temperature is T, is moved dry-adiabatically to its condensation level B, whence it is moved along the moist-adiabatic (*i.e.*, pseudo-adiabatically) upward until all water vapor has been condensed. The moist-adiabatic then approaches the dry-adiabatic asymptotically. The parcel is then moved dry-

adiabatically downward, and it arrives at the point D with a temperature T_{se}, which we shall call the *pseudo-equivalent temperature*.[1] If the parcel were moved further downward, it would arrive at the 1000-mb isobar with a temperature θ_{se}, which is called the *potential pseudo-equivalent temperature*.

It is readily seen that when a parcel of air is moved upward or downward, dry-adiabatically or moist-adiabatically, the pseudo-equivalent
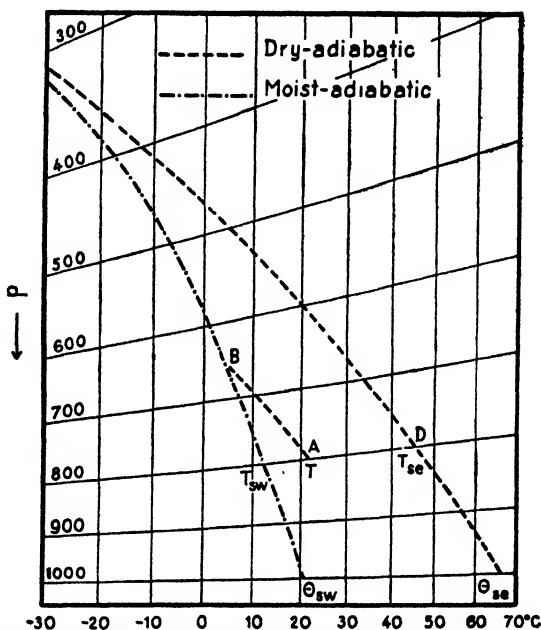
FIG. 12.—Showing the definition of pseudo-equivalent temperature.

temperature will vary dry-adiabatically, and the potential pseudo-equivalent temperature will remain unchanged. Hence, it follows that the *potential pseudo-equivalent temperature (θ_{se}) is conservative with respect to dry-adiabatic as well as moist-adiabatic changes*.

By aid of a thermodynamic diagram, it is readily shown that the pseudo-equivalent temperature is higher than the equivalent temperature. The difference may amount to 8°C. when the moisture content is high. Normally, the difference is small; and as the equivalent temperature is strictly conservative with respect to evaporation from falling rain, we

[1] Stüve called this temperature pseudo-temperature, Rossby called it equivalent temperature, and Bleeker equivalent adiabatic temperature. It is preferred here to introduce the designation *pseudo-equivalent temperature* in order to retain the qualifying word *equivalent* and at the same time to indicate that the process is a *pseudo*-adiabatic one.

may conclude that the pseudo-equivalent temperature is quasi-conservative with regard to such evaporation.

16. Pseudo-wet-bulb Temperature.—It was shown in Par. 14 that the equivalent temperature is uniquely determined by the wet-bulb temperature, and vice versa. Bleeker [7] has shown that it is possible to define another function of temperature and humidity which differs only slightly from the wet-bulb temperature and has the same thermodynamic properties as has the pseudo-equivalent temperature.[1]

In Fig. 12, a parcel of humid air A is moved dry-adiabatically upward to its condensation level B and thence moist-adiabatically down to the original isobar. It will then arrive there with a temperature T_{sw}, which is called the *pseudo-wet-bulb temperature* of the parcel at A. If the parcel were moved farther downward to the 1000-mb. isobar, it would arrive there with a temperature θ_{sw}, which is called the *potential pseudo-wet-bulb temperature.*

If the parcel A were moved upward beyond the level B, it would follow the moist-adiabatic through B. Whether the parcel moves upward or downward, dry-adiabatically or moist-adiabatically, its pseudo-wet-bulb temperature will be found on the moist-adiabatic running through B. During such processes, the potential pseudo-wet-bulb temperature will remain unchanged, and so will also the potential pseudo-equivalent temperature. θ_{sw} is therefore uniquely determined by θ_{se}, and vice versa; *they are both strictly conservative with respect to dry-adiabatic and moist-adiabatic changes and quasi-conservative with respect to evaporation from falling rain.*

It is readily seen from Fig. 12 that T_{sw} and θ_{sw} are more easily evaluated from a diagram than are T_{se} and θ_{se}. Moreover, as T_{sw}, together with T, is expressive of the degree of saturation, it is more convenient to use T_{sw} and θ_{sw} than T_{se} and θ_{se}.

17. Further Remarks on Humidity Elements.—It follows from Pars. 13 and 16 that the difference between T_w and T_{sw} is very small. The difference vanishes completely when the air is saturated, *i.e.*, when $T = T_w$. Only when the air temperature is high and the relative humidity is very low will there be any noticeable difference between them. The same also applies to θ_w and θ_{sw}.

It is readily seen that the following is true of humid nonsaturated air:

$$T_d < T_{sw} < T_w < T < T_e < T_{se}$$

The difference $T_w - T_{sw}$ is normally negligible against the inaccuracy of the humidity observations.

---

[1] The quantity defined by Bleeker was called the adiabatic wet-bulb temperature. It is preferred here to use the term *pseudo-wet-bulb temperature* by analogy with the term *pseudo-equivalent temperature* (see footnote, page 24).

If the air is saturated, we have

$$T_d = T_{sw} = T_w = T < T_e < T_{se}$$

The difference $T_w - T_{sw}$ vanishes, and the difference $T_{se} - T_e$ has then a maximum. Similarly, if the air is perfectly dry

$$T_d < T_{sw} < T_w < T = T_e = T_{se}$$

The difference $T_{se} - T_e$ then vanishes, and the difference $T_w - T_{sw}$ has a maximum. These relations, which follow from the definitions in Pars. 12 to 16, hold also for the corresponding potential temperatures.

18. Choice of Humidity Element.—It appears from the foregoing paragraphs that there are in use a considerable number of methods of indicating the humidity conditions of the air. Each of these methods may have advantages for special purposes, but from the point of view of air-mass analysis and forecasting the chief requirements are that the humidity elements contained in the synoptic reports should (1) indicate the degree of saturation, (2) be conservative with regard to dry-adiabatic and moist-adiabatic processes in the free atmosphere and with regard to nonadiabatic processes near the earth's surface, and (3) be readily used on aerological diagrams.

Table 1 summarizes the principal advantages and disadvantages of the various elements.

It will be seen that there are three humidity elements which are conservative with respect to nonadiabatic temperature changes. As nonadiabatic temperature changes are predominant near the earth's surface, it is most advantageous to use one of these elements in the analysis of the surface weather maps. It will be noticed that the dew-point temperature is the most convenient element to use because it expresses the degree of saturation, and it is most easily applied in forecasting fog. It is sufficiently conservative with regard to such pressure variation as may occur locally and such pressure differences as are due to differences in altitude between neighboring stations.

For the analysis of the upper-air data, it appears that the pseudo-wet-bulb temperature is most convenient. When plotted on a thermodynamic diagram, it shows at once the potential pseudo-wet-bulb temperature, and the advantages of both these elements are thus obtained. The fact that these elements are not conservative with respect to nonadiabatic temperature changes is of minor importance, for such processes are relatively unimportant in the free atmosphere during intervals of time as short as those between consecutive charts (see Par. 3). As the difference between wet-bulb temperature and pseudo-wet-bulb temperature is very small, it would also be satisfactory to use wet-bulb temperature in the analysis of upper-air data.

Owing to the great difference between the methods of analysis of surface maps and upper-air observations, there is hardly any inconvenience connected with the use of dew point in the surface data and pseudo-wet-bulb temperature in the upper-air data. Moreover, one of these elements is easily converted into the other by means of a diagram.

TABLE 1

Humidity element	Conservative with respect to			
	Dry-adiabatic temperature changes	Moist-adiabatic temperature changes	Nonadiabatic temperature changes	Evaporation from falling rain
Relative humidity.............	No	No	No	No
Absolute humidity.....	No	No	No	No
Ratio of mixing...	Yes	No	Yes	No
Specific humidity.............	Yes	No	Yes	No
Dew point...................	Quasi-conservative	No	Yes	No
Wet-bulb temperature.........	No	No	No	Yes
Equivalent temperature........	No	No	No	Yes
Pseudo-wet-bulb temperature...	No	No	No	Quasi-conservative
Pseudo-equivalent temperature.	No	No	No	Quasi-conservative
Potential wet-bulb temperature.	Quasi-conservative	Quasi-conservative	No	Yes
Potential equivalent temperature.	Quasi-conservative	Quasi-conservative	No	Yes
Potential pseudo-wet-bulb temperature.	Yes	Yes	No	Quasi-conservative
Potential pseudo-equivalent temperature.	Yes	Yes	No	Quasi-conservative

19. Condensation.—Active condensation occurs when the air is saturated or nearly so, provided that hygroscopic nuclei are present in the air. Slight condensation is known to occur in relatively dry air; but, in such cases, the drops are normally so rare and so exceedingly small that no clouds or fogs result. With condensation nuclei of normal hygroscopic properties, condensation would not be sufficiently active to produce a fog or cloud unless the relative humidity is 97 per cent or more, whereas mist may form with lower relative humidity.

Certain products of combustion are highly hygroscopic and may give rise to intense condensation. This is particularly true of sulphur trioxide which, under the direct influence of sunlight, forms from sulphur dioxide. The frequent fogs in industrial areas are caused by condensa-

tion on a variety of hygroscopic nuclei resulting from combustion. However, as condensation occurs effectively and frequently in unpolluted air, it is evident that the main source of condensation nuclei cannot be sought in combustion. Köhler has shown that sea salt sprayed up from the oceans is present in the atmosphere in abundant quantities and that most drops are condensed on nuclei of such salt.

At low temperatures, the condensation nuclei become inactive, and the sublimation nuclei become active. Ice crystals are then formed instead of water droplets, and the process is then called *sublimation*. But water droplets frequently form at temperatures considerably below freezing, and droplets that are carried upward in the ascending air currents often persist as water droplets even below −20°C. As large drops crystallize more easily than small drops, it is plausible that the drops which are carried upward by strong convective currents will crystallize at relatively high temperatures. In cumulo-nimbus clouds, the drops usually crystallize at temperatures about −10°C. Although the tops of the cumulo-nimbus usually consist of ice crystals and their bases of water droplets, there will be a portion of the cloud in which ice crystals and water droplets coexist. Similar conditions are frequently realized in the alto-stratus–nimbo-stratus cloud systems. We shall presently see that this feature is of considerable importance in the discussion of the formation of precipitation.

20. Classification of Clouds.—Even though the number of forms that clouds may take is almost unlimited, it is a fact that the number of *types* of cloud is limited. The international classification of clouds [34] consists of 10 main types, which for convenience are arranged according to height above the ground in the following manner:

TABLE 2.—CLASSIFICATION OF CLOUDS

Name	Abbreviation	Altitude
Cirrus	*Ci*	
Cirro-stratus	*Cs*	High
Cirro-cumulus	*Cc*	
Alto-stratus	*As*	
Alto-cumulus	*Ac*	Medium
Strato-cumulus	*Sc*	
Nimbo-stratus	*Ns*	
Cumulus	*Cu*	Low
Cumulo-nimbus	*Cb*	
Stratus	*St*	

Cirrus (*Ci*) is the highest of all clouds. It has a typical fibrous (threadlike) structure and a delicate silky appearance (Fig. 13). Cirrus

clouds are sometimes arranged irregularly in the sky as detached clouds without connection with cirro-stratus or alto-stratus. They are then
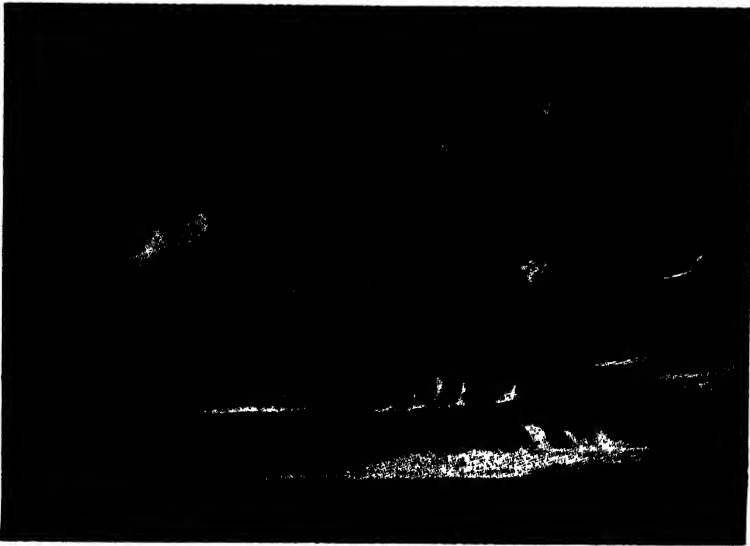
Fig. 13.—Cirrus. (*International Atlas of Clouds. Photograph by Fundacio Concepcio Rabell.*)
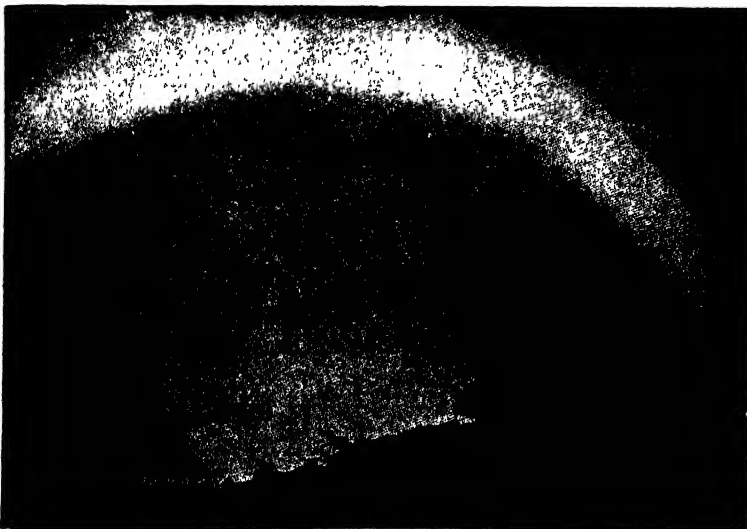
Fig. 14.—Cirro-stratus. Below, tops of cumulus. (*International Atlas of Clouds. Photograph by G. A. Clark.*)

called fair-weather cirrus. If the cirrus clouds are arranged in bands or connected with cirro-stratus or alto-stratus or otherwise systematically arranged, they are usually harbingers of bad weather. In "thundery"

or squally weather, a special kind of cirrus (*cirrus densus*) is frequently observed which originates from the anvils of cumulo-nimbus. These
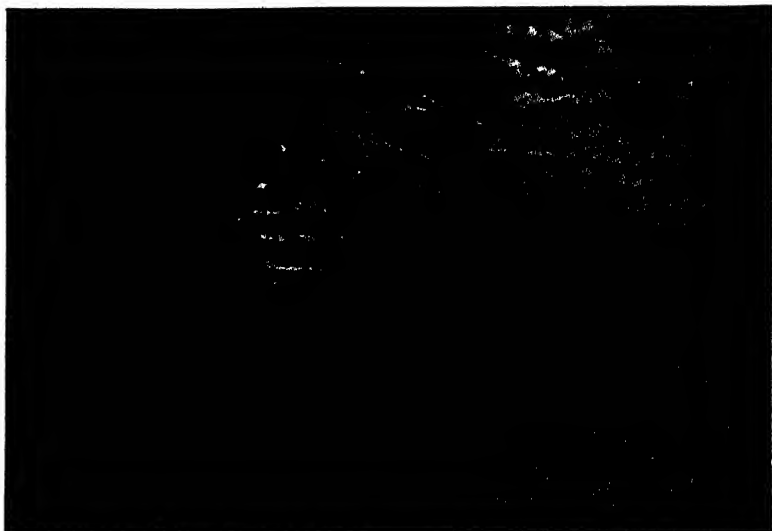
Fig. 15.—Cirro-cumulus.   (*International Atlas of Clouds.*)
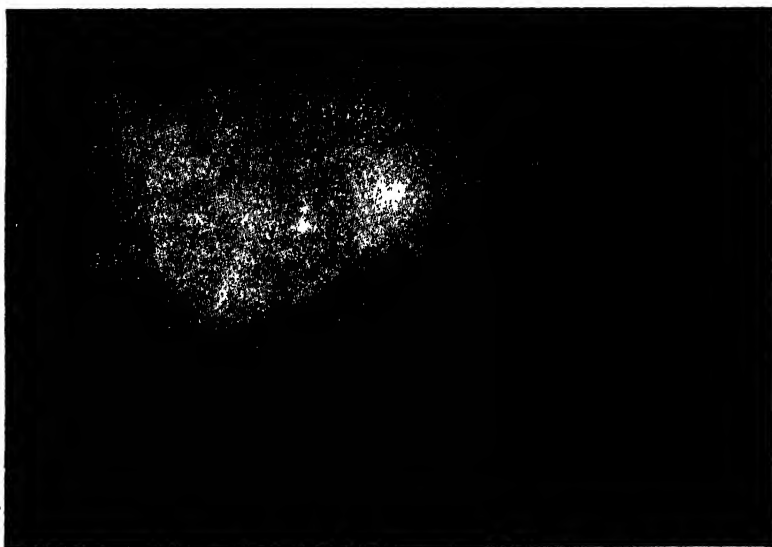
Fig. 16.—Alto-stratus.   (*International Atlas of Clouds.   Photograph by G. A. Clark.*)

clouds are often called *false cirrus,* because they are denser and usually lower than the ordinary cirrus.

Cirro-stratus (*Cs*) is a thin, whitish sheet of cloud, sometimes like a veil covering the whole sky and merely giving it a milky appearance, at other times showing signs of a fibrous structure like a tangled web

(Fig. 14).   Cirro-stratus often produces a halo around the sun or moon. It is often a sign of approaching bad weather.
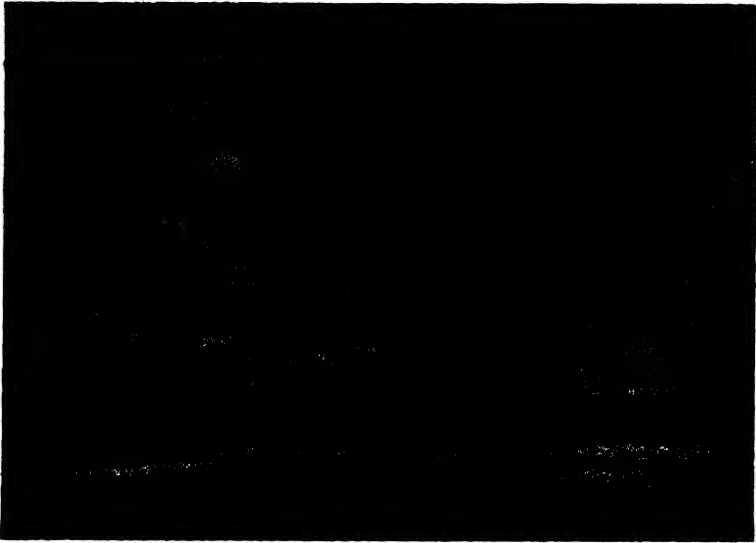
Fig. 17 —Alto-cumulus.   (*International Atlas of Clouds.   Photograph by G. A. Clark.*)
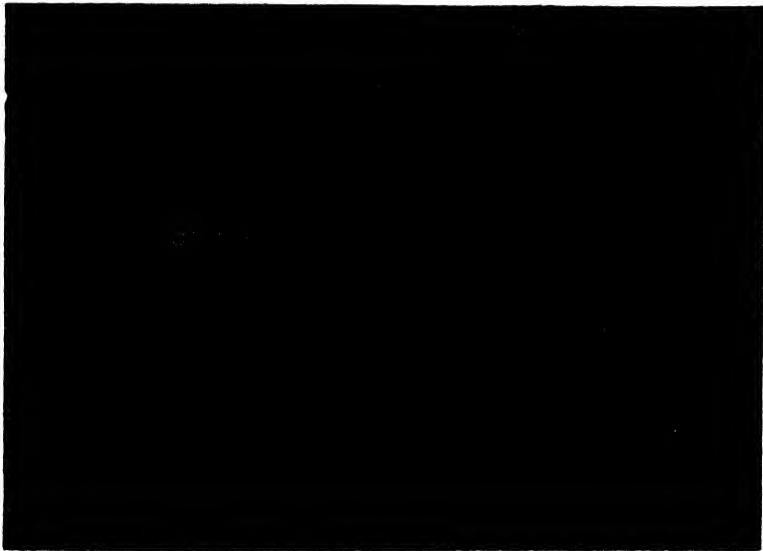
Fig. 18.—Strato-cumulus.   (*International Atlas of Clouds.   Photograph by G. A. Clark.*)

Cirro-cumulus (*Cc*) consists usually of small, white flakes of clouds without shadow, arranged in a regular pattern (Fig. 15).   Cirro-cumulus develops from cirro-stratus.   The pattern is due to a single or a double undulation of the cloud sheet.

Alto-stratus (*As*) is a dense sheet of gray or bluish color, often showing a fibrous structure (Fig. 16).   It often merges gradually into cirro-stratus.
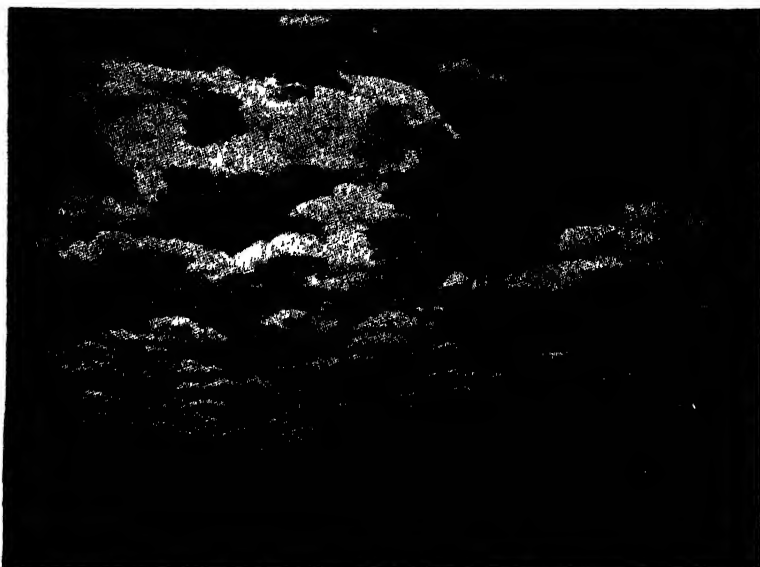
Fig. 19.—Cumulus humilis. (*International Atlas of Clouds. Photograph by O. N. M. Paris.*)

Fig. 20.—Cumulus congestus. (*International Atlas of Clouds. Photograph by Met. Obs. Potsdam.*)

Increasing alto-stratus is usually followed by precipitation of a continuous and lasting type.

Alto-cumulus (*Ac*) differs from cirro-cumulus in consisting of larger globules, often with shadows, whereas cirro-cumulus clouds show only indications of shadows or none at all (Fig. 17).   Alto-cumulus often develops from dissolving alto-stratus.   An important variety of alto-cumulus is called *alto-cumulus castellatus*.   In appearance it resembles

Fig. 21.—Cumulo-nimbus calvus.   (*International Atlas of Clouds.   Photograph by Baker.*)

Fig. 22.—Cumulo-nimbus incus.   (*International Atlas of Clouds.   Photograph by Baker.*)

ordinary *Ac*; but in places turreted tops develop that look like miniature cumulus.   Alto-cumulus castellatus usually indicates a change to a chaotic, "thundery" sky.

Strato-cumulus (*Sc*) is a cloud layer consisting of large lumpy masses or rolls of dull gray color with brighter interstices (Fig. 18).   The masses are often arranged in a regular way and resemble alto-cumulus.

Nimbo-stratus (*Ns*) is a dense, shapeless, and ragged layer of low clouds from which steady precipitation usually falls.   It is usually connected with alto-stratus which is present above the nimbus.   Fragments

Fig. 23.—Cumulo-nimbus arcus, or the line squall cloud.   (*International Atlas of Clouds Photograph by Fundacio Concepcio Rabell.*)

of nimbus that drift under the rain clouds are called *fractonimbus* or *scud*.

Cumulus (*Cu*) is a thick cloud whose upper surface is dome-shaped, often of a cauliflower structure, the base being usually horizontal. Cumulus clouds may be divided into two classes.   Flat cumulus clouds without towers or protuberances are called *cumulus humilis* or fair-weather cumulus (Fig. 19).   Towering cumulus clouds with typical

cauliflower structure showing internal motion and turbulence are called *cumulus congestus* (Fig. 20). They may develop into cumulo-nimbus.

Cumulo-nimbus (*Cb*) thunderclouds or shower clouds are great masses of cloud rising like mountains, towers, or anvils and having a base that looks like a ragged mass of nimbo-stratus. The tops are often anvil-shaped or surrounded by false cirrus. Figure 21 shows a cumulo-nimbus without anvil, and Fig. 22 shows one with anvil. The cumulo-nimbus clouds are accompanied by showers, squalls, or thunderstorms and sometimes hail. The *line squall cloud* is a variety of cumulo-nimbus that extends like a long line or arch across the sky (Fig. 23).
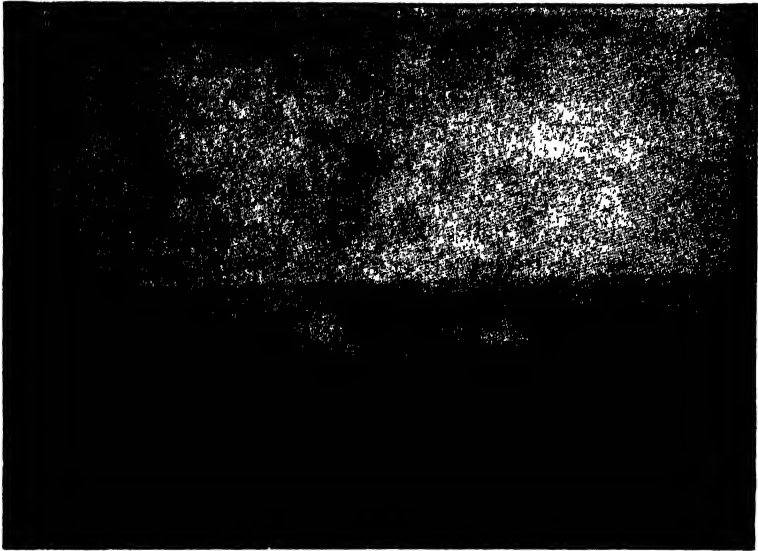
Fig. 24.—Stratus. (*International Atlas of Clouds. Photograph by Gain.*)

Stratus (*St*) is a uniform layer of low cloudlike fog, but not lying on the ground (Fig. 24).

The heights of the various types of cloud vary within wide limits. The high clouds are usually above 20,000 ft. (6000 m.) and below 30,000 ft. (10,000 m.). The medium clouds are most frequently between 8000 and 20,000 ft. (2500 and 6000 m.), and the low clouds below 8000 ft. (2500 m.). The tops of cumulus clouds, notably those of cumulo-nimbus, may reach to great heights, while their bases on the average are at or below 3000 ft. (1000 m.) above the ground.

21. Genetical Classification of Clouds.—From a genetical point of view the tropospherical clouds may be divided into four categories, *viz.*: (1) clouds that form in unstable air masses, (2) clouds that form in stable air masses, (3) clouds that form in connection with quasi-horizontal inversions, and (4) frontal clouds.

The categories (1) and (2) are typical air-mass clouds, or *internal* clouds, that characterize the stability conditions of the masses to which they belong.   The clouds belonging to (3) are most frequently related to the group (2), but sometimes they are in certain features related to (1).   The clouds of group (4) are formed because of upglide movement along frontal surfaces.   These clouds, too, are influenced by the stability conditions of the air.

The clouds typical of category (1) are: cumulus humilis (Plate 73)[1], cumulus congestus (Plate 79), cumulo-nimbus calvus (Plate 86), cumulo-nimbus incus (Plate 90), cumulo-nimbus capillatus (Plate 91), and cumulo-nimbus mammatus (Plate 96).   Other signs of instability are certain detached high clouds such as cirrus nothus (Plate 8) and cirrus densus (Plate 7), which originate from the anvils of cumulo-nimbus.

The most typical cloud forms belonging to category (2) are fog and stratus (Plates 66, 67 and 68), which are unmistakable signs of stable stratification.

Belonging to category (3) but being related to (2) are strato-cumulus (Plates 47 and 64) and certain types of alto-cumulus (Plate 27).   A great variety of clouds belong to category (3) but show signs of instability and are therefore related to category (1).   We mention here only the following: strato-cumulus vesperalis (Plate 56), strato-cumulus castellatus (Plate 55), strato-cumulus cumulogenitus (Plates 57 and 58), cumulus undulatus (Plate 74), and certain types of alto-cumulus castellatus (Plate 40).

The clouds belonging to category (4) are of a stratiform type when the air that takes part in the upglide movement is stable (*e.g.*, alto-stratus, Plate 43); and when the air is completely unstable, the frontal cloud system may be of the cumulus type (*e.g.*, cumulo-nimbus arcus, Plate 99).   When the air that takes part in the upglide movement is conditionally unstable, the lower part of the cloud system may be stratified, and cumulus or cumulo-nimbus towers project from the upper part of the frontal cloud layer, showing a vertical structure similar to Plate 120.

In later sections on stability and instability, air masses, fronts, and cyclones, the formation of clouds and the synoptic interpretation of clouds forms will be discussed more fully.   What we here wish to emphasize is that the various cloud forms give valuable information as to the processes in the atmosphere that depend on the stability and instability. Where aerological observations are lacking, the forms of clouds and precipitations are the only indicators of the conditions of the free atmos-

---

[1] The numbers refer to International Atlas of Clouds and States of Sky, I, General Atlas, Office *Nationale Météorologique*, Paris, 1932.

phere. The correct observation and interpretation of cloud forms and hydrometeors are therefore of immense importance.

22. Hydrometeors and Kindred Phenomena.—Bodies of solid or liquid water falling through the air are called hydrometeors. Together with the forms of clouds, the hydrometeors indicate to a certain extent the stability conditions in the free atmosphere and the thermodynamic processes in operation. The hydrometeors, when classified and reported in a rational manner, are of inestimable value as air-mass characteristics. The following descriptions of the most important hydrometeors are in agreement with the classification of Bergeron [3].

1. *Rain* is precipitation of liquid water in which the drops as a rule are larger than in drizzle (see below). Most drops have diameters greater than 0.5 mm., and they usually fall in still air with a velocity greater than 3 m./sec. The first drops, however, from an advancing alto-stratus–nimbo-stratus canopy may all have diameters less than 0.5 mm., but they can then be distinguished from drizzle by not being numerous and by the clouds from which they fall.

2. *Snow* is precipitation of solid water mainly in the form of branched hexagonal crystals or stars, sometimes mixed with simple ice crystals (see below). At temperatures above $-10°C$. they are often matted together in large flakes owing to the presence of a film of water or droplets of fog on the individual crystals.

3. *Sleet*[1] is precipitation consisting of snow and rain or melting snow.

4. *Drizzle* is rather uniform precipitation of very numerous minute drops (diameter less than 0.5 mm.), which seem almost to float in the air and visibly follow even slight air motion. Drizzle falls from fog or a continuous layer of thick stratus. In spite of the smallness of the drops, drizzle may sometimes give considerable amounts of precipitation (up to 1 mm./hr.), especially along coast and mountain ranges (*cf.* Fig. 25).

5. *Grains of ice* are precipitation consisting of transparent, globular or irregular, hard grains of ice, about 1 to 4 mm. in diameter; they rebound when falling on hard ground. This kind of precipitation occurs when rain from warm air aloft falls through a cold bottom layer of air whose temperature is below 0°C.

6. *Granular snow* is precipitation of white, opaque, snowlike grains, similar to soft hail, but more or less flattened or oblong in shape and generally less than 1 mm. in diameter, at least in one direction. They do not noticeably rebound or disintegrate when falling on hard ground.

---

[1] This description corresponds with the British use and that in publications of the International Meteorological Organization. The official definition of sleet of the U. S. Weather Bureau is "Frozen or partly frozen rain; frozen raindrops in the form of particles of clear ice." (See the paragraph on grains of ice.)

The grains consist mostly of small, unbranched or hexagonal ice crystals that have developed a soft rimelike cover or coating by falling through supercooled fog. Granular snow generally falls from stratus or fog; it falls in small quantities only and never as showers. It is the frozen product that corresponds to drizzle.

7. *Ice needles* are precipitation of very small, unbranched ice crystals in the shape of rods or plates often so small that they seem to float in the air like droplets of fog. When glittering in the sunshine, they become especially visible and often give rise to sun pillars or other halo phenomena. They occur under stable weather conditions, mostly as a result of strong frost in polar and typical continental winter weather and also in the high layers of the atmosphere (*e.g.*, diamond dust).

8. *Fog* consists of almost microscopically small waterdrops suspended in the air, or a mixture of such droplets and smoke or fine dust, that reduce the horizontal range of visibility to less than 1 km. At temperatures above 0°C., real fog can hardly exist when the relative humidity is less than 97 per cent. (If the relative humidity were less than 97 per cent, the condensation nuclei would have to be abnormally hygroscopic in order to produce a fog.) Thus, in a fog the air usually feels clammy and humid; and, on closer examination, one may even see the droplets floating past the eye. Fog is generally whitish in color, except in the vicinity of local sources of pollution where it may be of a dirty yellowish or grayish color.

9. *Mist*[1] consists of microscopically small waterdrops or of highly hygroscopic particles suspended in the air. The droplets in a mist are smaller and more scattered than in a fog; and, as a result, the horizontal range of visibility is greater than 1 km., the limit of visibility between fog and mist being fixed by international agreement. At temperatures above 0°C., the relative humidity in a mist may be below 97 per cent, and the air, therefore, does not feel as humid or so clammy as in a fog. Mist is of a grayish white color.

10. *Haze* consists of finely divided dust particles (from arid regions) or of salt particles which are dry and so extremely small that they cannot be felt or distinguished individually by the eye, but which diminish the visibility and give a characteristic smoky (hazy and opalescent) appearance to the air. Haze produces a uniform veil over the landscape and subdues its colors. The veil has a bluish tinge when viewed against a dark background ("blue mountains") but a yellowish or orange tinge when viewed against a white background (*e.g.*, clouds at the horizon,

---

[1] This definition corresponds with the British use and the one occurring in publications of the International Meteorological Organization. In North America, the word is often used synonymously with drizzle or fine rain.

snow-covered mountains, the sun, etc.). This distinguishes it from the grayish mist, the density of which it may sometimes attain.

At a certain distance, depending on the density of the haze, all details of the landscape and all details of color disappear and the object stands out as a silhouette against the sky. This characteristic distance at which the details disappear is in direct proportion to the distance at which the contours of a mountain disappear against the sky. In fine weather with sunshine on the object, the ratio between the two distances is 1:3, but in cloudy weather with shadow on the object, the ratio is 1:6.

11. *Soft hail* is precipitation of solid water in the form of white, opaque, round or occasionally conical grains of snowlike structure the diameter of which is 2 to 5 mm. The grains are crisp and compressible, and they rebound and disintegrate easily when they fall on hard ground. Soft hail occurs mainly at temperatures above 0°C. and mostly on land, often together with or before ordinary snow.

12. *Small hail* is precipitation of solid water in the form of semi-transparent, round or occasionally conical grains about 2 to 5 mm. in diameter. The grains generally consist of nuclei of soft hail surrounded by a thin crust of ice which gives them a glazed appearance. They are neither crisp nor easily compressed, and they do not generally rebound or disintegrate when they fall on hard ground. Small hail falls from cumulo-nimbus clouds, mostly at temperatures above 0°C. It often falls together with rain and is, therefore, usually wet.

13. *Hail* is precipitation of solid water in the form of balls or irregular lumps of ice of diameters ranging from 5 to 50 mm. or more. They are either transparent or composed of clear layers of ice alternating with opaque layers of snow, the clear layers being usually more than 1 mm. thick. Real hail falls almost exclusively in violent or prolonged thunderstorms and is very rare at temperatures below 0°C. at the earth's surface.

14. *Dust-* or *sandstorms* consist of dust or sand raised by the wind to such an extent that the horizontal range of visibility is considerably diminished. The dust and sand are never carried far from the source, and the conditions favorable for formation of dust- or sandstorms are extreme dryness of the ground, steep lapse rate of temperature, and high wind velocity.

15. *Drifting snow* is reported when there is no real precipitation but snow from the ground is carried up into the air by the wind to such an extent that the horizontal range of visibility is considerably diminished. When the vertical visibility, also, is considerably reduced, it may be difficult to distinguish drifting snow from real precipitation.

16. *Dew* is water deposited by direct condensation of aqueous vapor mainly on radiatively cooled horizontal surfaces.

17. *Hoarfrost* is ice crystals (scales, needles, feathers, or fans) deposited through sublimation in the same manner as dew.

18. *Soft rime* consists of white layers of ice crystals deposited chiefly on projected surfaces—especially on windward points and edges of objects—generally in supercooled fog or mist. The process of formation of soft rime is probably the same as that of soft hail.

19. *Hard rime* consists of opaque, granular masses of ice deposited in the same manner as soft rime, but in "wet air" or wet fog at a temperature below 0°C., thus developing a more compact and amorphous structure than soft rime, analogous to that of small hail.

20. *Glazed frost* is more or less homogeneous and transparent layers of ice that are deposited on horizontal as well as on projected surfaces from supercooled rain or drizzle. In the United States weather reports, rain and/or drizzle that produce glazed frost are reported as "freezing rain."

21. *Thunder and Lightning.*—When the difference in time is less than 10 sec., the phenomena are said to occur *"at the station"*; if the time difference is greater than 10 sec., the phenomena are said to occur *"in the neighborhood of the station."* When there is no audible thunder, the phenomenon is reported as "distant lightning."

22. *Pure air* indicates unusual clearness and transparency: distant objects and their details in shape and color stand out in full relief from the background with great hardness and distinctness (resembling the objects in a stereoscopic view) without any noticeable softening veil at a distance of 10 km. or more.

23. *Solar corona or lunar corona* is a luminous crown directly surrounding the sun or the moon, and whose radius seldom exceeds a few degrees, its inner part being bluish, whitish, or yellowish or sometimes showing faintly all spectral colors, whereas, the red colors always occupy the outer part of the ring. Sometimes series of spectral colors are observed. Solar corona or lunar corona is formed by the diffraction of the light of the luminary, generally by water droplets.

24. *Solar halo or lunar halo* is a ring round the sun or the moon at a distance of about 22°, mostly whitish, but sometimes showing spectral colors; in the latter case, the inner edge of the ring is always reddish. Inside the ring, the sky is darker than outside. Solar halo or lunar halo is formed by refraction of the light of the luminary in ice crystals.

23. Genetical Classification of Hydrometeors.—The foregoing classification of hydrometeors is based on morphological principles without regard to the processes that lead to their formation. With regard to atmospheric conditions, notably stability and vertical movement, it is important to distinguish between three main groups of hydrometeors, **viz.:**

1. *Hydrometeors of Frontal Cloud Systems.*—These hydrometeors are formed when huge bodies of air rise slowly because of the upglide movement due to a general convergence in the horizontal air flow along frontal surfaces; they originate from clouds of the alto-stratus–nimbo-stratus type and comprise rain, snow, or sleet as defined in the previous section. None of these hydrometeors is by definition indicative of frontal phenomena. What is characteristic of frontal (upglide) precipitation is the even falling of rain, snow, or sleet from a stratiform and extensive cloud system. The precipitation may be intermittent or of variable intensity, but its variations are never so pronounced as when it falls as showers or squalls (see below).

As mentioned in Par. 21, the upper portion of the alto-stratus system may be in an unstable state, and showers will then be superimposed on the more even frontal precipitation. This and other frontal phenomena will be discussed in later sections.

2. *Hydrometeors of Unstable Air Masses.*—These hydrometeors, which are formed when small bodies of air rise rapidly through the atmosphere, comprise all kinds of *showery* or *squally* precipitations. The showers or squalls may consist of rain, snow, sleet, or any kind of hail as defined above.

Rain, snow, and sleet are not by definition indicative of instability. Precipitation of a showery or squally type is characterized by the suddenness with which it starts and stops and by its rapid changes in intensity; also, by the aspect of the sky, which exhibits rapid variations in space and time from dark and threatening clouds (cumulo-nimbus) to clearings of short duration, often with an unusual blueness of the sky. Sometimes no definite clearing occurs between the showers, and the precipitation may not stop entirely between them; but, in such cases, the showery character is revealed by the sudden changes in intensity of precipitation and rapid alterations between lighter and darker clouds.

3. *Hydrometeors of Stably Stratified Air Masses.*—These hydrometeors, which are characterized by the smallness of their dimensions and the slowness of their fall, originate from clouds of the stratus or the fog type. The principal types are drizzle, granular snow, and ice needles. Grains of ice are not necessarily typical of the stably stratified air masses, because they form as raindrops in warm air aloft and solidify in the cold and stable ground layer of air. Apart from the hydrometeors just mentioned, stably stratified air is also characterized by fog and mist. Haze, even though it may be present in unstable masses, is often associated with the stable types. This particularly applies to continental tropical air masses that have become stable by moving to higher latitudes.

Figure 25 shows a typical example of the variations in intensity of warm-front rain, warm-sector drizzle, cold-front rain, and showers in the

rear of a depression that passed the southern part of Norway on May 9, 1938. The left-hand portion of the diagram shows the even increase in the rain intensity as the warm front approaches Lista (58°6′N, 6°34′E), the sudden but not discontinuous change to warm-sector drizzle at the passage of the warm front, and the similar change to cold-front rain, which in this case was of moderate intensity. The right-hand portion of the diagram shows the simultaneous rain intensities recorded at the station Sauda (59°39′N, 6°21′E) in the unstable northerly current of polar air in the rear of the passing depression.

From the foregoing discussion and examples and also from what has been said about forms of clouds, it appears that very important conclu-
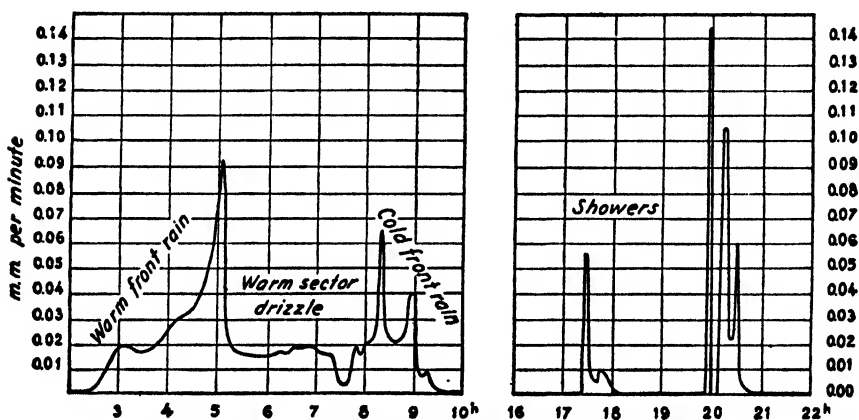
Fig. 25.—Rain intensities during the passage of a depression.

sions can be drawn from the cloud and hydrometeor observations with regard to the stability conditions of the air masses and the thermodynamic processes in operation. The clouds and hydrometeors of the free atmosphere are always representative, and their forms indicate the type of air mass or the type of front with which they are associated; they therefore give information that not even instrument records could easily divulge to the inquisitive forecaster.

24. Diurnal Variation of Clouds and Hydrometeors.—From the relation between stability and instability on the one hand and types of cloud and hydrometeor on the other, it follows that the diurnal heating and cooling will exercise a considerable influence as regards the formation, maintenance, and dissolution of clouds and hydrometeors. The influence acts directly through radiation on the clouds and indirectly through changes in lapse rate and turbulence.

The direct sunshine on the clouds will have a tendency to evaporate the cloud particles, and there will be a tendency for clouds to dissolve in sunshine. The effect is undoubtedly slight in comparison with other

effects such as turbulent mixing and transfer of heat from the earth's surface.   However, a thin cloud layer at a considerable distance from the ground would, perhaps, be appreciably influenced by the direct heating of the sun's rays.

The indirect influences are far greater.   As the insolation during the day tends to produce instability and the outgoing radiation by night tends to produce stability, it follows that the clouds and hydrometeors characteristic of unstable conditions will form more easily by day and dissolve more easily by night, whereas the reverse is true of the clouds and hydrometeors characteristic of stably stratified air.   Therefore, over land there is a definite tendency for the clouds of the cumulus family and the precipitation of the shower kind to have a maximum in the afternoon and a minimum at night or in the early morning.   This tendency is, of course, most pronounced in warm countries and in warm seasons.   At sea, the diurnal influence on such clouds and hydrometeors is slight and easily overshadowed by other effects (see Pars. 52 and 53).

The clouds and hydrometeors characteristic of stably stratified air masses show the reverse tendency: They form most frequently overnight and have a maximum at sunrise and a minimum in the afternoon.   Thus, the diurnal variation of cloudiness, clouds, and hydrometeors may be used, in conjunction with other evidence, for drawing conclusions as to the degree of stability and instability in the air.

The clouds connected with low inversions (see Pars. 21 and 54) often have a tendency to dissolve in the day because of increased altitude of the condensation level and the destruction of the inversion due to heating and increased turbulent mixing.   If the inversion is high above the ground, the clouds may persist day and night.

Certain types of local fog have a tendency to form after sunrise. This applies to fogs that form in industrial districts where the air contains considerable amounts of sulphur dioxide, which, through the action of the sun's rays, is changed into the highly hygroscopic sulphur trioxide, which then causes increased condensation.   Similarly, low clouds that form through mixing may sometimes show a maximum after sunrise; this condition is due to the circumstance that the mixing increases with the diurnal increase of wind velocity in the lower strata of the atmosphere.

25. Colloidal Stability.—Through the works of Wigand and Schmauss [72], Findeisen [26], and others, we know that clouds may be regarded as colloidal suspensions of water in the air.   The cloud is colloidally stable when the droplets do not coalesce, and it is colloidally unstable when the droplets have a tendency to coalesce.   Through coalescing, the drops grow in size and may become so heavy that they cannot be kept afloat in the cloud.   Precipitation, therefore, is a result of colloidal instability and an evidence of its presence in the cloud.

The conditions that some time ago were regarded as favorable for colloidal stability have been summarized by Bergeron as follows:

1. Uniform (equal, unipolar) electrical charge of cloud elements.
2. Uniform size of cloud elements.
3. Uniform temperature of cloud elements.
4. Uniform motion of cloud elements.

The nonfulfillment of any of these conditions would result in colloidal instability which, if of sufficient magnitude, would cause precipitation.

Bergeron [1, 2] has pointed out that colloidal instability caused by the failure of the above-mentioned factors is insufficient for producing precipitation of greater intensity than that of a wet fog or a drizzle. Not only is the failure of these factors insufficient for accounting for the intensity of precipitation other than wet fog or drizzle, but it also does not constitute a plausible reason why any or all of the stabilizing factors could fail so suddenly as would seem necessary to explain the *sudden release of precipitation* that is often observed to occur in cumulo-nimbus clouds.

According to Bergeron, the all-important cause of colloidal instability is the coexistence of water droplets and ice in the cloud. Owing to the difference in saturation pressure over water and ice, rapid condensation will take place round the frozen particles while water evaporates from the droplets. Thus, for example, at $-10°$C. the saturation water-vapor pressure over water is 0.24 mb. greater than over ice. In a cloud containing both ice and water, the water-vapor pressure adjusts itself to a value between the two saturation pressures, hence the evaporation from the water droplets and sublimation on the ice particles. When the cloud element has grown sufficiently, it falls through the cloud, and it is then readily seen that the stabilizing factors (2), (3), and (4), and perhaps also (1), are frustrated; the drop then continues to grow until it leaves the cloud or is broken up on account of its speed relative to the air.

The following evidence is in favour of Bergeron's theory:

1. Disturbed droplets and also drops larger than a certain size will crystallize more easily than undisturbed or small drops. With falling temperature, the smallest size or smallest disturbance necessary for crystallization of droplets will diminish, because the crystallization forces increase. There is, therefore, at every temperature below 0°C. within a water cloud a certain probability of crystallization and a corresponding frequency of crystals. Thus, within an ascending super-cooled water cloud, some elements may solidify spontaneously without any relative velocity of the cloud elements. Moreover, the ice part of a cloud may be infected by water droplets that are carried upward by ascending air currents.

2. The best evidence in support of the theory is the sudden release of precipitation when a cumulus turns into a cumulo-nimbus. This change is almost invariably preceded by the glaciation of the upper part of the cloud whereby the typical cauliflower structure of the tops of the cumulus congestus changes into the tangled web of the tops of cumulo-nimbus calvus, cumulo-nimbus capillatus, or cumulo-nimbus incus.

3. It is observed that a thin cloud frequently gives precipitation in the cold season in polar or subpolar regions, whereas much thicker clouds do not give any precipitation when the air temperature is high. Thus, the winter cumulo-nimbus clouds of the unstable maritime polar air do not reach nearly so high up in the atmosphere as do the summer cumuli; yet it will often rain or snow out of the former, and no precipitation falls from the latter.
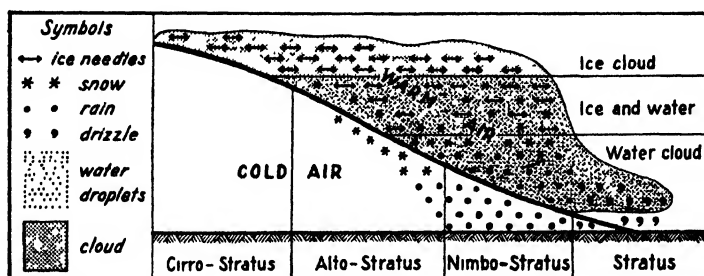
FIG. 26.—Idealised model of cloud genetics.   (*After Bergeron.*)

What has been said about the cumulo-nimbus clouds is likely to hold also for the alto-stratus–nimbo-stratus cloud systems. Figure 26 shows diagrammatically the vertical arrangement of cloud elements and forms of precipitation in a frontal cloud system with precipitation. In principle, the diagram also holds for cumulo-nimbus clouds.

In contradiction to Bergeron's theory are numerous observations of showers in tropical and equatorial regions from clouds whose tops do not reach the zero isotherm level and which, therefore, cannot contain ice crystals. This, however, does not disprove the theory; it merely shows that the ice-crystal effect is not the only important factor even though it is likely to be by far the most important.

In view of the fact that ice crystals cannot be held responsible for all precipitation of drops larger than drizzle, we turn to the four factors mentioned at the beginning of this discussion in order to see if any of them could account for the release of precipitation at temperatures above freezing. The only factor of importance seems to be differences in temperature between adjacent cloud elements.

In Fig. 27, curve Δe shows the difference between the saturation water-vapor pressure over water and over ice at various air temperatures.

It is seen that the maximum occurs at about $-12°C$., or in the region where the *a priori* probability of coexistence of ice and water is greatest. This gives additional weight to the ice-crystal theory of precipitation. The question now is whether or not the difference in temperature between adjacent cloud elements can produce an effect that is comparable with the ice-crystal effect.

Curve *A* shows the temperature difference between neighboring cloud elements that would cause a saturation water-vapor pressure difference of the same magnitude as the *maximum* difference between water and ice, *i.e.*, 0.27 mb. Curve *B* shows the temperature difference between adjacent cloud elements that would render a difference in saturation pressure equal to one-half the maximum ice-crystal effect
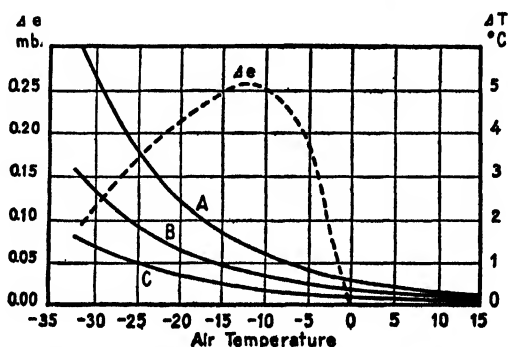
FIG. 27.—Explaining the formation of precipitation.

(*i.e.*, 0.13 mb.), and curve *C* shows the temperature difference that corresponds to one-fifth the maximum ice-crystal effect.

These curves show that, at very low temperatures, impossibly high temperature differences between adjacent water droplets are required, whereas, at high temperatures, only a minute fraction of a degree centigrade is required. It seems likely that such minute temperature differences between neighboring cloud elements can be produced as a result of intense mixing. But such differences are incapable of producing the desired effect at low temperatures where ice crystals are present. At high temperatures, however, temperature differences of less than 0.1°C. between adjacent droplets may effectively upset the colloidal stability, and precipitation of drops larger than 0.5 mm. may form if the cloud is deep enough to ensure the further growth of the drops while they fall through the cloud.

Another factor of importance is the electrical charge of the drops. It is true that the forces of electrical attraction and repulsion between cloud elements are small and insufficient, but on the other hand, laboratory experiments show that the coalescence of drops increases with the

electrical charge.   The conditions favorable for the formation of precipitation (other than wet fog or drizzle) at high temperature are:

1. Intense turbulence causing droplets of different temperatures to be brought together.

2. High electrical charge of the droplets.

3. Great thickness of the cloud to ensure further growth of the falling drops.

All these requirements seem to be fulfilled in tropical cumuli.   In high latitudes, precipitation of slight intensity is observed to fall from the strato-cumulus, notably during winter nights.   This release of precipitation is ascribed to temperature differences within the cloud. In tropical showers, the air temperature in the cloud is higher, the turbulence is more intense, and the cloud is thicker than in the winter strato-cumulus in high latitudes.   The precipitation falling from the former is, therefore, likely to be more intense than that which falls from the latter.   It is worthy of note that the tropical and equatorial thunderclouds show signs of ice crystals in their tops.   The formation of heavy precipitation, such as comes from thunderclouds, would, therefore, be released mainly by ice crystals, according to Bergeron's theory, whereas the cumuli that produce the slighter showers in warm regions need not reach up to the ice-crystal level.

Recent investigations by Simpson and Scrase, which will be referred to in Par. 43, have shown that the lower part of the showercloud is on the whole negatively charged whereas the upper portion is positively charged.   It is therefore plausible that turbulent mixing within such clouds may bring cloud elements of opposite charges so close to one another that electric attractions may also contribute slightly to the formation of precipitation.

It is highly desirable that the various theories of the formation of precipitation should be tested by direct observations.   Experience gained from the analysis of aerological ascents (see Chap. II) seems to show that the ice-crystal effect is the most important one.   At moderate and low temperatures, this effect seems to be all-important.

26. Visibility.—The term visibility is used to describe transparency of the air in the horizontal direction.   In some countries, visibility has been defined as the distance at which the outline of objects seen against the sky disappears.   In other countries, visibility means the distance at which objects seen against a background of the surface of the earth become indistinguishable.   In still other countries, it is the distance at which an object such as, for example, a tree or a house can be recognized as such.   The International Meteorological Organization [35] has recently agreed that the last definition of visibility should be adopted for future use.   The discrepancies between the various definitions are of slight

consequence when the visibility is bad, but they appreciably affect the measurements when the visibility is good.

The definition above refers to the daylight visibility. In darkness it is necessary to use lights of known candle power to determine the horizontal visibility.

Table 3a.—Visibility

Scale number	Daylight visibility	Night observations	
		Distance of object	Distance at which a light of 100 c.p. becomes indistinguishable
0	Less than 50 m.	50 m.	100 m.
1	50– 200 m.	200 m.	330 m.
2	200– 500 m.	500 m.	740 m.
3	500–1000 m.	1 km.	1340 m.
4	1– 2 km.	2 km.	2.3 km.
5	2– 4 km.	4 km.	4.0 km.
6	4– 10 km.	10 km.	7.5 km.
7	10– 20 km.	20 km.	12 km.
8	20– 50 km.		
9	Above 50 km.	At greater distances a 100 c.p. light is not suitable.	

The visibility is, at present, estimated or measured and reported on a scale ranging from 0 to 9. Table 3a gives the scale numbers, the corresponding daylight visibility according to the foregoing definition, and also the corresponding distances at which a light of 100 c.p. becomes indistinguishable.

Table 3b.—Normal Relation between Weather and Visibility

Scale number	Daylight visibility	Fog, mist, or haze	Snow	Drizzle	Rain
0	Less than 50 m.	Dense	Very heavy	—	—
1	50– 200 m.	Thick	Very heavy or heavy	—	Tropically heavy
2	200– 500 m.	Medium	Heavy	—	
3	500–1000 m.	Moderate	Moderate	Thick	Very heavy
4	1– 2 km.	Mist	Light	Moderate	Heavy
5	2– 4 km.	Slight mist or haze	Very light	Slight	Heavy
6	4– 10 km.	Slight mist or haze	Very light	—	Moderate
7	10– 20 km.	—	—	—	Light
8	20– 50 km.	—	—	—	Very light
9	Above 50 km.				

From this table, we see that a light of 100 c.p. is visible at greater distances than such objects as are used to determine the daylight visibility when the visibility is less than 4 km. For greater visibilities, the reverse is true. The definition of horizontal visibility and the methods of determining it are not satisfactory, and it is likely that modifications will have to be adopted in the near future.

The visibility depends greatly on the weather. Table 3b shows the normal relation between visibility and weather.

As the visibility varies between wide limits with the density of the precipitation, it is normally not a conservative property; nevertheless, it is often useful as an air-mass characteristic. In stably stratified air masses, it is fairly homogeneous, whereas, in unstable masses, it usually varies greatly in space and time. Moreover, as has been shown by Bergeron [1], the opalescent turbidity, which consists of finely and evenly divided dust in the air, is conservative as long as the air is not cleansed by precipitation. As the principal source of such turbidity is the arid subtropical regions, the presence of opalescent turbidity in considerable amounts in the air may be regarded as an indication that the air mass is of subtropical origin. Conversely, the absence of such turbidity may be taken as an indication of arctic or subpolar origin of the air. The difficulty in the way of using opalescent turbidity consistently in the analysis of weather maps originates from the circumstances that the visibility is defined and observed in a crude manner and that the conservative element of turbidity is often overshadowed by local pollutions of coarser matter or precipitation.

The haze is often arranged in layers in the atmosphere. In such cases, the vertical visibility may vary greatly in different directions. A pilot flying in sunshine above a haze layer may not be able to see the landing field, though the aircraft is perfectly visible from the ground. This condition is due to the reflection and scattering of light from the top of the haze layer.

CHAPTER II

STABILITY AND INSTABILITY IN RELATION TO WEATHER
PHENOMENA

As has been mentioned in the last chapter, most weather phenomena depend on the stability conditions of the air. It has been shown that the cloud forms and hydrometeors indicate roughly the degree of stability or instability and that the indirect aerological evidence which can be obtained from such observations is extremely valuable for the analysis and in forecasting; but only when aerological ascents are made sufficiently frequently and at a sufficiently dense network of stations will it be possible to obtain a satisfactory picture of the state of the free atmosphere.

The most comprehensive picture of the physical state of a large portion of the free atmosphere is obtained from maps representing the distribution of the significant elements in certain surfaces of reference, such as surfaces of standard elevations, standard isobaric surfaces, or standard isentropic surfaces. However, when the problem is to analyze in detail the stability conditions of the air and to draw conclusions with regard to the possible formation of clouds and cloud heights, showers, thunderstorms, etc., the most fruitful procedure will often be to analyze the individual aerologic ascent curves. This analysis does not render superfluous the construction and the analysis of upper-air maps.

27. Thermodynamic Diagrams.—The aerological reports in their simplest form give simultaneous values of pressure, temperature, and relative humidity in significant points on the ascent curve. More detailed reports contain the same basic information referred also to standard isobaric surfaces (1000,900,800 mb., etc.) and the corresponding geopotentials. In some countries, the reports also contain specific humidity and potential equivalent temperature or potential pseudo-equivalent temperature.

In order to draw the fullest possible thermodynamical conclusions from the records, it is essential that they should be plotted on a diagram which is an equivalent transformation of the Clapeyron's diagram. There are a great number of thermodynamic diagrams in use, but they do not all satisfy the foregoing requirement. Specimen diagrams, with summaries of the theories on which they are based, have been published by the Aerological Commission of the International Meteorological Organization [36]. For many purposes, and particularly for general use, the "aerogram" constructed by Refsdal [60, 61] is the most con-

venient of these, and it will therefore be used throughout this book. In this diagram, the abscissa is $\log T$, and the ordinate is $T \log p$.

Figure 28 shows the principal features of the aerogram. The vertical lines are isotherms (°C.), and the almost horizontal lines are isobars (millibars). In addition, there are three sets of curves crossing one
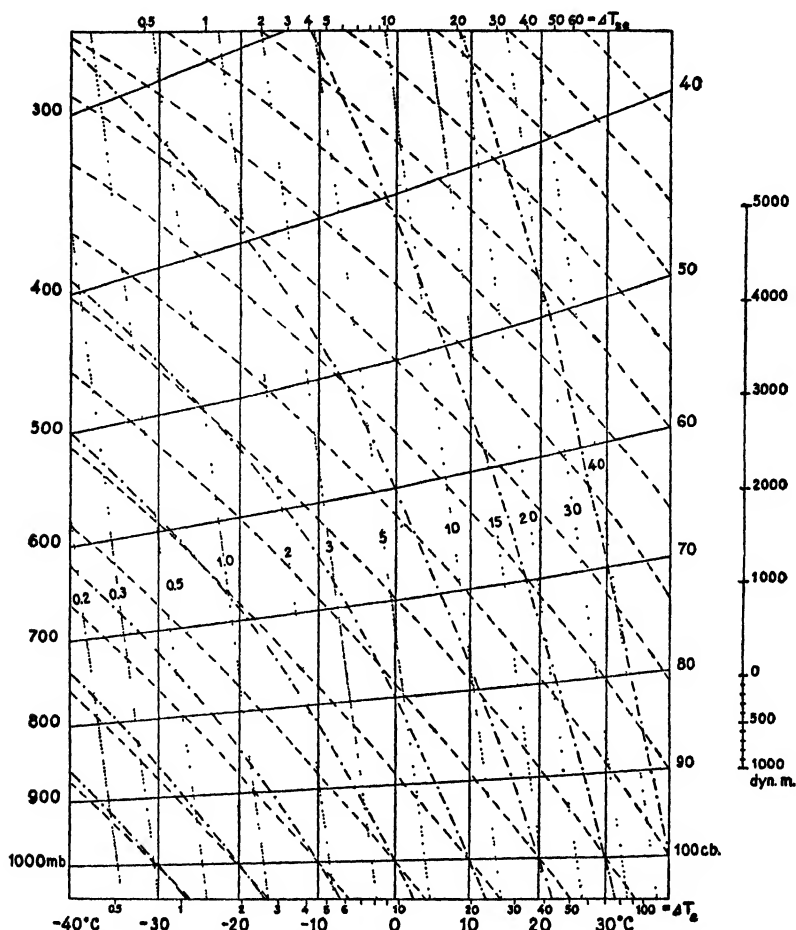
FIG. 28.—Showing the principal features of the aerogram. Intermediate isotherms and isobars, as well as some curves which serve special purposes, are omitted here.

another and crossing the coordinate curves. These curves are dry-adiabatic lines (broken lines), moist-adiabatic lines (broken dotted lines), and lines of constant maximum specific humidity or dew-point lines (dotted lines).

28. Evaluation of Basic Data.—The data obtained are represented on the diagram by plotting pressure versus temperature for each sig-

nificant point and writing alongside each point the corresponding relative humidity.

The specific humidity (q) at any point is determined in the following manner:

1. If the air is saturated $(R = 100$ per cent), the q-line running through the significant point gives the actual specific humidity for the saturated air at that point.

FIG. 29.—Showing how specific humidity (q), dew point (T_d), pseudo-wet-bulb temperature (T_{sw}), equivalent temperature (T_e), pseudo-equivalent temperature (T_{se}), potential temperature (θ), potential pseudo-wet-bulb temperature (θ_{sw}), potential equivalent temperature (θ_e) and potential pseudo-equivalent temperature (θ_{se}) are obtained by means of the aerogram.

2. If the air is not saturated $(R < 100$ per cent), the actual q can be found in one of two ways, *viz*: (a) Multiply the saturation q, as determined in (1) above, by R per cent. (b) Without multiplication, q may be determined by following the constant-humidity line through the significant point S (Fig. 29) till it intersects the isobar whose value in centibars equals the relative humidity at the significant point; and then following the isotherm down to the 100-centibar isobar. The q-line

at the intersection indicates the actual q of the significant point from which we started. This q-line is called the specific-humidity line, or the dew-point line, of the significant point S.

The dew-point temperature T_d of any point S is obtained by following the isobar through the significant point to intersection with the q-line that corresponds to that point; the isotherm running through this point indicates the dew-point temperature of the point S from which we started.

The wet-bulb temperature T_w is obtained by aid of humidity tables.

The pseudo-wet-bulb temperature T_{sw} of any point S is obtained by following the dry-adiabatic through the point to intersection with the q-line that corresponds to that point and thence along the moist-adiabatic down to intersection with the initial isobar. The isotherm running through this latter point of intersection indicates the pseudo-wet-bulb temperature of the point S from which we started. It should be noted that the difference $T_w - T_{sw}$ usually is so small that T_w and T_{sw} may be used interchangeably (see Par. 17).

The potential pseudo-wet-bulb temperature θ_{sw} is obtained as described above except that the moist-adiabatic is continued down to the 1000-mb. isobar. The isotherm running through the latter point of intersection indicates θ_{sw} of the point S from which we started.

The potential temperature θ is found by following the dry-adiabatic from the significant point S down to intersection with the 1000-mb. isobar. The isotherm running through the point of intersection indicates θ of the point S from which we started.

The equivalent temperature T_e is obtained by following the dry-adiabatic from the significant point S to intersection with the q-line corresponding to that point and thence along the q-line down to intersection with the 1000-mb. isobar. The equivalent-temperature difference ΔT_e is then found on a special scale of ΔT_e below the temperature scale. The equivalent temperature is the sum of the temperature of the significant point and the difference thus determined (*i.e.*, $T_e = T + \Delta T_e$).

The potential equivalent temperature θ_e is found by adding the equivalent-temperature difference to the actual temperature of the significant point S along the isobar through this point and then following the dry-adiabatic down to intersection with the 1000-mb. isobar. The isotherm running through this latter point of intersection indicates the potential equivalent temperature of the point S from which we started.

The pseudo-equivalent temperature T_{se} is obtained by following the dry-adiabatic from the significant point S to intersection with the q-line corresponding to that point and thence along the q-line down to intersection with the 1000-mb. isobar. The pseudo-equivalent temperature difference ΔT_{se} is then found on a special scale of ΔT_{se} at the top of the

diagram. The pseudo-equivalent temperature is then the sum of the temperature of the significant point and the difference thus determined (*i.e.*, $T_{se} = T + \Delta T_{se}$).

The potential pseudo-equivalent temperature θ_{se} is found by adding ΔT_{se} to T along the isobar through the significant point and then following the dry-adiabatic down to intersection with the 1000-mb. isobar. The isotherm running through this latter point of intersection indicates the potential pseudo-equivalent temperature of the point S from which we started.

The geopotential, or the dynamic height, of any significant point is obtained by applying the equal-area method. Let *abc* in Fig. 30 repre-

sent the ascent curve between two arbitrary pressure values p_0 and p_1. The difference in geopotential between the isobaric surfaces p_1 and p_0 is obtained by measuring the length of the segment of the isotherm between *e* and *d*, when the isotherm in question is chosen so that the two triangles *abe* and *bcd* equal one another.[1] The isotherm thus determined represents the mean temperature T_m of the layer of air between p_0 and p_1.

FIG. 30.—Evaluation of geopotential by means of the aerogram.

29. Condensation Levels.—Condensation within the atmosphere may be ascribed to four different processes, *viz.*:

1. Adiabatic cooling of air to such an extent that saturation occurs. Disregarding the slight adiabatic cooling that occurs by horizontal motion toward lower pressure or the adiabatic cooling that occurs on account of local pressure variations ($\partial p / \partial t < 0$), the principal cause of adiabatic cooling is upward displacement, or lifting, of the air. The level at which a parcel of air becomes saturated when it is lifted adiabatically is called the *lifting condensation level*.

2. Heating of air from below to such an extent that, on account of instability forces, it ascends adiabatically until it becomes saturated. The level at which condensation then occurs may be called the *convection condensation level*.

3. Isobaric cooling of air to its dew point, in which case condensation occurs without the particle changing its level (see Par. 56).

---

[1] The geopotential scale is printed on the aerogram. Geodynamical heights are easily converted into geometrical heights. The aerogram may also be used for determining specific volume and vertical acceleration.

4. Mixing of air of different temperatures and humidity content. In the case of vertical mixing, the level of condensation depends on the original distribution of humidity and temperature and also on the thickness of the mixed layer (see Par. 49).

The lifting condensation level may be determined from the aerogram by following the dry adiabatic from the point that represents the parcel of air to intersection with its q-line. The point of intersection is its lifting condensation level (Fig. 31). If the parcel were lifted beyond this level, condensation would occur. In the diagram the levels are represented by isobaric surfaces. We may therefore speak of condensation pressure instead of condensation level, meaning thereby the pressure at which the parcel of air becomes saturated.

In order to find the *convection condensation level*, we must answer the question: How much must the air be heated (with constant watervapor content) in order that it may subsequently rise adiabatically to its condensation level? This amount of heating is determined from the aerogram in the following manner: Follow the dry-adiabatic through the point A representing the parcel of air (Fig. 31) to intersection with the q-line B, thence follow the q-line to intersection with the ascent curve C, and thence follow the dry-adiabatic down to intersection with the initial isobar D. The temperature difference AD indicates the amount of heating necessary to start convection up to the condensation level. From what has been said above, it follows

FIG. 31.—Showing how lifting condensation level and convection condensation level are determined by means of the aerogram. AC, the ascent curve; B, the lifting condensation level of the parcel of air at A; C, the convection condensation level of the parcel at A; AD, the amount of heating necessary to make the parcel A ascend freely to the condensation level C.

that the point B represents the lifting condensation level and point C the convection condensation level.

It is easily understood that the latter level is higher than the former. Thus, for example, if AC were the ascent curve in the early morning and if the air were lifted without being heated (*e.g.*, along a frontal surface), condensation would occur in and above the level B. If the air were not lifted but heated (*e.g.*, diurnally) by the amount AD, convection would start and condensation would occur in and above the level indicated by C. It is also easily seen that the air at A cannot be heated by the amount AD unless the air above is heated by the amount corresponding to the horizontal distances between the lines DC and AC, for otherwise superadiabatic lapse rates would develop.

Usually the moisture content does not remain strictly constant during the heating. The increased temperature lowers the relative humidity which, again, favors evaporation. With increased water-vapor content, it is evident that the convective condensation level will become lower than that indicated by C in Fig. 31, and the amount of heating AD necessary to start convection up to the condensation level would decrease. Furthermore, as the air temperature in the thermometer screen on warm days is lower than the air temperature close to the earth in some places, it follows that convection up to the condensation level is likely to start before the air temperature in the screen has reached the point indicated by D.

From this we may conclude that, if the temperature during the day reaches the value D, convective clouds are bound to form, and such clouds are likely to form even if the temperature does not quite reach the value indicated by D.

30. Stability and Instability.—In the same manner as stability and instability are defined for rigid systems, we may say that the air is in a stable state of equilibrium if a parcel of air which is moved a small distance upward or downward and then brought to rest has a tendency to return to its original level. If such a parcel has a tendency to move farther away from its original level, the air is in an unstable state of equilibrium. If the parcel considered can be at rest at any level, the air is in a neutral or an indifferent state of equilibrium. Since any minute disturbance will upset the unstable systems and bring them to a stable state, it follows that unstable conditions cannot persist in the atmosphere for any appreciable interval of time. The transition from unstable to stable states of equilibrium involves a reduction of the potential energy, and all systems left to themselves will try to avoid instability and obtain a minimum of potential energy.

Thus, although it is perfectly easy to give an adequate definition of stability and instability, it is difficult to determine from actual observations whether the stratification is stable or not. This difficulty is due to several circumstances:

1. As the air is a compressible and continuous medium, the displacement of a parcel will cause compensation currents in the environment, and both the displaced parcel and its environment will change their density. As the acceleration which acts on the displaced parcel depends on the difference between its density and that of the surrounding air, it follows that this difference in density depends not only on the initial distribution of mass but also on the kinematics of the motion.

2. When the displacement results in condensation of aqueous vapor, the latent heat of vaporization is liberated, and this causes additional changes in the density distribution. Thus, for example, when saturated

air is displaced upward in a nonsaturated environment, the saturated air ascends moist-adiabatically and the environment descends dry-adiabatically. Depending on the distribution of vertical velocity, the rate of heating of the environment may then become smaller or greater than the rate of cooling of the ascending air.

3. When the degree of stability is slight, it may happen that the stratification is stable relative to small perturbations, whereas it is unstable relative to disturbances which are sufficiently large.

From the foregoing, it follows that the problem of determining the stability conditions of the air is not only a static problem, but also a dynamic one. In order to determine the stability conditions of the air, it is necessary to consider the following factors:

1. The initial distribution of mass.
2. The nature of the perturbation.
3. The changes in density that result from the motion.

With regard to the more complete discussion of the stability criteria that will be given in later paragraphs, it is of interest to remark that the foregoing definition of stability and instability may be expressed as follows: If the air is at rest and an impulse is applied, the stratification is stable when the air becomes decelerated in the direction of the impulse, and it is unstable when the air becomes accelerated in the direction of the impulse.

The state · of equilibrium is characterized by isobaric surfaces coinciding with the isosteric surfaces (barotropic conditions). When this condition is not fulfilled, the field is baroclinic, and accelerations develop that tend to establish barotropy. From this it follows that, when the equilibrium state is disturbed, positive solenoids must develop when there is instability, and negative solenoids must develop when stability is present.

It has been customary to determine the stability conditions by proceeding on the assumption that a parcel of air can be displaced adiabatically without causing any change in the density of the environment. This condition is approximately realized when a small parcel of air is displaced and the compensation currents affect a large mass. We shall, therefore, first deduce the stability conditions and classify them on the assumption that the environment of the displaced parcel remain uninfluenced; in later paragraphs, the changes of the environment and the nature of the perturbation will be discussed. On account of the complications that arise through the presence of aqueous vapor and liquid water in the air, it is convenient to discuss dry air, nonsaturated moist air, and saturated air separately.

31. Dry Air.—In Fig. 32, P represents a parcel of dry air. The curves **1, 2,** and **3** represent three hypothetical ascent curves plotted on an

aerogram. In case 2, the lapse rate of the air column is just equal to the dry-adiabatic rate; in case 1, the lapse rate is less than the dry-adiabatic; and in case 3, the lapse rate exceeds the dry-adiabatic rate.

Let an impulse displace the parcel of air at P a small distance Δz upward or downward. As the parcel assumes the pressure of its environment, its density will be inversely proportional to its temperature. During the displacement, the parcel changes its temperature dry-adiabatically. If the environment remains uninfluenced, it is seen from Fig. 32 that, in the case represented by curve 1, the density of the parcel would be such that it becomes accelerated back to its original level. By definition, the stratification is then a stable one. Similarly, if the lapse rate of the air column is greater than the dry-adiabatic rate (curve 3) the displaced parcel becomes accelerated away from its original level: the stratification is unstable. Finally, if the lapse rate of the air column is just equal to the dry-adiabatic rate (curve 2), the density of the displaced parcel would everywhere be equal to that of its environment: the equilibrium is then indifferent.
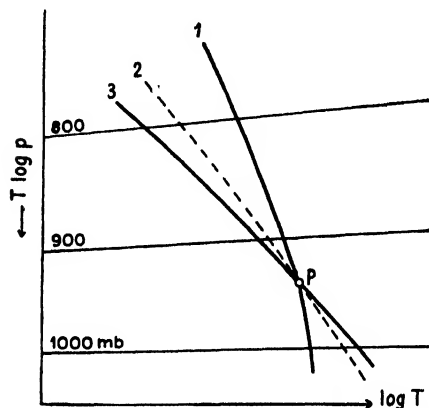
Fig. 32.—Stability conditions of dry air.

Let γ denote the lapse rate of the air column (*i.e.*, $\gamma = - \partial T/\partial z$), γ_d the dry-adiabatic rate, and θ the potential temperature. As θ is constant along a dry-adiabatic, it follows that the stability conditions of dry air may be expressed in the following manner:

$$(1) \qquad \gamma < \gamma_d \quad \text{or} \quad \frac{\partial \theta}{\partial z} > 0 \qquad \text{stable equilibrium}$$

$$(2) \qquad \gamma = \gamma_d \quad \text{or} \quad \frac{\partial \theta}{\partial z} = 0 \qquad \text{indifferent equilibrium}$$

$$(3) \qquad \gamma > \gamma_d \quad \text{or} \quad \frac{\partial \theta}{\partial z} < 0 \qquad \text{unstable equilibrium.}$$

32. Saturated Air.—In the discussion of saturated air, one may refer to the pseudo-adiabatic or the moist-adiabatic lapse rate. The first term applies to saturated air when the condensed water is immediately precipitated from the air, and the second refers to saturated air when the condensed water remains in the air. For all practical purposes, it suffices to consider the two lapse rates as identical. A parcel of saturated

air will change its temperature according to the moist-adiabatic law. By displacing a parcel of air *upward*, it is easily seen from Fig. 33 that the static equilibrium of saturated air is stable, indifferent, or unstable according to whether the lapse rate is less, equal to, or greater than the moist-adiabatic rate. If θ_{sw} denotes the potential pseudo-wet-bulb temperature of the air and γ_m the moist-adiabatic lapse rate, the three criteria similar to those in Par. 31 may be expressed as follows:

(1) $\qquad \gamma < \gamma_m \qquad$ or $\qquad \dfrac{\partial \theta_{sw}}{\partial z} > 0 \qquad$ stable equilibrium

(2) $\qquad \gamma = \gamma_m \qquad$ or $\qquad \dfrac{\partial \theta_{sw}}{\partial z} = 0 \qquad$ indifferent equilibrium

(3) $\qquad \gamma > \gamma_m \qquad$ or $\qquad \dfrac{\partial \theta_{sw}}{\partial z} < 0 \qquad$ unstable equilibrium

It should be borne in mind that these criteria are not so general as those pertaining to dry air. If $\gamma_d > \gamma > \gamma_m$ and if the air is saturated but not filled with water droplets, the foregoing conditions hold only for upward impulses; for a parcel of air that is displaced downward will be heated dry-adiabatically, and it would then be accelerated back to its original level. However, when the air contains a sufficient amount of liquid water which evaporates so quickly that the air is kept saturated while it is displaced downward, the above conditions would hold both for upward and downward impulses.

Fig. 33.—Stability conditions of saturated air. Broken line indicates the moist-adiabatic.

33. Nonsaturated Moist Air.— Owing to the influence of the moisture content on the specific heat of air, the adiabatic for moist nonsaturated air differs slightly from the adiabatic of perfectly dry air, but for all practical purposes the two may be regarded as identical. It follows then that the criteria of static stability and instability deduced for perfectly dry air are valid also for nonsaturated moist air as long as the motions set up by the perturbations do not surpass the limit where condensation occurs within the displaced air. Thus, although the criteria for perfectly dry air are applicable also to moist unsaturated air when the perturbations are small, they fail when the movements surpass the condensation limit. As the movements occurring within the troposphere often exceed this limit, it will be necessary to deduce criteria that hold also for large displacements in moist air.

Let *ACED* in Fig. 34 represent the ascent curve for nonsaturated air plotted on an aerogram or any other equivalent transformation of Clapeyron's diagram. Let the parcel of air of unit mass at *A* be displaced upward; it cools dry-adiabatically to *B* where it becomes saturated as a result of the dry-adiabatic cooling. From the level *B*, it cools moist-adiabatically as shown by the curve *BCD*. The area represented by *ABC* measures the amount of energy that must be supplied to the unit mass in order to raise it from the level *A* to the level *C*. The area *ABC*, therefore, measures the resistance against lifting. Below the level *C*, the lifted parcel of air is colder and denser than the surrounding air; and if it were left to itself, it would move back toward its original level (stability). However, if the parcel is lifted farther, beyond the level *C*, its representative point in the diagram would follow the line *CD*. Above the level *C*, therefore, the parcel would be warmer and less dense than its environment, and it would be accelerated upward until it reaches the level *D*. The area *CDE* expresses the amount of energy that is gained by a parcel of unit mass while it moves from the level *C* to the level *D*. This energy is used by the parcel to increase its kinetic energy and to overcome friction.
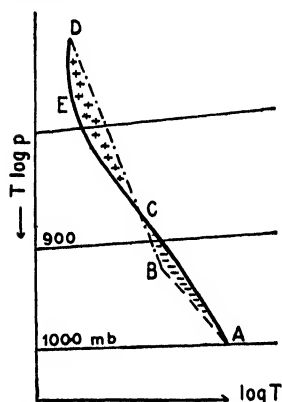
FIG. 34.—Example of conditional instability.

From the foregoing, it follows that the parcel *A* is stable relative to small perturbations (which do not bring it beyond the level *C*) but is unstable with respect to perturbations which are large enough to bring it above the level *C*. When the parcel passes the level *C*, it becomes accelerated upward. This level, then, may be called *the level of free convection*. This level as well as the *resistance against lifting* (area *ABC*) and the amount of *releasable energy* (area *CDE*) is usually different for each point on the ascent curve.

It is worthy of note that the layer between *E* and *D* is stably stratified. If the parcel at *E* were moved upward, it would resist lifting; but the parcel *A*, when lifted beyond *C*, would be unstable when it penetrates into the layer *ED*.

The above example shows that instability may be released by *upward* impulses in moist unsaturated air when the impulse is strong enough to bring the parcel of air beyond a certain level. It is easily seen, however, that, with the vertical temperature distribution indicated in Fig. 34, only upward displacements could release instability.

Owing to the difference in slope between the dry- and the moist-adiabatic lines, a great variety of conditions will be observed. Rossby [63] and Normand [49] distinguish between three principal cases, *viz.*, *absolute stability*, *absolute instability*, and *conditional instability*.

1. *Absolute stability* is characterized by a lapse rate of temperature in the moist air that is less than the moist-adiabatic rate, or $\gamma < \gamma_m$ as shown by curve 1 in Fig. 35. It is easily seen that the stratification will remain stable with respect to upward or downward impulses, however large the displacements may be.

2. *Absolute instability* is characterized by a lapse rate of temperature in the moist air that is greater than the dry-adiabatic rate, or $\gamma > \gamma_d$ (*e.g.*, curve 2 in Fig. 35). It is seen from Fig. 35 that the stratification is then unstable with respect to all upward or downward impulses, however small the displacements may be.

3. *Conditional instability* is characterized by a vertical lapse rate in the moist air that is greater than the moist-adiabatic and less than the dry-adiabatic rate, or $\gamma_d > \gamma > \gamma_m$. In this case, the distribution of humidity along the vertical decides whether or not instability can be released through vertical displacements.

FIG. 35.—Absolute stability, conditional instability, and absolute instability in relation to moist-adiabatic and dry-adiabatic lines.

a. The Stable Type.—Consider the ascent curve ABC (Fig. 36) and the curve $A'B'C'$ which represents the corresponding distribution of the pseudo-wet-bulb temperature. Let the parcel of air at A ascend dry-

FIG. 36.—Illustrating conditional instability of stable type.

adiabatically to its lifting condensation level a, whence it ascends moist-adiabatically along aa'. The curve $A'aa'$ represents the moist-adiabatic corresponding to A, or the potential pseudo-wet-bulb temperature line of the parcel A. Consider next a parcel of air at B whose pseudo-wet-bulb temperature is B'; its potential pseudo-wet-bulb temperature line is then the moist-adiabatic $B'bb'$. None of the potential pseudo-wet-bulb temperature lines intersects the ascent curve. It is seen that, throughout the lifting, any parcel of air belonging to the ascent curve will be colder than the environment. By definition, then, the stratification should be classed as a stable one. The critical point in Fig. 36 is B; but as the potential pseudo-wet-bulb temperature line through B' does not intersect the ascent curve, the parcel of air at B will remain colder (and denser) than its environment while it is lifted.

b. Latent Instability.—Consider next the ascent current *ABCDE* (Fig. 37) and the corresponding pseudo-wet-bulb temperature curve *A'C'D'*. Suppose the parcel at *A* is moved upward; it will follow the
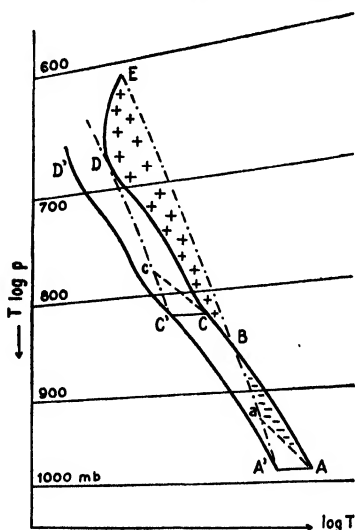
dry-adiabatic *Aa* to its lifting condensation level *a*, whence it will move along the moist-adiabatic running through the point *A'*. Below *B*, the parcel is denser than the environment, and it is stable with regard to small perturbations; but as it passes the level *B* (the level of free convection), it will be warmer and less dense than the surrounding air and hence will be accelerated upward till it arrives at *E*. Therefore, by lifting the parcel *A* from the level *A* to the level *B* or farther, instability, latent in the stratification, will be released. This type is called *latent instability.*

It is readily seen from the diagram that latent instability is present below the level *CC'*, whereas above the level the stratification is stable as none of the

potential pseudo-wet-bulb temperature lines belonging to the ascent curve above *CC'* intersects the ascent curve.

As mentioned above, the area *AaB* expresses the amount of energy that must be supplied to a unit mass at *A* in order to make it ascend to the level of free convection (*i.e.*, *B*). The area *BCDE* represents the amount of energy that a unit mass at *A* can release by being lifted beyond the level *B*. The difference between the areas *BCDE* and *AaB* represents the *amount of available* energy pertaining to a unit mass at *A*.

Normand [49] distinguishes between two cases of latent instability, *viz.*:

FIG. 38.—Illustrating conditional instability of pseudo-latent type.

i. *The area BCDE is greater than the area AaB* (Fig. 37). In this case, more energy is released by the displacement than is used to overcome the initial resistance against the displacement. The process thus leads to a net gain of energy that may be used to overcome fric-

tional forces and to create kinetic energy. This case is called *real latent instability*.

ii. The area BCDE is smaller than the area AaB. In this case, the net gain of energy is negative, and, in addition, energy must be used to overcome frictional forces. This type is called *pseudo-latent instability* (Fig. 38).

It will be shown later that the ratio of the positive to the negative area is an important factor in the prediction of showers, etc.; but it should not be forgotten that the upper positive area yields energy only after the lower negative area has been overcome. Therefore, this ratio is important only when the negative area is so small that the perturbations are able to lift the air above the level of free convection. In

TABLE 4.—CRITERIA OF STABILITY AND INSTABILITY DEDUCED ON THE ASSUMPTION OF AN UNDISTURBED ENVIRONMENT (THE PARCEL METHOD)

	Nonsaturated air: displaced parcel not becoming saturated	Saturated air: displaced parcel remaining saturated
Absolute stability..	$\gamma < \gamma_d$ or $\dfrac{\partial \theta}{\partial z} > 0$	$\gamma < \gamma_m$ or $\dfrac{\partial \theta_{se}}{\partial z} > 0$ or $-\dfrac{\partial T_{sw}}{\partial z} < \gamma_m$ or $\dfrac{\partial \theta_{sw}}{\partial z} > 0$
Indifferent state...	$\gamma = \gamma_d$ or $\dfrac{\partial \theta}{\partial z} = 0$	$\gamma = \gamma_m$ or $\dfrac{\partial \theta_{se}}{\partial z} = 0$ or $-\dfrac{\partial T_{sw}}{\partial z} = \gamma_m$ or $\dfrac{\partial \theta_{sw}}{\partial z} = 0$
Absolute instability	$\gamma > \gamma_d$ or $\dfrac{\partial \theta}{\partial z} < 0$	$\gamma > \gamma_m$ or $\dfrac{\partial \theta_{se}}{\partial z} < 0$ or $-\dfrac{\partial T_{sw}}{\partial z} > \gamma_m$ or $\dfrac{\partial \theta_{sw}}{\partial z} < 0$

	Nonsaturated air: displaced parcel becoming saturated
Absolute stability.. Conditional instability:	$\gamma < \gamma_m$
Stable type......	$\gamma_m < \gamma < \gamma_d$ and also no potential pseudo-wet-bulb temperature line intersecting the ascent curve (Fig. 36)
Pseudo-latent....	$\gamma_m < \gamma < \gamma_d$ and also some of the potential pseudo-wet-bulb temperature lines intersecting the ascent curve, and the positive area smaller than the negative area (Fig. 38)
Real latent......	$\gamma_m < \gamma < \gamma_d$ and also some of the potential pseudo-wet-bulb temperature lines intersecting the ascent curve, and the positive area larger than the negative area (Fig. 37)
Absolute instability	$\gamma > \gamma_d$ or $\dfrac{\partial \theta}{\partial z} < 0$

concluding this paragraph, it is appropriate to emphasize that the above criteria are derived on the assumption of an undisturbed, or mainly undisturbed, environment. In Pars. 35 to 37, the influences on the environment and the nature of the perturbation will be discussed in detail.

34. Summary of Criteria.—Table 4 contains in a condensed form the various definitions and criteria of stability and instability. The symbols used in the table have the following meanings: T = temperature, θ = potential temperature, T_{sw} = pseudo-wet-bulb temperature, θ_{sw} = potential pseudo-wet-bulb temperature, θ_{se} = potential pseudo-equivalent temperature, γ = lapse rate, γ_d = dry-adiabatic lapse rate, γ_m = moist-adiabatic lapse rate, z = distance along the vertical.

35. Influence of Descending Currents.—The criteria of stability and instability summarized in the previous paragraph were deduced on
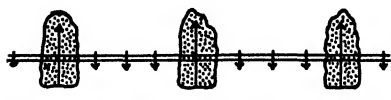
Fig. 39.

the assumption that an isolated parcel of air could ascend or descend and change its density adiabatically without causing any change in the density of its environment. However, the space occupied by an ascending parcel of air must immediately be filled by air from the environment, and the space that an ascending parcel of air is going to occupy must be evacuated. An ascending current must, therefore, have its counterpart in a descending current, and vice versa. But as the descending air also changes its density, it follows that the assumption of an undisturbed environment does not hold. It remains, therefore, to discuss how the coexistence of adjacent upward and downward currents modify the criteria of stability and instability. This question has been discussed by J. Bjerknes [8] and Petterssen [52].

With reference to a portion of the atmosphere that is large enough to contain several upward and downward currents, we may make the following assumptions:

1. The horizontal motion does not at any level maintain any net inflow to, or outflow from, the region under consideration.

2. The conditions are barotropic at the initial moment.

3. The temperature changes are adiabatic.

Assumption (1) involves equal transports of air upward and downward through any arbitrary isobaric surface or through any isobaric slice of air of unit thickness, the slice remaining stationary while the air passes through it. We may then write

$$(1) \hspace{3cm} M'v_z' = -Mv_z$$

where M' denotes the mass of ascending air and M the mass of descending

air contained within the slice; v_s' and v_s denote the mean upward and downward velocities, respectively.

Assumption (2) involves coincidence of the isobaric surfaces with the isosteric surfaces at the initial moment; and assumption (3) means that the temperature changes per unit time within the slice may be expressed by the following equations (see Par. 3):

(2)　　　$\dfrac{\partial T'}{\partial t} = v_s'(\gamma - \gamma_d)$　　　in ascending nonsaturated air

(3)　　　$\dfrac{\partial T'}{\partial t} = v_s'(\gamma - \gamma_m)$　　　in ascending saturated air

(4)　　　$\dfrac{\partial T}{\partial t} = v_s(\gamma - \gamma_d)$　　　in descending nonsaturated air

(5)　　　$\dfrac{\partial T}{\partial t} = v_s(\gamma - \gamma_m)$　　　in descending saturated air

In a later paragraph, the influence of the nonfulfilment of these assumptions will be discussed.

If the air were originally at rest and an impulse affecting the mass M' is applied, the isotherms, which were originally horizontal,[1] will not remain so, and solenoids will be created. The heat gained per second within the slice is expressed by

(6)　　$\dfrac{\partial Q}{\partial t} = c_p\left(M\dfrac{\partial T}{\partial t} + M'\dfrac{\partial T'}{\partial t}\right) = c_p(M + M')\dfrac{\partial T}{\partial t} + c_pM'\left(\dfrac{\partial T'}{\partial t} - \dfrac{\partial T}{\partial t}\right)$

The first term on the right-hand side represents a uniform heating (or cooling) of the entire slice at the rate $\partial T/\partial t$ equal to the heating (or cooling) of the descending mass; the last term represents the excess heating (or cooling) of the ascending air, at the rate $[(\partial T'/\partial t) - (\partial T/\partial t)]$ relative to the environment. Only the last term, which may be called the *solenoid-producing* term, contributes to the production or consumption of kinetic energy.

1. *Nonsaturated Air.*—In this case, the foregoing equations (1), (2), and (4) apply. It will be seen that, when $\gamma > \gamma_d$, an ascending current causes a local increase in temperature and a downward current causes a local decrease in temperature. When $\gamma < \gamma_d$, the reverse is true. Substituting from Eqs. (1), (2), and (4) into Eq. (6), we obtain

(7)　　$\dfrac{\partial Q}{\partial t} = -c_p\left(1 + \dfrac{M'}{M}\right)M'v_s'(\gamma - \gamma_d)$

$\qquad\qquad\qquad + c_p\left(1 + \dfrac{M'}{M}\right)M'v_s'(\gamma - \gamma_d) = 0$

[1] Strictly speaking, parallel to isobars.

Thus, the vertical velocities do not cause any net gain or loss of heat within the slice; but the isotherms will be perturbed, and the solenoid-producing term is expressed by

$$c_p \left(1 + \frac{M'}{M} \right) M' v_z'(\gamma - \gamma_d)$$

If the air were initially at rest ($v_z' = 0$) and a perturbation affecting the mass M' were applied, a parcel of air would be accelerated in the direction of the impulse when $\gamma > \gamma_d$; it would be retarded in the direction of the impulse when $\gamma < \gamma_d$, and no accelerations would occur when $\gamma = \gamma_d$. These conditions are independent of the magnitude of the impulse and the mass affected. Therefore, the stability criteria derived on the assumption of an undisturbed environment (*i.e.*, by the parcel method) hold without restriction when the air remains nonsaturated. However, as will be shown later, the two methods give different values for the amount of available energy.

The fact that the sign of the solenoid-producing term is independent of M' and M shows that nonsaturated air reacts in the same way whether the horizontal dimensions of the perturbations are large or small: we may say that *there is no selection of impulses.*

2. *Saturated Air.*—We shall next consider the case when both the ascending and the descending air are saturated. This occurs when the air is filled with droplets which evaporate so quickly that the descending air remains saturated. In this case, both the ascending and the descending masses follow the moist-adiabatic, and there is the same symmetry in the process as in the case described above. We may therefore substitute γ_m for γ_d into Eq. (7). This gives

$$(8) \quad \frac{\partial Q}{\partial t} = -c_p \left(1 + \frac{M'}{M} \right) M' v_z'(\gamma - \gamma_m)$$
$$+ c_p \left(1 + \frac{M'}{M} \right) M' v_z'(\gamma - \gamma_m) = 0$$

As in the previous case, there is no net gain of heat within the entire slice; but the isothermal surfaces, which were originally horizontal, will not remain so. As above, the term

$$(9) \qquad c_p \left(1 + \frac{M'}{M} \right) M' v_z'(\gamma - \gamma_m)$$

is the solenoid-producing term. If the air were originally at rest ($v_z' = 0$) and a perturbation affecting the mass M' were applied, it follows that the parcel of air would be accelerated in the direction of the impulse when $\gamma > \gamma_m$ and would be retarded in the direction of the impulse when

$\gamma < \gamma_m$. Thus, the criteria deduced on the assumption of an undisturbed environment hold without restriction when both the ascending and the descending currents are saturated. As in the previous case, the two methods give different values for the amount of available energy.

The fact that the sign of the solenoid-producing term is independent of M' and M shows that saturated air reacts in the same way whether the horizontal dimensions of the perturbations are large or small: *there is no selection of impulses.*
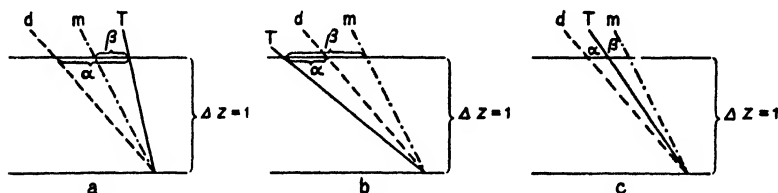
FIG. 40.—Showing the definition of α and β.

3. *Saturated Ascent through a Dry-adiabatically Descending Environment.*—In this case, the Eqs. (1), (3), and (4) apply. Substituting from them into Eq. (6), we obtain

$$(10) \quad \frac{\partial Q}{\partial t} = c_p v_z' M'(\gamma_d - \gamma_m) = c_p v_z' M' \left(1 + \frac{M'}{M}\right)(\gamma_d - \gamma)$$
$$+ c_p v_z' M' \left[\gamma - \gamma_m - (\gamma_d - \gamma)\frac{M'}{M}\right]$$

Putting $\gamma_d - \gamma = \alpha$ and $\gamma - \gamma_m = \beta$, as shown in Fig. 40, we obtain

$$(11) \quad \frac{\partial Q}{\partial t} = c_p v_z' M'(\alpha + \beta) = c_p v_z' M' \left(1 + \frac{M'}{M}\right)\alpha$$
$$+ c_p v_z' M' \left(\beta - \alpha\frac{M'}{M}\right)$$

It is important to note that at any level, or rather at any point, in a thermodynamical diagram

$$(12) \qquad \alpha + \beta = \delta = \text{constant} > 0$$

so that α can increase only as much as β decreases, and vice versa. Similarly, since $M' + M$ represents the mass contained in an isobaric slice of unit thickness over the area considered, it follows that

$$(13) \qquad M' + M = M_0 = \text{constant}$$

since the considered area is constant.

The term $c_p v_z' M'(\alpha + \beta)$ expresses the heat set free per second through condensation of aqueous vapor in the mass M' when its upward

velocity is v_z'. It is directly proportional to the upward velocity and the mass affected. It is also proportional to $(\alpha + \beta)$, or the angle between the moist-adiabatic and the dry-adiabatic. It will be seen from any thermodynamic diagram (*e.g.*, Fig. 28) that it decreases with decreasing temperature, because the two adiabatics approach one another as the temperature decreases.

The term $c_p v_z' M'[1 + (M'/M)]\alpha$, which represents the uniform heating (or cooling) of the entire slice, is directly proportional to $v_z' M'$; and it increases with α, or the angle between the ascent curve and the dry-adiabatic. When $\alpha > 0$ (see Fig. 40), the uniform heating term is positive, when $\alpha < 0$, it is negative. This term, which under normal conditions is positive, consumes a considerable part of the liberated heat.

The term

$$(14) \qquad\qquad c_p v_z' M' \left(\beta - \alpha \frac{M'}{M} \right)$$

which is the solenoid-producing term, represents *the portion of the liberated heat that is available for production or consumption of kinetic energy.* From the definition of stability and instability, it follows then that the equilibrium is stable when

$$(14a) \qquad\qquad \beta < \alpha \frac{M'}{M}$$

it is indifferent when

$$(14b) \qquad\qquad \beta = \alpha \frac{M'}{M}$$

and it is unstable when

$$(14c) \qquad\qquad \beta > \alpha \frac{M'}{M}$$

As the lapse rate of temperature is always important, we may distinguish between four cases (see Fig. 40), *viz.*:

i. $\beta < 0$, and $\alpha > 0$. In this case, $\gamma < \gamma_m$. From Eq. (14a), it follows that kinetic energy is consumed. If the air is at rest and then is given an impulse, it would be retarded in the direction of the impulse: the stratification is, by definition, a stable one. This applies irrespective of M' and M, which shows that the air behaves in the same manner regardless of the horizontal extent of the impulse.

ii. $\alpha < 0$, and $\beta > 0$. In this case, $\gamma > \gamma_d$. From Eq. (14), it follows that the sign of the solenoid-producing term is positive and the air would be accelerated in the direction of the impulse: the stratification is unstable. This applies irrespective of M' and M.

In the foregoing cases, there is no selection of impulses, and the criteria of stability and instability conform with the ones deduced on the assumption of an undisturbed environment, which, therefore, hold without restriction. As before, the amount of available energy determined by means of the parcel method differs from that found by aid of the slice method.

iii. $\beta = 0$, and $\alpha > 0$. In this case, $\gamma = \gamma_m$. From Eq. (14), it follows that kinetic energy is consumed. The equilibrium is indifferent only when Eq. (14b) holds, which implies that $\gamma > \gamma_m$. In this case, then, the criterion of indifferent equilibrium does not conform to the one deduced on the assumption of an undisturbed environment (*i.e.*, by the parcel method).

iv. $\beta > 0$, and $\alpha > 0$. In this case, $\gamma_d > \gamma > \gamma_m$. It is seen from Eq. (14) that the sign of the solenoid-producing term is no longer uniquely determined by β and α (or γ) but that the sign also depends on the ratio M'/M. If the air were initially at rest and an impulse were applied in an upward direction, it follows from Eq. (14) that the sign of the solenoid-producing term would be positive only when the horizontal dimensions of the mass effected are such that

$$(15) \qquad \frac{M'}{M} < \frac{\beta}{\alpha}$$

If this limit is exceeded, the mass M' would be retarded in the direction of the impulse. The meaning of the foregoing condition is perhaps best illustrated by the following example: Suppose that the slice of air considered is subject to a series of perturbations of variable horizontal extents. It would then react as an unstable medium relative to such perturbations as satisfy the inequality (15), whereas it reacts as a stable medium relative to such perturbations as do not agree with that condition. In this way, the atmosphere may "pick and choose" among the numerous perturbations that it receives from below. The air is then *selectively unstable*. As this case ($\alpha > 0$, and $\beta > 0$, *i.e.*, $\gamma_d > \gamma > \gamma_m$) occurs frequently in nature, it will be of interest to study this selection of perturbations in greater detail.

36. The Available Energy.—As in the last paragraph, we consider saturated air ascending through a dry-adiabatically descending environment. The solenoid-producing term is then the last term in Eq. *35*(11). Substituting from Eqs. *35*(12) and *35*(13) into the solenoid-producing term, we obtain

$$(1) \qquad c_p v_z' M' \left(\beta - \alpha \frac{M'}{M} \right) = c_p M_0 \, \delta \, v_z' S$$

where

(2)
$$S = \frac{M'/M}{1 + M'/M} \cdot \frac{\beta/\alpha - M'/M}{1 + \beta/\alpha}$$

As the solenoid-producing term is directly proportional to v_s' (which by definition is positive) and as c_p, M_0, and δ in any given case may be regarded as constants, it suffices to discuss the nondimensional quantity
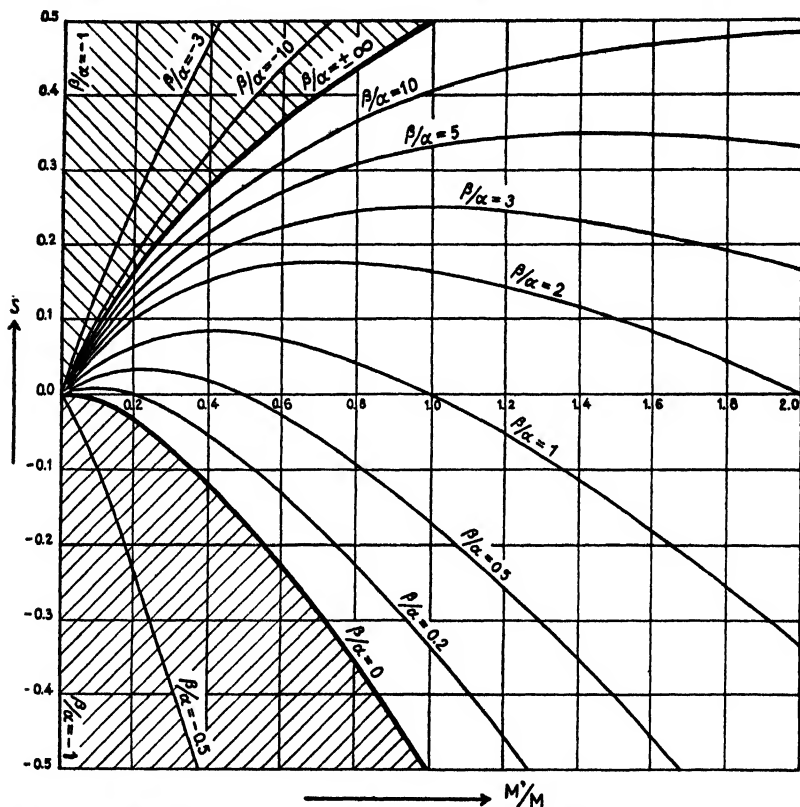
FIG. 41.—Showing the distribution of S as a function of M'/M for various values of β/α. S multiplied by v_s' is the variable factor in the solenoid-producing term.

S, which, multiplied by v_s', expresses the solenoid-producing term in relative units.

To facilitate the discussion, we suppose that the air initially is at rest, and that the portion M' of the slice is given an upward velocity $v_s' = 1$. Figure 41 then shows the distribution of S as a function of the ratio M'/M for various values of β/α. The diagram may be divided for convenience into three main portions, *viz.*:

1. *The area of absolute stability* represented by the lower hatched portion of the diagram. This area is characterized by $\beta < 0$ and $\alpha > 0$,

or $\gamma < \gamma_m$. The sign of the solenoid-producing term is negative independent of M' and M. This means that the kinetic energy of all impulses is consumed.

2. *The area of absolute instability* represented by hatching in the top part of the diagram. This area is characterized by $\alpha < 0$ and $\beta > 0$ or $\gamma > \gamma_d$. When γ approaches γ_d, β/α approaches $-\infty$. As the lapse rate normally does not appreciably exceed γ_d, only the portion above and close to the line indicated by $\pm \infty$ is of actual interest.

The sign of the solenoid term is positive independent of M' and M, which means that kinetic energy is produced by all impulses.

3. *The area of selective instability* represented by the unhatched portion of the diagram. This area is characterized by $\alpha > 0$ and $\beta > 0$ or $\gamma_d > \gamma > \gamma_m$ (*cf.* Fig. 40). In this case, the sign of the solenoid-producing term is not uniquely determined by the lapse rate (or β/α) but depends largely on the horizontal dimensions of the perturbations (or M'/M). When β/α is small (*i.e.*, when γ is close to γ_m), only such perturbations as cause M'/M to be exceedingly small can produce kinetic energy, and the amount of energy to be gained is then small. The air is then "highly particular" about its selection of energy-producing impulses. On the other hand, when β/α is large (*i.e.*, when γ is close to γ_d), the air reacts in an unstable manner relative to a great variety of impulses. The ratio M'/M may then vary within wide limits, and the amount of energy to be gained is large. This, interpreted, means that the energy-producing convective clouds can occupy only a small portion of the sky when γ is close to γ_m and that the spaces between individual clouds must be large. On the other hand, when γ is close to γ_d, the self-supporting individual clouds may occupy a considerable portion of the sky; large and small clouds may coexist, and the distances between the individual clouds may vary within wide limits.

The above deductions agree with observations: when the lapse rate above the condensation level is close to γ_m, the self-supporting convective clouds occupy only a small portion of the sky, and they are fairly uniformly spaced. However, when γ approaches γ_d, large and small clouds coexist, the sky is more chaotic, the clouds may fill a considerable portion of the sky, and wind squalls and strong or violent gusts occur frequently.

37. Selection of Perturbations.—As in the last paragraphs, we now consider the conditions in an isobaric unit slice when saturated air is given an upward impulse so that it is made to ascend in a dry-adiabatically descending environment. The condition for production of kinetic energy is

(1)
$$\beta > \alpha \frac{M'}{M}$$

It has already been shown that all impulses are suppressed when $\beta < 0$ and create kinetic energy when $\alpha < 0$. It remains to discuss in greater detail the frequently occurring case when $\beta > 0$ and $\alpha > 0$, or when $\gamma_d > \gamma > \gamma_m$.

Let us first remark that on account of the roughness of the ground, the unequal heating of the underlying surface, and other factors, the lower atmosphere is continuously subjected to a multitude of impulses of varying intensities and varying horizontal dimensions. But when the air is selectively unstable, it will react in an unstable manner only toward such impulses as satisfy the above inequality. Moreover, it follows from Eq. *36*(1) that the solenoid-producing term is directly proportional to the upward velocity v_z' of the impulse. Out of the multitude of the varying impulses, the air will "pick and choose" according to the intensity and the horizontal spacing of the impulses.

1. *Selection by Intensity.*—From what has been said above, it follows that the stronger the impulse the greater the upward acceleration in the ascending mass M' and the downward acceleration in the descending mass M. If two or more upward impulses coexist near one another, the stronger one will have a tendency to suppress the weaker one, because the latter will be counteracted by the downward acceleration created by the former. Thus, at the initial moment, there is a tendency for the stronger impulses to start convection and to suppress neighboring weaker impulses; what happens at the initial moment is controlled by the law of the survival of the fittest.

2. *Selection by Horizontal Extent.*—Other conditions being equal, the stratification is more unstable relative to such impulses as cause M'/M to be small than to such as cause M'/M to be large. That this is so is readily shown in the following manner: Let $v_{z1}'M_1'$ represent one impulse, and let $v_{z2}'M_2'$ represent the other impulse; and suppose that

$$v_{z1}'M_1' = v_{z2}'M_2'$$

The ratio r between the solenoid-producing terms is then

$$r = \frac{c_p v_{z1}'M_1'[\beta - \alpha(M_1'/M_1)]}{c_p v_{z2}'M_2'[\beta - \alpha(M_2'/M_2)]} = \frac{\beta - \alpha(M_1'/M_1)}{\beta - \alpha(M_2'/M_2)}$$

Hence, $r > 1$ when $M_1'/M_1 < M_2'/M_2$. Thus, there is a tendency for the impulse that causes the ratio M'/M to be a minimum to gain over other neighboring impulses. A similar result has been found by J. Bjerknes [8]. It should be borne in mind that this condition depends only on the ratio M'/M and not on the absolute magnitudes of M' and M. It is therefore not permissible to conclude that there is a tendency for narrow cloud towers to exist.

3. *Preference of Existing Circulations.*—It is reasonable to assume that the cross-sectional distribution of the vertical velocity resulting from an impulse is in principle as shown in Fig. 42. Let us suppose that a second upward impulse is applied somewhere between *B* and *D*. This impulse would add to the solenoids already produced; the upward velocity would be increased accordingly, and so would the descending velocity in the surrounding air.

Let us next suppose that the second impulse is applied somewhere near *A* or *E*. Here the impulse would be counteracted by the already existing downward velocities, and the impulse would be suppressed if it were not sufficiently intense to overcompensate the field of solenoids already created. Thus, an already existing upward energy-producing circulation has a tendency to suppress neighboring impulses and to feed on the impulses that occur within its own domain.

4. *Horizontal Growth of Energy-producing Circulations.*—Let us now suppose that a second impulse is applied at *B* or at *D*. Here, the vertical
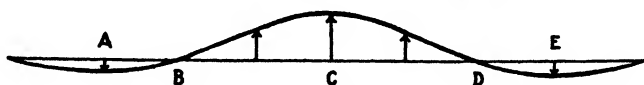
FIG. 42.—Diagrammatical distribution of vertical velocities in and around a cylindrical ascending current which satisfy Eq. 35(1).

velocities are slight or even nil. Additional impulses will then create kinetic energy, and the field of solenoids will grow and spread laterally, Thus, the circulation initially established by the strongest impulse has a tendency to grow laterally and to make its suppressing influence on more distant impulses felt over a wider region.

In this way, large cumulus clouds are built up of a great number of impulses the horizontal extent of each of which may be quite small compared with the horizontal dimensions of the entire cloud. That this is so is corroborated by observations of the growth and the structure of cumulus clouds. It would therefore be erroneous to assume that a cumulus cloud results from one single impulse or from one uniform ascending current.

5. *Limit of Horizontal Growth when $\beta/\alpha < 1$.*—To go a step further, we assume that at the initial moment there are several impulses over a wide area which start energy-producing circulations: none of these, then, clashes with the inequality (1) above. On account of the great multitude of impulses that the air receives from below, the existing circulations have a tendency to increase horizontally; and, if this continues, the state may be reached when the ratio M'/M approaches the ratio β/α. As the ratio M'/M thus increases from a value that is small compared with β/α to the final value equal to β/α, it is seen from Fig. 41 that it must pass the value at which there is a maximum of production of kinetic

energy, and it must gradually approach the state when no more solenoids are available.

The foregoing is not exact inasmuch as the convective currents have a tendency to change the lapse rate, so that the limit set for the final value of M'/M is determined, not by the initial value of β/α, but by the value that gradually develops. Moreover, as will be shown later, not all the available energy is used to create kinetic energy. It is important to bear in mind that when $\beta/\alpha < 1$, the ratio M'/M must, in virtue of the inequality (1), remain less than unity. This involves that the descending currents must be weaker than the ascending currents, as indicated by Eq. *35*(1).

6. *Limit of Horizontal Growth when $\beta/\alpha > 1$.* As above, we assume that widely scattered energy-producing circulations start and grow horizontally. As $\beta/\alpha > 1$, the *stratification* would allow the ratio M'/M to increase and approach the ratio β/α. But it is also necessary to consider the continuity of the motion. As M'/M approaches 1, the descending currents must be as strong as the ascending ones. When this state is reached, it is obvious that only excessive impulses that affect the mass M could overcompensate the descending velocity; and, in such cases, the circulation would be reversed so as to cause the already ascending air to descend. It follows, therefore, that the horizontal growth of upward energy-producing circulations will not surpass the limit set by $M' = M$, *i.e.*, when the upward currents occupy half the total area. This implies that *the energy-producing circulations must have an asymmetrical distribution of vertical velocity.*

It is of interest to note that the ratio M'/M is not expressive of the cloud cover as observed from the earth's surface. Thus, if the clouds were cylindrical and 1000 m. high with their bases about 1000 m. above the observer, a cloud cover of about $\frac{7}{10}$ to $\frac{9}{10}$ would be noted when $M' = M$.

7. *Lower Limit of M'/M.*—In discussions on convective clouds, it has been stated that the most favorable conditions exist when M'/M approaches zero; for the ascending motion would then be spread over a wide area, and the environment of the ascending currents would then remain sensibly unchanged. However, it is hardly reasonable to assume that such conditions can exist in the atmosphere. If an upward impulse affects the mass M', there seems no reason to justify the assumption that the descending compensation current would affect an area which is infinitely larger than that of the ascending mass. What regulates the lower limit of the ratio M'/M we do not know; it is plausible that the stratification is a determining factor. Thus, though it is certain that the distribution of vertical velocity in energy-producing circulations must be asymmetrical (*i.e.*, $v_s' > v_s$, and therefore $M' < M$), it is

plausible that there must also exist a lower limit of the ratio M'/M. This question can be decided only by further research. However, if M'/M could approach zero, it would imply that energy-producing circulations of saturated air could be started as soon as γ slightly exceeds γ_m. This follows from the inequality (1) above. Experience gained from the analysis of ascent curves seems to show that energy-producing clouds do not start unless γ is noticeably greater than γ_m. The exact limit is not known; and, with due allowance for this, we may say that the lower limit for M'/M is about at 0.1 or 0.2. The upper limit is set by β/α when $\beta/\alpha < 1$ and by $M'/M = 1$ when $\beta/\alpha > 1$. Thus, when the air is selectively unstable, all possible developments of energy-producing clouds should occur in the unhatched portion of Fig. 41 between the lines indicated by $M'/M = 0.1$ and $M'/M = 1$. The rest of the unhatched area is of theoretical interest only.

38. The Parcel Method and the Slice Method.—So far, we have described two different methods for determining the stability or instability conditions by means of ascent curves. The first, which is described in Pars. 30 to 34, may be called the *parcel method*. The second, which is described in Pars. 35 to 37, may be called the *slice method*. The parcel method is based on the assumption that an isolated parcel of air can move through an undisturbed environment; only the initial distribution of mass (or temperature) enters into the discussion. The slice method takes into consideration not only the initial distribution of mass but also the changes of the environment of the ascending air and the nature of the perturbation that starts the motion. Evidently, the slice method is more exact than the parcel method. However, in practice, the parcel method has certain advantages and a comparison between the two methods is therefore given below.

1. *Nonsaturated Air.*—According to Eq. *35*(6), the slice method gives the following solenoid-producing term:

$$c_p M' \left(\frac{\partial T'}{\partial t} - \frac{\partial T}{\partial .} \right)$$

If the environment remained unchanged (*i.e.*, by the parcel method), $\partial T/\partial t = 0$, and the solenoid-producing term would be

$$c_p M' \frac{\partial T'}{\partial t}$$

From Eqs. *35*(2) and *35*(4), it follows that the parcel method would give a solenoid-producing term which is numerically too small both when $\gamma > \gamma_d$ (instability) and when $\gamma < \gamma_d$ (stability). The parcel method, therefore, underestimates both the stability and the instability

of unsaturated air.   From both methods, it follows that the air is stable, indifferent, or unstable according to whether $\gamma \gtreqless \gamma_d$.

2. *Saturated Air.*—In the same manner as above, it follows from the deductions in Par. 35 that the solenoid-producing term, when determined on the assumption of an undisturbed environment, is numerically too small both when $\gamma > \gamma_m$ (instability) and when $\gamma < \gamma_m$ (stability). This applies when the descending air remains saturated. From both methods, it follows that the air is stable, indifferent, or unstable according to whether $\gamma \gtreqless \gamma_m$.

3. *Saturated Ascent through a Dry-adiabatically Descending Environment.*—From Eqs. *35*(3), *35*(4), and *35*(6), it follows that the following is true of the solenoid-producing term as deduced on the assumption of an undisturbed environment:

a. When $\gamma > \gamma_d$, the solenoid-producing term comes out with too small a positive value.

b. When $\gamma_d > \gamma > \gamma_m$, the solenoid-producing term comes out with too large a positive value.

c. When $\gamma < \gamma_m$, the solenoid-producing term comes out with too small a negative value.

From both methods, it follows that the air is unstable when $\gamma > \gamma_d$ and stable when $\gamma < \gamma_m$. When $\gamma_d > \gamma > \gamma_m$, the stability criteria of the slice method differ from those of the parcel method as has been shown in Par. 35.

From the foregoing and from Par. 33, it follows that when the air is conditionally unstable (*i.e.*, when $\gamma_d > \gamma > \gamma_m$) the parcel method underestimates the resistance against lifting and overestimates the available energy (see Fig. 34).   On the other hand, it underestimates the available energy when the air is absolutely unstable.

It is important to note that the error due to the assumption of an undisturbed environment vanishes when γ approaches γ_d; this follows from Eqs. *35*(4) and *35*(6).   Similarly from Eqs. *35*(1), *35*(4), and *35*(6), it follows that this error decreases when the ratio M'/M decreases and becomes insignificant when the cloud towers are very narrow relative to the width of the descending currents.

39. Discussion of the Assumptions.—The deductions in Pars. 35 to 37 were based on the three assumptions quoted at the beginning of Par. 35. As none is strictly fulfilled in the atmosphere, it is of interest to investigate how the nonfulfillment of these assumptions affects the results deduced above.

We consider first assumption (1).   If there is convergence toward the area under consideration, the descending velocity would be less than it would be if there were no convergence.   Conversely, if there is divergence from the area under consideration, the descending velocities

would be increased relative to the ascending velocities. It follows then from Eqs. *35*(4), *35*(5), and *35*(6) that horizontal convergence would increase the solenoid-producing term in all cases when the solenoid-producing term is positive, and diminish the solenoid-producing term when this term is negative. The reverse is true for horizontal divergence. It will be shown later that horizontal convergence is an important factor in releasing and maintaining convection. The methods of detecting horizontal convergence are described in Chap. IV.

As regards assumption (2), it suffices to remark that, if the conditions are not strictly barotropic at the initial moment, the initial solenoids would add to those created by the vertical displacements.

If assumption (3) is not fulfilled, it is necessary to consider whether the nonadiabatic changes act in such a way as to increase or decrease the instability forces. How this is done will be shown in later paragraphs.

40. Autoconvection and Convection.—From the equation of condition $(p = \rho RT)$ and the equation of static equilibrium $(-\partial p/\partial z = \rho g)$, it follows that the density of the air would be constant along the vertical when

$$-\frac{\partial T}{\partial z} = \frac{g}{R} = 3.4°C. \qquad \text{per 100 m.}$$

If this limit is exceeded, the density would increase along the vertical, and heavier air would then rest on top of lighter air; the layers would turn over without any initial perturbation. This is called *autoconvection*. Such conditions can exist only close to the earth's surface on very warm days. Under ordinary atmospheric conditions, such extreme lapse rates do not develop in deep layers of air, and the instability phenomena which will be discussed hereafter are such as develop when the lapse rate of temperature in nonsaturated air exceeds the dry-adiabatic or when the lapse rate of temperature in saturated air exceeds the moist-adiabatic. In such cases, an initial disturbance is necessary in order to start the overturning. This process of overturning is called *convection*.

41. Convective Currents.—It has been customary to consider convection only as rearrangement of infinitely thin strata of air, each layer maintaining its potential temperature (see Margules [41]). The initial state would than be characterized by decreasing potential temperature along the vertical; and the final result of convection would be a rearrangement of the individual strata in such a manner that the potential temperature increases along the vertical. This may be acceptable when we consider atmospheric systems of the order of magnitude of the average extratropical cyclone; but we know from experience (Rossby [63]) that local convection results in a fairly thorough mixing of the various layers affected by convection.

Let us first consider convection in a layer between two horizontal rigid boundaries. The isotherms are initially horizontal, the lower portion is unstable, and the upper portion is stably stratified (see Fig. 43). If a perturbation is applied, the air in the unstable layer would be accelerated in the direction of the impulse, and the air in the stable layer would be retarded in the direction of the impulse. The isotherms resulting from the vertical motions are shown in Fig. 43.

The vertical motions must vanish at the boundaries and attain a maximum somewhere between them. Kinetic energy is produced in the unstable layer and consumed in the stable layer. As continuity must be established, there must be horizontal convergence in the lower portion of each ascending current and horizontal divergence in the upper portion

→ 5m/sec. ____ Initial isotherms. ⌒ Perturbed isotherms.
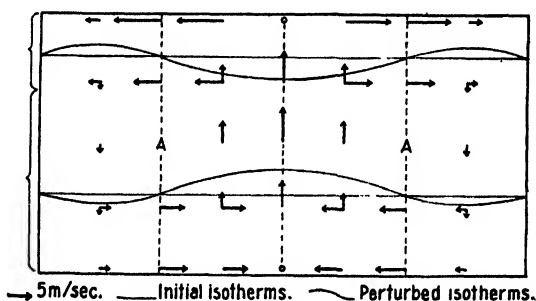
Fig. 43.—Diagrammatical distribution of vertical and horizontal velocities in a cylindrical convective current when $M'/M = \frac{1}{3}$.

of each ascending current. In the descending currents, the reverse is true. Figure 43 shows the horizontal velocities computed by aid of the equation of continuity that result when the vertical velocities are as indicated in the diagram.

We consider next the circulation round the point A in Fig. 43. The velocity of revolution round the point A varies with the distance from this point; and, as a result, the layers cannot arrange themselves in such a way that the potentially coldest air comes to the bottom of the layer and the potentially warmest air to the top of the layer. It is readily seen that the currents established will maintain solenoids until the various layers are thoroughly mixed into one another. *The final result of convection will, therefore, be an adiabatic lapse rate throughout the layer.*

Rossby [63] has shown that the foregoing conclusion holds also when there is no upper rigid boundary to the convective layer. Part of the energy that is released in the unstable layer is then used to establish an adiabatic lapse rate in the stably stratified air above. Figure 44 shows the initial distribution of temperature (curve A), and the final distribution (curve B) resulting from complete stirring. It will be seen that the convection layer has increased in thickness by the amount $H - h$.

In Fig. 43, there is no general horizontal velocity superimposed on the convective currents. Figure 45 shows the resulting stream lines when a slight translatory velocity (4 m./sec.) is superimposed on the currents shown in Fig. 43. It should be noted that the superimposition of a translatory movement changes nothing but the stream-line picture. The wind shift at the ground, which in Fig. 43 is found in the center of the ascending current, is displaced in a forward direction when the convective system is superimposed on a translatory motion. It should be noted that, when the translatory movement is slight, the convective cloud may be stationary while the air blows through it.

FIG. 44.—Showing the influence of convection on the vertical distribution of temperature.

What has been said above of the convective currents should be regarded only as vague suggestions. Further observations as well as dynamical and kinematical investigations will be needed to render an adequate picture of these complex phenomena.

It will be seen from Eq. $35(7)$ that the solenoid-producing term in nonsaturated air is directly proportional to $(\gamma - \gamma_d)$. As nonsaturated air is unstable relative to all impulses when $\gamma > \gamma_d$ and as perturbations are always present in abundant amounts, it follows that convection is released as soon as γ exceeds γ_d. As convection and mixing tend to make γ approach γ_d, it follows that γ will not appreciably exceed γ_d. The solenoid-producing term will therefore always remain small in nonsaturated air. The "dry convection," therefore, does not normally produce much kinetic energy. Only when the air is heated very rapidly by the underlying surface will strong wind gusts result (e.g., desert wind squalls).

FIG. 45.—Stream lines when a convective current, as shown in Fig. 43, is superimposed on a slight translatory movement. The eddies in the stream lines may vanish when the translatory movement increases.

When condensation occurs in the ascending current, γ may be considerably larger than γ_m. It follows, then, from Eq. $35(14)$ that the solenoid-producing term may be quite large. Strong wind gusts, therefore, often accompany convective clouds.

Referring again to Fig. 43, we see that, if condensation occurs in the ascending current, the cloud has a tendency to spread out in the top part of the ascending current where there is horizontal divergence. Here, then, the ratio M'/M (see Par. 35) will increase; and, if the strati-

fication is selectively unstable ($\beta > \alpha M'/M$), the growth of the ratio M'/M will tend to create stability. The cloud will flatten out, it ceases to grow upward, and it will eventually consume kinetic energy. *The divergent outflow from the top part of the ascending current is a stabilizing factor of great importance.*

42. Convective Clouds.—All clouds of the cumulus type form as a result of instability, either in the cloud layer or in the layer under the cloud. The various forms that these clouds may take depend on the
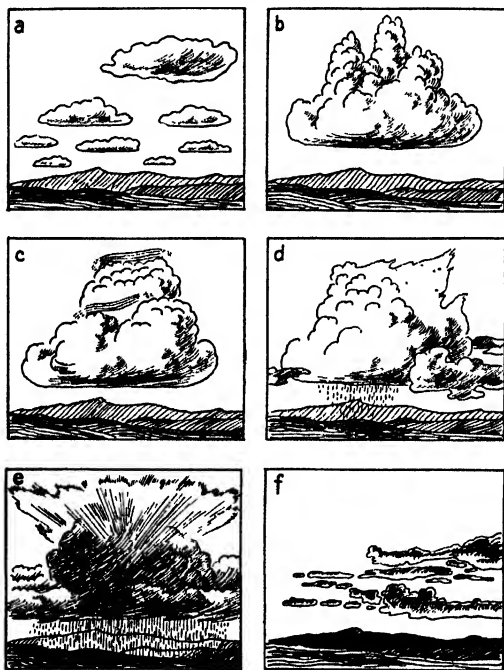
Fig. 46.—Types of convective clouds. *a*, cumulus humilis; *b*, cumulus congestus; *c*, cumulus pileus: *d*, cumulo-nimbus calvus; *e*, cumulo-nimbus incus; *f*, strato-cumulus vesperalis.

degree of instability, the depth of the unstable layer, and the distance from the condensation level to the top of the convective layer. In addition, we must consider the processes that contribute to the maintenance or frustration of instability. In this paragraph, we shall consider only the existing conditions, leaving the discussion of the processes that may produce or nullify instability to later paragraphs.

1. *Cumulus Humilis.*—These clouds (see Par. 20 and Fig. 46) form when the convection condensation level is close to the upper limit of the layer affected by the convective currents. They are sometimes entirely embedded in a layer of air that is absolutely stable (*i.e.*, $\gamma < \gamma_m$). In such cases, the clouds form in the upper, energy-consuming part of the

ascending currents.   The cloud air is then colder than the environment, and the cloud feeds on the energy-producing dry convection below the condensation level.

At other times, the cumulus humilis form in selectively unstable air (*i.e.*, $\gamma_d > \gamma > \gamma_m$) just under a layer of absolute stability.   The cloud is then embedded in the upper part of the ascending current, where the cloud, on account of the horizontal divergence (see Par. 41), has grown laterally to such an extent that it has become stable [*i.e.*, $\beta < \alpha(M'/M)$; see Par. 35]. In this case, too, the cloud air is colder than the environment, and it consumes kinetic energy. Cumulus humilis that form in the upper portion of a selectively unstable layer will usually grow upward until the dome reaches into a completely stable layer ($\gamma < \gamma_m$).   The cumulus humilis, therefore, develop when the condensation level is slightly above an unstable layer and, at the same time, not far below the layer where $\gamma = \gamma_m$.   Figure 46a shows the typical features of a cumulus humilis, or fair-weather cumulus.   It has a dead appearance and no active towers or protuberances.   Figure 47 shows the vertical distribution of temperature that is typical of clouds of this kind.   Related to the cumulus humilis are the cumulo-stratus and the cumulus undulatus
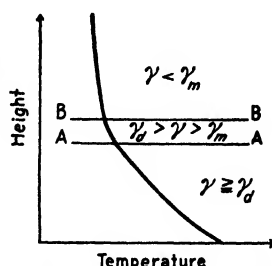
FIG. 47.—Vertical distribution of temperature typical of cumulus humilis.

(see Par. 21) both of which usually form in the layer under an inversion as a result of convection in the air below.

2. *Cumulus Congestus.*—These clouds (see Par. 20 and Fig. 46) form in deep layers of air that are either absolutely unstable or else selectively unstable.   The condensation level may be below or above the limit between absolute instability and selective instability.   If the condensation level is in absolutely unstable air, the rising masses will reach saturation while γ is close to γ_d.   It follows then from Pars. 35 and 36 that great amounts of kinetic energy will be released; towers and protuberances grow upward rapidly, and the cloud also grows horizontally.   As the towers grow upward into air that is selectively unstable, only those perturbations which cause M'/M to be less than β/α will produce kinetic energy.   If γ decreases upward, the towers must become narrower relative to the descending current around them.   Eventually, the towers may reach up to the heights where $\gamma = \gamma_m$.

FIG. 48.—Vertical distribution of temperature typical of cumulus congestus.

or where the divergent outflow from the upper portion of the ascending current is strong enough to make the cloud spread out horizontally, whereby the ratio M'/M becomes too large for further production of kinetic energy.

The typical features of a developing cumulus congestus are shown in Fig. 46b, and the temperature distribution typical for such development is shown in Fig. 48. It will be seen that the size of the convective elements in the cloud decreases upward and that the top of the cloud has a typical cauliflower structure, showing that the selective instability decreases with elevation.

The condensation level may also be situated slightly above the bottom layer, which is absolutely unstable. In such cases, the layer between the condensation level and the top of the absolutely unstable layer is energy-consuming. The convection is then, as a whole, less intense.

It is sometimes observed that the towers of cumulus congestus break through minor inversions in the upper atmosphere. In such cases, a veil (pileus) forms around or above the towers (Fig. 46c). This condition is due to the circumstance that turbulence has transported so much moisture up to the air under the base of the inversion that, when this air is lifted by the ascending towers, it becomes saturated. The cloud is then called cumulus pileus. The veil (or "scarf") usually consists of water droplets; but if the temperature is well below freezing, it may consist of ice crystals.

As the cumulus congestus grows further, several developments are possible: (a) It grows up into layers where the wind increases rapidly with height. The towers are then blown asunder and dissolve by mixing into the air above. (b) It grows into a stable layer and flattens out in its upper portion before it reaches temperatures that are low enough for ice crystals to form or for the supercooled water droplets to freeze. In such cases, the cloud usually does not produce precipitation.[1] (c) It grows into layers where the top part of the cloud changes into ice or snow crystals. It has then developed into a cumulo-nimbus, a shower cloud, or a thundercloud.

3. *Cumulo-nimbus.*—These clouds (see Par. 20 and Fig. 46) develop from cumulus congestus (or pileus). When this happens, the cloud loses its cauliflower structure; the towers and protuberances become less pronounced, the crevices gradually disappear, and the upper portion of the cloud changes gradually into a tangled web with only slight traces of convective elements. During this process, precipitation is usually released from the cloud. This type of cloud is called cumulo-nimbus calvus; its principal features are shown in Fig. 46d.

[1] For exceptions see Par. 25.

The calvus type usually develops into cumulo-nimbus capillatus or cumulo-nimbus incus, whose principal features are shown in Fig. 46e. The top part of such a cloud consists of ice crystals and is called cirrus densus or cirrus nothus. It resembles a tangled web surrounding the top of the water cloud. Such clouds give heavy precipitation in the form of showers or squalls and frequently, also, thunderstorms. The cumulo-nimbus clouds develop from cumulus congestus when the unstable layer is sufficiently high for the cloud to grow considerably above the zero isothermal level. The typical structure of the air is shown in Fig. 49.

It is possible with practice to forecast the weather for a few hours ahead by looking at the cumulus clouds and observing their development. It is then most important to observe the changes in the upper part of the clouds. If there are no towers (as in Fig. 46a), there is no chance of precipitation. If there are towers (as in Fig. 46b or c), it is possible that precipitation may develop. If some of the clouds show signs of presence of ice crystals, precipitation is sure to be released soon. Figure 46c often occurs as a transition from Fig. 46b to d, but Fig. 46d usually develops from Fig. 46b.
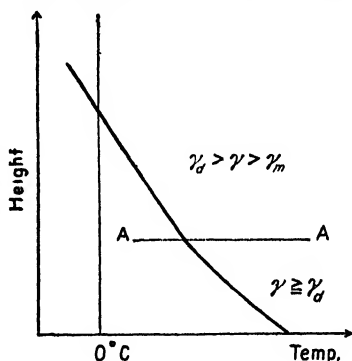
FIG. 49.—Vertical distribution of temperature typical of cumulo-nimbus.

The cumulus clouds sometimes dissolve by general shrinking and disappear gradually. This usually occurs when a sheet of high clouds (cirro-stratus or alto-stratus) develops above them. In dissolving in this way, they pass through the state of fair-weather cumulus (Fig. 46a). Most frequently, the cumulus clouds flatten out into rolls or bulging layers resembling strato-cumulus; this development is shown in Fig. 46f. This often occurs in the evening when the atmosphere is settling down after the diurnal heating (strato-cumulus vesperalis). In any case, the dissolution of cumulus clouds shows that the atmosphere is developing toward a stable stratification.

If the convection is caused by diurnal heating over land, it has a pronounced diurnal period with a maximum of cumulus clouds in the afternoon and clearing in the evening. Over oceans, the diurnal convection is only slight (except in tropical regions), and the maximum of cloudiness has a tendency to occur in the night.

If the convection is caused by the travel of air toward warmer regions, there is but slight diurnal variation, and cumulus and cumulo-nimbus may develop both day and night.

The precipitation caused by convection is always of a showery character; it begins and ends suddenly, owing to the rapid transition from ascending to descending currents (see Fig. 25). The sky is variable with frequent changes from a dark threatening appearance to clearing.

43. Thunderstorms.—Thunderstorms develop from clouds of the cumulo-nimbus type; they may be classified as frontal thunderstorms or air-mass thunderstorms. The former type occurs on account of instability released through ascent of air along frontal surfaces; the latter type develops on account of instability within the air masses. Both types have the same fundamental characteristics.

From the point of view of instability, the difference between a thunderstorm and a shower is only one of degree. The greater the instability is, the stronger are the vertical currents that develop. The falling velocity of raindrops depends on their size; and as the drops coalesce and increase in size, they fall more rapidly. A strong upward current may carry waterdrops upward. The largest drops (about 4 mm. in diameter) that can persist in the air can be kept up by an upward current of about 8 m./sec. When larger drops than these are formed, they are unstable and immediately break up into smaller drops. As the ascending current is not a steady one but blows in a succession of gusts and lulls, the drops may rise and fall intermittently, sometimes coalescing into larger drops and then breaking up into smaller drops. Moreover, they may repeatedly be carried from the water part of the cloud to the snow part. The waterdrop, being carried up to freezing temperatures, may freeze to solid ice and develop a covering of snow outside the ice. In a lull, it may fall down into the water cloud where it gathers a coating of water over the snow; and when it is again carried upward, the water may freeze to ice, and a fresh cover of snow develops. The structure of the hailstones shows conclusively the existence of large ascensional velocities in the thunderstorms; the hailstones often consist of concentric shells of clear ice and snow which shows that the hail must have been moved repeatedly from the liquid to the snow part of the cloud.

Simpson [75] has shown experimentally that, when a drop of water breaks up into smaller drops, there is a separation of positive and negative electricity, the waterdrops taking up a positive charge and the air a corresponding negative charge. By repeated splitting up of drops, enormous electric charges are made available for the thunderstorms. Since the air ascends much more rapidly than the drops which split up, it follows that the positive charge is accumulated in the part of the cloud where the ascending current is strongest, the rest of the cloud (except the top which consists of ice crystals) becoming negative or neutral.

Simpson and Scrase [76] have shown by balloon observations that the foregoing distribution of electric charge is found in most thunder-

storms.　In addition, it is found that the upper portion of the cloud, which consists of ice crystals, carries a positive charge.　The distribution of electricity in a model thundercloud is shown diagrammatically in Fig. 50.

A fully developed thunderstorm is accompanied by heavy rain or hail, lightning and thunder.　The wind freshens during the approach of the storm, blowing at first toward the storm.　As the thundercloud arrives overhead, the wind changes in direction (see Fig. 45), blowing out from the storm in a forward direction.　The barometer falls while the storm approaches, but when the wind changes a brisk rise amounting
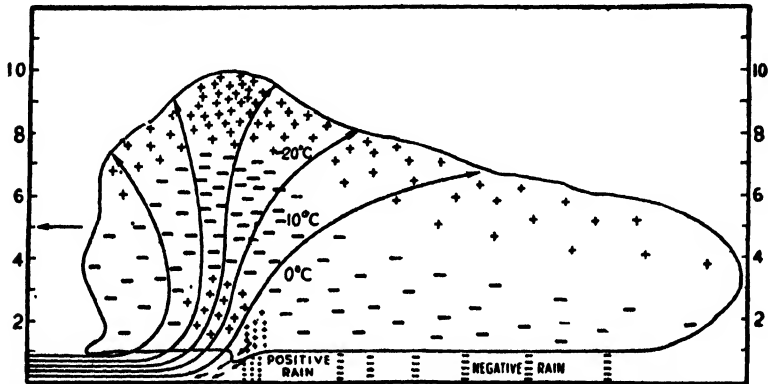
FIG. 50.—Showing the normal distribution of electric charge in a thundercloud.　(*After Simpson.*)

to a few millibars occurs.　The precipitation, which commenced as a sudden heavy downpour, changes into a more continuous rain which gradually decreases in intensity.

44. Conditions Favorable for Production of Stability and Instability.—In the practice of forecasting it is necessary to predict not only the developments that result from existing stability and instability, but also such processes as lead to development from stability to instability, and vice versa.　The factors that are of importance for changing the stability conditions are: (1) vertical movement of an air mass as a whole, (2) advection of air aloft, (3) mixing, (4) radiation, and (5) exchange of heat between the air and the underlying surface.

Although the reader is referred to general textbooks on meteorology (*e.g.*, Brunt [19]) for the detailed discussion of these factors, their significance for weather analysis and forecasting will be summarized below.

45. Ascent, Descent, and Lapse Rate.—We shall now consider a large mass of air that is moved upward or downward through the atmosphere in order to see what *internal* changes in lapse rate may occur.　Such displacements, which often take place along frontal surfaces and mountain

ranges, may also develop as a result of horizontal convergence or divergence within the air mass.

We consider first the simple case of dry air ascending or descending without horizontal divergence or convergence. It suffices to examine a slice of air between two isobaric surfaces p_1 and p_2, where $p_1 - p_2 = \Delta p$. As the air ascends or descends, the pressure difference Δp between the bottom and top face of the sheet must remain constant while the sheet expands or contracts vertically as it ascends or descends. Let θ denote potential temperature, and $\delta/\delta p$ differentiation with respect to p within the moving sheet. The expression $(1/\theta)(\delta\theta/\delta p)$ must then remain invariant within the ascending or descending air. Substituting from Poisson's equation and the equation of static equilibrium and remembering that $-(\delta T/\delta z) = \gamma$, we obtain

$$\frac{R}{p}\,(\gamma_d - \gamma) = \text{constant}$$

where R = gas constant.

T = temperature.

γ_d = dry-adiabatic lapse rate.

p = pressure.

If the stratification were initially stable $(\gamma_d > \gamma)$, the stability would decrease during the ascent, and γ would approach γ_d as p approaches zero; the stratification would approach the indifferent state, but it would never surpass it. Likewise, the initial stability would increase when the sheet descends, and the sign of γ may change from plus to minus.

If the stratification were initially unstable $(\gamma_d < \gamma)$, the instability would decrease and approach the indifferent state $(\gamma_d = \gamma)$ as p approaches zero.

The above results are modified to a certain extent by horizontal divergence and convergence. Let A denote the horizontal cross-sectional area of the lifted slice of air, and let the subscript 0 denote the initial state, and the subscript 1 denote the state after the lifting. The following equation then holds:

$$\frac{1}{p_0 A_0}\,(\gamma_0 - \gamma_d) = \frac{1}{p_1 A_1}\,(\gamma_1 - \gamma_d)$$

When there is horizontal divergence, $A_1 > A_0$; when there is horizontal convergence, $A_1 < A_0$. Thus, horizontal divergence or convergence may counteract the effect of the pressure variation. However, when the vertical displacements are appreciable, the effect due to variations in pressure is the predominant one.

46. Convective Instability.—Rossby [63] has shown that, when the distribution of temperature and humidity along the vertical is such

that the potential pseudo-equivalent temperature decreases with increasing altitude, a layer of ascending air becomes unstable when the air becomes saturated. This condition is called *convective instability*.

Owing to the relation between the potential pseudo-equivalent temperature θ_{se} and the potential pseudo-wet-bulb temperature θ_{sw} shown in Pars. 15 and 16, the condition of convective instability is expressed by:

$$\frac{\partial \theta_{se}}{\partial z} < 0 \qquad \text{or} \qquad \frac{\partial \theta_{sw}}{\partial z} < 0$$

or

$$-\frac{\partial T_{se}}{\partial z} > \gamma_d \qquad \text{or} \qquad -\frac{\partial T_{sw}}{\partial z} > \gamma_m$$

That is, there is convective instability in the layer when the pseudo-equivalent temperature T_{se} decreases more rapidly along the vertical than the dry-adiabatic or when the pseudo-wet-bulb temperature T_{sw} decreases more rapidly along the vertical than the moist-adiabatic.

It is readily seen from Fig. 51 that if such a layer of air were lifted above its condensation level, the lapse rate of temperature in the saturated air would be greater than the moist-adiabatic, and the layer would become unstable.

It is also readily seen (*e.g.*, from Figs. 37 and 38) that latent instability is always connected with convective instability in one or more layers. When convective instability is present and the air column is lifted, latent instability develops and results in absolute instability through continued lifting. This is seen from Fig. 51. Let AB represent the ascent curve in the layer AB. Let a mark the pseudo-wet-bulb temperature of the air at A and b the pseudo-wet-bulb temperature of the air at B. Regardless of the slope of AB, the layer is convectively unstable because the potential pseudo-wet-bulb temperature of B is less than that of A. Through lifting, A becomes saturated at A' and B at B'. When the whole layer has become saturated, it is completely unstable. In the state AB, none of the potential pseudo-wet-bulb temperature lines intersects AB; in the state $A'B'$ they all intersect $A'B'$. Thus, all transitions from absolute stability through latent instability to absolute instability fall between the initial state AB and the saturated state $A'B'$. If the parcel at A becomes saturated before the parcel at B, the former will move upward along the moist-adiabatic through A', and the instability will be increased.

Fig. 51.—Illustrating the development of instability through lifting of stably stratified air which is convectively unstable.

It is worthy of note that when a layer is convectively stable

$$\left(\frac{\partial \theta_{se}}{\partial z}\right) > 0 \quad \text{or} \quad \left(\frac{\partial \theta_{sw}}{\partial z}\right) > 0,$$

the layer is usually absolutely stable, because, otherwise, the humidity would have to increase so rapidly along the vertical that the effect of a contingent superadiabatic lapse rate would be overcompensated. On the other hand, convective instability is often present together with absolute stability. A typical example is shown in Fig. 52. The curve $ABCD$ represents an ascent curve showing a pronounced inversion of temperature in the layer 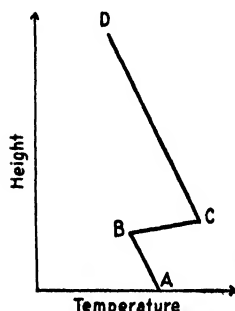BC. This layer is, of course, absolutely stable; but if the whole air column were lifted (*e.g.*, by a front), two developments are possible, *viz.*: (1) If the potential pseudo-equivalent temperature (or the potential pseudo-wet-bulb temperature) at B is smaller than at C, the inversion layer will retain its stable character while it is lifted. (2) If the potential pseudo-equivalent temperature (or the potential pseudo-wet-bulb temperature) at B is greater than at C, the layer will eventually become unstable by being lifted. The latter case, as is readily seen, occurs when the warm air above the inversion is exceedingly dry relative to the air below the inversion. Thus, an inversion with dry air aloft may form a complete hindrance against ordinary convection; but when the whole system is lifted, it may contribute substantially to convective phenomena. The latter case occurs quite frequently in the warm season in subtropical countries (see Chap. III).

Fig. 52.—Illustrating convectively stable and convectively unstable inversions.

From the foregoing, it follows that actual instability develops in convectively unstable air when it is lifted as a whole to its condensation level. This lifting may occur (1) at frontal surfaces, (2) along mountain ranges, and (3) as a result of convergence in the horizontal field of motion. Convective instability is a frequent occurrence in the equatorial and tropical continental air masses and also in the air that belongs to the western extremity of the subtropical cells (see Chap. III).

47. Advection of Air Aloft.—The development of instability in the atmosphere has often been ascribed to advection of colder air above warmer air. As the air temperature normally decreases with elevation, we are here concerned only with the conditions favorable for advection of potentially colder air above potentially warmer air.

1. *In the friction layer*, the wind normally increases with elevation, and the wind direction turns to the right relative to the direction of the surface wind. If the air temperature decreases in the direction opposite

to that of the wind, it is easily seen that potentially colder air will over-run potentially warmer air on account of the rapid increase in wind velocity along the vertical within the friction layer. This overrunning produces instability in addition to that caused by the heating of the air from below.

When the temperature distribution is such that the wind blows along the temperature gradient, the increase of wind velocity along the vertical within the friction layer causes potentially warmer air to overrun poten-tially colder air. This results in the production of stability in addition to that caused by the cooling of the air from below.

2. *In the free atmosphere*, the conditions are rarely favorable for poten-tially colder air to overrun potentially warmer air. This condition is mainly due to the variation in the distribution of pressure with increasing altitude. We consider first the left-hand portion of Fig. 53 in which the air along the surface blows from a colder toward a warmer region. The pressure distribution along the vertical satisfies with great accuracy the equation of static equilibrium, viz.,

$$-\frac{\partial p}{\partial z} = \rho g$$

FIG. 53.—Showing the normal change in the direction of the iso-bars with increasing elevation.

At the point B, $\partial p/\partial z$ is numerically smaller than at A, because ρ is smaller at B than at A. The isobars at a considerable altitude above the fric-tion layer will then run as shown by the broken lines. Thus, while a parcel of air near the surface moves from A to B, a parcel of air in the upper atmosphere will move from C to B. This means that poten-tially warmer air overruns potentially colder air. In the meantime, the air that streams from A to B is heated from below; this counteracts the effect of the advection of potentially warmer air aloft. Usually, the heating effect is the major one; but when air from the north streams southward toward the region occupied by the northern half of the sub-tropical anticyclones (see Chap. III), the strong westerlies at high alti-tudes may cause sufficient advection of warm air aloft to turn the upper portion of the air column stable.

We consider next the right-hand portion of Fig. 53. It is readily seen that potentially colder air may overrun potentially warmer air. But, in this case, the warm air in the lower layers moves toward a colder region so that it is cooled from below. The effect of the cooling from below is normally greater than the effect of the overrunning at higher levels: the air column develops stability. In the warm season it happens occasionally that the temperature gradient over warm continents is too
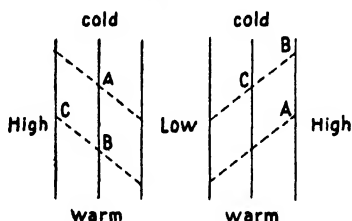
slight to overcompensate the effect of the overrunning. In such cases, which are rare, instability may develop above the friction layer.

3. *At cold fronts,* notably when orographic conditions are favorable, potentially colder air may overrun potentially warmer air. The conditions favorable for such developments are described in Par. 125.

48. Horizontal Mixing.—The wind is never a steady current; it consists of a succession of gusts and lulls of short period. This condition is mainly due to eddies that form on account of friction at the ground, horizontal and vertical stresses, and instability. An eddy that moves from one place to another may be regarded as an agency in the process of diffusion of heat, moisture, momentum, etc.

The mixing that occurs between *horizontally* adjacent air masses may be assumed to take place at constant pressure. Let M_1, T_1, e_1, and q_1 represent the total mass, the absolute temperature, the vapor pressure, and the specific humidity in the first component of the mixture; and let similar variables with the subscript 2 represent the second mass. Let T, e, and q represent the temperature, the vapor pressure, and the specific humidity in the air after complete mixing at constant pressure. The following formulae then hold:

(1)
$$q = \frac{M_1 q_1 + M_2 q_2}{M_1 + M_2}$$

(2)
$$e = \frac{M_1 e_1 + M_2 e_2}{M_1 + M_2}$$

(3)
$$T = \frac{M_1 T_1 + M_2 T_2}{M_1 + M_2}$$

On account of the variation in specific heat with the moisture content, the last formula is not exact, but it holds with a satisfactory accuracy for all practical purposes.

Let A and B in Fig. 54 represent two parcels of air. As both points fall to the right of the saturation line, it follows that neither of them is saturated. If the two parcels were completely mixed into one another, the conditions of the mixture would be represented by a point C on the straight line AB, C indicating the common center of gravity of the two parcels. As the saturation water-vapor pressure is not a linear function of the air temperature, it follows that the mixture of two nonsaturated parcels may be saturated or supersaturated. In the latter case, the superfluous water vapor will be condensed as a fog or a cloud. From this, it has been concluded that mixing is a frequent cause of formation of clouds and fogs. This conclusion, however, requires a more definite proof inasmuch as the order of magnitudes of temperature and humidity differences between adjacent air masses are concerned and it is also necessary to consider the effect of vertical mixing.

In order to show more accurately the maximum amounts of super-
fluous water that may result from complete mixing, we assume that
$M_1 = M_2$, so that $T = \frac{1}{2}(T_1 + T_2)$ and $e = \frac{1}{2}(e_1 + e_2)$.   We let sub-
script 1 indicate the warmer mass and R_1 denote the relative humidity
corresponding with T_1 and e_1, and R_2 the relative humidity corresponding
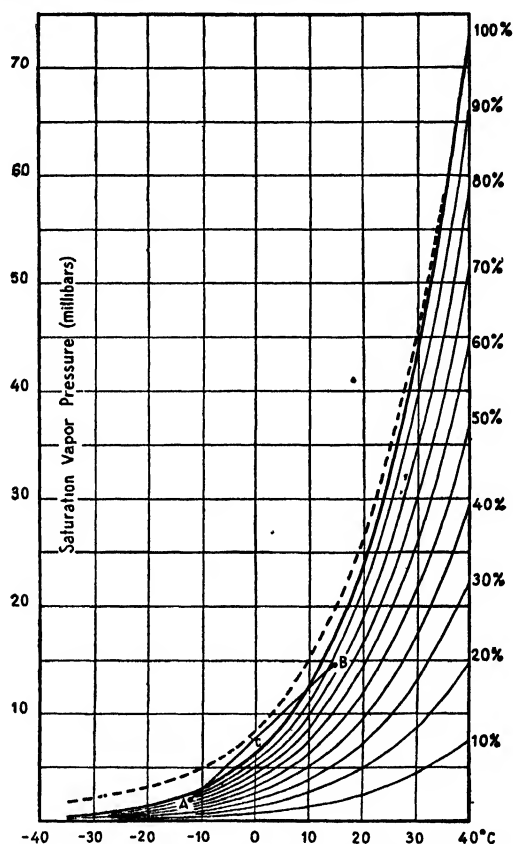

FIG. 54.—Relation between the water-vapor pressure and air temperature for standard
values of relative humidity.   The heavy curve represents saturation. . The broken curve
indicates the supersaturation which corresponds to saturated air plus 0.5 grams liquid water
per cubic meter of air.

with T_2 and e_2.   Table 5 then shows the resulting relative humidity or,
in the case of supersaturation, the amount of superfluous water expressed
in grams per cubic meter.

It is known that the content of liquid water in clouds and fogs may
vary from 0.1 to 5.0 grams/cu. m.   The horizontal distances between
the saturation curve and the broken curve in Fig. 54 represent the cooling
which saturated air must undergo in order to cause so much supersatura-
tion that the superfluous water amounts to 0.5 grams/cu. m.   If this

water were condensed, a fog or a cloud of slight density would result. It is readily seen from Fig. 54 that the temperature differences which normally occur between adjacent air masses are altogether insufficient for mixing to produce enough condensation that 0.5 gram of liquid water per cubic meter results.

TABLE 5.—RELATIVE HUMIDITY OR AMOUNT OF SUPERFLUOUS WATER RESULTING FROM COMPLETE HORIZONTAL MIXING

$T_1 - T_2$	R_2 / R_1	$T = -20°C.$			$T = 0°C.$			$T = 20°C.$		
		100%	95%	90%	100%	95%	90%	100%	95%	90%
2°C.	100%	*0.00*	98.1	95.7	*0.01*	98.0	95.6	*0.03*	97.8	95.5
	95%	97.5	95.3	93.0	97.6	95.3	92 9	97.5	95.2	92.8
	90%	94.7	92.6	90.3	94.9	92.6	90.3	95.3	92.5	90.1
4°C.	100%	*0.01*	99.3	97.2	*0.05*	98.8	96.6	*0.12*	98.5	96.3
	95%	98.4	96.3	94.2	98.1	95.9	93.8	97.8	95.6	93.4
	90%	95.4	93.3	•91.2	95.2	93.0	90.9	95.0	92.8	90.6
6°C.	100%	*0.03*	*0.01*	99.2	*0.10*	*0.01*	98.1	*0.26*	99.9	97.8
	95%	99.8	97.9	96.0	99.0	97.0	95.0	98.5	96.9	94.8
	90%	96.6	94.7	92.8	95.9	93.9	91.9	95.5	93 9	91.8
8°C.	100%	*0.06*	*0.04*	*0.02*	*0.18*	*0.09*	*0.00*	*0.46*	*0.13*	98.8
	95%	*0.02*	*0.00*	98.4	*0.02*	98.6	96.8	99.5	97.5	95.5
	90%	98.4	96.4	94.9	97.1	95.3	93.4	96.3	94.4	92.4

It will be seen from Table 5 and Fig. 54 that mixing at high temperatures will result in condensation only when both components are close to saturation. This condition is due to the small curvature of the saturation curve (Fig. 54). Furthermore, other conditions being equal, the amount of superfluous water increases with increasing temperature T, because of the mutual convergence of the saturation curve and the supersaturation curve. The conditions most favorable for supersaturation are when the warmest component has the highest relative humidity. At low temperature, the coldest component may be relatively dry; this condition is due to the convergence with decreasing temperatures of the relative humidity curves in Fig. 54.

The table shows that the amount of superfluous water is very small even under the most favorable conditions. It is important to note that Table 5 has been computed on the assumption that there is a perfect discontinuity between the two components. If there is a linear transition between them, the computed values of superfluous water would have to be reduced by about 50 per cent. Moreover, when the superfluous water condenses, the latent heat is liberated and the air temperature is

raised accordingly, and this reduces the amount of condensed water. It has been shown by Petterssen [53] that horizontal mixing is incapable of producing a cloud or a fog but that under favorable conditions it may produce a mist.

It is readily seen that the wet-bulb temperature and the pseudo-wet-bulb temperature do not mix according to Eq. (3). On the other hand, the equivalent temperature and the pseudo-equivalent temperature, which by definition are the temperatures of perfectly dry air, mix according to Eq. (3). From the relations that exist between T_w and T_e and between T_{sw} and T_{se}, T_w and T_{sw} of the mixture can be obtained from T_e and T_{se} computed from formula (3).

49. Vertical Mixing.—In this case, the pressure is not constant on the individual air particles, and it is necessary to consider adiabatic changes. The flux of heat in nonsaturated air across a horizontal unit area per unit time is expressed by [1]

$$(1) \qquad\qquad F_1 = -K_1 c_p \rho (\gamma_d - \gamma)$$

Here, K_1 is the coefficient of eddy transfer of heat, and ρ is density. If the air were saturated, γ_m should be substituted for γ_d.

When $\gamma_d > \gamma$, heat is transported downward; and when $\gamma_d < \gamma$, heat is transported upward by the eddies. If no heat is supplied to, or withdrawn from, the air from some external source and if no condensation takes place, the mean temperature of the air column will remain constant throughout the process. The same is true of the mean potential temperature of the column. The flux of heat along the vertical would continue until an adiabatic lapse rate is established. The final result of vertical mixing in nonsaturated air would then be characterized by

$$(2) \qquad\qquad \gamma = \gamma_d \qquad \text{or} \qquad \frac{\partial \theta}{\partial z} = 0$$

and the mean temperature and the mean potential temperature of the air column unchanged.

The eddy flux of specific humidity along the vertical is expressed by

$$(3) \qquad\qquad F_2 = -K_2 \frac{\partial q}{\partial z}$$

where K_2 denotes the coefficient of eddy transfer of specific humidity. It will be seen that moisture is transported upward when $(\partial q / \partial z) < 0$ and downward when $(\partial q / \partial z) > 0$. If no moisture is supplied to, or withdrawn from, the air and if condensation does not occur, the mean specific humidity of the air column will remain unchanged throughout

[1] See, for example, BRUNT [19].

the process. The final result of vertical mixing will then be characterized by

(4) $$\frac{\partial q}{\partial z} = 0$$

The final result of vertical mixing being characterized by Eqs. (2) and (4), it follows from Pars. 15 and 16 that the following is true of an air column that is completely stirred:

(5) $$\frac{\partial \theta_{sw}}{\partial z} = 0 \quad \text{and} \quad \frac{\partial \theta_{se}}{\partial z} = 0$$

This indicates that vertical mixing destroys convective stability and convective instability (see Par. 46) and produces a convectively indifferent state.   It should be noted that, whereas Eqs. (2) and (4) hold only when condensation does not occur, Eq. (5) holds in any case.

Under normal conditions, the air is stably stratified, and the specific humidity decreases along the vertical.   Vertical mixing will then transport heat downward from the top of the mixed layer and moisture upward to the air that is cooled by mixing.   It is readily seen that this may result in the condensation of water vapor.   It is, however, important to note that vertical mixing can cause condensation only in the upper portion of the mixed layer.   The lowest level at which condensation may occur as a result of vertical mixing is called the *mixing condensation level*.   The height of this level above the ground may be determined from the foregoing conditions, which indicate the final state in the following manner: (1) Find the temperature of the air column after complete mixing, and mark the dry-adiabatic that corresponds thereto.   (2) Find next the pseudo-wet-bulb temperature of the air column after complete mixing, and mark the moist-adiabatic that corresponds thereto.   (3) The intersection point of these adiabatic lines indicates the mixing condensation level.   It should be noted that the mixing condensation level can be defined only when the thickness of the mixed layer is known, and then it can be determined only on the assumption that the layer is completely stirred.   As complete stirring (*i.e.*, $F_1 = 0$ and $F_2 = 0$) occurs rarely, the actual cloud base is usually higher than the mixing condensation level determined as described above.

That vertical mixing of nonsaturated air does not cause condensation at the base of the mixed layer is readily verified by plotting the initial values of T and q on a thermodynamic diagram and applying the conditions that characterize the final state.'   It will then be seen that the conditions which are most favorable for condensation in the mixed layer are characterized by: $\gamma < 0$, and $(\partial q/\partial z) > 0$.   But, even then, the air

at the base of the layer remains nonsaturated for such inversions of temperature and humidity as occur in the atmosphere.

Figure 55 shows a typical example of the result of vertical mixing in a limited layer of air that is originally stably stratified and nonsaturated. It will be seen that the relative humidity in the lower portion of the layer has decreased during the process of mixing. It will also be seen that the mixing condensation level ($R = 100$ per cent) varies with the thickness of the stirred layer. Thus, when the layer between 1000 and 950 mb. is completely stirred, condensation occurs only in a very thin layer. If the mixed layer is shallower than that indicated by the lower right curve (1000 to 970 mb.), condensation does not result.
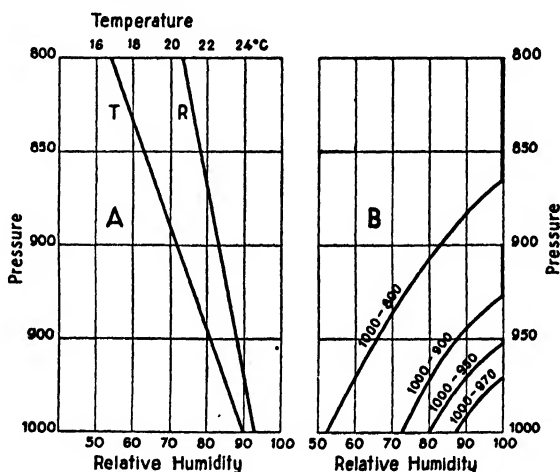

Fig. 55.—A, the initial state: T, air temperature; R, relative humidity. B, vertical distribution of relative humidity after complete stirring. The uppermost curve indicates the distribution of relative humidity when the entire layer between 1000 mb. and 800 mb. is completely stirred; the next curve shows the result when the layer between 1000 mb. and 900 mb. is stirred, etc.

Vertical mixing is a frequent cause of the formation of a stratus, either in nonsaturated air or from a fog that is dissipated. In such cases, there is usually a preexisting inversion at some distance above the ground. The mixing condensation level may then be computed on the assumption that the entire layer under the inversion becomes mixed.

50. Radiation.—The direct radiation of the sun is absorbed only to a slight extent in the atmosphere because the air is almost transparent to high-temperature radiation (short waves). About 43 per cent of the incoming radiation is reflected back to space, about 40 per cent is absorbed by the earth's surface, and the remaining 17 per cent is absorbed by the atmosphere. This means that only 57 per cent of the solar radiation is thermally effective. The reflective power of the earth (the albedo), which on the average is 43 per cent, varies within wide limits. Thus,

clouds and snow-covered ground may reflect up to 80 per cent of the radiation, and a water surface may reflect most of the incoming radiation, except when the sun is high in the sky.

The thermally effective 57 per cent of the incoming radiation must be reemitted by the earth and the atmosphere. The earth radiates as a black body according to the temperature of its surface (long waves). Part of this radiation is absorbed by the clouds, and a considerable portion is absorbed selectively by the aqueous vapor, which again radiate selectively. Part of the absorbed terrestrial radiation is radiated back to the earth. This "counterradiation," which protects the earth's surface from excessive cooling in the night, depends on the temperature, the water vapor content,[1] cloudiness, and other factors; but even on clear nights it may amount to about 75 per cent of the outgoing radiation. For this reason, it has been customary to compare the effect of the atmosphere on the temperature of the earth's surface to that of the glass in a greenhouse; but the conditions are in reality not so simple. The various motions in the atmosphere transport heat from one place to another. Thus, under normal conditions (see Par. 62) the eddy transfer of heat is about one hundred times as large as the radiative transfer which, again, is about ten thousand times as large as the molecular conduction of heat. In addition, heat is transported effectively by the large-scale air currents. Nevertheless, as has been shown by Emden [25] and others, the so-called greenhouse effect is considerable: it has a minimum at the equator and a maximum in high latitudes in winter.

51. Diurnal Heating and Cooling of Air over Land.—The amount of radiation absorbed by the earth after sunrise, depends on its color or its albedo. The portion that is absorbed is partly used to evaporate water and partly expended in chemical processes, but the major part goes to heat the earth. The heat thus absorbed is accumulated in the upper few centimeters of the earth, owing to the very slow conduction of heat in the earth. The air that comes into contact with the earth becomes heated, and the lapse rate in the very lowest layer of air increases rapidly. When the lapse rate surpasses the dry-adiabatic, the layer becomes unstable, and vertical currents are set up which carry heat and moisture, picked up from the surface, to higher levels. As the sun gets higher in the sky, the heating increases, and the unstable layer of air increases in thickness, the heat obtained from the surface being transported to higher and higher levels. The diurnal heating of the earth's surface results in a steep lapse rate and in stirring of the lower atmosphere.

As the temperature of the earth's surface increases, the outgoing radiation increases too; and, some two hours after the sun has reached

---

[1] See Brunt [19].

its maximum altitude, there is balance between the loss and gain of heat. The temperature of the earth reaches its maximum and begins to decrease. The cooling of the earth's surface affects the air temperature, and, as before, the influence is greatest near the surface, with the result that the air cools more quickly along the earth than above. The temperature lapse rate decreases, and the air becomes stable again. Figure 56 shows three typical temperature-height curves illustrating the diurnal variation of temperature in the lower atmosphere.

It is worthy of note that the midday temperature on sunny summer days is higher over macadam and sandy fields than over grassland, is lower over wet grounds and woods, and is still lower over water. These differences in temperature give impulses of considerable intensity to convective currents. Local currents of this kind are the main cause of the "bumpiness" experienced by pilots above level ground on warm days.

52. Diurnal Heating and Cooling of Air over Oceans.—It is important to note that the absorption of solar radiation by the sea surface does not appreciably affect its temperature. This condition is due to a variety of causes. If the sun is not overhead, or nearly so, the greater part of the incoming radiation is reflected from the surface of the sea and is lost as far as heating of the sea or the lower

Fig. 56.—Illustrating the diurnal variation in stability over land. *A*, early morning; *B*, midday; *C*, evening; broken line, dry-adiabatic. The arrows indicate the direction of the eddy flux of heat.

atmosphere is concerned. If the sun is near the zenith, the amount reflected by the sea is small; but, in this case, the radiation penetrates to a considerable depth before it is completely absorbed. Since the specific heat of sea water is very large, the effect of radiation on the temperature will be small, the heating being spread over a deep layer of water. Other effects help to reduce the diurnal temperature change in the sea surface. Part of the heat gained by the sea is used to evaporate water. Through evaporation, the salinity of the surface layer increases; it becomes denser than the water underneath and so sinks, to be replaced by colder water from beneath.

The outgoing radiation at night cools the sea surface. But when the top layer cools, it becomes denser and sinks, to be replaced by warmer and lighter water from underneath. Thus, both by day and night, the sea surface keeps a fairly constant temperature. The air that is in contact with the sea adapts its temperature to that of the sea surface.
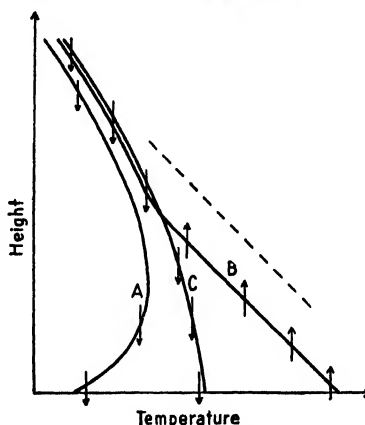
Observations show that the diurnal range of temperature at the sea surface is less than 0.5°C.

The regulating influence of the sea surface on the air temperature decreases with elevation. A few hundred meters above the sea, the temperature variation is controlled mainly by radiation, and the air has a diurnal variation in temperature that is greater than the variation at the surface of the sea. At still greater altitudes, the effect of radiation decreases on account of lack of absorbing substance (aqueous vapor), and the temperature remains almost constant day and night.

Figure 57 shows two characteristic temperature-height curves over sea. It is readily seen that the lower part of the atmosphere has a tendency to be stable by day and unstable by night. At greater heights, the reverse is true.
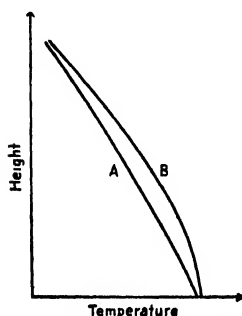

Fig. 57.—Illustrating the diurnal variation in stability over oceans *A*, night; *B*, midday.

The diurnal variation of stability and instability in the lower atmosphere over oceans is in sharp contrast to the conditions prevailing over land, and this has marked influence on the weather. Over land, all instability phenomena have a maximum frequency and intensity in the afternoon, whereas over oceans the diurnal variation is slight and the maximum frequently occurs at night.

53. Heating and Cooling of Traveling Air Masses.—An air mass that travels toward warmer regions will be heated from below; and if there is no other process in operation (such as subsidence or advection of warmer air aloft), it will develop instability. The heat and moisture absorbed from the underlying surface will then be carried to higher and higher levels. The changes in such an air mass are completely analogous to those occurring in air over land that is heated by sunshine on the earth's surface.

If such an air mass travels over land, it will have the effect of the diurnal heating and cooling superimposed on the effect originating from its movement toward warmer regions. The instability will then vary during the day, having a maximum in the afternoon and a minimum in the early morning. If the difference in temperature between the surface and the air is large, the air will remain unstable by day and night. If the difference is small, the air may become stable during the night. Referring back to Par. 24, it is of interest to note that pronounced diurnal variation of convective clouds is indicative of slight instability, whereas, other conditions being equal, a slight diurnal variation in convective clouds indicates pronounced instability.

Over the ocean, the conditions are different inasmuch as the diurnal variation in stability is slight. The development of instability over the

ocean is, therefore, mainly a result of the travel of the air toward warmer regions.

It was shown in Pars. 41 and 49 that the effect of convection and vertical mixing is to establish a dry-adiabatic lapse rate below the condensation level and a moist-adiabatic lapse rate above it. The heat (and moisture) absorbed from the underlying surface is then readily carried up to great heights, and a difference in temperature between the underlying surface and the air is maintained.

When air travels toward colder regions, it will be cooled from below and, unless other processes are in operation, will develop increasing stability in the lower layers. The increased stability diminishes the turbulence and prevents convective currents, so that the exchange of heat and moisture along the vertical decreases. The cooling effect of the underlying surface then affects mainly the friction layer, while the air above has a tendency to preserve its original temperature, except for the downward eddy flux of heat, which is small on account of the diminished turbulence. As the cooling mainly affects a shallow layer, it follows that the air temperature near the surface will adapt itself quickly to the temperature of the underlying surface. By continued cooling from below, isothermal

FIG. 58.—Types of temperature-height curves in traveling air masses. A, initial curve; B, after travel over a warmer ocean; C, after travel over a warmer continent; c, condensation level; D, after travel over a colder surface, slight wind velocity (slight turbulence); E, after travel over a colder surface, high wind velocity (strong turbulence).

conditions or temperature inversions may develop near the surface of the earth. As the intensity of the turbulence is roughly proportional to the wind velocity, it is readily seen that, when the wind velocity is slight, the result of continued cooling from below will be a minimum air temperature at the surface and higher temperature above, whereas, when the wind velocity is high, the mixing will cause sufficient exchange of heat within the friction layer to establish a normal lapse rate of temperature in the friction layer. A few principal types of development are illustrated in Fig. 58. It is worthy of note that the development from A to B results in numerous convective clouds and a low condensation level, whereas the development from A to C results in a smaller number of convective clouds at a considerably higher level. The development from A to D usually results in formation of fog, whereas the development from A to E results in formation of stratus or stratocumulus below the base of the inversion.
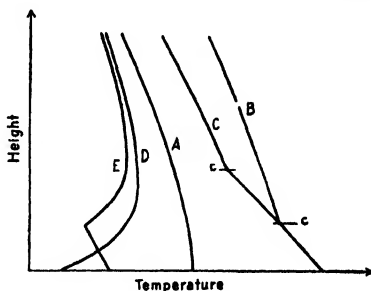
54. Inversions.—The air temperature normally decreases with elevation. Under special conditions, a reversal of the lapse rate may develop, showing a layer in which the temperature increases upward. This is called an inversion.

The essential feature of an inversion is a pronounced stability of the air in the inversion layer. A well-developed inversion acts as a lid through which no convection and only slight turbulent mixing can take place, for all upward or downward impulses are effectively suppressed by the excessive stability of the layer.

It was explained in the previous paragraph that a ground inversion may form on account of cooling of the air by the underlying surface. The cooling may be due to outgoing radiation from the surface or to advection of warmer air over a colder surface. If there is sufficient turbulent mixing in the ground layer, the inversion will not be found at the surface but at some distance above, as was shown in Fig. 58. Such inversions are present at low altitudes in most air masses that are cooled from below.

Inversions may form, and existing inversions may be substantially intensified, when subsidence develops in the free atmosphere. If the air above the inversion were originally stably stratified, the surfaces of constant potential temperature would be brought downward and accumulated in the inversion layer above which horizontal divergence balances the decrease in vertical velocity as the inversion layer is approached. Above the level where the downward velocity has a maximum, horizontal convergence must develop in order to establish continuity. It then follows from Par. 45 that a relatively steep lapse rate is maintained in the upper portion of the subsiding air while a slight, or even reversed, lapse rate is produced in the lower portion of the subsiding air.

The relative humidity decreases in proportion to the adiabatic heating, so that the subsiding air is recognized by its extreme dryness. Inversion layers formed through subsidence rarely come down to the earth's surface, as do those which are caused by cooling along the earth's surface. Moreover, the air above the latter type of inversion is not particularly dry.

It is typical of all inversions that the relative humidity is high under the inversion layer. If the inversion is produced by cooling only, the relative humidity would increase in the cooled air, but the specific-humidity temperature would not show any discontinuity in the inversion layer. If the inversion is caused by subsidence only, the flux of specifically dry air from aloft would tend to create a discontinuity in the specific humidity and the potential pseudo-wet-bulb temperature. If there is sufficient turbulent mixing in the air below the inversion, moisture would be steadily brought up from the surface to the base of the inversion layer.

In such cases, pronounced contrasts in specific humidity and potential pseudo-wet-bulb temperature are observed at the inversion layer.

From the foregoing, it follows that the type of inversion and the processes in operation may be recognized from the vertical distribution of temperature and humidity.   Figure 59 shows the principal types of inversion.

It is worthy of note that the inversions with dry air aloft may be convectively unstable, notwithstanding their pronounced stability (see Par. 46).   It should also be noted that the inversions are, from a dynamic
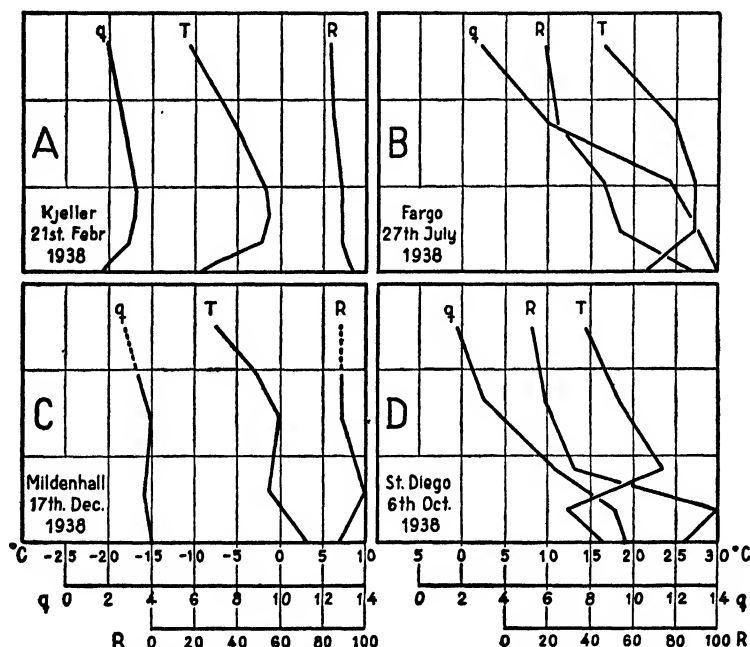

FIG. 59.—Types of inversions.   *A*, inversion produced by cooling from below; *B*, inversion produced by subsidence aloft and cooling from below; *C*, inversion produced mainly by cooling and turbulent mixing; *D*, inversion produced by subsidence aloft and heating and turbulent mixing below.

point of view, essentially different from fronts.   This condition is due to the difference in slope.   Inversions are mainly horizontal, whereas fronts are inclined discontinuities.   Bergeron [1] has shown that the number of isobaric-isosteric solenoids contained in a frontal surface is normally one hundred times larger than the number of such solenoids contained in an inversion layer.   The temperature contrasts in an inversion layer are, therefore, not available for production of kinetic energy.

55. Forecasting of Convective Phenomena.—In order to demonstrate the application of the principles discussed in previous paragraphs, we shall now analyze a few typical cases by means of actual observations.

It is well to remember that the ascents under discussion are made in the early morning (mostly at 5 A.M.) so that it is necessary to consider the changes which are likely to occur on account of the diurnal heating. It should also be borne in mind that it is, in general, not possible to predict convective phenomena unless a series of analyzed weather maps is at hand. In this paragraph, we shall discuss only some typical cases and draw such conclusions as are permissible without consulting the weather maps.
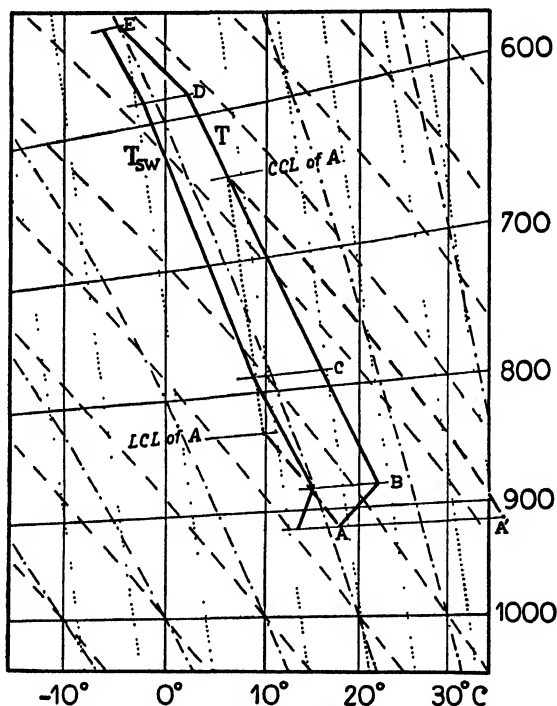

FIG. 60.—Example of conditional instability of stable type. For symbols see Fig. 28.

It will be understood that ascent curves which show either absolute instability or absolute stability without convective instability (see Par. 46) throughout the atmosphere do not present any difficulties; for, in the former case, convective clouds and showers are bound to form, and, in the latter case, such phenomena cannot form. Here, therefore, we shall discuss only the more difficult cases in which there is either conditional instability in one or more layers, or absolute stability together with convective instability.

CASE 1.—Figure 60 shows the ascent curve for Cheyenne, July 25, 1935, and the corresponding distribution of pseudo-wet-bulb temperature. The ascent was made in the early morning. Except for the

ground layer, it will be seen that the lapse rate is greater than the moist-adiabatic: the air is conditionally unstable (see Par. 34). Nevertheless, as none of the moist-adiabatics running through the points representing the pseudo-wet-bulb temperatures intersect the ascent curve, it follows from Par. 34 that the stratification is stable: it consumes the kinetic energy of all impulses.

Table 6 shows the result of the analysis of the ascent curve. It will be seen that the air is convectively stable except in the layer BC where

TABLE 6.*—CHEYENNE, JULY 25, 1935

Point	p	T	R	q	T_{sw}	θ_{sw}	ΔT
A	915	18	65	9.1	13.5	17.5	18.5
B	880	22	47	8.9	15.0	20.0	11.0
C	787	16	42	6.1	8.7	18.5	7.0
D	586	2	52	3.9	−2.2	19.5	—
E	535	−5	72	3.8	−6.4	19.5	—

* ΔT indicates the amount of heating necessary to start convection from the ground up to the convection condensation level.

the wet-bulb potential temperature decreases slightly along the vertical. If the air column were lifted as a whole, this layer would become unstable; but, in that case, the air column would have to be lifted 1500 m. or more. Whether or not such lifting, in the present instance, is probable can be decided only by studying the weather chart. However, if the convective instability were released through lifting, the layer BC would have stably stratified air below it as well as above it. The convective clouds would then be embedded in a shallow layer of air.

It remains now to discuss what would result if the air column were heated from below. The analysis of the ascent curve then shows that the convection condensation level is found at about the 635-mb. surface (i.e., about 2600 m. above station level); thus, the air at the surface would have to be heated about 19°C. during the day, which is improbable, particularly since considerable heating is also necessary at the levels B and C in order to start convective currents up to the convection condensation level.

Summarizing, we may say that the air is stably stratified in spite of γ being greater than γ_m. Furthermore, heat convection is highly improbable on account of the large amount of heating that is necessary to start the convection. As the convection condensation level is very high and the air is relatively dry, mixing between the ascending and the descending currents would counteract the cloud formation even if the air were heated so much that convection started. If the air column were lifted as a whole, convective clouds could form only in a shallow layer in

mid-air.   We may, therefore, conclude that the sky will remain cloudless unless the air were lifted sufficiently by a front, in which case a shallow layer of convective clouds might develop.

CASE 2.—Figure 61 shows the ascent curve for Omaha, July 26, 1935, and the corresponding distribution of pseudo-wet-bulb temperature. The ascent was made in the early morning (about 5 A.M.) when a shallow inversion was present near the ground.   Another inversion is present above the 820-mb. level.   The result of the analysis of this curve is given
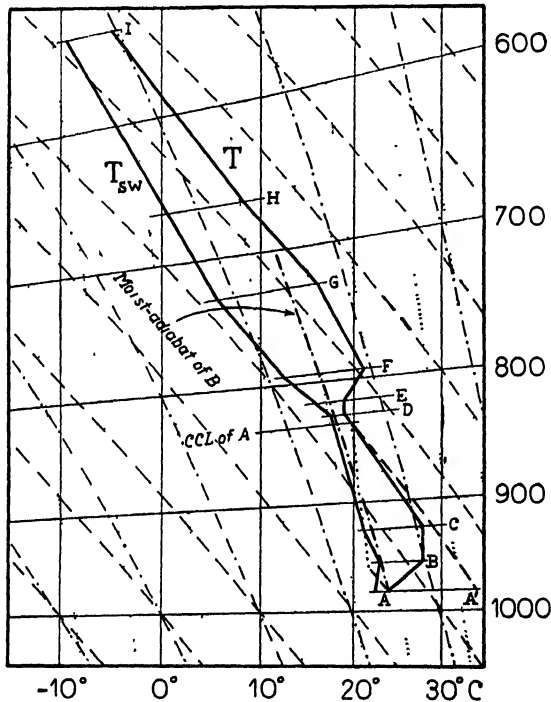

FIG. 61.—Example of convectively unstable inversion.   For symbols see Fig. 28.

in Table 7.   At the moment of observation, there is conditional instability between C and D, and also above F, the remaining layers being highly stable.   It will be seen that the air is convectively unstable above B, and the convective stability below B will be nullified by diurnal heating.   It is of interest to note that the inversion above D is convectively unstable (see Par. 46) so that, if the whole air column were lifted some hundred meters, the inversion would disappear, and the air in the inversion would become unstable.   This condition is due to the circumstance that the point D would soon become saturated whereas the point F would move for a long time along the dry-adiabatic and thus cool more rapidly than the point D.   Thus, it is seen that if the air were

lifted (*e.g.*, by a front) the entire mass might become unstable. The convective clouds would then not meet with any hindrance below the level where ice crystals could form; precipitation would then result.

TABLE 7.—OMAHA, JULY 26, 1935*

Point	p	T	R	q	T_{sw}	θ_{sw}	ΔT
A	980	24	90	17.1	22 5	23.5	10
B	955	28	66	16.5	23.0	24.5	4
C	923	28	57	14 8	21.0	24.0	1
D	825	19	86	14 6	17.5	24.0	—
E	815	19	76	12.9	16 0	23.5	—
F	793	21	40	8 0	12.5	21.5	—
G	727	16	26	4 2	5.5	18.5	—
H	662	8	31	3.4	0.5	18.0	—
J	540	−5	36	1.8	−9.5	17.0	—

* See footnote to Table 6.

Let us next consider the chances of heat convection producing convective clouds. The convection condensation level of the surface air is at point D, and the amount of heating that is necessary to start convection to this level is small (see ΔT in Table 7) considering the locality and the season and also that it is only a shallow layer that need be heated. If the air did not pick up moisture from the underlying surface, convective clouds could barely form at the level D, and they would have a stable layer of air above them. As the air is likely to absorb some moisture from the surface and as $(\partial q/\partial z) < 0$, there would be a flux of q upward to the base of the inversion; the result would then be that condensation could occur at a level somewhat lower than D. The clouds that form would then be exceedingly flat cumuli, of the cumulo-stratus type. They would perhaps also be sparse.

The next point to consider is whether or not the heating from below is likely to destroy the inversion above D. In that case, the convective clouds would build up into the layer above F, where the stratification then would be selectively unstable. It is readily seen from Fig. 61 that this could happen only if the surface air were heated from 24 to 40°C., and a heating of about 7°C. would be necessary in the deep layer between C and D. Summing up, we may say that heat convection would produce nothing more than cumulo-stratus or very flat cumulus humilis. However, if an advancing front lifted the entire air column, towering cumulus or cumulo-nimbus could result. Whether or not this latter development is likely to occur can be decided only from an analysis of the weather charts.

CASE 3.—Figure 62 shows the ascent curve of Murfreesboro, July 12, 1935. The ascent was made in the early morning so that an inversion

is recorded at the earth's surface. The result of the analysis of the ascent curve is shown in Table 8.

TABLE 8.—MURFREESBORO, JULY 12, 1935*

Level	p	T	R	q	T_{sw}	θ_{sw}	ΔT
A	993	23	90	15.8	21.6	22	7.5
B	970	27	62	14.2	21.5	23	2.0
C	882	20	79	13.2	17.5	22	1.0
D	815	15	58	7.6	10.0	19	—
E	756	10	71	7.1	7.0	18.5	—
F	735	8	79	7.9	6.0	18	—
G	684	5	63	4.9	1.0	17	—
H	670	4	75	5.6	1.5	18	—
I	637	2	57	3.9	−2.0	17	—
J	594	2	28	2.1	−5.5	17	—

* See footnote to Table 6.

It will be seen from Fig. 62 that the air is conditionally unstable between the levels B and H. The highest potential pseudo-wet-bulb temperature is observed at B. The moist-adiabatic through this point intersects the ascent curve at about D. It follows then from Par. 33 and Fig. 37 that the energy which can be released is considerable. The temperature at A is not representative. This point shows a large resistance against lifting, but this resistance will vanish on account of the diurnal heating of the surface air. The point B, which is representative, shows only a slight amount of resistance against lifting. It follows then that the available energy (the positive area minus the negative area) is considerable: the stratification belongs to the type called *real latent instability* (see Par. 34).

It is of interest to remark that, as the surface layer is heated during the day, the pseudo-wet-bulb temperature near the surface will increase, and so will also the positive area; simultaneously, the negative area decreases and may vanish altogether. It was shown in Par. 38 that the parcel method gives too large an amount of available energy when the air is conditionally unstable; but as the positive area increases while the negative area decreases as the air is heated from below, the error introduced by this method will not be significant. The ascent curve thus shows that convection of considerable intensity is possible. We shall, therefore, discuss in greater detail the various ways in which convection may be started.

1. *Lifting of the Entire Air Column.*—It will be seen from Table 8 that θ_{sw} decreases along the vertical between the levels B and G. The air is, therefore, convectively unstable. As T_{sw} will increase with the diurnal heating, the convective instability will also increase. If the air

is lifted, either along a frontal surface or along a mountain range, or
because of horizontal convergence near the earth's surface (see Chap. IV),
the air column below G will become absolutely unstable provided that it
is lifted to its saturation level. As the relative humidity varies along
the vertical in an irregular manner, the convective clouds thus produced
would probably occur at different levels. The convective instability
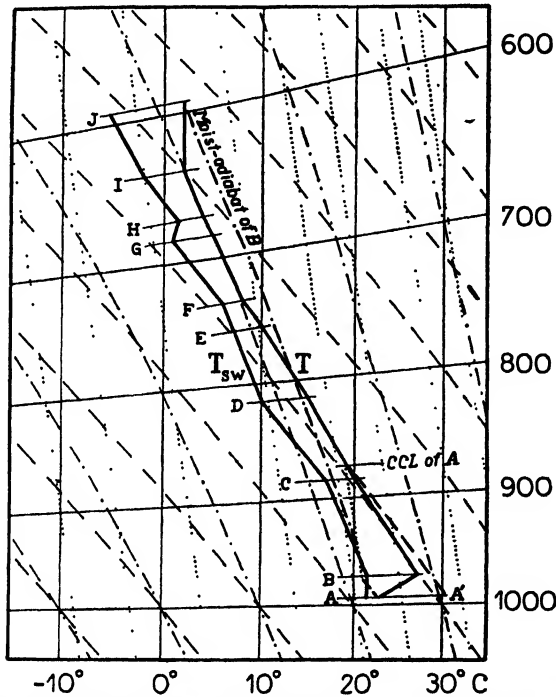is, however, slight; and it is not likely that violent convection would

FIG. 62.—Example of conditional instability of real latent type together with convective
instability. For symbols see Fig. 28.

result. Whether or not such lifting of the whole air column is likely
to occur can be decided only by studying the weather maps.

2. *Heat Convection.*—The convection condensation level of the surface
air is shown in Fig. 62, and the amount of heating necessary to start
convection up to the condensation level is indicated by ΔT in Table 8.
As the air is likely to absorb moisture from the surface while it is being
heated, it follows that the convection condensation level will be some-
what lower than shown in Fig. 62 and that the amount of heating will
be less than that indicated by ΔT. Considering the locality and the time
of the year, there can be little doubt that convection will start to the
convection condensation level. Above this level, γ is closer to γ_d than
to γ_m. From this it follows (see Par. 36) that $(\beta/\alpha) > 1$. It will then

be seen from Fig. 41 that the amount of energy to be released by convection is very great and, furthermore, that the convective clouds may occupy a considerable portion of the sky. The conditions are, therefore, highly favorable for convective clouds to form.

The next point to consider is to what height in the atmosphere the convective clouds will reach. It will then be seen from Fig. 62 that the ratio $\beta/\alpha = 0$ in the layer between F and I, above which isothermal conditions prevail. Above F, then, convective energy would be con-

Fig. 63.—Example of rapid increase in instability due to diurnal heating. For symbols see
Fig. 28.

sumed. It was shown in Par. 41 that the convective currents have a tendency to build up the adiabatic lapse rate in the air above the convective layer. Eventually, the convective clouds may reach considerably above the level F. But it is highly improbable that they would grow beyond the level I where the air is highly stable. It will be seen from Fig. 41 that the consumption of kinetic energy is very great when $\beta < 0$ and $\alpha > 0$ (in the layer above I, $\beta/\alpha = -\frac{1}{3}$ approximately). From this it follows that the convective clouds are not likely to grow above the zero isothermal level; the clouds will, therefore, remain water clouds, and no cumulo-nimbus (with ice crystals in their tops) will form. Precipitation is therefore unlikely.[1]

[1] For exceptions, see Par. 25.

The convective clouds that would form in the present case on account of heating from below would be of the cumulus congestus type. Their base would be somewhere between the 850- and the 900-mb. level. As the selective instability decreases upward, it follows from Par. 42 that only narrow towers could build up into the layer above F; but, below this level, considerable cloud masses might develop.

In the discussion above, we have not taken into account such factors as advection of air aloft and subsidence. These factors, which may modify the conclusions, could be studied only by means of weather charts and pilot-balloon observations.

CASE 4.—Figure 63 shows the ascent curve of Murfreesboro, July 24, 1935; and Table 9 shows the result of the analysis. Again, there is a night inversion at the ground which makes the temperature in the surface air nonrepresentative. Applying the parcel method, it will be seen that the point A has a very large negative area and a very small positive area. The point B, which is representative, shows a very small

TABLE 9.—MURFREESBORO, JULY 24, 1935*

Level	p	T	R	q	T'_{sw}	θ_{sw}	ΔT
A	994	23	91	16.0	21.5	22.0	7.5
B	950	26	56	12.3	19 5	21.5	1.0
C	808	14	90 ·	11 2	13.0	21.0	
D	775	13	74	9.0	10 0	20.0	
E	708	7	92	8 2	6.5	20.0	
· F	682	7	63	5.8	3 0	19.0	
G	668	6	52	4 6	1 5	18.0	
H	647	4	74	5.8	1.5	19.0	
I	537	−5	60	3.0	−7.6	18.0	

* See footnote to Table 6.

negative area below the 720-mb. level, above which there is a slight positive area. The positive and the negative areas balance one another, and from this one might conclude that no energy could be obtained from the stratification. It is, however, easily seen that the chances for violent convection are considerable.

1. The air is convectively unstable up to the level G. If the air column were lifted as described above, convection would result.

2. If the air near the earth's surface is heated as much as indicated by ΔT in Table 9, convection would develop from the surface up to the condensation level (the 870-mb. level). As the ascent was made in the early morning, a greater increase in temperature must be expected. Moreover, as the air also picks up moisture from the surface, convection would start before the air was heated as much as indicated by ΔT. As the air arrives at the convection condensation level, it begins to ascend

along the moist-adiabatic of A' shown in Fig. 63. It is then readily seen that the air is highly unstable, and considerable amounts of kinetic energy will be released. As the air ascends along the moist-adiabatic, it will be warmer than the surrounding air even when passing the shallow layers *CD* and *EF*, and it would be accelerated further into layers above the zero-isothermal level. The initial clouds would be of the cumulus congestus type; but, as the towers grow higher and higher, the cloud will reach into the layers where the supercooled water will freeze. The clouds will then develop into veritable cumulo-nimbus.

The outstanding difference between cases 3 and 4 is that in the former there is a stable layer of sufficient thickness to prevent the cloud from reaching the ice-crystal level, whereas, in the latter case, there is no such hindrance. Similarly, case 4 differs from case 1 in that the air in case 1 is so dry that the heating is insufficient to produce convection up to the condensation level.

CASES 5 AND 6.—Table 10 shows the observations of pressure, temperature, and relative humidity made at Norfolk, Virginia, in the early morning of July 24, 1935. The analysis of this ascent is offered as an exercise to the student. In this case, it is known that moderate heat thunderstorms occurred in the afternoon and that severe cold-front (lifting) thunderstorms occurred in the late evening. Table 11 gives another interesting case which deserves study.

Level	p	T	R
A	1017	26	89
B	950	24	91
C	907	24	84
D	825	19	83
E	740	14	73
F	660	7	89
G	635	6.5	76
H	600	2.5	86
I	565	1.5	75
J	510	−4.5	93

TABLE 10.—NORFOLK, VIRGINIA, JULY 25, 1935

Level	p	T	R
A	1017	27	85
B	1005	27	80
C	936	22	95
D	875	18	72
E	853	17	84
F	837	16	70
G	824	16	60
H	768	11	60
I	727	9	52
J	660	4	83
K	585	0	57
L	542	−2	62

TABLE 11.—PENSACOLA, JULY 23, 1935

56. Formation of Fog.[1]—The name fog is given to any cloud that envelops the observer and reduces the horizontal range of visibility to

[1] Most of the present and the following paragraphs on fog is based on a paper by Pettersen [53]. Extensive use has also been made of a paper by Taylor [83].

less than 1 km.[1] This definition is adequate at sea and over level ground, but it is inconsistent in hilly country, where the clouds may touch the hillsides without touching the lowland. In such cases, an observer in the lowland would report stratus and an observer at an elevated station would report fog. It is necessary to bear this distinction in mind both in analyzing weather charts and in predicting fogs. What we are here concerned with is to discuss the formation of such fogs as may develop in contact with the sea surface or level ground.

Nonsaturated air may become saturated in three different ways, viz.: (1) by evaporation of water into the air, (2) by mixing, and (3) by cooling. When a fog forms, it is necessary that these processes should take place at the surface of the earth. In most cases of fog formation, the three processes operate together. We shall, however, first discuss each of them separately and afterward comment on their various combinations.

1. EVAPORATION.—The evaporation of water, either from the underlying surface or from rain falling through the air, is proportional to the factor $(E - e)$, where E denotes the saturation vapor pressure corresponding to the temperature of the liquid water and e is the actual water-vapor pressure of the air. As e increases and approaches E, the evaporation decreases and approaches zero. It is convenient to consider three cases according to whether the air temperature is higher than, equal to, or lower than the temperature of the liquid water. In the following discussion, E_a denotes the saturation water-vapor pressure of the air.

a. *The Temperature of the Air Is Higher Than That of the Liquid Water.*—In this case, balance is reached when $E = e < E_a$, and the evaporation from the liquid water ceases before the air becomes saturated, because the saturation water-vapor pressure of the air is higher than the saturation pressure corresponding to the temperature of the liquid water. If evaporation takes place from a terrestrial source of water, the heat of vaporization is supplied mostly by the water, and the air temperature remains sensibly unchanged. It follows then that such evaporation will not cause condensation in the air.

If evaporation occurs from falling rain, the heat of vaporization is supplied mostly by the air, which is then cooled. Through continued evaporation, the air temperature will approach the wet-bulb temperature, which remains constant during the process. The air is then saturated with water vapor ($E \gtrless e = E_a$), and no further evaporation is possible from the falling rain. *As a fog consists not only of saturated air, but of air that contains a considerable amount of condensed water, it is evident that, when the temperature of the air is higher than that of the liquid water, a fog cannot form because of evaporation only.*

---

[1] Definition adopted by the International Meteorological Organization, 1929.

The foregoing conditions apply when the air is warmer than the underlying surface and also when rain from colder air aloft falls through the warmer air below. The latter case is the normal occurrence in the atmosphere. Thus, when the air temperature decreases along the vertical, the falling raindrops will be colder than the air through which they fall; the air will then remain nonsaturated until it has been cooled to its wet-bulb temperature, after which no further evaporation will occur.

b. The Temperature of the Air Equals That of the Liquid Water.—In this case, balance is reached when $E = e = E_a$; *i.e.*, when the air has become saturated. As above, it is evident that evaporation alone will not cause condensation to occur in the air.

c. The Temperature of the Air Is Lower than That of the Liquid Water.— In this case, water will evaporate into the air until $E = e > E_a$. If no condensation nuclei are present in the air, supersaturation will occur; but if such nuclei are present in sufficient amounts, the superfluous water will be condensed. In such cases, a fog, or a cloud, may result through evaporation only.

Here, too, we may distinguish between (i) evaporation from falling rain, and (ii) evaporation from the underlying surface.

i. When the air temperature increases along the vertical (*e.g.*, in inversion layers or along pronounced frontal surfaces), the falling raindrops may be slightly warmer than the air through which they fall. If the air is not saturated, its wet-bulb temperature will be lower than the air temperature and thus considerably lower than the temperature of the falling raindrops. Through evaporation of the falling rain, the air is cooled to its wet-bulb temperature. Condensation will then occur; and if the wet-bulb temperature of the air is sufficiently below the temperature of the falling raindrops, condensation will occur on the condensation nuclei, and the droplets thus formed may grow in number and size to such an extent that the horizontal range of visibility is reduced to 1000 m. or less. The cloud layer, from which the rain falls, then builds downward and may eventually touch the earth's surface; and hence a fog results. Such fogs may form under pronounced frontal surfaces when the temperature of the air above the frontal surface is much higher than the temperature of the air below it (*frontal fogs*). The same applies when rain from a cloud system aloft falls through a layer of cold air under a ground inversion.

What has been said above is illustrated in Fig. 64. In all four diagrams, the base of the rain cloud is at *aa*. In case *A*, the raindrops will be colder than the air below *aa*. Fog or stratus will not then result from evaporation of falling rain. In case *B*, the raindrops will be warmer than the air in the layer between *aa* and *bb*. A layer of stratus will then

build down from the frontal cloud system; below the level *bb*, the drops will be colder than the air, and condensation will not result. In case *C*, evaporation from the falling rain may fill the whole layer under *aa* with fog. It is readily seen that such fogs can develop only when the frontal surface is close to the ground; the fog area will then be close to the front. In case *D*, there is a shallow layer of cold air under a ground inversion. In this layer, the falling raindrops will be warmer than the air; a fog may then result under *bb*.

It should be borne in mind that fogs formed by evaporation of rain from warm air aloft falling into cold air below can occur only when the temperature difference is sufficiently large and when none of the fog-dissolving processes, which will be described later, overcompensates the effect of evaporation.

ii. Fogs are sometimes observed when cold air streams over a water surface the temperature of which is very much higher than the air temperature. These fogs are known as *steam fogs* or *arctic sea smoke*. In such cases, $E \gg E_a$, and the cause of the formation of such fogs is the intense evaporation from the water surface. For example, a water surface of 10°C. would have a saturation vapor

Fig. 64.—Types of temperature-height curves in relation to fog or stratus under the frontal rain area.

pressure of 12.3 mb. If the air above the water had a temperature of 5°C. and a relative humidity of 100 per cent, the vapor pressure of the air would be 8.7 mb., and the difference in water-vapor pressure between the surface and the air would be 3.6 mb. Water would evaporate quickly and fill the air with vapor, "steam" would pour forth from the surface, and the air be filled with a steam fog.

It is important to bear in mind that extreme temperature differences are required to produce a steam fog. This condition is due to the circumstance that the cold air above a warm surface will be heated from below to such an extent that the air becomes unstable. Through instability, vertical mixing sets in and prevents the steam from accumulating in the air. In general, light winds and a strong preexisting inversion near the sea surface are necessary for the steam to accumulate in the surface layer. In extreme cases, steam fogs are known to occur in strong winds. Thus, during a cold spell in February, 1934, steam fogs occurred at the harbor of East Boston; the air temperature was then about −28°C., probably 30°C. lower than the sea-surface temperature. On the other hand, when

warm rain drops fall through colder air, there is no tendency to produce instability, and a fog may result from comparatively small temperature differences. Moreover, the presence of a frontal surface close to the ground prevents the surface air from mixing with the air above.

Steam fogs are most frequently observed along the arctic coasts and in the fiords of cold continents [*e.g.*, Norway, where they are called *froströk* (frost smoke)]; they may also occur in the autumn in cold continental air masses over lakes and rivers.

2. MIXING.—It was shown in Par. 48 that horizontal mixing could cause only insignificant amounts of condensed water in the air; and it was shown in Par. 49 that vertical mixing, though it effectively produces condensation in the upper portion of the mixed layer, strongly counteracts condensation near the earth's surface. As horizontal mixing is always associated with vertical mixing (and vice versa), it follows that the former is counteracted and overcompensated by the latter.

If mixing (vertical and horizontal) occurs together with rain falling from warmer air aloft, the stratus layer caused by mixing and intensified by evaporation may build downward and may eventually reach down to the sea surface or level ground, thus forming a real fog. The conditions for this to occur are particularly favorable in the air under frontal rain areas as shown in Fig. 64c. Such fogs are therefore often called frontal fogs even though they form mainly as a result of evaporation and mixing. Again, it should be emphasized that the cloud can reach down to the ground only when the air from which the rain falls is considerably warmer than the air near the earth. This happens quite frequently in cold continents in winter. The conditions are then as shown in Fig. 64d.

It is, of course, obvious that the formation of such fogs is greatly facilitated when the surface air is simultaneously cooled by the underlying surface.

3. COOLING.—By far the most frequent and the most effective cause of fog formation is cooling of the air while it is in contact with the underlying surface. This cooling may be due to several causes. From the first theorem of thermodynamics, we obtain

$$(1) \qquad \frac{dT}{dt} = \frac{1}{c_p} \frac{dQ}{dt} + \frac{R}{c_p} \frac{T}{p} \frac{dp}{dt}$$

where dQ/dt denotes the heat added to, or withdrawn from, a unit mass of air per unit time. Let v_h denote the horizontal wind vector, v_z the vertical component of the wind velocity, and $-\nabla_h p$ the horizontal-pressure gradient. The preceding equation may then be written as

$$(2) \qquad \frac{dT}{dt} = \frac{1}{c_p} \frac{dQ}{dt} + \frac{RT}{c_p p} \frac{\partial p}{\partial t} + \frac{RT}{c_p p} v_h \cdot \nabla_h p + \frac{RT}{c_p p} v_z \frac{\partial p}{\partial z}$$

As we are here concerned with the formation and dissolution of fogs, we

need consider only air motion along the earth's surface. Equation (2) then shows that there are four factors which control the temperature changes of the moving air, viz.: (1) the nonadiabatic heating or cooling represented by the term containing dQ/dt, and three adiabatic influences resulting from (2) the local pressure variation $(\partial p/\partial t)$; (3) the flux of air across the isobars $(v_h \cdot \nabla_h p)$; and (4) vertical motion $[v_z (\partial p/\partial z)]$. It is convenient to discuss the various terms in the opposite order.

a. *The Slope Effect.*—The term $(RT/c_p p) v_z (\partial p/\partial z)$ vanishes at sea level and over level ground, where $v_z = 0$; but when the wind blows up or down a slope, the term may become larger than any of the other terms in Eq. (2). Even with a considerable upslope velocity, the air produces a fog only when it is stably stratified, because, if it were not, convective currents would develop. This implies that the air must also be *convectively stable* (see Par. 46) before saturation occurs, if an upslope fog is to develop. Furthermore, the relative humidity must be sufficiently high for the air to be cooled to its dew point during the ascent; and the vertical mixing must be slight or moderate. Thus, *stable stratification slight turbulence, and high relative humidity are favorable conditions for production of upslope fogs.*

It is typical of upslope fogs that they are very deep; this condition is due to the circumstance that the upslope velocity affects a deep layer of air. Upslope fogs are frequently observed with easterly winds in southeast Norway and also on the eastern slope of the Rocky Mountains. The "Cheyenne type" of fog belongs to this category (see Stone [78], and Clapp [22]).

b. *The Flux across the Isobars.*—The term $(RT/c_p p)v_h \cdot \nabla_h p$ is directly proportional to the pressure gradient and the wind component normal to the isobars. On account of the relation that exists between the wind velocity and the pressure gradient (see Chap. IV) the term can be important only when the wind velocity is high. But, when this is the case, the vertical mixing is appreciable and overcompensates the effect arising from the flux of air across the isobars. As an example, we assume that the horizontal-pressure gradient is 2×10^{-6} centibar/m. (which is a high value), and that the wind component normal to the isobars is 5 m./sec. With normal pressure and temperature, the term under discussion would amount only to 0.03°C. per hour, or 1°C. in 33 hr. The term is therefore insignificant in comparison with the other effects and need not be considered.

c. *Local Pressure Changes.*—The term $(RT/c_p p)(\partial p/\partial t)$ is important only when the air streams for a long time in an area of rapidly falling pressure. Let us assume that the barometer is falling 1 mb. per hour. The foregoing term would then amount to 0.08°C. per hour, or about 1°C. in 12 hr.

Barometric tendencies larger than these occur frequently in high and middle latitudes, but they are then accompanied by strong winds (strong pressure gradients). In such cases, vertical mixing is usually intense and counteracts the cooling influence caused by falling pressure. It should also be noted that the cooling caused by falling pressure is not confined to the layer of air close to the earth's surface, for $\partial p/\partial t$ is usually uniform throughout a deep layer of air. As p decreases more rapidly with elevation than does T, it follows that the term under discussion is apt to exert a greater influence in the upper atmosphere than at the earth's surface, where, in addition, the vertical mixing is most intense.

The conditions favorable for a fog to form on account of falling pressure are: (1) an intense isollobaric system which moves in the direction of the air current, (2) high relative humidity, (3) moderate or slight wind velocity, and (4) stable stratification so as to prevent vertical mixing. There is no evidence in support of the view that a fog forms only as a result of falling pressure; but when the foregoing conditions are favorable, the influence of falling pressure may add to the effect of the other fog-producing agencies.

4. NONADIABATIC COOLING.—The term $(1/c_p)(dQ/dt)$ constitutes the principal factor in the production of ordinary fogs. It is customary to distinguish between two principal types of fog formation, *viz.*, *radiation fog* and *advection fog*, the former being caused principally by radiative cooling of the underlying surface and the latter being mainly due to advection of warmer air over a colder surface. In both cases, the air gives off heat to the underlying surface. Most frequently, fogs form on account of the combined influence of radiative and advective cooling.

a. Radiation.—The influence of radiative cooling over land on the diurnal variation in air temperature is normally of the order of magnitude of 1°C. per hour. It is usually smaller than the upslope effect discussed above, and it is many times larger than the adiabatic cooling caused by falling pressure and flux of air across the isobars. The radiative influence is of a periodical nature; and, strictly speaking, if no other process were in operation, it would produce either fog every night or no fog at all. In discussing radiation fog, it is necessary to consider also the motion of the air.

We consider first the case where stably stratified, nonsaturated air streams along the isotherms of the underlying surface, so that there is no advective cooling. The eddy flux of heat is then directed downward, and this counteracts the radiative cooling of the underlying surface. Under normal atmospheric conditions, the specific humidity decreases upward, and the eddies transport water vapor upward through the air. Thus, *stable stratification and decreasing specific humidity along the vertical, together with turbulence, are unfavorable for the formation of radiation fog.*

However, when the wind velocity decreases, as it normally does in the evening, turbulence decreases rapidly (see Par. 57) and so, also, do the downward flux of heat and the upward flux of moisture. If the relative humidity is high enough, outgoing radiation from the surface may cool the surface air below its dew point, and a fog forms. As long as the specific humidity decreases along the vertical, fog usually does not form except in still air, and even then the cooling may result only in dew or rime on the ground.

When the specific humidity increases along the vertical, the eddy flux of moisture is directed toward the surface, and the conditions are favorable for formation of radiation fogs if the relative humidity is high and the wind is so slight that the radiative cooling of the surface is not substantially reduced by the eddy flux of heat from above. In addition, the sky must be clear or lightly clouded, for otherwise the counterradiation from the sky would reduce the outgoing radiation from the surface.

In short, we may say that the conditions favorable for formation of radiation fogs are: (1) *high relative humidity*, (2) *cloudless sky*, (3) *constant or increasing specific humidity along the vertical*, and (4) *lack of turbulence*. It should be noted that stable stratification involves a flux of heat toward the underlying surface which is unfavorable for radiative cooling. On the other hand, as turbulence depends greatly on the stability of the air, point (4) above may be replaced by (5) *stable stratification and lack of wind*.

The foregoing conditions (2) to (4) occur most frequently in continental anticyclones in the colder part of the year or in any uniform pressure distribution when there is enough subsidence in the upper air to dissolve the clouds. As high relative humidity is an important factor, radiation fogs develop most frequently in air of maritime origin when it becomes stagnant over cold continents.

On account of the slight diurnal variation of temperature at sea, radiation fogs do not normally develop over oceans.

b. Advection.—The term $(1/c_p)(dQ/dt)$ is an important factor when warmer air streams over a colder surface. The cooling of the traveling air depends mainly on the difference in temperature between the air and the underlying surface, which again depends on the speed with which the air streams across the isotherms of the underlying surface. In extreme cases, the cooling may amount to 1°C. per hour, but it is usually less than 0.5°C. per hour. As high wind velocities (strong turbulence and vertical mixing) are highly unfavorable for formation of fog and as a certain wind velocity is necessary to bring the air across the isotherms of the underlying surface, it follows that advection fogs develop as a compromise between the effects of vertical mixing and cooling from below. This explains why fogs are comparatively rare in the air currents from

warmer toward colder regions.   The conditions favorable for advection fogs are: (1) *large difference between the temperature of the air and that of the underlying surface,* (2) *not too high wind velocity,* (3) *high relative humidity initially, and* (4) *stable stratification initially.*

The factors (1) and (2) are of greatest importance.   As the turbulent mixing is somewhat proportional to the wind velocity and as a large temperature difference can be maintained only when the air streams across the isotherms of the underlying surface, it follows that the best
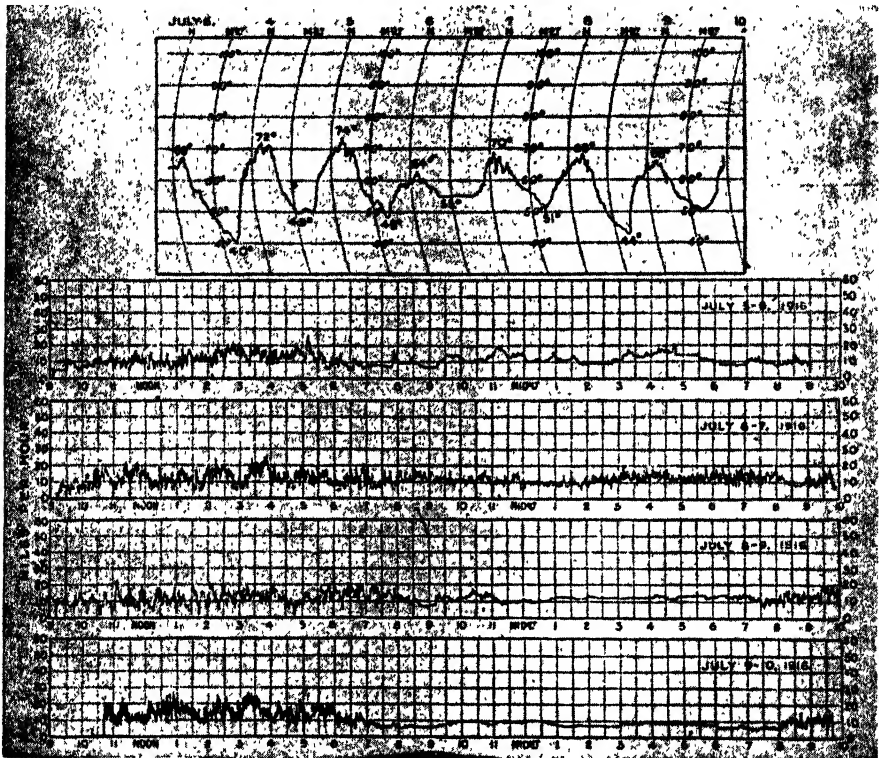
Fig. 65.—Anemograms from Pyestock, near Farnborough, 140 ft. above the ground, and the corresponding thermogram.

condition for the formation of advection fog is when the air streams with a moderate velocity normal to the isotherms of the underlying surface, for the cooling from the underlying surface will then be greatest in comparison with the downward eddy flux of heat.

Practically all sea fogs are of the advection type.   The winter fogs over land form most frequently in stagnant air from a warm and humid source which subsequently becomes cooled by outgoing radiation from the earth's surface.   In such cases, the cause of fog formation may be ascribed to *advection followed by radiation.*

57. Fog in Relation to Wind.—From the foregoing discussion, it follows that turbulence is a factor of basic importance, inasmuch as the vertical mixing that results from turbulence is highly effective in counteracting the fog-producing agencies. The intensity of the turbulence depends mainly on two factors: the stability of the air and the velocity of the wind. That this is so is shown clearly in a detailed study of fog by Taylor [83] from which the following passage is quoted (*cf.* Fig. 65):

It will be noticed that on all these days the wind speed was about 10 miles per hour both during the day and during the night. On the three days 5th-6th, 8th-9th, and 9th-10th the wind was gusty during the day, and practically free from gusts during the night. The anemometer trace for July 6–7, however, shows gustiness throughout the whole 24 hours, though the amount of gustiness at night is rather less than it is during the day.

The reason for this difference may be inferred from the record of the thermograph for the week July 3–10, which is also shown in Fig. 65. It will be seen that, during the evenings and nights of the 5th, 8th, and 9th the temperature fell through 26°, 25°, and 17°F. On the 6th, however, the temperature stopped falling at about 8.30 p.m. (owing to a sheet of cloud which came over the sky) after it had fallen only 9°F. below the maximum during the day. It seems, therefore, that the temperature gradient, due to the cooling of the ground on a clear night when the temperature of the surface air falls about 20°F., is sufficient to suppress practically all turbulent motion in a wind of 10 m.p.h. at a height of 140 feet (the height of Pyestock chimney), while the temperature gradient due to cooling of 9°F. on a cloudy night is not sufficient to suppress the turbulent motion due to the friction of a wind of about 10 m.p.h. over the ground.

The intensity of the turbulence increases with the speed of the wind; and when the wind increases beyond a certain value (which depends on the stability of the air), the fog may be dissipated or develop into a layer of stratus. The effect of the turbulent mixing accompanying strong winds is shown clearly in the following table which is quoted from Taylor's paper.

TABLE 12

Wind force, Beaufort's scale	Number of cases of fog	Mean value of air temperature minus water temperature
0	3	−0.5
1	20	0.3
2	30	1.0
3	46	1.0
4	26	1.1
5	12	1.8
6	3	2.6
7	1	4.1

It will be noticed that the maximum frequency is found neither at the extremely high values of the difference in temperature between air and sea nor at the lowest wind velocities, but somewhere between. This condition is due to the following circumstances: Great temperature differences occur only when the air moves rapidly across the isotherms of the surface; but in such cases fogs are rare on account of the intense mixing. On the other hand, when the wind velocity is slight, the difference in temperature is slight too; the air is then less stable, and even slight turbulence suffices to dissipate the fog. Thus, the sea fogs (which are advection fogs) are most likely to form when the wind speed is moderate and blowing more or less directly across the isotherms of the water. It will be seen from Table 12 that fogs may sometimes persist in air that is slightly colder than the sea surface. This happens only in almost still air. Such fogs must be formed while the air is blowing from warm toward cold sea.[1]

Table 12 refers to advection fog. Over land, it is difficult to distinguish between advection fog and radiation fog. Table 13, which is quoted from Taylor's paper, shows the frequencies of wind forces at different hours on the 70 occasions when fog was reported at Kew in the night during the years 1900 to 1905.

TABLE 13.—FREQUENCIES OF WIND FORCES PRECEDING NIGHT FOGS AT KEW, 1900 TO 1905

Wind veloc- ity, m.p.h.	Wind force, Beaufort's scale	4 P.M.	6 P.M.	8 P.M.	10 P.M.	Midnight
0 – 3.3	0–1	24	35	50	58	62
3.3– 5.5	1–2	23	20	18	10	5
5.5– 9.2	2–3	16	13	1	2	3
9.?–13.6	3–4	7	2	1	0	0

The table shows the normal decrease in wind velocity from the afternoon toward midnight. On looking at the 6 P.M. column of Table 13, it will be seen that it happened only twice in 5 years that a wind greater than 9.2 m.p.h. at 6 P.M. was followed by a fog in the night. Similarly, it happened only twice in 5 years that a wind greater than 5.5 m.p.h. at 8 P.M. was followed by fog in the night. The table may be used for forecasting; for if "no fog" were predicted at Kew every time the wind at 8 P.M. was greater than 5.5 m.p.h., only two errors would have been made in 5 years.

---

[1] "Arctic smoke" could form only if the air temperature were considerably below the sea-surface temperature (see Par. 56).

Thus, although it is practically certain that a fog does not form at Kew when the wind at 8 P.M. is greater than 5.5 m.p.h., there are still, naturally, many cases when the wind at 8 P.M. is less than 5.5 m.p.h. without fog forming later in the night. The reason for this is that the formation of fog depends, also, on the temperature of the surface and the temperature and the humidity of the air.

It is of interest to remark that, although Table 13 holds only for Kew, there can be little doubt that it is applicable, also, in a general way, to other land stations similarly situated. In view of the many local factors that influence fog formation on land, it is highly probable that local studies, on the lines indicated by Taylor, would substantially improve the forecasting of fog.

On comparing Table 12 with Table 13, it is seen that the upper limit of wind force at which fog can exist is much greater at sea than at Kew. This condition is partly due to the increased friction over-land which causes increased vertical mixing and partly due to the circumstances that land fogs are mostly radiation fogs, which cannot form unless the wind is slight, and that sea fogs are advection fogs, which require a certain wind velocity to bring the air across the isotherms of the underlying surface.

58. Fog in Relation to Temperature.—Whether fog is produced by radiation, advection, or any of the adiabatic processes described in Par. 56, the forecaster will have to estimate the amount of cooling that is likely to occur within the forecasting period. Whether or not the expected cooling suffices to produce a fog depends on the humidity of the air.

Figure 66 shows a diagram from which the amount of cooling necessary to produce a fog can be determined when the air temperature and the relative humidity are known. Let *A* denote a point in the diagram to which correspond a certain relative humidity and a certain air temperature. The horizontal lines then indicate the corresponding dew point. The distance from *A* to *B* measures the amount of cooling that is necessary to make the air saturated, provided that the moisture content remains constant during the cooling.

It should be borne in mind that fog is not just saturated air, but air which contains an amount of liquid water sufficient to reduce the horizontal range of visibility to 1000 m. or less. The visibility is primarily a function of the amount of liquid water, but it also depends on the size of the droplets and the pollution. As it is known that the amount of liquid water in fogs and clouds may vary between 0.1 and 5.0 grams/cu. m., it seems probable that a moderate fog would not contain less than 0.5 gram liquid water/cu. m. Whether or not this value is exact is a matter of minor importance. What we are here desirous of emphasizing is that, after the air has become saturated, a certain amount of

cooling is necessary in order to produce so much condensed water that the horizontal visibility is reduced to 1000 m. or less. This is shown in Fig. 66, where, for example, the air represented by the point *A* must be cooled by the amount *AB* in order to become saturated, after which it must be cooled still further, by the amount $\Delta T = BC$, in order that the air should contain 0.5 gram liquid water/cu. m.

While the air is being cooled from *B* to *C*, it will be misty, but a real fog will not develop until the amount of liquid water has reached a
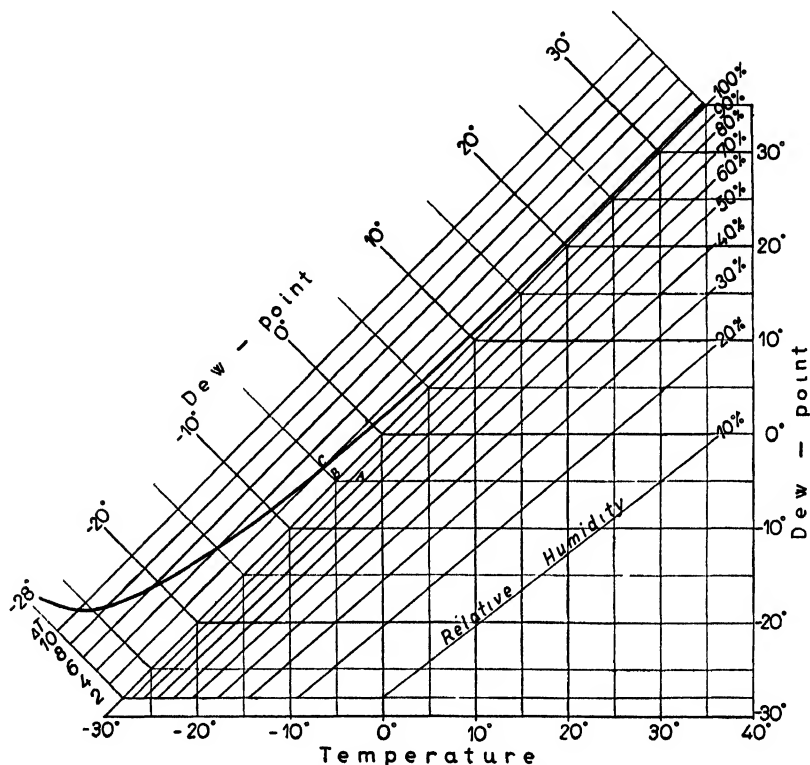
FIG. 66.—Fog prediction diagram.

certain value. It is of interest to note that the "mist interval" is very small when the air temperature is high and increases as the temperature decreases. When the temperature approaches −28°C., the "mist interval" widens rapidly, because almost the total amount of aqueous vapor in the air must then be condensed in order to produce a sufficient amount of liquid water. Thus, at −25°C., saturated air must be cooled about 9°C. in order to condense 0.5 gram water, whereas, at +20°C., a cooling of 0.4°C. produces the same effect. It follows then that, at low temperatures, the amount of cooling necessary to produce a fog becomes greater

than the diurnal amplitude of temperature and no fog will form as a result of nocturnal cooling.   We shall see later that the drying influence of the snow has a tendency to counteract the formation of fog over snow-covered ground and to dissipate fog transported to such areas.

For prediction of radiation fogs, it is of basic importance to estimate the amount of cooling that is likely to occur.   As radiation fogs do not form when the wind velocity is high or the sky is cloudy, it suffices to consider the conditions when the cloudiness is small and the wind velocity is slight or moderate.   Suppose the observation to be made at a certain hour h and that we know the normal diurnal fall in temperature under
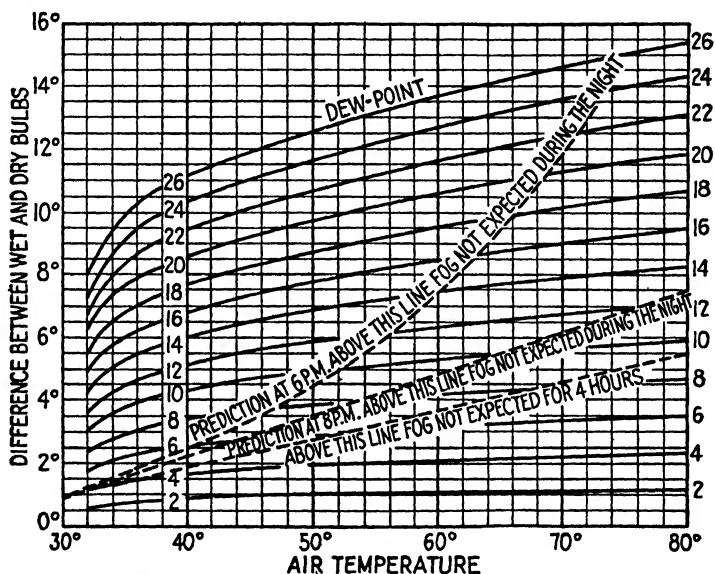
FIG. 67.—Taylor's fog prediction diagram for Kew on calm, clear nights.   The "fog prediction lines" may conveniently be plotted on Fig. 66.

calm and cloudless conditions after the hour h.   From the temperature-moisture diagram (Fig. 66), we may determine the amount of cooling necessary to produce saturation.   If this amount is less than the normal fall in temperature, fog is likely to develop; if it is greater, fog is unlikely.

It is well known that the diurnal amplitude of temperature for any given locality is greater on warm days (in the warm season) than on cold days (in the cold season).   The normal fall in temperature on almost calm and clear nights must be determined statistically for representative stations.   It is then possible to draw a line on a temperature-humidity diagram in such a way that it separates the combinations of temperature and humidity at which fog can form, from those at which fog is improbable.   Figure 67 shows such a diagram prepared by Taylor for Kew. Taylor found that the same diagram holds also for Oxford, Nottingham,

and Potsdam.   As regards the method of construction of such diagrams, the reader is referred to Taylor's paper.

In estimating the chances for formation of radiation fogs, it is necessary to know not only the normal variation of air temperature on clear, calm evenings, but also the normal variation in dew point.   As was pointed out in Par. 12, the dew-point temperature has a diurnal variation that is slight as compared with that of the air temperature.   Figure 68 shows this.

It will be noticed that the dew-point temperature normally remains constant during the day, but a slight fall sets in after sunset on account of dew that forms on the ground.   When a fog forms, the dew point
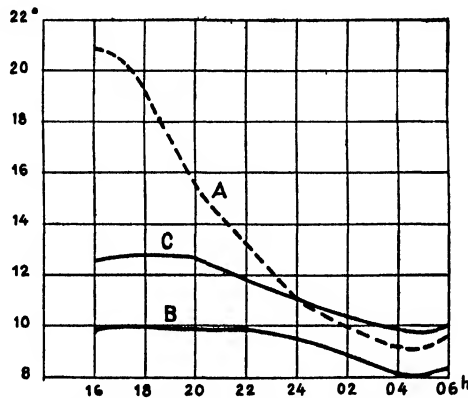
FIG. 68.—Curve *A*, the normal fall in temperature in calm and clear nights at Kew; curve *B*, the normal variation in dew point on calm and clear nights without fog; and curve *C*, the normal variation in dew point when fog developed in the night.   See also Par. 12.

decreases still further owing to the condensation of water vapor.   In the morning, the dew point rises again, as the dew, or the fog, evaporates.

If aerological ascents are available, one may go a step further and try to estimate the diurnal heating and cooling by considering the actual stability conditions of the air.   It was shown in Par. 8 that the more stable the air the greater the diurnal amplitude of temperature.   It was also pointed out that the presence of an inversion above the ground has a marked influence on the magnitude of the diurnal variation.

The foregoing discussion refers mainly to radiation fogs, but similar reasoning holds for all types of fog (except arctic smoke) since it is immaterial whether or not the cooling is caused by radiation.   However, in predicting nonradiation fogs, one must estimate the probable changes of temperature along the trajectory of the air.   The knowledge of average local conditions (such as are illustrated in Fig. 67) is then less useful.

Radiation fogs are always connected with an inversion of temperature at the ground (*e.g.*, Fig. 59*A*).   The same is true, in most cases, of advec-

tion fogs. If the wind is strong enough to raise the inversion, the fog dissipates or develops into a layer of stratus. In rare cases, however, advection fogs may persist even when the inversion is at some distance above the ground. This only happens when the air travels over a surface that is so much colder than the air that the cooling from below over-compensates the effect of the vertical mixing. Fogs that exist together with strong winds are usually very deep, for they fill the entire layer below the inversion that has been raised by the turbulent mixing.

59. Fog in Relation to Snow.—As cooling from the underlying surface is the primary cause of formation of fog, it is surprising to observe how rarely fogs develop over cold continents, such as Siberia and Canada, in winter. It is frequently observed that moist air from the Atlantic Ocean enters the snow-covered regions of north Europe and Siberia without producing fog. On the other hand, when Atlantic air comes
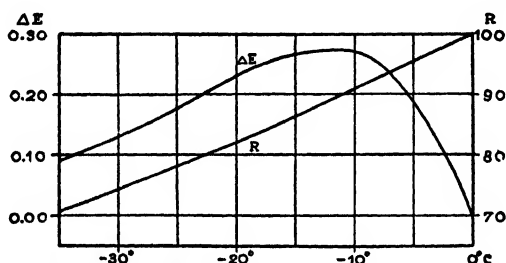
FIG. 69.—Difference in saturation pressure over water and over ice (curve ΔE); and relative humidity (curve R) of air which is saturated over ice.

over the Labrador Current, it produces fog very quickly. In the first case, the air may be cooled from 15 to −40°C.; in the latter case, it may be cooled only from 15 to 5°C. Even when the air is perfectly calm and clear, fogs do not easily form over cold snowfields. The principal reason for this may be sought in the depression of the saturation vapor pressure over ice.

In Fig. 69, the curve ΔE represents the difference in saturation pressure over water and over ice. It is zero at 0°C.; it has a maximum (0.27 mb.) when the air temperature is about −12°C., and it decreases as the air temperature decreases still further. The curve R represents the relative humidity of the air when the vapor pressure equals the saturation pressure over ice. It will be seen that R decreases linearly with decreasing temperature.

When air over a snow-covered surface is cooled to such an extent that its relative humidity increases to the value indicated by R in Fig. 69, water vapor is condensed on the snowy surface. As this continues, the air obtains a minimum of specific humidity near the surface. The eddy flux of moisture will then be directed downward, and the air column gives

off moisture to the snow.   When the air temperature is slightly below zero, ΔE is small, and, if the air is cooled with a sufficient speed, a fog may easily form.   But the fog must then give off moisture to the snow. The fog can persist only when the air is steadily cooled (*e.g.*, by advection) or when the downward eddy flux of moisture is strong enough to over-compensate the loss of moisture caused by condensation on the snow.

As the air temperature decreases to -10 or $-15°C.$, ΔE increases to its maximum value, and the drying influence increases accordingly; it becomes increasingly difficult for a fog to form; and a fog that is brought over a cold snow-covered surface has a marked tendency to dissipate.

As the diurnal amplitude is very small when the air temperature is very low, a fog will not form over a cold snow-covered surface as a result of nocturnal cooling alone.   The fogs that are sometimes observed over cold continents in winter are caused by advection of moist air from warmer regions.   When such air is cooled, it may produce fog, which gradually dissipates as the air temperature decreases.   As was shown in the last paragraph, the "mist interval" is very wide at low temperatures. Most of the water fogs that occur over cold snow fields are very light and so shallow that the sky is discernible.

The foregoing conditions apply when the air temperature above the snow is below 0°C.   The conditions are, however, different when the air temperature above the snow is higher than 0°C.   The snow is then melting.   Under such conditions, as has been shown by Sverdrup [80], the air that is in direct contact with the melting snow has a temperature close to 0°C. and a relative humidity of 100 per cent.   The vapor pressure of the air that is in contact with the melting snow is then 6.11 mb.   If the specific humidity increases along the vertical (as it is likely to do when the air temperature increases along the vertical), there is an eddy flux of moisture downward, and moisture from the air is condensed on the snow. This implies that condensation occurs on the melting snow whenever the *relative humidity* of the air exceeds a limiting value which depends on the air temperature above the snow.   These limiting values are given in Table 14.   If the relative humidity for any given air temperature is less than the limiting value, water evaporates from the snow.   Relative humidities less than the limiting values are seldom encountered over melting snow, and, as a result, condensation of water vapor is the normal occurrence in spring after the air temperature has become greater than 0°C.   The observations of Ahlmann and Sverdrup show that water is condensed on the melting snow in considerable amounts and that the latent heat thereby liberated results in appreciable ablation.

The foregoing results are of considerable interest in connection with our discussion of formation and dissipation of fog over snow.   Suppose that an air temperature of 4°C. is measured at a height of 2 m. above the

snow.   If the air were saturated, there would be a vapor-pressure gradient
of about 1 mb./m. in the layer below the thermometer.   The water vapor
would then condense quickly on the snow which would retain a temper-
ature of 0°C.   The downward flux of moisture would continue until
the relative humidity has been lowered to the limiting value, 77 per cent
(see Table 14).   In order to maintain saturation, the advection of
warmer air would have to be strong enough to overcompensate the loss
of moisture toward the snow.   The higher the air temperature above the
snow, the more difficult would it be for saturation (or fog) to be main-
tained.   It follows then that fogs can form only in exceptional cases when
the air temperature at some distance above the ground is much above
0°C.   Similarly, fogs that are transported over melting snow will have a
marked tendency to dissipate.   From this, we may conclude that fogs
over melting snow can exist only when the air temperature is not far
removed from 0°C.

TABLE 14

Air temperature at some distance above the ground, °C.	Saturation vapor pressure, mb.	Limiting value of relative humidity, %
0	6.11	100
2	7.05	87
4	8.13	77
6	9.35	67
8	10.73	58
10	12.28	51

When the air temperature falls below 0°C., the dissipating influence
due to the depression of the saturation water-vapor pressure over snow
commences and increases as the temperature decreases.   It follows then
that *the highest frequency of fog over snow-covered ground in spring would
be observed when the air temperature is close to 0°C.*

The arctic fogs, which are so frequent in summer, form because of
advection of warm air over cold sea.   Such fogs often invade the arctic
fields of ice, where they gradually dissipate, unless the advection of moist
air from the open sea is sufficiently intense to overcompensate the effect
of condensation on the melting snow.   The arctic summer fogs are,
therefore, essentially advection fogs.

The dissipating influence of snow on fogs is brought to light by statis-
tical evidence.   An example is shown in Table 15.   Let f denote the
frequency of occurrence of fog in the various temperature intervals, and
let F be the frequency of air temperatures observed within these intervals.

Table 15 then shows the percentage frequency (100 f/F) of occurrence of fog for any given temperature in Oslo.

Table 15.—Fog Frequencies (100 f/F), Oslo, 1920 to 1931
(Total number of observations 4365)

Temperature intervals, °C.	October	January–February	March
20 to 15	0.0	—	0.0
15 to 10	0.5	—	0.0
10 to 5	3.0	0.0	0.0
5 to 0	5.7	5.6	3.3
0 to −5	12.3	5.0	8.7
−5 to −10	0 0*	4.6	6.0
−10 to −15	—	4.1	0.0
−15 to −20	—	0 0	—
−20 to −25	—	0.0	—

* There are only three temperature observations in this interval.

It is of interest to note that October in Oslo is a snowless month, that January and February normally have snow with freezing temperatures, and that March frequently has snow with temperatures above freezing (melting snow).[1]   It will be seen from the above table that the frequency of fog in October is highest when the air temperature is lowest.   This is what one would expect over snowless ground; the lower the temperature sinks, the greater, on the average, the probability of formation of fog. This particularly applies to radiation fogs.

In January and February, when the ground is covered by snow, the conditions are quite different.   The highest frequency of fog over snow occurs when the temperature is about 0°C., whereas, for lower temperatures, the fog frequency decreases.   The circumstance that the highest frequency of fog occurs at high temperatures in mid-winter seems to indicate that the mid-winter fogs in Oslo are mainly advection fogs which form when there is a strong transport of warm and moist air over the cold surface.   The fogs then persist as long as the advection is strong enough to overcompensate the dissipating influence of the snow.   As the air temperature approaches −10 to −15°C., the difference in saturation pressure over water and ice increases to its maximum value (0.27 mb.), and sublimation on the snow increases accordingly.

In March, when the mean air temperature is above freezing, the snow is normally melting.   Fogs with air temperature considerably above 0°C. are then very rare.   The highest frequency occurs at temperatures just below zero, and the frequency decreases as the temperature decreases

[1] In the period examined, the average number of days with ground completely covered by snow is as follows: October, 0.6; January, 21.3; February, 21.8; March, 14.6.

further.   The spring fogs in Oslo are apparently mainly of the advection type, also, and it is plausible that advection is the all-important cause of the formation of fogs over snow-covered ground.

What has been said above applies to *water fogs*.   At low temperatures, the water vapor of the air sublimates on the sublimation nuclei, and *ice-crystal fogs* result.   Such fogs are sometimes observed at temperatures of about −10°C.; but, most frequently, sublimation begins at about −20°C. At still lower temperatures (−30 to −50°C.), ice-crystal fogs are the normal occurrence (*e.g.*, in Siberia and north Canada in winter).   At such low temperatures, the specific humidity of the air is insufficient for producing a water cloud of such density that the horizontal range of visibility is reduced to 1000 m. or less.   However, when sublimation occurs, a much smaller amount of aqueous vapor is needed in order to produce ice crystals whose size and number suffice to reduce the horizontal visibility below the fog limit.   At extremely low temperatures, the density of the cloud is such that it appears as a thin mist or haze ("frost haze").

It is of interest to remark that *snow on the ground has no dissipating influence on ice-crystal fogs*.   It is, therefore, to be expected that the fog frequency would show an increase in the temperature intervals below −20°C. or so, where ice-crystal fogs are predominant.   In order to test this assumption, fog frequencies have been computed for 10 synoptic stations in the Siberian lowland east of the Ural Mountains.   The result is shown in Table 16.

TABLE 16.—Fog Frequency ($100\ f/F$) at 10 Siberian Lowland Stations, October
to March
(Total number of observations 4389)

Temperature intervals, °C.	Fog frequency, %	Temperature intervals, °C.	Fog frequency, %
+15 to 11	0.0*	−20 to −24	7.0
+10 to 6	9.0*	−25 to −29	5 0
+5 to 1	9.1	−30 to −34	4.4
0 to −4	4.9	−35 to −39	6.5
−5 to −9	3.3	−40 to −44	12.8
−10 to −14	2.7	−45 to −49	15 4
−15 to −19	2.7	−50 to −55	0.0†

* Probably no snow on the ground.
† There is only one temperature observation in this interval.

It will be seen that here, too, the fog frequency decreases rapidly as the air temperature sinks below 0°C.   The decrease continues until the air temperature approaches −20°C., where there is a hump, which perhaps is due to the circumstance that water fogs as well as ice-crystal

fogs may occur within this temperature interval. The frequency then decreases slightly and increases again as the temperature decreases to $-50°C$. At still lower temperatures, the frequency would be likely to decrease, on account of the slight amount of specific humidity which the air can hold at such low temperatures.

Summing up, we may say that melting snow has a marked dissipating influence on fog, when the air temperature is above freezing. The dissipating influence is greater the higher the air temperature rises above $0°C$. As the air temperature falls to $0°C$., this dissipating influence vanishes; but when the air temperature sinks below $0°C$., another dissipating influence, due to the depression of the saturation pressure over ice, commences and increases in intensity until the air temperature reaches -10 to $-15°C$., where it has a maximum. This dissipating influence is identical with the "ice-crystal effect" found in the upper portion of clouds, where ice crystals and water droplets coexist. Bergeron [2] ascribes the release of precipitation from clouds to this effect. As the air temperature sinks to approximately $-20°C$., sublimation nuclei become active, and ice-crystal fogs form. The presence of snow on the ground has then no dissipating influence on the fogs.

It is of interest to remark that the dissipating influences mentioned above are not sufficiently strong completely to prevent the formation of fog. However, when they are present, a corresponding fog-producing process (*e.g.*, advection) is necessary for its production and maintenance. It should also be mentioned that the deposition of water from the air on the snowy surface is of considerable importance in the production of polar continental air masses in winter (see Chap. III).

60. Classification of Fogs.—In the above paragraphs, an attempt has been made to explain the physical processes that, under favorable conditions, may lead to the formation of fogs. Mention has also been made of the processes that counteract the fog-producing agencies and may lead to the dissipation of existing fogs. With reference to this discussion, fogs may be classified according to the identity of the process that constitutes the principal cause of their formation. This is shown in the left-hand portion of Table 17. A summary of the fog-dissipating agencies is given in the right-hand portion of the same table.

61. Inversion Fogs.—In many cases, it will be found that fogs are produced as a result of several of the above-mentioned fog-creating agencies. This is particularly true of fogs that build down from a layer of stratus under an inversion at some distance above the ground (*i.e.*, inversion fogs). In such cases, the formation of a stratus layer is primarily caused by vertical mixing in the air under the inversion; but, as was shown in Par. 49, vertical mixing alone cannot cause condensation in the lower portion of the stirred layer. Therefore, when the cloud

layer builds downward to the earth's surface, other fog-producing factors must be present, and these must be sufficiently strong to over-compensate the effect of vertical mixing.

TABLE 17.—CLASSIFICATION OF FOGS

Fog-producing Processes	Fog-dissipating Processes
1. Evaporation from	1. Sublimation or condensation on
a. Rain that is warmer than the air (rain-area fog, or *frontal fog*).	*a.* Snow with air temperature below 0°C. (excepting ice-crystal fogs).
b. Water surface that is warmer than the air (*steam fog*).	*b.* Snow with air temperature above 0°C. (melting snow).
2. Cooling due to	2. Heating due to
c. Adiabatic upslope motion (*upslope fog*).	*c.* Adiabatic downslope motion.
d. Flux of air across the isobars toward lower pressure (*isobaric fog*; effect negligible).	*d.* Flux of air across the isobars toward higher pressure (effect negligible).
e. Falling pressure (*isallobaric fog*; unimportant).	*e.* Rising pressure (unimportant).
f. Radiation from the underlying surface (*radiation fog*).	*f.* Radiation absorbed by the fog or the underlying surface.
g. Advection of warmer air over a colder surface (*advection fog*).	*g.* Advection of colder air over a warmer surface.
3. Mixing	3. Mixing
h. Horizontal mixing (unimportant by itself, and strongly counteracted by vertical mixing).	*h.* Vertical mixing (important in dissipating fogs and producing stratus).

It was shown in Par. 56 that evaporation from falling rain may cause the stratus layer to build down to the earth's surface when the rain is warmer than the air through which it falls; but, in the absence of such rain, it is necessary that the air along the earth's surface be cooled while the layer is mixed. This cooling may be due to (1) advection of warm air over a colder surface, (2) radiative cooling of the underlying surface, (3) radiative cooling of the top of the stratus layer, and (4) the normal diurnal variation in temperature.

The most typical inversion fogs occur along subtropical west coasts. We shall therefore first describe the formation of such fogs and afterward comment on other cases of inversion fogs. The following is a summary of a recent investigation of such fogs in Southern California (Petterssen [54]), but the conditions are similar along other subtropical coasts similarly situated (*e.g.*, the coast of Africa from Casablanca to Senegal).

Climatological records show a high frequency of coastal fogs in summer and early autumn. Aerological ascents show that the foggy air is rather *unstable* and that a pronounced inversion is present at some distance above sea level, with very warm and exceedingly dry air aloft. A dense layer of stratus is normally present under the inversion. Over land, the stratus usually dissolves by day and re-forms in the evening,

sometimes building down to sea level and forming a dense fog. The investigation already mentioned showed that fog and stratus form as a result of vertical mixing and the four cooling influences listed above. In addition, subsidence in the air above the inversion is an important factor.

1. *Cooling from Below.*—Figure 70 shows the normal sea-surface temperature in August. It will be seen that there is a distinct minimum of temperature north of San Francisco with increasing temperatures to the north and south. The low sea-surface temperature along the coast is the result of the upwelling of water caused by the prevailing northwesterly winds along the coast in summer.
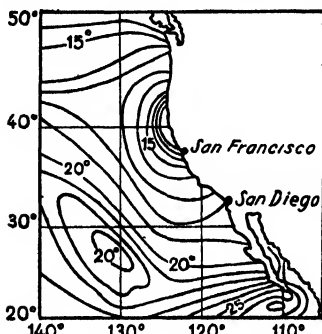
FIG. 70.—Sea-surface temperature in August. (*After Thorade.*)
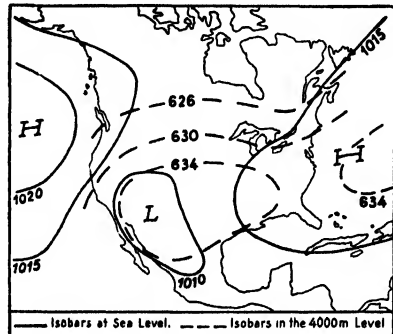
FIG. 71.—Mean atmospheric pressure at sea level and at the level of 4 km., July, 1935.

The air that moves in over the colder water will be cooled from below and might well produce fog, but, in that case, the air ought to be stable, not unstable, as it actually is. This cooling effect of the sea surface cannot be the direct cause of the fog, for it is frequently observed in San Diego that fogs form with the air current from the northwest. The air would then be heated and not cooled from below. The presence of cold upwelling water along the coast is an important factor inasmuch as it causes the air temperature to be generally low and the relative humidity generally high, and this favors the formation of the fog (or stratus).

2. *The High-level Anticyclone.*—Figure 71 shows a typical distribution of atmospheric pressure in the level of 4 km. in summer (see also Reed [59]). At low levels, particularly in the southwest portion, there is a quasi-permanent area of low pressure, which vanishes with increasing altitude and changes into a high-level anticyclone. The descending motion in the anticyclone results in adiabatic heating of the air and a corresponding decrease in relative and specific humidity above the inversion. The upper air is, therefore, exceedingly dry. A typical example of the vertical structure of this type of air was shown in Fig. 59D.

3. *Maintenance of the Inversion.*—The inversion separates the warm and dry air aloft from the cold and humid air below. This inversion

acts as a lid through which practically no transport or mixing of air takes place. The only way in which the two air masses can exchange properties to any considerable extent is through radiation; and since the upper air is considerably warmer than the air below, it might seem plausible that radiation would be highly effective in destroying the inversion; in that case, it would be difficult to explain why the inversion is an almost permanent phenomenon during the foggy season. The radiation within the atmosphere, however, depends also on the distribution of moisture.

The radiation R follows the well-known Stefan's law

$$(1) \qquad\qquad R = cT^4$$

where c is a constant characteristic of a black body, and T is absolute temperature. Brunt [19] has shown that the radiation R' of moist air can be expressed with great accuracy by the following formula:

$$(2) \qquad\qquad R' = cT^4(0.526 + 0.065\sqrt{e})$$

where e denotes the partial pressure of the aqueous vapor. It is then readily seen that the net radiation from the warm and dry air aloft toward the cold and humid air underneath is greatly reduced on account of the large difference in water-vapor content; for extreme differences in water-vapor content, the cold and humid layer may lose heat toward the warmer air above.

This applies to nonsaturated air. When the saturation point is reached and stratus (or fog) forms under the inversion, the outgoing radiation at night from the upper surface of the cloud layer will be almost that of a black body [Eq. (1)], whereas the outgoing radiation from the warmer and dryer air above the cloud layer will be that given by Eq. (2), which rarely amounts to more than 70 per cent of the black-body radiation. Thus, on foggy nights, the air under the inversion radiates more heat outward than the air above. In this way, the inversion is maintained and even increased during the night. Since the air under the inversion is thus cooled from above, it follows that instability is produced in the layer below the inversion. During the day, when the fog dissipates, the earth's surface absorbs heat, and the layer under the inversion is heated from below. There is therefore a tendency to produce instability both by day and by night. The unstable state of this air is directly observable from the internal motion of the clouds and is also experienced as bumpiness by pilots.

4. *Formation and Dissolution.*—The stratus layer forms under the inversion as a result of vertical mixing and convection in the unstable air. It was found that the base of the stratus layer coincides with the condensation level of the surface air. As the air is heated diurnally,

the condensation level rises, and the stratus layer dissolves as the condensation level coincides with the base of the inversion. The sky remains cloudless until the air is cooled so much in the evening that the descending condensation level coincides with the base of the inversion, when it reforms and builds down as the cooling proceeds. Eventually, the cloud layer may reach down to the earth's surface.

Thus, it was found that (1) all cases of unbroken stratus (or fog) occurred when the condensation level of the surface air was lower than the base of the inversion, (2) all cases of scattered stratus occurred when the condensation level was close to the base of the inversion, and (3) all cases without stratus occurred when the condensation level was higher than the base of the inversion.

The results above may be used for forecasting purposes. As the base of the cloud coincides with the condensation level *CL* and the upper surface of the cloud coincides with the base of the inversion *BI*, it follows that, the greater the distance *BI-CL*, the thicker the cloud layer and the greater the amount of heating (in the morning) which is necessary to dissipate the fog. For San Diego, it was found that the correlation coefficient between (*BI-CL*) and the hour when the fog broke was 0.84, which shows that the relation is almost linear.

There can therefore be little doubt that the distance from the condensation level to the base of the inversion is the primary factor as far as the hour of dissolution is concerned; but it is also plausible that the height of the inversion above the ground exerts an influence. Since the air under the inversion is mostly unstable, the heat gained from the surface by the air after sunrise will be distributed over the whole air column under the inversion. When the inversion is high, the diurnal amplitude of temperature at any level will be small, and its effect on dissolving the cloud will be small, too. When the base of the inversion is low, the diurnal amplitude of temperature will be large, and its effect on the cloud will be large. The table in Par. 8 shows the average diurnal amplitude of temperature in relation to the height of the base of the inversion above San Diego. It will be understood that fog forms later and dissolves earlier when the base of the inversion is low than it does when it is high.

The records from San Diego showed furthermore that the height of the condensation level of the surface air has a large diurnal amplitude, varying from 500 m. at 6 A.M. to 960 m. at 3 P.M. On the other hand, the diurnal variation in the height of the base of the inversion is less than 50 m. The condensation level of the surface air, therefore, moves in a regular rhythm in time with the diurnal variation of temperature. The fog "burns off" in the morning when the condensation level of the surface air coincides with the base of the inversion, and the sky remains clear

till the descending condensation level again comes down to the base of the inversion.

Although the height of the base of the inversion has no appreciable diurnal variation, it moves aperiodically, and its variations depend on the changes in the general weather situation. These variations are closely related to the wind direction, as is shown in the table below:

Wind direction (quadrant).....................	N	E	S	W
Height of base of inversion, m.................	210	200	640	450

The above results refer to San Diego, where the meteorological conditions are extremely simple and regular. The inversion fogs which are encountered in middle and high latitudes form in connection with inversions which are neither so persistent nor so regular in behavior as are those which form along the subtropical west coasts in summer. The mechanism of the formation of stratus and fog is, however, in principle as described above, with the exception that the difference in humidity content between the air above and below the inversion is not so extreme.

The inversion fogs along the coasts of California and north Africa are essentially summer phenomena, for only in summer is there sufficient upwelling of cold water along these coasts. Inversion fogs over continents in higher latitudes occur most frequently in winter. Certain valleys with access to the sea have frequent winter fogs. The fog develops after an invasion of warm and humid maritime air which becomes trapped in the valley, where it is cooled from below under stagnant anticyclonic conditions. The subsiding air aloft intensifies the inversion above the foggy air, which is gradually cooled by outgoing radiation. This leads to prolonged fogs which dissipate when the anticyclone breaks down. This is the typical winter fog in several of the California valleys, particularly in the San Joaquin Valley, which has a higher frequency of winter fogs than any other region in the United States. It should be noted that vertical mixing is relatively unimportant in the formation of these valley fogs; they form mainly as a result of advection followed by radiation, and they are connected with an inversion because of the anticyclonic subsidence.

62. Further Remarks on Fog.—Sea fogs are invariably of the advection type. They[1] form mostly over cold ocean currents or in regions where the sea surface is considerably colder than the adjacent continents. The following regions are noted for their high frequency of fogs.

[1] Excepting the steam fogs; see Par. 56.

The Labrador Current and the Oya Shio have frequent fogs throughout the year with a maximum in summer. In winter, it is mostly the warm maritime air masses that produce fog; in summer, fogs are frequently produced, also, in warm air from the adjacent continents.

The cold equatorward currents off the west coasts of California and north Africa (between Casablanca and Senegal) have frequent fogs in summer. Frequent fogs are also observed in the Benin Bay (November to May), along the west coasts of south Africa from 8 to 32°S (June to August), along the east coast of Africa south of Cape Guardafui (June to September), along the east coast of South America from Rio de la Plata and southward (July to September), and along the west coast of South America from 4 to 31°S (August to September). These fogs are formed on account of the cooling of the air by the passage over the cold coastal currents.
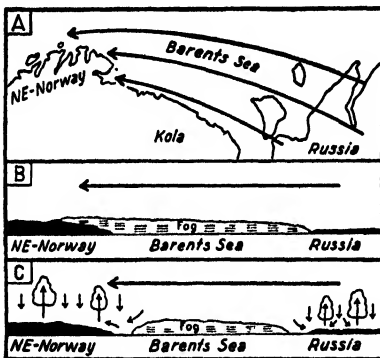
Fig. 72.—Example of arctic sea fog in north Norway. *A*, prevailing winds; *B*, night fog at sea and in coastal regions; *C*, coastal fog dissolved through convection over land.

The Norwegian Sea and the Barents Sea have frequent fogs in summer which form through advection of warm air from the adjacent continents. The same also applies to the North Sea and the Baltic, but the fogs occur here most frequently in spring or early summer when the sea surface is cold, partly on account of ice water from northern countries, while warm air is produced over central Europe and other warm sources.

Another type of sea fog is produced by the gradual cooling of air that streams poleward. Such fogs may occur everywhere on the northern oceans. Representative of this type is the *tropical-air fog* that is often observed in the warm sector of cyclones in middle or high latitudes. The same type of fog formation occurs quite frequently in returning maritime polar air in advance of a depression. In both of these cases, the advective cooling, sometimes assisted by evaporation from falling rain, is the main cause of the formation. Such fogs frequently invade the adjacent continents in winter where additional cooling causes increased density and prolonged duration of the fog. In summer, the fog usually dissolves in the first day's sunshine.

A certain type of fog formation in coastal districts may be ascribed to returning continental air. This is a typical summer phenomenon which occurs when air from a warm continent has been in contact with considerably colder sea for some time and then returns to the coast. The return of the air may be due to a change in the general weather

situation, but most frequently the foggy air is brought inland in the evening by the dying sea breeze after the land has cooled below the dew point of the sea air. Coastal night fogs of this type are sometimes observed in summer in west Norway, and also along other coasts adjacent to cold sea. Perhaps the most typical examples of this kind of fog are found along the north and northeast coast of Norway when warm air from Russia takes part in the summer monsoon that blows from an easterly direction so that the air before it reaches the coast of Norway has passed over the Arctic Sea. The conditions are illustrated in Fig. 72. In the day, when there is convection over land, the fog remains at sea in spite of moderate to fresh sea breezes. In the evening, when the convection ceases and the wind weakens, the fog is carried in over land, where it usually dissolves the next day. During the day, the fog may be seen at sea as a stationary bank in spite of the on-land component of the wind. Coastal night fogs of this kind may form even when there is no fog at sea. This happens when the air in the night cools below its dew point.

CHAPTER III

PRODUCTION AND TRANSFORMATION OF AIR MASSES

An air mass is defined as a huge body of air whose conservative properties, notably temperature and humidity or functions thereof, are more or less homogeneous in the horizontal direction. The horizontal and vertical dimensions of an air mass are normally of the same order of magnitude as those of the large systems of circulation, such as anticyclones and depressions. The various portions of an air mass must be of common "origin," and the "development," or "life history," of the various portions must be essentially the same. For example, a vast mass of air remaining over the snow-covered arctic regions for a sufficient length of time will acquire physical properties characteristic of that region. When such a mass moves toward warmer regions, it will change its properties and develop weather phenomena that are determined by the arctic origin of the mass and its movement from a cold toward a warm region. When classified according to origin and development, the air masses often appear as distinct types, and the recognition of this fact is of substantial assistance in the forecasting of weather.

63. The Chief Agencies.—The sun may be regarded as the only source of the energy that is supplied to the earth's surface and the atmosphere. The ultimate cause of all changes and motions in the atmosphere may, therefore, be sought in the heat energy radiated from the sun. The atmosphere, being almost transparent for high-temperature radiation, absorbs only a small portion of the direct solar radiation, and the earth's surface, which is a good absorbing medium, absorbs a considerable portion thereof (see Par. 50). The earth's surface may therefore be regarded as the direct source of the main supply of heat for the lower atmosphere.

The heat energy received in one place may be transported to other places by conduction, radiation, turbulence, and advection. The transfer of temperature T by conduction, radiation, or turbulence may be described by the formula[1]

$$\frac{\partial T}{\partial t} = K \frac{\partial^2 T}{\partial s^2}$$

where t denotes time and s distance and K may be interpreted as the

[1] See, for example, Brunt [19].

coefficient of molecular conduction, the coefficient of radiative transfer, or the coefficient of eddy transfer of heat.

The order of magnitude of K in c.g.s. units is, under normal conditions,

Molecular conduction.. 10^{-1}
Radiative transfer... 10^3
Eddy transfer.. 10^5

The molecular conduction of heat within the atmosphere is therefore altogether negligible, and the radiative transfer is normally small in comparison with that caused by turbulence. The advective transfer of heat, which depends on the temperature gradient and the wind velocity, may under favorable conditions greatly exceed the other agencies. In stagnant conditions, the advective and turbulent transfer of heat may become as small as, or smaller than, the radiative transfer. But in our study of how the vast air masses are formed we may consider advection and turbulence as the dominating factors.

Through the action of turbulence and convective currents, heat may be conducted effectively from one portion of the atmosphere to another. This exchange of heat is particularly active in the vicinity of the surface of the earth. As the specific heat of air is small in comparison with that of the earth's surface (land or sea), it follows that the exchange of heat between the atmosphere and the surface will have a great influence on the temperature conditions of the atmosphere. In the study of how vast air masses are formed, the properties of the earth's surface constitute a factor of prime importance.

Heat may also be transported from one place to another by advection, or large-scale air currents. Since these are mainly horizontal currents, the advective transfer of heat is mainly in the horizontal direction, whereas turbulence and convective currents transport heat mainly along the vertical. Though the turbulent exchange of heat has a tendency to smooth out temperature contrasts, the advective process may create or destroy temperature contrasts according to whether the large-scale currents are convergent or divergent. Large-scale divergent air currents, having a homogeneizing influence, are of great importance in the production of air masses within the meaning defined above, and convergent air currents are of importance in the formation of fronts (see Chap. V).

Thus, there are two chief agencies that deserve to be considered as the primary factors in the production of air masses, *viz.*:

1. The properties of the surface of the earth on which depend the amounts of heat and moisture that the air can absorb from below and that turbulence and convective currents distribute mainly in the vertical direction. The radiative exchange of heat between the surface and the air is to be recognized as a modifying factor of less importance.

2. The large-scale air currents which, when divergent, tend to produce homogeneous conditions in the air. The widespread, vertical velocities (*e.g.*, subsidence) that result from horizontal divergence and convergence are also of importance.

64. The Earth's Surface in Winter.—If the air remains over a region long enough, it will acquire a distribution of temperature and moisture
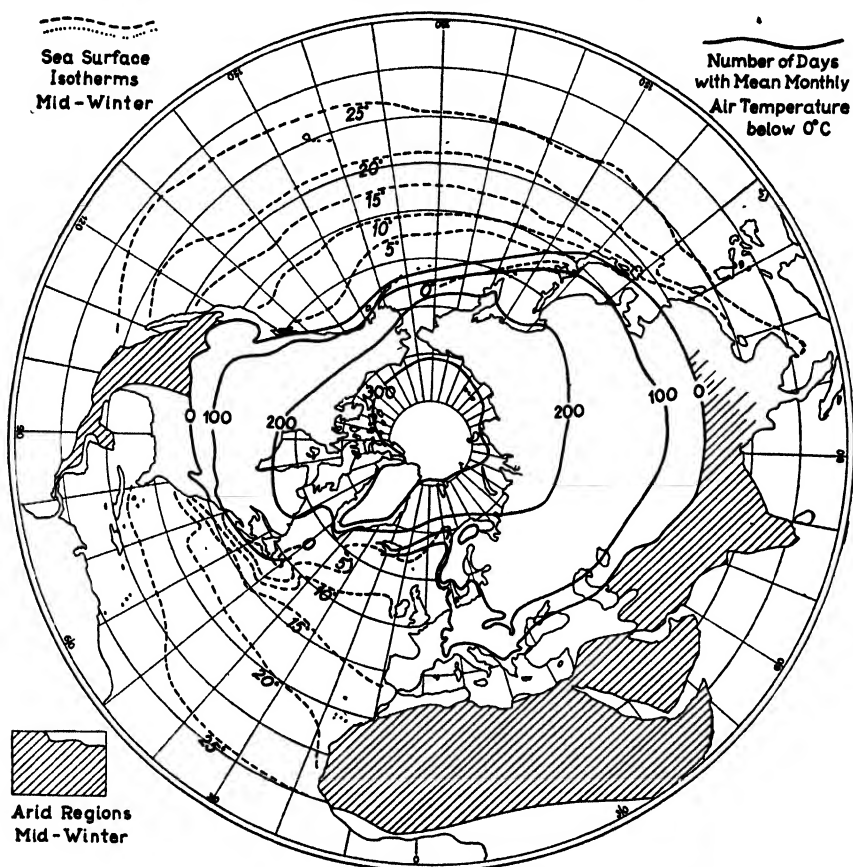
Fig. 73.—The properties of the earth's surface in winter. The curves over land indicate the average number of days with mean monthly air temperature below freezing. The curves over oceans indicate the mean sea-surface temperature in midwinter. Hatching indicates regions without snow and with pronounced winter dryness.

content that gives equilibrium with the surface underneath, and the air-mass properties will then be characteristic of the type of underlying surface. As approximate horizontal homogeneity is a characteristic feature of an air mass, it is natural to seek the regions of origin of air masses in those parts of the world where the earth's surface is fairly homogeneous and where, simultaneously, the air currents are favorable

for the formation of air masses. Such regions are called *air-mass sources* or *source regions*.

Although the normal surface temperature of most oceans is known with satisfactory accuracy, similar information regarding the temperature and humidity conditions of the continental areas is generally lacking. In winter, however, a factor of crucial importance is the distribution of snow or ice on the ground. Unfortunately, books on climatology do not contain sufficient data on snow cover, but from tables of mean monthly air temperatures it is possible to compute with sufficient accuracy the average number of days when the mean monthly air temperature is below freezing. Figure 73 shows this for the continents of the northern hemisphere.

It will be seen that the curves indicating the number of days with temperature below freezing are centered round the North Pole; otherwise, their trend is determined by the distribution of land and sea. In detail, it is not quite certain how these curves are related to the curves showing the number of days with snow on the ground, but there can be little doubt that a close correlation must exist between the two sets of curves. Taking this for granted, it appears evident that the most effective source regions for the production of cold air in winter are the arctic region and the northern parts of North America and Eurasia, for the snow-covered ground ensures fairly homogeneous surface properties.

Figure 73 also contains the normal sea-surface isotherms in midwinter. It is seen that the equatorial belts of the oceans are extremely homogeneous; also fairly homogeneous are the subtropical regions of the Atlantic and Pacific and the northeastern part of the Atlantic Ocean. In view of the great contrasts which exist in high latitudes in winter between the temperature of the sea surface and that of the adjacent continents, it appears that the northern parts of the oceans cannot be classed as source regions of air masses of low temperature in winter. These regions, particularly the eastern portions of the northern oceans, may rather be described as producers of air masses that are warmer than those of the adjacent continents.

In Fig. 73 are also indicated the snowless areas of the continents which are particularly arid. These comprise the deserts, the steppes, and the savannas with pronounced winter dryness.

With regard to the problem under discussion, we may distinguish between the following types of extensive underlying surface that influence the production of air masses in winter:

1. The arctic fields of ice, and the snow-covered parts of the continents.

2. The southern parts of the continents which are not covered by snow. The greater portion of these areas is conspicuously arid.

3. The large ocean areas which are warm and fairly homogeneous.

How these various types of surface act with respect to the formation of air masses will depend mainly on the large-scale air currents.

It will be seen from Fig. 73 that certain parts of the northern hemisphere have no place in the above classification. These areas (*e.g.*, southwest Europe and the southeastern part of the United States) are regions of frequent invasions of air masses from the neighboring sources.

65. The Earth's Surface in Summer.—As far as production of air masses is concerned, the best indication of the properties of the earth's solid surface in summer is, perhaps, the distribution of the mean annual maximum temperature. It has been found that the large-scale distribution of this element is expressive of the capacity of the underlying surface for transferring radiation into heat. As a compromise between intensity and diurnal duration, the sum of incoming radiation in midsummer attains a maximum in middle latitudes. Nevertheless, both the mean monthly temperature and the mean annual maximum temperature have their maxima south of this latitude. This condition is partly due to advection of air and partly to reflection of radiation from the clouds, but it is also due to the nature of the underlying surface. Thus, the deserts and the summer-dry steppes accumulate the absorbed heat in the upper few centimeters of the sandy soil, and practically all the absorbed radiation is converted into heat. In the northern moister regions of grass and woodland, part of the absorbed radiation is expended in evaporating water, and part is expended in chemical processes. As a result, the midsummer maxima of temperature are found in regions that are conspicuously arid. These regions are characterized by a mean annual maximum temperature of about 40 to 45°C.

It will be seen from Fig. 74 that the great expanses of grassland and forests have a fairly *uniform* mean annual maximum temperature of about 30 to 35°C., whereas great contrasts occur along the coasts. It is important to bear in mind that the extreme temperatures are largely independent of advection, for they develop mostly in rather stagnant air. We may, therefore, take the mean annual maximum temperature as an indication of the fitness of the region in question for producing warm air masses. Disregarding the coastal regions and the tundra areas, it follows from Fig. 74 that we may distinguish between three principle types of continental area in summer, *viz.*:[1]

1. The equatorial belt of high temperature and high moisture content (*i.e.*, the *A* climates: tropical forests and savannas).

2. The subtropical arid regions of extremely high temperature (*i.e.*, the *B* climates: deserts and steppes). .

3. The forest regions in high and middle latitudes with moderate temperature and moisture content (*i.e.*, the *D* climates).

[1] See the classification of climates by Köppen [40].

Figure 74 also contains the mean isotherms of the sea surface in mid-summer. It will be noticed that, on the whole, the temperature of the sea surface is much more homogeneous in summer than in winter (see Fig. 73).

FIG. 74.—The properties of the earth's surface in summer.

How the various regions of the northern hemisphere act with respect to the production of air masses will depend mainly on the large-scale air currents. This will be discussed in later sections.

66. Circulation of the Free Atmosphere.—In older literature on this subject, it was customary to consider the general circulation of the free atmosphere as being purely of a zonal character and consisting of trades, antitrades, and prevailing westerlies. The fact that the subtropical anticyclones do not consist of a uniform girdle of high pressure was either overlooked or considered to be of minor importance. Bergeron [1, 4] was the first to emphasize the importance of the separate anti-

cyclones with intermediary cols for the production of fronts and air masses. J. Bjerknes [13], and later V. Bjerknes [17] have developed a "cell theory" of the general circulation that accounts for the existence of separate anticyclones and intermediary cols arranged as a belt in the sub-tropics. In view of its importance for the understanding of the production of air masses, fronts, and cyclones, the essential features of this theory are summarized here.

1. If no temperature differences were in action, friction would annihilate every internal relative motion, and the earth and its atmosphere would rotate like a rigid body. The atmosphere would then form a simple barotropic circular vortex, isobaric and isosteric surfaces coinciding with the equipotential surfaces of the resultant of gravitational attraction and centrifugal force.

2. In the troposphere, the temperature decreases from the equator toward the poles. This temperature field is too weak to overcome the internal stability of the rotating atmosphere, except, perhaps, at very low latitudes. The result is a balanced circular vortex in which the wind velocity increases from the ground to the tropopause, when we ascend along a direction parallel to the earth's axis. The difference between the vortex (1) and the vortex (2) is that, in the latter, the lower tropospheric strata become displaced toward the equator whereas the higher tropospheric strata become displaced toward the poles.

3. It is thus seen that circles at the ground have expanded as a result of the transition from vortex (1) to vortex (2); they have obtained reduced circumferential velocity and, therefore, have smaller circumferential velocity than the ground below them at their new latitudes. They will be accelerated by frictional stresses from the ground, and this will cause the total angular momentum of the atmosphere to increase, and the accelerated circles near the ground to be displaced toward the
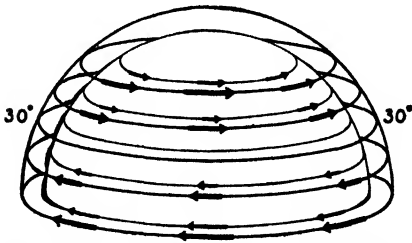
Fig. 75.—Idealized zonal circulation. *(After V. Bjerknes.)*

equator, while, in compensation, circles in the upper atmosphere will be displaced poleward. The latter circles, on account of their contraction, will obtain a higher angular velocity than the solid earth below. They descend toward the ground in the polar regions where they form a layer of greater angular velocity than the earth; this layer becomes retarded by friction from the ground.

In this way, two zones are formed (Fig. 75), one in low latitudes where the earth accelerates the motion of the atmosphere, and one in high latitudes where the earth decelerates this motion. The steady state is

reached when the moments of the accelerating and retarding frictional forces have become numerically equal. Experience shows that this balance is attained when the two zones are more or less equal in area, the lines of demarcation running approximately along the parallels 30°N and S.

Excepting a shallow layer of easterly winds at the poles, the above explains some of the observed facts, *viz.*, an intertropical zone of easterly winds (of angular velocity less than that of the earth), and two extratropical zones of prevailing westerlies (of angular velocity greater than that of the earth). The pressure distribution that corresponds to the above-mentioned circulation is as follows: a uniform belt of high pressure over each hemisphere in the subtropics, a deep low-pressure area centered at each pole, and also a uniform belt of low pressure along the equator. The foregoing deductions, therefore, do not explain the existence of centers of highs and cols in the tropical belt of high pressure. Moreover, the purely zonal circulations do not allow of any meridional exchange of heat.

4. It remains now to discuss the secondary effect of friction within each zone. On account of their excess of centrifugal force, the frictionally accelerated circles near the ground in the intertropical zone tend toward the equator, and the frictionally retarded circles near the ground in the extratropical zones tend toward the poles because of their deficit of centrifugal force. These meridional circulations in the lower layers involve, for continuity reasons, opposite meridional circulations in the upper atmosphere. The resulting motion would be helicoidal (screw motion), and the intertropical zone would contain two such currents, one on each side of the equator. As the frictional effect decreases rapidly along the vertical, the equatorward current would be shallow and strong, and the upper poleward current would be deep and weak. In the extratropical zones, the conditions would be similar, with a shallow layer of strong poleward component along the surface and a deep current of moderate equatorward component above. In both zones, the zonal components of velocity would be predominating.

Even though the foregoing explains in broad outlines the observed zonal distribution of the circulation, there are admittedly considerable difficulties in the way of explaining the meridional circulations. The most obvious difficulties are those connected with the energetics and the stability of the extratropical circulations. Thus, outside the intertropical zone, the currents revolve in a negative sense relative to the solenoids, which means that they constantly give off kinetic energy. The only source of energy for the maintenance of this motion would be the frictional coupling with the trade currents; but this coupling is highly imperfect on account of the subtropical belt of calms between them.

In considering the question of stability, we meet with the obvious difficulty that there is no uniform zonal distribution of pressure which can account for the winds observed. The helicoidal currents (Fig. 76) running zonally around the earth cannot, therefore, represent a stable state of motion.

FIG. 76.—Helicoidal currents. (*After V. Bjerknes*.)
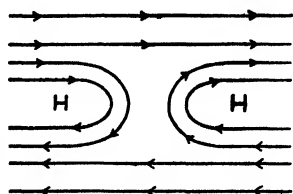
FIG. 77.—Cols in the subtropical belt of high pressure.

As has been shown by J. Bjerknes [13], a stable state can exist only when the subtropical belt of high pressure is divided into separate anticyclones, or cells, separated from one another by cols (Fig. 77). Theoretically, these cols should be regarded as disturbances which would then migrate (as they often do); but, on account of the distribution of land and sea, certain regions (*e.g.*, coasts) have a tendency to develop quasi-stationary cols which predominate in the average picture. With the division of the high-pressure belt into separate anticyclonic centers, the two helicoidal currents on either side of the subtropical belt join in the vicinity of the cols and form the stable circulations of the subtropical anticyclones (Fig. 78).
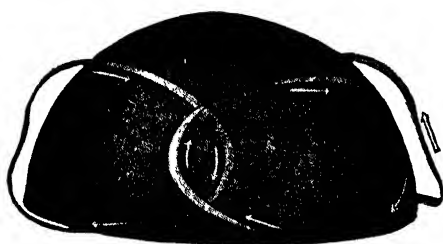
FIG. 78.—Cellular anticyclonic circulations. (*After V. Bjerknes*.)

It should be mentioned that Rossby [67] has attacked the problem of the general circulations of the free atmosphere from a different point of view. His theory gives a satisfactory relation between the solenoids and the prevailing winds. According to Rossby's theory, the mean field of solenoids in the middle latitudes (the polar front region) creates the prevailing westerlies, which throw off large anticyclonic eddies on their equatorial side. These eddies constitute the necessary brakes in the system of circulations.

It will be understood that the theories of the general circulations are as yet incomplete. The strength of these theories lies in the circumstance that the deductions seem to agree in the main with what is observed in the free atmosphere.

67. Consequences of the Cell Theory.—Although the reader is referred to the works cited above for a detailed discussion of the assumptions and facts on which the cell theory is based, it is of interest to summarize here those consequences of the theory that are of importance for the understanding of how air masses and fronts are formed.

1. As the two helicoidal currents north and south of the subtropical anticyclone join in the vicinity of the cols and form a cellular circulation round the anticyclonic center (Fig. 78), the air on the equatorial side will ascend as it moves westward and descend as it moves eastward in the northern half of the cell.[1] A zonal inclination of the "planes of orbit" of 1/10,000 suffices to make the air circulate in a positive direction round the solenoids, and no frictional coupling is required to maintain the circulation. As the longest axis of a subtropical cell is of the order of magnitude of 4000 to 9000 km., it follows that the air, while moving from the eastern to the western end of the cell, will ascend about 400 to 900 m. and will descend the same distance while moving eastward. The planes of orbit are, of course, horizontal when close to the surface of the earth. The maximum inclination of the planes of orbit is found at about 5000 m. above the earth's surface. As ascent favors instability and descent is conducive to stability (see Par. 45), it follows *that the air in the eastern part of the cell will be more stable than the air in the western part.*

2. Where the opposite currents belonging to contiguous cells pass through the same col, the one coming from the equatorial side will be warmer than that coming from the temperate zone. The surface of separation between the two currents must therefore be inclined, *the warmer current overrunning the colder. The so-called "antitrade" exists only above the surface of separation between two adjacent cells.*

3. In the space above the friction layer and below the level of maximum inclination of the planes of orbit, the air will converge horizontally in the region of ascent (on the equatorial side) and diverge horizontally in the region of descent (on the poleward side). A closed horizontal curve within the ascending air contracts, and a corresponding curve expands in the area of descent. These curves (being horizontal) comprise no solenoids and, therefore, conserve their circulation in absolute motion. Observed from the rotating earth, the westward-moving contracting curve is then seen to reduce its anticyclonic circulation, and the eastward-moving expanding curve to increase its anticyclonic circulation. Consequently, there will be a minimum of anticyclonic curl relative to the earth at the western end and a maximum of anticyclonic curl at the eastern end of the cell.

In the space above the level of maximum vertical velocity, the conditions are reversed, and there will be a maximum of anticyclonic curl at

[1] The discussion is henceforth limited to the northern hemisphere.

the western end and a minimum at the eastern end of the cell.   The axes of the anticyclones will therefore tilt from east to west; and although the highest pressure at low levels is observed (on the average) in the eastern half of the anticyclone, the highest pressure in the free atmosphere will be observed farther to the west.

4. The tilting of the axes of the subtropical anticyclones may also be deduced from the equation of static equilibrium (see Par. 47),

$$- \frac{\partial p}{\partial z} = \rho g$$

As ρ is inversely proportional to the temperature, it follows that the pressure decreases more slowly with altitude in warm air than in cold air. As the air in the eastern portion of the cell is colder than in the western portion, it follows that the center of highest pressure must be displaced toward the warmer half of the anticyclone as the altitude increases.   From this, it follows that *the axis of a subtropical anticyclone tilts westward and equatorward.*

5. In the above deduction, the divergent outflow in the friction layer has not been considered.   On account of this outflow, *a general subsidence develops above the friction layer to compensate for the outflow.*
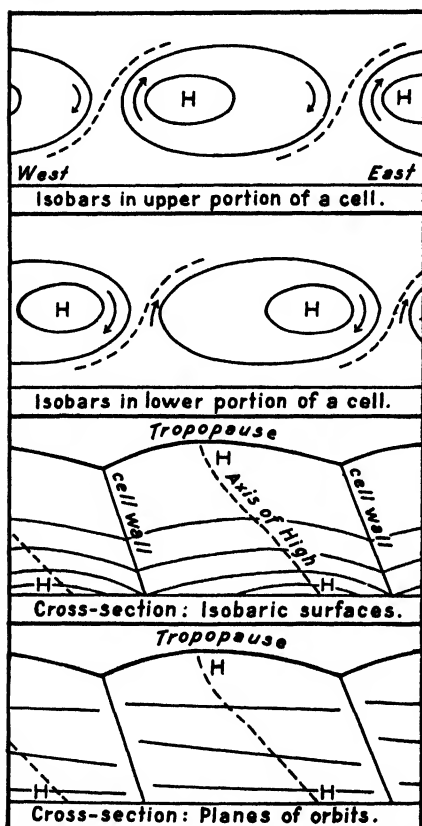
FIG. 79.—Showing the structure of a subtropical cell.

This descending motion is often strong enough to overcompensate the ascent that results from the orbital movement.   Figure 79 shows the predominant features of the subtropical cells under normal conditions.

68. Further Remarks on Subtropical Anticyclones. 1. *Pressure Distribution in Various Levels.*[1]—Figures 80 and 81 show the mean distribution of pressure at sea level in winter and in summer.   The conditions in the 2-km. level are shown in Figs. 82 and 83.   It will be seen from Figs. 80 and 82 that the cold winter anticyclones vanish with increasing altitude.   Thus, already in the 2-km. level, the cold continental

[1] Figures 80 to 85 are based essentially on Shaw's maps [73a] modified with the use of more recent data.

anticyclones of Siberia and North America are completely submerged, and the general circulation above this level in winter is, on the average, controlled by an immense area of low pressure centered at the North Pole. It will be observed from Figs. 81 and 83 that the warm continental lows in summer vanish with increasing altitude and change into anticyclones. This applies to south Asia, north Africa, and the southwestern
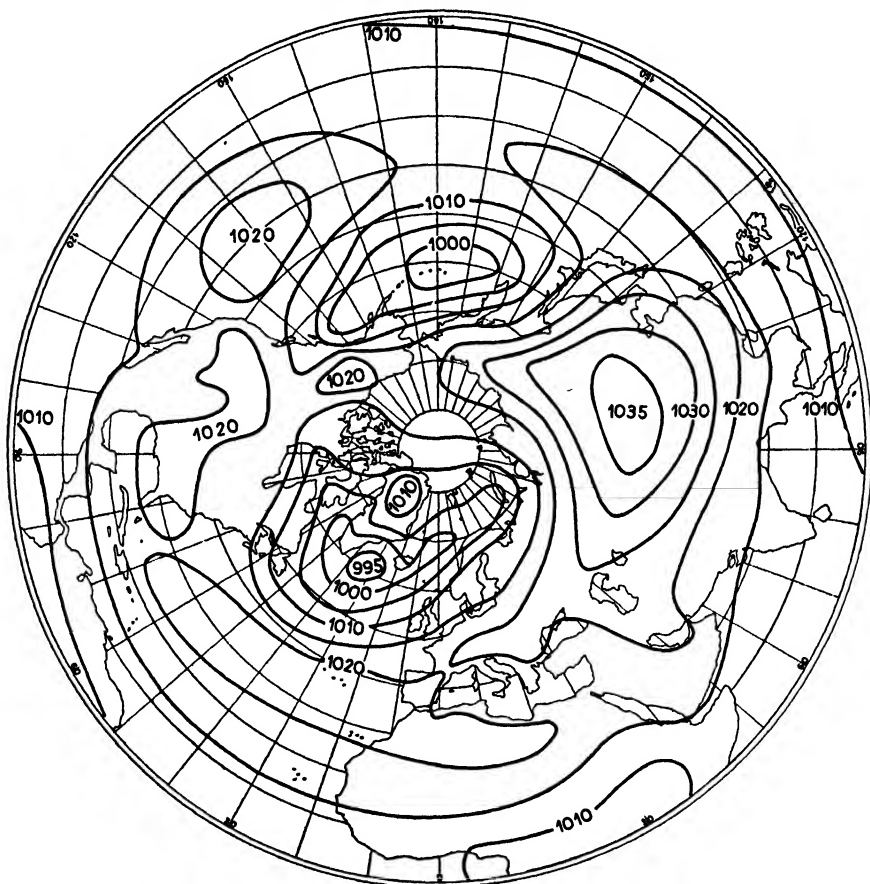
Fig. 80.—Mean distribution of pressure at sea level in winter.

part of the United States. It will also be noticed that the anticyclones, which are warm at sea level, predominate in the upper atmosphere and that their axes tilt toward the warmer regions. Figures 84 and 85 show the mean pressure distribution in July in the levels of 4 and 8 km., respectively. The anticyclonic centers in these levels are situated above the warm continental low-pressure areas. It will be noticed that the observed pressure distribution, in the main, corroborates what was inferred from the cell theory of the general circulation.

2. *Size of Subtropical Anticyclones.*—It is important to note that the maps presented above represent the mean conditions averaged
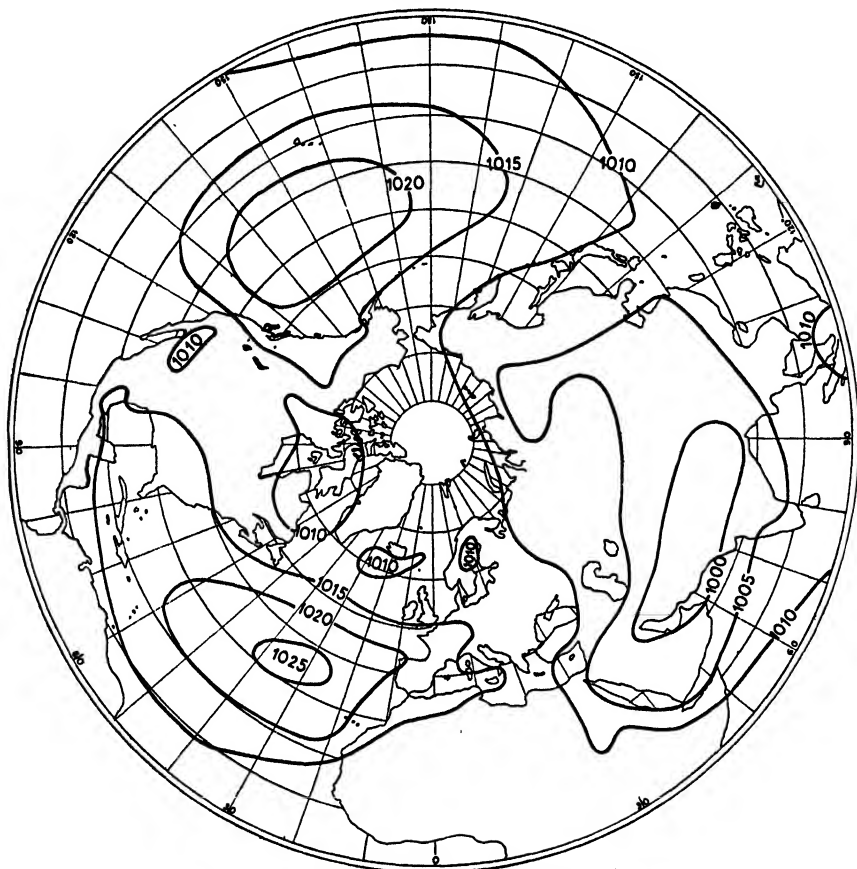
Fig. 81.—Mean distribution of pressure at sea level in summer.

over a large number of years. The maps, therefore, give only a blurred picture of the actual subtropical cells. It will be noticed (*e.g.*, from Figs. 80 and 81) that the average subtropical anticyclones at sea level

TABLE 18.—Percentage Frequency of Length of Longest Axis of Subtropical Anticyclones on the North Pacific Ocean, 1930 to 1934

Length, km.	Summer	Winter	Length, km.	Summer	Winter
Less than 3000.......	4	18	6000–7000...........	14	9
3000–4000...........	17	36	7000–8000...........	18	4
4000–5000...........	22	20	8000–9000...........	16	0
5000–6000...........	8	13	Larger than 9000.....	2	0

occupy about 90° long. This is due to the circumstance that the migratory cols are suppressed in the mean picture. The zonal dimensions of the actual subtropical cells are, therefore, smaller than those brought to light by the mean maps. That this is so, is shown clearly by the data contained in Tables 18 and 19.

TABLE 19.—PERCENTAGE FREQUENCY OF NUMBER OF SIMULTANOEUS SUBTROPICAL ANTICYCLONES ON THE NORTH PACIFIC OCEAN, 1930 TO 1934

Number	0	1	2	3	4
Summer..	1	71	28	0	0
Winter..	2	43	55	1	0
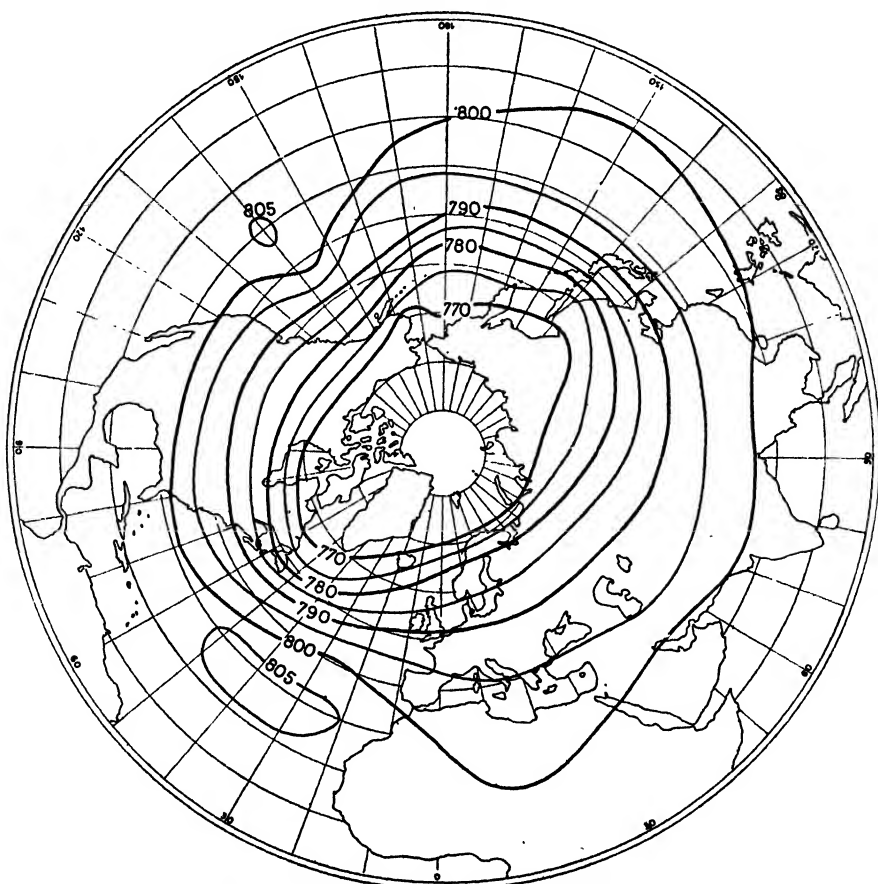
FIG. 82.—Mean distribution of pressure in the 2-km. level in winter.

It will be seen that the winter cells are most frequently less than 5000 km. in length and that there are normally two simultaneous cells

on the North Pacific. In summer, the cells are, on the whole, larger, and most frequently there is only one cell present. Therefore, on the weather maps, the actual cells are not nearly so large as those shown on the mean-pressure maps. Moreover, the actual cells are more distinct than those shown on the mean maps.
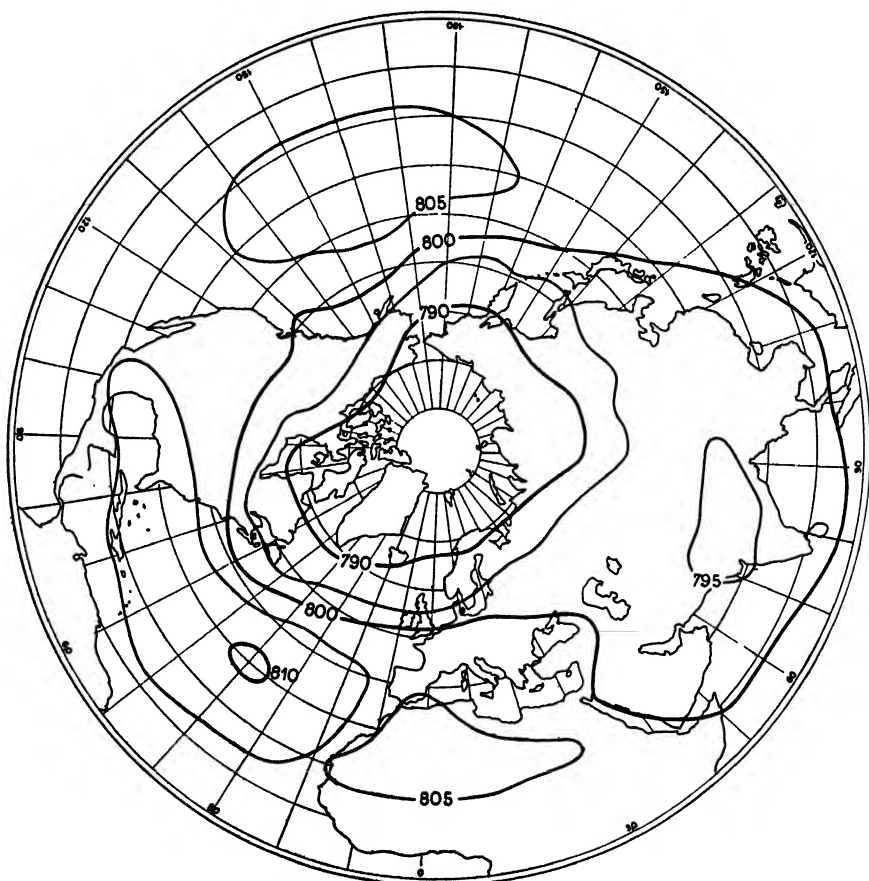
FIG. 83.—Mean distribution of pressure in the 2-km. level in summer.

3. *Anticyclonic Eddies in the Free Atmosphere.*—It is frequently observed[1] that anticyclonic eddies of quite small dimensions (1000 km., or so) form in the free atmosphere, notably in the southern region of the prevailing westerlies, and move into the belt of subtropical anticyclones. According to Rossby, these eddies are necessary links in the general circulation; and it is plausible that the actual subtropical anticyclones in the upper atmosphere often consist of a series of such eddies. These eddies are, of course, eliminated in the mean-pressure maps. Aerological

[1] ROSSBY [67].

observations from the United States show that such eddies, of high-level anticyclones, are often present in the free atmosphere in the warm season and sometimes also in the cold season.

The air motion in these eddies is characterized by marked subsidence which often produces a warm and exceedingly dry air mass aloft (see Par. 83).
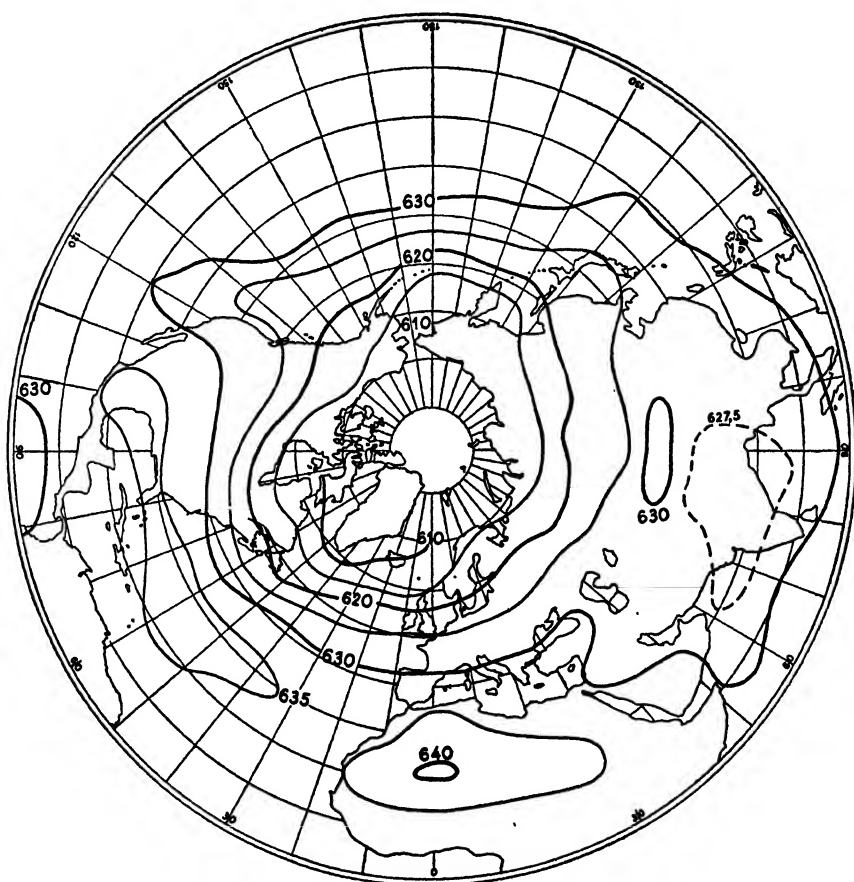
Fig. 84.—Mean distribution of pressure in the 4-km. level in summer.

69. The Larger-scale Air Currents in Winter.—It was mentioned in Par. 63 that the physical properties of the earth's surface and the large-scale air currents in the lower atmosphere are factors of primary importance for the production and transformation of air masses. We shall, therefore, discuss in greater detail the air currents in the lower atmosphere. These are shown in Fig. 86. With a view to the problem under discussion, we may distinguish between the following types of circulation:

1. Anticyclonic systems, or regions of stagnant air surrounded by divergent air currents.

2. Cyclonic systems, or regions of stagnant air surrounded by convergent air currents.

3. Belts of convergence.
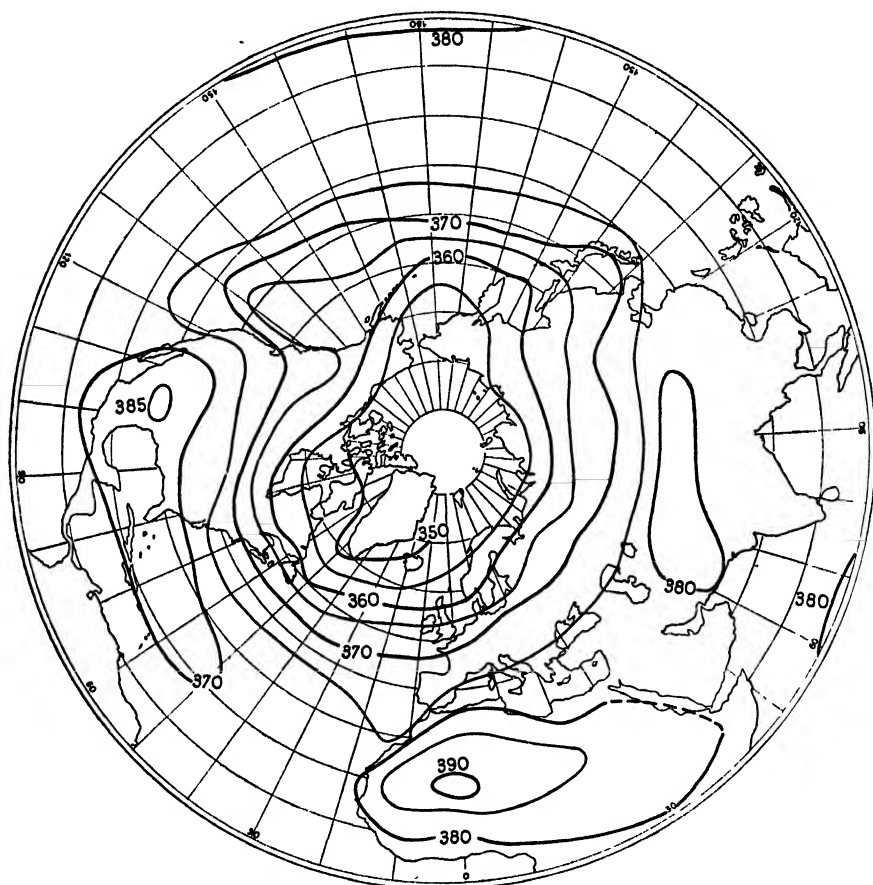
FIG. 85.—Mean distribution of pressure in the 8-km. level in summer.

4. More or less straight currents of considerable extent or persistence which transport air from cold to warm regions, or vice versa.

1. *Anticyclones.*—In the central parts of anticyclones, or belts of high pressure, the air is stagnant or slowly moving; it therefore has sufficient time to adjust its temperature and moisture content to the underlying surface. The same also applies to air that travels with considerable speed over a homogeneous surface or along the isotherms of the surface underneath.

The currents round the anticyclones are divergent. The properties absorbed in the central parts will, therefore, be spread over large areas, while turbulence and convective currents gradually distribute the absorbed properties to great heights. A phenomenon accompanying divergence is a general subsidence in the upper atmosphere. It was shown in Par. 45 that subsidence diminishes the lapse rate of temperature,

Fig. 86.—Surface air currents in mid-winter.

and this has a stabilizing effect on the air. This stabilizing effect is counteracted by the heating of the air from below; but, in regions where cold air is produced, subsidence in the upper air and cooling from below will tend to make the stratification extremely stable, and this will hinder the turbulent transfer of properties upward. On the other hand, great stability favors horizontal (lateral) mixing.[1] Horizontal divergence

[1] Rossby [68].

and lateral mixing, therefore, combine to produce horizontal homogeneity in the air masses produced in anticyclonic regions.

Anticyclones with their longest axes orientated along the isotherms of the underlying surface are more effective air-mass producers than those which have their longest axes along the gradient of the surface temperature. As warm anticyclones extend to great heights and cold anticyclones reach only to moderate heights, it is evident that the former will produce air masses of great vertical extent and the latter will produce air masses of moderate vertical extent.
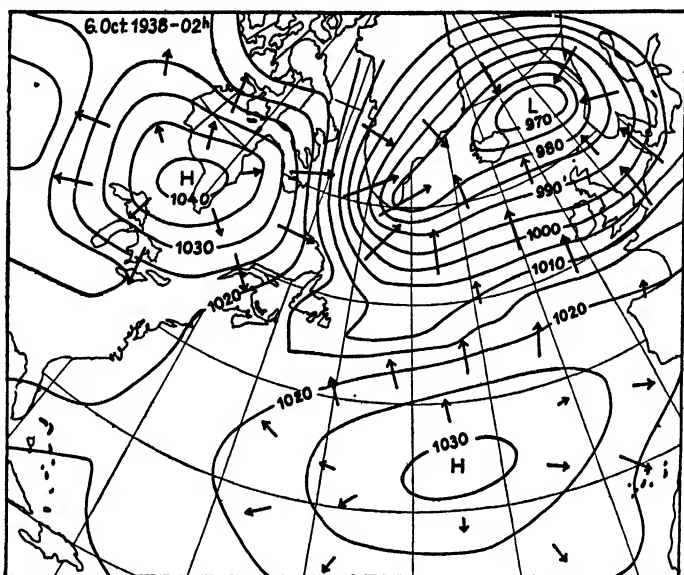
FIG. 87.—Showing an example of divergence and convergence in anticyclones and cyclones, respectively.

2. *Cyclones.*—The regions of stagnant air surrounded by converging winds are not air-mass sources. The areas of stagnant air in the cyclonic systems (*e.g.*, the Icelandic low and the Aleutian low) are of small extent, and the convergence toward the center of lowest pressure will tend to create temperature contrasts. Moreover, the air that is brought toward the center ascends and thus loses contact with the underlying surface. As will be shown in a later chapter, cyclones form along the border between adjacent air masses, and the paths of cyclones most frequently follow the zone where there is a maximum temperature gradient in the underlying surface. None of the conditions that are required for formation of quasi-homogeneous air masses is normally fulfilled in cyclones. The air that partakes in the cyclonic systems will be subject to considerable changes, but these do not result in the creation of a uniform mass of air.

Figure 87 shows an example of the order of magnitude of the divergent outflow and the convergent inflow in anticyclones and cyclones, respectively. The arrows indicate the distances that the air near the earth's surface would flow in a direction normal to the isobars in 24 hr. under stationary pressure conditions. The amount of subsidence in the anticyclones and the amount of ascent in the cyclones are in direct proportion to the horizontal outflow or inflow, respectively.

3. *Belts of Convergence.*—Belts or zones of convergence are found in the doldrums (Fig. 86) and also across the Pacific and Atlantic oceans between air of polar and tropical origin. Pronounced convergence is also found along a belt extending from the southwest of Iceland toward the Taimyr Peninsula, and slight convergence is found along the Mediterranean basin, between the Siberian high and Alaska, and between the small high over Alaska and the larger high farther to the south. These zones of convergence are of no direct importance in the production of air masses, but they are of fundamental interest in understanding the formation of fronts. It suffices here to mention that the zones of convergence often form the natural limitation of the air masses produced in the anticyclonic systems.

4. *More or Less Straight Currents.*—Large areas of the world are occupied by more or less straight currents which transport air from colder to warmer regions, or vice versa. These currents have their origin in anticyclonic regions and terminate in cyclonic systems or belts of low pressure. Near their origin, they are under the influence of the anticyclonic divergence and subsidence, and they usually end in areas of low pressure with convergence and ascending motion. Such currents are most pronounced on the equatorial sides of the subtropical high-pressure belts (*e.g.*, the trade winds and the northeast monsoon). As these currents are mostly directed across the isotherms of the underlying surface and are of considerable strength and persistence, they are producers of air masses only where the temperature gradient over the underlying surface is small. Outside the anticyclonic control, subsidence is no longer operative, and the air partaking in these currents becomes less stable. This favors the turbulent exchange of heat between the surface and the higher strata of the atmosphere.

70. The Large-scale Air Currents in Summer.—The current systems in the lower layers of the troposphere are considerably modified as the northern continents become warmer than the adjacent oceans. It will be seen from Fig. 88 that we may distinguish between the following types of circulation:

1. Two huge anticyclonic systems in subtropical latitudes, one over the North Atlantic Ocean and another over the North Pacific Ocean.

The winds invade the adjacent continents on the western sides of the anticyclones as summer monsoons.

2. A huge monsoon system with winds blowing across the equator and converging toward the continental low pressure area over south Asia.

3. Weak and variable winds in the interior of the northern continents.
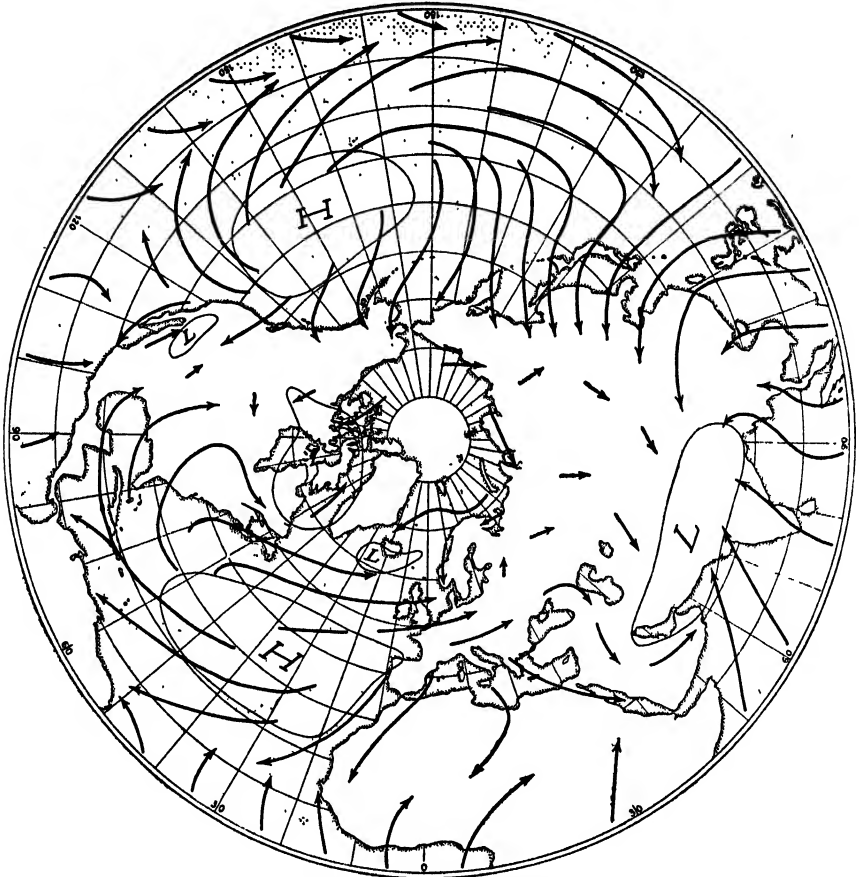
FIG. 88.—Large-scale air currents in summer.

4. Weak anticyclonic winds over the arctic fields of snow.

5. A belt of converging trade winds (the doldrums) across the Pacific and Atlantic oceans, continuing across north Africa.

71. Air-mass Sources in Winter.—The temperature and humidity conditions of the earth's surface and the large-scale air currents being the predominant factors in the production and transformation of air masses, we may now combine the discussion of their influence in order to localize the principal source regions of the northern hemisphere in winter.

Roughly speaking, we may distinguish between five principal zones, or regions, which are more or less distinctly separated from one another by the nature of the underlying surface or by the type of circulation.

1. The polar region comprising the arctic fields of snow and ice and the snow-covered portions of northern continents in which the surface is extremely cold and the wind system predominantly of the anticyclonic type.

2. The region of the subtropical anticyclones in which the temperature of the earth's surface is fairly uniform and the wind system predominantly anticyclonic.

3. The region of transition between (1) and (2).

4. The equatorial region in which the temperature of the earth's surface is extremely uniform.

5. The region of transition between (1) and (4), or the monsoon region in Asia.

Each of these principal zones may be subdivided as shown in Fig. 89.

1. The *source region of cold air* occupies the arctic fields of snow and ice, and at least, also, the snow-covered portions of the continents. On account of its snow cover, the surface is fairly uniform and is characterized by excessive outgoing radiation and reflection of insolation, a large negative temperature anomaly, and slight evaporation. Within the entire region, the air is either stagnant or slowly moving, or it moves mainly along the isotherms of the underlying surface. The prevalent anticyclonic divergence contributes to the homogenification of the air. Thus, within the entire region, both the surface properties (Fig. 73) and the prevailing winds (Fig. 86) are favorable for production of a fairly uniform mass.

Figure 73 shows that the zone between the isolines for zero and 100 days with monthly mean temperature below freezing is very narrow. There is, therefore, a rapid transition from ground without snow cover to the region with snow cover for 100 days or more. Throughout the winter months, snow-covered ground is typical for the region. In Köppen's classification of climates, the southern limit of effective snow cover is drawn along the −3°C. isotherm in the coldest month. On the whole, this isotherm falls in the zone between the isolines for 50 and 100 days with mean monthly temperature below freezing. With minor exceptions, the source region of the winter-cold air masses comprises the arctic and the boreal climates, and also parts of the winter-cold arid climatic zones, or, in Köppen's [40] classification, the *E, D, BWk* and *BSk* climates.

On account of advection of air from the Atlantic (Fig. 86) toward the Barents Sea and because of the prevailing cold easterly current farther to the north, the source region of cold air may be divided into two distinct

parts, *viz.*, one that is mainly under the influence of the arctic and American circulations, and a polar continental region that is controlled by the Siberian circulation.

The border between the Siberian and the arctic circulation is quite distinct west of Novaya Zemlya and less distinct farther to the east;
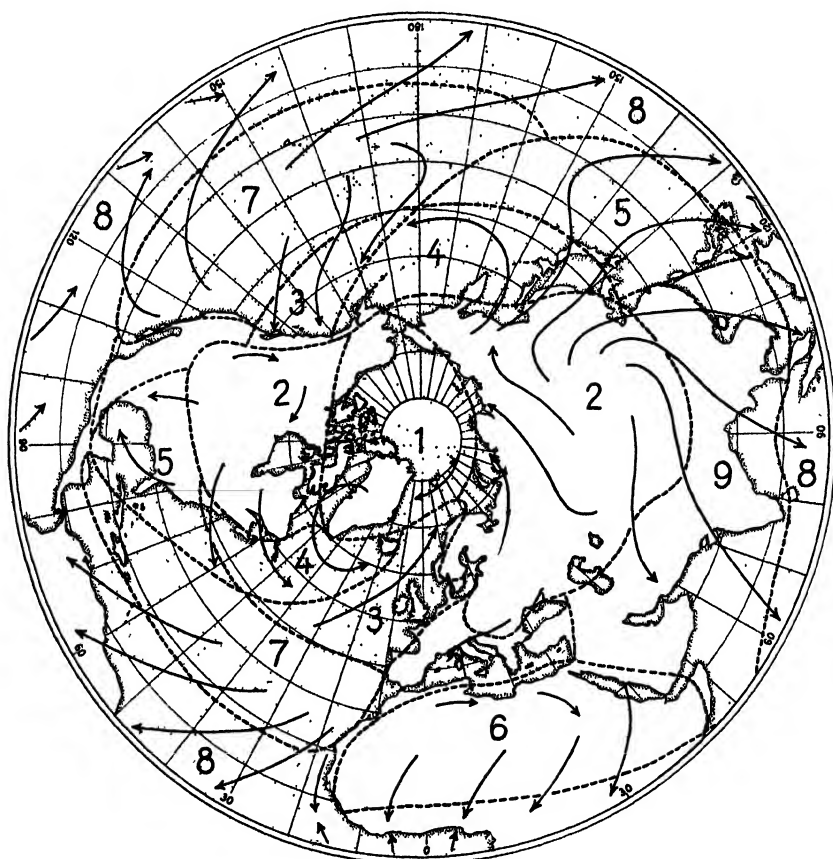
Fig. 89.—Air-mass sources of the northern hemisphere in winter.   1, arctic; 2, polar continental; 3, polar maritime, or transitional; 4, transitional; 5, transitional, or tropical maritime; 6, tropical continental; 7, tropical maritime; 8, equatorial; 9, monsoon.

but, in perturbed cases, the Siberian circulation may be completely separated from the arctic one.   On the American side, there is no distinct limit between the arctic and polar continental circulations; but in certain cases, notably when the North American high is dislocated toward the south, such a separation may develop, though most frequently there is a gradual transition from the arctic source to the polar continental source of North America.

Thus, the source region of the winter-cold air masses may be sub-divided in three portions, viz.,

a. The arctic source (*i.e.*, the region indicated by 1 in Fig. 89).

b. Two polar continental sources (*i.e.*, the regions indicated by 2 in Fig. 89), of which only the Siberian is frequently and clearly separated from the arctic source.

2. The *source regions of tropical air* occupy the subtropical high-pressure belt which may be divided into three main divisions, viz., two oceanic sources (*i.e.*, the regions indicated by 7 in Fig. 89), and one continental source (6, in Fig. 89). On account of the monsoon in South Asia, there is no proper subtropical high over the Indian Ocean.

The Pacific and the Atlantic anticyclones, or cells of circulation, are situated over fairly homogeneous water; and, on account of the prevalent divergence (see Fig. 86), these regions are excellent air-mass sources. On the poleward side, these regions are separated from the arctic and polar continental sources by a zone of transition (see below). The northern limit of the Atlantic subtropical source is drawn in Fig. 89 along the line indicating about equal frequencies of occurrence of polar and subtropical air masses. North of this line, the anticyclonic control (divergence and subsidence) is normally negligible. In the Pacific area, the corresponding line of separation has been drawn by analogy with that over the Atlantic Ocean.

On the equatorial side of the high-pressure belt, the subtropical region gradually merges into the equatorial region, and there is no distinct limit between them. The line of separation in Fig. 89 has been drawn where the anticyclonic divergence vanishes. This line coincides mainly with the zone where there is a distinct maximum in the southward increase in humidity, cloudiness, and precipitation.[1] Moreover, south of this line, the sea-surface temperature is extremely uniform.

The north African high is separated distinctly from the source of continental polar air over Eurasia by the low-pressure area over the Mediterranean basin. On the equatorial side, the air from the north African high flows over extremely arid ground, and only when it comes over the wetter ground close to the doldrums does it absorb so much moisture that it deserves to be classed as equatorial air. Along the Atlantic Coast, there is a distinct limit between the tropical continental and the tropical maritime sources, though, on the Arabian side, there is no distinct limit, Arabia sometimes being under the influence of Asiatic and sometimes under the influence of African circulation.

3. The *zone of transition between polar and tropical air* occupies mainly the northern portions of the Atlantic and Pacific oceans. Considering

[1] See, for example, GERHARD SCHOTT, "Geographie des Indischen und Stillen Ozeans," Verlag von C. Boysen, Hamburg, 1935.

the distribution of sea-surface temperature and prevailing winds, the Atlantic and the Pacific transitional zones may each be subdivided into three portions.

In the Atlantic region 3 (Fig. 89), the sea surface is extremely homogeneous in winter (see Fig. 73) and the prevailing air current is from the southwest, or along the isotherms of the sea surface. Under favorable conditions, region 3 in the Atlantic may produce a typical air mass of polar maritime character. This happens when a broad and stationary current from the southwest lasts for some days or when a migrating anticyclone settles down in this area. However, when a depression moves up to north Scandinavia, Spitsbergen or the Barents Sea, arctic air, sometimes in strong outbreaks, occupies region 3 where it rapidly becomes transformed. At other times, air of tropical origin (from region 7 and very rarely from region 6) streams northward into region 3, which then transforms tropical air into maritime polar air.

On the whole, region 3 is a region of transition; most frequently, it is occupied by air from the arctic or the polar continental sources, and sometimes by air from the tropical source. These masses usually do not remain in region 3 long enough to acquire typical properties. Sometimes, however, the wind circulation allows the air to remain within this region long enough to become uniform. In such cases an air mass results that in many ways resembles the tropical air, and it is then often difficult to draw a definite limit between the tropical and the polar maritime masses.

The conditions in the North Pacific are analogous to those in the North Atlantic, except that the Pacific region 3 is on the whole smaller and less homogeneous than the corresponding Atlantic region. It is worthy of note that, in winter, the area of the arctic and polar continental sources greatly exceeds that of the polar maritime sources. The winter maritime polar masses usually form through consenescence of air from the neighboring sources.

The Pacific and the Atlantic region 4 occupy mainly the area of the cold east coastal ocean currents in which the sea-surface temperature exhibits a veritable maximum of gradient. In these regions, the air current is mainly against the gradient of the temperature of the underlying surface. The region 4 can therefore under no circumstances be a source region of air masses, but the invading air masses are rapidly transformed. In these regions, the polar continental air is rapidly changed from a dry and stable to a humid and unstable mass.

In the two regions indicated as 5 in Fig. 89, the sea-surface temperature is high, and the main air currents are from polar continental sources. Most frequently, these regions act as regions of transformation of polar continental air into tropical air. This happens pronouncedly when a

depression is situated in or near region 4. At other times, when the subtropical highs are displaced far to the west, the two regions indicated by 5 will act as effective sources of tropical air.

Thus, the transitional zones over the Atlantic and Pacific oceans between polar continental and tropical air may each be divided into three regions, *viz.*: (*a*) an easterly warm region which is frequently invaded by air from arctic, polar continental, and tropical sources and which sometimes produces uniform masses of maritime polar air, (*b*) the region of the cold ocean currents and northwesterly winds in which polar continental and arctic air are rapidly transformed into maritime polar air, and (*c*) a southwesterly region in which polar continental air is transformed into tropical air and which under favorable wind conditions may act as a good source of tropical air.

The Mediterranean region forms a special zone of transition that is frequently invaded by air from all adjacent sources. The same also applies to southwest Europe and the western part of the United States.

4. *The equatorial region* (8) occupies a considerable portion of the surface of· the earth between the subtropical anticyclones of the northern and southern hemispheres. In this region, which is mainly oceanic, the temperature of the earth's surface is extremely uniform so that a homogeneous equatorial air mass is produced on each side of the doldrums regardless of the type of wind circulation.

5. *The monsoon region* (9) occupies a vast area in which there is a direct and gradual transition of air from the Siberian polar continental source to the truly equatorial air of the Indian Ocean. On account of the monsoon, the subtropical high in this region is completely submerged, which accounts for the lack of a region of tropical air between the polar and equatorial air.

Toward the north, the monsoon region is distinctly separated from the Siberian source by the mountain ranges. As most of south Asia is pronouncedly dry in winter, the air does not absorb much moisture until it comes over the Indian Ocean. On the average, subsidence is more pronounced in the western than in the eastern part of the Indian Ocean, so that the monsoon air soon becomes transformed into equatorial air in the eastern part. In the western part, it remains relatively dry almost down to the equator.

The above discussion of the principal source regions is based upon average conditions. In individual cases, the significant regions may be displaced. Thus, when central Europe is snow-covered, the source of polar continental air may spread westward over Germany and France, and sometimes southward to Asia Minor, where a mild type of polar continental air may be produced. Similarly, the source of maritime

tropical air may spread northward into the southern part of region 3 (Fig. 89) when the Azores anticyclone moves toward the north.

In the southern hemisphere, the system of source regions is simpler and the zonal distribution more pronounced than in the northern hemisphere, but the principles of classification are essentially the same as shown above. In the southern hemisphere, we meet with the following types of source: the antarctic, polar maritime, tropical, and equatorial. The polar continental sources of the northern hemisphere in winter coincide mainly with the regions of boreal climates. In the southern hemisphere, there is no such climatic zone, and there is no typical source of polar continental air.

72. Air-mass Sources in Summer.—On the same principle as in the foregoing paragraph, the combined influence of the underlying surface (Fig. 74) and the prevailing wind systems (Fig. 88) has been used to locate the air-mass sources in summer. This is shown in Fig. 90 where a distinction is drawn between the following zones, or regions:

1. The *source region of arctic air* (*i.e.*, 1 in Fig. 90) is mainly occupied by melting snow and ice or icy water and mostly swept by light anticyclonic winds. In the upper atmosphere, the circulation is cyclonic (see Figs. 83 to 85). The lower layers of air become cooled to about 0°C. by the melting ice. The air is extremely stable with a pronounced temperature inversion in the surface layer. Stratus and strato-cumulus occur frequently, and fog is a very frequent phenomenon, particularly near open water (see Par. 59).

Above the cloud layer, the absorption of solar radiation continues day and night throughout the summer. As the air is usually stagnant, it becomes fairly warm aloft so that extreme stability develops throughout the mass. The ice-cooled layer of air is usually so shallow that it soon loses its source characteristics when the air is set in motion toward warmer regions.

2. The *source regions of tropical continental air* (*i.e.*, 4 in Fig. 90) are two in number, both characterized by light and variable winds over arid ground.

One of these regions contains central and southwest Asia, Arabia, south Europe, and north Africa. The winds are on the whole from a northerly direction; the air is therefore normally under a continental influence before it enters this region. Apart from the Mediterranean Sea, the Black Sea, and other enclosed seas, the region is extremely arid. It comprises the deserts and steppes and the adjoining areas characterized by summer dryness (*i.e.*, the *B* and *C*'s climates). On account of the areas of water that are embedded in this region, the humidity conditions of the tropical continental air masses in Eurasia are very variable.

The second source region of continental tropical air (4) in the northern hemisphere is to be found in western part of the United States. This region is arid. The eastern portion of the United States, in which the prevailing winds bring oceanic air into the continent, is a region of transi-
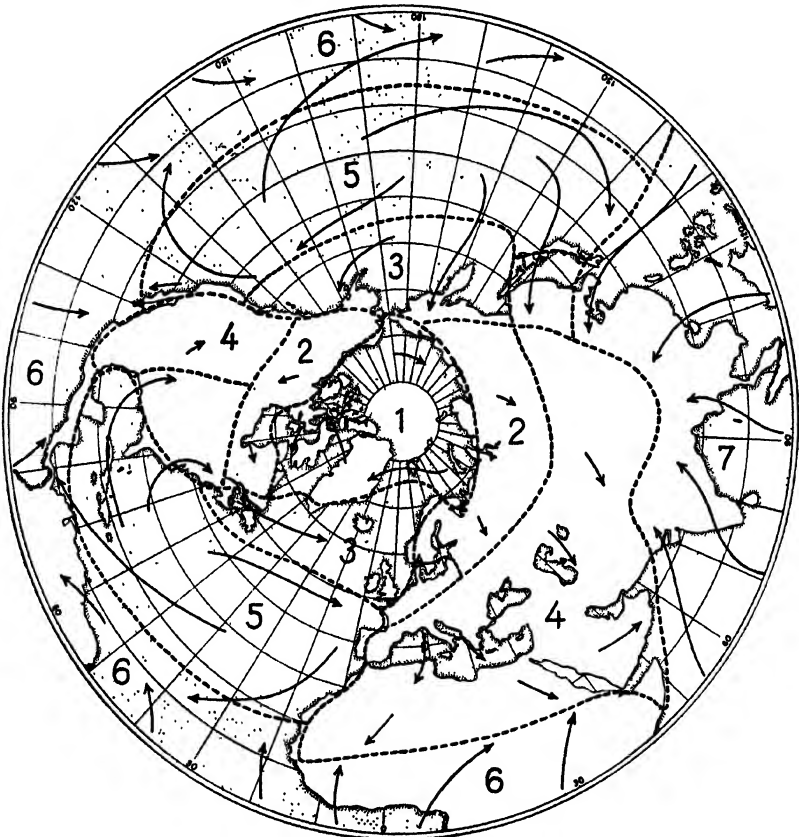
FIG. 90.—Air mass sources of the northern hemisphere in summer. 1, arctic; 2, polar continental; 3, polar maritime; 4, tropical continental; 5, tropical maritime; 6, equatorial; 7, monsoon.

tion of maritime tropical air. In many ways, it resembles the monsoon region in Asia, but the monsoon winds in Asia are more persistent and more humid than are the winds in the eastern portion of the United States.

3. The *source regions of tropical maritime air masses* (*i.e.*, 5 in Fig. 90) are characterized by conditions that are in principle the same as in winter, except that the sea-surface temperature is higher and the subtropical anticyclones are larger and situated farther to the north.

4. The *subpolar zones of transition* between the arctic and the sub-tropical sources run as a fairly narrow belt round the world, roughly between 50 and 70°N lat. Within this belt, the winds are mostly light and variable, the underlying surface is moderately warm, and the continental areas are fairly humid. The belt may be subdivided into four portions. Two are continental regions (2 in Fig. 90). These occupy the subpolar forest belts and are the principal sources of *polar continental air* in summer. Remaining are two oceanic regions (3 in Fig. 90), and these are the main sources of *polar maritime air*.

5. The *source region of equatorial air* (6 in Fig. 90) is in principle the same as in winter, except that it is displaced slightly northward, and a considerable portion of the equatorial belt north of the equator is occupied by equatorial air from the southern hemisphere.

6. The *monsoon region* (7 in Fig. 90) occupies about the same position as in winter; but the winds are reversed, so that the summer monsoon brings equatorial air into the interior of Asia. As in winter, the monsoon region is separated distinctly from the tropical continental source by the mountain ranges in south and east Asia.

73. Classification of Air Masses.—From the above discussion, it follows that the general circulation of the atmosphere has a tendency to produce vast masses of air whose conservative properties are more or less uniform within each typical source region, whereas the transition from one source mass to another is somewhat abrupt. If the physical properties were strictly conservative, the air masses could be identified by means of these properties after they leave their sources. However, when an air mass leaves its source region, it begins to change its properties; but if one air mass were originally "blue" and a neighboring air mass originally "red," they could still be identified by their "colors" even though these may "fade" more or less rapidly while the masses travel. On their journeys, the "colors" of the air masses may fade completely, and the air may enter another type of source region so that a mass that was, say originally "red," may become "yellow." Again, the mass may start on another journey, and the "yellow color" begin to fade. The synoptician is satisfied when he can trace the air back to its last source region, and it is of no interest to the forecaster to account for the changes that take place during successive sojourns in various source regions. The forecaster is interested in the properties that the mass acquired in its last source and the changes that have developed after leaving it, because the weather phenomena that develop depend entirely on the *life history* of the air mass.

In studying the life history of an air mass, the following factors should be considered: (1) the source from which the air mass obtained its fundamental properties, (2) the path by which it has traveled and the nature of the underlying surface, and (3) the time it has spent on its journey.

The idea of air masses was first introduced into forecasting practice and meteorological literature by Bergeron [1, 4], who has laid down the fundamental principles of air-mass theory. Bergeron introduced a dual classification of air masses, *viz.*, (1) a geographical classification comprising four principal source air masses, and (2) a thermodynamic classification depending on whether the air mass is colder or warmer than the underlying surface.

The *geographical* classification of Bergeron comprises the following four principal source air masses:

1. Equatorial air masses E, or air typical of the equatorial part of the trade-wind belts.

2. Tropical (or subtropical) air masses T, or air typical of the subtropical anticyclones.

3. Polar (or subpolar) air masses P, or air typical of the subpolar anticyclones.

4. Arctic air masses A, or air typical of the anticyclones over the arctic fields of snow and ice.

Each of these four principal groups may be subdivided into maritime (m) or continental (c) masses, according to whether the source in question is oceanic or continental.

The *thermodynamical* classification comprises two main types, *viz.*:

1. Cold air masses K, or air that is colder than the underlying surface. An air mass of this type will absorb heat from below.

2. Warm air masses W, or air that is warmer than the underlying surface. An air mass of this type will give off heat to the underlying surface.

Whereas the geographical classification refers rather to the *integral* result of the processes that lead to formation of quasi-homogeneous conditions in the quasi-conservative properties during the sojourn of the air mass in its source, the thermodynamic classification is essentially *differential* in character and refers mainly to the recent developments that have led to the formation of clouds, hydrometeors, and other passing phenomena in the air.

The above classification, which has been widely accepted in synoptic works and studies, has not always been used consistently. Thus, the polar continental (Pc) air is frequently denoted as arctic air just because it may be extremely cold near the earth's surface, regardless of its trajectory, vertical extent, and coldness aloft. Similarly, the notations maritime (m) and continental (c) are now most frequently used for recent maritime or continental influences irrespective of whether the air originally came from a maritime or a continental source. Furthermore, there is a tendency, particularly in southern countries, to indicate extremely warm air as equatorial without regard to its trajectory or its vertical structure.

In Bergeron's thermodynamic classification, the terms *cold* (*K*) and *warm* (*W*) refer to whether the air is *colder or warmer than the underlying surface*. Hence, it follows that equatorial or continental tropical air, for example, will frequently have to be classed as a cold mass, whereas the extremely cold arctic or continental polar air in its source should be classed as a warm mass. Furthermore, the warm-sector air in a depression should sometimes be designated as a cold mass; and, in other cases, the cold air in advance of a warm front should be referred to as a warm mass.

The essential feature in the thermodynamic classification is not so much the actual loss or gain of temperature by the air in contact with the underlying surface as the *production and maintenance of stability or instability*, because the formation of clouds and hydrometeors within the masses and the exchange of properties along the vertical depends ultimately on the stability conditions of the air. But, as we shall see in Par. 75, an air mass that is colder than the underlying surface may become increasingly stable as it moves toward warmer regions. This condition is due to the circumstance that the effect of subsidence in the free atmosphere sometimes overcompensates the heating from below. Similarly, instability may develop without heating from the underlying surface.

TABLE 20.—GEOGRAPHICAL (SOURCE) CLASSIFICATION OF AIR MASSES

Symbol	Denomination	Winter source (Fig. 89)	Summer source (Fig. 90)	Remarks
A	Arctic	1	1	Unimportant in midsummer
Pc	Polar continental	2	2	Prominent in winter
Pm	Polar maritime	3	3	—
Tc	Tropical continental	6	4	Prominent in summer
Tm	Tropical maritime	7 and 5	5	—
E	Equatorial	8	6	—
M	Monsoon	9	7	—
S	"Supérieur"	Formed in the free atmosphere through subsidence in anticyclonic eddies in middle or subtropical latitude (see Par. 83).		

Auxiliary notations: *t* = transitional, *r* = returning.

Willet [89], who has studied the air masses of North America, and Schinze [71], who has studied the air masses of central Europe, have preferred to use local classifications based on Bergeron's principles. Local classifications are, naturally, useful for detailed investigations

within limited areas; but, with the extension of synoptic charts to cover a whole hemisphere or a large portion thereof, it becomes urgently necessary to develop a general classification which, when necessary, may be supplemented by local designations.

From the above, it appears that, although Bergeron's classifications should be maintained in principle, there are both linguistic and physical reasons for making minor changes and introducing some new subdivisions in order to make the classification both broad and detailed enough to cover all main types of air mass and development.

Based on the discussions in the foregoing paragraphs regarding the normal properties of the earth's surface and the prevailing wind systems, the classification shown in Table 20 is proposed for reference of air masses to their source regions.

The *geographical* classification shown in Table 20 should be supplemented by an *influence* classification, the object of which should be to indicate appreciable or systematic changes in the stability of the air after it has left its source region.

The most significant changes in the air-mass properties are those which lead to development from stability to instability, or vice versa. These changes depend primarily on the exchange of heat between the surface and the air. But, as has been shown in Pars. 45 to 53, the stability conditions may also change appreciably on account of ascent, subsidence, and advection in the free atmosphere. Instead of Bergeron's "cold-warm" classification, we propose a classification that directly indicates the stability conditions and their changes without specifying the processes that actually caused them. Table 21 shows such significant types of instability condition as can be inferred from the analysis of the surface weather maps.

TABLE 21.—INFLUENCE CLASSIFICATION OF AIR MASSES

Symbol	Denomination	Clouds, hydrometeors, etc.
S	Stable stratification	Stratus, strato-cumulus, fog, drizzle, granular
S^+	Stability increasing	snow, ice crystals
S^-	Stability decreasing	Dissolution of stable clouds and hydrometeors. Development toward instability
U	Unstable stratification	Cumulus, cumulo-nimbus, showers, squalls, hail,
U^+	Instability increasing	thunderstorms, etc.
U^-	Instability decreasing	Dissolution of unstable clouds and hydrometeors, development toward stability

74. Source Properties of Arctic and Polar Continental Air Masses in Winter.—From the nature of the underlying surface and the character

of prevailing wind systems, definite conclusions may be drawn with respect to the properties of the air which invades a cold source region and remains there so long that it adjusts itself to the underlying surface.

In the first place, the air should be cooled from below.   On account of outgoing radiation, the cooling of the surface is most intense in the divergent part of the wind system where subsidence dissolves the clouds so as to allow the surface to radiate freely.   In the stagnant parts of the anticyclones, the turbulent transfer of heat along the vertical is insufficient for the maintenance of a normal lapse rate of temperature.   Isothermal conditions, or inversions, develop near the surface.   As the lapse rate is diminished, turbulence decreases in intensity, and the further growth of the inversion is favored.   As the cooling of the air along the surface continues without sufficient turbulent exchange of heat with the air above, the outgoing radiation from the surface is checked by radiation from the warmer air aloft.   As has been shown by Wexler [86], the amount of temperature inversion is not likely to exceed 20°C.

The divergent flow from the central part of the anticyclones spreads the cooled air over large areas, while subsidence, which compensates for the outflow, contributes to the intensification of the inversion.   The final result will then be an extremely cold layer of air along the surface with relatively warm air above.   The intensity and the vertical extent of the inversion will depend greatly on the turbulence, which, again, is mainly a function of wind velocity.   Thus, the temperature conditions that gradually develop depend on the cooling of the surface, turbulence, and subsidence.   The amount of radiative cooling of the surface depends greatly on the temperature of the air aloft.

The moisture content of the air adapts itself to the temperature so as not to exceed saturation.   In the lower layers, moisture is withdrawn from the air by frost deposited on the ground (see Par. 59) or formation of "frost haze" or of ice-crystal fogs.   As the air close to the ground is considerably colder than in the thermometer screen, considerable amounts of frost may be deposited on the ground without the air above the ground becoming saturated.   Thus, the air in the central parts of the anticyclones is gradually desiccated, and the cooled and dried air is spread over larger areas by the divergent flow.

On account of subsidence and turbulent transfer, the air throughout the air column gradually becomes drier and colder; but the air along the surface will, throughout the process, be colder and usually also drier than the air at some height above the ground.

In the outer regions of the anticyclone where the wind velocity is higher, turbulence is usually sufficient to maintain a normal lapse rate. Air that has been cooled under stagnant conditions and that afterward is set in motion will become warmer in the lower layers and colder in the

upper layers (see Par. 49). Thus extremely low temperature at the surface and moderately low temperature aloft are characteristic of stagnant conditions, and moderately low temperature at the surface and extremely low temperature aloft are characteristic of stirred continental polar air in winter. But, regardless of the state of motion, the specific humidity is extremely low as long as the underlying surface is dry. A typical example of stagnant and stirred conditions is shown in Fig. 91.

The vertical extent of the cold air mass that is formed in the manner described above depends greatly on topographical conditions. Almost the entire source region of the cold air masses (*A* and *Pc*) is encircled by mountain ranges, *viz.*, the east Asiatic ranges, the Himalayan ranges, and their continuation westward to Balkan and central Europe. Mountain ranges are also found along the border of the source region in Scandinavia and in North America. Where the source is limited by extensive mountain ranges, the cold air produced will be prevented from streaming out of its source until it has attained a considerable ·height, and air from adjacent sources of different nature will be prevented from streaming into the source. Above the mountain range, air from foreign

FIG. 91.—Examples of temperature conditions in stagnant (Irkutsk) and stirred (Moscow) polar continental air.

sources may be present. This happens frequently in northwest Europe where the prevailing westerlies proceed far eastward above the *Pc* air.

In North America, the mountain range along the west coast is, in most cases, high enough to form an effective barrier against the westerlies from the Pacific Ocean; and when Pacific air invades Canada above the range, it does so without making its influence much felt at the ground. Pacific air sometimes invades Canada and adjacent regions around the Alaskan peninsula where the barrier is less effective. Across the North American continent, from east to west, there is no effective barrier; cold air from the northern snow-covered regions may, under favorable pressure distributions, stream freely toward the south and southeast, and foreign air masses may invade the northern territory from these directions.

The arctic region is frequently invaded by air masses of warm origin. This happens most frequently between Spitsbergen and north Russia and less frequently along the west coast of Greenland and west to Alaska. These invasions of foreign air masses may not sweep away the source air

entirely, but they will be present aloft and sometimes quite close to the ground.

The most extremely cold and specifically dry air would naturally be found in north Siberia and north Canada and also in the Arctic; but as ascents from these regions are not available, the properties of the polar continental and arctic air masses will be demonstrated by means of ascents from less extreme regions. The following tables contain mean values of the various air-mass properties under source conditions. The tables, which are based on a varying number of ascents, may be interpreted as representing *typical conditions, but not climatological normals.* The coordinates of the stations referred to are given in the Index of Stations, and the symbols used are defined in the List of Symbols.

Table 22 shows the typical properties of *Pc* air in North America[1] under typical source conditions. The ascents on which the table is based were for the most part made under fairly stagnant conditions. Ellendale is particularly typical of *Pc* air in its source. It will be seen from the table that the vertical structure of the air is precisely as one would expect, considering the coldness of the surface and the stagnant anticyclonic conditions.

TABLE 22.—POLAR CONTINENTAL AIR (*Pc*) IN THE UNITED STATES

Elevation, km.	Ellendale			Royal Center		
	T	q	θ_{se}	T	q	θ_{se}
Surface	−26	0.32	−23	−23	0.45	−21
1	−25	0.35	−17	−20	0.48	−11
2	−20	0.60	−1	−16	0.48	4
3	−22	0.50	7	−18	0.85	13
4	−25	0.45	15	—	—	—

Table 23 shows the average properties of *Pc* air in Siberia and Russia under typical source conditions. Comparison between Tables 22 and 23 shows that the Ellendale type of vertical structure is representative of vast expanses of the northern snow-covered regions under anticyclonic control. In north Canada and north Siberia, the temperature and humidity content would be lower than at the stations referred to, but the vertical structure would be essentially the same.

Under favorable conditions, notably when the ground is covered with snow, *Pc* air may form also in continental anticyclones over central Europe. These masses are usually rather shallow and seldom reach above the 2-km. level. However, when the upper-air current is from an

[1] The air masses of North America have been studied in great detail by Willet [89], from which the tables below concerning the United States are taken.

TABLE 23.—POLAR CONTINENTAL AIR (Pc) IN SIBERIA AND RUSSIA

Station	p	Φ	T	q	θ	θ_{sw}	θ_{se}	Remarks
Irkutsk.	1000	—	−25	0.40	−25	−26	−25	Mostly stagnant
	900	750	−21	0.56	−13	−15	−12	When quite stagnant,
	800	1600	−26	0.46	−9	−12	−8	surface temperature
	700	2550	−30	0.37	−4	−9	−3	lower than shown
	600	3600	−35	0.26	2	−5	3	here
	500	4850	−41	0.18	11	−1	11	Note the low specific humidity in the surface layer
Novo-sibirsk.	1000	—	−28	0.39	−28	−28	−27	
	900	750	−22	0.56	−14	−16	−13	
	800	1600	−22	0.58	−6	−10	−4	
	700	2550	−26	0.43	1	−5	2	
	600	3650	−32	0.28	6	−3	6	
	500	4900	−40	0.17	12	0	12	
Archangel.	1000	—	−26	0 36	−26	−26	−25	Mostly stagnant
	900	800	−19	0.85	−11	−13	−9	
	800	1650	−21	0.80	−4	−8	−2	
	700	2600	−27	0.50	0	−6	1	
	600	3700	−36	0.25	2	−5	3	
	500	4950	−42	0.16	9	−1	10	
Moscow and Smolensk.	1000	—	−17	1.0	−17	−17	−15	Mostly stirred conditions. Air from East Russia
	900	800	−14	1.0 .	−6	−9	−4	
	800	1650	−16	1.0	1	−4	3	
	700	2600	−23	0.56	4	−3	5	
	600	3700	−32	0.39	6	−2	7	
	500	4950	−41	0.20	10	−1	11	

TABLE 24.—POLAR CONTINENTAL AIR (Pc) IN CENTRAL EUROPE

Station	p	Φ	T	q	θ	θ_{sw}	θ_{se}	Remarks
Munich and Fried-richshafen.	1000	—	—	—	—	—	—	Mostly stirred conditions
	900	800	−11	1.4	−3	−6	1	
	800	1700	−17	1.0	0	−5	3	
	700	2650	−21	0.60	6	−2	8	
	600	3750	−26	0.38	9	2	14	
	500	5050	−36	0.16	17	3	18	
Nancy, Cologne, and Frankfurt.	1000	—	−6	2.0	−6	−7	0	Mostly stirred conditions
	900	800	−9	1.5	−1	−5	3	
	800	1700	−15	1.1	2	−4	5	
	700	2650	−20	0.72	8	−1	10	
	600	3800	−25	0.50	14	2	16	
	500	5100	−34	0.20	19	4	20	

easterly direction, central Europe may be invaded by Pc air from east Europe. Table 24 shows the vertical structure which is typical of such cases.

Over the Arctic Ocean, the surface-air temperature will never reach the extremely low values recorded in Siberia and north Canada. This condition is due to conduction of heat through the ice from the warm water underneath. The arctic air, however, is cold aloft, extends to great heights, and may sometimes fill the entire space below the tropopause. Table 25 shows the typical structure of highly stirred arctic air.

Table 25.—Arctic Air (A) in the Arctic

Station	p	Φ	T	q	θ	θ_{sw}	θ_{se}	Remarks
Buchta	1000	—	—	—	—	—	—	The table is based on
Tichaja.	900	750	−30	0.29	−23	−24	−22	only three ascents,
	800	1550	−34	0.21	−18	−20	−18	all of which are
	700	2450	−38	0.16	−12	−15	−12	stirred air
	600	3500	−42	0.12	−6	−10	−6	
	500	4650	−49	0.07	0	−6	0	

A comparison between the above tables will show that the Pc source air has remarkably uniform characteristics above the ground layer. This particularly applies to specific humidity. Thus, in these tables the specific humidity in the 700-mb. level varies only between 0.4 and 0.7 grams; in the 500-mb. level, it varies only between 0.17 and 0.20 grams. In the truly arctic air, the specific humidity is somewhat lower. The typical Pc air is further characterized by pronounced absolute stability $[(\partial\theta/\partial z) > 0]$ and convective stability $[(\partial\theta_{sw}/\partial z) > 0$, or $(\partial\theta_{se}/\partial z) > 0]$. The cloud forms characteristic of Pc air in its source are low stratiform clouds.

The time required for a Pc air mass to form depends greatly on the cloudiness and the air temperature aloft. Under cloudy or overcast conditions, the radiative cooling of the underlying surface is hindered, and the mass approaches the normal conditions very slowly. Similarly, when there is advection of warm air aloft, the radiative cooling of the surface is reduced. Under such conditions, several days are required for a typical Pc mass to form. On the other hand, when the air is cloudless, the underlying surface cools rapidly and if the wind velocity is high enough to produce sufficient turbulence the whole air column is cooled quickly. A typical Pc mass may then form in less than 48 hr.

75. Modification of Arctic and Polar Continental Air in Winter.—
Following the initial outflow of the Pc mass from the source region where its vertical structure is essentially as shown in Tables 22 to 25 of the

previous paragraph, there are five important influences at work to change the source properties. Observed changes in its properties are then to be explained in terms of one or more of the following influences:

1. Supply of heat from the underlying surface.
2. Supply of moisture from the underlying surface.
3. Turbulent transfer of heat and moisture along the vertical. •
4. The effect of subsidence.
5. The liberation of latent heat of vaporization.

Although influences 1 and 3 tend to reduce the original stability of the mass and to transform it into an unstable state $(S \rightarrow U)$ and influences 1 and 2 tend to produce convective instability, influence 4 tends to counteract the production of instability. Moreover, subsidence is most effective at the beginning of the outflow from the source while the air is still under anticyclonic control, whereas the liberation of latent heat is most active in the later stages of the outflow, notably when influence 2 overcompensates influence 1, and when influence 4 is absent.

The type of air mass that develops from a source Pc mass when it moves toward warmer regions will depend on which of the five influences mentioned above are predominating, and it is of interest to note that the movement toward warmer regions does not necessarily result in instability. In fact, we may distinguish between the following types of development:

1. Absorption of heat from an underlying dry surface together with pronounced subsidence. In this case, which is most pronounced in anticyclonic currents over land, the original stability may be maintained or even increased $(S+)$ while the air temperature increases and the relative humidity decreases at all levels.

2. Absorption of heat from an underlying dry surface and no appreciable subsidence. In this case, which is typical of air in strong currents that are not under anticyclonic control, the absorption of heat and turbulent mixing raises the air temperature and lowers the relative humidity in the lower layers while the temperature and relative humidity are not appreciably affected at high levels. In this case, the mass develops rapidly toward instability; but, on account of the lack of moisture supply, convective clouds and showers do not easily form.

3. Absorption of heat and moisture from the underlying surface and pronounced subsidence in the higher layers. This combination, which is typical of currents with anticyclonic subsidence over wet ground or water, often results in an inversion at some distance above the ground. If the subsidence is not strong and the heating is considerable, inversions do not form, and convective clouds may develop.

4. Absorption of heat and moisture from below and no subsidence. This combination, which is typical of cyclonic currents or currents

outside anticyclonic control over wet ground or water, is highly favorable for the development of a deep layer of unstable air with convective weather phenomena, such as cumulus, cumulo-nimbus, showers, squalls, and thunderstorms.

Type 1.—Table 26 shows the average properties of *Pc* air from the Ellendale region (see Table 22) which, under the influence of pronounced subsidence, has moved over dry, snow-covered ground down to Groesbeck. The development corresponds to case 1 described above.   Comparing

TABLE 26.—MODIFICATIONS OF POLAR CONTINENTAL (*Pc*) AIR

Elevation, km.	Groesbeck (type 1)			Boston (type 2)		
	T	q	θ_{ee}	T	q	θ_{ee}
Surface	−13	0.9	−12	−6	0.9	−6
1	−9	0.9	1	−14	0.6	−5
2	−1	1.2	21	−18	0.5	1
3	—	—	—	−23	0.3	6
4	—	—	—	−29	0.2	10

the data for Ellendale (Table 22) with those for Groesbeck, it will be seen that the temperature has increased at all levels, and so, also, has the potential pseudo-equivalent temperature.   It is of interest to note that the stability of the air has increased in spite of the heating from below.   This condition is due to subsidence in the free atmosphere. Through subsidence, the convective stability has also increased.   The specific humidity has increased slightly, but the air is relatively drier at Groesbeck than at Ellendale.

Type 2.—The data for Boston (Table 26) illustrate the development described with respect to case 2 above.   This air, too, is originally of the Ellendale type, but it arrives at the New England coast as a moderate or strong nonsubsiding current, in which vertical mixing is a prominent feature.   Comparing the Boston data with those for Ellendale, it will be seen that the temperature has increased considerably in the lower layers and decreased slightly above the 2-km. level.   This change is due partly to heating from below and partly to stirring of the air column. During this process, the specific humidity has increased at the ground and decreased in the upper air.   This development is due to stirring of the air column and a slight absorption of moisture.   The air has developed toward instability ($S-$); but, on account of lack of moisture supply, convective clouds do not easily form.   It is worthy of note that the air has retained its convective stability [$(\partial\theta_{ee}/\partial z) > 0$].

The Boston *Pc* air is typical of east coasts in high latitudes.   Here, air from the polar continental sources streams freely toward the adjacent

oceans.   It is therefore to be expected that the same type of air would be found also along the east coast of Asia.   Table 27 shows the average conditions in Pc air from the Siberian source (January to February, 1937 to 1938) that arrives at Khabarovsk and Vladivostok, partaking in the winter monsoon.   Extremely cold air from the Siberian source often retains its fundamental properties as far south as Peiping[1] (see Table 28).

TABLE 27.—POLAR CONTINENTAL AIR FROM THE SIBERIAN SOURCE

Station	p	Φ	T	q	θ	θ_{sw}	θ_{se}	Remarks
Khabarovsk	1000	—	−25	0.40	−25	−26	−24	Modification of type
	900	750	−27	0.39	−19	−20	−18	2. In most cases,
	800	1600	−28	0.37	−12	−14	−11	strong winds from
	700	2500	−32	0.30	−6	−10	−6	northwesterly di-
	600	3500	−38	0.20	0	−7	0	rection at all levels
	500	4750	−44	0.13	7	−2	7	
Vladivostok	1000	—	−19	0.55	−19	−20	−18	As above
	900	750	−22	0 50	−14	−16	−13	
	800	1600	−25	0.45	−8	−12	−7	
	700	2550	−32	0.22	−6	−10	−6	
	600	3600	−39	0.16	−2	−8	−2	
	500	—	—	—	—	—	—	

TABLE 28.—POLAR CONTINENTAL AIR AT PEIPING

H, m.	T	q	θ_{se}	Remarks
Surface	−9	0.4	−10	Modification of type 2. This part of the table is bas-
500	−13	0.3	−9	ed on only three ascents made in Pc air from the true
1000	−18	0.2	−10	Siberian source with strong northwesterly winds at
1500	−22	0.2	−10	all levels
2000	−27	0.1	−9	
Surface	−1	0.9	0	This part of the table is based on only eight ascents
500	−5	0.7	−1	in Pc air of less extreme source conditions than
1000	−9	0.6	0	above. All ascents were made during January and
1500	−13	0.5	1	February, 1933 to 1934
2000	−15	0.5	4	
2500	−19	0.4	6	

Bearing in mind that the source properties of Pc air are essentially the same in North America and over the Eurasian continent and having regard to the differences in latitude and continentality of the stations referred to in Tables 26 to 28, we may say that the different stages in the development of Pc air, which, under nonsubsident conditions, streams

[1] The author is greatly indebted to Professor Hsia-Cien Huang [33] for permission to use the data concerning Peiping.

over dry ground toward warmer regions, are represented by the above stations in the following sequence: Khabarovsk, Vladivostok, Boston, and Peiping. It will be seen that the development is characterized by *almost invariant specific humidity, development toward instability and convective instability*. When such air has passed the coast, it absorbs heat and moisture in the lower levels; *absolute instability and convective instability develop rapidly*. It is often observed that such air, on account of its low relative humidity, is cloudless on the coast, whereas, at a distance of 100 to 150 km. off the coast, towering cumulus and cumulo-nimbus develop. It is important to bear this in mind when forecasting the weather conditions off the coast.

Type 3.—It is not possible to present tables showing the average conditions in *Pc* air exposed to the modifying influences mentioned with respect to case 3 above. The development is typical of *Pc* air when, after having passed the coast, it streams in an anticyclonic current over an ocean. Subsidence aloft maintains a low specific humidity in the upper air, while the lower layers become heated and moistened by the underlying surface. In cases of pronounced subsidence, an inversion may develop in mid-air. The typical cloud forms are then cumulus humilis, strato-cumulus, or stratus.

Type 4.—The combination of modifying influences mentioned with respect to case 4 above is typical of air from the polar continental and the arctic sources when it moves in a strong, preferably cyclonic current over an ocean. Heat and moisture are then absorbed in a deep layer of air; cumulus, cumulo-nimbus, showers, and squalls are the typical weather phenomena in such air masses.

Table 29 shows the average properties of arctic air from the Greenland region which, in strong outbreaks, arrives in west Europe, and Table 30 shows the properties of the corresponding types of air along the west coast of North America.

Most of the cases used in compiling Table 29 are those of strong outbreaks of arctic air, the air taking only 20 to 50 hr. on its journey from the Arctic to west Europe. In comparing the data of Tables 29 and 30 with the characteristics of polar continental and arctic air masses in their sources (see Par. 74), it will be seen that the combination of modifying influences referred to as type 4, causes radical changes in the vertical structure of the air.

It is of interest to note that the development referred to as type 1 is typical of continental areas south of the center of the *Pc* source; that referred to as type 2 occurs most frequently over the continents in the NW currents to the east of the *Pc* sources, *i.e.*, when *Pc* air moves from the source toward regions 4 and 5 (see Fig. 89); while the development referred to as type 3 is typical of *Pc* air after it has left the continent

TABLE 29.—ARCTIC AIR (*tA*) IN WEST EUROPE AFTER HAVING PASSED THE NORWEGIAN SEA

Station	p	Φ	T	q	θ	θ_{sw}	θ_{se}	Remarks
Nancy, Cologne, and Frankfurt.	1000	—	2	3.6	2	1	13	Modification of type 4. Moist-adiabatic stratification up to the −20°C. isothermal level
	900	800	−3	2.9	5	1	14	
	800	1700	−10	1.9	8	1	14	
	700	2700	−17	1.1	11	1	14	
	600	3850	−26	0.45	14	2	14	
	500	5100	−36	0.21	17	3	17	
Trappes, Dijon, Lyon, and Chateauroux.	1000	—	4	3.6	4	2	14	As above
	900	800	−2	2.6	6	2	14	
	800	1700	−8	2.0	9	2	15	
	700	2700	−16	1.2	12	2	15	
	600	3850	−25	0.52	15	3	16	
	500	5150	−32	0.25	21	5	22	
Hamburg, Kiel, and Norderney.	1000	—	3	3.8	3	2	15	As above
	900	800	−2	3.0	6	2	15	
	800	1700	−8	1.7	10	2	15	
	700	2750	−14	0.9	14	2	16	
	600	3900	−21	0.5	19	4	20	
	500	5150	−30	0.27	24	6	24	
Lindenberg, Berlin, and Breslau.	1000	—	2	3.7	2	2	14	As above
	900	800	−2	2.9	6	2	15	
	800	1700	−9	2.0	9	2	15	
	700	2700	−15	1.1	13	2	16	
	600	3850	−23	0.56	17	4	18	
	500	5150	−32	0.26	21	5	22	

TABLE 30.—ARCTIC AIR (*tA*) ON THE PACIFIC COAST

Elevation, km.	Seattle			San Diego			Remarks
	T	q	θ_{se}	T	q	θ_{se}	
Surface	8.3	4.4	19	13.5	6.1	28	Modification of type 4.
1	0.0	2.7	16	7.5	5.3	29	
2	−8.3	1.5	15	0.5	2.8	27	
3	−14.3	0.8	16	−6.0	1.3	26	
4	−19.3	0.4	21	—	—	—	

when it enters the southern portion of the prevailing westerlies and becomes exposed to subsidence in passing anticyclones and wedges òf high pressure. Here, advection of warmer air aloft (see Par. 47) constitutes another stabilizing factor. Finally, the development referred to as

type 4 is the normal occurrence in Pc air when it enters the regions referred to as No. 4 in Fig. 89. The same applies to regions 3 when arctic air streams southward. It should be noted that the Pc air within these regions is more unstable than that shown by the data contained in Table 29.

76. Polar Maritime Air in Winter.—The abode of this type of air is the Atlantic region 3 (Fig. 89) and also the corresponding region in the Pacific Ocean. On account of the small areas of these regions and the strong wind circulation, the air only rarely has sufficient time to acquire the typical properties to their full extent. Most frequently, the air masses occupying these regions are still in a state of transformation; and, depending on the trajectory and the time during which the air mass has been in contact with the ocean, a great variety of conditions will be observed.

Most of the air that comes to the Atlantic region 3, has come from the American region 2 via the Atlantic region 4 in which it travels mainly against the gradient of the sea-surface temperature. The general air current in this region is cyclonic; there is, therefore, no appreciable subsidence, and as the air is rapidly heated from below, it becomes transformed into an unstable mass $(U+)$, which, on account of turbulence and convection, becomes heated and moistened at all levels.

When such air enters region 3, south of the Icelandic low-pressure area, it begins to move mainly along the isotherms of the underlying surface; the heating from below gradually ceases while part of the latent heat of vaporization is made free at high levels. Owing to this development, the instability decreases $(U-)$; and when the air has moved far enough into region 3, it becomes increasingly stable $(S+)$. On its journey farther toward the northeast, the air may eventually enter the arctic or the Siberian polar continental source where it gradually becomes cooled from below and develops an extremely stable stratification.

While the air is in the Atlantic region 4, it should be classified as tPc; when it occupies region 3, it should be noted as Pm; and, finally, after it has entered the polar continental source in north Europe, it should be referred to as tPm after which it develops into a Pc mass. Its successive thermodynamic changes from the Canadian to the European polar continental source would then be indicated by the symbols $S-$, $U+$, $U-$, and $S+$.

When the wind velocity is high, the air that comes from the Canadian polar continental source, may arrive in west Norway as an unstable mass, but usually it arrives there in a neutral or slightly stable state. When the winds are moderate or slight, a stable stratification is attained before the air reaches as far east as the Faeroe Isles.

The conditions described above are typical of situations with the Icelandic depression in its normal position or displaced to the west thereof. However, when a depression moves towards north Scandinavia or the Barents Sea, the North Atlantic is invaded by air that comes directly from the Greenland-Spitsbergen area. In such cases, the conditions in region 3 will be similar to those in region 4 as described above.

It happens sometimes that a migrating anticyclone settles down over the Atlantic region 3 for some time. The *Pm* mass that is then produced resembles the type of *Pm* air that has come from the Canadian *Pc* source and moved south of the Icelandic low; but the air in the anticyclone will be warmer, and its stability more pronounced. In certain cases, particularly when there is a trough of low pressure from Iceland down to the Azores, tropical air (from region 7, and very rarely from region 6) invades region 3. In such cases, the tropical air, being cooled from below, develops an extremely stable stratification. This, naturally, is the warmest type of air that is observed in region 3, and its appropriate designation should be *tTm*.

What has been said above concerning the North Atlantic applies also in principle to the conditions in the North Pacific.

On the whole, we may say that the so-called polar maritime air masses develop in the transitional zones through consenescence of air masses from the neighboring sources. It follows then that the *Pm* air will exhibit a great variety of conditions, the masses sometimes resembling the tropical maritime type *Tm* and sometimes approaching the transitional polar continental or transitional arctic type. Tables 31 and 32 show the average properties of *Pm* masses in Europe and in the United States, respectively. The typical air temperatures observed in ships are given in the illustrations in Par. 86.

77. Tropical Continental Air in Winter.—As was mentioned in Par. 71, there is only one source region of continental tropical air in the northern hemisphere in winter, *viz.*, the north African region (6, Fig. 89). In the south of Asia, the winter monsoon prevents the air from becoming stagnant and thereby absorbing the properties characteristic of the latitude. On account of the southward convergence of the coast lines of North America, there is not sufficient continental area in this region to form a source of continental tropical air in North America. Apart from the coastal regions, which are under maritime influence, most of Mexico and Central America is high plateau or mountain country which is quite cool in winter. Air masses that settle down in these regions acquire no distinguishing warmth by which they may be traced during their later life history (see Willett [89]).

The *Tc* air of North Africa (region 6, Fig. 89) is characterized by the extreme dryness of the ground and the prevalent anticyclonic circulation. It is moderately warm, stably stratified, and very dry.   No aerological observations are as yet available to show its average properties in the upper atmosphere.   It is of interest to note that the African *Tc* air in

TABLE 31.—POLAR MARITIME AIR (*Pm*) IN WEST EUROPE

p	Φ	T	q	θ	θ*sw*	θ*se*	p	Φ	T	q	θ	θ*sw*	θ*se*
Trappes, Dijon, Lyon, and Chateauroux							Hamburg, Kiel, and Norderney						
1000	—	5	4.5	5	3	18	1000	—	4	4.4	4	3	15
900	850	2	3.9	11	6	22	900	850	1	3.5	9	4	20
800	1750	−4	2.9	14	6	23	800	1750	−5	2.2	14	4	20
700	2300	−9	1.9	20	7	26	700	2750	−10	1.3	18	5	22
600	3950	−16	1.3	25	9	29	600	3950	−18	0.8	22	6	24
500	5250	−24	0.6	32	10	33	500	5250	−27	0.5	27	8	28
Nancy, Cologne, and Frankfurt							Lindenberg, Berlin, and Breslau						
1000	—	4	4.7	4	3	18	1000	—	2	4 1	2	2	14
900	850	2	4.1	10	5	22	900	850	0	3.3	8	3	18
800	1750	−5	2.8	13	5	22	800	1750	−4	2.3	14	5	20
700	2750	−11	1.6	17	5	22	700	2750	−11	1 1	17	5	20
600	3950	−19	0.9	22	6	24	600	3950	−19	0.7	22	6	24
500	5250	−30	0.5	24	7	25	500	5250	−28	0.4	27	8	28

TABLE 32.—TRANSITIONAL POLAR MARITIME (PACIFIC) AIR (*tPm*) IN THE UNITED STATES

Elevation, km.	Ellendale			Broken Arrow			Groesbeck			Royal Center			Due West		
	T	q	θ*se*	T	q	θ*se*	T	q	θ*se*	T	q	θ*se*	T	q	θ*se*
Surface*	−1	3.0	11	4	3.9	15	6	4 7	19	0	3.1	9	5	3.2	14
1	7	3.0	26	8	3.3	27	10	2 2	24	3	2.3	19	9	1.7	23
2	1	2.2	27	4	2.4	29	4	1.2	27	1	1.4	24	7	1.4	31
3	−7	1.5	28	−2	1.8	32	3	0.4	32	−4	1.0	29	2	0.7	33
4	−14	1.1	29	—	—	—	—	—	—	—	—	—	—	—	—

* Surface air nonrepresentative on account of cooling over land.

winter constitutes the main heat supply of the Mediterranean depressions which form along the front between this *Tc* air and the *Pc* air from Europe and western Asia.   These depressions generally move eastward.   Only in exceptional cases does the *Tc* air invade Europe; and when this happens, it does so at great altitudes without making its influence much felt at the ground.

78. Tropical Maritime Air in Winter.—*Tm* air masses are continuously formed within regions 7, Fig. 89, and frequently within the regions 5, Fig. 89, when an anticyclone settles down in these areas. The vertical structure of the *Tm* masses is characterized by (1) the warmth and the oceanic conditions of the regions in question, (2) the anticyclonic subsidence caused by divergent outflow in the lower layers, and (3) the cellular movement within the subtropical cells.

As the air is heated from below, there will be a tendency toward the production of instability. On the other hand, the effect of the heating from below is counteracted by the prevalent subsidence which tends to produce stability. Furthermore, as the air takes part in the cell circulation described in Par. 67, additional subsidence develops while the air moves eastward in the northern half of the cell, and a general ascending motion (which counteracts the subsidence caused by the divergent outflow in the lower layers) occurs while the air moves westward in the southern half of the cells. As a result of this, the air in the southwestern part of the cell is fairly unstable, whereas the air in the northeastern part of the cell is fairly stable. In this connection, it is of importance to note that the sea-surface temperature (see Fig. 73) is higher in the western half of the cell than it is in the eastern half. For this reason, too, the air in the western part of the cells is warmer and less stable than in the eastern part.

While the air partakes in the circulation in the subtropical anticyclones, it absorbs moisture from the underlying surface. Part of this moisture is transported upward by turbulence, but this transport is somewhat hindered by the general subsidence which tends to cause a slow transport of moisture downward. As a result of this, $\partial q/\partial z$ is negative and fairly large, so that the air becomes convectively unstable [*i.e.*, $(\partial\theta_{sw}/\partial z) < 0$] when $\partial q/\partial z$ is sufficiently large. This happens particularly in the western part of the subtropical cells.

Aerological ascents in the subtropical oceanic anticyclones are as yet too scanty to permit tabulation of the average conditions in the free atmosphere over the oceans. All that we can do here, therefore, is to give tables that illustrate the typical conditions in tropical maritime masses after they have invaded the adjacent continents. Table 33 shows the typical properties of *Tm* air in Europe, and Tables 34 and 35 show the same for air masses in the United States.

It will be seen from Table 34 that the *Tm* air which comes most directly from the western part of the subtropical cell is convectively unstable. This applies to the data for Groesbeck, Broken Arrow, Royal Center, and Due West. At Boston, however, the air is pronouncedly stable, and there is marked convective stability. This condition is due partly to cooling from below and partly to increased upward flux of

specific humidity as the air leaves the anticyclonic *régime*.   It appears from Table 34 that the specific humidity may vary considerably in

TABLE 33.—TROPICAL MARITIME AIR (Tm) IN WEST EUROPE (WINTER)

p	Φ	T	q	θ	θ_{sw}	θ_{se}	p	Φ	T	q	θ	θ_{sw}	θ_{se}
Trappes, Dijon, Lyon, and Chateauroux							Nancy, Cologne, and Frankfurt						
1000	—	10	7.0	10	9	31	1000	—	9	6.7	9	8	29
900	850	6	5.4	15	9	31	900	850	7	5.2	16	10	33
800	1800	3	4.1	21	10	34	800	1800	3	4.0	21	10	34
700	2850	−2	2.7	27	11	36	700	2850	−3	2.5	26	10	34
600	4050	−9	1.8	33	12	39	600	4000	−11	1.4	31	11	36
500	5400	−18	1.0	39	13	42	500	5400	−19	1.0	37	13	41
Hamburg, Kiel, and Norderney							Lindenberg, Berlin, and Breslau						
1000	—	9	6.2	9	8	28	1000	—	6	5.5	6	5	22
900	850	5	5.4	14	9	30	900	850	5	5.5	13	9	30
800	1800	2	3.7	20	10	32	800	1800	1	4.2	20	10	32
700	2850	−4	2.2	25	10	32	700	2850	−6	2.7	24	10	32
600	4000	−12	1.4	30	11	34	600	4000	−11	1.8	31	11	36
500	5400	−19	0.8	38	13	40	500	5400	−19	1.1	38	13	41
Königsberg and Swinemünde							Moscow and Slutsk						
1000	—	—	—	—	—	—	1000	—	—	—	—	—	—
900	—	4	5.6	13	9	30	900	—	—	—	—	—	—
800	—	1	3.4	19	9	30	800	—	−3	3.4	15	7	26
700	—	−6	2.1	23	8	30	700	—	−10	2.0	19	6	24
600	—	−14	1.5	28	9	32	600	—	−15	1.4	26	9	30
500	—	−18	1.3	38	13	42	500	—	−23	0.8	32	11	35

TABLE 34.—TROPICAL MARITIME AIR FROM THE ATLANTIC SOURCE IN THE UNITED STATES IN WINTER

Elevation, km.	Groesbeck			Broken Arrow			Royal Center			Due West			Boston		
	T	q	θ_{se}	T	q	θ_{se}	T	q	θ_{se}	T	q	θ_{se}	T	q	θ_{se}
Surface	19	12.6	54	20	11.8	55	18	11.3	51	17	10.5	47	14	8.5	37
1	14	10.4	53	14	9.7	51	13	9.6	49	13	9.1	47	14	6.5	41
2	13	4.1	45	12	4.8	45	8	4.5	41	8	5.3	42	9	6.2	46
3	8	1.2	39	7	3.1	45	—	—	—	3	4.0	43	2	4.6	45
4	—	—	—	—	—	—	—	—	—	—	—	—	−4	2.9	46

the same level at the various stations.   This, apparently, is due to the circumstance that the distribution of specific humidity along the vertical

depends on the amount of vertical mixing which has occured within the air column. The mean specific humidity q_m in the column below the 3-km. level is, however, almost constant, as will be seen from the following data:

Station	Groesbeck	Broken Arrow	Due West	Boston
q_m	7.1	7.3	7.2	6.8

Hence, if the air were thoroughly mixed, the specific humidity would be practically constant at all stations.

TABLE 35.—TROPICAL MARITIME AIR FROM THE PACIFIC SOURCE IN THE UNITED STATES IN WINTER

Elevation, km.	San Diego			Seattle			Ellendale		
	T	q	θ_{se}	T	q	θ_{se}	T	q	θ_{se}
Surface	19	9.1	43	13	7.4	32	—	—	—
1	17	6.1	42	8	5.7	35	5	2.8	24
2	11	5.3	46	2	4.3	35	1	3.7	32
3	5	3.7	45	−2	2.9	36	−5	2.8	34

The Atlantic Tm air that arrives in Europe is pronouncedly stable in the lower layers, and temperature inversions occur quite frequently. Above the ground layer, the lapse rate is not far removed from the moist-adiabatic and the air is convectively indifferent from the ground layer up to about 3 km. The same also applies to the Pacific Tm air that comes to the Pacific Coast. The Tm air that comes to the west coast in high latitudes has had a long trajectory over a colder surface since it left its source in the subtropical anticyclone. Its original convective instability has been nullified by cooling from below and upward flux of moisture. As a result of the latter process, the specific humidity in each level does not vary much from one station to another (see Table 33). The uniformity in specific humidity appears more distinctly when we consider the mean specific humidity below the 700-mb. level. Thus, at the stations Trappes, Dijon, Lyon, Chateauroux, Nancy, Cologne, Frankfurt, Hamburg, Kiel, Norderney, Lindenberg, Berlin, and Breslau the mean specific humidity below the 700-mb. level varies only from 4.5 to 4.8 grams. Seattle (see Table 35), which is similarly situated, has a mean specific humidity of 5.1 grams below the 3-km. level.

It should be noted that the tropical maritime air is the most homo-geneous of all air masses that arrive in middle and high latitudes. The mean specific humidity of the air column is perhaps more conservative

and more uniform than any other characteristic.   Not only is the tropical maritime air very homogeneous, but its characteristics vary but little from one case to the next, so that the conditions in individual cases do not differ considerably from the mean values given in the tables above. *Tm* air has fairly constant properties owing to the almost invariant conditions in its source and the slight variations in the trajectories of the tropical air masses.   Furthermore, very little precipitation is released within *Tm* air masses, appreciable amounts being released only in the *Tm* air that ascends along frontal surfaces.

The air temperatures observed in ships and typical of *Tm* masses will be discussed in Par. 86.

79. Arctic (*A*) and Polar Maritime (*Pm*) Air in Summer.—The coldest air masses in midsummer are those which form over the arctic fields of snow and ice; but these masses are usually so shallow that they lose their characteristics when they move southward.   This is particularly true of the conditions from the later half of June to the later half of August.   It is then difficult to recognize the arctic characteristics of the air after it has moved south of 60 to 65°N lat.   Earlier or later in the summer, arctic air may be recognized as such in west Europe as far south as 45°N lat.   Table 36 shows the typical properties of arctic air in north Russia.

TABLE 36.—ARCTIC AIR (*A*) IN SUMMER: MURMANSK AND ARCHANGEL

p	Φ	T	q	θ	θ_{sw}	θ_{se}
1000	0	9	5.1	9	6	24
900	850	2	3.7	10	5	23
800	1750	−2	3.5	16	8	28
700	2800	−11	1.8	18	6	23
600	3850	−16	0.8	25	8	27
500	5150	−27	0.3	28	8	28

It will be seen from Fig. 88 that there is a general outflow of air from the arctic region.   The ice-cooled air gradually becomes transformed into polar continental or polar maritime air.   The latter process takes place within the two regions 3, Fig. 90.   The *Pm* air within these regions is relatively cold and humid.   During its southward movement, it becomes heated from below and develops a moderately steep lapse rate. The vertical structure of such air is shown in Tables 37 and 38.

It will be seen that the *Pm* air that has moved southward has become slightly convectively unstable up to about 2 to 3 km.

Pm air may also form when warm air from the continents invades the regions 3, Fig. 90.   Such air masses develop extreme stability in the lower layers.   Stratus and fogs occur as a rule in such masses.

80. Polar Continental (Pc) Air in Summer.—These air masses originate in the northern parts of the continents (regions 2, Fig. 90). They do not usually form in well-defined anticyclones as does, for example, Pc air in winter. The summer Pc air masses form most frequently through consenescence of arctic and polar maritime air masses that invade the northern continents. Through an extended sojourn over a

TABLE 37.—POLAR MARITIME (Pm) AIR IN WEST EUROPE (SUMMER)

p	Φ	T	q	θ	θ_{sw}	θ_{se}
Hamburg, Kiel, Norderney, Swinemünde, and Königsberg						
1000	—	15	8.5	15	13	41
900	850	10	6.3	18	12	38
800	1800	4	4.7	22	12	38
700	2850	−2	3.1	27	12	38
600	4050	−9	1 8	33	12	39
500	5400	−17	1 0	39	13	42
Helsinki, Utti, and Slutsk						
1000	—	14	7 4	14	11	37
900	850	11	6 0	20	12	38
800	1800	4	4 0	23	11	35
700	2850	−2	2.8	28	11	36
600	3950	−9	1.9	33	12	39
500	5300	−19	1.2	37	13	41

TABLE 38.—POLAR MARITIME (Pm) AIR AT SEATTLE (SUMMER)

Elevation, *km.*	T	q	θ_{se}
Surface	17	7.1	35
1	9	6.3	35
2	5	3.9	34
3	1	2.3	36

warm continent, the Pc air may change gradually and become as warm as the tropical continental air. The summer Pc air masses, therefore, may exhibit all degrees of transition from cold and stable arctic air to warm and unstable tropical continental air. The properties of the Pc air will therefore vary considerably with latitude. It should also be remembered that the Pc air has a greater annual variation in temperature, moisture content, etc., than has any other air mass. Its properties will therefore vary rapidly from month to month.

In general, Pc air is characterized by: (1) A fairly low specific humidity. This is particularly true of the Pc air that forms directly out of

arctic air, *i.e.*, when air streams from the arctic region into the northern continents without coming into contact with the oceans. (2) A moderately low temperature. (3) Instability and convective instability in the lower layers (at least, in the middle of the day), becoming more pronounced as the air streams southward. (4) Convective stability aloft. (5) A relatively high condensation level, and lack of condensation phenomena, except in the later phases of its development when convective clouds and showers occur quite frequently.

TABLE 39.—POLAR CONTINENTAL (*Pc*) AIR IN NORTH AMERICA (SUMMER)

Ele-vation, km.	Ellendale			Royal Center			Broken Arrow			Pensacola			Due West		
	T	q	θ_{se}	T	q	θ_{se}	T	q	θ_{se}	T	q	θ_{se}	T	q	θ_{se}
Surface	19	6.3	39	17	8.3	41	15	8.3	39	23	13.4	59	22	10.0	51
1	16	5.6	40	13	5.8	38	17	5.8	42	20	9.8	57	17	7.3	47
2	10	3.9	39	6	4 5	37	12	2.9	39	12	7 2	52	9	4.8	42
3	4	3.1	41	2	2.6	38	6	1.7	41	7	5.0	51	4	3.0	42
4	−3	2.9	45	−2	1.4	41	1	1.2	44	—	—	—	—	—	—

TABLE 40.—POLAR CONTINENTAL (*Pc*) AIR IN EUROPE (SUMMER)

p	Φ	T	q	θ	θ_{sw}	θ_{se}
Berlin, Lindenberg, Breslau, Swinemünde, and Königsberg						
1000	—	17	9.6	17	15	46
900	850	14	7.5	23	15	46
800	1850	8	5.7	27	14	44
700	2900	2	3.9	32	15	45
600	4050	−6	2.3	36	14	44
500	5450	−14	1.3	43	15	45
Helsinki, Utti, and Slutsk						
1000	—	19	9.2	19	15	48
900	900	14	7.3	23	15	46
800	1850	8	5.0	27	14	43
700	2900	1	3.5	31	14	43
600	4100	−7	2.2	35	13	42
500	5450	−17	1.1	40	14	43

Table 39 shows the typical structure of the *Pc* air in the United States. The relative coolness and deficit of specific humidity of the American *Pc* air becomes more evident when its characteristics are compared with the data of continental tropical air (Table 43). It will be seen from Table 39 that the *Pc* air at Royal Center is considerably colder than, for

example, that at Ellendale. According to Willet [89], this condition is due to the cooling influence of the Hudson Bay and the Great Lakes which the air must traverse before it arrives at Royal Center.

It will be seen from Fig. 88 that the American Pc air borders upon the tropical continental air along a sharp line of demarcation in the wind field (the American polar front), so that the Pc air appears as a definite type of air on account of its great contrast relative to the warmer air masses that originate farther to the south. In Europe, there is generally no such distinct line of separation in the wind field (see Fig. 88); and, as a consequence, the contrast between the Pc air and the continental tropical

TABLE 41.—POLAR CONTINENTAL (Pc) AIR IN EAST EUROPE (SUMMER)

p	Φ	T	q	θ	θ_{sw}	θ_{se}
		Moscow, Smolensk, Cracow, and Kiev				
1000	—	17	7.4	17	14	42
900	900	16	7.0	25	16	50
800	1850	9	5.1	28	15	44
700	2900	2	3.5	32	13	43
600	4100	−5	2.2	38	14	44
500	5500	−14	1.1	43	15	47
		Murmansk and Archangel				
1000	—	14	8.6	14	12	40
900	850	11	7 3	20	14	43
800	1800	5	5.6	22	13	41
700	2850	−1	4.0	28	13	42
600	3950	−5	2.4	38	14	46
500	5350	−15	1.9	42	15	48

air is often quite indistinct. The typical properties of Pc air in Europe are shown in Tables 40 and 41. A comparison of these data with those contained in Table 42 will show that European Pc air is only slightly colder and drier than Tc air in west Europe. It will also be seen that European Pc air is, on the whole, moister than American Pc air. This condition is due to the circumstance that Pc air in Europe often develops from air which has previously been in contact with the ocean. Finally, it is of interest to remark that Pm air (Table 37) is considerably colder than Pc air in west Europe.

The vast expenses of northern Russia and Siberia have a type of Pc air that is similar to the American type. Here, air from the arctic region is brought into the interior of the warm continent; and as the air does not absorb much moisture from the underlying surface, it remains dry and cloudless. The warm and moist air that the monsoon in south and

east Asia brings into the interior of the continent gives off a considerable part of its moisture content on the windward side of the extensive mountain range.   The air of tropical or equatorial origin that arrives in Siberia is therefore relatively dry.   In stagnant situations, notably when an anticyclone settles down in Siberia, the *Pc* air may eventually become as warm as air of southern origin.   Whether the *Tc* air in Siberia originally came from the monsoon region or from the arctic region, it will be convectively unstable and will produce showers or thunderstorms whenever it is lifted sufficiently either along a front or in an area of converging winds.

TABLE 42.—TROPICAL CONTINENTAL (*Tc*) AIR IN GERMANY (SUMMER)

p	Φ	T	q	θ	θ_{sw}	θ_{se}
Königsberg and Swinemünde						
1000	—	21	11.6	21	18	57
900	900	17	8.7	27	17	54
800	1850	11	6.6	29	16.5	52
700	2925	3	4.6	32	15.5	49
600	4125	−4	2.9	39	16	49
500	5500	−12	1.6	46	16	51
Berlin, Lindenberg, and Breslau						
1000	—	20	9.5	20	16	49
900	900	18	8.5	27	17	53
800	1850	11	6.5	30	16	50
700	2925	4	4.6	35	16	50
600	4150	−3	2.7	40	16	49
500	5500	−14	1.6	44	15	48

81. Tropical Continental (*Tc*) Air in Summer.—The typical *Tc* air in summer is continuously produced in the subtropical arid regions (4, Fig. 90).   The *Tc* air that develops over deserts and steppes (*i.e.*, in the zones of the *B* climates in Köppen's classification) is extremely warm and unstable.   On account of its lack of moisture, the counterradiation of the sky at night is small, and the air develops a large diurnal amplitude of temperature.   On account of its relative dryness, the condensation level is high; and as the wind conditions in the upper air are predominantly anticyclonic (see Figs. 84 and 85), subsidence in the upper air prevents the formation of convective clouds.   A typical example of the stability conditions of such air was shown in Fig. 60.   The *Tc* air that develops in north Africa and Asia Minor is excessively dry; but when it streams northward, it absorbs a considerable amount of moisture before it arrives

in south Europe and southwest Siberia. The absorption of moisture in the lower levels reduces the height of the condensation level and increases the convective instability. These masses, therefore, contribute much to the summer showers and thunderstorms in south and east Europe and in southwest Siberia. The weather charts of July and August, 1938, show numerous examples of this condition.

TABLE 43.—TROPICAL CONTINENTAL (Tc) AIR IN EAST EUROPE (SUMMER)

p	Φ	T	q	θ	θ_{sw}	θ_{se}
			Murmansk and Archangel			
1000	—	17	9.7	17	15	47
900	850	15	8.9	24	16	52
800	1850	10	6 8	29	16	51
700	2900	3	5 4	33	16	51
600	4100	−4	3 6	39	16	50
500	5500	−12	1 8	46	16	52
			Helsinki, Utti, and Slutsk			
1000	—	20	10.4	20	17	52
900	900	17	8.0	26	16	51
800	1850	10	5.8	29	15	48
700	2900	4	4.1	34	15	47
600	4150	−4	2.6	39	15	47
500	5500	−12	1.3	46	16	52
			Moscow, Smolensk, Kiev, and Cracow			
1000	—	—	—	—	—	—
900	900	23	9.3	32	20	62
800	1900	15	7.2	34	18	58
700	3000	6	4.5	36	16	51
600	4200	−1	3.0	42	17	52
500	5600	−10	1.6	48	17	54

A less extreme type of Tc air develops in midsummer in the northern portion of the Eurasian region 4. This happens mostly in anticyclonic conditions and when the ground is relatively dry. This type of Tc air is, on the whole, more stable than that which develops farther to the south. Consequently, summer thunderstorms occur within the Eurasian region 4 more frequently when Tc air from southern regions is brought northward than in the Tc air which develops in the anticyclones in high latitudes. Table 42 shows the typical structure of Tc air that forms over central Europe in midsummer. It will be seen that it is only slightly

warmer than the Pc air within the same region; its convective instability is, however, more pronounced.   The lack of instability below the 900-mb. level is due to the fact that the ascents were made in the early morning. Table 43 shows the typical properties of Tc air in Russia, and Table 44 shows the same for Tc air in North America.

TABLE 44.—TROPICAL CONTINENTAL (Tc) AIR IN THE UNITED STATES (SUMMER)

Elevation, km.	Ellendale			Broken Arrow		
	T	q	θ_{oo}	T	q	θ_{oo}
Surface	27	11.3	62	27	9.5	56
1	28	8.0	60	27	7.9	59
2	22	6.1	59	19	6.5	57
3	15	4.6	59	10	5.0	54
4	6	3.3	56	—	—	—

82. Tropical Maritime (Tm) Air in Summer.—The abode of the tropical maritime air masses in summer is the two regions indicated by 5 in Fig. 90.   The conditions within these regions are principally the same as in winter; but the subtropical anticyclones arc larger and more permanent, and the sea-surface temperature is, on the whole, higher and more uniform.   In the eastern portion of the subtropical anticyclones, the northerly winds increase in summer; and, as a result, there is a considerable upwelling of cold water along the subtropical west coast.   Simultaneously, the sea-surface temperature rises to its summer maximum in the western portions of these anticyclones.   In summer, there is therefore a considerable zonal temperature gradient in the sea surface in subtropical latitudes.   The air that moves westward on the equatorial side of the subtropical anticyclones will therefore be heated from below, whereas the air that moves eastward on the poleward side of the anticyclone will be cooled from below.   In addition, the air is subject to the influences due to the cell circulation (see Par. 67).   The Tm air in summer is therefore rather unstable in the western portion and highly stable in the eastern portion of the cell.   This has a great influence on the distribution of rain.   Thus, though Funchal (Madeira) has 0.1 in. of rain in July, Miami (Florida) (on the same parallel) has more than 5 in.

Table 45 shows the typical properties of the Tm air that arrives in the eastern part of the United States from the western portion of the Atlantic cell, and Table 46 shows the properties of Tm air that arrives in southwest Europe.   It will be seen that the American Tm air is convectively unstable and the European type is convectively stable.

It is of interest to note that most of the rain which falls in the warm season in the United States originates from Tm air, either as air-mass

showers and thunderstorms or as frontal rain. On account of the pronounced convective instability, convective clouds and thunderstorms occur frequently when the *Tm* air is lifted along frontal surfaces. A further reason for the high frequency of convective phenomena within the *Tm* air in the United States may be sought in the circumstance that the air, before it arrives at the south coast, has passed the West Indies where, on account of the diurnal heating of the islands, it has become engrained with convective elements.

Observations from Peiping show that the structure of the *Tm* air there is the same as that shown in Table 45 for Pensacola. The structure of Pacific *Tm* air, when it arrives at the coast of California, is similar to that of the Atlantic *Tm* air that arrives in southwest Europe. Observations are as yet too scanty to allow compiling of tables of the normal properties for the Pacific region.

TABLE 45.—TROPICAL MARITIME (*Tm*) AIR IN THE UNITED STATES (SUMMER)

Eleva-tion, km.	Pensacola			Due West			Broken Arrow			Royal Center		
	T	q	θ_{se}	T	q	θ_{se}	T	q	θ_{se}	T	q	θ_{se}
Surface	29	20.7	86	29	18.4	83	30	15.4	75	29	15.9	76
1	23	15.6	77	25	12.8	72	27	12.3	72	25	13.9	75
2	17	12 5	72	18	10.3	67	20	9.9	69	19	11.5	71
3	11	9.5	68	10	8.1	63	13	8.2	66	11	8.6	66
4	—	—	—	4	5.9	60	7	5.4	63	—	—	—
5	—	—	—	—	—	—	2	3.5	63	—	—	—

TABLE 46.—TROPICAL MARITIME (*Tm*) AIR IN EUROPE (SUMMER)

p	Φ	T	q	θ	θ_{sw}	θ_{se}

Hamburg, Kiel, Norderney, Königsberg, and Swinemünde

p	Φ	T	q	θ	θ_{sw}	θ_{se}
1000	—	20	8.9	20	15	46
900	900	14	7.5	23	15	46
800	1850	9	6.2	28	16	48
700	2900	3	4.6	33	16	48
600	4100	−4	3.3	39	16	50
500	5500	−11	2.1	47	17	54

83. Supérieur Air.—It was mentioned in Par. 68 that a distinct type of air mass develops in anticyclonic eddies in the free atmosphere. These masses, which develop entirely on account of subsidence, stand in no direct relation to the properties of the earth's surface. They develop above inversion layers, and only rarely do they descend to the earth's surface. They are most frequently recorded in the zone consisting of the

southern half of the prevailing westerlies and the northern half of the subtropical anticyclones.   The symbol S (or T_s) has been introduced for this type of air by American meteorologists, S being suggestive of *supérieur, sèche,* and subsidence. It was first thought that this type of air developed out of tropical air, but it was found later that such a type of air may also develop in a subsiding polar current.

TABLE 47.—TYPICAL PROPERTIES OF S-AIR AT THE 2-KM. LEVEL

Station	January		July	
	T	q	T	q
San Antonio............................	10	3	24	5
Omaha.................................	5	2	22	5

The vertical structure of a *supérieur* air mass is essentially as shown by Figs. 59D and 60. Above the inversion layer, the S-air is warmer than any other air mass; but, on account of the steep lapse rate in higher levels, its temperature above the 5-km. level would probably decrease below the temperature of neighboring tropical masses.
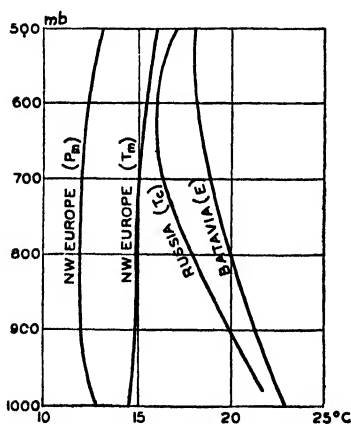
FIG. 92.—Vertical distribution of potential pseudo-equivalent temperature in summer.

Extreme dryness is the outstanding feature of the S-air. The relative humidity is frequently below 30 per cent and sometimes falls below 10 per cent. The conditions typical of the S-air in the United States are shown in Table 47.

It is worthy of note that the S-air is similar to the continental tropical air masses which develop in subtropical anticyclones in arid regions.

84. Equatorial Air.—The abode of this air mass is the region indicated by 8, Fig. 89 (winter), and the region indicated by 6, Fig. 90 (summer). The belt that is occupied by equatorial air coincides with the doldrums, and it moves northward and southward in an annual rhythm as do the subtropical anticyclones. The equatorial air mass is extremely uniform in space and time. It is characterized by high temperature and high humidity content, indifferent or unstable equilibrium, and pronounced convective instability.

Figure 92 shows the mean distribution of potential pseudo-equivalent temperature along the vertical at Batavia compared with similar curves

for stations in other latitudes. It will be seen that the equatorial air is characterized by pronounced convective instability in a deep layer of air. The curve for Batavia may be regarded as representative for all seasons in the entire area occupied by equatorial air.

85. Monsoon Air.—In the region occupied by the winter monsoon in Asia and adjoining seas (*i.e.*, region 9, Fig. 89), *Pc* air is gradually transformed into equatorial air. The northern limit of this air mass is marked quite distinctly by the mountain ranges, but the southern limit is very diffuse.

TABLE 48.—MONSOON (*M*) AIR IN INDIA (WINTER)

p	Φ	T	q	θ	θ_{sw}	θ_{se}	R
				Agra			
996		19	4.3	19	10	33	32
900	850	10	4.2	19	10	32	50
800	1800	5	3.5	23	10	34	51
700	2850	1	3.1	32	13	41	51
600	4050	−5	1.7	37	14	43	50
500	5400	−14	1.2	47	15	46	49
				Poona			
—	—	—	—	—	—	—	—
900	1000	22	6.8	31	17	54	38
800	2000	14	4.6	33	15	47	39
700	3200	7	2.8	38	15	46	32
600	4300	0	1.4	44	15	48	21
500	5700	−9	0.6	49	16	51	16
				Karachi			
1000	—	18	6.6	18	12	39	51
900	900	15	5.0	24	13	41	43
800	1850	8	3.4	27	12	38	41
700	2900	4	3.4	34	14	47	48
600	4150	−3	2.6	40	18	58	53
500	—	—	—	—	—	—	—

Pc air that streams across the mountain range is heated adiabatically, and it is also heated by traveling toward warmer regions. Over the continent, the moisture supply is sparse, and the relative humidity decreases as the air streams southward. Over land, the monsoon air in winter is exceedingly dry. The typical properties are shown in Table 48.

In summer, the winds are reversed, and air of the equatorial type is brought into south Asia on the eastern side of the line indicated in Fig. 90.

To the west of this line, either the air is of continental origin, or its trajectory over water is so short that it has absorbed only a small amount of water vapor. Furthermore, the dry westerly winds at high levels that come from Afghanistan and Baluchistan hinder condensation and precipitation in the western part of India in summer (Simpson [77]). The air in western India is therefore, on the whole, of a continental (Arabian) type. The structure of the monsoon air in India in summer is shown in Table 49.

TABLE 49.—MONSOON (*M*) AIR IN INDIA (SUMMER)

p	Φ	T	q	θ	θ_{sw}	θ_{ss}	R
Madras							
1000	—	31	18.0	31	26	88	65
900	950	25	17.0	34	25	87	76
800	1950	17	13.5	37	24	82	87
700	3050	10	10 0	41	23	74	89
600	4300	3	7.0	47	22	71	89
500	5700	−5	4.2	54	21	68	83
Agra							
1000	—	—	—	—	—	—	—
900	900	28	19.0	38	27	103	73
800	1900	21	15.0	41	26	93	79
700	3000	15	12 0	47	25	87	78
600	4250	6	7.5	51	23	78	74
500	5700	−1	5.0	59	23	78	77

It should be noted that the southwest monsoon in summer crosses the Western Ghats before it arrives at the stations given in Table 49. The monsoon air is therefore more humid on the west coast of India than at the stations referred to.

86. Air-mass Temperatures on the North Atlantic Ocean.—Aerological observations on the oceans are as yet so sparse that it is not possible to compute tables of the normal air-mass characteristics. However, as the air temperature observed in ships is representative, it is possible to compute the normal values of the air temperature in the principal types of air mass. Maps containing such normals have been computed by aid of an extended series of carefully analyzed synoptic maps. As ship observations are rather scanty, it is often difficult to identify the air masses and to locate the fronts. However, when the normal air temperature of the various air masses is known for each month and for each 5° square, the individual observations may be compared with these normal temperatures and with the temperature of the

sea surface.   It will then often be possible to decide even from scanty observations what type of air mass one is concerned with.

Figure 93 shows the mean air temperature in the various 5° squares when the square in question is occupied by maritime tropical air.   Except-
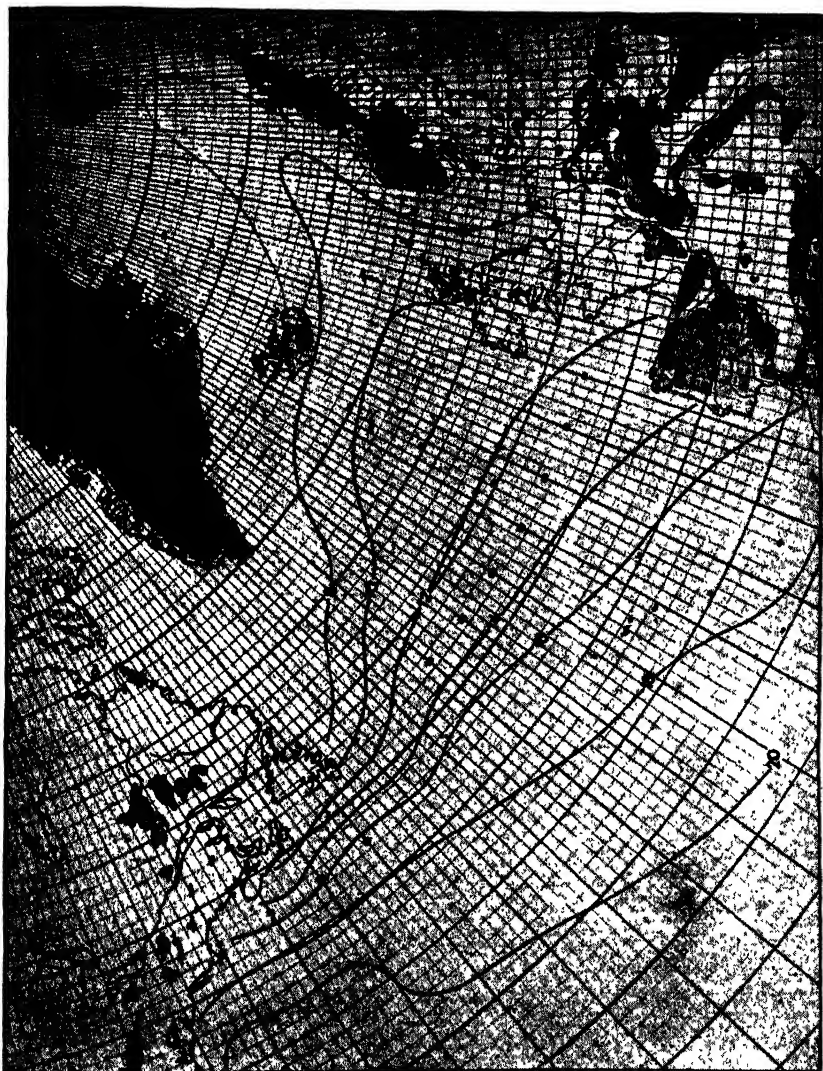
FIG. 93.—Mean air temperature in tropical maritime air in January.

ing the area occupied by the Labrador Current, it will be seen that the temperature of the *Tm* air is exceedingly uniform, its horizontal temperature gradient being even less than that of the underlying surface (see Fig. 73).

The statistical investigations on which the map is based showed that the dispersion of the individual Tm air temperatures within each 5° square is very small. In the eastern part of the North Atlantic, it was
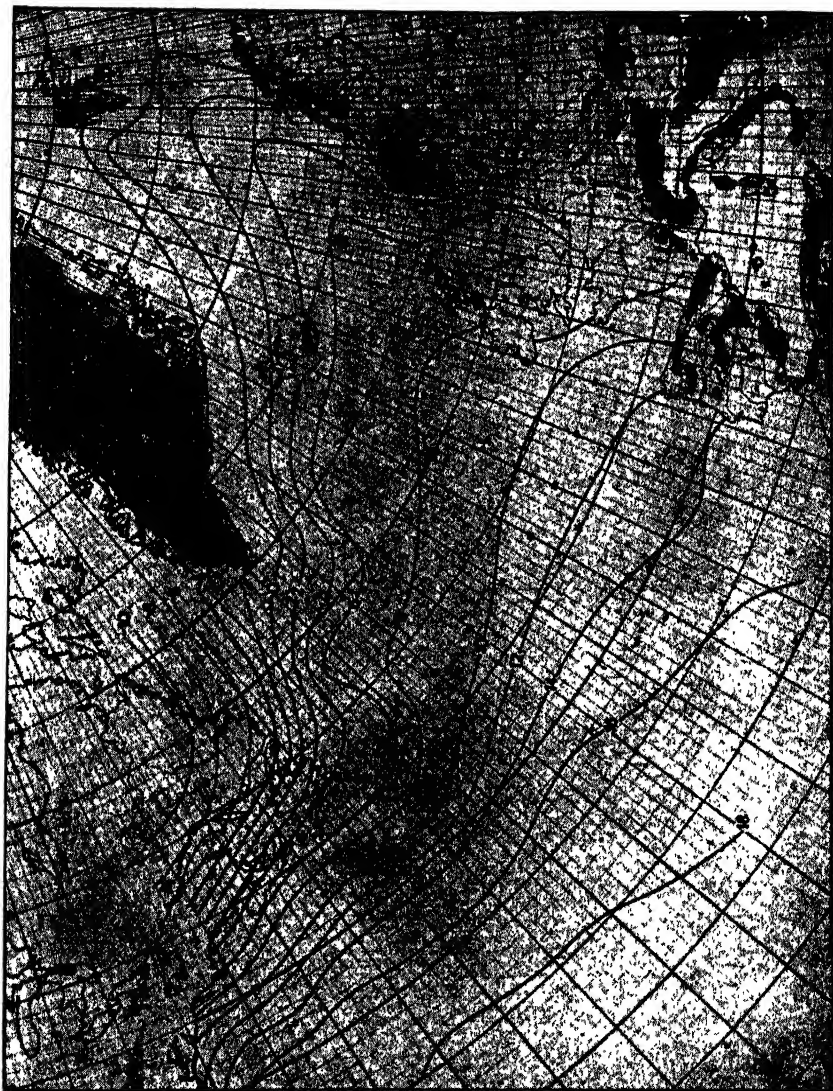
FIG. 94.—Mean air temperature in returning polar air in January.

found that the temperature of Tm air varied about the mean values for the significant squares by 1 or 2°C. Thus, during the several years under investigation, it was found that true Tm air appeared in a given square with an almost constant temperature. This condition is due to the well-defined source of the Tm mass and to the slight variation in the

trajectories of the individual *Tm* masses. In the region of the Labrador Current, it was found that the temperature of *Tm* air varied considerably from one case to another, the extreme variations being up to ±4°C.
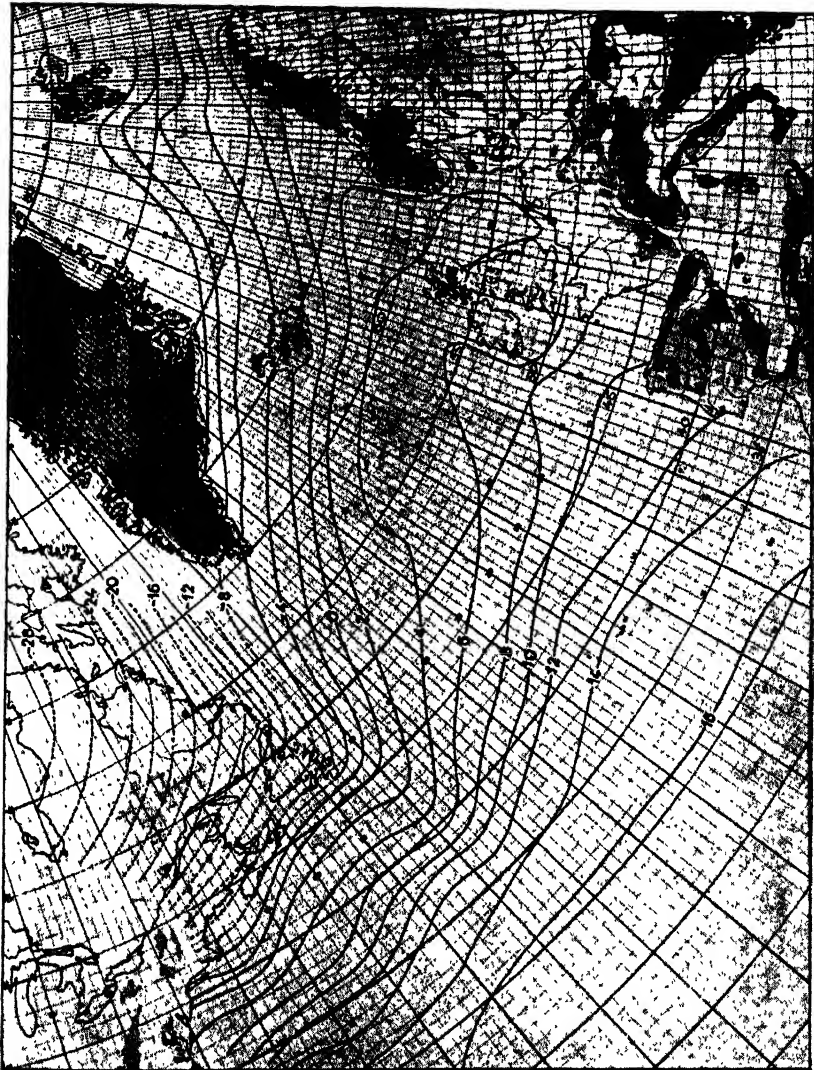
FIG. 95.—Mean air temperature in direct outbreaks of polar continental and arctic air in January.

This condition is due to the great variations in the temperature of the sea surface that are encountered in and near the Labrador Current.

The polar continental and the arctic air masses that invade the North Atlantic Ocean in winter are not so uniform as are the *Tm* masses. Figure 94 shows the mean air temperature of returning polar air, *i.e.*, air

from polar continental or arctic sources that again returns northward. Figure 95 shows the mean air temperature in direct outbreaks of air from the arctic and the polar continental sources in January.   Figures 96 to 98 show the same conditions in summer.
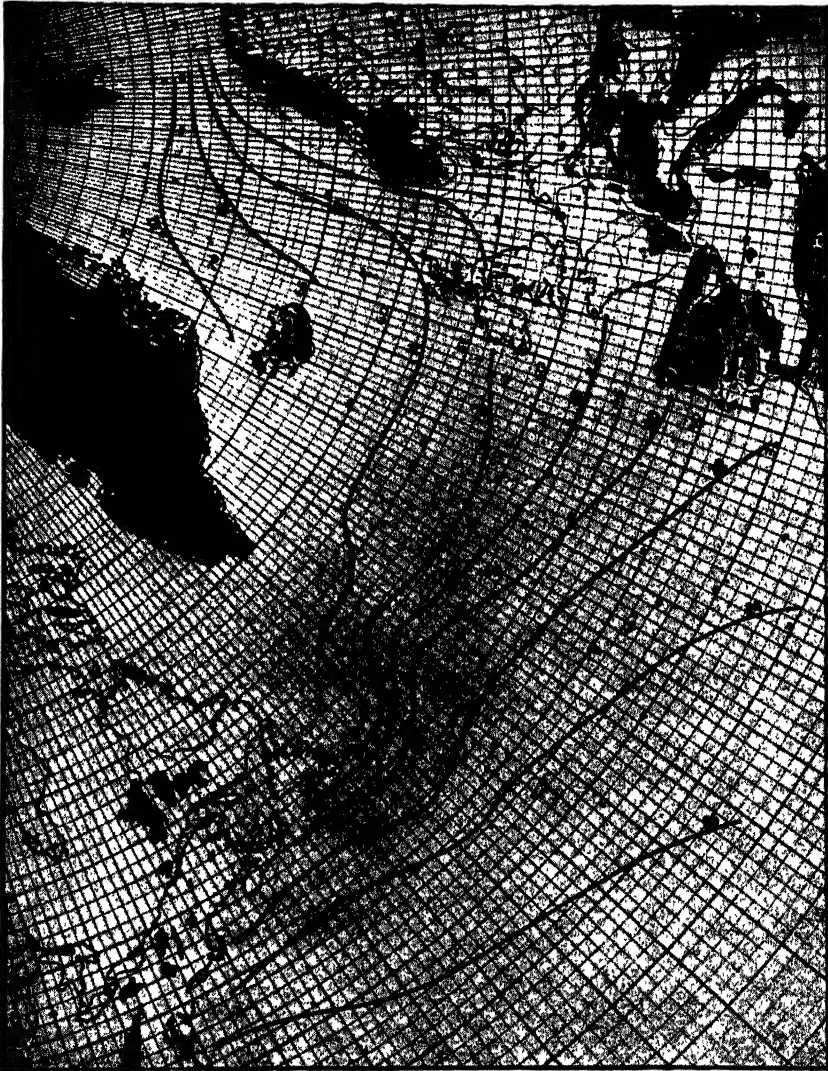
FIG. 96.—Mean air temperature in tropical maritime air in July.

It will be shown later that important conclusions with regard to frontogenesis may be drawn from these maps.

87. Use of Air-mass Characteristics.—The following remarks will supplement what has been said in the foregoing paragraphs.

Even though the air masses usually appear as distinct types, it should be borne in mind that this is not always so. Thus, when arctic air arrives into the region west of Portugal and Morocco, the changes due to

Fig. 97.—Mean air temperature in returning polar air in July.

a lengthy trajectory over the Atlantic Ocean are so great that the air can hardly be distinguished from the air that comes from the tropical maritime source. On the other hand, in the Labrador region, there is a pronounced difference between *Pc* and *Tm* air. That this is so is readily seen from the maps shown in Par. 86. As a general rule, it may be stated

that the air masses appear as distinct types where extreme air-mass sources are adjacent to one another.   This is true of the eastern part of the United States and the western part of the North Atlantic Ocean
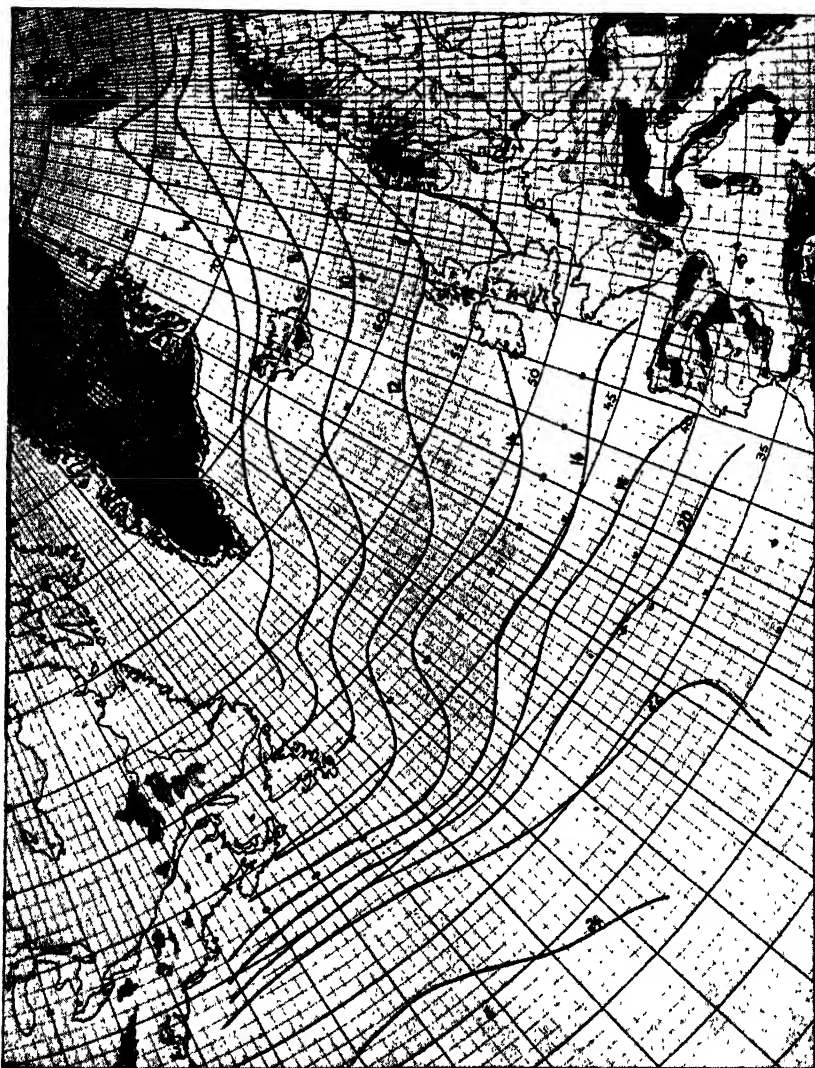
Fig. 98.—Mean air temperature in direct outbreaks of polar and arctic air in July.

in winter (see Fig. 89) where the extremely cold *Pc* and the warm *Tm* air are brought into juxtaposition by the prevailing winds.   The same also applies to the western part of the Pacific Ocean and the east coast of Asia.   In these regions, the air masses are separated from one another

by strong fronts, and rapid and pronounced changes occur when one air mass replaces another.

In the eastern parts of the oceans, the differences in properties between adjacent air masses are often so small that it is difficult to identify the air masses by comparing the actual observations with the normal values. In such cases, the actual trajectories of the air masses must be considered.

The quasi-conservative properties are more conservative in the free atmosphere than near the earth's surface. The traveling masses may therefore be more readily recognized by aid of observations made above, say the 2-km. level, than by those made below this level. Furthermore, the air masses that
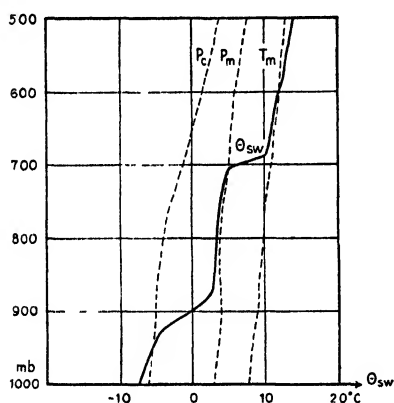
Fig. 99.—Air-mass-type diagram. Broken lines indicate the normal distribution of θ_{sw} in principal types of air masses. Full line indicates the actual distribution of θ_{sw}. It will be seen that the ascent goes through a shallow layer of P_c air, above which is a layer of P_m air which is separated from T_m air aloft by a well-defined frontal surface.

Fig. 100.—Showing temperature changes in various levels. (*Courtesy of M. Bureau, Office Nat. Met. de France.*)
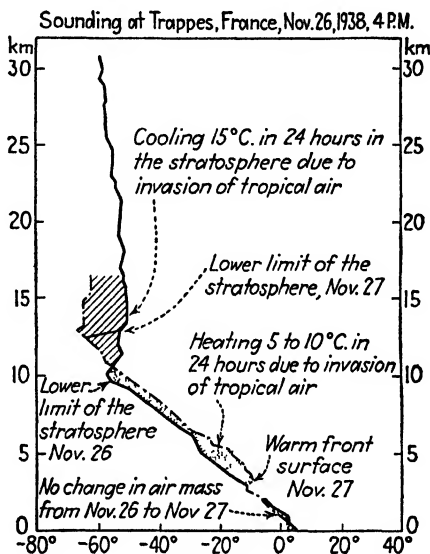
develop stability while they move from their sources are more conservative in the free atmosphere than are those which develop instability. Thus, the Tm masses are particularly conservative aloft. It is therefore always important to trace the Tm masses; other masses, which have more variable characteristics, may then be recognized by their contrasts relative to the Tm mass. In northern latitudes, it is important to extend the analysis so far southward that the movements of the Tm and Tc masses can be traced. It is along the northern border of these masses that the principal source of energy for atmospheric disturbances is found.

Schinze [71], who has studied in great detail the air-mass characteristics in Germany, has made a diagram that facilitates the identification of air masses. In Schinze's diagram, the abscissa is potential equivalent

temperature θ_e, and the ordinate is height.   From what was said in Chap. I, it follows that it would be more appropriate to use a diagram in which θ_{sw} is abscissa and p ordinate.   On such a graph, the normal θ_{sw} lines of the air masses may be printed.   The actual observations, when plotted on this diagram would, in most cases, show what type of air mass is above the station in question.   The principle of this diagram is shown in Fig. 99.

In tracing the movement of the air masses aloft, it is often useful to plot consecutive ascents on one graph so as to see the changes that occur in the various levels.   For this, one may use a temperature-height diagram or any type of T-p diagrams.   An example is shown in Fig. 100.

CHAPTER IV

KINEMATIC ANALYSIS: WIND AND PRESSURE

Considered from a theoretical point of view, the forecasting problem is closely related to the study of the field of motion of the air. A rational treatment of the observed wind is, however, very difficult. This condition is due to a number of circumstances. In the first place, the mathematical structure of the equations of motion is so complicated that solutions can be obtained only on the basis of numerous simplifying assumptions. Theoretical results, thus obtained, are therefore not strictly comparable with what is observed. Secondly, the wind is never a steady current; it varies in a succession of gusts and lulls of short period, so that it is difficult to obtain representative values of the direction and the speed of the wind. Furthermore, the wind observations are made within the friction layer close to the earth's surface, where the wind varies rapidly along the vertical. The observed winds, therefore, depend greatly on local conditions, and there is perhaps no other meteorological element that is influenced locally to such an extent as are the wind observations. In the free atmosphere, the winds are computed from observations of pilot balloons. These observations are equally inaccurate, for the wind must be computed from the observed angles on the assumptions that the rate of ascent of the balloon is constant and that there are no vertical currents in the air. Moreover, the pilot-balloon observations are as yet too scanty to permit a detailed analysis of the winds aloft.

It will therefore be understood that the analysis of the directly observed winds, either near the earth's surface or in the free atmosphere, often gives inaccurate results. However, on account of the numerous relations that exist between the direction and the speed of the wind on the one hand, and the distribution of the physical variables of the atmosphere on the other, it is possible to study the wind field by means of these variables. The aim of this chapter will be to demonstrate a number of relations between the wind and the other elements that have proved useful in the analysis of daily weather charts and upper-air charts.

88. The Terms in the Equations of Motion.[1]—The equations of motion state a relation between the acceleration that the air undergoes

---

[1] Most of the content of this and the two following paragraphs is based on a paper by Jeffreys [39]. Reference is also made to Brunt [19].

and the forces that act upon the air. The forces are: (1) gravity, (2)
hydrostatic pressure, and (3) friction. When the motion is referred to
the rotating earth, the so-called deviating force due to the earth's
rotation enters into the equations of motion. Choosing a right-angled
system of coordinates with the z-axis along the vertical and using the
notations in the list of symbols, we may write

(1)
$$\frac{dv_x}{dt} + 2\omega(v_z \cos \varphi - v_y \sin \varphi) = -\frac{1}{\rho}\frac{\partial p}{\partial x} + K\frac{\partial^2 v_x}{\partial z^2}$$

(2)
$$\frac{dv_y}{dt} + 2\omega v_x \sin \varphi = -\frac{1}{\rho}\frac{\partial p}{\partial y} + K\frac{\partial^2 v_y}{\partial z^2}$$

(3)
$$\frac{dv_z}{dt} - 2\omega v_x \cos \varphi = -\frac{1}{\rho}\frac{\partial p}{\partial z} - g$$

In the first place, the pressure terms in the equations are always
important; otherwise, each portion of the air would move more or less
independently of the adjacent parcels of air.

The terms on the left-hand side of Eq. (3) are usually negligible
because they are small as compared with gravity. Even when the wind
is of hurricane force (e.g., $v_x = 30$ m./sec.) and when $\varphi = 0°$, the term
$2\omega v_x \cos \varphi$ amounts only to 0.004 m./sec.², which is negligible against g.
It has been found that the acceleration term dv_z/dt in violent convective
currents may amount to 0.5 m./sec.² Even though vertical acceleration
and vertical velocity are important factors in local convective currents,
as was shown in Chap. II, they are altogether negligible in the discussion
of the large-scale wind systems. Therefore, neglecting v_z and dv_z/dt and
putting $2\omega \sin \varphi = \lambda$, we may write

(4)
$$\frac{dv_x}{dt} - \lambda v_y = -\frac{1}{\rho}\frac{\partial p}{\partial x} + K\frac{\partial^2 v_x}{\partial z^2}$$

(5)
$$\frac{dv_y}{dt} + \lambda v_x = -\frac{1}{\rho}\frac{\partial p}{\partial y} + K\frac{\partial^2 v_y}{\partial z^2}$$

(6)
$$0 = -\frac{1}{\rho}\frac{\partial p}{\partial z} - g$$

89. Classification of Winds.—Since the pressure term is always
important, it follows that at least one of the other terms must be com-
parable in magnitude with it. The winds may, therefore, be classified
according to the identity of the term or terms in question.

Case 1.—Rotational and frictional terms negligible. Here

(1)
$$\frac{dv_x}{dt} = -\frac{1}{\rho}\frac{\partial p}{\partial x} \quad \text{and} \quad \frac{dv_y}{dt} = -\frac{1}{\rho}\frac{\partial p}{\partial y}$$

or in vector notations

$$\frac{dv}{dt} = -\frac{1}{\rho}\nabla p$$

The acceleration coincides with the pressure gradient, and the air will eventually blow *normal* to the isobars from high to low pressure. Jeffreys calls this class of wind "Eulerian." Winds of this type are seldom observed, except in low latitudes, for the rotational term increases with the wind velocity, so that the deviating force gradually becomes important and tends to balance the pressure term. The Eulerian (*i.e.*, the accelerational) component of the wind is, however, always important even though it is usually overshadowed by the winds arising from the rotational term. A special type of Eulerian wind occurs in equatorial regions, notably in tropical cyclones. This type is characterized by an accelerational term which consists mainly or solely of the centrifugal force due to the curvature of the path of the air particle (see below).

Case 2.—Frictional terms exceeding the rotational and the accelerational terms. The equations of motion then reduce to

$$(2) \qquad K\frac{\partial^2 v_x}{\partial z^2} = \frac{1}{\rho}\frac{\partial p}{\partial x} \qquad \text{and} \qquad K\frac{\partial^2 v_y}{\partial z^2} = \frac{1}{\rho}\frac{\partial p}{\partial y}$$

The wind will in general blow along the pressure gradient, friction preventing its velocity from increasing steadily. Jeffreys calls this class of wind "antitriptic." Such winds are of small horizontal extent; they are exceedingly shallow and of short duration. Land and sea breezes and mountain and valley winds are mostly antitriptic winds.

Case 3.—Rotational terms far in excess of both accelerational and frictional terms. The equations of motion now reduce to

$$(3) \qquad -\lambda v_y = -\frac{1}{\rho}\frac{\partial p}{\partial x} \qquad \text{and} \qquad \lambda v_x = -\frac{1}{\rho}\frac{\partial p}{\partial y}$$

The gradient of pressure is here balanced by the deviating force. Winds of such a type are called "geostrophic."

Letting $v_{g_\bullet} = +\sqrt{v_x^2 + v_y^2}$ = geostrophic wind, and

$$\frac{\partial p}{\partial n} = \sqrt{\left(\frac{\partial p}{\partial x}\right)^2 + \left(\frac{\partial p}{\partial y}\right)^2} = \text{horizontal pressure gradient,}$$

we obtain

$$(4) \qquad v_{g_\bullet} = \frac{\partial p/\partial n}{\rho\lambda} = \frac{\text{pressure gradient}}{\rho\lambda}$$

or in vector notations

$$(4a) \qquad v_{g_\bullet} = -\frac{1}{\rho\lambda}\nabla p \times k$$

where k is a vertical unit vector. It follows from Eqs. (3) and (4a) that the geostrophic wind blows along the isobars with high pressure to

the right of the direction of motion (in the northern hemisphere); further-more, the velocity of the geostrophic wind is proportional to the pressure gradient, or inversely proportional to the distance between the isobars. It should be borne in mind that the geostrophic wind is derived on the assumption that the accelerational term is negligible. This assumption applies when *the isobars are straight and parallel, and when the pressure gradient does not change.*

Case 4.—The frictional terms are negligible, and so, also, are the accelerational terms except the centrifugal acceleration due to the curva-ture of the path. The motion of the air is then balanced by the following forces: (*a*) the pressure gradient acting from high to low pressure, and at right angles to the isobars, (*b*) the deviating force acting at right angles to the direction of the motion and toward the right (in the northern hemisphere), and (*c*) the centrifugal force acting at right angles to the direction of the motion.

It is convenient to distinguish two cases, according to whether the forces *a* and *c* are in the same or in opposite directions, *i.e.*, according to whether the path is curved in the same sense as anticyclonic or cyclonic isobars. The wind that corresponds to this balance is called the gradient wind v_{gr}. Equating the forces and solving with respect to wind velocity, we obtain the gradient-wind equations

$$(5) \qquad v_{gr} = \frac{\text{pressure gradient}}{\rho \lambda} + \frac{v_{gr}^2}{\lambda r} \qquad \text{(anticyclonic curvature)}$$

$$(6) \qquad v_{gr} = \frac{\text{pressure gradient}}{\rho \lambda} - \frac{v_{gr}^2}{\lambda r} \qquad \text{(cyclonic curvature)}$$

In these equations, r is the radius of curvature of the path. Equation (6) may be regarded as included in Eq. (5) when we consider r as being negative when the path is curved cyclonically.

v_{gr} in the above equations defines the *gradient wind*. It is readily seen that the forces *a*, *b*, and *c* mentioned above can balance one another only when the wind blows along the isobars: *the gradient wind has no radial component.* The gradient wind is a good approximation to the true wind above the friction layer when the isobars do not diverge or converge appreciably.

From Eqs. (4), (5) and (6), we obtain

$$(7) \qquad\qquad v_{gr} - v_{ge} = \pm \frac{v_{gr}^2}{\lambda r}$$

The difference between the gradient wind and the geostrophic wind decreases as r increases. The geostrophic wind may therefore be used as a good approximation to the true wind (above the friction layer) when the radius of curvature of the path is not too small.

The term on the right-hand side in Eq. (7) is called the *cyclostrophic term*.   In most cases, in high and middle latitudes, r is so large that the cyclostrophic component is negligible.   In low latitudes, where λ is small, the geostrophic component may become negligible in comparison with the cyclostrophic component.   Multiplying Eq. (6) by λ and letting λ converge to zero, we obtain

$$(8) \qquad \pm \frac{v_{gr}^2}{r} = \frac{\text{pressure gradient}}{\rho}$$

As v_{gr}^2/r must always be positive, it follows that steady cyclostrophic motion is possible only when the pressure increases along the radius of curvature of the path, *i.e.*, when the isobars are curved cyclonically. Closed anticyclonic isobars are not possible as stable systems near the equator.

90. Application of the Classification.—Following Jeffreys, the winds of the globe may be classified according to their horizontal extent as follows:

1. World-wide phenomena, including the general circulation and its seasonal variation.

2. Phenomena on a continental scale, including monsoon winds and associated changes of pressure.

3. Phenomena on a scale comparable with the British Isles.   As it is known that an island as large as Australia produces only modifications of secondary importance in the general circulation, it seems likely that small islands do not to any great extent modify the general and continental circulations in their neighborhood.

4. Small-scale phenomena, including atmospheric disturbances whose horizontal dimensions, at least in one direction, are of the order of magnitude of kilometers or tens of kilometers.   This category includes tropical cyclones, tornadoes, land and sea breezes, mountain and valley winds, and local winds of the Föhn type.

TABLE 50.—HORIZONTAL DIMENSIONS OF PERTURBATION WHEN ACCELERATIONAL TERM EQUALS ROTATIONAL TERM

v_x φ	10 m./sec.	20 m./sec.	30 m./sec.	70 m./sec.
90°	70	140	210	480
30°	140	270	410	960
20°	200	400	600	1400
10°	400	800	1200	2800

The acceleration dv_x/dt is comparable with v_x^2/l, where l is the linear dimension of the disturbance.   This may then be compared with the rotational term.   The accelerational term equals the rotational term

when $l = v_x/\lambda$. Some values of l are shown in Table 50. If l is greater than shown in the table, then the rotational term is predominating, and the winds are mainly geostrophic.

A strong wind of any of the first three classes has a velocity of 20 m./sec. It is therefore clear that these winds cannot be Eulerian but are either geostrophic or antitriptic. In the tropical cyclones, the wind velocities frequently reach 70 m./sec., whereas the dimensions in typical cases are of the order of 100 km. The dimensions are therefore such that the accelerational term greatly exceeds the rotational one. The winds in the tropical cyclone are therefore not geostrophic as long as the storm is in low latitudes.

Observations show that the winds of types 1, 2, and 3 deviate from the direction of the isobar by not more than 20 to 40° near the surface and by much less at heights above 0.5 km. These winds are therefore essentially geostrophic above the friction layer, with an antitriptic (frictional) influence close to the earth's surface.

In the tropical storm, a particle performs one revolution around the center in a few hours, whereas the storm center lasts for several days. The frictional term must thus be much smaller than the accelerational term; the motion must therefore be mainly cyclostrophic (*i.e.*, Eulerian).

91. The Effect of Changing Pressure Distribution.—It is evident that all winds which are mainly geostrophic will be influenced by changes in the distribution of pressure. Thus, when the pressure distribution changes, the winds must be accelerated in such a manner that they tend to adapt themselves to the geostrophic balance. The various aspects of this problem have been discussed by Sverdrup [82], Brunt and Douglas [20], and Pettersj1en [55].

The equations of frictionless motion in the horizontal plane are

$$(1) \qquad \frac{dv_x}{dt} = -\alpha \frac{\partial p}{\partial x} + \lambda v_y$$

$$\frac{dv_y}{dt} = -\alpha \frac{\partial p}{\partial y} - \lambda v_x$$

where $\alpha = (1/\rho)$. Let k denote a unit vector along the vertical. The above equations may then be written in vector form as follows:

$$(2) \qquad \frac{dv}{dt} = -\alpha \nabla p + v \times k\lambda$$

Multiplying vectorially by k, solving with respect to v, and introducing the geostrophic wind, we obtain

$$(3) \qquad v = -\frac{\alpha \nabla p}{\lambda} \times k + \frac{1}{\lambda} k \times \frac{dv}{dt} = v_{gs} + \frac{1}{\lambda} k \times \frac{dv}{dt}$$

This equation shows that the wind vector v is the sum of two vectors,

of which one is the geostrophic wind and the second is in magnitude proportional to the acceleration, its direction being at right angles and to the left of the acceleration vector. *When $dv/dt = 0$, the wind equals the geostrophic wind.*

Differentiating Eq. (3) partially with respect to time, we obtain, when α is constant locally,

$$(4) \qquad \frac{\partial v}{\partial t} = -\frac{\alpha}{\lambda}\frac{\partial(\nabla p)}{\partial t} \times k + \frac{1}{\lambda}k \times \frac{\partial}{\partial t}\left(\frac{dv}{dt}\right)$$

Here, $-[\partial(\nabla p)/\partial t] = -\nabla(\partial p/\partial t) = -I =$ the isallobaric gradient. According to Brunt and Douglas, the last term in Eq. (4) is negligible against $\partial v/\partial t$, and hence

$$(5) \qquad \frac{\partial v}{\partial t} = -\frac{\alpha}{\lambda}I \times k$$

This equation shows that the local acceleration ($\partial v/\partial t$) is related to the isallobaric gradient as the geostrophic wind is related to the pressure gradient. *The isallobars, therefore, represent local acceleration as the isobars represent geostrophic wind.*

We shall next find a relation between the wind v and the isallobaric gradient. Writing

$$\frac{dv}{dt} = \frac{\partial v}{\partial t} + v \cdot \nabla v$$

and substituting from Eq. (5), we obtain

$$(6) \qquad \frac{dv}{dt} = -\frac{\alpha}{\lambda}I \times k + v \cdot \nabla v$$

Brunt and Douglas have shown that the term $v \cdot \nabla v$ is negligible against dv/dt, except when the curvature of the path is excessively large. Neglecting this term and substituting from Eq. (6) into Eq. (3), we obtain

$$(7) \qquad v = v_{gs} - \frac{\alpha}{\lambda^2}I$$

This shows that the wind may be regarded as being composed of two vectors, *viz.*: (1) *the geostrophic wind*, which blows along the isobars, and (2) *the isallobaric wind*, which blows along the *isallobaric gradient*.

Equation (7), which is applicable only when the curvature of the path is not excessively large, shows that the geostrophic wind is a good approximation to the true wind when the isallobaric gradient is small.

92. The Effect of Friction.—The motion of the air near the earth's surface is noticeably influenced by friction. For a detailed discussion of the theory of friction, the reader is referred to general textbooks, *e.g.*, Brunt [19]. In this discussion, we are concerned only with such con-

ditions as are of direct use in the analysis of weather maps. As a first approximation, it may be assumed that the frictional force due to the roughness of the ground is proportional to the wind velocity and that its direction is opposite to that of the wind. A steady state of motion of geostrophic character is obtained when there is balance between (1) the pressure gradient, (2) the deviating force, and (3) the frictional force. As (2) acts at right angles to the direction of the wind and (3) acts against the wind, it is readily seen that balance between the three forces can be established only when the wind has a component normal to the isobar, in such a manner that the component of the pressure gradient in the direction of the motion balances the frictional force. This is shown in Fig. 101,
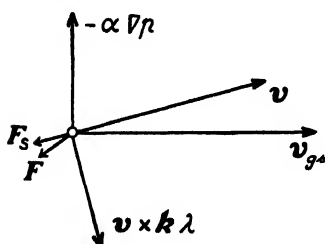
Fig. 101.—Motion under balanced forces: gradient force $(-\alpha \nabla p)$, deviating force $(v \times k\lambda)$, and frictional force (F_s) due to the roughness of the ground. $(F =$ the frictional force resulting from surface friction and the frictional drag of the air above.)

which applies to the conditions in the northern hemisphere. If the path is not a straight line, the centrifugal force adds to, or deducts from, the deviating force. The frictional force, which acts against the direction of the wind, must then be balanced by the component of the gradient force along the direction of the wind. In this case, too, friction causes the air to flow with a component normal to the isobar.

The friction along the earth's surface influences not only the direction of the wind but also its velocity. That this is so is readily deduced from Fig. 101. If there were no friction, the gradient force would be balanced by the deviating force, and the wind would be equal to the geostrophic wind. With friction, part of the gradient force is balanced by the frictional force, and a wind velocity smaller than the geostrophic wind suffices to balance the remaining component of the gradient force. Hence, it follows that the wind which corresponds to balance between the gradient force, the deviating force, and the frictional force is deviated to the left of the geostrophic wind, and its velocity is less than that of the geostrophic wind.

In addition to the frictional force due to the roughness of the ground, a layer of air near the earth's surface is exposed to the frictional drag from the air above it. This drag is proportional to $\partial^2 v/\partial z^2$. As the effect of the ground friction decreases along the vertical, it follows from Fig. 101 that the wind will approach the geostrophic wind with increasing elevation. The frictional drag that is proportional to $\partial^2 v/\partial z^2$ is therefore equivalent to a force that acts to the right of the surface wind. Hesselberg and Sverdrup [32] have shown that the frictional force (F) which results from the surface friction and the frictional drag of the air above is deviated to the right of the direction of the wind and makes an angle

with it which is slightly less than 180°. Observations show that the friction due to the roughness of the ground is the predominant factor in the layer of air close to the earth's surface.

The layer of air between the earth's surface and the level where the wind equals the geostrophic wind (or the gradient wind when the path is curved) is called the *friction layer*. The thickness of the friction layer depends on many factors, *e.g.*, the speed of the wind, the stability of the air, and the curvature of the path. When the wind speed is high and the air is unstable, the air within the friction layer becomes thoroughly stirred and the winds recorded at anemometer level will be closer to the geostrophic wind (or the gradient wind) than when there is less vertical mixing. Haurwitz [31] has shown that the wind in the friction layer approaches the gradient wind more rapidly along the vertical when the isobars are cyclonically curved than when they are curved anticyclonically. This is due to the circumstance that the centrifugal force in cyclonically curved motion tends to drive the air to the right and thus make it move more along the isobar than it does when the isobars are straight. Under normal conditions, the wind distribution along the vertical, projected on a horizontal plane, is in good agreement with the well-known Ekman spiral.

93. Comparison of the Gradient Wind with the Observed Wind.—A detailed comparison of the gradient wind with the observed wind was made byGold [28], who found that at a height of 500 m. above the ground the direction of the wind was almost exactly along the isobars at sea level, whereas the velocity was slightly below the computed gradient wind. Later investigations have shown that the influence of surface friction over land is noticeable to greater heights, but the difference between the gradient wind and the observed winds is too small to be of any practical significance above, say 500 to 1000 m. above the ground. It is therefore legitimate to consider the gradient wind as a satisfactory approximation to the actual wind at the top of the friction layer within the limits of the errors of observation. When the isobars are straight lines or their curvature is small, the curvature of the path is negligible, and the geostrophic wind may be used as a good approximation to the true wind in the upper portion of the friction layer and above it.

When the pressure systems are not stationary, or nearly so, the curvature of the path may differ considerably from the curvature of the isobars (see Par. 99), and care must then be exercised in using either the geostrophic wind or the gradient wind as an approximation of the true wind above the layer that is appreciably influenced by friction.

In the layer of air which is directly influenced by friction, the observed winds differ appreciably from the computed geostrophic wind, or gradient wind. Over land, the conditions vary greatly on account of the varia-

tions in the roughness of the ground, and it is generally found that the ratio of the observed wind speed to that of the geostrophic wind varies with the direction of the wind. At sea, the conditions are fairly simple, and the analysis of the weather charts has shown that the ratio of the observed wind to the geostrophic wind is approximately as 2:3. The direction of the observed wind at sea is usually 15 to 30° to the left of the isobars (in the northern hemisphere). This applies to the conditions in middle and high latitudes where the curvature of the isobars is such that the wind is mainly geostrophic. In tropical and subtropical latitudes, the geostrophic control is slight, and the observed winds may be mainly Eulerian or antitriptic in nature. In such cases, there is no simple relation between the pressure gradient and the wind.

The relation between the pressure gradient and the observed winds is of great importance both for the drawing of the isobars at sea, where pressure observations are scanty, and for the forecasting of the displacements of air masses and fronts. We shall therefore return to this relation in Chaps. IX and XI.

Attention is again directed to the fact that the relation between the observed wind and the pressure gradient is considerably modified and may become fictitious when the pressure gradient is changing rapidly. This is due to the fact that the motion is then not under balanced forces. Under such conditions, the motion tends to adapt itself to the pressure gradient; but the balance is incomplete, and a velocity component along the isallobaric gradient results.

94. The Gradient Wind Equation.—The gradient wind equation may be written

(1) $v_{gr}^2 - \lambda r(v_{gr} - v_{gs}) = 0$ (anticyclonic curvature)
(2) $v_{gr}^2 + \lambda r(v_{gr} - v_{gs}) = 0$ (cyclonic curvature)

Each of these equations has two solutions, but only those which give $v_{gr} = v_{gs}$ when the radius of curvature increases indefinitely have any physical meaning. Solving Eq. (1), we obtain

$$v_{gr} = \tfrac{1}{2}\lambda r \left(1 \pm \sqrt{1 - \frac{4v_{gs}}{\lambda r}} \right)$$

Expanding the expression under the radical, we find that only the following solution has a physical meaning:

(3) $v_{gr} = \tfrac{1}{2}\lambda r \left(1 - \sqrt{1 - \frac{4v_{gs}}{\lambda r}} \right)$ (anticyclonic curvature)

When the curvature is cyclonic, the gradient-wind equation is the same as for anticyclonic curvature, with the sign of r changed. The appro-

priate solution is therefore

$$(4) \qquad v_{gr} = \tfrac{1}{2}\lambda r \left(\sqrt{1 + \frac{4v_{gs}}{\lambda r}} - 1 \right) \qquad \text{(cyclonic curvature)}$$

95. The Geostrophic-wind Scale.—The relation between wind and pressure expressed by the above equations (3) and (4) may be transferred to a celluloid sheet, taking into account the projection and the scale of the weather chart. It is then convenient to convert the variables into convenient units.

In the first place, the wind speed may be converted into Beaufort units by means of Table 51.

TABLE 51.—THE BEAUFORT SCALE OF WIND FORCE WITH VELOCITY EQUIVALENTS

Beaufort number	General description	Limits of velocity 6 m. above level ground			
		M./sec.	Km./hr.	M.p.h.	Knots
0	Calm	Less than 0.5	Less than 2	Less than 1	Less than 1
1	Light air	0.6– 1.7	2– 6	1– 3	1– 3
2	Slight breeze	1.8– 3.3	7– 12	4– 7	4– 6
3	Gentle breeze	3.4– 5.2	13– 18	8–11	7–10
4	Moderate breeze	5.3– 7.4	19– 26	12–16	10–14
5	Fresh breeze	7.5– 9.8	27– 34	17–22	15–19
6	Strong breeze	9.9–12.4	36– 44	23–27	19–24
7	Moderate gale	12.5–15.2	45– 55	28–34	24–30
8	Fresh gale	15.3–18.2	56– 66	35–41	30–35
9	Strong gale	18.3–21.5	67– 77	42–48	36–42
10	Whole gale	21.6–25.1	78– 90	49–56	42–49
11	Storm	25.5–29.0	91–104	57–67	49–56
12	Hurricane	Above 29.1	Above 105	Above 68	Above 56

The speed of the geostrophic wind is obtained from Eq. *89*(4), *viz.*:

$$(1) \qquad v_{gs} = \frac{1}{\rho\lambda} \frac{\partial p}{\partial n}$$

Using the meter-ton-second system of units, p should be expressed in centibars and ρ in tons per cubic meter. If isobars are drawn for each fifth millibar (*e.g.*, 995, 1000, 1005, etc.), we may put

$$\frac{\partial p}{\partial n} = \frac{0.5}{H}$$

where H is the distance between neighboring isobars. As $\rho = p/RT$ and $\lambda = 2\omega \sin \varphi$, we obtain from Eq. (1)

$$(2) \qquad H = \frac{RT}{p} \frac{1}{4\omega \sin \varphi \, v_{gs}} \qquad \text{(meters)}$$

From this, we may compute the distances between neighboring isobars which correspond to the velocity equivalents given in Table 51. Thus, to any given H there corresponds a certain geostrophic wind (which varies with T, p, and φ), and vice versa. The variations depending on T and p are, however, so slight that it suffices, in most cases, to use mean values of these variables. The relation between H and v_{gs} (for $p = 1000$ mb. and $T = 283°A.$) is given in Table 52, and the corrections for varying p and T are given in Table 54.

TABLE 52.—RELATION BETWEEN PRESSURE GRADIENT ($0.5/H$) AND GEOSTROPHIC
WIND (v_{gs}) AND GEOSTROPHIC DISPLACEMENT IN 6 HR. (D) WHEN $p = 1000$
MB. AND $T = 283°A.$

(Corrections for varying p and T are given in Table 54)

Limits of Beaufort numbers	Geostrophic wind, m./sec.	$D = 21,600v_{gs}$ geostrophic displacement in 6 hr., km.	Corresponding values of H, km., in various latitudes			
			40°	50°	60°	70°
2– 3	3.4	75	1280	1080	945	875
3– 4	5.3	120	825	690	610	565
4– 5	7.5	160	580	490	430	400
5– 6	9.9	215	440	370	325	300
6– 7	12.5	270	350	295	255	240
7– 8	15.3	335	280	240	210	195
8– 9	18.3	390	240	200	175	165
9–10	21.6	465	200	170	150	140
10–11	25.2	542	175	145	130	120
11–12	29.1	625	150	125	110	105

For use on weather charts, it is sometimes convenient to replace v_{gs} by the distance D that the air would travel in 6 hr. if the wind were strictly geostrophic. We find that

$$D = 21,600v_{gs} \quad \text{(meters)}$$

It was shown in Par. 93 that the wind velocity at sea in middle and high latitudes, where the geostrophic control is predominant, is very nearly two-thirds of the geostrophic wind. Let v denote the wind speed observed at sea. We may then write

$$v = \tfrac{2}{3}v_{gs}$$

which substituted into Eq. (2) gives

$$(3) \qquad H = \frac{RT}{p} \frac{1}{6\omega \sin \varphi \, v}$$

From this, it follows that, when the direction and the speed of the wind

are observed at sea, the pressure gradient in the environment of the ship may be inferred from the observed wind. The corresponding values of H and v are given in Table 53 for $T = 283°A$. and $p = 1000$ mb. The influence due to varying pressure and temperature is slight and may be corrected for by aid of Table 54.

TABLE 53.—DISTANCE (H) BETWEEN NEIGHBORING ISOBARS AND OBSERVED WIND
SPEED (v) AT SEA WHEN $p = 1000$ MB. AND $T = 283°A$.
(Corrections for varying p and T are given in Table 54)

Limits of Beaufort numbers	Distance between isobars, km., in various latitudes			
	40°	50°	60°	70°
2– 3	855	720	630	585
3– 4	550	460	415	375
4– 5	390	325	285	275
5– 6	295	245	215	200
6– 7	235	195	170	160
7– 8	190	160	140	130
8– 9	160	135	115	110
9–10	135	120	100	95
10–11	115	100	85	80
11–12	100	85	75	70

TABLE 54.—PERCENTAGE CORRECTIONS TO TABLE 52 AND 53 FOR VARYING T, °C.,
AND p, MB.

T / p	−10°C.	0°C.	10°C.	20°C.
1040	−11	−7	−4	0
1020	−8	−5	−2	2
1000	−6	−4	0	3
980	−4	−2	2	6
960	−2	0	4	8

The above relations apply when the geostrophic control is predominant, when the curvature of the path is not excessively large, and when the pressure distribution does not change rapidly. The relations between the curvature of the isobars and the curvature of the path will be discussed in Par. 99. If the curvature of the path is considerable, the gradient wind should be used instead of the geostrophic wind. In high and middle latitudes, the curvature of the path is often so small that the cyclostrophic term is negligible.

Table 55 shows the relation between the gradient wind and the geostrophic wind for various cyclonic curvatures in various latitudes.

When the curvature is anticyclonic, the wind speed is rarely very high, and the radius of curvature is usually large. The difference between the geostrophic wind and the gradient wind is then small.

TABLE 55.—RELATION BETWEEN GEOSTROPHIC WIND AND GRADIENT WIND (CYCLONIC CURVATURE)

Geostrophic wind, m./sec.	Latitude, degrees	Gradient wind, m./sec.			
		$r = 10,000$ km.	$r = 1000$ km.	$r = 500$ km.	$r = 200$ km.
10	10	10	8	7	5
	20	10	9	8	6
	40	10	9	8	7
	70	10	9	9	8
20	10	19	13	11	8
	20	19	15	13	10
	40	19	17	15	12
	70	19	18	16	13
30	10	26	18	14	10
	20	28	21	18	13
	40	29	24	21	16
	70	29	25	23	18
50	10	43	25	20	14
	20	46	31	25	18
	40	47	36	30	23
	70	48	39	33	26
70	10	57	31	24	16
	20	62	39	31	22
	40	65	47	38	28
	70	66	51	43	32

The above data concerning the relation between the pressure gradient and the wind may be transferred to a celluloid sheet as shown in Fig. 102. In doing so, it is necessary to take into account the projection and the scale of the weather chart. The International Meteorological Organization [38] has recommended three conformal (orthomorphic) projections, of which the Lambert conformal conic projection is recommended for middle latitudes, the cone cutting the sphere at 30 and 60°. The scale of such maps is a function of latitude, and this has been accounted for in constructing Fig. 102.

The construction of the wind scale may be explained as follows: The distances between neighboring isobars are marked along the scale AB. The numerals between the vertical lines indicate the geostrophic wind

(in Beaufort numbers) which corresponds to the measured distance between neighboring isobars. The vertical distances from the line AB to the curve CDE indicate the distances that the air would travel in 6 hr. if the wind were strictly geostrophic. These data are obtained from Table 52.

Corrections for curvature of the path may be plotted as shown by the curve c (for cyclonic curvature) and curve a (for anticyclonic curvature). The necessary data are obtained from Table 55 or Eq. *94*(3). Thus, when the radius of cyclonic curvature is 800 km., the distance that the air would travel with the speed of the gradient wind in 6 hr. is indicated
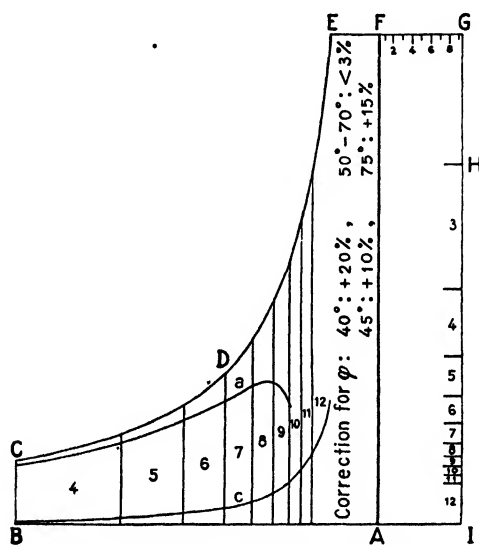
Fig. 102.—The geostrophic wind scale.

by the distance from the curve c to the curve CDE. If the curvature were anticyclonic, the air would travel faster than the geostrophic wind by the amount indicated by the lines between the curve a and the curve CDE. A sufficient number of such correction curves may be drawn on the graph. It is worthy of note that large anticyclonic curvatures with strong winds are rare. It will be shown in later paragraphs that, in computing the displacements of fronts and air masses, it is preferable to choose points on the map where the curvature of the path is so small that the corrections are of negligible magnitude.

The diagram is constructed for 60° lat.; but on account of the combined influence of the latitudinal variations in the geostrophic wind and the scale of the map, the diagram holds with a satisfactory accuracy for a wide range of φ in middle latitudes. The latitude corrections that should be applied to the distances traveled in 6 hr. are indicated on the graph.

The part of the geostrophic wind scale to the left of the line *AF* may be used for determining the approximate wind at the top of the friction layer and the displacement of fronts and air masses. How this is done will be described in later sections. The right-hand portion of the diagram serves two other purposes. The scale *IH* is computed by means of Eq. (3), which gives the relation between the observed (representative) wind at sea and the pressure gradient. The data are tabulated in Table 53. For example, if a ship reports wind force 7 on the Beaufort scale, the distance along *IH* from *I* to the interval indicated by 7 would be the approximate distance between the isobars in the vicinity of the ship. This relation is particularly useful in drawing isobars at sea when observations are scanty. The scale *IH* may also be used for determining the approximate wind force from the isobars where direct observations are lacking.

The applications of the geostrophic wind scale described above are not valid in tropical and subtropical latitudes where the geostrophic balance is less rigid. Nor are they valid in middle and high latitudes when the wind velocity is slight. But when the isobars are drawn consistently, considerable use may be made of the wind scale north of, say 35°, when the wind force is above 4 Beaufort.

The scale indicated by *FG* in Fig. 102 is used for correcting the barometric tendencies observed in ships. Let $\delta p/\delta t$ denote the pressure variation recorded in a ship that moves with the velocity V where the horizontal pressure gradient is $-\nabla p$. The true pressure variation at a fixed station is then

$$\frac{\partial p}{\partial t} = \frac{\delta p}{\delta t} - V \cdot \nabla p$$

Place the scale *FG* along the course of the ship. The scale numbers represent the code figures for the speed of the ship. The distance from *F* to the appropriate code figure indicates the distance made good by the ship during the last 3 hr. (*i.e.*, the tendency interval). The difference in pressure (as interpolated from the isobars) between the point on the map coinciding with *F* and the point coinciding with the appropriate code figure indicates the correction that must be applied to the observed barometric tendency in order to obtain the barometric tendency that would be recorded if the ship did not move. After such correction, isallobars may be drawn at sea.

96. Boundary Conditions.—Apart from the equations of motion given in Par. 88, the motion must satisfy certain boundary conditions and the condition of continuity. Suppose that a surface of discontinuity (*e.g.*, a frontal surface) divides the atmosphere into two portions. The kinematic boundary condition then requires that the motion in the vicinity

of the surface of discontinuity must be such that no fissure develops at the surface. Let the vectors v and v' denote the wind velocities in two points on either side of such a surface and infinitely near one another, and let n denote a unit vector perpendicular to the surface of discontinuity. The kinematic boundary condition may then be written in the form

$$(1) \qquad\qquad (v - v') \cdot n = 0$$

This is the same as saying that the velocity components normal to the surface must be equal on both sides.

Let α, β, γ denote the direction cosines of the unit vector n. Then

$$(2) \qquad (v_x - v_x')\alpha + (v_y - v_y')\beta + (v_z - v_z')\gamma = 0$$

If we choose a system of coordinates with the z-axis along the vertical and the y-axis along the contour lines of the surface of discontinuity, Eq. (2) reduces to

$$(3) \qquad\qquad (v_x - v_x')\alpha + (v_z - v_z')\gamma = 0$$

or, when θ_d denotes the inclination of the surface of discontinuity,

$$(4) \qquad\qquad \tan \theta_d = \frac{v_z - v_z'}{v_x - v_x'},$$

It will be shown in Chap. IX that the velocity of fronts and the vertical velocity of air along frontal surfaces may be obtained from the above equations.

Let us next consider a surface of discontinuity coinciding with the earth's surface, and let letters without indices refer to the condition in the air. n is then a vertical unit vector, and $v' = 0$. It follows then from Eq. (1) that the wind velocity can have no component perpendicular to the earth's surface. We may therefore put $v_z = 0$ close to the earth's surface.

In addition to the kinematic boundary condition, the motion must be restricted in such a manner that the pressure must be equal at both sides of a surface of discontinuity, or

$$(5) \qquad\qquad p - p' = 0$$

This condition, which is usually referred to as the dynamic boundary condition, originates from the principle of equal action and reaction. It will be shown in Chap. IX that the velocity and the acceleration of fronts may be obtained from Eq. (5) without recourse to the equations of motion.

97. Trajectories.—The trajectory of a parcel of air may be defined as the curve described by its successive positions. Let

$$(1) \qquad v_x = v_x(x,y,t) \qquad \text{and} \qquad v_y = v_y(x,y,t)$$

represent the distribution of wind velocity on a map. If the functional relations between v_x and v_y on the one hand and x, y, and t on the other were known, the position of any parcel at any future instant could be obtained. In practice, a graphical picture of the above relations can be obtained from successive wind charts. However, as the direct wind observations are nonrepresentative, it is found more advantageous to compute trajectories by the aid of the relations between wind and pressure. The trajectories thus obtained would apply to the air motion above the layer that is directly influenced by friction along the earth's surface.

Suppose that the pressure distribution is known over a large area at frequent intervals. Using the geostrophic wind (or the gradient wind), we may compute the displacement D_1' of the parcel P (see Fig. 103) during the space of time between map 1 and the map 2 on the assumption that the parcel travels with a constant speed equal to the geostrophic
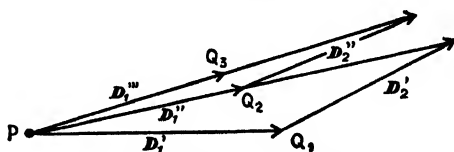
Fig. 103.—Showing the method of constructing trajectories by successive approximations.

wind (or the gradient wind) of the point P on map 1. On the next map, the parcel would then arrive at the point Q_1. In the meantime, the pressure distribution may have changed so that the displacement D_1' represents only a first approximation to the true displacement. From map 2, we may compute the displacement D_2' of the point Q_1 which this parcel has made good during the time interval elapsing between maps 1 and 2. The two vectors D_1' and D_2' carry equal weights, and a better approximation to the true displacement of the parcel during the interval between maps 1 and 2 would be

$$(2) \qquad D_1'' = \tfrac{1}{2}(D_1' + D_2')$$

With this approximation, the parcel P would arrive at the point Q_2. Next, we may find the displacement D_2'' of the point Q_2, which may differ slightly from the displacement D_2'. A further approximation to the true displacement would then be

$$(3) \qquad D_1''' = \tfrac{1}{2}(D_1'' + D_2'')$$

The operation may be repeated, and it will then be found that the points Q_1, Q_2, etc., converge toward a point which marks the position of the air parcel in question.

It should be noted that the vector D_1' represents the displacement which would result if there were no acceleration. The vector D_1'' represents the displacement when the first approximation to the accelera-

tion has been taken into account; the vector D_1''' represents the displacement when the second approximation to the acceleration has been considered.

In general, it will be found that the approximation represented by Eq. (2) is sufficiently accurate. The construction of displacements may be repeated from map 2 to map 3, etc., and the displacements thus found indicate the trajectory of the parcel in question. Figure 104 shows as an example the displacements computed from four successive
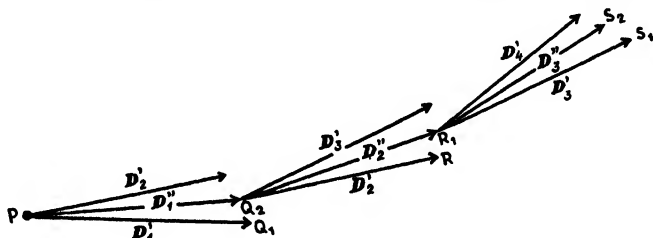
FIG. 104.

maps, the first approximation to the acceleration being taken into account.

It is worthy of note that the definition of geostrophic wind involves constant speed along the trajectories. When the construction of displacements shows that the speed varies considerably along the path, the true wind differs from geostrophic wind. Although the construction of trajectories often is a laborious task, the drawing of streamlines is a simple operation. A useful relation between the curvature of the trajectories and the curvature of the streamlines will be given in Par. 99.

98. Streamlines.—Let the vector v with the components v_x and v_y represent the velocity of the air in a horizontal plane. At any given moment, $(t = t_0)$, v_x and v_y may be regarded as functions of x and y, *viz.*:

(1) $$v_x = v_x(x,y) \quad \text{and} \quad v_y = v_y(x,y)$$

The streamlines of the wind velocity may then be defined as the lines that everywhere are tangential to the wind vector. It is important to note that the streamlines indicate the direction of the motion at a given instant, and the trajectories indicate the actual paths which the air parcels travel. Only under stationary conditions will the streamlines coincide with the trajectories.

Let (x,y) represent an arbitrary point on a streamline. It follows then from the definition that the streamlines must satisfy the following relation:

(2) $$\frac{dy}{dx} = \frac{v_y}{v_x} = \frac{v_y(x,y)}{v_x(x,y)}$$

Through integration, the streamlines are found.

A graphic method of obtaining streamlines from observed winds has been rendered by Sandström [70]. The streamlines derived from the observed surface winds are of but little interest in the analysis of weather maps; for the surface winds are often nonrepresentative, and, when the winds are representative, the streamline picture thus obtained would vary rapidly with height so as to approach the isobars at the top of the friction layer. In middle and high latitudes where the winds at the top of the friction layer do not differ much from the geostrophic wind (or the gradient wind), it suffices, in most cases, to consider the isobars as streamlines. This approximation holds with sufficient accuracy when the isallobaric gradients are small. When this is not the case, it will be necessary to consider also the isallobaric component of the wind (see Par. 91).

99. Relation between Trajectories and Streamlines.—Let r denote the radius of curvature of the trajectory, r_s the radius of curvature of the streamline, and ψ the wind direction. Then, as has been shown by Blaton [6], the following relation holds:

$$(1) \qquad v\left(\frac{1}{r} - \frac{1}{r_s}\right) = \frac{\partial \psi}{\partial t}$$

where v denotes the speed of the wind. Under stationary conditions, $\partial \psi/\partial t = 0$, and therefore

$$r = r_s$$

Furthermore, as both the streamline and the trajectory are tangential to the wind vector, it follows that streamlines and trajectories are identical when the conditions are stationary. In such cases, the isobars represent both trajectories and streamlines of the motion at the top of the friction layer.

When $(\partial \psi/\partial t) \gtrless 0$, the trajectories differ from the streamlines.

In general, it is permissible to substitute the curvature of the isobars for the curvature of the streamlines. From Eq. (1), a rough idea of the curvature of the trajectories is then readily obtained without constructing actual trajectories. A few typical cases are discussed below.

1. *Cyclonic Centers.*—We consider the air motion around a cyclonic center that moves across the chart with a velocity c. We choose the x-axis along the velocity of the center, and let ψ denote the angle between the x-axis and the direction of the wind. Let $\delta/\delta t$ denote variation with respect to time in a system of coordinates that moves with the center. Then

$$\frac{\delta \psi}{\delta t} = \frac{\partial \psi}{\partial t} + c\frac{\partial \psi}{\partial x}$$

Here, $\delta\psi/\delta t$ indicates the variations in ψ caused by internal changes in structure of the moving cyclone, and the term $c\ \partial\psi/\partial x$ denotes the changes caused by the travel of the cyclonic center. Neglecting the small term $\delta\psi/\delta t$, we obtain

$$\frac{\partial\psi}{\partial t} = -c\frac{\partial\psi}{\partial x}$$

It is readily seen that $\partial\psi/\partial x = \cos\psi/r_s$, and therefore

$$\partial\psi/\partial t = -c\frac{1}{r_s}\cos\psi$$

which, substituted in Eq. (1), gives

(2)
$$\frac{1}{r} = \frac{1}{r_s}\left(1 - \frac{c}{v}\cos\psi\right)$$

Above the layer directly influenced by friction, r_s may be interpreted as the radius of curvature of the isobar (r_i), v as the gradient wind, and ψ as the angle between the path of the center and the tangent to the isobar. This gives

(3)
$$\frac{1}{r} = \frac{1}{r_i}\left(1 - \frac{c}{v}\cos\psi\right)$$

Comparing Eq. (3) with Fig. 105, we see that $\cos\psi = 0$ where the isobars are perpendicular to the path of the center. Here, then, *the curvature of the trajectories equals the curvature of the isobars.* To the left of the path, $\cos\psi < 0$, and *the greatest curvature of the trajectories is found where the isobars are parallel to the path* (*i.e.*, $\psi = 180°$). The curvature of the trajectories may then be considerably greater than the curvature of the isobars. To the right of the path of the center, $\cos\psi > 0$, and the curvature of the trajectories is smaller than that of the isobars, with a *minimum where the isobars are parallel to the path of the center* (*i.e.*, $\psi = 0$).
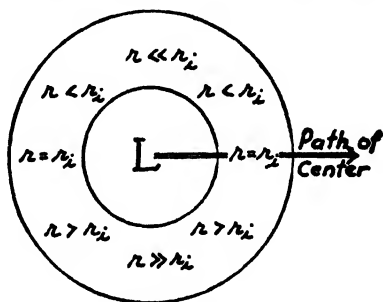
Fig. 105.—Showing the relation between the curvature of trajectories and the curvature of the isobars.

It should be noted that the difference $[(1/r) - (1/r_i)]$ depends also on ratio c/v. Normally, the speed of the wind is larger than the speed with which the center moves. Then $v > c$, and the trajectories are curved in the same sense as the isobars. In rare cases, notably in the immediate vicinity of the center of depressions, c may be larger than v.

In such cases, the trajectories are curved in a sense opposite to that of the isobars in the areas where the angle between the isobars and the path of the center is small (*i.e.*, ψ not far removed from 0°).

2. *Warm-sector Cyclone.*—We consider next a warm-sector cyclone as shown in Fig. 108*B*. In the warm sector, $1/r_i = 0$. The same is true of the areas in the rear of the cold front and in advance of the warm front where the isobars are almost straight lines. In these regions, therefore, the trajectories are almost straight lines. Within the region north of the path of the center, $\cos \psi < 0$, and the curvature of the trajectories is larger than that of the isobars.

3. *Anticyclonic Centers.*—The conditions are similar to those described under (1) above, but the sign of $\cos \psi$ is reversed. Therefore, the
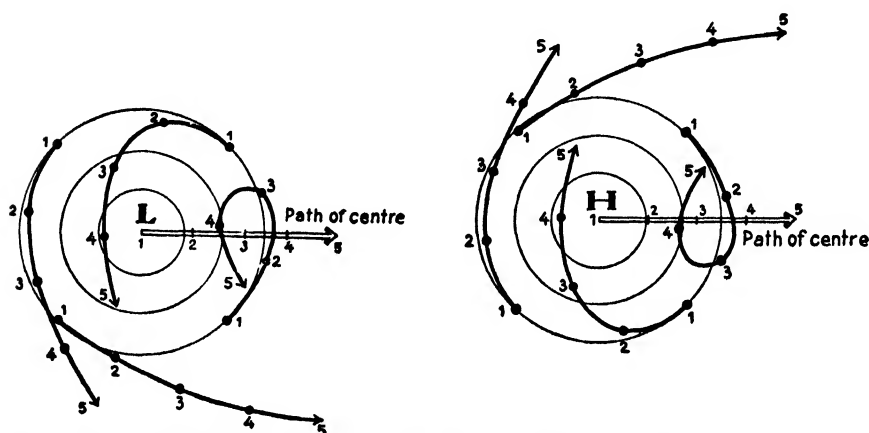
Fig. 106.—Showing same typical trajectories in the vicinity of moving cyclonic and anticyclonic centers.

curvature of the trajectories has a minimum to the left of the path of the center where the isobars are parallel to the path; the curvature of the trajectories equals that of the isobars where the isobars are perpendicular to the direction of the path of the center; and the maximum of curvature is found to the right of the path where the isobars are parallel to the path. Similar rules are readily deduced for troughs and wedges.

With reference to Par. 95, it is of interest to remark that the geostrophic wind is a good approximation to the true wind only when the curvature of the path is not large and when the isallobaric gradient is small. From the above, it is evident that both these conditions are fulfilled in the region between cyclonic and anticyclonic centers where the air motion is in the same direction as that of the pressure systems. For this reason, *the geostrophic wind scale will give results of great accuracy in warm sectors, to the right of the path of cyclonic centers and to the left of*

the path of anticyclonic centers. It will be shown in Chap. IX that the displacement of fronts and air masses may be obtained from the isobars by the aid of the geostrophic wind scale. If the geostrophic wind scale is used in the regions where the curvature of the trajectories is large (*e.g.*, to the left of the path of cyclonic centers or to the right of the path of anticyclonic centers), it will be necessary to apply corrections for the difference between geostrophic wind and gradient wind (see Par. 95). Figure 106 shows typical trajectories during an extended interval of time around a moving cyclone and anticyclone.

100. Divergence and Convergence.—In a rectangular system of coordinates, the divergence of the three-dimensional motion is defined by

$$(1) \qquad \text{div } v = \nabla \cdot v = \frac{\partial v_x}{\partial x} + \frac{\partial v_y}{\partial y} + \frac{\partial v_z}{\partial z}$$

The equation of continuity is then

$$(2) \qquad \frac{1}{\alpha}\frac{d\alpha}{dt} = \text{div } v$$

or

$$(2a) \qquad -\frac{1}{\rho}\frac{d\rho}{dt} = \text{div } v$$

where α denotes specific volume and ρ density.

It was shown in Par. 96 that $v_z = 0$ near the earth's surface. In middle and high latitudes where the geostrophic control is predominant, the motion is approximately isobaric when $v_z = 0$. Only in tropical cyclones and in tornadoes are the pressure variations of horizontally moving air parcels sufficiently large to cause important changes in specific volume. Under ordinary conditions, we may therefore consider the motion near the earth's surface as horizontal and isobaric. The specific volume (or density) can then vary only on account of nonadiabatic temperature changes. It follows then that div $v > 0$ when the air is heated and div $v < 0$ when the air is cooled. When the air is cooled or heated through extended intervals of time, this effect is important. Thus, the cooling of air over cold continents in winter results in convergence, or accumulation of air, which again results in the formation of cold continental anticyclones. Likewise, thermal low-pressure areas will develop on account of prolonged heating over warm continents in summer. These processes, which last for extended periods, give rise to the monsoon winds. However, when the heating or cooling lasts for only short intervals, the nonadiabatic effects are negligible. Therefore, when we consider changes during short intervals of time, we may neglect the three-dimensional divergence in the vicinity of the earth's surface. This gives

$$\text{div } v = 0$$

or

(3)
$$-\frac{\partial v_z}{\partial z} = \frac{\partial v_x}{\partial x} + \frac{\partial v_y}{\partial y} = \text{div}_2 \, v$$

where div$_2$ stands for the two-dimensional (horizontal) divergence.

As $v_z = 0$ at the surface itself, it follows that *there must be ascending motion at some distance above the ground when there is convergence in the horizontal motion and that there must be descending motion (subsidence) at some distance above the ground when there is divergence in the horizontal motion.* It is therefore at least theoretically possible to find the regions of ascending and descending motion in the lower atmosphere from the analysis of weather charts. As most weather phenomena depend on vertical motion, the importance of this analysis is readily appreciated.

In special cases, when

$$\text{div}_2 \, v = 0$$

the streamlines indicate both the direction and the speed of the wind. The streamlines then form tubes of constant flow; the speed of the wind is thus inversely proportional to the distance between the streamlines. In such cases $\partial v_z/\partial z = 0$, and the motion is horizontal.

It was emphasized at the beginning of this chapter that the direct observations of wind direction and force are too inaccurate to allow of a satisfactory analysis of the wind observations. On the other hand, the relations between pressure and wind given in previous paragraphs may be used to find areas of appreciable convergence and divergence.

1. *Divergence of the Gradient Wind.*—Let n denote a unit vector along the horizontal pressure gradient (*i.e.*, normal to the isobars), t a unit vector along the wind velocity, and k a unit vector along the vertical. The gradient wind is then defined by

(4)
$$\left(\lambda v_{gr} \pm \frac{v_{gr}^2}{r}\right) n = -\alpha \nabla_2 p$$

Multiplying vectorially by k and noting that $n \times k = t$, we obtain

(5)
$$\left(\lambda v_{gr} \pm \frac{v_{gr}^2}{r}\right) t = -\alpha \nabla_2 p \times k$$

Here, the vector $v_{gr}t$ defines the gradient wind. Taking the divergence of this vector and choosing the x-axis toward the east and the y-axis toward the north, we obtain after some elementary but somewhat lengthy computations

(6) $$\text{div}_2 \, v_{gr} = \frac{N - \frac{1}{a}\left(\alpha \frac{\partial p}{\partial x} \mp \frac{v_{gr}}{r} v_y\right) \cotan \varphi \pm \frac{1}{r}\frac{\partial v_{gr}}{\partial t} \pm \frac{v_{gr}}{r^2} v_{gr} \cdot \nabla r}{\lambda \pm \frac{v_{gr}}{r}}$$

where the upper sign applies to cyclonic curvature of the path. Here, N denotes the number of isosteric-isobaric solenoids contained in a horizontal unit area, a the radius of the earth, and v_y the northward component of the gradient wind.

Equation (6) shows that the divergence of the gradient wind is controlled by the following three factors:

a. The temperature effect, or the solenoid effect, which depends on the term containing N. This effect depends mainly on the distribution of temperature; it vanishes in homogeneous air; and it also vanishes when the isotherms coincide with the isobars, for the gradient of specific volume then coincides with, or is opposite to, the pressure gradient. The temperature term is negative when the air blows from a warm toward a cold region and is positive when it blows in the opposite direction. As the number of solenoids contained in a horizontal unit area is exceedingly small, the temperature term is usually negligible against the other terms in Eq. (6).

b. The latitude effect, which depends on the term containing cotan φ. This effect depends on the meridional transport of air. The first term within the parentheses is independent of the radius of curvature of the path; the second term, however, depends on the curvature of the path. When $(\partial p/\partial x) > 0$, $v_y > 0$, and vice versa. The two terms within the parentheses therefore counteract one another when the motion is cyclonic. The last term within the parentheses is usually the larger one, except when the radius of curvature is very large. But for such curvatures as occur in moving cyclones, the last term is larger than the first. In such cases, the latitude term as a whole gives convergence in air that moves northward and divergence in air that moves southward. The effect of the latitude term on the divergence is usually much larger than the effect of the solenoid term.

c. The curvature effect, which depends mainly on the last two terms in Eq. (6). These terms, which usually are very small, vanish with increasing radius of curvature of the path of the moving parcel of air. Even when the radius of curvature is small, these terms are usually much smaller than the term containing cotan φ. Moreover, the next to the last term vanishes when the motion is steady, or nearly so; and the last term vanishes when the wind is perpendicular to the gradient of r. As r is mainly a function of the distances from the pressure center and as the wind direction is normal to r, it follows that the last term must be very small, particularly since it contains r^2 in the denominator.

In view of the above, we may neglect the first, third, and fourth terms in Eq. (6). We then obtain

$$(7) \qquad \text{div}_2\, v_{gr} = -\frac{\alpha(\partial p/\partial x) \mp (v_{gr}v_y/r)}{a\lambda[1 \pm (v_{gr}/\lambda r)]}\, \text{cotan}\ \varphi$$

Here the upper sign refers to cyclonic and the lower sign refers to anti-cyclonic motion.

2. *Divergence of the Geostrophic Wind.*—The geostrophic wind is identical with the gradient wind when the radius of curvature of the path is infinitely large. The divergence of the geostrophic wind (v_{gs}) is therefore obtained from Eq. (6) by putting $r = \infty$. This gives

$$(8) \qquad \operatorname{div}_2 v_{gs} = \frac{1}{\lambda} N - \frac{1}{a\lambda} \alpha \frac{\partial p}{\partial x} \cotan \varphi$$

or, when we neglect the solenoid term,

$$(9) \qquad \operatorname{div}_2 v_{gs} = -\frac{1}{a\lambda} \alpha \frac{\partial p}{\partial x} \cotan \varphi = -\frac{v_y \cotan \varphi}{a}$$

where v_y is the meridional component of the geostrophic wind. From this, it follows that the divergence of the geostrophic wind vanishes when the wind blows along the parallels. If the wind has a component along the meridian, there is convergence when the wind blows from south to north and divergence when it blows in the opposite direction.

Returning to Eq. (5) and putting $r = \infty$, we obtain for the geostrophic wind

$$v_{gs} = -\frac{\alpha \nabla_2 p}{\lambda} \times k$$

If α and λ be regarded as constants horizontally, we obtain

$$(10) \qquad \operatorname{div}_2 v_{gs} = -\frac{\alpha}{\lambda} \operatorname{div} (\nabla_2 p \times k) = 0$$

Therefore, the divergence expressed by Eq. (8) is due to the horizontal variations in α and λ. The actual divergence of the geostrophic wind is usually small and may be neglected unless great accuracy is required. If we consider a small area on the weather map, or motion with only slight meridional component, it suffices to use Eq. (10), which states that the geostrophic wind has no divergence or convergence. However, if we integrate the divergence over large areas, it will be necessary to use Eq. (9), which is more accurate. If the curvature of the motion is considerable, Eq. (7) should be used. It will be shown in Chap. VII that the divergence of the geostrophic wind and the gradient wind is of importance for the development of cyclones.

3. *Divergence of Antitriptic Winds.*—It was shown in Par. 92 that the frictional force near the earth's surface is proportional to the wind velocity and to the roughness of the underlying surface. Therefore, if the roughness increases in the direction of the wind (*e.g.*, when the wind blows from sea to land), the winds will be retarded and this may cause con-

vergence in the flow.   Far more important is the circumstance that the frictional force causes the air to flow across the isobars toward lower pressure.   This antitriptic component of the wind may cause considerable convergence or divergence within the friction layer.   This effect is most pronounced in pressure fields consisting of closed isobars.   The antitriptic component of the wind will then cause an export of air from the regions bounded by closed anticyclonic isobars and a corresponding import of air into the regions bounded by closed cyclonic isobars.   The divergence and convergence of the antitriptic wind component increase with the horizontal pressure gradient and the curvature of the isobars. Frictional convergence will therefore be particularly strong in the inner portion of cyclones.   The accumulation of air in the central part of cyclones that is brought about by frictional convergence will tend to fill up the cyclone, unless a corresponding amount of air is removed at higher levels.

4. *Divergence of Eulerian Winds.*—It was shown in Par. 89 that the accelerational term in the equations of motion will cause the air to flow across the isobars toward lower pressure when the wind is accelerated and that there will be a component across the isobars toward high pressure when the wind is decelerated.   The influence of the centrifugal acceleration due to the curvature of the path has already been discussed in connection with the gradient wind.   It remains to discuss the effect of acceleration when the path is straight.

We shall first consider stationary pressure fields consisting of converging and diverging isobars.   If the air moves in the direction of converging isobars, it will obtain a Eulerian component toward the left, whereas air that moves in the direction of diverging isobars will obtain a similar component toward the right.   From this, it follows that there must be divergence of the flow in a current when there are converging isobars to the left of and diverging isobars to the right of the direction of the motion. Conversely, there must be convergence of the flow in a current when there are diverging isobars to the left and converging isobars to the right of the direction of the motion.   Examples of such convergence and divergence are shown in Par. 132, Fig 158.

It was shown in Par. 91 that changes in the pressure distribution influence the acceleration and the velocity of the wind.   It was found that, when the curvature of the path was not too large, the velocity of the wind could be expressed by Eq. *91*(7).   As this is only a rough approximation to the actual wind, it is not necessary to consider the temperature effect and the latitude effect as was done under (1) and (2) above.   Equation *91*(7) then gives

(11) $$\mathrm{div_2}\, v = \frac{\alpha}{\lambda^2}\,\mathrm{div_2}\,(-I)$$

This shows that the divergence of the wind is directly proportional to the divergence of the isallobaric gradient. Even though the mathematical basis for Eq. *91* (7) is weak, Eq. (11) renders results that agree fairly well with what is observed. From Eqs. (3) and (11), we obtain

$$(12) \qquad \frac{\partial v_z}{\partial z} = -\frac{\alpha}{\lambda^2} \operatorname{div}_2 (-I)$$

As $v_z = 0$ at the earth's surface, it follows that $v_z > 0$ (*i.e.*, ascending motion) above areas where the isallobaric gradients converge and $v_z < 0$ (*i.e.*, descending motion) above areas of diverging isallobaric gradients. *There will therefore be a tendency for clouds and precipitation to form and for convective instability to be released in areas of isallobaric minima.* This agrees well with what is observed in regions where there are no fronts. In the vicinity of fronts, these rules hold in a modified form which will be discussed in Par. 166.

5. *Relation between Divergence and Curl.*—The equations of frictionless motion in the horizontal plane may be written in vector form as follows:

$$(13) \qquad \frac{dv}{dt} = -\alpha \nabla_2 p + \lambda v \times k$$

where k is a vertical unit vector. From this, we obtain

$$(14) \qquad \operatorname{curl}_2 \left(\frac{dv}{dt} \right) = -\nabla \alpha \times \nabla p - \lambda k \operatorname{div}_2 v$$

The first term on the right-hand side expresses the number of solenoids in the horizontal plane. This term is exceedingly small, except in pronounced frontal zones. Within the air masses, this term may be neglected. Multiplying Eq. (14) scalarly by the vertical unit vector k, we obtain

$$(15) \qquad \operatorname{div}_2 v = -\frac{1}{\lambda} k \cdot \operatorname{curl}_2 \left(\frac{dv}{dt} \right)$$

As

$$\frac{dv}{dt} = \frac{\partial v}{\partial t} + v \cdot \nabla v$$

we obtain, from Eq. (15),

$$(16) \qquad \frac{d}{dt} (\operatorname{curl}_2 v) = -\operatorname{div}_2 v(\lambda k + \operatorname{curl}_2 v)$$

The term λk is always positive; and when there is cyclonic vorticity, $\operatorname{curl}_2 v > 0$. When there is anticyclonic vorticity, $\operatorname{curl}_2 v < 0$; but as the magnitude of the anticyclonic vorticity in frictionless motion cannot

surpass the value set by λ, it follows that the factor $(\lambda k + \text{curl}_2 v)$ is always positive. From this, it follows that *the sign and the rate of change in vorticity of a moving parcel of air are determined by the divergence of the flow.*

If it were possible to map the distribution of divergence and vorticity with sufficient accuracy, it would be possible to forecast future changes on a hydrodynamic basis. This is not possible as yet, but the above relations will be useful for the qualitative discussions in Chaps. V and VII.

As the vectors in Eq. (16) coincide with the vertical, we may drop the vector notations and put $\text{curl}_2 v = K$. We then obtain

$$(17) \qquad \text{div}_2 \, v = -\frac{dK}{dt} \frac{1}{\lambda + K}$$

6. *Divergence in Moving Pressure Systems.*—The above equation may be used to obtain a qualitative picture of the distribution of $\text{div}_2 \, v$ in moving pressure systems. We consider a system of coordinates that moves with a pressure system traveling across the chart with a velocity c. Let $\delta/\delta t$ denote differentiation with respect to time in the moving system of coordinates. Then,

$$(18) \qquad \frac{dK}{dt} = \frac{\delta K}{\delta t} + (v - c) \cdot \nabla K$$

where the vector $(v - c)$ denotes the velocity of the wind relative to the moving pressure center. Let β denote the angle between the wind direction and the vector represented by ∇v; then,

$$(19) \qquad K = |\nabla v| \sin \beta + \frac{v}{r_s}$$

where r_s represents the radius of curvature of the streamlines. From Eqs. (17), (18), and (19), we obtain[1]

$$(20) \quad (\lambda + K) \, \text{div}_2 \, v = -v \cdot \nabla \left(|\nabla v| \sin \beta + \frac{v}{r_s} \right) +$$
$$c \cdot \nabla \left(|\nabla v| \sin \beta + \frac{v}{r_s} \right) - \frac{\delta}{\delta t} \left(|\nabla v| \sin \beta + \frac{v}{r_s} \right)$$

The last term on the right-hand side represents variations due to internal changes in the structure of the moving pressure system. These variations are, in general, negligible against the first two terms, which represent the changes due to the horizontal pressure gradients and the travel of the pressure system. Above the layer directly influenced by friction, it is, in

---

[1] This equation was first derived by R. Fjörtoft at a seminar in Bergen, Norway, May, 1939.

general, permissible to substitute the radius of curvature of the isobar (r_i) for the radius of curvature of the streamline (r_s). Moreover, in high and middle latitudes where the geostrophic control is predominant, the wind velocity vanishes in the pressure centers where the geostrophic wind also vanishes. Where the pressure gradient is considerable, the actual wind will differ slightly from the geostrophic wind, the actual wind having a component normal to the isobars, but the vorticity of the actual wind will not differ much from the vorticity of the geostrophic wind. We may therefore substitute curl₂ v_{gs} for curl₂ v in Eq. (19). With these minor simplifications, Eq. (20) reduces to

$$(21) \quad (\lambda + K) \operatorname{div}_2 v = -v_{gs} \cdot \nabla \left(\mid \nabla v_{gs} \mid \sin \beta + \frac{v_{gs}}{r_i} \right)$$
$$+ c \cdot \nabla \left(\mid \nabla v_{gs} \mid \sin \beta + \frac{v_{gs}}{r_i} \right)$$

This equation shows that the horizontal divergence depends on the velocity of propagation of the pressure system. Suppose that the isobars are circular and concentric. The vector $\nabla [\mid \nabla v_{gs} \mid \sin \beta + (v_{gs}/r_i)]$ is then everywhere perpendicular to v_{gs}, and the scalar product of these vectors vanishes. Equation (21) then reduces to

$$(22) \quad (\lambda + K) \operatorname{div}_2 v = c \cdot \nabla \left(\mid \nabla v_{gs} \mid \sin \beta + \frac{v_{gs}}{r_i} \right)$$

Let ψ denote the angle between the path of the pressure center and the isobar through the point that we consider. From Eq. (22), we then obtain

$$(23) \quad (\lambda + K) \operatorname{div}_2 v = c \left[\frac{\partial^2 v_{gs}}{\partial r_i{}^2} + \frac{1}{r_i} \left(\frac{\partial v_{gs}}{\partial r_i} - \frac{v_{gs}}{r_i} \right) \right]$$

In the vicinity of a cyclonic center, the distribution of v_{gs} along the radius is in principle as shown in Fig. 107. It will be seen that the geostrophic wind has a maximum close to the center, and there is one inflection point close to the center and another at some great distance from the center. Between these inflection points, the term

$$\frac{\partial^2 v_{gs}}{\partial r_i{}^2} < 0$$

The sign of the term

$$\frac{1}{r_i} \left(\frac{\partial v_{gs}}{\partial r_i} - \frac{v_{gs}}{r_i} \right)$$

is determined in the following manner: Draw the line through the origin

(Fig. 107) that is tangent to the velocity curve. In the interval between the maximum point and the point P in Fig. 107, $\partial v_{gs}/\partial r_i$ is positive and smaller than the term v_{gs}/r_i, which is positive everywhere. To the right of the maximum point, $\partial v_{gs}/\partial r_i$ is always negative. The term
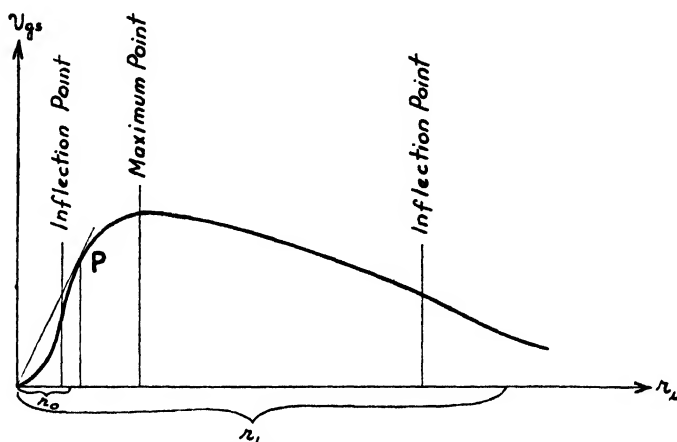
FIG. 107.—Distribution of v_{gs} as a function of r_i in the vicinity of a cyclonic center with circular isobars.

$(1/r_i)[(\partial v_{gs}/\partial r_i) - (v_{gs}/r_i)]$ is therefore negative everywhere to the right of the point P. Furthermore, since $(\partial^2 v_{gs}/\partial r_i{}^2) < 0$ between the inflection points, it follows that

$$\frac{\partial^2 v_{gs}}{\partial r_i{}^2} + \frac{1}{r_i}\left(\frac{\partial v_{gs}}{\partial r_i} - \frac{v_{gs}}{r_i}\right) < 0$$

within the interval between r_0 and r_1 in Fig. 107. Since $(\lambda + K)$ and c are positive, the following relation holds for the values of r_i between r_0 and r_1:

(24) $\mathrm{div}_2\, v = -\sin\psi \times$ (a positive quantity)

Close to the center, the sign may be reversed. Equation (24) shows that $\mathrm{div}_2\, v$ vanishes where $\psi = 0°$ and $\psi = 180°$, or along the line that is perpendicular to the path of the center. In advance of the center, $\sin\psi > 0$ and there is convergence in the horizontal flow, with a maximum of convergence in the direction in which the center is moving. In the rear of the center, $\sin\psi < 0$. There is therefore divergence in the horizontal flow, with a maximum of divergence in the direction from which the center is moving. The distribution of divergence and convergence around a moving cyclonic pressure system is shown diagrammatically in Fig. 108.

Equation (24) holds also for anticyclonic centers, but the sign of sin ψ is then reversed. There would then be divergence in advance of a moving anticyclone and convergence in its rear.

From the above discussion and from Eq. (6), it follows that there must be convergence and ascending motion in advance of a moving cyclone and also in the rear of a moving anticyclone, and divergence and descending motion in the rear of moving cyclones and in advance of moving anticyclones. These rules agree well with what is actually observed, since there is a marked tendency for cloud systems and precipitation to form in advance of moving cyclones, clearing weather usually occurring in the rear of moving cyclones.
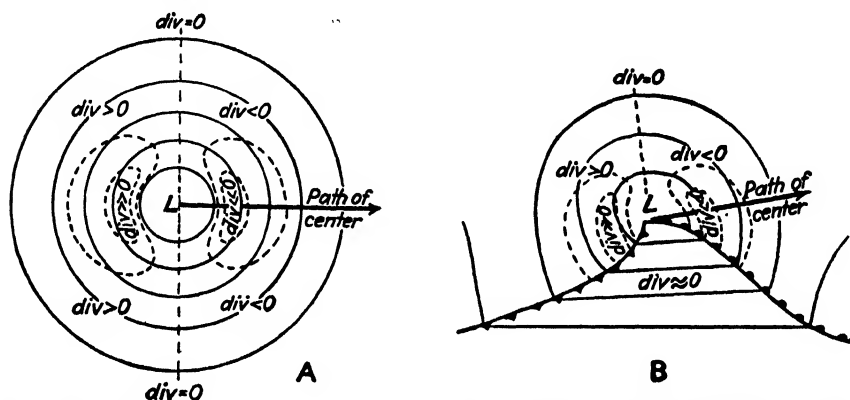
Fig. 108.—Distribution of convergence and divergence in the vicinity of pressure centers. *A*, circular isobars; *B*, warm-sector cyclone.

As convergence in the horizontal flow means accumulation of air and divergence depletion of air, it might be expected that there would be rising pressure in advance of moving cyclones and falling pressure in the rear of such cyclones. As a cyclone must move in the direction from rising pressure to falling pressure (see Chap. IX), there is an apparent paradox in the above result. This question will be discussed further in Chap. VII. It will then be shown that the pressure variations which are due to the convergence and divergence in the vicinity of closed isobars are overcompensated by (1) advection of air of different density along sloping frontal surfaces, (2) vertical motion, and (3) removal of air at high levels where the isobars (above cyclonic centers) are not closed.

In conclusion, a few remarks concerning warm-sector cyclones (Fig. 108*B*) may be of interest. In the warm sector, the isobars are usually straight (*i.e.*, $r_i = \infty$) and parallel, and the vector c is parallel to the isobars. Both terms on the right-hand side of Eq. (21) will then vanish, and $\mathrm{div}_2\, v$ in the warm sector must then be due to the last term in Eq. (20), which is small. This gives

$$(\lambda + K)\,\mathrm{div}_2\,v = -\frac{\delta\,\lvert\,\nabla v\,\rvert}{\delta t}$$

There is then convergence in the warm sector when the cyclone deepens. This question will be discussed further in Chaps. VII and X.

To return now to Fig. 106, it will be seen that a parcel of air moving in advance of an approaching cyclonic system will perform a loop. In its northernmost position, it will be closest to the center. In this position, it will have a maximum of cyclonic shear. Furthermore, since its path then has a maximum of cyclonic curvature, it follows from Eq. (19) that the parcel will then also have a maximum of cyclonic vorticity. This increase in cyclonic vorticity during the northward movement of the parcel must obey Eq. (16), from which it follows that increase in cyclonic vorticity on a moving parcel of air is only possible when the parcel moves in a field of convergence. Equation (16) and the equivalent equation (17) may therefore be used for estimating the formation of and changes in the vorticity of moving air masses. This equation will be used in Chap. V in the discussion of the sequence of streamline patterns. It will also be used in Chaps. VII and X in the discussion of moving cyclones.

CHAPTER V

KINEMATIC ANALYSIS: FRONTOGENESIS

The large-scale wind systems have a considerable influence on the distribution of the conservative (or quasi-conservative) air-mass properties. Through diverging winds, large quasi-homogeneous air masses may be formed; through converging winds, air masses from different and distant source regions may be brought into juxtaposition. The influence of the large-scale wind systems on the production of air masses was discussed in Chap. III. The aim of this chapter will mainly be to discuss the wind conditions that may lead to production of frontal surfaces.

Soon after the discovery of the polar front, it was realized that the fronts were subject to processes which either diminished or increased their intensity. It was also found that fronts developed sometimes out of a continuous distribution of air-mass properties. Bergeron, who was the first one to offer an adequate theory for the formation of fronts, introduced the term *frontogenesis* for the processes that lead to formation of new fronts or intensification of existing fronts and the term *frontolysis* for the processes that lead to decreasing front intensity. Bergeron [1] discussed the behavior of the isotherms of a linear field of temperature superimposed on a linear field of motion. Under these special conditions, he found that fronts may form along the axis of dilatation in fields of deformation when the isotherms have a favorable orientation relative to this axis. The theory of frontogenesis has been developed further by Bjerknes [16] and Petterssen [56]. For a detailed discussion of frontogenesis and types of motion, the reader is referred to the last-mentioned paper.

101. Definition of Frontogenesis.—We consider a scalar quantity S which has a continuous distribution in the horizontal plane (x,y). S may then be represented by means of its equiscalar curves on a map. When time t varies, the S-curve (*e.g.*, isotherms) will, in general, move relative to the coordinates of the chart. We then say that *we have frontogenesis if the S-curves move in such a way that they tend to create a discontinuity along a line in the field.* The meaning of this definition is shown in Fig. 109, which also explains the meaning of the term *frontolysis.*

The line along which frontogenesis takes place is called the *line of frontogenesis.* It may be a stationary or moving, curved or straight line. Let $|\nabla S|$ denote the magnitude of the gradient of S, and let $\delta/\delta t$ denote

differentiation with respect to time in a system of coordinates that moves with the line of frontogenesis. Then,

$$(1) \qquad F = \frac{\delta| \nabla S |}{\delta t}$$

measures the variation in the magnitude of the gradient of S per unit time in a system of coordinates that moves with the line of frontogenesis. It will then be seen that the development from A to B to C in Fig. 109 is characterized by $F > 0$, whereas the opposite development would be characterized by $F < 0$.
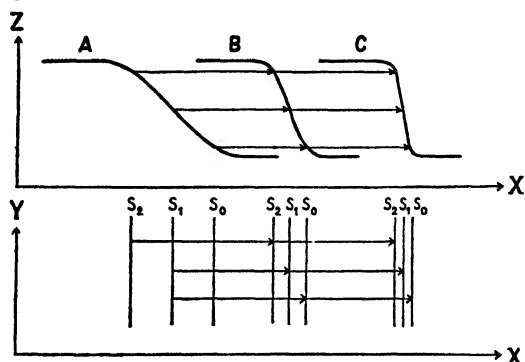
FIG. 109.—Upper portion shows a cross-section through an S-surface that moves from A to B to C while it is exposed to frontogenesis. The isolines of S on a horizontal map will then change as shown in the lower portion. If the motion were reversed so that the profile changed from C to B to A, there would be negative frontogenesis, or *frontolysis*.

In order to have frontogenesis, it is obviously necessary that F must have a maximum on the line of frontogenesis. This means that the magnitude of the gradient of S must increase more rapidly on the line of frontogenesis than outside this line. Thus, if n measures length along an axis normal to the line of frontogenesis, it will be seen that frontogenesis occurs when

$$(2) \qquad F > 0, \qquad \frac{\partial F}{\partial n} = 0 \qquad \text{and} \qquad \frac{\partial^2 F}{\partial n^2} < 0$$

This means that the quantity $| \nabla S |$ must increase, and the rate of increase must have a maximum along the line of frontogenesis.

The conditions (2) are necessary but not sufficient for frontogenesis to occur. In order to obtain frontogenesis, the line of frontogenesis must be a *substantial line* consisting of the same individual air parcels; for otherwise the frontogenetical effect would steadily act on fresh air parcels, and no discontinuity would tend to result. But then we may write instead of Eq. (1)

$$(3) \qquad F = \frac{d| \nabla S |}{d t}$$

and this quantity measures the intensity of the frontogenetical effect. When simultaneously the conditions (2) are fulfilled along the line of frontogenesis, a real front may form if the process lasts for a sufficiently long space of time. Thus, the problem of predicting the formation of a front involves three aspects, *viz.:* (1) the instantaneous distribution of the quantity F, (2) the position and the future movement of the line of frontogenesis, and (3) the duration of the frontogenetic effect.

102. Frontogenesis in a Conservative Field of Property.—There can be little doubt that frontogenesis in the atmosphere is mainly a kinematic phenomenon. When air masses from different and distant source regions are brought into juxtaposition, there will be formed a discontinuity, or a front, in the conservative properties of the masses. It was shown in Chap. I that no air-mass property is strictly conservative. Though radiation, conduction, and mixing invariably counteract the formation of discontinuities and thus counteract the kinematic frontogenesis, experience shows that the transport of property by the large-scale air currents is the predominant factor in the production of fronts. As a first approximation, we may therefore assume that the property S is strictly conservative. In a later paragraph, the nonfulfillment of this assumption will be discussed.

We consider the distribution of S in a horizontal plane, and write

$$S = S(x,y,t)$$

As S is conservative

$$\frac{dS}{dt} = 0$$

and hence

(1) $$\frac{\partial S}{\partial t} = -v \cdot \nabla S$$

where v denotes the wind velocity. Substituting from Eq. (1) into Eq. *101*(3), we obtain

(2) $$F = -\frac{(\nabla S \cdot \nabla v) \cdot \nabla S}{|\nabla S|}$$

which expresses the intensity of the frontogenetic effect when S is a conservative property. Frontogenesis is then characterized by

$$F > 0, \qquad \frac{\partial F}{\partial n} = 0 \qquad \text{and} \qquad \frac{\partial^2 F}{\partial n^2} < 0$$

For practical purposes, it is of interest to obtain a graphical interpretation of Eq. (2). In the first place, we consider the conditions near the earth's surface where the vertical component of v vanishes. Let s denote

the unit vector of ∇S. Then

$$s = \frac{\nabla S}{|\nabla S|}$$

and is perpendicular to the isolines of S and points from low to high values of S. Let v_s denote the component of the wind velocity in the direction of s. Then,

$$(3) \qquad F = -|\nabla S|\frac{\partial v_s}{\partial s}$$

As $|\nabla S|$ is positive by definition, it is seen that $F > 0$, *where v_s decreases in the direction from low to high values of S.*

In order to obtain a clear picture of the meaning of formula (3), we let S denote air temperature T. Then $|\nabla T|$ represents the magnitude of the horizontal gradient of T, and v_s denotes the wind component normal to the isotherms reckoned positive in the direction from low to high temperatures. The above theorem may then be expressed as follows:

Frontogenesis in the field of temperature is possible (1) *when the wind blows from low to high temperatures and decreases in this direction (Fig. 110a) or* (2) *when the wind blows from high to low temperatures and decreases in this direction (Fig. 110b).*

Figure 110c shows a wind field that is a combination of the cases 1 and 2. Figures 110d to e show the wind fields in which $F < 0$. Such fields will dissolve existing fronts and develop quasi-homogeneous conditions in the horizontal distribution of the property in question.

It should be borne in mind that the wind component along the isotherms has no influence on the transport of isotherms; it is only the wind component (v_s) normal to the isotherms that counts.

The conditions represented in Figs. 110a to c are necessary but not sufficient conditions for frontogenesis to occur. In order to obtain frontogenesis, F must have a maximum arranged along a line that makes a small angle with the isotherms. The representative isotherms and the wind distribution are obtained from the analysis of the weather maps. The zones forming important maxima and minima of F are then readily visualized without computations. It may be remarked that in this analysis it usually suffices to use the geostrophic wind (or the gradient wind) instead of the actual wind, and the large-scale distribution of temperature. Even when the distribution of wind and temperature is imperfectly known, it will, in most cases, be possible to find the areas where the value of F is particularly large. When F is small, the changes are unimportant.

When Eq. (3) is applied to temperature, we obtain

(4) $$F = -\mid \nabla T \mid \frac{\partial v_s}{\partial s}$$

As F must have a maximum along the line of frontogenesis, it is readily seen that this maximum occurs where the temperature gradient has a
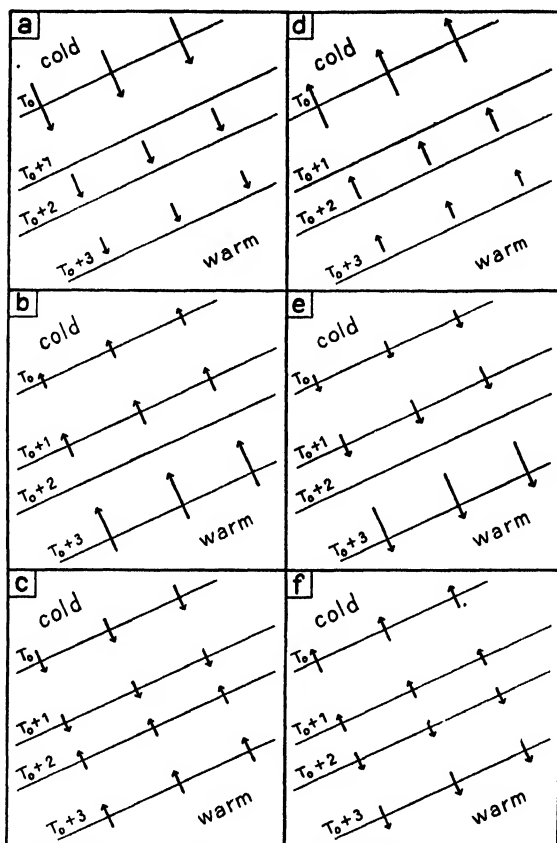
Fig. 110.—a and b show the relation between the isotherms and the wind component normal to the isotherms when frontogenesis is possible (*i.e.* $F > 0$). The magnitude of the horizontal gradient of temperature then increases, and crowding of the isotherms and creation of solenoids result. c shows a wind field resulting from a combination of the types a and b. d, e and f show wind fields and isotherms when $F < 0$. The distance between the isotherms decreases and the air develops toward horizontal homogeneity (*i.e.* frontolysis).

maximum or where the wind component v_s decreases most rapidly; otherwise, the maximum of F may result as a compromise between these two maxima.

It is readily seen from Eq. (3) that F cannot have a maximum when the fields of wind and temperature are linear fields; for when both fields

are linear, F = constant. It follows then that frontogenesis is possible only when T or v or both are nonlinear functions of x and y. It is of interest to note that the distribution of temperature between neighboring source regions is always nonlinear, the temperature varying from a maximum value in one source region to a minimum in the other and the temperature gradient having a maximum in the zone of transition between the two regions. *The conditions are therefore particularly favorable for frontogenesis to occur in the transitional zone between air-mass source regions where* $|\nabla T|$ *has a maximum.* Frontogenesis will then always occur whenever the wind distribution is as shown in Figs. 110a to c.

103. Linear Fields of Motion.—The formulae developed in the foregoing paragraph hold for any distribution of wind and property, and no simplifying assumptions are necessary to render them applicable to the weather charts.   In spite of this, we shall now introduce some simplifying assumptions concerning the wind field in order to find certain frequently occurring types of wind distribution that are favorable for frontogenesis. Let

$$v_x = v_x(x,y) \quad \text{and} \quad v_y = v_y(x,y)$$

represent the distribution of the wind components v_x and v_y in a horizontal plane at a given moment. Expanding in a Taylor series and neglecting terms of second and higher orders, we obtain a linear field of motion, *viz.*:

$$(1) \qquad \begin{cases} v_x = v_{x0} + v_{x1}x + v_{x2}y \\ v_y = v_{y0} + v_{y1}x + v_{y2}y \end{cases}$$

By appropriate choice of system of coordinates, we may write

$$(2) \qquad \begin{cases} v_x = v_{x0} + ax + bx - cy \\ v_y = v_{y0} - ay + by + cx \end{cases}$$

where a is positive and the other coefficients may be positive or negative. The method of determining the constants a, b, and c from v_{x1}, v_{x2}, v_{y1}, and v_{y2} is described in most textbooks on vector analysis.   The coefficients a, b, and c have the following meanings:

$$2a = \frac{\partial v_x}{\partial x} - \frac{\partial v_y}{\partial y} \quad \text{(deformation)}$$

$$2b = \frac{\partial v_x}{\partial x} + \frac{\partial v_y}{\partial y} = \text{div } v$$

$$2c = \frac{\partial v_y}{\partial x} - \frac{\partial v_x}{\partial y} = \text{curl } v$$

By parallel translation of the system of coordinates to the point where

$v_x = v_y = 0$, the translatory components v_{x0} and v_{y0} vanish, and we may write

(3)
$$\begin{cases} v_x = ax + bx - cy \\ v_y = -ay + by + cx \end{cases}$$

Equations (2) show that a linear field of motion may, in general, be divided into four elementary fields, *viz.*:

1. *A translatory field* represented by the velocity components v_{x0} and v_{y0}. In such a field, the velocity is constant, the mutual distances between individual air parcels will be preserved, and neither frontogenesis nor frontolysis is possible. This type of motion is shown in Fig. 111*A*.

2. *A deformative field* represented by the velocity components $v_x = ax$ and $v_y = -ay$. These components are shown in Figs. 111*B* and *C*. We consider a substantial circular curve in Fig. 111*B*. The circle will be transformed into an ellipse whose shortest axis will be parallel to the y-axis and remain equal to the diameter of the circle at the initial moment and whose longest axis will be parallel to the x-axis while it steadily increases. Any axis parallel to the x-axis is called the *axis of dilatation*.

We consider next two isotherms superimposed on Fig. 111*B*. If the isotherms were parallel to the axis of dilatation, the distance between them would be preserved; but if the isotherms make an angle with the axis, the distance between them would increase, and they would rotate and tend to become parallel to the axis of dilatation. The increase in distance between neighboring isotherms would be most rapid when the isotherms are perpendicular to the axis of the dilatation. The rotation of the isotherms would then vanish. It follows then that a field of motion as shown in Fig. 111*B* can never be frontogenetical. In general, it is frontolytical; and when the isotherms are parallel to the axis of dilatation, it is neutral.

Let us next consider a substantial circular curve in Fig. 111*C*. The circle would be transformed into an ellipse whose longest axis would be parallel to the axis of dilatation and remain equal to the diameter of the circle at the initial moment and whose shortest axis would be parallel to the y-axis while it steadily contracts. Any axis parallel to the y-axis is called the *axis of contraction*.

Let us next consider two isotherms superimposed on Fig. 111*C*. If the isotherms were parallel to the axis of contraction, they would remain stationary, and there would be neither frontogenesis nor frontolysis. If the isotherms form an angle with the axis of contraction, they would move and approach one another while they rotate and tend to become parallel to the axis of dilatation. If they were parallel to the axis of dilatation initially, they would not rotate but would then approach one another with a maximum of speed. Eventually, the isotherms would crowd

along the axis of dilatation where $v_y = 0$. From the above, it follows that a field of motion as shown in Fig. 111C is in general frontogenetical. Only when the isotherms are parallel to the axis of contraction is the field neutral; under no circumstance is it frontolytical.
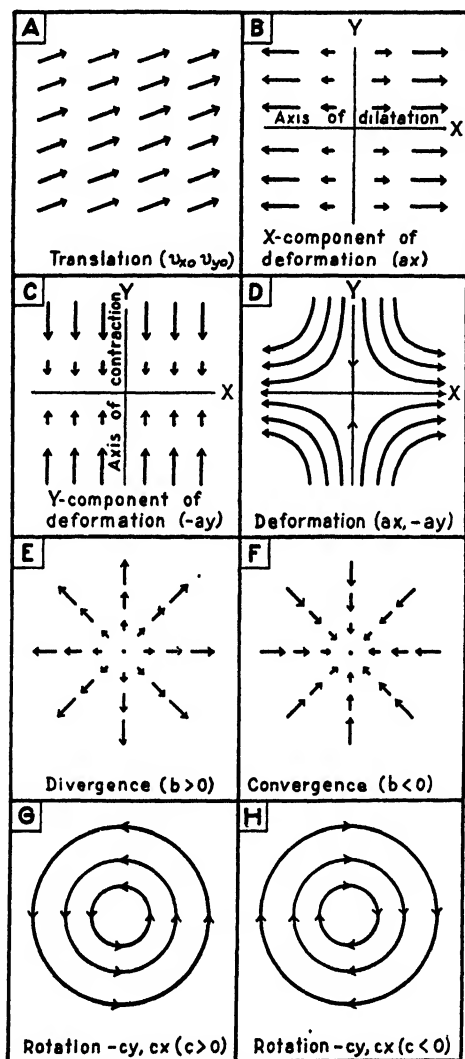
Fig. 111.—Showing the elementary linear fields of motion.

The types of motion represented by Figs. 111B and C cannot exist individually as stable systems in the atmosphere, for there is no pressure distribution that corresponds to either of them. However, the field of motion resulting from the superimposition of the fields shown by Figs.

111B and C represents the well-known type of motion in the vicinity of a col in the pressure distribution (see Fig. 111D). In this field of motion, which is represented by

$$v_x = ax \quad \text{and} \quad v_y = -ay$$
$$\text{div } v = 0$$

and the wind speed is inversely proportional to the distance between the streamlines (see Par. 100).

From what has been said above, it follows that this type of motion is frontogenetical when the isotherms form an angle with the axis of dilatation which is less than $\pm 45°$; it is frontolytical when they form an angle with this axis larger than $\pm 45°$.

3. *A field of divergence* represented by the velocity components

$$v_x = bx \quad \text{and} \quad v_y = by$$

When $b > 0$, the motion diverges from a center (Fig. 111E); when $b < 0$, the motion converges toward a center (Fig. 111F). It is readily seen that, in the case of convergence, the distance between neighboring air parcels decreases and, when there is divergence, the distance increases. Thus, a field of convergence is always frontogenetical, whereas a field of divergence is always frontolytical.

It should be borne in mind that the types of motion represented in Figs. 111E and F cannot exist as stable systems in the atmosphere because there is no pressure distribution that corresponds to such motion. Divergence and convergence are often present in small amounts superimposed on stable systems of motion. Although the field of deformation has a tendency to arrange the isotherms along a line, the field of convergence has no such tendency, and, although it may add to the frontogenesis caused by fields of deformation, it is rarely alone responsible for production of extensive fronts.

4. *A rotational field* represented by the velocity components

$$v_x = -cy \quad \text{and} \quad v_y = cx$$

The streamlines of this type of motion are concentric circles. The wind speed v along each such circle is expressed by

$$v = c\sqrt{x^2 + y^2}$$

which is constant along each circle. When $c > 0$, there is cyclonic rotation as shown by Fig. 111G; when $c < 0$, the rotation is anticyclonic (Fig. 111H). It is readily seen that the distance between individual parcels of air and the distance between neighboring isotherms will be preserved. The rotational fields are therefore incapable of bringing

distant air masses together: they are neither frontogenetical nor frontolytical.

The fields of motion found in nature will usually be composed of several or all of the elementary types discussed above. In such cases, it is only the deformative and the convergent types that affect frontogenesis. It is therefore important to be able to detect the presence of these fields when they are more or less overshadowed by rotational and translational fields. Important types of such fields of motion will be discussed in later paragraphs.

104. Frontogenesis in Linear Fields of Motion.—We return to the fundamental formula for the frontogenetical effect [*i.e.*, Eq. *102*(2)] and put

$$(1) \qquad \nabla S = |\nabla S|(mi + nj)$$

where m and n are the direction cosines of the vector ∇S, and i and j are the unit vectors of the x- and y-axes, respectively. From Eq. *103*(2), we obtain

$$(2) \qquad v = i(v_{x0} + ax + bx - cy) + j(v_{y0} - ay + by + cx)$$

Substituting this into Eq. *102*(2), we obtain

$$(3) \qquad F = -|\nabla S|[b + a(m^2 - n^2)]$$

Let α denote the angle between the axis of dilatation (*i.e.*, the x-axis) and the vector ∇S, and let β denote the angle between the axis of dilatation and the isolines of S. Then,

$$m = \cos \alpha = -\sin \beta$$
$$n = \sin \alpha = \cos \beta$$

which substituted into Eq. (3) gives

$$(4) \qquad F = |\nabla S|(a \cos 2\beta - b)$$

In agreement with the results of the graphical analysis in the foregoing paragraph, Eq. (4) shows that translation (v_{x0}, v_{y0}) and rotation $(-cy, cx)$ have no influence on frontogenesis, which depends entirely on the fields of deformation $(ax, -ay)$ and divergence (bx, by) and on the angle between the axis of dilatation and the isolines of the property in question. Furthermore, Eq. (4) shows that divergence $(b > 0)$ deducts from, and convergence $(b < 0)$ adds to, the frontogenetical effect. The part of the frontogenetical effect that is due to deformation vanishes when $\beta = \pm 45°$ and becomes negative when β is larger than $\pm 45°$. This, too, is in agreement with the results of the graphical analysis in the foregoing paragraph.

In any given case, a, β, and b are constants, whereas $|\nabla S|$ varies with x and y. Since F must have a maximum along the line of fronto-

genesis, it follows that the line of frontogenesis in a linear field of motion coincides with the line along which $|\nabla S|$ has a maximum. Therefore, *the line of frontogenesis in the field of temperature coincides with the line along which the horizontal temperature gradient has a maximum.* If $F > 0$ along this line, there is frontogenesis; if $F < 0$, there is frontolysis.

105. Frontogenetical and Frontolytical Sectors.—Equation *104*(4) shows that the sign of F, for any given field of motion, depends entirely on the angle β between the axis of dilatation and the tangent to the isolines of S. $F = 0$ along a line in the field determined by

$$(1) \qquad\qquad \cos 2\beta' = \frac{b}{a}$$

If, at a given point, $\beta' > \beta > -\beta'$, then $F > 0$, and $|\nabla S|$ increases. On the other hand, when $\pi - \beta' > \beta > \beta'$, then $F < 0$, and $|\nabla S|$
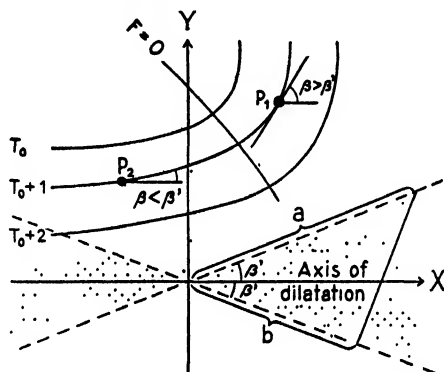
Fig. 112.—Showing the definition of frontogenetical and frontolytical sectors.

decreases. Owing to the duplicity of Eq. (1), we see that there are, in general, two symmetrical sectors in which $F > 0$ and two in which $F < 0$. These sectors are called sectors of frontogenesis and sectors of frontolysis, respectively.

Figure 112 shows the meaning of these sectors: Consider the tangent to the isotherm in the point P_1. Here, $\beta > \beta'$, and F is therefore negative. In the point P_2, $\beta < \beta'$, and F is positive. $F = 0$ along the line where $\beta = \beta'$. The area to the left of this line is called the *frontogenetical area,* and the area to the right of this line is called the *frontolytical area.* Within the frontogenetical area, the temperature gradient increases; within the frontolytical area it decreases. The two sectors $2\beta'$ symmetrical with respect to the x-axis (*i.e.,* the axis of dilatation) are called the *frontogenetical sectors,* and the two remaining sectors symmetrical with regard to the y-axis (*i.e.,* the axis of contraction) are called the *frontolytical sectors.*

When there is no divergence or convergence, $b = 0$ and Eq. (1) then gives $\beta' = \pm 45°$. When there is convergence, $b < 0$ and $\beta' > \pm 45°$; when there is divergence, $b > 0$ and $\beta' < \pm 45°$. As the divergent (or convergent) component of the motion is usually small, it follows that β' will not be far removed from $\pm 45°$. That this is so will be shown in a later paragraph on types of streamline patterns.

Theoretically, it is possible that $b > a$ or that $-b > a$. In these cases, Eq. (1) becomes meaningless, which shows that F does not vanish anywhere. The case $b > a$ then indicates that $F < 0$ throughout the field, and the case $-b > a$ gives $F > 0$ everywhere.

106. Classification of Streamlines.—For the following discussion of the practical aspects of frontogenesis, it is useful to classify the streamline patterns. The types of motion that are encountered on the weather charts are such as may exist as more or less stable systems. To such types, there will always be a pressure distribution that satisfies the motion. Other types of motion may be observed occasionally and locally; but when there is no pressure distribution that corresponds to them, they cannot exist for any appreciable length of time.[1]

The types of motion with which we are here concerned may be referred to as belonging to either central streamline patterns or patterns without a center. The first type is predominant in the atmosphere inasmuch as the large-scale wind systems are mainly controlled by centers of highs and lows and by cols in the pressure distribution. The central patterns may be grouped according to the number of straight streamlines through the center.

The linear field of motion is expressed by Eq. $103(2)$, viz.:

(1)
$$\begin{cases} v_x = v_{x0} + (b + a)x - cy \\ v_y = v_{y0} + cx + (b - a)y \end{cases}$$

The field has a center (x_0, y_0) when v_x and v_y vanish simultaneously in one point only within the region that we consider. Putting $v_x = v_y = 0$ and solving Eq. (1) with respect to x and y, we obtain

(2)
$$x_0 = \frac{\begin{vmatrix} -v_{x0}, & -c \\ -v_{y0}, & b - a \end{vmatrix}}{\begin{vmatrix} b + a, & -c \\ c, & b - a \end{vmatrix}}, \qquad y_0 = \frac{\begin{vmatrix} a + b, & -v_{x0} \\ c, & -v_{y0} \end{vmatrix}}{\begin{vmatrix} b + a, & -c \\ c, & b - a \end{vmatrix}}$$

The following three cases may occur:

1. x_0 and y_0 are finite. In this case, there is a center in which the motion vanishes.

2. x_0 and/or y_0 are indeterminate. In this case, the field of motion has no center, but there is a line along which the motion vanishes.

[1] For a more detailed discussion of streamline patterns, see Petterssen [56].

3. x_0 and y_0 are infinite. In this case, there is no center, and the motion will resemble what is observed in the vicinity of extensive troughs of low pressure or extensive ridges of high pressure.

1. *Central Patterns.*—The condition for having a center requires that the denominator in Eq. (2) does not vanish, or

$$(3) \qquad b^2 - a^2 + c^2 \gtrless 0$$

When this is so, there are always finite values for x_0 and y_0, which means that the center exists.

The central patterns may be subdivided into four classes according to the number of straight streamlines through the center.

By parallel translation of the system of coordinates to the center, Eqs. (1) reduce to

$$(4) \qquad \begin{cases} v_x = (b + a)x - cy \\ v_y = cx + (b - a)y \end{cases}$$

The condition for having straight streamlines through the center is

$$(5) \qquad \frac{dy}{dx} = \frac{v_y}{v_x} = \frac{y}{x}$$

Substituting from Eq. (4), we obtain, when A denotes the angle between the x-axis, *i.e.*, the axis of dilatation, and the straight streamline,

$$(5) \qquad \tan A = \frac{a \pm \sqrt{a^2 - c^2}}{c} \qquad \text{(independent of } b)$$

Four classes of central patterns may be distinguished.

(*a*) $a = c = 0$. In this case, there is neither deformation nor rotation; the field of motion is one of pure divergence ($b > 0$) or convergence ($b < 0$), and there is an infinite number of straight streamlines through the center. This type of motion is shown in Fig. 111*E* and *F*. As already stated, this type of motion cannot exist individually as a stable system, for there is no pressure distribution that corresponds to it. However, divergence or convergence of slight or moderate intensity is usually superimposed on other types of motion. Their importance in the production of rotational motion was explained in Chap. IV, and further comments will be found in the paragraphs to follow.

(*b*) $a^2 > c^2$. In this case, the deformation field (*i.e.*, Fig. 111*D*) predominates relative to the rotational field (*i.e.*, Fig. 111*G* or *H*). The condition $a^2 > c^2$ in connection with inequality (3) above gives the following two possibilities:

$$(6) \qquad b^2 > a^2 - c^2 > 0$$
$$(7) \qquad b^2 < a^2 - c^2 > 0$$

As $a^2 > c^2$, it will be seen from Eq. (5) that there are two straight streamlines through the center. Integration of the streamline equation shows that inequality (6) corresponds to parabolic streamline patterns around the center. As such motion does not correspond to any possible pressure distribution, it will not be discussed here.

Integrating the streamline equation under consideration of inequality (7), it will be found that the streamlines are hyperbolic and correspond to the motion around a col in the pressure distribution. It is in such fields of motion that frontogenesis may be most active. The significant types are discussed in connection with Fig. 113.

(c) $a^2 = c^2 > 0$. In this case, there is only one straight streamline through the center, and the remaining streamlines are S-shaped. As such motion does not correspond to any possible pressure distribution, it will not be discussed here.

(d) $a^2 < c^2$. In this case, the rotational field (*i.e.*, Figs. 111G and H) predominates relative to the deformative field (*i.e.*, Fig. 111D). It will be seen from Eq. (5) that there is no straight streamline through the center. This class is highly important because it represents all types of motion around cyclonic and anticyclonic centers. The various types of such motion will be discussed in connection with Fig. 116.

2. *Straight Streamlines.*—We consider next the case when Eqs. (2) are indeterminate, or when

$$b^2 - a^2 + c^2 = 0$$

and

(8)
$$\frac{v_{y0}}{v_{x0}} = \frac{c}{b + a} = -\frac{b - a}{c}$$

This, substituted into Eq. (1), shows that v_x and v_y vanish everywhere on a straight line whose slope relative to the axis of dilatation is

$$\frac{b + a}{c} = -\frac{c}{b - a}$$

By parallel translation of the system of coordinates so that the origin falls on this line, we obtain

(9)
$$\begin{cases} v_x = (b + a)x - cy \\ v_y = cx + (b - a)y \end{cases}$$

The slope of any streamline is expressed by

$$\frac{dy}{dx} = \frac{v_y}{v_x}$$

Substituting from Eqs. (8) and (9), we obtain

$$\frac{dy}{dx} = \frac{c}{b + a} = -\frac{b - a}{c}$$

independent of x and y. This means that all streamlines are straight throughout the field. Eight qualitative different cases may occur,[1] but they show only slight resemblance to what is actually observed. Moreover, fields of motion consisting of straight streamlines are only special cases of the category that will be discussed below.

3. *Curved Streamlines without Centers.*—This case occurs when the numerators in Eqs. (2) differ from zero and the denominators vanish. We then have

$$\frac{v_{y0}}{v_{x0}} \gtrless -\frac{b-a}{c} = \frac{c}{b+a}$$

On comparing this with Eq. (8), it is easily seen that the field of motion in this case may be divided into two parts: one that is congruent with the cases discussed under (2) (straight streamlines), and another that is a constant translation superimposed on and forming an angle with the straight streamlines. The significant types of motion are shown in Fig. 117.

107. Frontogenesis in the Vicinity of Cols.—In Fig. 113, the x-axis is chosen along the axis of dilatation and the y-axis along the axis of contraction. In all types of motion with hyperbolic streamlines, the deformative field predominates relative to the rotational and divergent (convergent) fields. The straight streamline with outflow from the center is called the *axis of outflow*, and the one with inflow toward the center is called the *axis of inflow.*

When $c = 0$, there is no rotational motion. It follows then from Eq. *106*(5) that the angle A equals either zero or 90°. This means that the axis of outflow coincides with the axis of dilatation and the axis of inflow coincides with the axis of contraction.

When $b = 0$, it follows from Eq. *105*(1) that the angle $\beta' = \pm45°$. This means that the frontogenetical sector is 90° with the axis of dilatation as bisectant.

Figures 113A, B, and C show the various types of hyperbolic streamline when there is no rotational motion. The angle between the axis of outflow and the axis of inflow is then 90°, and these axes coincide with the axes of dilatation and contraction, respectively. In Fig. 113A, $b = 0$, indicating that there is no convergence or divergence. The frontogenetical sectors are then 90°. In Fig. 113B, there is divergence ($b > 0$) superimposed on a field of pure deformation. In this case, the frontogenetical sector is less than 90° (see Eq. *105*(1)). In Fig. 113C, there is convergence superimposed on the deformative field. The frontogenetical sector is then larger than 90°. Thus, when convergence and deformation operate together, frontogenesis will more readily take place than when divergence and deformation cooperate.

[1] See footnote to p. 249.

In Figs. 113D, E, and F, there is cyclonic rotation ($c > 0$) super-imposed. It will be seen from Eq. *106*(5) that, when $a > c > 0$, tan $A \lessgtr 0$. This means that the axis of outflow deviates from the axis of dilatation and the axis of inflow deviates from the axis of contraction. Comparison between Figs. 113A to C and Figs. 113D to F shows
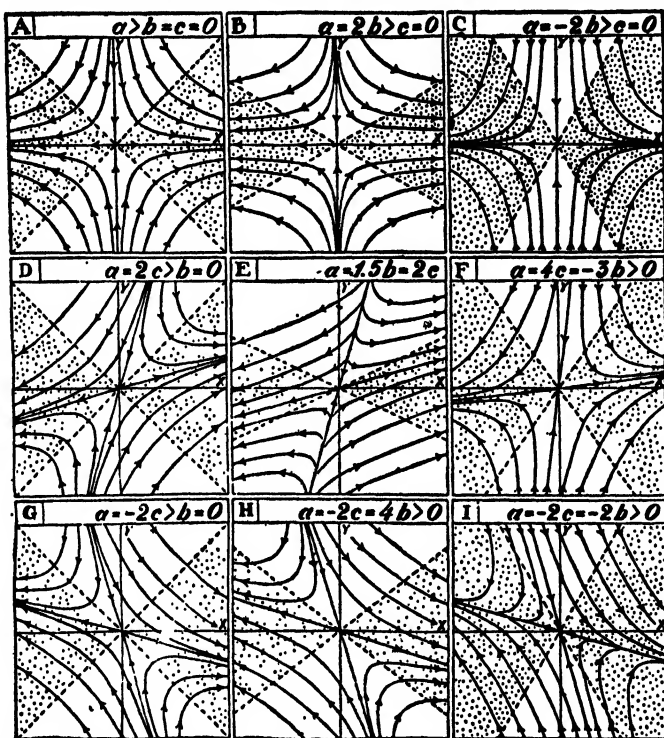
Fig. 113.—Showing types of motion with hyperbolic streamlines. The dotted areas indicate the sectors of frontogenesis. A represents pure deformation; B, deformation plus divergence; C, deformation plus convergence; D, deformation plus cyclonic rotation; E, deformation plus divergence plus cyclonic rotation; F, deformation plus convergence plus cyclonic rotation. G, H and I are principally the same as those represented by D, E and F, but with anticyclonic instead of cyclonic rotation.

The diagrams are obtained by integration of the streamline equation for definite values of the constants in order to show the relative importance of the deformative, the divergent (convergent) and the rotational fields. By comparing these diagrams with what is actually observed on the weather charts, it is possible to obtain a rough idea of the composition of the wind field.

that the cyclonically curved streamlines become more cyclonically curved when a cyclonic rotation is superimposed and that anticyclonically curved streamlines obtain a diminished curvature.

The sectors of frontogenesis are not affected by the superimposition of rotation.

Figures 113G to I are characterized by anticyclonic rotation. In this case, $c < 0$, the curvature of the anticyclonic streamlines are

increased, and the curvature of the cyclonic streamlines is diminished. The axis of outflow then suffers a negative rotation relative to the axis of dilatation, whereas the axis of inflow suffers a positive rotation relative to the axis of contraction.

It will be seen from the figures that whenever there is rotation superimposed on the field of motion (*i.e.*, $c \gtreqless 0$), the axes of dilatation and rotation are not visible in the streamline picture: they become "hidden." What is always visible in the streamline picture are the axis of outflow and the axis of inflow. However, as it is the angle between the axis of dilatation and the isotherms (*i.e.*, the angle β; see Par. 104) that decides
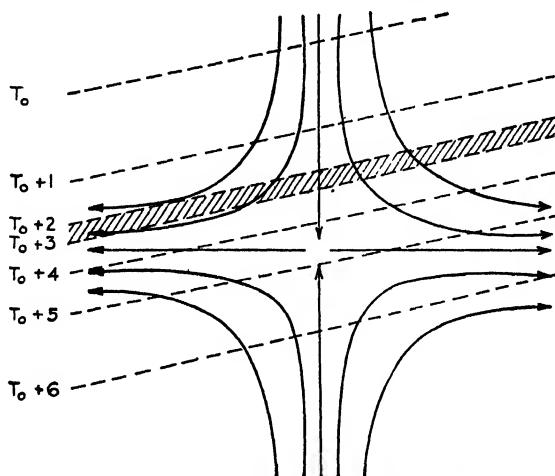
FIG. 114.—Illustrating the movement of the line of frontogenesis in the vicinity of a col.

whether or not, there is frontogenesis, it is important to determine the direction of the axis of dilatation. This is done in the following manner: *Bisect the angle between the axis of inflow and the axis of outflow, and draw lines forming angles of $\pm 45°$ with a bisectant. The line along which there is a wind component out from the center is the axis of dilatation, and the other line is the axis of contraction.* That this is so is readily verified by aid of Fig. 113.

We shall next return to Eq. *104*(4) which expresses the intensity of the frontogenetical effect. In any given case (wind and temperature distribution) a, b, and β are given. F then has a maximum along the line where the gradient of the property in question (*e.g.*, temperature) has a maximum. This line then is the line of frontogenesis.[1]

In order to obtain a clear idea of the process of frontogenesis, we shall consider Fig. 114, where the wind field is one of pure deformation. The line of frontogenesis coincides with the hatched zone where the tempera-

---

[1] It is important to note that the line of frontogenesis need not coincide with the axis of outflow or with the axis of dilatation.

ture gradient has a maximum. The line of frontogenesis will move toward the axis of dilatation, and, when it does so, it will rotate and tend to become parallel to this axis. As it does so, the angle between the axis of dilatation and the isotherms will decrease, and the frontogenetical effect will increase accordingly. As the line approaches the axis, it will tend to become stationary and thus be exposed to continued frontogenesis. It is for this reason that the wind distribution in the vicinity of a neutral point (col) is particularly favorable for frontogenesis. If the process lasts long enough, a veritable front will form, which will usually be found close to the axis of outflow. We may therefore say that *the axis of outflow*
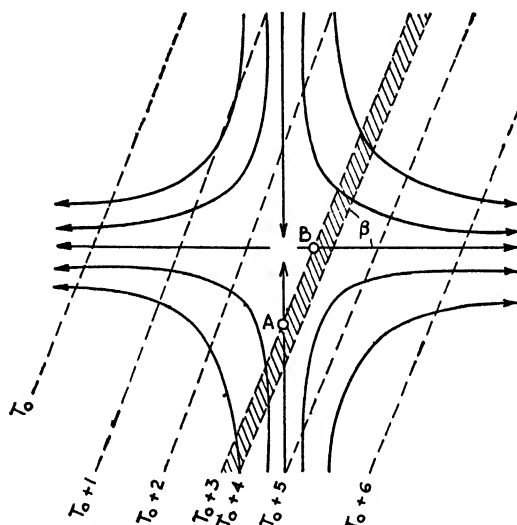
FIG. 115.—Illustrating frontolysis followed by frontogenesis.

is not a creator of fronts but a collector of fronts; for though frontogenesis may occur anywhere in the field, the line of frontogenesis will move toward this axis, and the resulting front will be found at this axis, or close to it.

Let us next assume that a line of frontogenesis is embedded in Fig. 113*D*, somewhere above the axis of outflow. The line would then move toward the axis of outflow and tend to become parallel to it. But, in this case, it will not become parallel to the axis of dilatation, in which position the frontogenetical effect would have a maximum of intensity (*i.e.,* $\beta = 0$).

We shall now consider Fig. 115. The zone in which there is a maximum of temperature gradient forms an angle with the axis of dilatation that is larger than 45°. In this case, $F < 0$, and there is frontolysis. However, the point A will move toward the neutral point, and the point B will move to the right along the axis of dilatation. The line of frontolysis

will rotate and tend to become parallel to the axis of dilatation. As the angle between this axis and the isotherms passes the critical value, $F = 0$, and, when the angle decreases below the critical value, the line of frontolysis changes into a line of frontogenesis. Eventually, it may approach the axis and develop a veritable front.

In the hyperbolic wind systems, frontolysis is usually a passing phenomenon; for if the wind system retains its character for a sufficiently long interval of time, the isotherms will have a tendency to move and crowd along the axis of outflow.

It is of importance to note that the intensity of the frontogenetical effect is proportional to the temperature gradient and the wind gradient. When these gradients are small, the kinematic frontogenesis will be slight; and as the kinematic effect is always counteracted by physical processes (*e.g.*, radiation, conduction, mixing, etc.), no effective frontogenesis will result unless there are sufficient gradients in the fields of temperature and wind.

108. Frontogenesis in the Vicinity of Cyclones and Anticyclones.— The significant types of cyclonic and anticyclonic wind systems are shown in Fig. 116. Figure 116*A* represents pure cyclonic rotation in the northern hemisphere, or anticyclonic rotation in the southern hemisphere; Fig. 116*B* represents pure anticyclonic rotation in the northern hemisphere, or cyclonic rotation in the southern hemisphere. In these cases, $a = b = 0$, and there is no frontogenetical effect [see Eq. *104*(4)]. Figures 116*C* and *D* result from *A* and *B*, respectively, when a field of divergence ($b > 0$) is superimposed. In these cases, $a = 0$, and $b > 0$. The frontogenetical effect is then negative [see Eq. *104*(4)], and the isotherms will move away from one another. This results in homogenification of the air masses that partake in the circulation. The importance of horizontal divergence in the production of quasi-homogeneous air masses was explained in Chap. III.

Figures 116*E* and *F* result from *A* and *B*, respectively, when a field of convergence ($b < 0$) is superimposed on them. In this case, we obtain from Eq. *104*(4)

$$F = -|\ \nabla S\ |b$$

As $b < 0$, there is frontogenesis throughout. This means that the isolines of S (*e.g.*, isotherms) will approach one another, and they will do so most rapidly where the gradient of S (*e.g.*, the temperature gradient) has a maximum.

On account of the convergence, the frontal zone thus created will move toward the center, forming a boundary between two sectorially distributed air masses. It should be noted that convergence is rarely sufficiently effective to produce fronts of appreciable intensity. Such

fronts are formed only when a field of deformation of sufficient intensity is present.
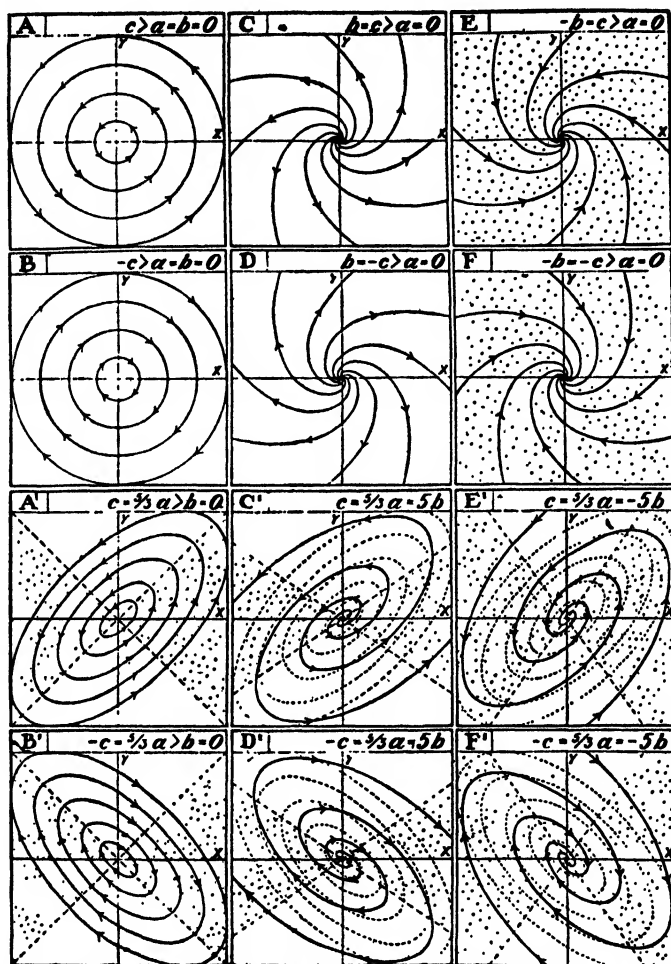
Fig. 116.—Showing the various types of cyclonic and anticyclonic streamline patterns. All these types are characterized by $c^2 > a^2$ which means that the rotational field predominates relative to the deformative field. If $c^2 < a^2$, we would obtain hyperbolic types of motion (compare Fig. 113). In the diagrams $A - F$, $a = 0$, and in those indicated by $A' - F'$, $a > 0$. The frontogenetical sectors are indicated by dotted areas. Note that when deformation is present, the streamline patterns become oblong, and the more so the more intense the deformation is relative to the rotation. Conversely, from the observed wind field, we may obtain an idea of the intensity of the deformation relative to that of the rotation.

Figures 116A to F are symmetrical in all directions. This is due to the circumstance that there is no deformation in the motion.

Figures 116A' to F' result from the corresponding figures A to F when a field of deformation is superimposed on them. In the patterns

A' to F', the x-axis indicates the direction of the axis of dilatation. It will be seen that the trough line in cyclonic systems and the wedge line in anticyclonic systems bisect the angle between the axis of dilatation and the axis of contraction. Therefore, the axes of dilatation and contraction may be determined by drawing lines that form $\pm 45°$ with the trough or the wedge line. The line that has a wind component outward from the center is the axis of dilatation, and the other line is the axis of contraction. Frontogenesis will then result in oblong systems when the isotherms form an angle with the axis of dilatation that is less than half the angle of the frontogenetical sector.

It is instructive to discuss hypothetical temperature distributions in connection with Figs. 116A' to F' in order to see what temperature distributions are most favorable for formation of fronts. We shall here discuss only the case in which a line of frontogenesis runs through the center of an oblong cyclonic system (*e.g.*, Fig. 116A'). To simplify the discussion, we assume that the y-axis points northward and toward the colder air mass. We then see that a line of frontogenesis which, for example, is situated in the frontogenetical sector to the west of the center will be accentuated. The line will then move with the air current and approach the trough line. If the center and the trough do not move, the line will be brought into the frontolytical sector to the south of the center, where it will gradually dissolve. Thus, unless the trough line moves approximately with the speed of the air current, the frontogenetical effect will not have sufficient time to build up a real front: there will be only a temporary concentration of isotherms in the rear of the cyclonic center. However, when the trough line moves in a forward direction (*e.g.*, toward the east), the line of frontogenesis will remain for a long interval of time in the frontogenetical part of the wind field. A real front may then result.

With reference to the discussion of the hyperbolic types of motion in Par. 107, it is seen that the field of deformation has a much greater chance of producing a real front when the streamlines are hyperbolic than when they are as shown in Figs. 116A' to F'. This circumstance is due, not to any difference in intensity of the deformation, but to the fact that, in the case of hyperbolic streamlines, the line of frontogenesis will become stationary along the axis of outflow where the frontogenetical effect is considerable, whereas, in the case of trough-shaped streamlines (*e.g.*, Fig. 116A'), the line will move out of the frontogenetical area. Thus, frontogenesis in troughs is a rather perfidious phenomenon. Even when there is a considerable frontogenetical effect at a given instant, it may not last long enough to produce a front. Whether or not a front will be formed in a trough depends greatly on the movement of the trough. How the movement of a trough is evaluated from the data of the weather maps will be discussed in Chap. IX.

It will be seen from the foregoing discussion and Figs. 116A' to F' that the following rules hold:

1. Fronts that move toward a trough line increase in intensity.
2. Fronts that move away from a trough line will dissolve.
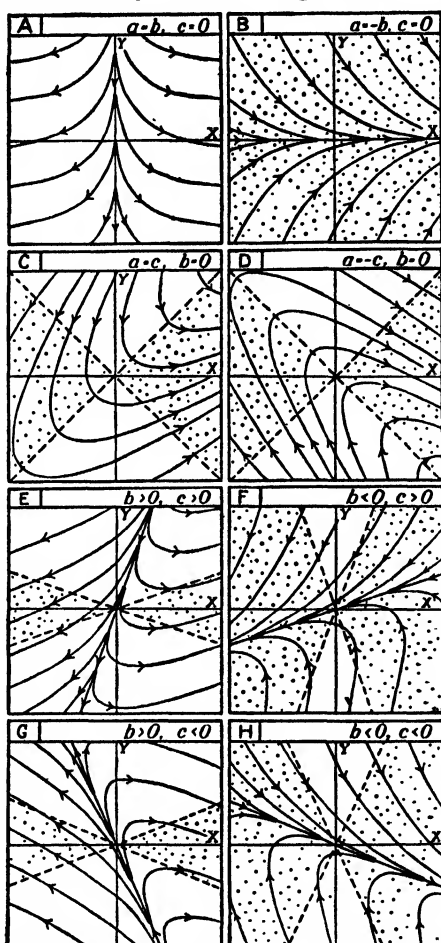
FIG. 117.—Showing frontogenesis in curved streamlines without center.

109. Frontogenesis in Curved Motion without Center.—The significant types of motion discussed under (3), Par. 106 are illustrated in Fig. 117 for characteristic values of the constants a, b, and c. These diagrams may be discussed on the principles outlined in Pars. 107 and 108. In all cases, the x-axis indicates the direction of the axis of dilatation, and the dotted areas indicate the sectors of frontogenesis. Whenever the angle between the axis of dilatation and the isotherms is smaller than half the angle of the frontogenetical sector, there will be frontogenesis provided that there is a sufficient gradient of temperature present.

Figures 117*A*, *E*, and *G* resemble the conditions that are encountered in areas occupied by extensive ridges of high pressure. In these systems, frontogenesis is either impossible or highly improbable.

Figures 117*B*, *F*, and *H* represent the conditions along extensive troughs of low pressure, such as, for example, the doldrums. It will be seen that the kinematic conditions are highly favorable for fronts to form, for any line of frontogenesis will move toward the line that separates the opposing currents, and it will thus either coincide with the axis of dilatation or else form a small angle with it. The frontogenetical effect is then large. It should, however, be borne in mind that the intensity of the frontogenetical effect is proportional to the horizontal gradient of temperature. As the gradient of temperature usually is small in the equatorial regions, it is only under special circumstances that the converging winds there result in fronts of considerable intensity.

Figures 117*C* and *D* are essentially the same as the cyclonic troughs in the northern and the southern hemisphere, respectively. Frontogenesis in such troughs was discussed in Par. 108.

110. The Sequence of Streamline Patterns.—It was shown in Par. 103 that the parameters *b* and *c* in the equations for the linear field of motion have the following meanings:

$$2b = \operatorname{div} v \qquad \text{and} \qquad 2c = \operatorname{curl} v$$

Substituting this in Eq. *100*(16) and dropping the vector notations, we obtain

$$\frac{dc}{dt} = -b(\lambda + 2c)$$

where $\lambda = 2\omega \sin \varphi$. As $(\lambda + 2c)$ is always positive, it follows that *whenever there is horizontal divergence or convergence (i.e., $b \gtrless 0$), the rotational field must change.* This circumstance may be used for estimating the nature of the change with time in the wind systems.

The various possibilities are shown in the table below.

Initial state	Convergence ($b < 0$)	Divergence ($b > 0$)
No rotation ($c = 0$)........	Creation of cyclonic rotation	Creation of anticyclonic rotation
Cyclonic rotation ($c > 0$)...	Increasing cyclonic rotation	Decreasing cyclonic rotation, and, possibly, creation of anticyclonic rotation
Anticyclonic rotation ($c < 0$)	Decreasing anticyclonic rotation and, possibly, creation of cyclonic rotation	Increasing anticyclonic rotation

The foregoing principles are illustrated in Figs. 118 and 119. In Fig. 118*A*, there is deformation plus divergence. Anticyclonic rotation will then develop and the streamline pattern will change as shown in Figs. 118*B* to *F*.

A   B   C   D   E   F
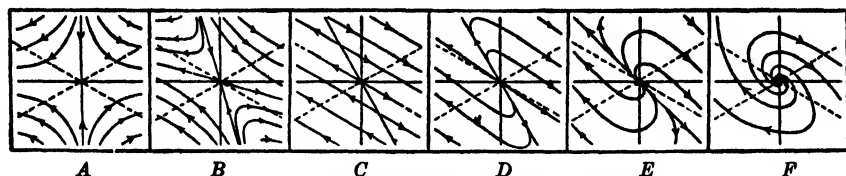
FIG. 118.—Anticyclogenesis through divergence.

In Fig. 119*A*, there is deformation and convergence. Cyclonic rotation will then develop, and the motion will change as shown in Figs. 119*B* to *F*. If frontogenesis occurs simultaneously, the development would result in a wave cyclone; but it is also possible to have cyclogenesis without an original front.

A   B   C   D   E   F
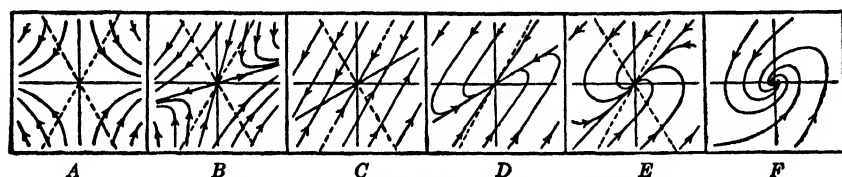
FIG. 119.—Cyclogenesis through convergence.

111. The Nonconservative Influences.—The foregoing deductions were based on the assumption that the air-mass property in question is strictly conservative (see Par. 102). Bjerknes and Bergeron [16] have shown that frontogenesis in the field of temperature is slightly modified on account of the heating or cooling that the air masses undergo while they move across the isotherms of the underlying surface. This modification is such that the temperature contrast which actually results at the front is always less than what it would have been if the temperatures were strictly conservative.

The temperature variation per unit time in a fixed point is expressed by Eq. *3*(5). The last term, which contains the vertical velocity, vanishes at the earth's surface. The second term on the right-hand side may be written as $-(\partial T/\partial s)v_s$, where s measures length along a line that is normal to the isotherms, s being positive in the direction from low to high temperature. $-(\partial T/\partial s)$ thus expresses the magnitude of the horizontal gradient of temperature, and v_s is the component of the wind velocity in the direction of s. Equation *3*(5) then reduces to

$$\frac{\partial T}{\partial t} = \frac{1}{c_p}\frac{dQ}{dt} - \frac{\partial T}{\partial s}v_s$$

Suppose that v_s is positive; the wind then blows from a colder toward a warmer region.   In this case, the air will be heated by the underlying surface so that the term $(1/c_p)(dQ/dt) > 0$ while the term $-(\partial T/\partial s)$ $v_s < 0$.   If, on the other hand, v_s is negative, the air moves from a warmer toward a colder region, and the term $(1/c_p)(dQ/dt) < 0$, while $-(\partial T/\partial s)v_s > 0$.   Thus, in either case, the nonadiabatic term $(1/c_p)$ dQ/dt counteracts the transport of isotherms, with the result that the
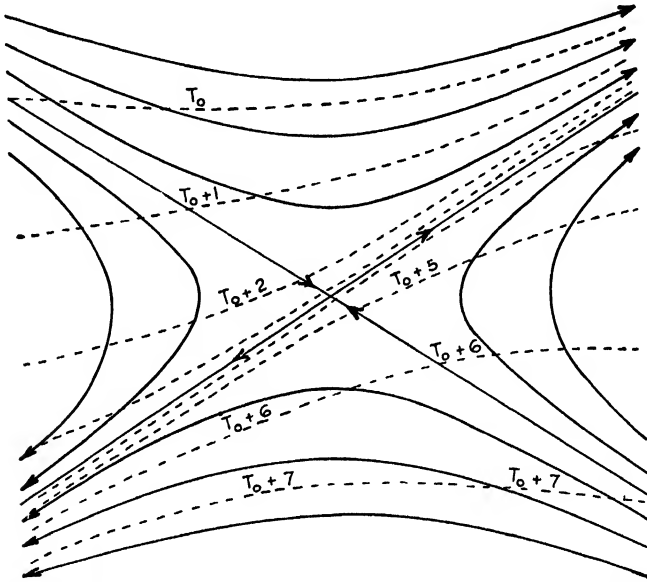
FIG. 120.—Showing the influence of heating and cooling on the arrangement of isotherms in a frontogenetical wind field.

isotherms move more slowly than the air itself.   The isotherms would remain stationary when the two terms balance, *viz.:*

$$\frac{1}{c_p}\frac{dQ}{dt} = \frac{\partial T}{\partial s} v_s$$

The isotherms that originally were close to the axis of outflow in a system of hyperbolic motion would soon be brought toward this axis; but more distant isotherms will not reach this axis, because the heating or cooling that the air undergoes during its long journey across the isotherms of the underlying surface would cause these isotherms to become stationary.

If the axis of outflow initially coincides with the isotherms, the front that results would contain the same bundle of isotherms throughout. However, when the axis of outflow initially forms an angle with the isotherms, the resulting front would not contain the same individual

isotherms throughout. The isotherms would then coincide with the front only in a comparatively short interval and would then branch off as shown in Fig. 120.
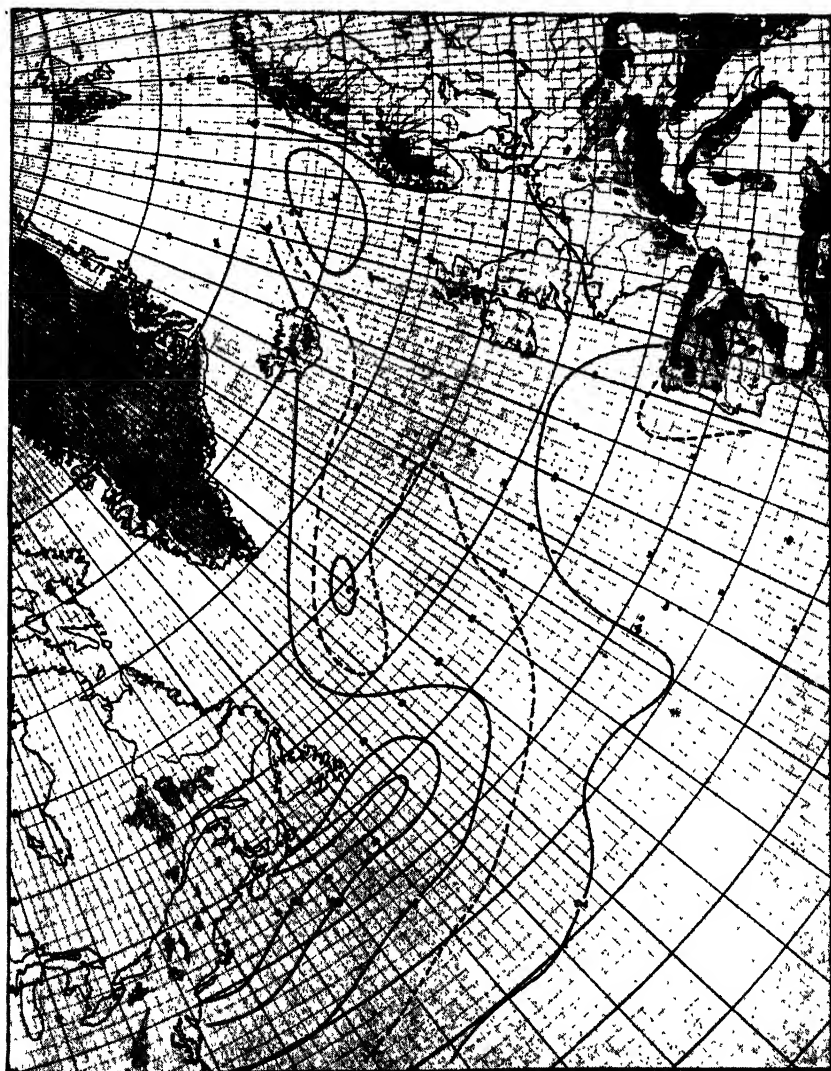
Fig. 121.—Normal difference in air temperature between tropical air and returning maritime air in midwinter. Compare Figs. 93 and 94.

The influence of heating and cooling of the air masses during the formation of fronts is important for the understanding of the geographical position of the principal frontal zones and their intensities.

Figures 93 to 95 show the mean air temperature of the three principal types of air masses in midwinter. Figure 121 shows the difference

between the maps in Figs. 93 and 94.   In other words, it shows the
normal difference in temperature between tropical maritime air and
returning polar air.   It will be seen that the difference in temperature
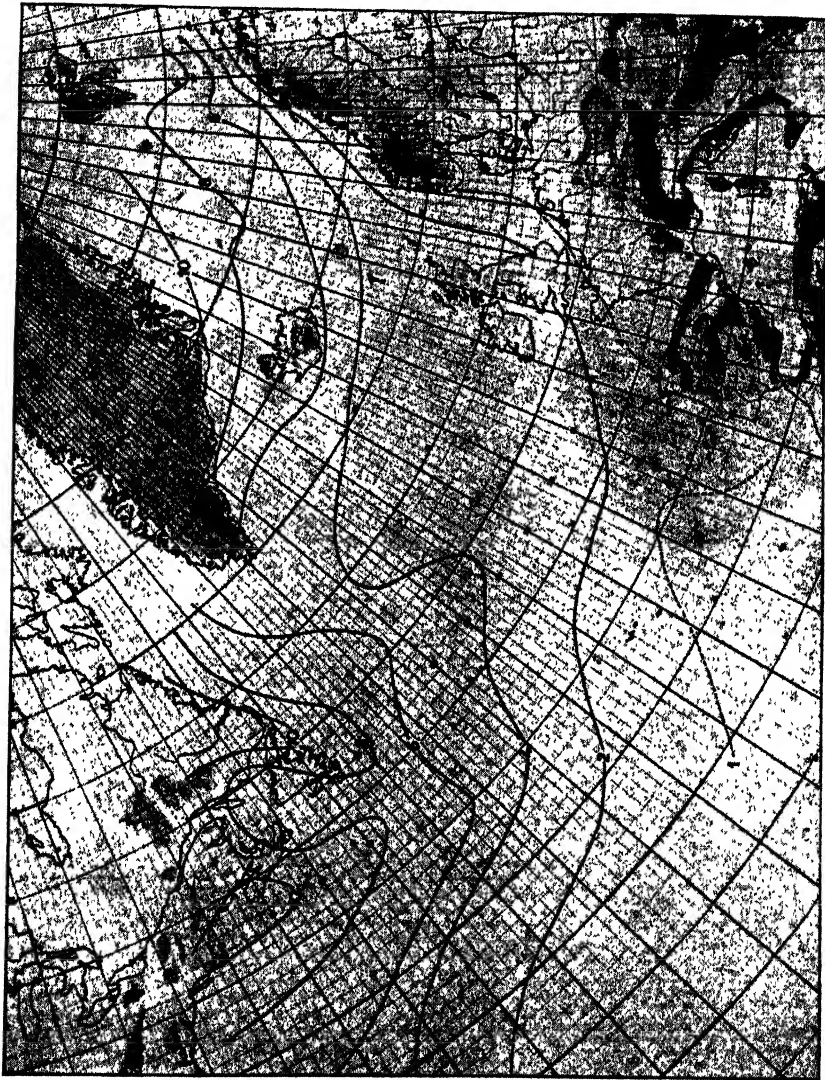
Fig. 122.—Normal difference in air temperature between returning polar air and arctic air in midwinter. Compare Figs. 94 and 95.

between these air masses is small in the eastern and southern part of the
North Atlantic.   This is due to the circumstance that the polar air in
such cases has absorbed so much heat from the ocean surface that its
temperature approaches that of the tropical air in the same latitude.
However, in the western portion, notably near Newfoundland and Nova

Scotia, the difference is considerable. Therefore, a frontogenetical wind system may produce a strong front between Tm and Pm air masses in the western part of the North Atlantic Ocean, whereas a similar field can produce only a weak front in the eastern part of the North Atlantic.
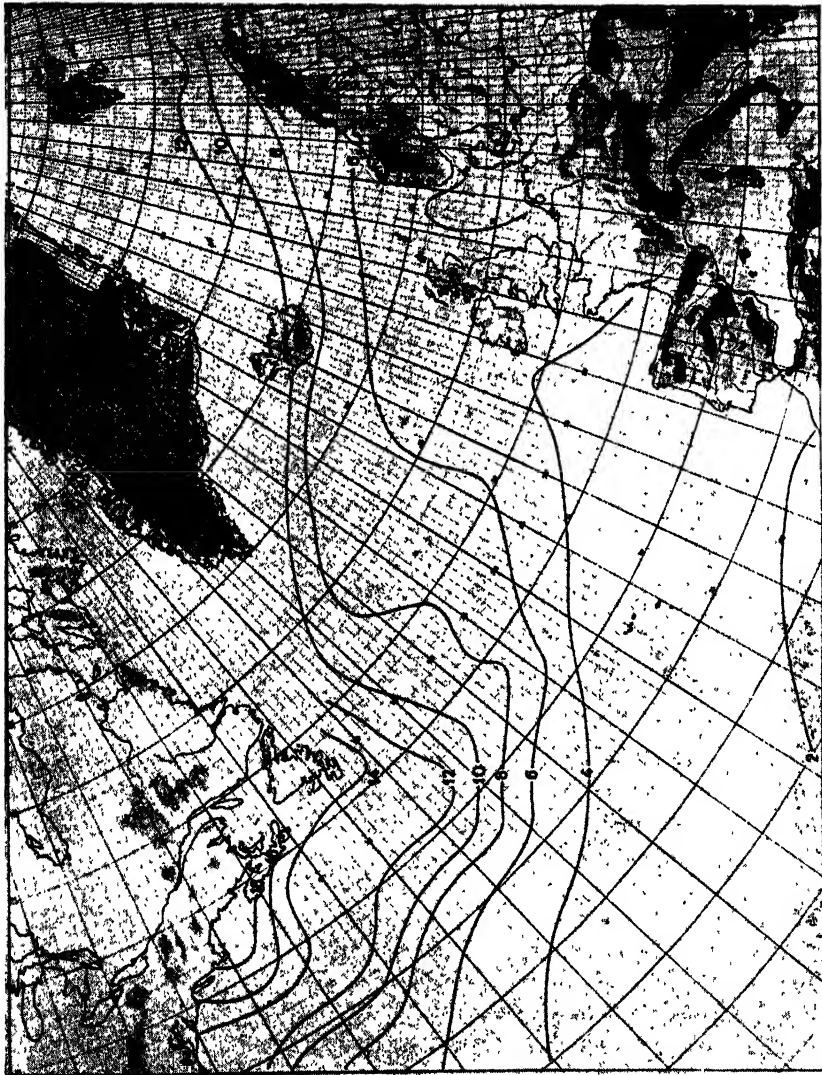
FIG. 123.—Normal difference in air temperature between tropical air and direct outbreaks of arctic air in mid-winter. Compare Figs. 93 and 95.

Figure 122 shows the corresponding difference between Figs. 94 and 95, *i.e.*, between returning polar air and arctic air. It will be seen that the differences between these air masses are, on the whole, larger than between tropical maritime air and returning polar air. The maximum

of temperature difference is found in the zone from Spitsbergen to Newfoundland and Nova Scotia, where there is a maximum of temperature gradient in the underlying surface. A frontogenetical wind field within this zone will produce strong fronts, whereas a similar wind field in the southeastern part of the North Atlantic will produce only a weak front.

Figure 123 shows the difference between the maps in Figs. 93 and 95. It will be seen that strong fronts will result over the entire northern part of the North Atlantic whenever there is a frontogenetical wind field between direct outbreaks of arctic air and the tropical maritime air. It should be noted that tropical air is rarely brought into juxtaposition with fresh arctic air in the eastern part of the North Atlantic, whereas this often occurs along the east coast of North America.

It will be seen from the maps (Figs. 121 to 123) that most strong fronts must form in the western part of the North Atlantic, say west of about 40°W. Such fronts are normally carried eastward with the traveling cyclones in the prevailing westerlies. The fronts then normally decrease in intensity on account of the heating that the polar air sustains over the warm ocean. The fronts then arrive in west Europe as comparatively weak fronts.

Figures 121 to 123 show the conditions in midwinter. Similar conditions hold also in summer except that the zone of maximum temperature difference between the principal types of air mass is moved farther to the north.

The conditions described above for the North Atlantic in midwinter apply also to the North Pacific Ocean. On the whole, we may say that strong fronts develop when frontogenetical wind fields are present within the air-mass zones 4 and 5 (in Fig. 89) on the Atlantic and on the Pacific Ocean.

112. The Principal Frontal Zones in the Northern Hemisphere in Winter.[1]—In order to obtain a picture of the geographical distribution of the principal zones of frontogenesis and the principal frontal zones, it is necessary to consider the distribution of temperature and wind. In general, it may be stated that the "source" of temperature difference is partly the normal meridional temperature gradient and partly the temperature contrasts between oceans and continents. The "agency" that creates fronts out of these sources of temperature differences is mainly the deformative part of the wind field. In individual cases, fields of convergence may add to the frontogenetical effect. Moreover, it is

---

[1] The frontal zones of the northern hemisphere in winter and summer have been described by Bjerknes and Bergeron [16]. The results presented here agree in all essentials with those obtained by Bjerknes and Bergeron, the slight differences being due to the fact that the present results are based on more detailed study of the temperature field in relation to the wind distribution.

necessary to consider the heating and cooling that the air undergoes during the process of frontogenesis (see Par. 111). The most favorable conditions for the formation of fronts will therefore be found where the circulation is such that air from widely different source regions is brought into juxtaposition by a minimum of travel. In winter, these conditions are most ideally fulfilled along the east coasts of northern continents.

It was shown in Pars. 102 and 108 that the line of frontogenesis has a tendency to coincide with the zone in which the temperature gradient has a maximum. The line or zone of frontogenesis will then move with the air current and tend to approach the axis of outflow from a col in the pressure distribution or the trough line in an oblong cyclonic system.

Consequently, the regions within which frontogenesis should be particularly active are those where the wind circulation is such that the air moves from a zone of maximum gradient in the mean temperature distribution toward an axis of outflow or a trough line. Although the frontogenetical process might commence in the zone of maximum temperature gradient, the resulting front should most frequently be found near the axis of outflow or near the trough line in the mean motion. Statistical investigation of the frequency of occurrence of fronts in the North Atlantic area (Petterssen [57]) has shown that the theoretical considerations are verified by actual observations.

In Fig. 124, the zones of maximum temperature gradient in midwinter are indicated by hatching. The wind chart (Fig. 86) or the pressure chart (Fig. 80) will show the mean positions of the axes of outflow and the trough lines. Figure 124 then shows the average, or the mean positions of the principal frontal zones in midwinter.

Some brief comments on these frontal zones may be of interest.

1. *The Atlantic Area.*—The principal frontal zone in this area is the so-called *Atlantic polar front.* The principal source of temperature contrast is the difference in temperature between the cold continent of North America and the warm ocean adjacent to it. The kinematic background for this front is the field of deformation between the subtropical cell and the cold continental high. The closeness of these extreme airmass sources accounts for the remarkable intensity and persistency of this frontal zone.

The front usually oscillates between the West Indies and the Great Lakes. A maximum of front intensity is usually observed when the front coincides with the coast line. Disturbances that develop on this front usually form to the south or to the southwest of Newfoundland and travel eastward with the prevailing westerlies. In this way, fronts that originally formed in the western portion of the Atlantic are carried eastward to Europe or farther. The Atlantic polar front is sometimes prolonged in an eastward direction through the action of frontogenetical

wind systems of a temporary character. In the eastern part of the North Atlantic, the polar front oscillates within wide limits, depending on the actual wind distribution.

Outbreaks of polar or arctic air, notably from Greenland, often sweep southward in the rear of passing cyclones and bring the front southward to the Canary Islands or farther. On account of the heating of the polar air and the anticyclonic (divergent) wind distribution in these regions, the front usually dissolves in the area west of Portugal, while it is steadily maintained or re-formed in the Bermuda region.

Occasionally the Atlantic subtropical cell splits in two. In such cases, there may be two coexisting polar fronts on the Atlantic, the one nearest to the American coast usually being the stronger one.

Next in importance to the polar front in the Atlantic Area comes the *Atlantic arctic front.* Its temperature source is the difference between the cold air over the arctic field of snow and ice and the warmer air from the Atlantic that streams along the northwest and north coast of Europe (see Fig. 86). Its kinematic background is the field of deformation that is manifest in the extensive pressure trough extending from the Icelandic low toward Novaya Zemlya and sometimes along the entire coast of Siberia. Frontogenesis in this region is particularly active when the Icelandic low is situated further to the east than normal. In such cases, there is usually an active supply of warm air from the southwest to make a strong contrast to the arctic air farther to the north. The arctic front usually is nonexistent when the cold air from the European continent streams toward the northwest. Thus, though the Atlantic polar front is always present, the arctic front may sometimes disappear.

Third in importance and persistency is the *Mediterranean frontal zone.* The energy of this zone is drawn from the contrast in temperature between the cold winter air over the European continent and the warm air over the Mediterranean and Africa. The kinematic background for this front is the mutual convergence of the winds from Europe and those from north Africa into the Mediterranean low-pressure trough (see Fig. 86).

This front is by no means a permanent phenomenon; but when the temperature distribution is favorable, it may be well developed. Disturbances that form on this front usually travel eastward. Some of them may branch off to the northeast into south Russia and west Siberia, and others will travel across Asia Minor and eventually arrive in India. It is typical that the winter storms in India come from the west. The disturbances that develop on the Mediterranean front are responsible for the winter maximum of the rain that occurs in the Mediterranean countries. In summer, the front disappears, and dry weather prevails.

Fronts of secondary importance are sometimes formed along the west coast of Europe when the wind conditions are favorable for accentuating

the contrast between the continental and maritime air.   In situations of pronounced maritime circulation, such fronts may move across the European continent and enter west Siberia.

2. *The Pacific Area.*—The conditions on the Pacific Ocean are similar to those on the Atlantic Ocean, with the exception that there are usually
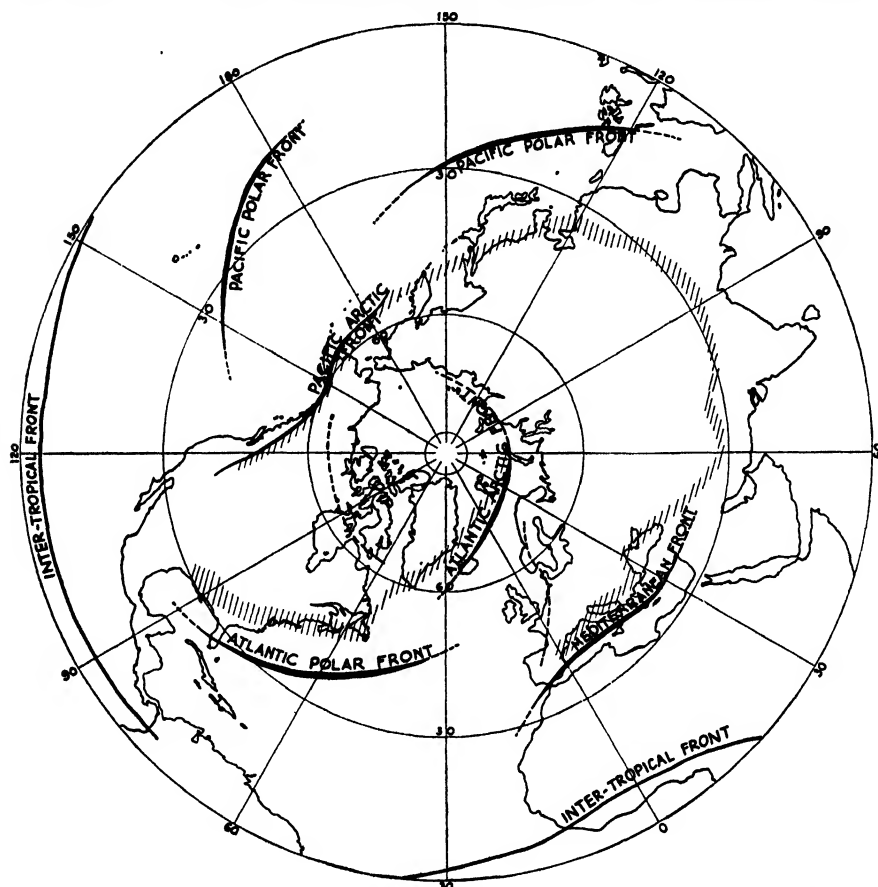
FIG. 124.—The principal frontal zones in winter.   Hatched zones indicate zones of maximum temperature gradient.   While frontogenesis may commence in these zones, the resulting fronts will be found near the axes of outflow, or near the trough lines in the wind distribution.

two subtropical Pacific cells in midwinter (see Par. 68).   The high frequency of two Pacific cells is not brought out in the mean wind chart (Fig. 86), owing to the variable position of these cells.

When there is only one cell present on the Pacific, the frontal zone (*i.e.*, the *Pacific polar front*) will usually form in the western part of the ocean.   Its source of energy is the difference in temperature between the cold north monsoon and the tropical maritime air.

When there are two cells present, there will be a field of deformation between them. A second Pacific polar front will then form somewhere in the vicinity of the line indicated in Fig. 124. The source of energy of this front will then be the temperature contrast between the southerly wind in the western part of the easternmost cell and the northerly wind in the eastern part of the other cell.

When there are two Pacific polar fronts, a double system of cyclonic disturbances will be observed.

On account of the high mountains along the west coast of North America, a sharp temperature contrast will be found in winter along the west coast. Under favorable wind conditions, this temperature contrast may be made available for creation of a front. This front often extends across Alaska and the Aleutian Islands, where it corresponds to the Atlantic arctic front.

A front of secondary importance, and usually of slight intensity, sometimes forms in an east-west direction across Canada. This only happens when the arctic and the North American anticyclones are well developed and when the air over North America is warmer than that over the arctic region.

Sometimes, when both the Siberian and the American highs are well developed and the truly arctic anticyclone is missing, a field of deformation will be present across the Arctic Ocean. Evidence of frontogenesis in that region was found by Sverdrup [81], who called this frontal zone the *interarctic front*. It is not indicated in Fig. 124.

3. *The Equatorial Area.*—The convergence of the trade winds from both hemispheres forms excellent kinematic conditions for frontogenesis to occur in the doldrums. However, as the temperature gradient is but
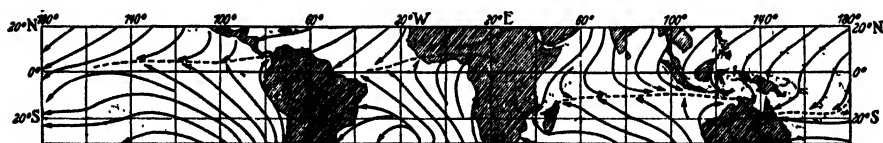
FIG. 125.—The intertropical (or the equatorial) front in midwinter.   (*According to Bjerknes and Bergeron.*)

slight, it is only under special circumstances that fronts of appreciable intensity form. A slight temperature difference is due to the circumstances that the trade winds from the winter hemisphere are somewhat colder than those from the summer hemisphere. This temperature difference rarely amounts to more than 1 or 2°C. However, in exceptional cases, when an active outbreak of polar air occurs in the winter hemisphere, relatively cold air may be brought into juxtaposition with equatorial air along the zone of convergence. In such cases, fronts of appreciable intensity may form in the doldrums. The greatest transport of air toward the equator occurs in spring and autumn as a rearrangement

of the atmosphere owing to the heating (in spring) and cooling (in autumn) of the continents. However, as the temperature is about equal in both hemispheres at the equinoxes, fronts of appreciable intensity are then rarely observed. The strongest fronts are usually found in late summer and late winter when the temperature difference between the two hemispheres has a maximum. It is in these seasons that tropical cyclones obtain a maximum of frequency and intensity.
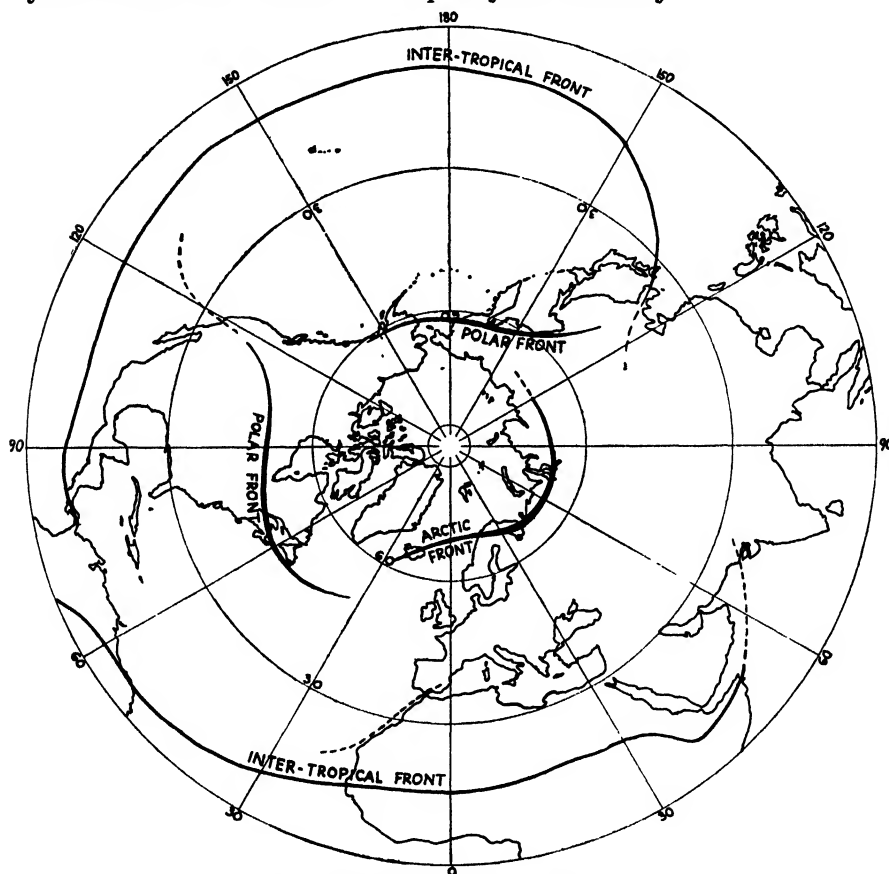
FIG. 126.—The principal frontal zones in summer.

The front that forms in the equatorial belt of convergence has been called by Bjerknes and Bergeron [16] the *intertropical front*. Its position in midwinter is shown in Fig. 125. Figure 127 shows its position in midsummer.

113. The Principal Frontal Zones in the Northern Hemisphere in Summer.—In accordance with the theory of frontogenesis and the principles outlined in the foregoing paragraph, the mean position of the more or less permanent frontal zones in midsummer may be mapped as

shown in Fig. 126. In this connection, it is of interest to note that the temperature difference between the oceans and the continents is small in middle latitudes, whereas it is very large along the northern coasts of America and Eurasia. In tropical regions, the difference is considerable and gives rise to monsoon winds. In middle latitudes, it is therefore chiefly the normal meridional temperature gradient that supplies the energy of the frontal zones. As this gradient is slight, the summer fronts in middle latitudes will be of slight intensity. Pronounced fronts will form in frontogenetical wind fields in high latitudes where the temperature between arctic air and air from warm continents is available.

In summer, the wind circulation is relatively weak, and the fields of deformation that occur are usually of slight intensity. For this reason, too, the summer fronts are usually weak.
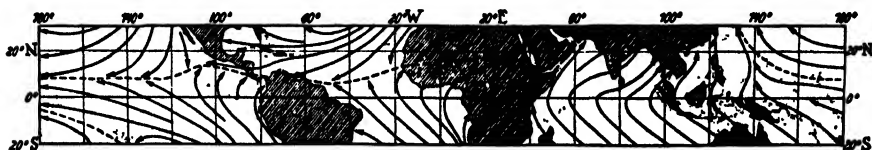
Fig. 127.—The intertropical (or the equatorial) front in midsummer. (*According to Bjerknes and Bergeron.*)

In summer, the subpolar lows are indistinct, whereas the oceanic subtropical cells are pronounced and situated farther to the north than in winter (*cf.* Figs. 80 and 81). This, in connection with the circumstance that the northern continents are relatively warm in summer, causes the polar frontal zones to be displaced northward relative to their winter positions. (*Cf.* Figs. 126 and 125.)

Figure 127 shows the position of the intertropical front in summer.

114. Vertical Extent of Frontogenesis.—The previous paragraphs contained a discussion of frontogenesis in the vicinity of the earth's surface. It was found that frontogenesis would occur when the isotherms were favorably arranged relative to the axis of dilatation in fields of deformation. The fronts would then eventually be found near the axis of outflow. If we consider frontogenesis as a three-dimensional problem, it will be found that the axis of outflow represents the intersection of a plane in which the two opposing currents meet. The frontal surface, while it is being formed, will tend to become parallel to this plane and approach it.

It will be shown later that a surface of discontinuity in moving air will obtain a stable state of equilibrium when it is inclined relative to the horizontal plane, the angle of inclination being of the order of magnitude of about $\frac{1}{100}$. As a frontal surface cannot be far removed from the equilibrium position, it follows that the actual inclination, whether the surface is stable or not, will be of the order of magnitude mentioned above.

The vertical extent of the frontal surfaces is the same as that of the wind fields that form them. They may reach from the earth's surface to the tropopause, but in most cases they do not reach such great heights.

The height to which the frontal surfaces may reach depends not only on the wind fields but also on the processes that create the air masses. It was shown in Chap. III that the tropical air masses reach up to great heights. Thus, a front that separates real tropical air from any other air mass is likely to have great vertical extent. This then is true of the
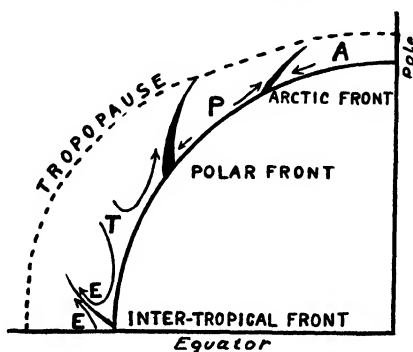
FIG. 128.—Diagrammatical cross section showing the vertical structure of the principal air masses and frontal zones of the northern hemisphere.

polar fronts as indicated in Figs. 124 and 126. Furthermore, the processes that create typically continental polar air masses in winter do not normally reach up to great heights, for the anticyclones in which these air masses are formed are usually shallow (2 to 3 km.). The vertical extent of the polar continental air masses in winter depends also on the height of the mountain ranges that surround their source regions (see Par. 74). Therefore, the fronts that separate polar continental air from transitional types of air are usually shallow fronts. Although these are general rules, exceptions will be encountered in many cases. In general, it may be stated that *the air masses which form through heating from below will be deep and those which form on account of cooling from below will be shallow.* The depth of the air masses will increase in proportion to the length of the duration of the process that forms them.

Figure 128 shows diagrammatically the frontal structure in a meridional section. The diagram is intended to show only the principal features of the main frontal zones in the troposphere.

CHAPTER VI

FRONTAL CHARACTERISTICS

It was explained in the previous chapter how fronts are formed and how they would be arranged in the normal circulation of the atmosphere. The aim of this chapter will be to give a detailed description of the phenomena that characterize the fronts as such and the weather phenomena that are associated with the various types of fronts. Throughout, less stress will be laid on purely theoretical considerations than on such aspects as have proved to be directly applicable in the forecasting of the weather. The disturbances that develop at frontal surfaces and lead to the formation of waves and cyclones and the forecasting of the movement. and the development of such disturbances will be treated in the following chapters.

115. Preliminary Remarks on Fronts.—It is of interest to note that the frontogenetical process, described in the previous chapter, has a tendency to create a discontinuity in the field of temperature but that the process does not result in a discontinuity in the strict mathematical sense of the word. The reason for this is: (1) In a continuous medium, two distant particles will approach one another asymptotically, so that an infinite interval of time will be required to bring two distant particles into juxtaposition. (2) Radiation and turbulence will usually tend to smooth out temperature differences, the effect of friction being to maintain a layer of transition between the neighboring air masses. Frontogenesis, therefore, results in a narrow zone of transition instead of a perfect discontinuity.

On account of the motion of the air, the surface of discontinuity, or the layer of transition, will be in equilibrium when it forms an angle with the horizontal plane. A *frontal surface* may therefore be defined as an inclined narrow layer of transition in which the meteorological elements vary abruptly. A *front* may then be defined as the line or zone of intersection between a frontal surface and a horizontal plane (*e.g.*, the earth's surface).

The layer of transition which constitutes a frontal surface and the zone of transition which constitutes a front are usually so narrow that their widths are negligible in comparison with the dimensions of the adjacent air masses. Whether a frontal zone will appear on the weather charts as a perfect discontinuity or as a zone of transition depends primarily on the scale of the map. In most cases, the scale of the weather charts is such that even comparatively broad zones of transition

appear as distinct discontinuities. However, when vertical cross sections are drawn, the vertical scale is usually exaggerated relative to the horizontal scale. In such cases, the frontal surface may appear as a fairly broad layer of transition, whereas the front on the weather map appears as a quasi-discontinuity. It has been shown by Petterssen [55] that the boundary conditions which hold for perfect discontinuities are valid also for frontal surfaces. It is therefore permissible to treat the frontal surfaces as if they were mathematical discontinuities.

From a dynamic point of view, the essential feature of a frontal surface is the difference in density between the adjacent air masses. Let letters with indices indicate the conditions in the warm mass and similar letters without indices refer to the conditions in the cold mass. From the equation of condition, we then obtain

$$T' = \frac{p'}{R\rho'} \quad \text{and} \quad T = \frac{p}{R\rho}$$

According to the dynamic boundary condition, the pressure p must be continuous at the front. The difference in temperature between two points at either side of the front and infinitely near one another is then

$$T' - T = \frac{p}{R\rho'\rho} (\rho - \rho')$$

Thus, the density difference is directly proportional to and of opposite sign from the temperature difference, the colder air having the larger density. If we introduce specific volume α instead of density ρ, we obtain

$$T' - T = \frac{p}{R} (\alpha' - \alpha)$$

As the isobaric surfaces are almost horizontal and the isothermal surfaces often have great slopes, it follows that the isosteric surfaces (*i.e.*, surfaces of equal specific volume) will coincide approximately with the isothermal surfaces. Figure 129 shows, as an example, a cross section through a frontal surface.

On account of the slope of the isosteric surfaces relative to the isobaric surfaces, a bundle of isosteric-isobaric solenoids will be concentrated in the transitional layer which constitutes the

Fig. 129.—Cross section through a frontal surface (*FS*). Full lines are isobars, dotted lines isosterics. Vertical scale exaggerated 300 times relative to the horizontal scale.

frontal surface. According to V. Bjerknes [18], the increase in circulation along a closed curve equals the number of isosteric-isobaric unit solenoids contained within the curve. This applies to the conditions on a

nonrotating earth. On a rotating earth, there is a tendency for the earth's rotation to balance the isosteric-isobaric solenoids. It has not been possible to apply the circulation theorem quantitatively to actual forecasting on account of the fact that it is difficult to determine how many of the isosteric-isobaric solenoids are balanced by the earth's rotation. However, as the rotational influence comes in only after wind has been created, it will be understood that when solenoids are created there will also be creation of circulation. In any case, the isosteric-isobaric solenoids concentrated in the frontal surfaces constitute the principal supply of energy for the creation of winds.

116. Discontinuities of Zero and First Order.—From a mathematical point of view, one may define discontinuities of different orders, according to whether it is the element itself or some of its derivatives that are discontinuous. Let f denote a variable; if f is discontinuous at a surface, the discontinuity is of zero order. If, on the other hand, f is continuous but the first derivative of f is discontinuous, then the discontinuity is of first order. In a similar manner, discontinuities of any order may be defined. In the atmosphere, we are concerned only with the elements themselves or with their gradients. We are therefore interested only in discontinuities of zero and first order.

From what was explained in the previous paragraph, it follows that frontal surfaces are discontinuities of zero order with respect to temperature, density, and specific volume. It will be shown later that frontal surfaces are discontinuities of zero order also with respect to wind. From the dynamic boundary condition, it follows that the atmospheric pressure varies continuously through a frontal surface. Therefore, such surfaces cannot be discontinuities of zero order with respect to pressure. It will be shown later that frontal surfaces are discontinuities of first order with respect to pressure, because the pressure gradient varies discontinuously through frontal surfaces.

It is of interest to note that the tropopause, which separates the air masses of the troposphere from those of the stratosphere, is a surface of discontinuity of first order with respect to temperature, density, and wind, whereas frontal surfaces are discontinuities of zero order with respect to these elements.

117. Inclination of Frontal Surfaces.—We choose a system of coordinates with the x-axis normal to the front and the z-axis positive upward. Let indices refer to the less dense (*i.e.*, the warmer) air mass. Then the pressure variation along the frontal surface is expressed by

(1)
$$\begin{cases} dp = \dfrac{\partial p}{\partial x}\, dx + \dfrac{\partial p}{\partial y}\, dy + \dfrac{\partial p}{\partial z}\, dz \\[2mm] dp' = \dfrac{\partial p'}{\partial x}\, dx + \dfrac{\partial p'}{\partial y}\, dy + \dfrac{\partial p'}{\partial z}\, dz \end{cases}$$

whence

$$(2) \quad dp - dp' = \left(\frac{\partial p}{\partial x} - \frac{\partial p'}{\partial x}\right) dx + \left(\frac{\partial p}{\partial y} - \frac{\partial p'}{\partial y}\right) dy + \left(\frac{\partial p}{\partial z} - \frac{\partial p'}{\partial z}\right) dz$$

According to the dynamic boundary condition (see Par. 96), $p - p' = 0$. Therefore,

$$(3) \qquad dp - dp' = 0 \quad \text{and} \quad \frac{\partial p}{\partial y} - \frac{\partial p'}{\partial y} = 0$$

Let θ_d denote the angle between the x-axis and the frontal surface. Then

$$(4) \qquad\qquad\qquad \tan \theta_d = \frac{dz}{dx}$$

Substituting (3) and (4) into Eq. (2), we obtain

$$(5) \qquad\qquad \tan \theta_d = -\frac{(\partial p/\partial x) - (\partial p'/\partial x)}{(\partial p/\partial z) - (\partial p'/\partial z)}$$

The inclination of the frontal surface is therefore exclusively determined by the pressure distribution in its vicinity. For the following discussion, it is convenient to transform Eq. (5). From the equation of static equilibrium, we obtain

$$\frac{\partial p}{\partial z} = -\rho g \quad \text{and} \quad \frac{\partial p'}{\partial z} = -\rho' g$$

which, substituted into Eq. (5), gives

$$(6) \qquad\qquad \tan \theta_d = \frac{(\partial p/\partial x) - (\partial p'/\partial x)}{g(\rho - \rho')}$$

As the denser mass must form a wedge under the warmer mass (the opposite arrangement would be highly unstable), it follows that $\tan \theta_d > 0$ when the x-axis points from the warmer toward the colder air and $\tan \theta_d < 0$ when the x-axis is chosen in the opposite direction. From this, it follows that

$$(7) \qquad\qquad\qquad \frac{\partial p}{\partial x} - \frac{\partial p'}{\partial x} \gtrless 0$$

according to whether the x-axis points from the warmer toward the colder air, or vice versa.

It should be noted that, whereas Eq. (5) is quite general, Eq. (6) is derived on the assumption that the vertical acceleration of the air is negligible in comparison with the acceleration of gravity. This simplification is always permissible.

Instead of the horizontal pressure gradients, we may introduce the slope of the isobaric surface. Let $\tan \theta_p = dz/dx$ indicate the slope of the isobaric surface. Then,

$$\frac{\partial p}{\partial x} = -\frac{\partial p}{\partial z} \tan \theta_p = \rho g \tan \theta_p$$

$$\frac{\partial p'}{\partial x} = -\frac{\partial p'}{\partial z} \tan \theta_p{}' = \rho' g \tan \theta_p{}'$$

which substituted into Eq. (6) gives

$$(8) \qquad \tan \theta_d = \frac{\rho \tan \theta_p - \rho' \tan \theta_p{}'}{\rho - \rho'}$$

A simple and useful expression for the inclination of a frontal surface may be obtained by combining Eq. (6) with the equations of motion. Neglecting the accelerational and frictional terms, we obtain from Eq. *88*(4)

$$0 = -\frac{1}{\rho} \frac{\partial p}{\partial x} + 2\omega \sin \varphi v_y$$

$$0 = -\frac{1}{\rho'} \frac{\partial p'}{\partial x} + 2\omega \sin \varphi v_y{}'$$

which substituted into Eq. (6) gives

$$(9) \qquad \tan \theta_d = \frac{2\omega \sin \varphi}{g} \cdot \frac{\rho v_y - \rho' v_y{}'}{\rho - \rho'}$$

which is the well-known Margules formula.[1] Usually, the density discontinuity is slight in comparison with the wind discontinuity. We may therefore put

$$\rho' = \rho = \rho_m = \tfrac{1}{2}(\rho' + \rho)$$

which substituted into Eq. (9) gives

$$(10) \qquad \tan \theta_d = \frac{2\omega \sin \varphi}{g} \rho_m \frac{v_y - v_y{}'}{\rho - \rho'}$$

It should be noted that this formula is derived by neglecting, also, the horizontal accelerations. However, experience shows that the formula holds with sufficient accuracy.

Referring to Par. 96, it is of interest to note that, if $\tan \theta_d$ were known, it would be possible to compute the vertical velocities by the aid of the observed wind velocities at the front. In order to observe the slope of the frontal surface, it would be necessary that the aerological ascents should be *strictly* synchronous, which usually is not the case. The slope of the frontal surface may be computed from the above equations; but such computations are not very reliable, as the factors involved usually are not known with sufficient accuracy. In the next two paragraphs, we

---

[1] If the x-axis were chosen along the front, the formula would be

$$\tan \theta_d = -\frac{2\omega \sin \varphi}{g} \cdot \frac{\rho v_x - \rho' v_x{}'}{\rho - \rho'}$$

shall see that some fundamental properties of frontal surfaces and fronts may be derived from these formulae.

The above formulae hold for surfaces of discontinuity of zero order with regard to density and temperature. If the discontinuity is of first order,

$$(11) \qquad\qquad \rho - \rho' = 0$$

From Eq. (6), it follows that tan θ_d can have a finite value only when

$$(12) \qquad\qquad \frac{\partial p}{\partial x} - \frac{\partial p'}{\partial x} = 0$$

This means that the pressure gradient is continuous through such a surface. The tropopause belongs to this category of discontinuities.

118. Thermal Structure of Fronts.—If the frontal surface were a perfect discontinuity, the ascent curve would appear as shown in Fig.
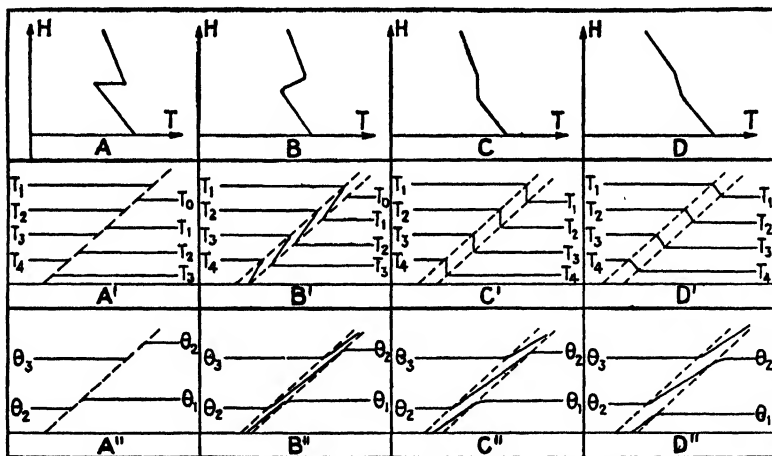
FIG. 130.—Thermal structure of fronts. Top row: temperature-height curves; A, ideal discontinuity; B, well-developed frontal surface; C, frontal surface of moderate intensity; D, frontal surface of slight intensity. Middle row: Temperature cross sections corresponding to diagrams $A-D$. Bottom row: Potential-temperature cross sections corresponding to diagrams $A-D$.

$130A$. However, as there always will be a layer of transition between the two masses, an ascent through a well-developed frontal surface would show a distribution of temperature as shown in Fig. $130B$. It is important to note that it is not necessary that the temperature increase with elevation within the frontal zone. Even an isothermal layer (Fig. $130C$) and a layer with decreasing temperature and a minimum of lapse rate (Fig. $130D$) will, when they are inclined, constitute layers of maximum of solenoids and are therefore frontal surfaces.

Figures $130A'$ to D' show the temperature distribution in cross sections which correspond to Figs. $130A$ to D. As the isobaric surfaces are

almost horizontal and the isosteric surfaces coincide approximately with the isothermal surfaces, it is readily seen that even a "weak" front may contain a considerable number of solenoids.

Figures 130A'' to D'' show in principle the distribution of potential temperature in cross sections through frontal surfaces corresponding to Figs. 130A to D and A' to D'. As the warm mass usually moves relatively to the cold mass, and as the processes in the free atmosphere are mainly adiabatic, there will be a tendency for the surfaces of potential temperature to coincide with the frontal surface. This is particularly true when there is no cloud system connected with the front. When condensation occurs, the potential temperature is no longer conservative, and the air will move through the surfaces of potential temperature. A detailed discussion of the relation between fronts and isentropic surfaces will be given in Chap. VIII.

It was shown in Chaps. I and III that the most conservative air-mass properties are the potential pseudo-wet-bulb temperature θ_{sw} and the potential pseudo-equivalent temperature θ_{se}. Under normal conditions, the warm mass will have the higher humidity content, so that there will usually be a maximum of specific humidity above the frontal surface. There will then also be a maximum of potential pseudo-wet-bulb temperature and a maximum of potential pseudo-equivalent temperature above the frontal surface. It should, however, be borne in mind that exceptions to these rules may occur. These exceptions are mainly due to two reasons and are, moreover, indicative of two processes in the atmosphere that require the attention of the analyst.

1. When the warm air slides down the frontal surface, it will bring with it its dryness from aloft. It may then happen that the specific humidity and also θ_{sw} and θ_{se} are smaller in the warm air above the frontal surface than in the cold air below it.

2. If the cold air is unstable, or nearly so, turbulence will transport appreciable amounts of moisture upward under the frontal surface. Through this process, the humidity discontinuity at the frontal surface may be nullified or even reversed. In such cases, the discontinuity in θ_{sw} and θ_{se} may become annulled or, in rare cases, reversed. Usually a reversal of the humidity discontinuity results only when there is subsidence above the frontal surface and, simultaneously, eddy transfer of humidity upward in the air under the frontal surface. Such abnormal distributions of specific humidity, θ_{sw}, and θ_{se} are therefore indicative of these processes.

A diagrammatic cross section through the tropopause is shown in Fig. 131. If the scale of Figs. 130B', C', and D' were reduced sufficiently, the transitional zones would appear as perfect discontinuities as shown in Fig. 130A'. However, if the scale of the cross section through the

tropopause (Fig. 131) is reduced, the diagram will retain its principal features: the isotherms will remain continuous, and the temperature gradient will vary discontinuously. The tropopause is therefore a discontinuity of first order with regard to temperature, and from this it follows that it is also a discontinuity of first order with regard to density. This distinguishes the tropopause from frontal surfaces.
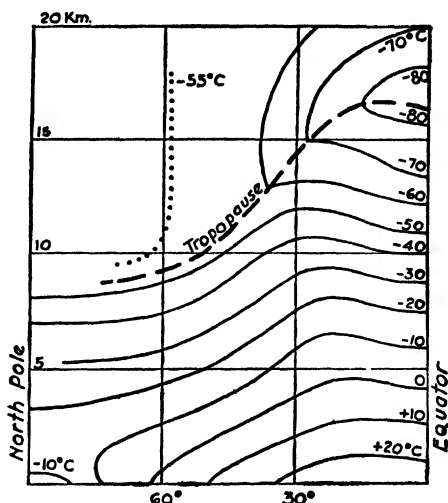
FIG. 131.—Diagrammatical temperature cross section through the tropopause.

119. Fronts in Relation to Pressure.—The dynamic boundary condition

$$(1) \qquad\qquad p - p' = 0$$

states that the pressure must be continuous at the frontal surface. The isobars must therefore be continuous at the fronts. If we choose the y-axis tangential to the front, it follows that

$$(2) \qquad\qquad \frac{\partial p}{\partial y} - \frac{\partial p'}{\partial y} = 0$$

because, otherwise, the isobars could not be continuous.

It was shown in Par. 117 that the pressure gradient normal to the front is discontinuous, or

$$(3) \qquad\qquad \frac{\partial p}{\partial x} - \frac{\partial p'}{\partial x} \gtrless 0$$

according as the x-axis points from the less dense (*i.e.*, warmer) toward the denser (*i.e.*, colder) mass, or vice versa. Choosing the x-axis so that it points from the warmer toward the colder mass,

$$\rho - \rho' > 0$$

From Eq. *117*(6), we then see that

(4)
$$\frac{\partial p}{\partial x} - \frac{\partial p'}{\partial x} > 0$$

This means that *the isobars are always refracted at the front in such a way that the kink points from low to high pressure; i.e., the isobars have an infinite*
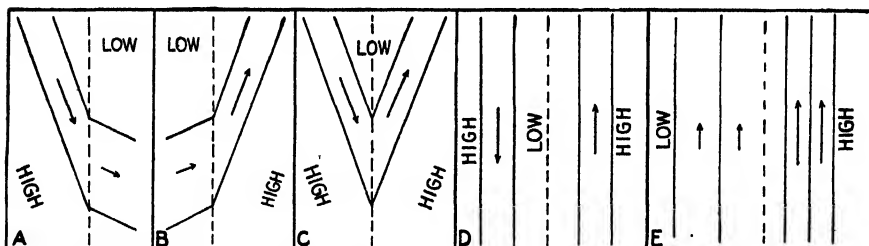
Fig. 132.—Principal types of isobars in the vicinity of fronts. In these diagrams it is immaterial whether the warm air is to the right or to the left of the front.

cyclonic curvature at the front. These rules are of great importance for the analysis of weather charts.

The principal types of isobar in the vicinity of fronts are shown in Fig. 132.
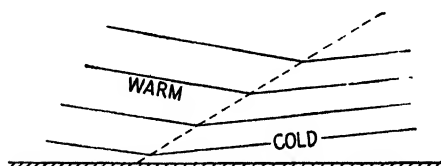
Fig. 133.—Vertical cross section through the isobaric surfaces in the vicinity of a frontal surface.

In a similar manner, it follows from Eq. *117*(8) that the isobaric surfaces have a trough of infinite curvature at the frontal surface, with the edge of the trough pointing downward. This is shown in Fig. 133. It is well to remember that the slope of the isobaric surfaces is so slight that the kinks shown in Fig. 133 become noticeable only when the vertical scale is greatly exaggerated relative to the horizontal scale.

We consider next a system of coordinates that moves with the front. The x-axis is perpendicular to the front, and the front moves along this axis with a velocity c_x. Let $\delta/\delta t$ denote time differentiation in the moving system of coordinates. Then,

$$\frac{\delta}{\delta t} = \frac{\partial}{\partial t} + c_x \frac{\partial}{\partial x}$$

According to the dynamic boundary condition [Eq. (1)], the pressure must be continuous at the front. Therefore,

$$\frac{\delta(p - p')}{\delta t} = 0$$

and

$$(5) \qquad c_x = -\frac{(\partial p/\partial t) - (\partial p'/\partial t)}{(\partial p/\partial x) - (\partial p'/\partial x)}$$

It has already been shown that the denominator differs from zero. Therefore, when the front moves, the numerator must differ from zero, or *the barometric tendency must be discontinuous at the front.*

We can always choose the direction of the x-axis in such a manner that c_x is positive. Equation (5) in connection with Fig. 132 then shows that the kink in the barogram which marks the discontinuity in the slope of the barograph trace must always point downward. A few typical examples are shown in Fig. 134.

FIG. 134.—Types of barograph traces during frontal passages. The types A, B, and C occur most frequently when the front moves in the direction from the warm to the cold mass (*i.e.* warm fronts), and the types D, E, and F occur most frequently when the front moves in the opposite direction (*i.e.* cold fronts).

The above characteristics apply to fronts and frontal surfaces but not to the tropopause. It was shown in Par. 117 that the pressure gradient varies continuously through the intersection between a horizontal plane and the tropopause. The isobars will then show, not kinks, but a finite cyclonic curvature that has a maximum along the line of intersection. This circumstance is due to the fact that the tropopause is a discontinuity of first order in density, whereas the frontal surface is of zero order. The discontinuity in pressure will always be one degree higher than the density discontinuity.

Further remarks on fronts, etc., in relation to the fields of pressure and pressure tendencies will be found in Chap. IX.

120. Fronts in Relation to Wind.—Returning to Eq. *117*(10) and solving with respect to $v_y - v_y'$, we obtain

$$v_y - v_y' = \frac{g}{2\omega \sin \varphi} \cdot \frac{\rho - \rho'}{\rho_m} \tan \theta_d$$

This shows that the wind component tangential to the front is discontinuous when the density is discontinuous. *A frontal surface is, therefore, a discontinuity of zero order with respect to wind.*

In the above formula, g, ω, $\rho - \rho'$, and ρ_m are always positive, whereas $\tan \theta_d$ is positive only when the x-axis points from the less dense toward the denser mass (*i.e.*, from the warmer to the colder mass). Choosing

the x-axis so that tan $\theta_d > 0$ for warm fronts and tan $\theta_d < 0$ for cold fronts, it will be seen[1] that the following relations hold

Northern hemisphere ($\varphi > 0$)...........	tan $\theta_d > 0$	$v_y - v_y' > 0$
	tan $\theta_d < 0$	$v_y' - v_y > 0$
Southern hemisphere ($\varphi < 0$)...........	tan $\theta_d > 0$	$v_y - v_y' < 0$
	tan $\theta_d < 0$	$v_y' - v_y < 0$

This shows that *the wind discontinuity at a front is such that the wind shift is cyclonic; i.e., the surface curl is cyclonic at frontal surfaces.*

These rules agree with the rules concerning the trend of isobars in the vicinity of fronts (*cf.* Fig. 132) if we imagine that the wind blows mainly along the isobars. It should, however, be borne in mind that the rules concerning the isobars are valid without exception, whereas those concerning the wind are less rigid. This is due to the circumstance that the latter are deduced on the basis of the simplifying assumptions which underly Eq. *117*(10). In rare cases, it may happen that the horizontal accelerations are so large that the cyclonic wind shift at the front is suppressed. Such exceptions, which may occur locally, are very rare and of short duration. On the whole, the fronts can be recognized by the cyclonic wind shift that accompanies them, and the wind shifts will be cyclonic whether the colder air is to the right or to the left of the front (*cf.* Figs. 132 and 135).

From the above, we have the following rule: *If the observer stands with his back toward the wind in advance of a front, the wind will shift toward the left when the front passes.* This rule, too, holds whether the colder air is in advance of the front or in its rear.

Thus, although a front is always accompanied by a wind shift, it does not follow that a wind-shift line necessarily is a front. A wind-shift line can be a front only when there is a discontinuity in the density or, what is equivalent, in the temperature. Only when this is the case will there be a maximum of solenoids along the wind-shift line, and this is the fundamental front characteristic.

As the colder air must form a wedge under the warmer air,[2] the above rules may be modified to hold also for the distribution of wind along the vertical. This is shown diagrammatically in Fig. 135. It will be seen that in the left-hand portion of the diagram $\theta_d > 90°$. The wind then turns to the left when we ascend through the frontal surface. In the right-hand portion, $\theta_d < 90°$; the wind turns to the right when we ascend through the frontal surface. In this way, the pilot-balloon ascents may

[1] See "Physikalische Hydrodynamik," Par. 128.
[2] For exceptions, see Par. 122.

be used for locating the position of the fronts in the free atmosphere. Again, it should be emphasized that the wind shifts of the types shown in Fig. 135 are indicative of a frontal surface only when there is a discontinuity in density (or temperature). The analysis of the winds must therefore be checked by aerological ascents. The pilot-balloon observa-
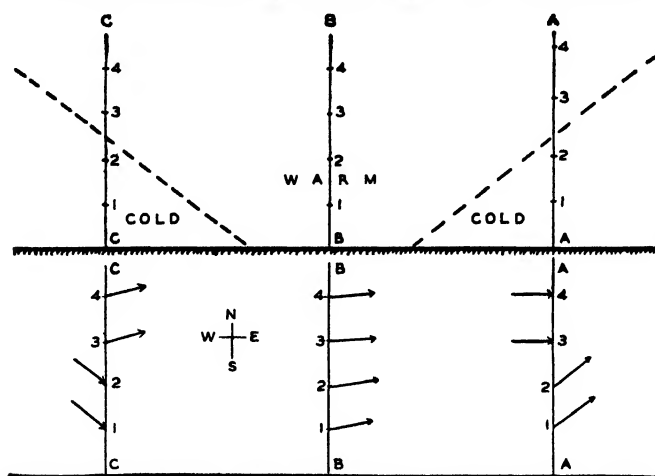
FIG. 135.—Vertical distribution of wind in the vicinity of frontal surfaces.

tions may then be used to fill in the gaps between the aerological stations It is then important to remember that when the wind shifts to the right (*e.g.*, as along the vertical AA) the altitude of the frontal surface increases in the direction toward which the wind blows. However, when the wind shifts to the left (*e.g.*, as along the vertical CC), the altitude of the frontal surface decreases in the direction toward which the wind blows.
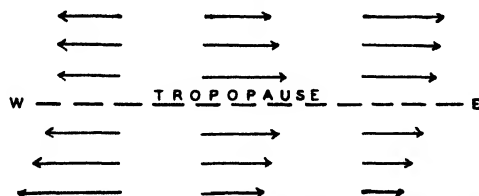
FIG. 136.—Wind distribution in a horizontal plane intersecting the tropopause.

The analysis of the winds aloft is of great importance for the isentropic analysis, as will be shown in Chap. VIII.

As the tropopause is a discontinuity of first order in density, it will be a discontinuity of first order with regard to wind. Hence, the wind (and pressure gradient) must vary continuously through the tropopause. Under normal conditions, the tropopause slopes downward toward the poles. A mathematical discussion, which will not be reproduced here, has shown what types of wind distribution are possible at

the tropopause. These are shown in Fig. 136. If the plough-shaped curve that connects the points of the wind arrows is drawn, then the plough must point eastward. The same also applies to the distribution of the wind along the vertical.

121. Classification of Fronts.—The frontal characteristics described so far are such as apply to all fronts whether the cold air replaces warm air, or vice versa, or whether the front remains stationary. These characteristics may therefore be called *general front characteristics*. Depending on the movement of the fronts, the position of the cold air relative to the warm air, and the stability conditions of the air masses involved, a series of additional characteristics may be described. It is therefore appropriate to classify the fronts in order to be able to specify *the special front characteristics* that apply to each of the significant types. By means of the general front characteristics, the analyst will be able to decide that *a front* is present. From the special front characteristics, he will be able to decide *what kind of front* he is concerned with and to identify this front with a known model.

The choice of a rational classification of fronts will naturally depend on the purpose that the classification is intended to serve. Moreover, care should be exercised in devising a classification, for a too rigid system of classification may be misleading.

1. *Geographical Classification.*—It was shown in Chap. III that there are four principal types of air mass in each hemisphere, *viz.:* arctic, polar, tropical, and equatorial. It was shown in Chap. V that the polar air is often separated from the arctic air by the arctic front. The tropical air is almost invariably separated from the polar air by the polar front. On the other hand, the tropical air usually merges gradually into equatorial air, whereas a more or less distinct front (the intertropical front) separates the equatorial air of the summer hemisphere from that of the winter hemisphere.

Consequently, from a geographical point of view, there are three principal frontal zones, *viz.:* the arctic front, the polar front, and the intertropical front. The mean positions of these principal frontal zones are shown in Figs. 124 to 128.

In addition to these principal fronts, *secondary* fronts may form temporarily within the air masses when the distribution of temperature and wind is favorable for frontogenesis. Such fronts form rarely within the equatorial, the tropical, and the arctic air masses because these masses are usually so homogeneous that the horizontal temperature gradient is insufficient for production of fronts. Secondary fronts form most frequently within the polar air masses, notably between "old" and "fresh" polar air or between polar continental and polar maritime air. The secondary fronts are usually neither extensive nor long-lived, whereas

the principal fronts are both extensive and more or less permanent. Experience shows that most fronts occurring on the weather charts originate from the principal frontal zones. Weather charts with numerous secondary fronts are usually indicative of an inconsistent analysis.

Apart from the general front characteristics, which apply to all fronts, there are no particular characteristics that can be allotted to the geographical classification. Nevertheless, the usefulness of the geographical classification is obvious. As the principal fronts predominate relative to the secondary fronts, both with respect to frequency, extent, and persistence, it is wise, as a general rule, to try to explain the frontal weather phenomena that are encountered on the maps in terms of the principal fronts. Only when such an explanation appears improbable should resort be made to secondary fronts. Moreover, before a secondary front is introduced in the analysis, a plausible reason for its genesis should be indicated. Conversely, when a secondary front is allowed to disappear from the maps, a plausible reason for its dissolution (frontolysis) should be given.

A weather forecaster in northwest Europe should, therefore, endeavor to explain the weather phenomena that may be of frontal origin by means of the Atlantic polar front and/or the Atlantic arctic front. In like manner, a forecaster in California should try to explain the weather phenomena on the eastern part of the Pacific Ocean by the aid of the Pacific polar front and/or the Pacific arctic front. In doing this, one should exercise meticulous care in tracing these fronts consistently from one map to the next, letting the fronts on the maps move in accordance with the prevailing winds. When this is done consistently, it will usually be found that it is only in rare cases that secondary fronts need be introduced.

2. *Classification According to Motion.*—The most significant classification of fronts is the one that refers to the motion of the air masses involved. This classification, which was introduced by Bjerknes and Solberg [14], distinguishes between the following types of fronts:

a. A *cold front* is a front along which cold air replaces warmer air.

b. A *warm front* is a front along which warm air replaces colder air.

c. A *stationary front* is a front along which one air mass does not replace the other.

d. An *occluded front* is a front resulting when a cold front overtakes a warm front, provided that there still is a temperature discontinuity between the cold air that originally was in advance of the warm front and the cold air that originally was in the rear of the cold front.

It is usually easy to recognize cold and warm fronts even when the temperature difference at the earth's surface is indistinct. As will be shown later, the systems of clouds and hydrometeors, the fields of pres-

sure and pressure tendencies, and the life history of the air masses involved will usually afford decisive distinctions.

The ideal stationary front is seldom found in nature, but it often occurs that the frontal movement is such that no appreciable displacement takes place. The front is then said to be *quasi-stationary*. Such fronts constitute the most intricate forecasting problem, for (1) as the velocity of the front is nil, its future movement will depend on the acceleration, which is exceedingly difficult to evaluate or even estimate, and (2) the stationariness of the front is highly favorable for the formation of cyclonic disturbances. The theory of wave formation and the structure of developed cyclonic waves will be discussed later in Chap. VII, and an account of the various symptoms of nascent waves will be given in Chap. IX.

The occluded front has a complex structure resulting from a cold front overtaking a warm front. If the air in the rear of the cold front is colder than the air in advance of the warm front, the occlusion will be of a cold-front character, while when the temperature conditions are reversed, it will resemble a warm front. The occluded front usually results from unstable cyclonic waves. This process will be discussed, theoretically and practically, in later paragraphs.

3. *Classification According to Vertical Velocity and Stability.*—The cold-warm classification referred to above is based on the movements of the fronts and the sequence of the air masses. As will be shown later, the weather phenomena that accompany these fronts may be classified roughly in the same manner. However, in order to cover all significant types of frontal weather phenomenon, it will be necessary to consider the distribution of vertical velocity and the stability conditions in the air masses close to the fronts.

Let v_z and v_z' denote the vertical velocities in the cold and in the warm air, respectively. Table 56 then shows the combinations of vertical velocities that are theoretically possible.

TABLE 56.—COMBINATIONS OF VERTICAL VELOCITIES AT FRONTAL SURFACES

Type	Warm air	Cold air
A	$v_z' > 0$	$v_z > 0$
B	$v_z' > 0$	$v_z < 0$
C	$v_z' < 0$	$v_z < 0$
D	$v_z' < 0$	$v_z > 0$

Experience shows that most of these combinations of vertical velocities actually occur. Thus, each of the types of front referred to in the cold-warm classification may be subdivided into several categories according to the distribution of vertical velocity.

Although the primary cause of frontal cloud systems is the ascending motion of the air, it will be understood that the types of cloud which develop and the nature of the precipitation which occurs will depend greatly on the stability conditions of the air masses which partake in the ascending motion. No classification of fronts that is intended to have bearing on the weather phenomena will be complete unless the distribution of vertical velocity and the stability conditions are taken into account. A detailed discussion of this topic will be given in Par. 122.

In the above, fronts have been classified according to geographical origin and the sequence of the cold and warm air masses. In addition, an auxiliary grouping has been introduced according to the distribution of vertical velocity and the stability conditions of the air masses. In the following paragraphs, these various principal and subordinate types of front will be discussed in a manner intended to facilitate the analysis of the weather charts.

In conclusion, it may be remarked that fronts are often referred to as being accelerated or retarded and as being exposed to frontogenesis or frontolysis. For the analysis and for the forecasting it is not sufficient to determine the position of the fronts and whether they are cold, warm, or occluded. From the type and distribution of clouds and hydrometeors and from other frontal characteristics, the analyst should endeavor to make out the sign of the vertical velocity and the stability conditions (when not directly observed), and from kinematic considerations (see Chap. IX) the displacement of the fronts should be determined. Finally, from the principles explained in Chap. V, it should be determined whether the fronts are exposed to frontogenesis or frontolysis.

122. Fronts and Clouds.—We shall now take into consideration the stability conditions of the air masses and describe the types of frontal cloud system that correspond to the various distributions of vertical velocities specified in Table 56.

Experience shows that the frontal cloud systems are mainly embedded in the warm air. This indicates that the upward velocity of the warm air is larger than that of the cold air. This relation between v_z' and v_z is a dynamic necessity when the fronts in question are subjected to a wave disturbance (see Par. 129). It is also rendered plausible by the fact that the cold air, which is limited by the earth's surface below and the frontal surface above, is under a greater kinematic restraint than is the warm air. For these reasons, the development of frontal cloud systems depends mainly on the vertical velocity of the warm air (*i.e.*, v_z').

TYPE A.—We consider first the case when $v_z' > v_z > 0$. The warm air will then ascend relative to the cold air. Clouds may then form in both air masses, but mostly in the warm mass. The types of cloud that

develop will then depend on the stability conditions of the air masses involved.

We shall first assume that the front is stationary and that both air masses have a convergent movement toward the front, resulting in ascend-
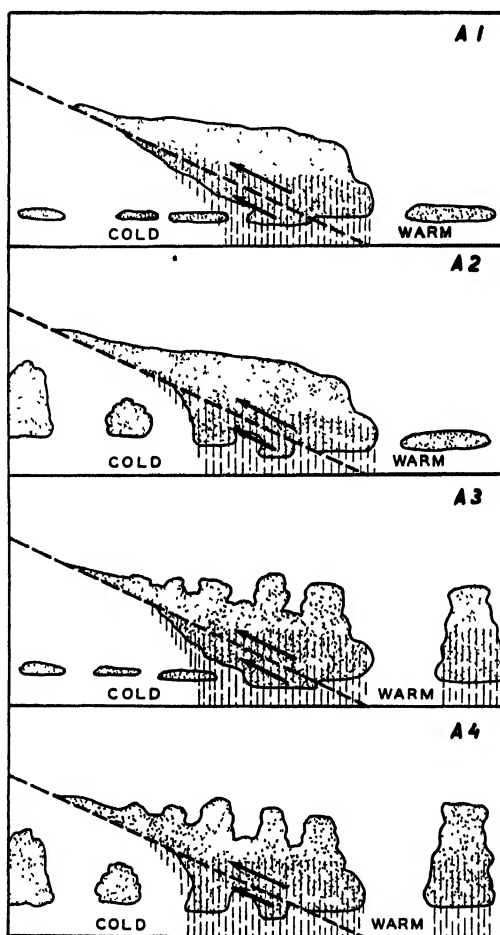
Fig. 137.—Cross sections through frontal systems of the type A (*i.e.* $v_s' > v_s > 0$). $A1$, both masses are stably stratified; $A2$, the warm air is stable while the cold air is unstable; $A3$ the warm air is unstable or convectively unstable while the cold air is stable; $A4$, both masses are unstable or convectively unstable.

ing motion. Figure 137 then shows cross sections through the cloud systems that develop under the various stability conditions.

Figure 137$A1$ corresponds to the case where both masses are stably stratified, and $A2$ shows the case where the warm mass is stable and the cold mass is unstable, the difference between the two cases being that the

clouds under the frontal surface are of the stratiform type (*St* or *Sc*) in the former case, whereas they are of the cumulus type (*Cu* or *Cb*) in the latter case.

It is of interest to note that the case *A*2 occurs frequently when the quasi-stationary front runs in a north-south direction with cold air streaming southward and the warm air streaming northward. The cold air will then be heated from below, and the warm air will be cooled from below.

Figure 137*A*3 corresponds to the case where the cold air is stable and the warm air is either unstable or convectively unstable. It was shown in Par. 46 that, when the air is convectively unstable, it becomes unstable when it reaches its condensation level. The ordered ascending velocity above the frontal surface will then cause a cloud system to form, but convective clouds will grow up from the frontal cloud system as indicated in Fig. 137*A*3.

If the cold air, too, were unstable, there would be instability clouds, also, in the cold air under the frontal surface. This is shown in Fig. 137*A*4.

If the cloud systems reach up to sufficient altitudes, precipitation will be released (see Par. 25). The precipitation that falls from cloud systems of the type *A*1 will be of a continuous character and of even intensity, whereas, when the conditions are as shown in the Fig. 137*A*2, slight convective precipitation may be superimposed on the more even frontal precipitation. If the conditions are as shown in Fig. 137*A*3, showery or squally precipitation of considerable intensity will be superimposed on the frontal precipitation. In extreme cases, the convective currents may even

Fig. 138.—Profiles of warm (*W*), cold (*C*) and quasi-stationary (*S*) fronts.

break up the frontal cloud system above the frontal surface. In the case represented by Fig. 137*A*4, the convective nature of the cloud system and the precipitation is more pronounced than in the case represented by Fig. 137*A*3.

In discussing Fig. 137, it was supposed that the front was quasi-stationary. If the front moved in the direction from the warm mass toward the cold mass, its profile would be slightly deformed, owing to the normal increase of wind velocity along the vertical. The effect of this would be most pronounced within the friction layer. The profile of a warm front is indicated diagrammatically by curve *W* in Fig. 138. This change in profile does not alter the conditions for the formation of frontal cloud systems along warm-front surfaces. The diagrams shown in Fig. 137, which were deduced for quasi-stationary fronts, will therefore hold also for warm fronts as long as the stability conditions and the

distribution of vertical velocity are as indicated.   *Quasi-stationary fronts and warm fronts have, therefore, principally the same type of cloud system,* though the cloud systems belonging to warm fronts are usually more pronounced and more active than are those connected with quasi-stationary fronts.

Although experience shows that warm fronts and quasi-stationary fronts have principally the same cloud systems, it also shows that cold fronts develop cloud systems of a different type when they move with a considerable velocity.   However, cold fronts that are slowly moving will usually be accompanied by cloud systems of the types shown in Fig. 137. This is particularly true of cold fronts which approach the quasi-stationary state, notably when they are exposed to frontogenesis.

The diagrams shown in Fig. 137 *may therefore be regarded as representative of warm fronts, quasi-stationary fronts, and also of slowly moving cold fronts that are exposed to frontogenesis.*

The sequence of cloud forms from the upper to the lower portion of the frontal surface will, in most cases, be as follows: *Ci, Cs, As* translucidus, *As* densus, nimbo-stratus.   When either or both of the air masses involved is unstable or convectively unstable, convective clouds (*Cu, Cu* congestus, *Cb*, etc.) may develop in connection with the frontal clouds. Moreover, strato-cumulus, stratus, and frontal fogs may occur in the stably stratified air masses, as explained in Pars. 56 to 62.

TYPE B.—We consider next the case where $v_s' > 0$ and $v_s < 0$.   The cold air will then descend, no clouds will appear under the frontal surface, but frontal clouds will form above it.

It is of interest to remark that fronts with this type of distribution of vertical velocity will be exposed to effective frontolysis.   The reason for this is that the cold descending air will be heated adiabatically whereas the warm ascending air will be cooled adiabatically.   As a result, the temperature discontinuity between the air masses will be nullified, and the front will perish.   There is no evidence to show that descending velocities of appreciable magnitude occur extensively under quasi-stationary or warm-front surfaces, but there is copious evidence that such velocities occur along the *lower portion* of cold fronts which move with a moderate or high speed.   The lower portion of such fronts is, therefore, exposed to frontolysis.   The distribution of vertical velocity along the upper portion of such fronts will then be that indicated as type *C* in Table 56.   The further discussion of the frontal cloud systems will be given in connection with type *C*.

TYPE C.—Here, $v_s' < 0$ and $v_s < 0$.   For the reasons indicated in the discussion of type *A*, the warm air will have a descending velocity greater than that of cold air.   As the warm air then will be heated adiabatically more rapidly than the cold air, it is evident that such fronts

will maintain or increase their intensity. Moreover, as both masses descend, there will be no cloud system connected with the front.

This type of velocity distribution occurs quite frequently at the upper portion of cold-front surfaces and also, under certain circumstances,
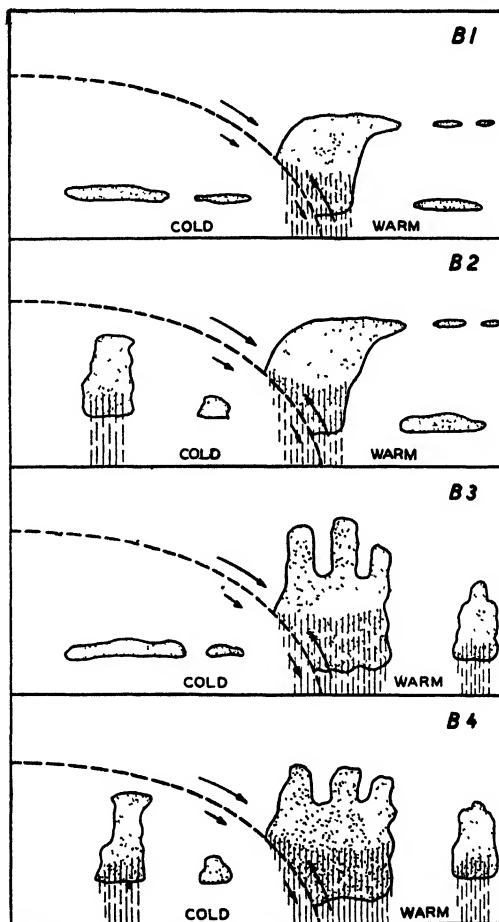
FIG. 139.—Cross sections through frontal systems of type B (*i.e.* $v_s' > 0$ and $v_s < 0$). $B1$, both masses are stably stratified; $B2$, the warm air is stable and the cold air unstable; $B3$, the warm air is unstable or convectively unstable while the cold air is stable; $B4$, both masses are unstable or convectively unstable. Along the upper portion of the frontal surfaces the front is of type C (*i.e.*, $v_s' < 0$ and $v_s < 0$).

along the upper portion of warm-front surfaces. We shall first discuss the cold front.

The most frequently occurring case is a cold-front surface of type B along its lower portion and of type C along its upper portion. This is shown in Fig. 139, where the stability conditions of the air masses have been taken into account. At these cold fronts, the cloud systems some-

times extend far into the warm air ahead of the front at the ground. The cold-front precipitation is usually of short duration and of variable intensity (see Fig. 25). After the passage of the front a clearing occurs, after which, if the cold air is unstable, instability showers will follow.

Cold fronts of this type usually move with a considerable velocity, and the warm air above the upper portion of the cold front surface moves in a forward direction with a speed that is greater than the speed of the cold air. Thus, the conditions shown in Fig. 137 are typical of slowly moving cold fronts and those shown in Fig. 139 are typical of rapidly moving cold fronts. For reasons explained above, the latter type of front is exposed to frontolysis in the lower atmosphere. The intensity of frontolysis is particularly great within the friction layer, where mixing (vertical and horizontal) is most intense. Such fronts will
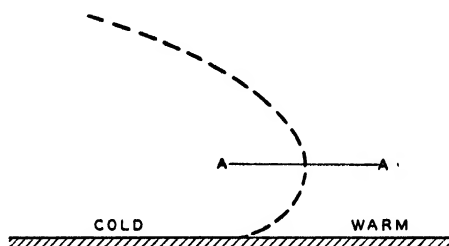
Fig. 140.—Profile of rapidly moving, overrunning cold front. Great instability below the level *A*.

therefore often be very indistinct in the temperature distribution near the earth's surface. In rare cases, when the cold front moves rapidly and when the wind increases rapidly with elevation, it is observed that such cold-front surfaces become very steep. Within the friction layer, the cold air may even overrun the warmer air. The front has then a vertical cross section as shown in Fig. 140. The temperature gradient in the transitional zone where the cold air overruns warm air may approach or surpass the dry-adiabatic rate. Great instability will then develop under the projecting cold wedge aloft. Line-squall clouds (cumulo-nimbus arcus) are often associated with such fronts.

Although Figs. 137 and 139 represent typical cases, it will be found that many cold fronts show features of transition between the types shown. The typical transitional states are characterized by lack of cirrus and cirro-stratus along the upper portion of the cold-front surface. The cloud observations will therefore furnish valuable information as to the kinematic conditions along the frontal surfaces aloft.

The distribution of vertical velocity of type *C* is often observed along the upper portion of warm fronts, notably above the southern extremity of the cold tongues of polar air. It has been shown by Bjerknes [10, 16]

that the warm air, when it ascends along a warm-front surface, obtains an anticyclonically curved trajectory which tends to become parallel to the contour lines of the frontal surface and, eventually, obtains a component down the slope. This is shown diagrammatically in Fig. 141. The cloud system of such fronts would be as shown in Fig. 137, but the frontal clouds would not extend to the top of the dome of the cold air. In southern latitudes, where the wedge of cold air usually is shallow, the upper frontal cloud system may be lacking, and cirrus and cirro-stratus may occur at higher altitudes. In such cases, it will often appear as if frontal clouds were present in several layers.

TYPE D.—In this case, the warm air would descend, and the cold air would ascend. This would lead to a cloud system in the cold air under the frontal surface, whereas the warm air above would be cloudless. There is no observational evidence to show that such distribution of vertical velocity actually occurs along frontal surfaces.

On the Use of Cloud Observations.—If the vertical velocities along the frontal surfaces were known, one could draw conclusions as to the cloud systems that would occur. In actual practice, it is the cloud systems that are known, and from the analysis of the cloud observations one should try to infer the kinematic conditions. This can only be done in a qualitative manner by referring the fronts to one of the types discussed above.

Most fronts, and particularly the warm fronts, are characterized by a zone of continuous cloud

FIG. 141.—Topography of a warm-front surface and streamlines of the warm air relative to the moving cold wedge. To the left of the dotted line the frontal surface would be of type *A*, while to the right it would be of type *C*. The dotted line indicates the forward edge of the warm-front cloud system.

cover over the cold wedge. Warm fronts will, therefore, often be found near the windward limit of the zone of complete overcast. This limit usually coincides with the windward limit of precipitation of frontal character (see Par. 23).

If the warm air is relatively dry and/or if the slope of the frontal surface is slight, the zone of complete overcast may commence slightly in advance of the front at the ground, and the area of active precipitation will then be found at some distance ahead of the front. This is particularly characteristic of warm fronts when the warm air is of tropical continental origin (*i.e.*, of low relative humidity and high temperature).

The presence of a front will also be noticed in the "past-weather" phenomena. Thus, a front that has moved from a position *A* to a position *B* during the interval between two observations should cause an area of "past overcast" and/or an area of past precipitation within this zone. Only when this is so will the front fully explain the weather that actually occurs as a logical consequence of what has occurred. No frontal or air-mass analysis is complete unless it conforms with the principle of *historical sequence*. This principle will be explained in Par. 181.

123. Fronts and Wind Structure.—A passage of a well-marked front is often accompanied by gusts and wind squalls, which, in violent cases, may cause difficulties for aircraft operations. These gusts and squalls depend mainly on three factors: (1) the speed of the wind, (2) the stability conditions in the air masses, and (3) distribution of vertical velocity at the front.

The speed of the wind is somewhat proportional to the pressure gradient. Thus, a frontal squall is to be expected at the passage of a front when the pressure gradient in the rear of the front is larger than that in advance of the front. Such squalls are always associated with a wind shift of cyclonic character (*i.e.*, veering). Conversely, a lull would occur at the passage of the front if the pressure gradient in the rear is weaker than in advance of the front.

The intensity of turbulence depends on the speed of the wind and the stability conditions of the air masses. Other conditions being equal, the turbulent gusts are most intense in the air mass that is least stable. Thus, strong gusts are likely to occur along fronts where rapidly moving unstable air replaces slowly moving stable air. Such conditions occur most frequently along cold fronts with northerly or northwesterly currents in the rear.

The intensity of the frontal squalls that occur near the ground depends greatly on the distribution of vertical velocity along the frontal surface The reason for this is best understood by comparing Fig. 137 with 139. If the air ascends along the frontal surface in both masses (Fig. 137), there must be a convergent flow toward the front. The air that arrives at the front at the ground will then be exposed to the frictional drag along the earth's surface for an extended interval of time; as a result, its speed will be much below the geostrophic value. However, when the air in the rear of the front descends (Fig. 139), it will come from higher levels where the speed is close to the geostrophic wind. From the above, it follows that frontal wind squalls of considerable intensity may occur during the passage of cold fronts of type *B*, notably when the cold air is unstable and the pressure gradient in the cold air is greater than that in the warm air. The most violent wind squalls occur in connection with overrunning cold fronts (see Fig. 140) where instability is produced and

maintained through the overrunning of the warm air by the cold air in the rear of the front.

124. Summary of Frontal Characteristics.—On the basis of the foregoing discussion, the general frontal characteristics, which apply to all fronts, and the specialized frontal characteristics are summarized below. These characteristics, together with the life history of the air masses and the fronts, will assist the analyst in locating the fronts.

1. *General Characteristics.*

a. Coinciding lines of discontinuity (or narrow zones of transition) in the fields of temperature, density, pressure gradient, and wind.

b. Cyclonic wind shift.

c. Cyclonic kinks in the isobars.

d. Barometric tendencies of the types shown in Fig. 134, except when the front is stationary.

e. Temperature-height curves as shown in Fig. 130.

f. Temperature and potential-temperature cross sections as shown in Fig. 130. As the frontal zone is characterized by a maximum of stability, it follows that the vertical distances between neighboring isothermal surfaces must have a maximum, and the vertical distances between neighboring potential isothermal surfaces must have a minimum within the frontal zone. This rule is of fundamental importance for analyzing aerological cross sections (see also Chap. VIII.)

g. Wind distribution along the vertical as shown in Fig. 135. In rare cases, exceptions to this rule may occur (see Par. 120).

2. *Warm Fronts.*—In addition to the above general characteristics, the following special characteristics will apply to warm fronts:

a. A pronounced cloud system (*Ci, Cs, As, Ns*) in advance of the front at the ground (Fig. 137).

b. A zone of overcast sky and usually also an area of continuous precipitation in advance of the front. If the ascending air is unstable or convectively unstable, showery precipitation will be superimposed on the even frontal precipitation.

c. Representative temperatures higher in the rear than in advance of the front.

d. Usually, falling barometer in advance of the front and slight fall or stationary barometer in the rear. In rare cases, the barometer may rise in advance of a warm front; but, in that case, the barometer rises still more in the rear (*cf.* Fig. 134).

e. Usually, wind shift from a southerly to a westerly direction (in the northern hemisphere).

f. Clockwise wind shift in ascending through the frontal surface.

g. Usually rapid increase in potential pseudo-wet-bulb temperature or potential pseudo-equivalent temperature in ascending through the frontal surface (for exceptions, see Par. 118).

3. *Cold Fronts.*—In addition to the general characteristics, the following special characteristics will apply to cold fronts:

a. A cloud system of type A or B (see Figs. 137 and 139) depending on the kinematic and dynamic properties of the front.

b. A zone of overcast sky in the rear of the front (type A) or a cloud system both in advance and in the rear of the front (type B). If the front moves rapidly and dissolves, the frontal cloud system may be narrow and broken. Usually, an area of precipitation in the rear of fronts of type A, and mainly in advance of fronts of type B. The precipitation connected with cold fronts of type B is more uneven and less continuous than that connected with warm fronts or cold fronts of type A. If the warm air is unstable or convectively unstable, squally precipitation will occur.

c. Representative temperatures lower in rear of than in advance of the front.

d. Usually, falling barometer in advance of the front and briskly rising barometer in the rear. Occasionally, the barometer may rise in advance of cold fronts; but, in that case, it rises still more in the rear (*cf.* Fig. 134). Conversely, the pressure may fall in the rear of a cold front; but, in that case, it will fall still more in advance of it.

e. Usually, wind shift from a southerly to a westerly or from a westerly to a northerly direction.

f. Counterclockwise wind shift in ascending through the frontal surface.

g. Usually, rapid increase in potential pseudo-wet-bulb temperature or potential pseudo-equivalent temperature in ascending through the frontal surface. Exceptions to this rule may be found along the upper portion of cold fronts of type B (see also Par. 118).

h. Gusts and wind squalls, particularly in connection with fronts of type B and overrunning cold fronts (see Fig. 140).

4. *Stationary Fronts.*—In addition to the general frontal characteristics, the quasi-stationary fronts are recognized by the characteristics that apply to warm fronts, except those depending essentially on the motion of the front.

5. *Occluded Fronts.*—As an occluded front results from the overtaking of a warm front by a cold front, its characteristics will be partly of warm-front type and partly of cold-front type, and the general characteristics will apply. Since occlusions form as a result of the development of wave cyclones, their properties will be discussed in detail in connection with cyclones.

125. Influence of Mountain Ranges.—The speed of the fronts, the inclination of the frontal surfaces, and the weather phenomena that accompany them are greatly influenced by mountain ranges. These

influences depend on the height and horizontal extent of the range and also on the angle between the front and the main direction of the range. Moreover, the effect of mountain ranges differs according to whether the front in question is cold or warm. We shall here discuss only a few typical cases.

1. *Warm Fronts.*—To simplify the discussion, we assume that the mountain range runs in a north-south direction along a west coast (*e.g.,*
as in Scandinavia and in California) and that the warm front is parallel to the range. Figure 142 then shows successive cross sections through the warm-front surface while it passes the range. In the upper section, the frontal surface is too far away from the range to be influenced by it. In the next section, the lower portion of the cold wedge is about to be cut off. A more or less stationary front will then be maintained to the west of the range, while the inclination of the frontal surface above the range decreases and approaches the horizontal. At still greater altitudes, farther to the east, the frontal surface retains its original slope. The stationary cold wedge to the west of the range forms a surface of upglide motion which causes prolonged frontal rain on the windward side, whereas the absence of appreciable ascending motion above the eastern slope of the

FIG. 142.—Successive cross sections through a warm-front surface passing a mountain range.

range either prevents precipitation from forming or causes only slight amounts to fall.

The subsequent stage in the development is shown in the lower middle section. The descending warm air to the east of the range causes the warm-front cloud system to dissolve, while the upper portion of the system may proceed eastward. A clearing will then occur to the east of the range, while the warm front proceeds eastward as an upper front. In the pressure trough that accompanies this front, frontogenesis may occur. The frontal surface then gradually builds downward; and, as

the front moves away from the range, a warm front may again appear at the surface.

The conditions for frontogenesis to occur under these circumstances are particularly favorable in winter, for the air to the east of the range will then be colder than the invading air. In summer, the conditions are usually reversed, and the lower portion of the warm-front surface may then be completely destroyed dur-
ing the passage across the range.

The cold air under the frontal surface to the west of the range will gradually mix with the warm air. The stationary frontal surface to the west of the range will then disappear, and the cloud system will dissolve or change into a layer of stratus caused by mixing. The cold air that remains over the lowlands to the east of the range will also mix in with the
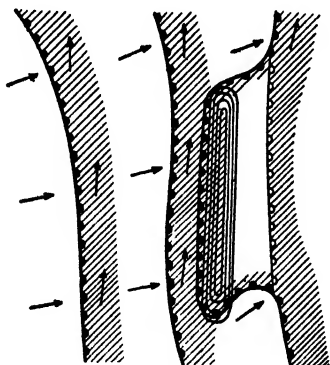
Fig. 143.—Warm front passing a mountain range. Hatching indicates area of precipitation.
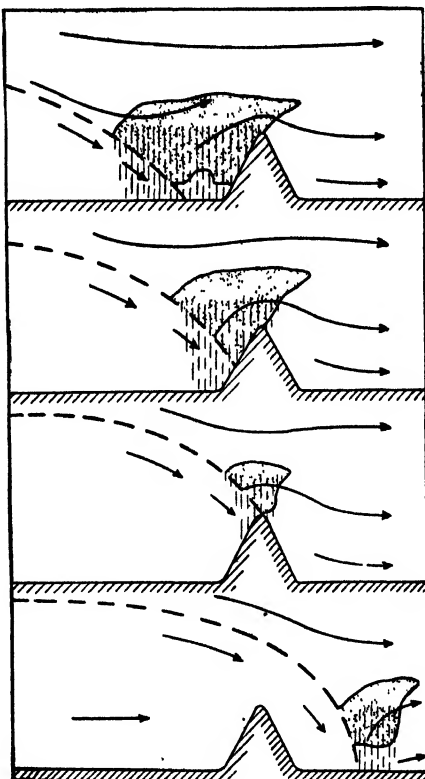
Fig. 144.—Successive cross section through a cold-front surface passing a mountain range.

air above and become absorbed by it; but as the air aloft is warm and relatively dry, the mixing does not result in the formation of stratus. Thus, eventually, the entire range will be surrounded by the warm invading air.

From the above, it follows that the effect of a mountain range is to widen the warm-front precipitation area and to prolong the duration of precipitation on the windward side of the range and to narrow the precipitation area, or to dissolve it, on the lee side of the range.

If the front forms an angle with the direction of the range, the conditions may become more complicated.

2. *Cold Fronts.*—Figure 144 shows successive cross sections through a cold front that passes a mountain range, the front being originally more or less parallel to the range. The cold wedge will be retarded on the windward side of the slope while the front itself climbs up the slope. As the front reaches the crest of the range, the cold air will begin to stream down the slope. The influence of the development on the cold-front cloud systems is shown in the diagrams.

If the air to the lee of the range is warmer than the air in the rear of the cold front, the cold wedge will sweep the warm air away, and the conditions will be as shown in Fig. 144. Under

Fig. 145.—Successive positions of cold-front surface passing a mountain range. 1 and 2, frontal surface before passing the crest; 3, frontal surface after having passed when the air to the lee of the range is colder than the air in the rear of the cold front.

such conditions, clearing weather develops on the lee side of the range.

If the air on the lee side of the range is colder than the air in the rear of the cold front, the front will proceed aloft above a layer of cold and stagnant air, as shown in Fig. 145.· This stagnant air will gradually mix into the air above, the surface of separation becoming more and more diffuse. Such conditions are often encountered to the east of the Scandinavian range and also to the east of the Rocky Mountains during the winter.

If the air on the lee side of the range is stagnant and much warmer than the air in the rear of the front, the latter may overrun the former after the front passes the crest of the range. The conditions will then be as shown in Fig. 146. Such conditions are often encountered in the Po Valley in summer, with cold fronts passing the range from the north. As the cold air overruns the warm air that fills the Po Valley, heavy showers and thunderstorms occur. However, as the cold air streams southward, clearing weather prevails.

Figure 147 shows successive positions of a cold front during the passage of a mountain range. It will be seen that the front develops a bulge, or wave, after the passage. Within the region of the bulge, the slope of the frontal surface will be increased. This is due to the fact that the front has been retarded below the level of the range while the frontal surface has moved unhindered aloft. This increase in slope is favorable for the formation of waves on the front. Under favorable conditions,

cyclonic waves may develop after the cold front has passed the range. This will be discussed in greater detail in Chap. VII.   In fact, it was the study of a passage of such a cold front across the Scandinavian range that led to the idea underlying the wave theory of cyclones.

3. *Occluded Fronts.*—When a warm front followed by a cold front approaches a mountain range, the warm front will be retarded while the cold front is still moving unhindered.   This leads to a speeding up of the occlusion process. The occluded front that results will pass the range more or less as a warm front if the air in the rear of the cold front is warmer than the air in advance of the

STAGNANT WARM AIR

OVERRUNNING COLD AIR   GREAT INSTABILITY

STAGNANT WARM AIR
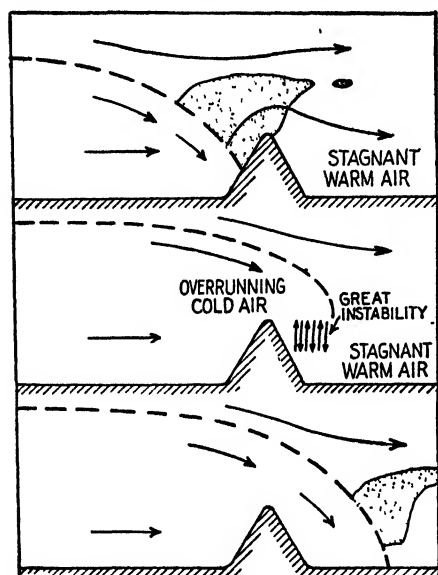
Fig. 146.—Cold front passing a mountain range and overrunning warm stagnant air at low levels to the lee of the range.
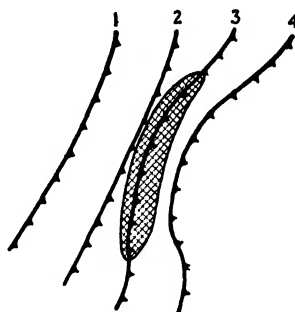
Fig. 147.—Successive positions of a cold front passing a mountain range.

warm front.   With the reverse temperature distribution, the front will pass the range as if it were a cold front.

Summing up, we may say that the influence of a mountain range on a front is characterized by: (1) Widening of the frontal area of precipitation as the front approaches the range.   (2) Prolonged duration and increased intensity of the frontal precipitation on the windward side.   (3) Narrowing of the area of precipitation or dissolution of the frontal cloud system on the lee side of the range, except, under the special conditions discussed above, when cold air aloft overruns the warm air to the lee of the range; in such cases, heavy showers or thundery weather may occur on the lee side during the passage.   (4) Retardation of the fronts as the range is passed and, occasionally, formation of cyclonic waves after the passage of cold fronts.   (5) Speeding up of the occlusion process during the approach and passage of a warm front followed by a cold front.

CHAPTER VII

WAVES AND CYCLONES

Even though the development of the theory and practice of fronts, waves, and cyclones is of a comparatively recent date (from 1918 onward), indication of concepts of frontal ideas can be traced back to the early writings of Dove, Helmholtz and Blasius. A study of the history of these early indications has been given by Gold [29] and other European writers.

Dove, in his "Law of Storms" (1861), noted that, when a cold current breaks through, it is observed first at the surface and later at high levels, whereas, when a warm current replaces a colder one, the warm current is observed at higher levels before it is found at the surface. This implies that adjacent air masses of outstanding temperature discontinuity are separated from one another by a sloping surface with warm air above cold air.

Helmholtz, in his first paper on Atmospheric Motion (1888), suggests that the cold air from the north, in its endeavor to flow southward, will form a stratum of cold air at the surface, that it advances irregularly, and that vortex motion will develop at the surface of separation.

Blasius, in his studies of tornadoes (1851), arrived at the conclusion that storms arise from the interaction between air currents of polar and equatorial origin. Similar indications of more or less vague ideas about the development of storms through the contrasts between neighboring air masses are found in the writings of Luke Howard and Fitzroy.

The same ideas are more clearly brought to light by Clement Ley (1878), Köppen (1882), Durand-Greville (1892), and Abercromby (1892). Through these investigations, the squall line was found; but it was apparently assumed that a squall line was a rare occurrence and not a general feature in the development of extratropical cyclones.

Margules, in his "Energy of Storms" (1902), showed that the energy available through the juxtaposition of air masses of different temperatures was sufficient to account for the kinetic energy of cyclones. He also computed the slope of the dividing surface for various temperature and wind discontinuities and found that the surface could not be horizontal.

Shaw and Lempfert studied the air currents around extratropical cyclones (1906) and found that the changes of wind were not continuous but discontinuous, the wind discontinuity being particularly pronounced

along squall lines.   Indications of atmospheric discontinuities were also found by von Ficker in his study of cold waves in Siberia.

A discovery of outstanding importance was made in 1898 by V. Bjerknes, who proved that the increase in circulation per unit time around a closed curve was equal to the number of isosteric-isobaric solenoids comprised by the curve.   This theorem showed that temperature (or density) contrasts were of great importance for the creation of atmospheric motion.   Although Bjerknes' theorem greatly accelerated the development of dynamic oceanography, its influence on the development of dynamic meteorology is of more recent date.

In 1910, V. Bjerknes presented some results concerning the relation between lines of flow, convergence and divergence, and ascending motion and their relation to the formation of clouds and precipitation.   About the same time, Shaw (1911) published his famous diagram of the air flow around a depression and its relation to the cyclonic rain areas.

The various ideas and observations on atmospheric discontinuities were rather vague and disconnected, and their importance with respect to the formation and development of cyclones was not realized. A synthesis coordinating the evidence into a dynamic, genetic picture was not arrived at.   The next outstanding step in this direction was taken by J. Bjerknes [9] in 1918.   By examining a great number of cyclones by means of observations from a dense network of stations and following the lines indicated by V. Bjerknes, who then was the leader of the Norwegian group of meteorologists, certain general results of great importance were deduced.   The principle of these results was that every moving cyclone has two outstanding lines of convergence distinguished by characteristic thermal properties.   According to J. Bjerknes, the cyclone consisted of a warm sector surrounded by cold air (see Fig. 148). The line of discontinuity on the forward side where warm air replaces cold air was called the *steering line,* and the line of discontinuity in the rear of the cyclone was called the *squall line.*   The two lines of discontinuity joined in the center of the depression.   From this picture, the three-dimensional structure of moving cyclones was deduced.   To the steering line corresponded a sloping surface of discontinuity along which warm air overruns cold air, resulting in an extensive cloud system and precipitation in advance of the steering line.   To the squall line corresponded a sloping surface of discontinuity along which cold air underruns warm air.   Through lifting of the warm air, a cloud system and precipitation result along the squall line.

Concerning this discovery, Gold [29] writes:

This paper of Bjerknes contains only eight pages; but they are the most remarkable eight pages in the literature of synoptic meteorology: they form the

pattern for subsequent investigation, though in points of detail later developments have necessitated correction as well as extension.

In 1921, J. Bjerknes and H. Solberg published their paper entitled Meteorological Conditions for the Formation of Rain. In this paper, the original cyclone model was modified as shown in Fig. 148. The terms "steering line" and "squall line" were abandoned, and the terms. "warm front" and "cold front" introduced. The middle part of the diagram
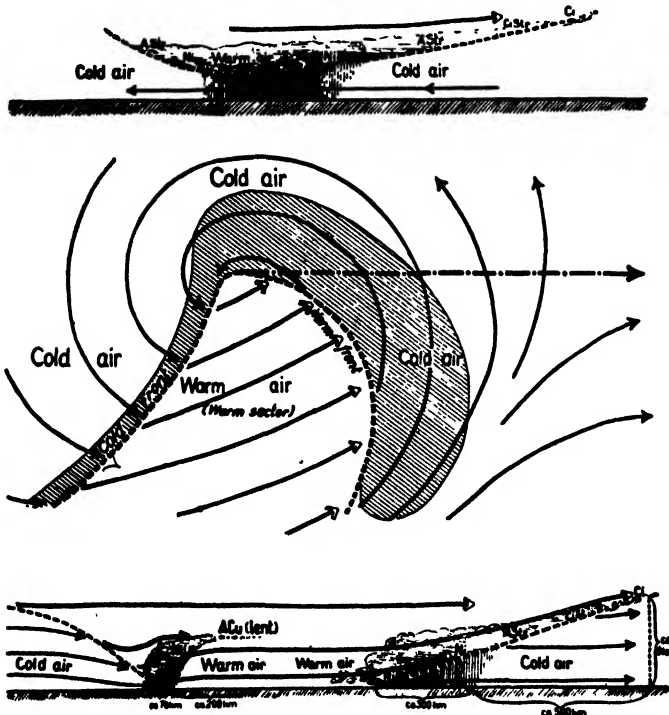
Fig. 148.—Idealized cyclone. (*According to J. Bjerknes and H. Solberg.*)

represents a horizontal picture of the air flow, the fronts, and the frontal cloud systems. The top part of the diagram represents a vertical cross section north of the cyclonic center, and the lower portion represents a similar section to the south of the center. In view of the discussion in Chap. VI, the diagram is self-explanatory.

This model of the idealized cyclone shows, so to speak, the anatomy of the cyclone; but it does not explain its genesis and its future development, nor does it explain how the fronts are created.

A year later, J. Bjerknes and H. Solberg published a short paper on the Life Cycle of Cyclones and the Polar Front Theory of Atmospheric Circulation. In this paper the authors showed that the cyclone model

shown in Fig. 148 represents only a special case, or a single stage, in the development of a cyclone.

The importance of this paper lies in the fact that the authors explain the genesis and the development of a cyclone. The surface of discontinuity was interpreted as the surface of separation between polar air and tropical air; hence the name *polar front*. Furthermore, the authors showed that the nascent cyclone is a wave of small amplitude on the polar front surface which gradually develops into the cyclone model shown in Fig. 148. Therefore, the cyclone model (Fig. 148) is preceded by the stages shown in Figs. 149A to C. Furthermore, the authors showed that
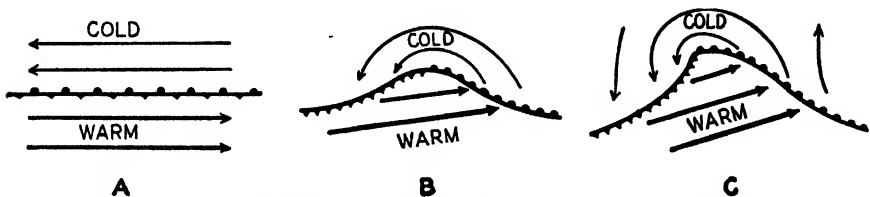
Fig. 149.—Formation of a wave cyclone which develops through the stage represented by Fig. 148 into the stages shown in Fig. 150.
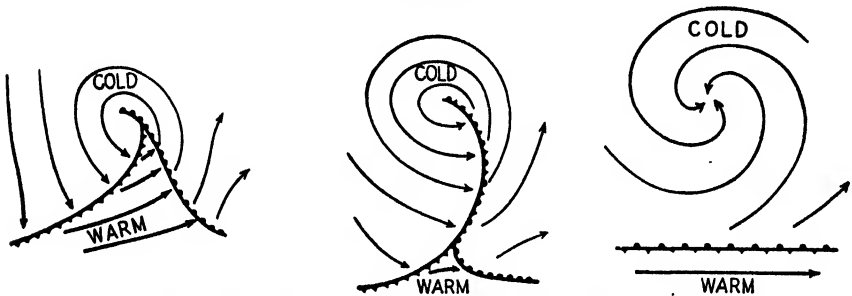
Fig. 150.—Late stages in the development of a cyclone.

the cyclone, after having reached the stage represented by Fig. 148, develops further through destruction of the fronts into a dying vortex. This development is characterized by a number of intermediate stages in which the cold front gradually overtakes the warm front; the cyclone then *occludes*, and the resulting front was called an *occluded front*. Normally, the cyclone would reach a maximum of intensity when it is partly occluded; and, through the later development, the kinetic energy, created from potential energy, heat energy, and liberation of latent energy, would be dissipated. The later stages in the development of a cyclone are shown in Fig. 150. Thus, the nascent cyclone originates as a slight wave, the amplitude of which increases while the cyclone occludes. This development is characteristic of *unstable* waves. The synoptic studies indicated further that these waves had a period of oscillation of about 24 hr. and a wave length of 1000 to 2000 km.

It is of interest to note that the occlusion process was originally discovered by Bergeron through his study of the behavior of cold and warm fronts on synoptic maps.

The next discovery of paramount importance was the theory for the formation of fronts presented by Bergeron (1926). Through these discoveries, fronts and cyclones became living entities, forming through some genetical process, developing into a maximum of intensity, and then degenerating through consenescence.

Although the attention of the Bergen school of meteorologists initially was directed toward the frontal phenomena, Bergeron soon emphasized the importance of the air masses themselves. In 1926, he published his paper outlining the principles of air-mass analysis.

In recent years, Rossby and his collaborators, favored by the comparatively dense network of aerological stations in North America, have developed a method of analysis of the free atmosphere known as *isentropic analysis*. These methods, which are now widely used in the United States, have yielded a mass of new knowledge about the processes in the free atmosphere.

The empirical studies of cyclones referred to above gave indications but not adequate proofs of the correctness of the wave theory of cyclones. In recent years, extensive theoretical researches, notably by Solberg, V. Bjerknes, and Godske, have shown that the original ideas of the wave theory are soundly founded on hydrodynamic principles. Of paramount importance is Solberg's theory of unstable waves in which the force of inertia is taken into account. Although the development of this theory has not yet been brought to a conclusion, the rapid advances in recent years seem to promise much for the future.

Parallel to the theoretical investigation, important synoptic studies of the structure of cyclones have been made by many authors, notably by J. Bjerknes, Bergeron, Douglas, Palmén, Swoboda, and others. Simultaneously, the kinematic properties and the differential mechanics of fronts and cyclones have been investigated by Giao and Petterssen. Thus, at present, our knowledge of extratropical cyclones may be referred to three categories, *viz.:* (1) the wave theory, which explains the formation of unstable waves of small amplitude; (2) the empirical knowledge derived from the analysis of weather situations and furnishing a quasi-theoretical explanation of the development of cyclones from the initial wave disturbance through the deepening and occlusion processes to the final frontless structure; and (3) the kinematic relations which, though they do not explain the physical processes, are useful for prognosticating the movement and development of cyclones.

A brief outline of the principles of the wave theory, together with a detailed description of the structure and development of cyclones, will be

given in this chapter; the kinematic relations and their application to actual forecasting will be discussed in Chaps. IX to XI.

126. Idealized Initial State.—We shall first consider the case when the polar front coincides with a parallel circle, say at 50°N lat. If there were no motion in the atmosphere, the isobaric surfaces would be parallel to the earth's surface as shown in Fig. 151A. If the air moves zonally from the east, there would be high pressure over the poles, and the isobaric surfaces would have a curvature which is greater than that of the earth's surface (Fig. 151B). On the other hand, if the air moved from the west, there would be high pressure to the south, and the isobaric surfaces would be less curved than the earth's surface (Fig. 151C).
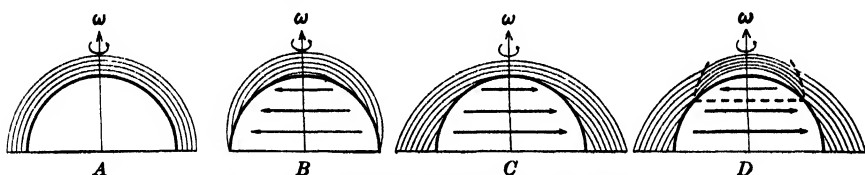
FIG. 151.—Isobaric surfaces in initial state.

If the air north of the polar front moves from the east while the warm air to the south moves from the west, the isobaric surfaces would be as shown in Fig. 151D. In the latter case, the kink in the isobaric surfaces would indicate the position of the polar front surface in agreement with formula 117(8). Along such a frontal surface, there would be cyclonic vorticity in agreement with the principles explained in Par. 120.

The frontal surface would then separate the dense polar air from the less dense warm air above and to the south of the frontal surface. Even though the conditions described above are somewhat idealized, they nevertheless are similar to those which actually occur in the atmosphere.

In the equilibrium position, the slope of the frontal surface would be given by the Margules formula 117(9). Under ordinary atmospheric conditions, the inclination would be about $\frac{1}{100}$.

From the different branches of fluid mechanics, it is a well-established fact that a small perturbation of the state of equilibrium would result in wave motion. Correspondingly, one should expect to find waves developing on the frontal surface. It is of interest to note that the waves actually occurring on frontal surfaces differ qualitatively and quantitatively from those forming on the surface of separation between the ocean and the atmosphere. The reason for this is due partly to the difference in dimensions and partly to the fact that other wave-generating forces occur in large-scale atmospheric motion.

127. Small Oscillations.—We start from a fluid system in equilibrium or in a state of stationary motion and add to this system a small perturbation. The perturbation is supposed to be infinitely small in comparison

with the motion in the undisturbed state.   Furthermore, the perturbation is supposed to depend on time according to an exponential law, thus containing the factor

$$e^{i\nu t}$$

where i is the imaginary unit, ν the frequency, or

$$\nu = \frac{2\pi}{t_0}$$

where t_0 is the period of oscillation.

When the equations of motion and the mutual boundary conditions are taken into account, the method of small oscillations will furnish an equation between the frequency ν, the wave length L, and the physical parameters of the fluid system.

If ν is *real*, the perturbation diminishes with time, and we have a *stable* state of motion.   However, if ν is *imaginary*, the perturbation increases with time, and the general state of motion is *unstable*.   With the aid of this method, it was found long ago that the waves in a fluid medium were essentially of two different types, *viz.*, either *longitudinal* or *transversal*, the former belonging to the category of sound waves, and the latter belonging to the category of gravitational waves.   Whereas the sound waves obtain their energy from the elasticity of the medium, the gravitational waves receive their energy from the force of gravity. Apart from these wave-generating forces, it is necessary, in dealing with large-scale atmospheric motion, to consider also the inertia force and the shearing stresses at the frontal surface.

128. The Wave-generating Forces.   1. *Sound Waves.*—These waves, which are longitudinal and draw their energy from the elasticity of the air, travel with a speed of about 330 m./sec. and have a period of a few seconds. They have no resemblance to the cyclonic waves.

2. *Gravitational Waves.*—The nature of these waves is best illustrated by the waves on an ocean surface.   The water particles oscillate in vertical planes, each particle describing a circle or an ellipse.   The particles at the wave crest have a maximum of potential energy, and those in the wave trough have a minimum of potential energy.   In these waves, potential energy is transferred into kinetic energy, and vice versa. The process is reversible, and the waves are essentially stable.   Gravitational waves may develop on surfaces of discontinuities in the atmosphere; but, as instability is an essential feature of the cylonic waves, it follows that the influence of the gravitational force on the cyclonic waves must be less than the influence of the other wave-generating factors.   Waves that are mainly of gravitational type occur along inversion layers and become visible through the formation of billow

clouds (Helmholtz' *Wogenwolken*). These waves are of short wave length, and their periods of oscillation are of the order of magnitude of some minutes.

3. *Inertia Waves.*—In order to find waves that resemble the cyclone waves of the weather maps, it is necessary to take the earth's rotation into account. We then find another source of wave energy which is due to the *force of inertia*. This force may be neglected in the discussion of sound waves and gravitational waves, for the periods of oscillation of these waves are so small that the deviating force due to the earth's rotation does not appreciably influence the motion.

That the inertia force is of importance is readily shown by the aid of a tank experiment: A cylindrical vessel partly filled with water is rotated on its axis, which is vertical. The free surface then obtains the shape of a parabola, as shown in Fig. 152. Consider an arbitrary particle on the
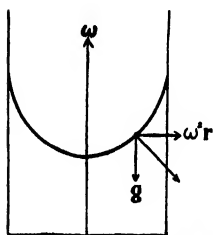
Fig. 152.—Illustrating the wave-generation force due to inertia.

free surface. The gravitational force acts in a direction parallel to the axis of the cylinder, and the inertia force acts perpendicularly to this axis, the resultant force being normal to the free surface. If the free surface is disturbed, it would oscillate in the direction of the resultant force, and both the inertia force and the gravitational force would supply energy to the wave motion on the surface. If the angular velocity of the vessel were increased, the inertia force would increase relative to the gravitational force, and the waves on the free surface would be predominantly of the inertia type.

In order to obtain a clearer idea of the role of the inertia force in the production of waves, it suffices to consider the motion in a circular vortex in a homogeneous and incompressible fluid. We consider a substantial circle of radius r and angular momentum $M = \Omega r^2$, Ω being the angular velocity of the fluid. If the circle is perturbed horizontally outward so that r increases to r_1, the angular momentum will be preserved, and the angular velocity will change from M/r^2 to M/r_1^2. The centrifugal force will then change from M^2/r^3 to M^2/r_1^3. Before the perturbation, the centrifugal force on the circle r_1 was M_1^2/r_1^3.

If the displaced particle were in equilibrium initially, it would not remain so after being displaced: it would be subjected to an acceleration that is equal to the difference between the two centrifugal forces, *viz.*:

$$\frac{M^2 - M_1^2}{r_1^3}$$

Thus, when $M_1 > M$ (*i.e.*, the circulation and the angular momentum increasing with increasing distance from the axis), the acceleration would

tend to drive the displaced particle back toward its equilibrium position. Conversely, when $M_1 < M$, the displaced particle would be accelerated away from its original position.

4. *Dynamic Stability.*—If the perturbed particle is displaced the distance Δr, we may write

$$r_1 = r + \Delta r$$

and as

$$M_1 = M + \frac{dM}{dr}\,\Delta r + \cdots$$

we obtain the following expression for the acceleration where terms of second and higher order are neglected,

$$\frac{M^2 - [M^2 + 2M(dM/dr)\Delta r]}{(r + \Delta r)^3} = -2\frac{\Omega}{r}\frac{d}{dr}\,(\Omega r^2)\Delta r = -2\Omega|\ \text{curl}\ v\ |\Delta r$$

because in polar coordinates

$$|\ v\ | = \Omega r \qquad \text{and} \qquad |\ \text{curl}\ v\ | = \frac{1}{r}\frac{d}{dr}\,(\Omega r^2)$$

If the rotation of the fluid is constant, we have

$$|\ \text{curl}\ v\ | = 2\Omega$$

and the acceleration reduces to

$$\frac{d^2(\Delta r)}{dt^2} = -4\Omega^2\Delta r$$

which is the equation for harmonic oscillations with the frequency 2Ω and the period $\frac{1}{2}t_0$ (*i.e.*, half the period of the rotating fluid).

In the general case when Ω is not constant, we obtain the frequency

$$\nu = \sqrt{2\Omega|\ \text{curl}\ v\ |}$$

and the period

$$t_0' = \frac{t_0}{2}\sqrt{\frac{1}{1 + (r/2\Omega)(d\Omega/dr)}}$$

Now, if the rotation increases with r, the period will be less than $\frac{1}{2}t_0$; if the rotation decreases with r, the period will be greater than $\frac{1}{2}t_0$. Furthermore, when the circulation increases with r [*i.e.*, $(d/dr)(\Omega r^2) > 0$], we obtain real values for ν, which means that the oscillations are stable. This case is called *dynamic stability*. On the other hand, if the circulation decreases with r, [*i.e.*, $(d/dr)(\Omega r^2) < 0$], the frequency is imaginary, indicating that the motion is unstable. This case is called *dynamic instability*. In the limiting case when $(d/dr)(\Omega r^2) = 0$, the state is *dynamically indifferent*.

The conditions prevailing in the atmosphere are usually such that the circulation increases with increasing r. Therefore, the inertia force will usually produce stable waves. On the other hand, the inertia waves are of great lengths and their periods are of several hours. In this respect, they resemble cyclone waves. But, as dynamic instability is an essential feature of the cyclone waves, it will be necessary to find some unstabilizing factor which, together with the inertia force, will give waves of the types encountered on the weather maps.

5. *Shearing Waves.*—The shearing motion at the frontal surface (*cf.* Figs. 151*D* and *E*) will cause certain types of waves to become unstable. Helmholtz considered two infinite strata of incompressible fluids separated from one another by a horizontal surface of discontinuity. For the velocity of propagation c of waves on the surface of separation, he found the formula

$$(1) \qquad c = \frac{\rho v + \rho' v'}{\rho + \rho'} \pm \sqrt{\frac{gL}{2\pi} \cdot \frac{\rho - \rho'}{\rho + \rho'} - \rho \rho' \left(\frac{v - v'}{\rho + \rho'}\right)^2}$$

Here, ρ denotes density, v wind velocity along the front, L wave length, and g acceleration of gravity. Indices refer to the less dense mass. The theory of shearing waves has been improved by Solberg and Godske, but the above formula will suffice for this qualitative discussion.

Equation (1) shows that the velocity of a wave of this type is composed of two factors, *viz.*:

a. The convective term represented by

$$c_c = \frac{\rho v + \rho' v'}{\rho + \rho'}$$

As the density discontinuity usually is slight in comparison with the wind discontinuity, we may write $\rho = \rho' = \frac{1}{2}(\rho + \rho') = \rho_m =$ the mean density. The convective term then reduces to

$$(2) \qquad c_c = \frac{v + v'}{2}$$

b. The dynamic term represented by the radical. The first term under the radical depends on the static stability, or on gravity, and is always positive at frontal surfaces, since the indices refer to the less dense mass. This term decreases with decreasing wave length L and becomes unimportant when L is small.

The last term under the radical depends on the shearing motion. This term, which is independent of the wave length, deducts from the gravity term. For suitable wave lengths, the two terms balance, and, if the wave length is below this critical value, the dynamic term becomes imaginary; the wave is then *unstable.*

It is of interest to note that the gravity term decreases as the density discontinuity decreases. Therefore, when ρ approaches ρ', this term vanishes, and waves of all wave lengths become unstable. In the atmosphere, the stratification is usually stable. For small waves, the static stability may be overcompensated by the shearing instability; but as the wave length increases, the static-stability term will predominate, and all waves become stable. With the commonly observed values of density and wind discontinuities in the atmosphere, the transition from unstable to stable waves occurs when the wave length is of the order of magnitude of a few kilometers. Equation (1) applies to waves that are generated through the combined action of gravity and shearing motion. These waves are short waves. However, for longer waves, it is necessary to take into consideration the inertia force.

129. Cyclone Waves.—Following the theory of cyclone waves as outlined in "Physikalische Hydrodynamik," we proceed to describe the kinematics of the waves that may develop along frontal surfaces. Comparison of the results with what is actually observed on the weather charts will show that the wave theory actually renders results which in principle harmonize with nature.

The kinematics of the wave motion is illustrated in Fig. 153. *I* and *II* show the motion in vertical cross sections through the frontal surface. *I* shows the case of stability, and *II* shows the case of instability. It will be seen that, in the case of stability, a center of counterclockwise rotating motion is present at the crest of the wave and a center of clockwise rotating motion is present at the trough of the wave. In the case of instability (*i.e.*, *II*) the centers of clockwise and counterclockwise motion are displaced one-fourth of the wave length toward the left. In the case of instability, the amplitude of the wave would increase with time.

A, *B*, and *C* illustrate the shearing motion that should be added to the wave motion. In all three cases, the upper layer has the greatest velocity toward the right (*i.e.*, toward the east). Adding the three types of shearing motion to *I*, we obtain the pictures *IA*, *IB*, and *IC*. The counterclockwise rotating whirls at the crests are suppressed, whereas the clockwise rotating whirls at the troughs are maintained. The waves propagate to the right with constant amplitudes.

Adding now the shearing motions *A*, *B*, and *C* to the unstable wave *II*, we obtain *IIA*, *IIB*, and *IIC*, which can be interpreted as results of either static or dynamic instability. The whirls are centered midway between the crests and the troughs. The surface of discontinuity would then roll up around the clockwise rotating whirls.

From the formula of Helmholtz, it is seen that in general we have a velocity of propagation. In the case of instability, the velocity c is complex, or, $c = c_e + ic_d$, where c_d is the dynamic term. When c_e

approaches c_d, the velocity of propagation will be of the same order of magnitude as the increase in amplitude, with the result that the clockwise
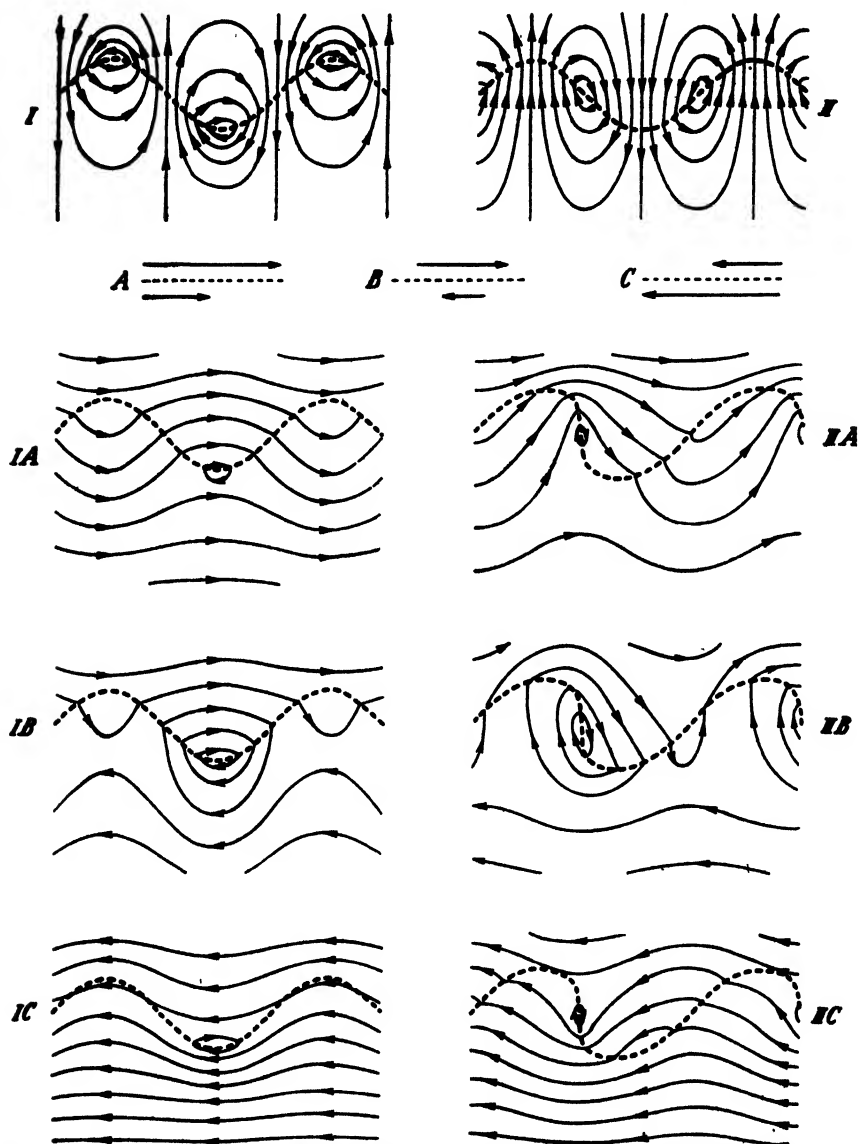
Fig. 153.—Resulting streamlines of wave motion without and with shearing motion. *I*, stable waves; *II*, unstable waves.   (*After V. Bjerknes.*)

rotating whirls are centered about one-eighth of the wave length to the left of the troughs.

As long as the period of oscillation is small, the deviating force due to the earth's rotation has no sensible effect on the motion; the particles will then oscillate in vertical planes. However, when the period of oscillation is large, the deviating force becomes important, and it is necessary to consider its effect on the oscillations.

In the first place, the deviating force affects the slope of the surface of discontinuity in such a manner that it obtains a slope relative to the horizontal. In the equilibrium position, the slope would obey the Margules formula; it amounts to about $\frac{1}{100}$ to $\frac{1}{200}$.

Far more pronounced is the effect of the deviating force on the trajectories of the oscillating particles and on the stream surfaces containing these trajectories. In a vertical plane along the direction of propagation of the wave, the gravitational force and the pressure gradient will be large as compared with the deviating force. Therefore, the earth's rotation will have but slight influence on the motion in this vertical plane. The influence of the deviating force on the horizontal motion is far greater because the acting forces in this direction are far smaller. The deviating force will have a tendency to produce horizontal motion of inertia with clockwise rotation. As a result of the combined effect of the vertical oscillations of the Helmholtz wave and the far larger horizontal motion of inertia, we obtain a quasi-horizontal motion with clockwise rotation of the particles in their stream surfaces. The greater the period, the greater is the wave length, and the smaller will be the angle between the horizontal and the stream surface.

Although the effect of the deviating force on the surface of discontinuity is to cause the surface to be inclined to the horizontal by the amount $\frac{1}{100}$ to $\frac{1}{200}$, when the wave length is of cyclone dimensions the effect of the same force on the stream surfaces is to cause them to be inclined to the horizontal by an amount of about $\frac{1}{1000}$. The oscillations will therefore be mainly horizontal when the wave length is as large as what is observed on the weather maps.

The diagrams shown in Fig. 153 represent vertical cross sections, but they will hold in principle also in any section that is inclined to the vertical and intersects the frontal surface along the direction of the propagation of the waves. The diagrams will therefore hold in principle also for quasi-horizontal sections. In the vertical sections, the cold air would be situated under the warm air. If the sections be interpreted as quasi-horizontal pictures, the cold air would be situated to the south of the warm air, and the diagrams would then represent the conditions in the southern hemisphere where the polar front separates the cold air to the south from the warm air to the north. In the case of stability (*I*), the clockwise rotating whirls are centered at the southernmost portion of the warm tongue; in the case of instability (*II*), they are centered one-fourth

of a wave length to the left of these tongues. In the intermediate case, they would be situated slightly to the left of the warm tongues, and the resulting · motion in the quasi-horizontal stream surfaces will have a marked resemblance to what is actually observed in rapidly developing cyclones in the southern hemisphere.

To obtain the corresponding streamline pictures of cyclones in the northern hemisphere, the vertical stream surfaces are to be turned in the opposite direction so that the warm air comes to the south. The reversed pictures will then apply to the northern hemisphere. These are shown in Fig. 154. The clockwise rotating whirls in the vertical sections will appear as counterclockwise whirls in the quasi-horizontal stream surfaces. The whirls are situated slightly to the left of the northernmost end of the warm tongues. These streamlines show a remarkable resemblance to the wind distribution that is actually observed in the lower atmosphere (*e.g.*, at the earth's surface) in the northern hemisphere.

The greater the wave length, the smaller will be the angle between the stream surface and the horizontal, and, therefore, the smaller will be the effect of gravitation on the wave motion. The gravitational stabilizing effect will therefore decrease with increasing wave length. But, simultaneously, the stabilizing influence of the inertia force will increase with increasing wave length. These stabilizing forces are counteracted by the effect of shearing, and this effect is independent of the wave length, as can be seen from Eq. *128*(1). On account of the variation with wave length of the stabilizing forces, it is readily seen that unstable waves can occur only when the wave length is such that the effect of the stabilizing forces is less than that of the shearing motion along the frontal surface.

Fig. 154.—Streamlines in cyclonic waves in the northern hemisphere. (*After V. Bjerknes.*)

The effects of the various forces are illustrated qualitatively in Fig. 155. The stabilizing influence of gravity increases with wave length as long as the wave length is small. As the wave length increases, the deviating force comes into action, and the stream surfaces become more and

more inclined.   As the wave length increases further, the gravitational influence decreases and approaches asymptotically to zero with increasing wave length.   The inertia force vanishes for small wave lengths and increases at a progressive rate as the wave length increases.   The sum of these forces is always positive as long as the stratification is statically stable (*i.e.*, $\rho > \rho'$); but the sum has a minimum for wave lengths somewhere between 500 and 3000 km.   Within this interval, then, the unstabilizing effect of the shearing motion may overcompensate the stabilizing forces, and unstable waves result.   The same also applies to very short waves where the gravitational and the inertia effects are small.
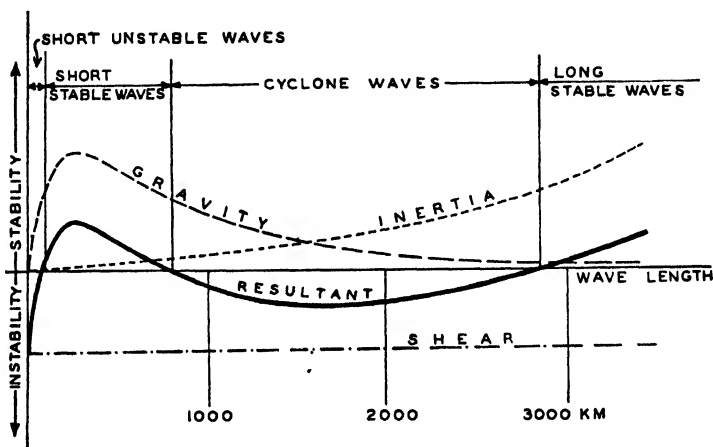
Fig. 155.—Qualitative diagram showing the variation of stabilizing and unstabilizing forces with the wave length.   The heavy curve shows the resultant of these forces.

The heavy curve in Fig. 155 shows the resultant of the stabilizing and unstabilizing forces.   Unstable waves occur when the wave lengths are of the order of magnitude of meters or a few kilometers. Waves greater than these become stable on account of the maximum of the gravitational influence.   But waves whose lengths are of the order of magnitude of 500 to 3000 km. will become unstable when there is sufficient shearing motion along the frontal surface.   If the wave length increases beyond this interval, the waves become stable on account of the stabilizing effect of the inertia force.

Thus, there are four different types of wave that may occur at frontal surfaces:

1. *Short unstable waves* with wave lengths up to a few kilometers and with periods of some minutes.   These waves, which frequently give rise to billow clouds, will cause the frontal surface to become a layer of transition; but as the wave length is short, the layer of transition will be fairly shallow.

2. *Short stable waves* with wave lengths ranging from a few kilometers to about 500 km. or more. These waves are controlled by gravity, inertia, and shearing motion; they are stable because the unstabilizing effect of the shearing motion is insufficient to overcompensate the stabilizing force of gravity and inertia.

3. *Cyclone waves* with wave length in the interval between about 500 and 3000 km. These waves are unstable because the unstabilizing effect of the shear overcompensates the stabilizing effect of gravity and inertia.

4. *Long stable waves* with wave lengths in excess of about 3000 km. These waves are mainly of the inertia type, and they are stable because the effect of shearing motion is overcompensated by the effect of inertia.

The short stable waves (2) and the long stable waves (4) are not observed on the weather maps for, as they are stable, their amplitudes will remain small.

The period of oscillation varies with the wave length. According to the theory summarized above, a period of 12 to 15 hr. would correspond to a wave length of 1000 km. This period is somewhat shorter than what is actually observed. In this connection, it is of interest to remark that Solberg's theory is based on some simplifying assumptions that cause some discrepancy between theoretical and observed results. Thus, Solberg assumes that the two atmospheric layers which partake in the oscillations are isothermal, whereas, in nature, the temperature would decrease with altitude within each of the air masses. Solberg's assumption, therefore, involves a static stability that is far greater than what actually occurs, and this causes the computed period of oscillation to be too small. What is actually observed is a period of about 24 hr.; but, in extreme cases, the period may vary between 15 and 40 hr.

In the theoretical deductions, it is assumed that the two layers are of infinite thickness and the frictional influence is neglected. The theoretical results are, therefore, likely to be less valid close to the earth's surface than in the free atmosphere. Finally, it should be borne in mind that the theory is developed by the aid of the method of small oscillations. The results are therefore applicable only to the nascent cyclone where the perturbations are small as compared with the fundamental motion. When the amplitude of the waves grows and the perturbation increases, the method of small oscillations is no longer applicable. Our knowledge of the structure and the development of such cyclones is based on the studies of weather maps and aerological ascents.

Summing up, we may say that the wave theory of cyclones is capable of explaining the spontaneous formation of unstable waves whose length and velocity of propagation agree with what is actually observed. As these waves are unstable, it follows that their amplitude must increase with time. The waves therefore develop toward occlusions. The theory

also shows that the stream surfaces in each of the oscillating air masses are inclined relative to the horizontal. The inclination is of the order of magnitude of $\frac{1}{1000}$, and it is greater in the warm mass than in the cold mass. Furthermore, the oscillating particles will ascend when they move northward and descend when they move southward. These rules agree in principle with what was explained in Par. 100. They are also corroborated by observations.

Synoptic studies, notably by J. Bjerknes and Palmén [15] have shown that cyclone waves will, while their amplitudes grow, induce wave motion on the tropopause and that these upper perturbations have a marked influence on the development of the cyclones in the later stages. The problem is then no longer a "two-layer" but a "three-layer" problem; for, in addition to the two atmospheric layers that are separated from one another by the polar-front surface, a third layer, the stratosphere, comes into action. In later paragraphs, it will be shown that this has a profound influence on the development of cyclone waves of large amplitudes.

In the discussion of Eq. *128*(1), it was pointed out that the velocity of propagation of the Helmholtz waves consist of a convective and a dynamic term. The waves are stable when the dynamic term is real and unstable when the dynamic term is complex. In the Helmholtz waves (short waves), the inertia force was disregarded. If the inertia force is taken into account, the formula becomes more complicated. However, as the cyclone waves are unstable, it follows that the dynamic term must be complex: it accounts for the increase in the amplitude, and the convective term accounts for the velocity of propagation tangential to the crest of the wave. The convective term is therefore expressive of the translatory velocity of the wave. The velocity of propagation of cyclonic waves will thus depend only on the translations of the warm and cold layers. A mathematical analysis by Godske [27] gives the following result: "*The velocity of propagation of the cyclone wave is intermediate between the translation of the warm layer and the cold layer, but much nearer to the translation of the warm layer.*" This rule agrees well with what is observed.

The above is a brief and incomplete summary of the wave theory of cyclones. Readers who are interested in the mathematical analysis of this theory are referred to the papers and books cited in the references to the literature. Although the wave theory gives results that are of great importance, it is as yet not directly applicable to the analysis of weather charts. In the following paragraphs, we shall therefore turn to the aspects of cyclones that are brought to light by synoptic studies. These aspects will form the real working knowledge of the practical forecaster.

130. Structure of Moving Cyclones.—The salient features of the formation of a wave cyclone and its development from an unstable wave

of small amplitude to a vortex are shown schematically in Fig. 156. For convenience, the development is shown in five different stages, each stage being illustrated by means of two horizontal maps, one at the earth's surface and the other in the warm air above the polar front surface, and two vertical cross sections, one north of the cyclonic center and the other south of it.

Stage 1.—In Fig. 156*A*1, the cold air to the north moves from the west with a speed which is less than that of the warm air to the south. In many cases, it will be found that the cold air to the north moves from an easterly direction, and the warm air to the south moves from a westerly
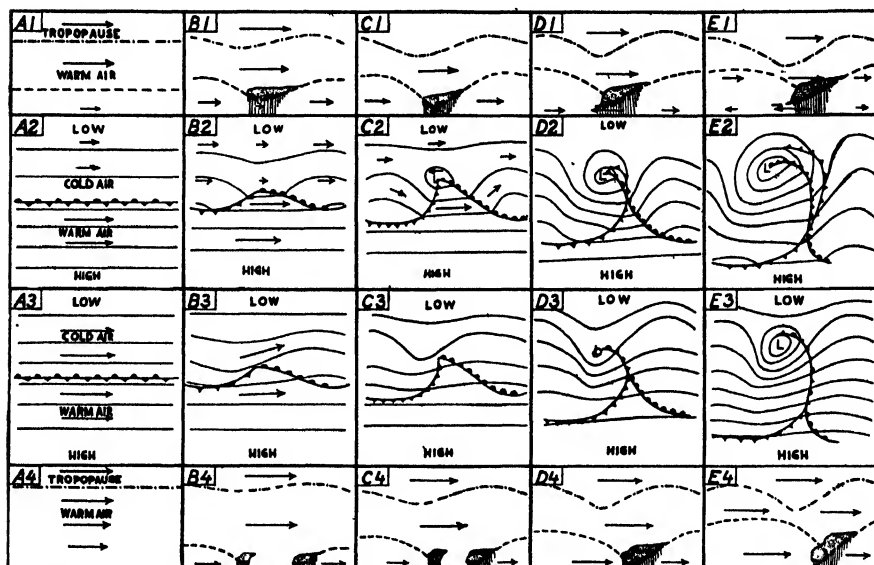
Fig. 156.—The structure of moving cyclones. Row 1, E-W section north of center; row 2, fronts and isobars at the earth's surface; row 3, fronts at the surface and isobars above the cold air; row 4, E-W section south of center.

direction. The front is then situated in a trough of low pressure. The two cases are dynamically equivalent inasmuch as they both give cyclonic shear at the frontal surface. As the former case is the most general one, it will serve as a basis for our discussion.

In the initial state (Fig. 156*A*2) the front is quasi-stationary and more or less parallel to the isobars. The frontal surface slopes toward the cold side, its inclination being about $\frac{1}{100}$. In a vertical cross section parallel to the front and north of it (Fig. 156*A*1), the intersection of the frontal surface will be a horizontal line, and so, also, will be the intersection with the tropopause. An ascent through the frontal surface will show a rapid increase in the westerly wind as the front is passed, showing that the shearing motion is concentrated at the frontal surface. No such

shear is observed by ascending through the tropopause, for the tropopause is a discontinuity of first order whereas the front is a discontinuity of zero order with respect to wind (compare Par. 120).

The cross section to the south of the front (Fig. 156A4) does not intersect the frontal surface, but it intersects the tropopause which normally slopes downward from the south to the north. The isobars in the warm air above the frontal surface (Fig. 156A3) will be more or less parallel and running from the west toward the east, with low pressure to the north and high pressure to the south.

Stage 2.—Under the conditions described in the foregoing paragraphs, unstable waves (cyclone waves) will form on the frontal surface. The amplitude of these waves will grow; and, after a few hours, the stage will be reached when the amplitude is as shown in Fig. 156B. The trend of the front at the earth's surface will then be as shown in Fig. 156B2. The wave motion will cause an increase in the westerly wind velocity to the south of the center and a decrease in the westerly wind velocity to the north of the center. The pressure field would adapt itself to the motion, and there will be a tendency for a cyclonic pressure center to form at the northern end of the tongue of warm air. Depending on the degree of instability, this center would be more or less displaced toward the left. This accounts for the asymmetry in the bend of the front.

If the cold air to the north of the front moved from the east, the front would be situated in a pressure trough. The wave motion would then tend to increase the easterly wind to the north of the forming center.

It was explained in the foregoing paragraph that the cause of the instability of the cyclone waves is the shearing motion along the frontal surface. There is no such shear along the tropopause. But as the warm air moves in an eastward direction faster than the cold air, it will oscillate vertically as it moves up or down the slope of the bulging frontal surface. Thus, the wave motion, originally set up along the frontal surface, will gradually affect the upper strata of the atmosphere; and, as a result, the tropopause is set in an oscillatory motion. As the tropopause slopes downward from the south toward the north and the frontal surface slopes in the opposite direction, the vertical distance between the frontal surface and the tropopause will decrease northward. The waves induced on the tropopause by the frontal waves will therefore have larger amplitudes above the northern part of the cyclonic disturbance than above the southern part of it.

Theoretical and empirical investigations by J. Bjerknes [10, 16] have shown that the waves on the tropopause are not in phase with those on the frontal surface. The crests of the tropopause waves will be found above the warm-front surface and the trough above the cold-front surface. The tropopause waves are therefore retarded about one-fourth of

a wave length relative to the frontal waves.   This circumstance is due to the distribution of vertical velocity in cyclone waves, which will be discussed later.

The warm air between the frontal surface and the tropopause will also perform an oscillatory motion horizontally and vertically, and these oscillations are accompanied by pressure variations.   Figure 156*B*3 shows the principal features of the distribution of pressure in a horizontal plane above the cold air.   The fronts at the earth's surface are drawn to indicate how the pressure distribution aloft is related to the fronts at the ground.   It will be seen that there is a tendency for a trough of low pressure to form in mid-air in the rear of the wave cyclone and for a wedge of high pressure to form above the warm-front surface.

Stage 3.—The nascent cyclone develops gradually into a vortex through the increasing of its amplitude and deepening of its pressure system.   A center of low pressure with cyclonic circulation develops at the upper left portion of the warm tongue (Fig. 156*C*2).   The westerly winds to the north of the center decrease and change into increasing easterly winds, whereas the westerly winds to the south of the center are strengthened.   In the vertical cross sections (Figs. 156*C*1 and *C*4), the undulations of the frontal surface and of the tropopause become more pronounced, and so, also, does the sinusoidal trend in the isobars in mid-air (Fig. 156*C*3).

During the development from stage 2 to stage 3, an important change is usually observed along the northern part of the cold front.   In the quasi-stationary state, there is usually convergence superimposed on the winds shown in Fig. 156*A*2, with the result that the warm air ascends over the wedge of cold air.   The cloud system that is connected with a quasi-stationary front is of the type *A* shown in Fig. 137.   The frontal cloud system retains its principal characteristics when the quasi-stationary front changes into a cold front.   However, as the wave develops, the cloud system along the northern part of the cold front changes from the type *A* (Fig. 137) to the type *B* (Fig. 139).   *This change usually occurs only where the isobars in the rear of the cold front are curved cyclonically.*   Proceeding along the cold front from the center of the cyclone in a backward direction, the cloud system changes from the type *B* to the type *A*. The presence of a cloud system of type *B* along the northern part of the cold front therefore indicates (see Par. 122) that the warm air above the upper portion of the cold-front surface slides down the slope of the cold-front surface.   It will be shown later that this descending motion is due to the oscillating motion in the upper atmosphere.

Stage 4.—Figures 156*D* show the subsequent stage in the development when the cold front overtakes the warm front and the warm air that was in the northern part of the warm sector is lifted to higher levels.   The

cyclone then occludes.   The occlusion process involves that horizontally adjacent air masses of different density become arranged in such a way that the potentially denser mass becomes situated under the potentially less dense mass.   This means a reduction of the potential energy of the whole system, which is the principal source for the creation of kinetic energy.   In addition, a considerable portion of the latent heat of vaporization is liberated through the condensation and precipitation that occur in the frontal cloud systems.

In Figs. 156*D*2 and *D*4, it is assumed that the cold air in the rear of the cold front is warmer than the cold air in advance of the warm front. This distribution of temperature is most frequently observed in winter in regions adjacent to the west coasts of northern continents where the air in the rear of the cold front has a long trajectory over oceans, whereas
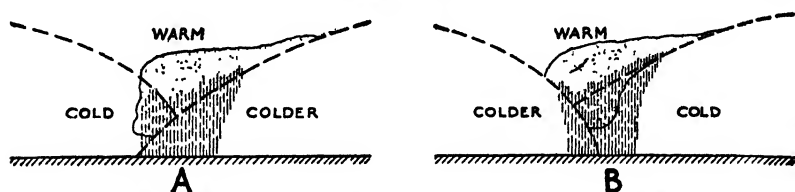
Fig. 157.—Cross sections through occlusions: *A*, warm-front type occlusion; *B*, cold-front type occlusion.

the air in advance of the warm front may come directly from a cold continent.   We then have a *warm-front type of occlusion.*   In regions adjacent to east coasts of northern continents, the reverse temperature distribution is the normal occurrence.   The cold air in the rear of the cold front will then underrun the cold air in advance of the warm front. We then have a *cold-front type of occlusion.*   The two types of occlusion are shown in Fig. 157, and further remarks on occluded fronts will be found in Pars. 134 and 135.

In connection with Fig. 156*D*3, it is of interest to remark that there is a tendency for a cyclonic whirl to form in the warm air above the frontal surface in partly occluded cyclones.   This whirl, or center of low pressure, results from an intensification of the trough of low pressure above the cold-front surface.   This cyclonic whirl in the warm air, which was first found by Bjerknes and Palmén [15], is a consequence of the oscillation of the upper atmosphere and the difference in phase between the frontal wave and the upper perturbation.   Further remarks on the formation of this whirl will be found in Par. 135.

Stage 5.—Figure 156*E* shows the structure of an occluded cyclone following the stage shown in Fig. 156*D*.   Comparing *B*, *C*, *D* , and *E*, it will be seen that the development of a cyclone is characterized by the formation of a wave which gradually develops into a whirl.   The whirl is first found at the earth's surface at the northern left portion of the

tongue of warm air. The whirl grows in intensity and spreads to higher and higher levels. In the final stage, it may affect the entire atmosphere; the tropopause is sucked downward in the region of the whirl, and there is some evidence to show that this suction effect reaches up to the ozone layer or farther.

During the development of a cyclone, parts of the fronts may be exposed to frontogenesis, and other portions may be exposed to frontolysis. The principles outlined in Chap. V should therefore be used to distinguish between frontogenetical and frontolytical fronts. Other methods of detecting the symptoms of frontogenesis and frontolysis will be described in Chap. IX.

Stage 6.—On the whole, it may be said that the occlusion process generally results in frontolysis and in destruction of the frontal surfaces. The final stage of a cyclone is therefore characterized by an occluded front which is rolled up around the center of the depression. Usually, the fronts are then so weak that they can hardly be detected. There is then no supply of energy, and the cyclone lives on for a while as a dying whirl that feeds on the kinetic energy created in the earlier stages. As this energy is dissipated, the cyclone dies as a steadily weakening frontless whirl.

It is of interest to note that the cylonic whirl first forms near the earth's surface and gradually spreads upward. The same sequence is found also in the destruction of the whirl. The whirl first dissipates in the lower atmosphere, whereas it may be intensified in the upper layers. It is therefore often found that cyclonic whirls of considerable intensity exist in the upper atmosphere long after they have been completely dissipated at the earth's surface.

131. The Tendency Equation.—The development of a cyclone is characterized by the increase in amplitude and occlusion. This process is accompanied by a *deepening* of the pressure system that accompanies the cyclone. Let $\delta p/\delta t$ denote the variation in pressure per unit time in a system of coordinates that moves with the cyclone in question. Then the cyclone deepens when

$$\frac{\delta p}{\delta t} < 0$$

and it fills up when

$$\frac{\delta p}{\delta t} > 0$$

Let the vector c denote the velocity of propagation of the center of the cyclone. Then,

(1)
$$\frac{\delta p}{\delta t} = \frac{\partial p}{\partial t} + c \cdot \nabla p$$

where $-\nabla p$ is the horizontal pressure gradient, and $\partial p/\partial t$ is the pressure variation per unit time in a fixed system of coordinates. When c is determined from the weather maps, the deepening may be computed from the observed barometric tendency (*i.e.*, the isallobars) and the horizontal pressure gradient (*i.e.*, the isobars). The method for determining the velocity and the deepening of cyclones will be explained in Chaps. IX and X. Here it suffices to remark that

$$\frac{\delta p}{\delta t} = \frac{\partial p}{\partial t}$$

in the center of the cyclone (because $\nabla p = 0$) and along trough lines and wedge lines (because c is perpendicular to ∇p).

A convenient equation for the pressure variation $\partial p/\partial t$ has been deduced by J. Bjerknes [12]. The atmospheric pressure at a level h is equal to the weight of the atmosphere above that level. Therefore,

$$(2) \qquad\qquad p_h = \int_h^\infty g\rho \, dz$$

The equation of continuity is

$$\frac{1}{\rho}\frac{d\rho}{dt} = -\operatorname{div} v = -\left(\frac{\partial v_x}{\partial x} + \frac{\partial v_y}{\partial y} + \frac{\partial v_z}{\partial z}\right)$$

This gives

$$(3) \qquad \frac{\partial \rho}{\partial t} = -\rho\left(\frac{\partial v_x}{\partial x} + \frac{\partial v_y}{\partial y} + \frac{\partial v_z}{\partial z}\right) - \left(v_x\frac{\partial \rho}{\partial x} + v_y\frac{\partial \rho}{\partial y} + v_z\frac{\partial \rho}{\partial z}\right)$$

Differentiating Eq. (2) with respect to time, we obtain the following expression for the pressure variation in a fixed point at the level h:

$$(4) \qquad\qquad \left(\frac{\partial p}{\partial t}\right)_h = \int_h^\infty g\frac{\partial \rho}{\partial t}\, dz$$

Combining this with the equation of continuity, and rearranging the terms, we obtain

$$\left(\frac{\partial p}{\partial t}\right)_h = -\int_h^\infty g\rho\left(\frac{\partial v_x}{\partial x} + \frac{\partial v_y}{\partial y}\right) dz - \int_h^\infty g\left(\rho\frac{\partial v_z}{\partial z} + v_z\frac{\partial \rho}{\partial z}\right) dz$$
$$- \int_h^\infty g\left(v_x\frac{\partial \rho}{\partial x} + v_y\frac{\partial \rho}{\partial y}\right) dz$$

Here,

$$\frac{\partial v_x}{\partial x} + \frac{\partial v_y}{\partial y} = \operatorname{div}_2 v = \text{horizontal divergence}$$

and

$$-\int_h^\infty g\left(\rho\frac{\partial v_z}{\partial z} + v_z\frac{\partial \rho}{\partial z}\right) dz = (g\rho v_z)_h$$

Substituting this in the above equation, we obtain the so-called *tendency equation* which will form the basis for the subsequent discussion:

$$(5) \quad \left(\frac{\partial p}{\partial t}\right)_h = -\int_h^\infty g\rho \text{ div}_2 \, v \, dz + (g\rho v_s)_h - \int_h^\infty g\left(v_x \frac{\partial \rho}{\partial x} + v_y \frac{\partial \rho}{\partial y}\right) dz$$

This equation shows that the barometric variation in a fixed point at the level h is controlled by three factors, *viz.*:

1. The horizontal divergence in the air column above the level h, convergence of flow causing rising pressure, and divergence of flow causing falling pressure. The first term on the right-hand side, therefore, measures the disappearance of mass through horizontal outflow from an air column of unit cross section extending from the level h to the upper limit of the atmosphere.

2. The transport of air through the base of the said air column; upward transport into the air column, causing rising pressure; and downward transport out of the air column, causing falling pressure. The second term on the right-hand side, then, expresses the accumulation or depletion of mass in the air column through vertical motion. If we consider an air column with its base on the earth's surface, the term vanishes because $v_s = 0$; *i.e.*, no mass disappears from, or is brought into, the air column through the earth's surface.

3. The advection of density by horizontal motion. The third term on the right-hand side is important when the horizontal gradient of density is considerable, *e.g.*, when cold and warm air masses replace one another; it is positive when cold air replaces warm air, and it is negative when warm air replaces cold air. The advective term vanishes in homogeneous air. It also vanishes when the wind blows along the lines of equal density. Although the advection term is important in the lower atmosphere, its influence decreases rapidly with elevation because (1) the density gradient decreases with the density and (2) the winds in the upper atmosphere have a marked tendency to blow along the lines of equal density.

The tendency equation in connection with the deepening equation [*i.e.*, Eq. (1)] may now be used for discussing the deepening of cyclones. It will be seen from Eq. (5) that the pressure variations depend primarily on the distribution of wind. As direct wind observations are unreliable, we shall here resort to the relations between wind and pressure given in Chap. IV in order to discuss the types of wind distribution that occur at different levels in moving cyclones.

132. Divergence and Convergence in Simple Isobaric Systems.—The tendency equation has been used by J. Bjerknes[1] to explain the pressure variations that occur in connection with moving cyclones.

---

[1] Part of his results were published in the paper quoted in Par. 131. Additional results were presented in four lectures at the Massachusetts Institute of Technology, November, 1939.

We shall first discuss the first term on the right-hand side in Eq. *131*(5) in connection with simple models of isobaric patterns that occur in moving cyclones and shall apply the expressions for divergence and convergence developed in Par. 100. The results may then be checked by the aid of the vorticity equation [*i.e.,* Eq. *100*(16)].

1. *Straight Isobars.*—Neglecting the influence of friction, we may say that the wind distribution is controlled by three terms (*cf.* Par. 89), *viz.*: the geostrophic, the cyclostrophic, and the accelerational term. Figures 158*A* and *B* show systems of straight isobars: *A*, with converging isobars
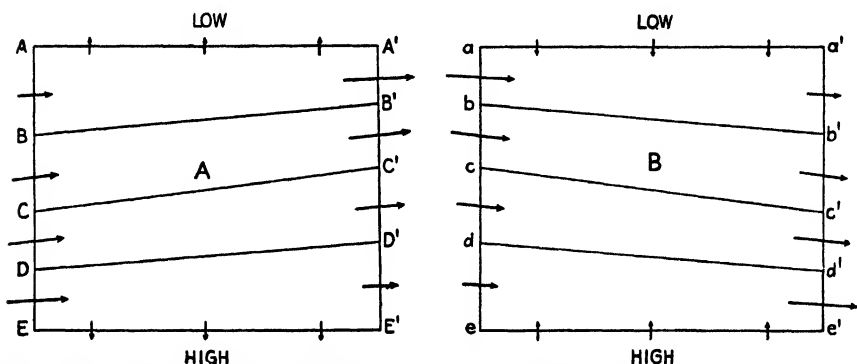
Fɪɢ. 158.—Convergence and divergence in fields of straight isobars. *A*, divergence; *B*, convergence.

to the north and diverging isobars to the south; and *B*, with diverging isobars to the north and converging isobars to the south. In these fields, the cyclostrophic term vanishes, and the wind is determined by the geostrophic term and the accelerational term. The divergence of the geostrophic wind is expressed by Eq. *100*(8). As the solenoid term is very small and as the isobars in Fig. 158 on the whole run from east to west, the latitute effect integrated over the areas in Fig. 158 will vanish. Under the conditions shown in Fig. 158, the divergence of the geostrophic wind is altogether negligible. This, interpreted, means that the geostrophic import of air across the line *AE* will be the same as the geostrophic export of air across the line *A'E'*. The same also applies to the lines *ae* and *a'e'*.

It was shown in Par. 100 that the accelerational term will cause the air to flow across the isobars, with a component toward lower pressure when the wind is accelerated and a component toward higher pressure when the wind is decelerated. Therefore, when the air moves from the section *AB* toward the section *A'B'* or from *de* toward *d'e'*, it will have a component of velocity to the left of the isobars. Conversely, the air will have a component of velocity to the right of the isobars along the border lines *EE'* and *aa'*. From this, it follows that *the accelerational*

term will cause divergence of air from the area $AA'E'E$ and convergence of air into the area $aa'e'e$.

2. *Parallel Sinusoidal Isobars.*—Following Bjerknes, we consider equidistant isobars of sinusoidal shape as shown in Fig. 159. The pressure gradient is constant along each isobar. Assuming that the wind everywhere is gradient wind, Eq. *100*(7) expresses the horizontal divergence. This equation may be integrated over suitable areas. As the gradient wind everywhere is parallel to the isobars, the integral of div$_2$ v over an
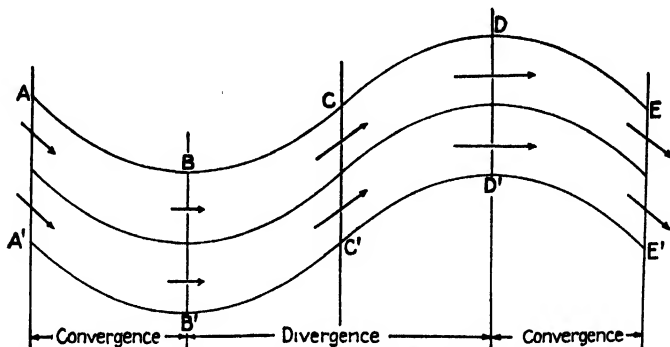
Fig. 159.—Convergence and divergence in fields of sinusoidal equidistant isobars.

area bounded by two isobars and cross sections normal to the isobars would be equal to the difference between the import of air across one and the export of air across the other section. These transports of air can be computed directly from the gradient-wind equation. We have

$$(1) \qquad v_{gr} = \frac{1}{2\rho\omega \sin \varphi} \frac{\partial p}{\partial n} \pm \frac{1}{2\omega \sin \varphi} \frac{v_{gr}^2}{r}$$

where the first term on the right-hand side is the geostrophic wind. We consider the air transport through vertical cross sections at BB' and DD', and let letters with indices refer to the section DD'. Let H denote the distance $BB' = DD'$ and Δz the height of the cross section. Then the transport of air per unit time through the cross sections at DD' is

$$(2) \qquad v_{gr}' H \, \Delta z = \left(\frac{1}{2\omega} \frac{\partial p}{\partial n} \frac{1}{\rho' \sin \varphi'} + \frac{1}{2\omega \sin \varphi'} \frac{v_{gr}'^2}{r} \right) H \, \Delta z$$

and the transport through the section at BB' is

$$(3) \qquad v_{gr} H \, \Delta z = \left(\frac{1}{2\omega} \frac{\partial p}{\partial n} \frac{1}{\rho \sin \varphi} - \frac{1}{2\omega \sin \varphi} \frac{v_{gr}^2}{r} \right) H \, \Delta z$$

The divergence (ΔD) from the area $BCDD'C'B'$ is therefore

$$(4) \quad \Delta D = H \, \Delta z \frac{1}{2\omega} \frac{\partial p}{\partial n} \left(\frac{1}{\rho' \sin \varphi'} - \frac{1}{\rho \sin \varphi} \right) + H \, \Delta z \frac{1}{2\omega r} \left(\frac{v_{gr}'^2}{\sin \varphi'} + \frac{v_{gr}^2}{\sin \varphi} \right)$$

The first term on the right-hand side is due to the latitude effect on the divergence of the geostrophic wind in conformity with Eq. *100*(8). The difference between $1/\rho'$ sin φ' and $1/\rho$ sin φ contains the solenoidal effect, which usually is negligible. Moreover, as the air in the northernmost section will have larger density than the air in the southernmost section and as $\varphi' > \varphi$, it follows that the first term on the right-hand side of Eq. (4) is negative. The geostrophic wind, therefore, causes convergence in those compartments of Fig. 159 where the air moves from south to north. Conversely, the geostrophic wind causes divergence in those compartments of Fig. 159 where the air moves from north to south. This agrees with the results derived in Par. 100.

The second term in Eq. (4) represents the cyclostrophic divergence of air from the compartment $BCDD'C'B'$. This term gives divergence from the compartment $BCDD'C'B'$ and convergence into the compartments $ABB'A'$ and $DEE'D'$.

The question then arises: Which of the two terms predominates? The following computations will show the order of magnitude and the relative importance of the geostrophic and the cyclostrophic terms. Suppose that the points B', B, D', and D have the latitudes 40, 50, 50, and 60°N, respectively, that the pressure gradient is 5 mb./200 km., and that the radius of curvature is 1000 km. We then obtain the following values for the transports in 3 hr. when $\Delta z = 2000$ m.:

1. Geostrophic transport of air through the section

$$DD' = 4.48 \times 10^{11} \text{ tons.}$$

2. Geostrophic transport of air through the section

$$BB' = 5.25 \times 10^{11} \text{ tons.}$$

3. Difference between (1) and (2) $= -0.77 \times 10^{11}$ tons.
4. Cyclostrophic transport of air through the section

$$DD' = 1.06 \times 10^{11} \text{ tons.}$$

5. Cyclostrophic transport of air through the section

$$BB' = -0.81 \times 10^{11} \text{ tons.}$$

6. Difference between (4) and (5) $= 1.87 \times 10^{11}$ tons.
7. Sum of (3) and (6) $= 1.10 \times 10^{11}$ tons.

This shows that there is divergence from the area $BCDD'C'B'$. When the radius of curvature of the path is 1000 km. or less, the cyclostrophic term is by far the larger one. The net result is therefore divergence of air from the compartment $BCDD'C'B'$ and convergence of air into the compartments $ABB'A'$ and $DEE'D'$. As convergence means accumulation and divergence means depletion of air, it follows from Eq.

131(5) that horizontal convergence would cause falling pressure in the compartment $BCDD'C'B'$ and rising pressure in the other compartments of Fig. 159. The limits between areas of convergence and divergence coincide with the lines BB' and DD'. Along these lines, there would be no pressure variations; the pressure fall caused by horizontal divergence would have a maximum along the line CC', and the pressure rise caused by convergence would have a maximum along the lines AA' and EE'. With this distribution of barometric tendencies, the troughs and wedges would move in the direction of the wind (*i.e.*, from the left toward the right in Fig. 159), but the wind would have to move faster than the pressure systems. Bjerknes ascribes the propagation of the upper perturbations mentioned in Par. 130 to this effect.

It is of interest to note that if the wave length in Fig. 159 increases, the cyclostrophic contribution would decrease relative to the geostrophic contribution. For very large wave lengths, the two contributions would balance, and there would be neither convergence nor divergence. There would therefore be no pressure variations, and the waves would be stationary. Such waves, which were first studied by Rossby [67a], have wave lengths of the order of magnitude of the large centers of action in the general circulation. For such wave lengths as occur in connection with moving cyclones, the cyclostrophic term predominates, and the distribution of divergence and convergence will then be as shown in Fig. 159.

In the discussion of Fig. 159, it was assumed that there was no acceleration except what is due to the centrifugal force. It is, however, easily seen that this assumption does not appreciably alter the results. That this is so may be shown in the following manner: When a parcel moves from AA' to BB', it increases its cyclonic vorticity; when it moves from DD' to EE' it decreases its anticyclonic vorticity. According to Eq. *100*(16), it is necessary that there be convergence within the compartments $ABB'A'$ and $DEE'D'$. Likewise, if a parcel moves from BB' to CC' it decreases its cyclonic vorticity; when it moves from CC' to DD', it develops anticyclonic vorticity. According to Eq. *100*(16), there must then be divergence within the compartment $BCDD'C'B'$. The lines separating areas of divergence and convergence must then be the lines BB' and DD'. The vorticity equation, therefore, gives the same results as do the simplified computations of the convergence and divergence of the gradient winds.

3. *Diverging and Converging Sinusoidal Isobars.*—The case discussed above consisting of sinusoidal isobars with constant distance between them is seldom found in the atmosphere. What is actually found, particularly in the upper atmosphere, are pressure fields that resemble certain combinations of Figs. 158 and 159. We need here discuss only

those combinations which show a resemblance to the pressure fields with sinusoidal isobars, shown in the third row in Fig. 156. Such fields result through the superposition of Fig. 158B on the compartments $AA'BB'$ and $DD'EE'$, and Fig. 158A on the compartment $BCDD'C'B'$ in Fig. 159. The resultant pressure field is illustrated schematically in Fig. 160. Comparison between the diagrams shows that the accelerational effect shown in Fig. 158 adds to the effect of the gradient wind and increases the intensity of convergence and divergence.

The accumulation of air to the right of the wedge would cause rising pressure, and the removal of air to the right of the trough would
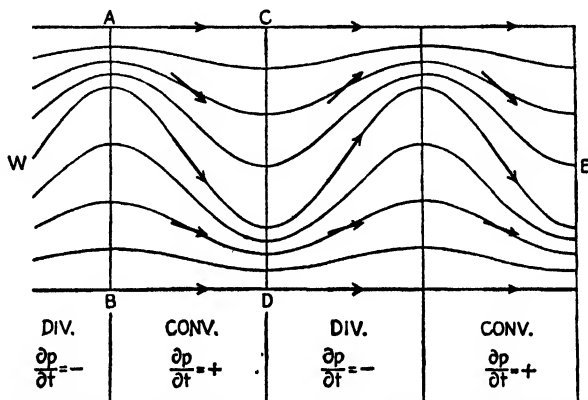
FIG. 160.—Divergence and convergence in diverging and converging sinusoidal isobars.
(After J. Bjerknes.)

cause falling pressure. The wedges and troughs in Fig. 160 would propagate from the left toward the right, in the direction of the general air flow.

If, in the above superimposition of simple isobaric fields, Figs. 158A and B were interchanged, we should obtain other types of motion that give a minimum of divergence and convergence. As these types are not observed in connection with moving cyclones, they will not be discussed here.

4. *Closed Isobars.*—Just as the transport of air through various cross sections was computed from Fig. 159, we may compute the gradient-wind transport through vertical cross sections north and south of the center in cyclonic and anticyclonic systems. Such computations have been made by J. Bjerknes, who has shown that there is convergence within the two quadrants of closed cyclonic isobars in which the air moves northward and divergence within the two quadrants in which the air moves southward. These results agree in the main with those deduced in Par. 100 by means of the vorticity equation. The distribution of

convergence and divergence in systems consisting of closed cyclonic iso-
bars will therefore be as shown in Fig. 108.

As convergence would tend to cause rising pressure and divergence
would tend to cause falling pressure, one arrives at the paradoxical result
that the pressure ought to rise in advance and fall in the rear of moving
cyclones; this distribution of barometric variations is contradictory to the
fact that cyclones must move in the direction from rising to falling pres-
sure.   The paradox is, however, only an apparent one.   It will be seen
from Fig. 156 that the pressure distribution aloft is of the type illustrated
in Fig. 160, which causes divergence of the flow above the closed isobars
in the lower atmosphere.   This is particularly true of cyclones in the
early stages of development.   As the pressure variations at the ground
depend on the integral of divergence throughout the air column, it follows
that the convergence in advance of a cyclonic center at the ground may
be overcompensated by the divergence at higher levels.   Moreover, as is
seen from the tendency equation, the barometric variations depend not
only on the divergence but also on the vertical velocity and the advection
of air of different density.   We shall therefore turn to the tendency equa-
tion in order to explain the development, the propagation, and the
deepening of the pressure systems that accompany moving cyclones in
extratropical latitudes.

133. The Pressure Variations in Moving Cyclones.—The deepening
Eq. *131*(1) shows that the pressure variation in a fixed point (*i.e.*, $\partial p/\partial t$)
is composed of two parts: one that depends on the velocity of propagation
of the pressure system (*i.e.*, $c \cdot \nabla p$), and one that depends on the deepen-
ing or filling (*i.e.*, $\delta p/\delta t$) of the pressure system.   Consequently, there are
two aspects to consider, *viz.*: the pressure variations that cause the pres-
sure system to move, and the pressure variations that cause the pressure
system to deepen or fill.   Following J. Bjerknes and applying the results
developed in Pars. 130 to 132, we shall discuss below the two aspects of
pressure variations.

We consider first the pressure distribution in the nascent cyclone
(Fig. 156*B*).   In advance of the warm front, the trend of the isobars at
the earth's surface is such that there will be divergence.   This will cause
the pressure to fall in advance of the warm front.   In addition, the motion
is such that warm air replaces cold air.   According to Eq. *131*(5), the
advection term would cause falling pressure.   The first and the last term
in the tendency equation will therefore combine to cause falling pressure
in the air under the warm-front surface.   At the earth's surface, the term
$(g\rho v_z)_h$ in the tendency equation vanishes because $v_z = 0$ at the surface.
The pressure variation at the ground is therefore solely controlled by the
advection term and the divergence term.   In the cold air under the warm-
front surface, there is slight ascending velocity.   This would then cause

a slight pressure rise; but since v_z is small in the cold air, the term depending on the vertical velocity will be small. The net result, therefore, is that there is falling pressure at all levels under the warm-front surface. As the advection term in Eq. *131*(5) depends on the density gradient, it is readily seen that advective pressure fall will be proportional to the temperature contrast at the front and the slope of the frontal surface.

In the warm sector of Fig. 156*B* at the ground, both the last two terms in Eq. *131*(5) tend to vanish because $v_z = 0$ at the ground and because the air in the warm sector is quasi-homogeneous. The falling pressure that is observed in the warm sector at the ground must therefore be due to the first term in the tendency equation, *i.e.*, to horizontal divergence in the air column. This agrees with Fig. 156*C*. The air above the warm sector at the ground moves from a trough of low pressure toward a wedge of high pressure. According to Pars. 132 to 133, this gives divergence and a falling barometer. But as the advection term tends to vanish in the warm sector though it does not vanish over the area under the warm-front surface, it follows that the pressure at the ground must fall more in advance of the warm front than in the rear of it. The passage of a warm front will therefore give a kink in the barogram as shown in Figs. 134*a* and *b*.

At the peak of the warm sector of the nascent cyclone, the pressure variation must be negative. That this is so follows from the deepening equation: in the warm sector the horizontal pressure gradient is perpendicular to the velocity of propagation of the wave. It follows then that

$$\frac{\delta p}{\delta t} = \frac{\partial p}{\partial t}$$

and as an unstable wave must deepen, $\partial p / \partial t < 0$. Within the warm sector, the air is fairly homogeneous; the advection term is therefore very small. However, as the tropopause also is set in wave motion, we must consider the advective influence at this level. The air immediately under the crest of the tropopause wave is colder than the air above the trough of the tropopause wave. That this is so follows from the fact that the air under the tropopause has a steep lapse rate, whereas the air above the tropopause is more or less isothermal. The stratospheric air in the trough of the tropopause wave must therefore be less dense than the tropospheric air under the crest of the tropopause wave. As the wave passes over a station, cold air at the tropopause level will be replaced by warm air. Thus, at this level, the advective term in the tendency equation gives a negative contribution to the pressure variation in the warm sector at the ground. Thus, the falling pressure that is observed at the ground in the warm sector must be due to divergence and advection

aloft. Within the friction layer there may be frictional convergence, but the effect of this is overcompensated by the divergence and advection aloft.

We consider next the conditions in the rear of the cold front. Here the sloping frontal surface will cause a marked rise in pressure on account of advection. Moreover, the trend of the isobars below the frontal surface is such (*cf.* Fig. 160) that convergence should occur. For both these reasons, the pressure at the ground must rise. The conditions above the cold-front surface are, however, different. The isobars in the warm current above the cold air have a trough at some distance behind the front at the ground. Within the region from the cold front to the trough line aloft, there would be divergence as shown in Fig. 160. This would then deduct from the advective pressure rise at the ground. Moreover, in advance of the trough of the tropopause wave, there would be advection of less dense air; and this, too, would give a negative contribution to the barometric variation at the ground. Within the region behind the cold front at the ground and in advance of the trough of the tropopause wave, the upper and the lower strata would cause opposite pressure variations, with the result that the pressure rise in the rear of the cold front at the ground is less than what the advection in the lower atmosphere would cause. In the nascent cyclone, the upper perturbation is slight, and the pressure variations at the ground conform fairly closely with what one should expect from advection in the lower atmosphere. However, as the cyclone develops further, the upper perturbation becomes more pronounced and gives an increasing contribution to the pressure variations at the ground.

The next question to consider is: How do the upper perturbations increase in magnitude? In order to answer this question, we consider the isobars in Fig. 156 above the frontal surface. Comparing these isobaric patterns with Fig. 160, we see that horizontal convergence and divergence would give $\mathrm{div}_2\, v = 0$ at the trough lines and wedge lines. The horizontal convergence and divergence would therefore cause no change in pressure along the trough lines and wedge lines. The distribution of pressure variations caused by convergence and divergence would therefore cause the upper perturbations to move but not to deepen or fill. That this is so is deduced from the deepening equation. On the trough line and wedge line, $c \cdot \nabla p = 0$; therefore, if $\partial p/\partial t = 0$, the deepening term $\delta p/\delta t = 0$.

Furthermore, at the trough and at the crest of the tropopause wave, the advective term vanishes because the tropopause is there horizontal. In order to obtain an increase in the upper perturbation, it is necessary to have $(\partial p/\partial t) < 0$ along the trough line and $(\partial p/\partial t) > 0$ along the wedge line. But as neither the advection term nor the divergence term

in the tendency equation gives such pressure variations at the upper troughs and wedges, it follows that the term $(g\rho v_z)_h$ must be responsible for the increase in amplitude of the upper pressure wave aloft. This term is positive where the air ascends and negative where the air descends. As the warm air in Figs. 156*A* and *B* supposedly moves faster than the cold air, it follows that the warm air must descend above the cold-front surface and rise above the warm-front surface. The term will therefore give falling pressure in the trough above the cold-front surface and rising pressure on the wedge above the warm-front surface. This is exactly the distribution of barometric tendencies that results in increasing amplitude of the upper pressure waves. As these waves develop, they reflect their influence on the pressure distribution at the ground.

The pressure variations aloft, expressed by the term $(g\rho v_z)_h$, will therefore cause the upper perturbation to increase; the isobars in the upper layers will become more sinusoidal, and this results in the increasing of the latitude effect of the cyclostrophic flow and of horizontal divergence in the layers above the cyclone at the ground. According to J. Bjerknes (*loc. cit.*, Par. 132), this depletion of air aloft is the essential cause of the deepening of cyclones.

As the nascent cyclone deepens in this way, the effect accumulates downward through the warm air, and a maximum effect is observed at the ground. Closed isobars develop at the earth's surface, as shown in Figs. 156*C* and *D*. Within the region of closed isobars, there must be convergence of flow in advance of the center and divergence in the rear. This gives a positive contribution to the pressure at the ground in advance of the cyclone and a negative contribution in the rear. This effect is counteracted by the divergence and convergence and other factors aloft. The result is that the cyclone continues to deepen until the cyclonic whirl in the regions of closed isobars have spread through a deep column of air (*cf.* Fig. 156*E*). The effect of convergence and divergence within the closed isobars will then be balanced by the opposite distribution of convergence and divergence aloft. The deepening at the ground then ceases; and as the development goes on, the center begins to fill up at the ground, though it may still develop at high altitudes. This development is corroborated by synoptic maps at high and low altitudes.

The convergence within the closed isobars in advance of the center and the divergence within the isobars in the rear of the cyclone would cause pressure variations that would tend to decrease the speed of the cyclonic center. This agrees with what is actually observed. The nascent and the young cyclones travel with considerable speed; but when closed isobars develop and when these become crowded around the center, the speed decreases. That this is so will appear also from the kinematic considerations in Chap. IX.

The result of the above discussion is perhaps better illustrated in terms of barograms. Figure 161 shows a cross section through a young cyclone and the barogram that would result at various levels during the passage of such a cyclone. The upper perturbation causes the barograph trace at the ground to be asymmetrical. If there were no upper perturbation, $\partial p/\partial t = 0$ in the warm sector. On account of the upper wave, there will be a pressure fall [*i.e.*, $\partial p/\partial t) < 0$] in the warm sector. Since $c \cdot \nabla p = 0$ in the warm sector, it follows that $(\delta p/\delta t) < 0$, which means that the cyclone deepens. A further result of the upper perturbation is that a dent develops in the barogram in the rear of the cold front. As the cyclone develops, this dent increases, and an elongated trough of low
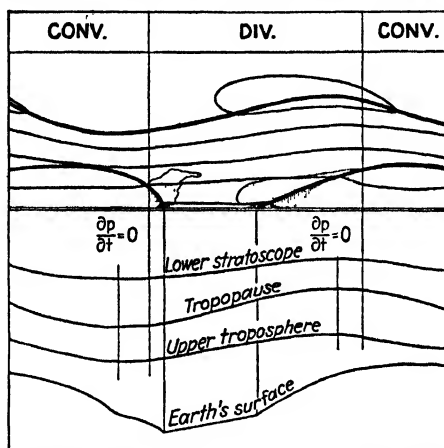
Fig. 161.—Thermo-isopleths (upper portion) and barograms (lower portion). (*According to J. Bjerknes.*)

pressure develops in the rear of the cyclone in the isobars at the ground. This trough, which is nothing but the reflection of the upper pressure wave in the pressure distribution at the ground, is often erroneously interpreted as a frontal trough, and a "bent-back" occlusion is often drawn in it.

On the basis of the above discussion, it is possible to indicate the normal distribution of barometric tendencies in the vicinity of moving cyclones. It suffices to illustrate the principle by means of a young cyclone, as shown in Fig. 162. If advection of cold and warm masses were the only factor in operation, there would be no barometric change in the warm sector since there is no appreciable component of temperature gradient in the warm mass in the direction of the motion. The largest falling tendencies would occur in advance of the warm front where the slope of the frontal surface in the direction of the velocity of the center has a maximum. In a similar manner, the largest rising tendencies

would be in the rear of the northern part of the cold front. The distribution of the "advection" barometric tendencies is shown in Fig. 162A.

The tendencies due to the upper perturbation are shown in Fig. 162B. The upper perturbation would diminish with increasing distance from the center in the north-south direction. In a zonal cross section, $\partial p/\partial t = 0$ along the lines indicated in Fig. 161. The greatest pressure fall would occur in advance of the trough of low pressure in the upper atmosphere, and the greatest rise would occur in the rear of the trough. Through superimposition of Figs. 162A and B, we obtain the resulting barometric tendencies at the ground as shown in Fig. 162C. This agrees well with what is observed. It is worthy of note that the "advection" tendencies are discontinuous at the front because of the frontal discontinuity, whereas the "upper-perturbation" tendencies are continuous through the front. The resulting tendencies must therefore be discontinuous. This agrees with the deduction in Par. 119. It will be shown in Chap. X that the deepening tendency $\delta p/\delta t$ is continuous whereas the observed resultant tendency is discontinuous at the fronts.

The theory of the pressure variations outlined above explains in a qualitative manner the observational facts. If detailed pressure maps could be drawn for different levels in the troposphere and in the lower

Fig. 162.—Distribution of barometric tendencies around a young cyclone. *A*, tendencies due to advection of cold and warm masses; *B*, tendencies due to the upper perturbation; *C*, resultant tendencies.

portion of the stratosphere, it would be possible to integrate the tendency equation, and the contributions of the various layers to the pressure variations could be evaluated. On the basis of such charts, the future pressure charts could be computed to show the movement and the development of pressure systems. The upper-air data are as yet too scanty for a detailed analysis, but the method of attack inaugurated by Bjerknes seems to promise much for the future. In this connection, it may be remarked that nature itself integrates the equation of static equilibrium and the tendency equation. The pressure and pressure tendencies observed at the ground represent such integrals. These integrals do not tell us how much variation is due to divergence, vertical velocity, or advection; they give only the sum total of these effects.

However, as the movement and the development of the pressure system depend on this sum total, it is possible to compute the displacement and the development of pressure systems. Chaps. IX and X deal with these problems.

134. Bent-back Occlusions.—It was shown in the last paragraph that there is a tendency for a trough of low pressure to form in the rear of moving cyclones, particularly in their later stages of development. As a pressure trough may also occur along fronts, it has become customary to prolong the occluded front from the center of the depression into the pressure trough in its rear. These fronts are understood to be part of the occlusion that has been caught by the easterly and northerly currents to the northwest of the center and brought down with the current so as to approach the original cold front. Such fronts are called bent-back occlusions.

FIG. 163.—Showing the formation of a bent-back occlusion.

There can be little doubt that most of the bent-back occlusions drawn on the weather maps are not real fronts. The best evidence for this statement is the fact that the pressure trough in which the front is placed moves with a speed less than the wind velocity normal to the trough line. If the trough were of frontal origin, it would have to move with the front, which could not move slower than the wind. As was explained in Par. 133, the trough in the rear of a developed depression is the reflection of the pressure trough belonging to the upper perturbation. The movement of this trough is, of course, independent of the wind distribution at the earth's surface.

On the other hand, it happens sometimes that a real bent-back occlusion exists. It is therefore of interest to indicate under which circumstances the formation of a bent-back occlusion is possible or impossible.

We consider first an occluded cyclone whose center is stationary. Since the surface winds converge toward the center, it follows that the occluded front cannot prolong itself backward into the current in the rear of the cyclone. The front would be rolled up around the center while it dissipates. Bent-back occlusions, therefore, cannot form in stationary or slowly moving cyclones.

Let us next consider a partly occluded cyclone as shown in Fig. 163. If the center A fills up while a considerable deepening takes place at the peak of the warm sector B, a new center of low pressure will form at B while B moves eastward to C and the warm sector occludes. When the new center is formed, the part of the occlusion that was between A and B

will be caught by the current set up around the center *B*. It is then obvious that a bent-back occlusion will result. This development is not a frequent occurrence; but whenever it does occur, a bent-back occlusion should be drawn. The front and the pressure trough that accompanies it must then move with the air current. Moreover, it must be ascertained that the front thus drawn satisfies the general frontal characteristics described in Par. 124.

It was shown in Chap. V that an elongated trough of low pressure may be frontogenetical if the isotherms are favorably arranged in the field of motion. The trough in the rear of the cyclone may therefore develop a front, but this front will then be a secondary cold front and not a bent-back occlusion. Whether or not the trough is frontogenetical can be decided by applying the principles outlined in Chap. V.

In connection with Fig. 163, it is of interest to note that frontogenesis may also occur in the vicinity of the cols in advance and in the rear of the center. This will happen if the field of deformation is strong and if the isotherms north and south of the center are favorably arranged relative to the axis of dilatation. In old occluded cyclones, where the original front may be brought far to the south, the air between the front and the regime of the cols will be heated, and the southernmost parts of the front will be situated in frontolytical fields of motion. In such cases, the original fronts may dissolve while new fronts form within the regime of the northern cols. Many errors in the analysis of weather maps are due to the circumstance that it is not realized that fronts have a tendency to dissolve when they come into the regime of the subtropical anticyclones, while, simultaneously, new fronts may form within the domain of the cols in higher latitudes.

135. Examples Showing the Structure of Moving Cyclones.—The above diagrams of the structure of moving cyclones are idealized models intended to show the typical features. It is therefore well to present some diagrams showing actual cases in order to show to what extent the models may be expected to correspond to reality. The diagrams shown in this paragraph are taken from a recent paper by J. Bjerknes and E. Palmén [15].

On Feb. 16, 1935, at 6 P.M., an occluded front had arrived at the west coast of Norway. The rapid occlusion in the northern part was partly due to the influence of the mountain range (*cf.* Par. 125). To the south of the mountain range, there is a wide warm sector with an indication of a secondary disturbance east of Scotland. The pressure in the center of the occluded cyclone was about 968 mb., and the analysis of the tendencies showed that the center would fill up rapidly. Simultaneously, there was some deepening in the trough of low pressure between Denmark and Norway. A new center is therefore forming over Skagerrak, while the
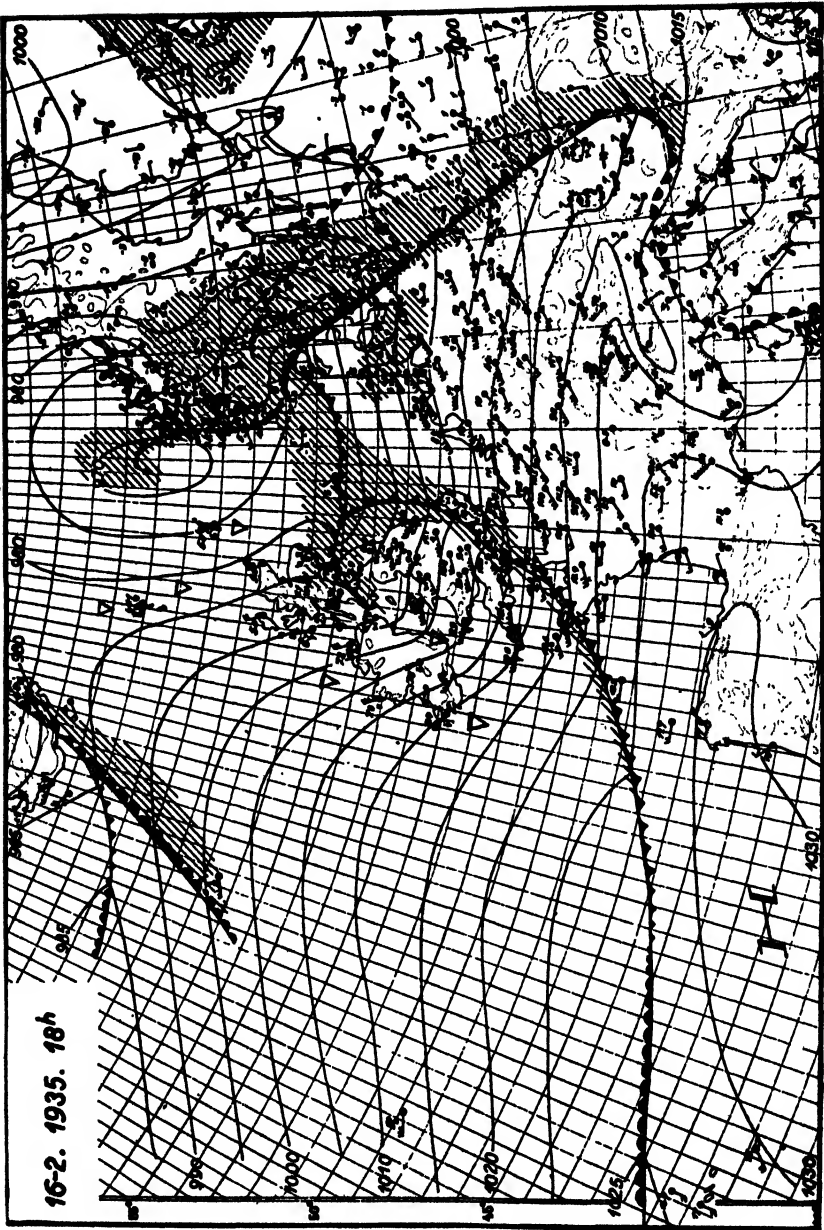
Fig. 164.—Surface weather map, Feb. 16, 1935, 6 p.m., GMT.   (*After Bjerknes and Palmén.*)

old center farther to the north will tend to disappear.   This is just the
case when the conditions are favorable for a bent-back occlusion to form.
The situation the next morning is shown in Fig. 165.   The deepening at
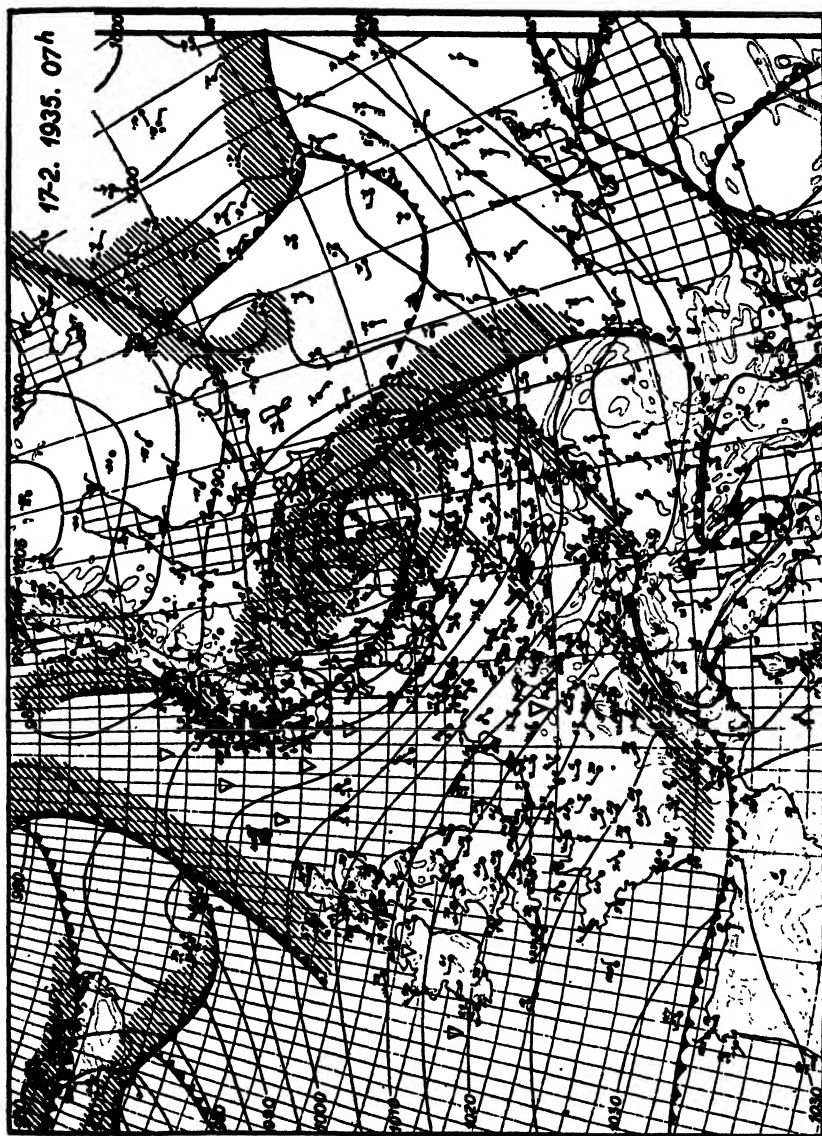
FIG. 165.—Surface weather map, Feb. 17, 1935, 7 A.M., GMT.   (*After Bjerknes and Palmén.*)

the peak of the warm sector has caused a deep center to form, and the
center has moved toward the east, leaving a bent-back occlusion in its
rear.   The polar front in the southwest portion of the map is brought

southward into the subtropical anticyclone where it gradually dissolves. Simultaneously, frontogenesis must have occurred in the region of the col southwest of Iceland, for a system of fronts appears in the Iceland region. The complicated system of fronts in the northwestern and in the northeastern portion of the map will not be discussed here.

Broadly speaking, Fig. 165 contains three principal air masses, *viz.*: tropical maritime air, polar maritime air, and arctic air.   Figure 166 shows the difference between these air masses.   In agreement with what was pointed out in Chap. III, the temperature difference between arctic air
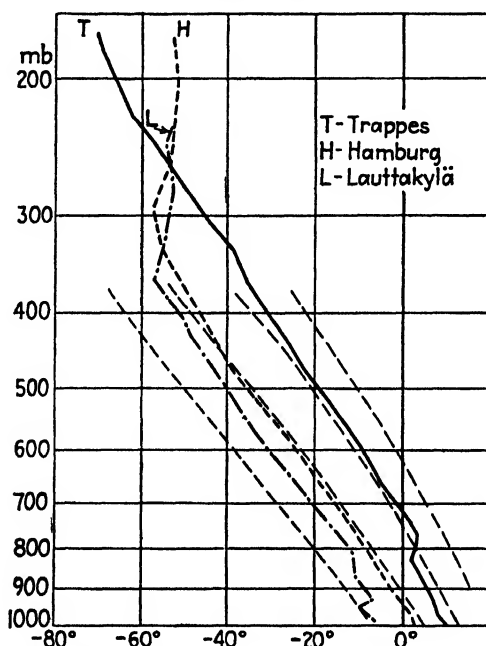
FIG. 166.—Sample ascents in arctic (Lauttakyla, Finland), maritime (Hamburg, Germany), and tropical air (Trappes, France). Stippled lines indicate moist adiabatics. (*After Bjerknes and Palmén.*)

and polar maritime air is greater than the difference between maritime polar air and tropical air.   It is of interest to note from Fig. 166 that the tropopause is found at high altitudes in tropical air and at much lower altitudes above arctic or polar air.   Another interesting feature is the homogeneity of the tropical maritime air.   This is shown in Fig. 167. The temperature within the tropical mass is practically constant in each isobaric surface at Sealand (England), Trappes (France), Madrid (Spain), and Rabat (north Africa), showing that the conditions are quasi-barotropic.

Having a large number of ascents at their disposal, Bjerknes and Palmén were able to carry out a detailed analysis of the structure of the

disturbances shown in Figs. 164 and 165 at various levels and in various cross sections.   Figure 168 shows a cross section from Madrid to Moscow corresponding to Fig. 165.   The diagram intersects the front over Germany just north of the peak of the warm sector.   It will be seen that the warm-front surface reaches up to the tropopause.   This is by no means always so; but when it occurs, the tropause may be vertical, or even "overrunning," as shown in the left portion of the diagram.   Normally, the cold air under the warm-front surface does not fill the entire
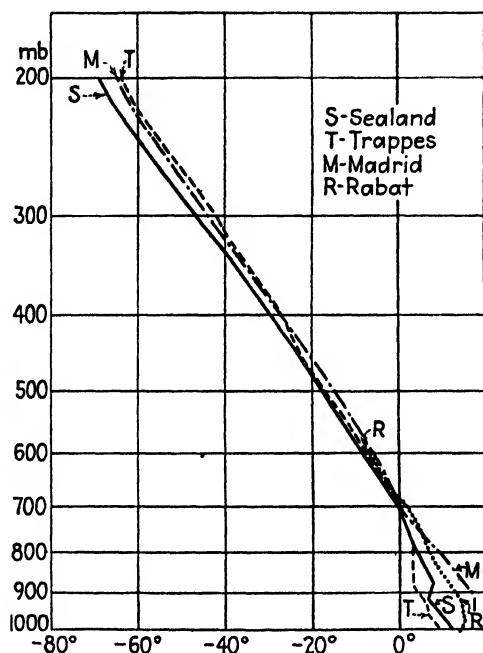
Fig. 167.—Four ascents in tropical air showing quasi-barotropic conditions.   (*After Bjerknes and Palmén.*)

troposphere.   The cross sections will then be as shown diagrammatically in Fig. 156.

A feature of considerable interest is the structure of the tropopause itself.   It is frequently observed that the tropopause consists of two or three layers.   An explanation of the formation of the multiple tropopause has been suggested by Bjerknes and Palmén [15].   The relation between the undulations of the tropopause and the polar-front wave shown in Fig. 168 is found practically in all cases that have been analyzed in detail and agrees with the theoretical models in Fig. 156.

Figure 168 shows that the frontal surfaces are fairly wide zones of transition.   The stable stratification and the concentration of solenoids in the transitional zone are features of general interest.   So also is the

track of the isentropes, with a marked tendency to follow the frontal surfaces. These features agree with the theoretical models shown in Fig. 130.

The motion of the warm air relative to the cold air is of considerable interest, for on it depends the up- or downglide motion that is responsible
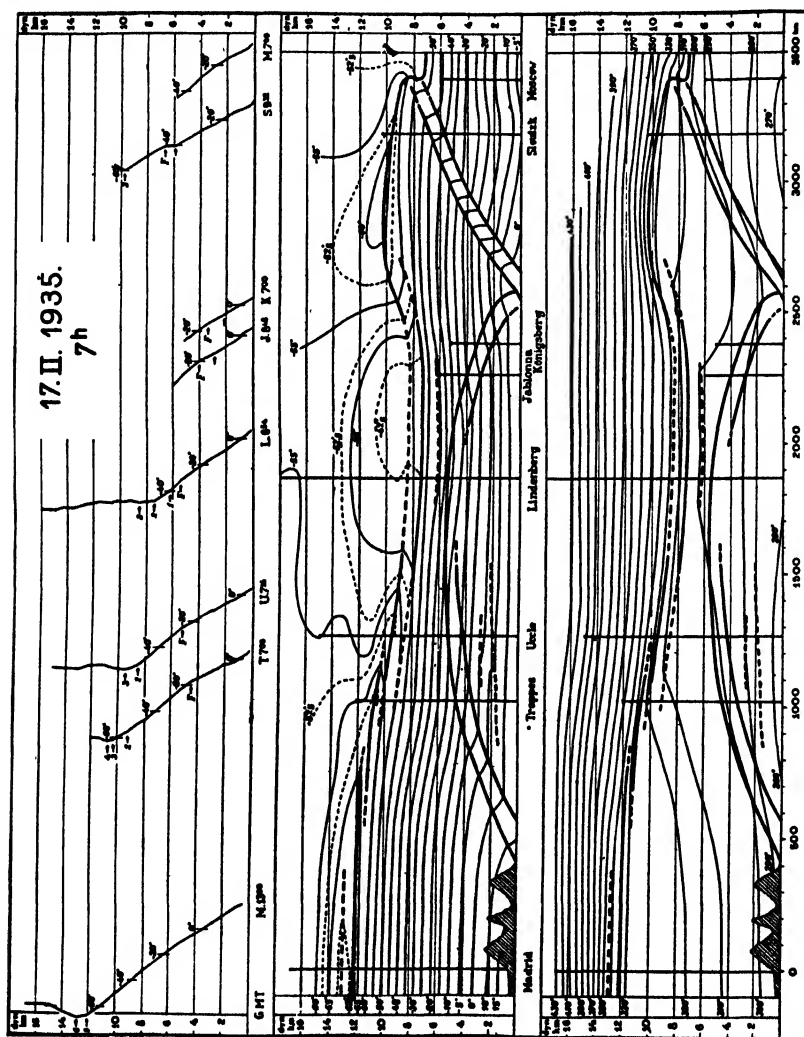
Fig. 168.—Vertical cross section from Madrid to Moscow, morning of Feb. 17, 1935. Top, ascent curves; middle, isotherms; bottom, isentropes or potential isotherms. (*After Bjerknes and Palmén*.)

for the formation or dissolution of cloud systems. Figure 169 shows the conditions at cold and warm fronts and also north of the cyclonic center. It will be seen that the warm air slides downward along the upper portion of the cold-front surface while the warm air at low levels

is forced upward. This distribution of vertical velocity is characteristic of rapidly moving steep cold fronts (see Par. 122). The warm air ascends above the warm-front surface; but on account of the fact that it moves in a field of divergence (see Par. 132), it develops anticyclonic
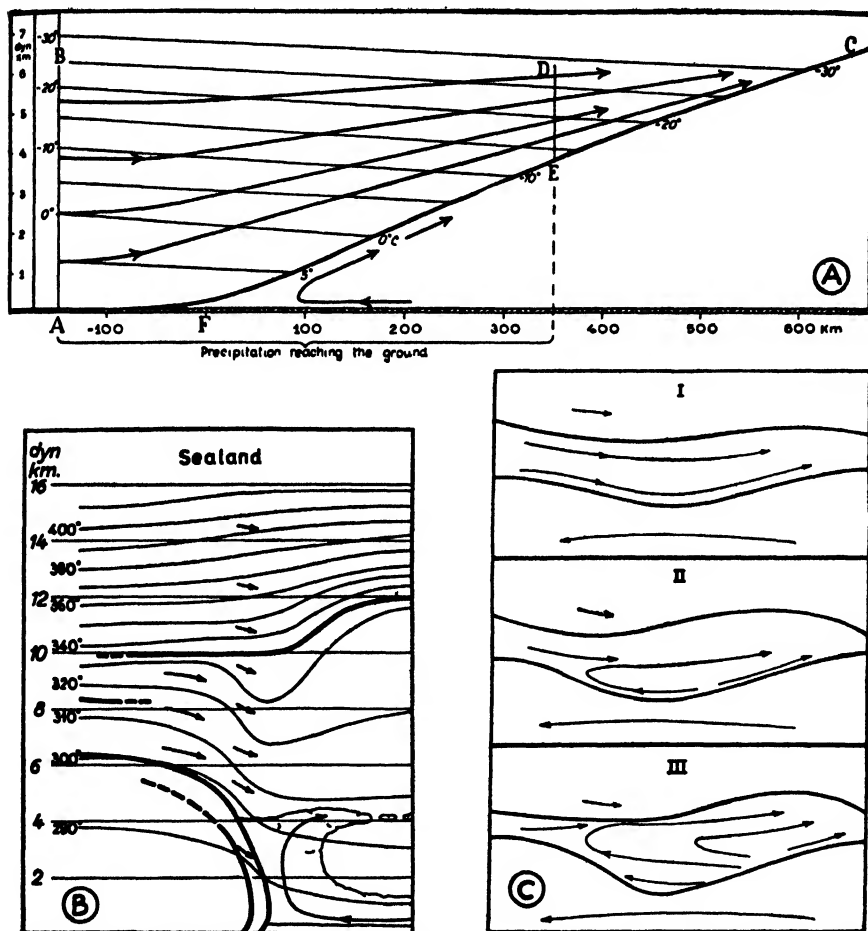
FIG. 169.—*A*, streamlines of motion relative to the moving warm-front surface. *B*, projected motion of the warm air relative to the cold front. *C*, sections north of the moving cyclonic center showing the projected streamlines of the motion relative to the moving center; *I*, nascent cyclone; *II* and *III*, later stages of the deepening cyclone. (*After Bjerknes and Palmén.*)

vorticity. Its steamlines relative to the moving frontal surface will then be curved to the right, with the result that the motion gradually becomes parallel to the contour lines of the frontal surface. A good example of this is shown in Fig. 170. It will be seen that the motion at the 6-km. level is almost parallel to the contour lines. As the frontal cirrus clouds indicate the direction of the flow in the upper portion of the

ascending warm air, their motion will indicate the horizontal direction of the flow at that level. The result of numerous observations of the movement of cirrus clouds in moving young cyclones is shown diagrammatically in Fig. 171. In old cyclones, the cyclonic whirl in the upper atmosphere (see Fig. 156*E*3) will cause the cirrus near the center to move cyclonically around the whirl whereas the frontal cirrus farther to the south will move as shown in Fig. 171. It is of interest to note that the first frontal cirrus that appears ahead of a warm front in a young or partly occluded cyclone often moves from the northwest, whereas the center of the cyclone moves from a westerly or southwesterly direction (*cf.* Fig. 171).
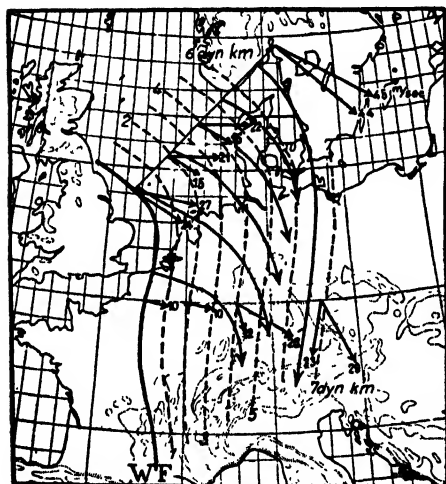
Fig. 170.—Streamlines of the geostrophic motion of tropical air relative to the moving warm-front surface, Feb. 15, 1935, 6 P.M. (*After Bjerknes and Palmén.*)

To return to the weather situation over west Europe as shown by Fig. 165, it is of interest to comment on the structure of the cyclone in the upper atmosphere. This is shown in Fig. 172. It will be seen that the pressure center of the occluded cyclone is well developed
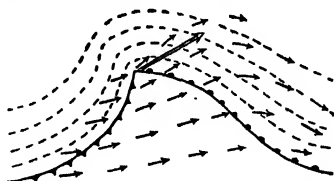
Fig. 171.—Contour lines of frontal surface and direction of motion of cirrus. Double arrow indicates the approximate direction of the movement of the cyclone center.

near the earth's surface where there are four closed contour lines. In the 80-cb. level (*i.e.*, 800 mb.), there are three closed contour lines; in the 40-cb. level (*i.e.*, 400 mb.), there is barely a closed contour line. At higher levels, there are none. This distribution of pressure in the higher levels is in complete agreement with the theoretical models shown in Fig. 156 for developing cyclones.

The upper left map in Fig. 172 shows the topography of the tropopause in relation to the fronts at the ground and the topography of the frontal surface. It will be seen that the cyclone is accompanied by a trough in the tropopause and that this trough is situated in the rear of the cyclone. The minimum altitude of the tropopause is found in the rear of the cyclone where, in this case, the contour lines are closed curves.
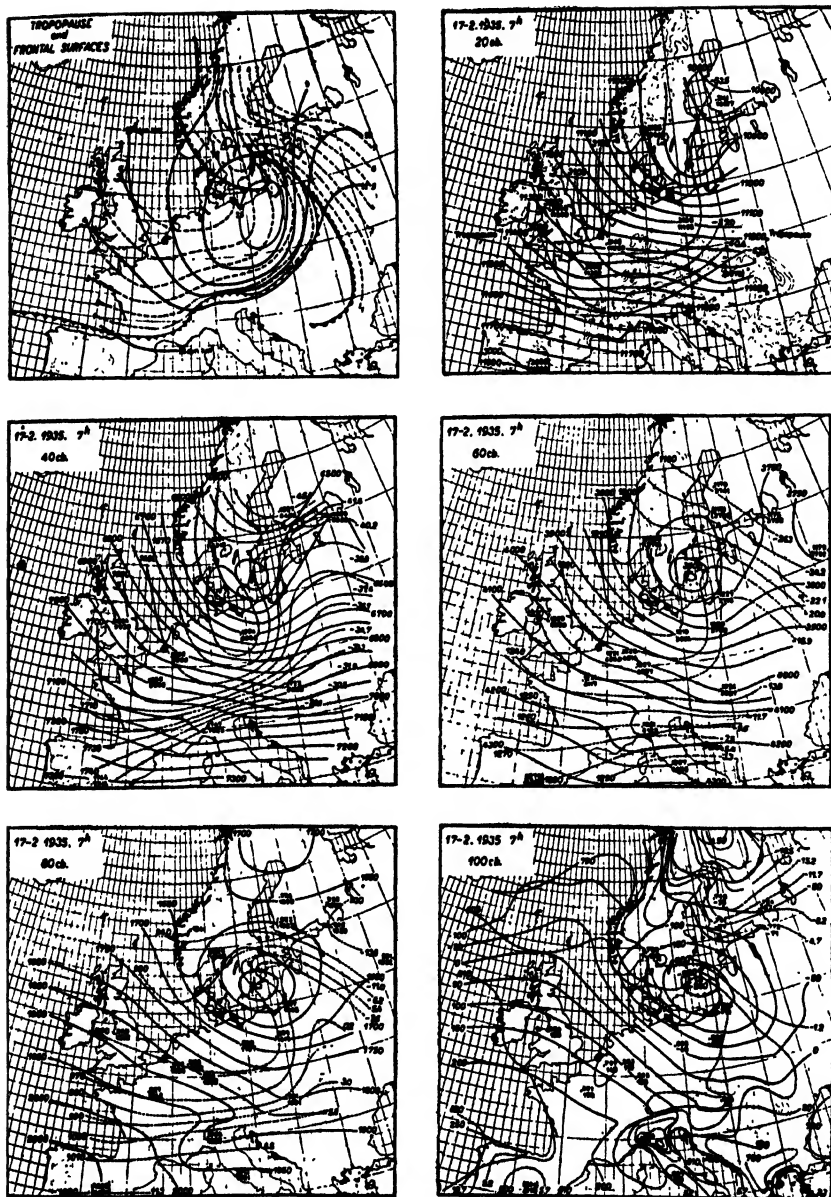
FIG. 172.—Upper left: Topography (dyn. km.) of the tropopause (full lines) and topography of frontal surface (stippled lines). Other maps: Topography of standard isobaric surfaces (full lines) and distribution of specific volume (stippled lines). (*After Bjerknes and Palmén.*)

The low altitude of the tropopause in the rear of the cyclone is due partly to horizontal and partly to vertical oscillations. The horizontal oscillations shown in Fig. 156 would bring southward the lower tropopause from the north in the rear of the cyclone and bring northward the higher tropopause from the south in advance of the center. In addition, the vertical oscillations would lower the tropopause in the rear and raise the tropopause in advance of the cyclone.

Our knowledge of the structure of moving cyclones in the upper atmosphere has been greatly advanced by the investigations of Bjerknes and Palmén. Their paper, referred to above, is recommended as a model of detailed and consistent analysis of an intricate weather situation.

136. Transformation of the Quasi-permanent Circulations through Frontal Action.—It was shown in Chap. V that the general circulation of the troposphere has a tendency to produce fronts along which there is a concentration of isosteric-isobaric solenoids and cyclonic vorticity (shear). On account of the combined effect of the shearing motion and inertia, unstable waves (cyclone waves) form at the tropospheric fronts and develop into large cyclonic whirls. Depending on the degree of instability and the amount of available energy, the cyclones may develop into such dimensions that they substantially affect the large-scale circulation of the atmosphere.

If the polar front were continuous around the entire hemisphere, there would not be a sufficient exchange of heat between high and low latitudes. In order to effect this exchange, it is necessary that polar and arctic air, either continuously or intermittently, be transported into the tropical latitudes and that air from tropical latitudes be transported into polar or subpolar latitudes. Such an exchange of air goes on in almost every cyclone through the horizontal oscillations of the polar front and the occlusion process of the wave disturbances.

A more effective way of exchanging air between high and low latitudes is established through intermittent changes in the quasi-permanent centers of action in the general circulation. The following description, which applies to the Atlantic region, is summarized from "Physikalische Hydrodynamik."

The cyclones of the North Atlantic travel normally toward the east or northeast with the Atlantic subtropical high to the right of their path and the Icelandic low to the left of their path. If the cyclone develops only to a moderate strength, it will not be deeper than the quasi-permanent Icelandic low. It will then appear as a "secondary" depression which travels with the current around the Icelandic low till it arrives in the region of the arctic front. However, if the polar-front cyclone develops to a considerable strength, it will eventually become deeper than the Icelandic low, and, when such a cyclone eventually becomes stationary, it will replace the Icelandic low.

The deeper the cyclone is, the stronger is the southward current in its rear, and the more intense is the meridional exchange of air. The polar front will then be displaced far to the south, and there are then two possibilities for the further development:

1. The southwest current north of the Atlantic subtropical high is strong enough to "repulse" the advancing polar air (Fig. 173). The polar front will then remain north of the subtropical high, and, for every new wave that forms on the front, there will be a wedge of cold air that
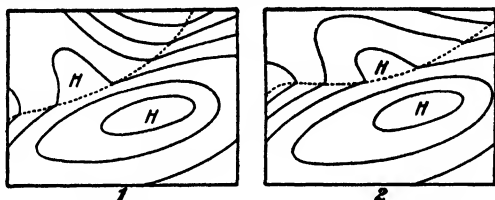
Fig. 173.—Migrating wedges of polar air north of the subtropical anticyclone. (*After Bjerknes and Bergeron.*)
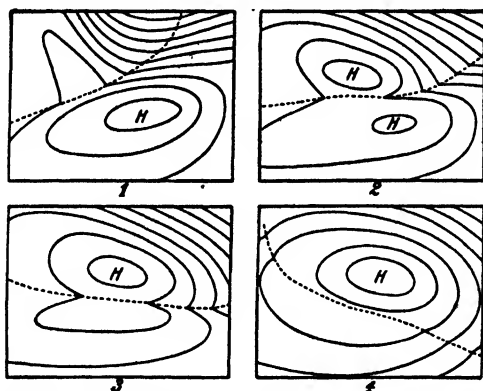
Fig. 174.—Transformation of subtropical anticyclone. (*After Bjerknes and Bergeron.*)

moves eastward. This is shown in Fig. 173. Occasionally, a secondary high with closed isobars may form on the migratory wedge.

2. If the Atlantic subtropical high and the southwesterly current north of it are not strong enough to withstand the onrush of polar air, the polar front will gradually penetrate the high. This will usually take place as illustrated in Fig. 174. The influx of cold air from the north builds up a cold anticyclone north of the polar front while the original warm anticyclone decreases. The front is steadily pushed farther to the south, and the air of polar origin gradually occupies the space of the tropical air. Throughout this development, the polar front will have to pass through a field of motion that is frontolytical. The front will then gradually dissolve. But the result of the development is that polar air has been brought into the source region of tropical air where it gradually is transformed into a *Tm* mass. Simultaneously, the

field of deformation to the west and northwest of the anticyclone forms a new polar front between the Atlantic anticyclone and the high over the American continent. A new front with waves and cyclones will then appear in the normal position. Similar conditions hold also for the Pacific polar front.

This large-scale exchange of polar and tropical masses has a tendency to occur quasi-periodically. Though there is no regular rhythm in these large outbreaks of polar air, the *average* period between them is about 5½ days, and each outbreak lasts for 1 or 2 days. It was shown in Par. 129 that the normal period of oscillation of cyclone waves is about 1 day. Under average conditions, then, there would be about four cyclone waves on the polar front between each outbreak of polar air. This quasi-periodicity in the behavior of cyclones in the North Atlantic region was found in 1921 by J. Bjerknes and H. Solberg [14] and conforms with a somewhat indistinct period of equal length in the weather phenomena found earlier by Defant [23].

FIG. 175.—The cyclone family. (*After J. Bjerknes and H. Solberg.*)

In the space of time between two consecutive outbreaks of polar air, there are then usually four cyclones that travel toward the east or northeast. The first of these, which usually is occluded, travels farthest to the north, and each of the following waves is younger and less developed than its predecessor. With the steady accumulation of polar air north of the front, the front is forced farther and farther to the south, so that the last wave tends somewhat farther to the south than the first one. Such a series of polar-front cyclones was called a cyclone family by J. Bjerknes and H. Solberg (see Fig. 175). The cyclone family is found most regularly over northern oceans in winter. Its period may vary from 3 to 7 days, and the family may consist of three to six members. Its significance for forecasting for ocean areas consists in the fact that, when the forecaster has seen the first and the second member of the family and studied their behavior, he may be on the lookout for the following members, and the expectance of a new member may assist him in interpreting the scanty observations available from the oceans. It would, however, be too risky for the analyst to base his forecast, without observational evidence, on the assumption that a new member would develop. In summer, the cyclone period is highly irregular and sometimes nonexistent. Over continents, the period is highly irregular in all seasons.

CHAPTER VIII

ISENTROPIC ANALYSIS

by Jerome Namias

Through the work of Rossby and his collaborators, a new method of analysis (*i.e.*, isentropic analysis) has been introduced in meteorological literature and forecasting practice in recent years. This method, apart from supplementing the methods of frontal and air-mass analysis, has brought to light a mass of new knowledge of the physical and dynamic processes in the free atmosphere. Many of the results obtained are as yet unpublished. The aim of this chapter will be to give a brief summary of the principles and practice of the isentropic analysis in order to supplement the discussions in Chaps. I, II, III, and VII of this book. An example of isentropic analysis will be found in Chap. XI.

137. Basis for the Analysis.—In Chap. I, we discussed the need in synoptic meteorology for conservative elements by means of which parcels of air may be identified from day to day. It was pointed out that two of the most conservative of these elements are potential temperature and mixing ratio or specific humidity, neither of which changes during adiabatic processes as long as the air remains unsaturated and as long as turbulent redistribution of heat and moisture may be neglected. These two quantities are used as coordinates of the Rossby diagram [63]; and if the points of an aerological sounding are plotted on such a diagram, we obtain the "characteristic" curve. This curve is unaltered during any adiabatic process involving the same particles; for, in this case, the individual points of the curve stay fixed. Thus the characteristic curve may be used to identify vertical air columns as they move over the surface of the earth. Under the assumptions made above, each potential temperature in a series of characteristic curves obtained at different stages in the history of a moving air column will then be characterized by a practically unchanging mixing ratio. We may therefore choose some particular surface of potential temperature and use the mixing ratio on this surface as an identifying element by means of which parcels of adiabatically moving air having the chosen potential temperature may be traced from day to day. The equation (see Par. 4)

$$S = c_p \log \theta + \text{constant}$$

expresses the fact that a surface of constant potential temperature is also a surface of constant entropy, and hereafter we shall speak of it as an *isentropic surface*. Since the atmosphere is normally stable, the potential temperature increases steadily with elevation. We may then consider the atmosphere as consisting of an infinite number of thin isentropic sheets limited by the surfaces $\theta =$ constant, $\theta + d\theta =$ constant, etc.

The above considerations, in part, led Rossby [68, 69] to suggest that upper-air charts be drawn along isentropic surfaces, rather than along constant levels where the comparison of elements from point to point is at times misleading because of ascending and descending motion of the air through these level surfaces. Sir Napier Shaw [73] suggested several years ago that weather maps be drawn along isentropic surfaces and actually constructed a few such charts containing isotherms. He pointed out that isotherms on an isentropic surface were also lines of constant density and constant pressure. But Shaw did not make use of the mixing ratio as a second identifying element to be used on isentropic charts. For numerous reasons, probably mainly because of lack of aerological data at the time, Shaw's suggestion was not put into practice, and the method of analyzing conditions along isentropic surfaces lay dormant until reawakened by Rossby several years later. But other considerations, the fruit of later studies, helped to indicate that isentropic surfaces should be used.

FIG. 176.—Forces resisting displacements from isentropic sheets.

In a study of the Gulf Stream, Rossby [64] found that there is much evidence of large-scale cross current mixing between the Gulf Stream water and its environment and that this mixing takes place along surfaces of constant density.[1] In the atmosphere, where compressibility must be taken into account, it is readily seen that this type of mixing must operate chiefly along isentropic surfaces. In Fig. 176, for example, we have a normal atmospheric stratification in which the potential temperature increases with elevation. A parcel of air originally resting at A, if displaced to the point B, will be subjected to a downward force F_1, since it finds itself colder than its environment (see Chap. II). Similarly, if the parcel is displaced to C, a force F_2 resists the displacement. These restoring forces are proportional to the vertical gradient of potential temperature. But if A is displaced to D, *i.e.*, along an isentropic surface, there is no resisting force, since at each point the particle has the same

[1] Strictly speaking, surfaces of constant potential density.

temperature and density as its environment. Thus, lateral mixing in the atmosphere must take place chiefly along the surfaces of constant potential temperature (isentropes). In saturated air, the mixing operates chiefly along lines of constant equivalent potential temperature. There has also been accumulated considerable evidence in support of the view that the intensity of vertical mixing decreases and the intensity of lateral mixing increases as the vertical stability increases. The latter conclusion is known as Parr's principle [50].

The importance of isentropic mixing in the atmosphere lies in the fact that, if it is of appreciable magnitude, this mixing must lead to sizable shearing stresses operating in nearly horizontal planes (isentropic surfaces) whenever there are variations in wind velocity in a broad current flowing along the isentropic surface. If a westerly current flowing along an isentropic surface is of such character that the velocities are larger to the north and diminish to the south, shearing stresses will tend to speed up the westerlies to the south and retard the eastward flow along the northern edge of the current. In other words, the shearing stresses tend to distribute momentum uniformly over all filaments of the current. As a result of the frictional stresses, frictional volume forces are set up that act in the direction of the axis of the current, retarding in the regions of velocity maxima, accelerating in the regions of velocity minima. Under steady-state conditions, these axial forces must be balanced by Coriolis forces associated with slight motions normal to the current axes. Thus, as pointed out by Ekman [24], in the northern hemisphere an accelerating force F, per unit mass, acting eastward, produces a southward motion whose velocity is

$$v = \frac{F}{2\omega \sin \varphi}$$

Figure 177 shows diagrammatically the accelerating and retarding forces F_a and F_r, respectively, which operate on account of lateral mixing within a broad westerly current whose velocity profile is indicated by the curve. The motions which result from the Coriolis forces are given by the arrows marked v.

It will be seen from Fig. 177 that air motions created by shearing stresses may result in regions of convergence and divergence. For example, at P, air is being flung to the south, whereas at O, it is being flung to the north, so that between these two filaments divergence must set in. Similarly, convergence must set in in the region between O and Q. At the ground in regions above which convergence of this nature is taking place at all levels, the pressure rises, whereas below regions of divergence the surface pressure falls. Far to the right of the stream,

the lateral shearing stresses will also produce convergence, for, to the extreme south, the velocities are hardly accelerated at all. Therefore, it is highly probable that *lateral shearing stresses may be important in producing cross-isobar wind components* and thus also pressure variations that are of purely dynamic rather than thermal advective nature. There has been accumulated an increasing mass of evidence, both on theoretical and observational grounds, that the magnitude of these lateral shearing stresses is sufficient to account for such pressure variations. Thus, by equating isentropic shearing stress within sloping parallel isentropic surfaces that intersect the ground at a normal angle and stress due to ground friction (and assigning reasonable values of lapse rate and wind velocity in temperature latitudes), Rossby [66] obtained a lateral stress of 167 dynes/cm.^{2} corresponding to an isentropic shear of 2.5×10^{-5} per second and an isentropic eddy viscosity of 6.7×10^6 grams/cm. sec. These values agree fairly well in order of magnitude with those obtained from a study of the diffusion of water vapor actually observed in isentropic charts (Grimminger [30]). These values lie between those found by Richardson and Proctor for diffusion over small distances and those obtained by Defant by considering cyclones and anticyclones as large-scale turbulent elements in the general circulation. The analysis of isentropic charts has shown that eddies of appreciably smaller size than extratropical cyclones and anticyclones occur almost daily in the isentropic flow patterns.

FIG. 177.—Accelerating and retarding forces operating on an isentropic-current profile in which velocity varies in neighboring filaments.

There is being gathered an increasing mass of observational evidence to substantiate the theory summarized above.[1] In the following pages, we shall discuss briefly the practical results of studies of some of this material.

Before proceeding with this discussion, it is well to repeat that the isentropic analysis suggests itself as a practical tool in synoptic meteorology for the following two reasons:

[1] A complete quantitative treatment of the underlying theory is at present in preparation by C. G. Rossby and his colleagues.

1. It provides a method of identifying and following large-scale moist and dry currents and of anticipating their subsequent thermodynamic modifications.

2. It provides a method for taking into consideration lateral shearing stresses and their hydrodynamic effects on the prevailing flow pattern.

138. Plotting Routine.—The mechanical operation of preparing upper-air data in a form suitable for isentropic analysis is quite simple. We require for the analysis two sets of upper air charts; isentropic charts, for which an ordinary geographical base map suffices, and atmospheric cross sections that represent vertical planes cutting through the atmosphere along desired lines. The choice of some convenient isentropic surface or surfaces for analysis must then be made. The deciding factor in this regard is the general elevation of the surface, which again depends upon the general temperature distribution. Thus the isentropic surface $\theta = 290°$ which has been found useful in the United States during the winter months is far too low during the summer months. In general, the isentropic sheet finally chosen should be high enough to be above the layer influenced by surface friction and, at the same time, low enough to show a large range of specific-humidity values. It is obvious that, over a large area of diverse topographical and climatic features, these two criteria cannot be completely satisfied. However, it is in general possible to find an isentropic surface that satisfies these conditions well enough for a reasonably sound analysis:

In North America, suitable values of potential temperature for the individual seasons are:

Season	Potential Temperature, °A.
Winter	290–295
Spring	295–300
Summer	310–315
Fall	300–305

The abrupt increase from spring to summer values is due to the normally rapid increase of free air temperatures as summer convection sets in.

During periods of unusual weather, it is sometimes necessary to change to a different surface for a few days and then to return to the normal for the season. It should be pointed out, however, that such changes carry with them a certain loss of continuity—and it cannot be emphasized too strongly that continuity is the primary requirement of isentropic analysis. For this reason, it is most advantageous to follow from day to day the flow patterns in a given isentropic surface and, when an abnormal period suggests a change in surface, to construct an additional set of charts for a more representative surface for this particular period.

The elements plotted along the isentropic surface are the mixing ratio, saturation mixing ratio, and atmospheric pressure.[1] The appropriate values for plotting on the isentropic chart are readily extracted from aerological soundings with the help of some convenient thermodynamic diagram (see Chap. II). The pilot-balloon wind observations are then entered along the isentropic surface for those stations where the height (or pressure) of the isentropic surface is already evaluated. In addition to the above data, it is helpful to indicate the form and motion of clouds as well as hydrometeors observed at the aerological sounding stations together with the levels in which these phenomena are reported.

The atmospheric cross-section diagrams (see Fig. 243 to 245) have pressure (on a logarithmic scale) as ordinate and horizontal distance as abscissa. The values of mixing ratio and potential temperature are plotted at the significant levels for each station. It is convenient to plot, also, the relative humidity and the temperature. By constructing lines of constant moisture and constant potential temperature in the cross sections, we obtain a picture of the moisture and temperature distribution along the vertical plane represented by the cross section, as well as a view of the moisture pattern in the isentropic surfaces. Pilot-balloon wind observations, clouds, and hydrometeors are also plotted in the cross sections.

139. Technique of Analysis.—In order to enter all available pilot-balloon winds on the isentropic surface, it is necessary to sketch a set of lines of constant pressure. We shall refer to these as contour lines. Usually, it suffices to draw such lines for every fiftieth millibar. The number of aerological soundings is in general insufficient for drawing the contour lines in a purely mechanical fashion. Contour lines may be drawn more accurately by taking into consideration the guiding factors mentioned below. It is, indeed, necessary to make use of these aids when one wishes to extend the analysis into regions in which the data are sparse.

The particular isentropic surface or surfaces to be analyzed may be sketched immediately in the cross sections, and the positions of troughs or ridges may thus be determined and indicated on the isentropic map. In sketching the isentropes on the cross sections, one should bear in mind that, in the case of adiabatic lapse rates [*i.e.*, $\partial\theta/\partial z = 0$], the isentropes run vertically. In general, one can determine the lapse rate directly from the isentropes by making use of the following simple derivation. As an approximation, we may write

$$\theta = T + z$$

where T is the temperature and z the height above sea level expressed in

[1] Byers [21] has suggested the use of condensation pressure instead of mixing ratio.

hundreds of meters. Differentiating with respect to elevation, we obtain

$$\frac{\partial \theta}{\partial z} = \frac{\partial T}{\partial z} + 1 \quad \text{or} \quad \frac{\partial T}{\partial z} = \frac{\partial \theta}{\partial z} - 1$$

If one chooses for dz a unit distance, say 1000 m., then $\partial T/\partial z$ is easily determined by simply noting the difference of potential temperature in the vertical range; or the distance between two successive isentropes may be estimated, and $\partial T/\partial z$ quickly determined. This method is especially helpful when lapse-rate diagrams are not at hand.

The domes and ridges in the isentropic surfaces are found in regions occupied by cold air masses, and the troughs in the isentropic surfaces are found in the warm air masses. To the extent that the surface pressure changes are due to advection of cold and warm masses, the slope of the isentropic surfaces will be greatest above the isallobaric maxima.

Fronts on the surface weather map also offer a great deal of information about the structure and pattern of the contour lines. Regions in the vicinity of well-marked fronts are characterized by a crowding of the contour lines. Since cold fronts are generally much sharper and steeper than warm fronts, this steep gradient of contour lines on the isentropic chart is usually at its maximum just behind cold fronts. Moreover, as is to be expected, the contour lines usually run parallel to the surface fronts. Experience shows that most well-defined fronts are characterized by constant, or almost constant, potential temperature, so that the frontal surfaces have a marked tendency to coincide with the isentropic surfaces. Moreover, since a frontal surface is characterized by stable stratification, $\partial \theta/\partial z$ should have a maximum within the transitional zone (see Fig. 130). Since lateral mixing occurs mainly along isentropic surfaces, it follows that frontal surfaces that are parallel to isentropic surfaces will not be destroyed by mixing. On the other hand, frontal surfaces that intersect the isentropic surfaces will dissolve on account of lateral mixing, unless the front is situated in a field of motion that is pronouncedly frontogenetical (see Chap. V). When the front is associated with large areas of precipitation, the process is no longer isentropic, and lateral mixing does not take place along isentropes, but along surfaces of constant potential pseudo-equivalent temperature or surfaces of constant potential pseudo-wet-bulb temperature. In such cases, the isentropic surfaces will cross the frontal surfaces. At cold fronts, however, the area of precipitation is normally relatively narrow so that, in most cases, cold fronts lie along isentropic surfaces above the frictional layer.

The warmest air is normally found just ahead of the surface cold front. Thus, the trough in the contour lines is usually found slightly

in advance of the cold front, with a steep upward slope of the isentropic surface in the rear of the cold front.

The parallelism of contour lines with well-marked cold fronts many times enables one to construct contour lines in regions where upper-air observations are sparse. The application of this principle to frontal-wave disturbances is apparent, for here there must be a wavelike pattern in the contour lines roughly parallel to the frontal waves in the synoptic surface chart.

Sharp warm fronts show up in the contour-line pattern in much the same manner as do cold fronts, the gradient increasing abruptly at the front whereas the lines remain fairly parallel to the front. There
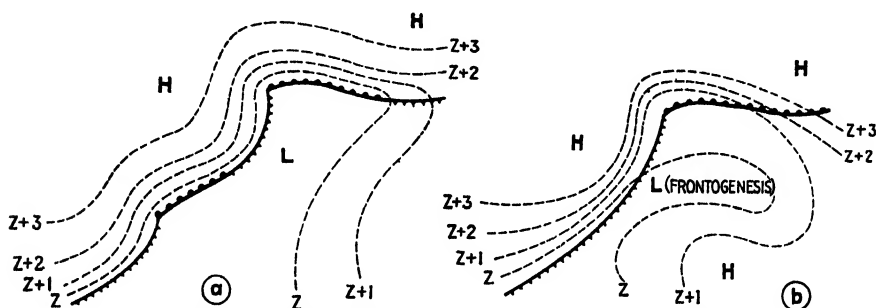
Fig. 178.—Relation of contour-line pattern to surface fronts.

are, however, many warm fronts on the surface weather maps that are not associated with this simple contour-line pattern above. Moreover, the surface maps frequently indicate a homogeneous air mass in the warm sector, whereas the isentropic charts show conclusively that the warm air is far from homogeneous aloft, but rather is characterized by troughs in the contour lines suggestive of fronts. Some time after their appearance in the contour-line pattern, these troughs may appear in surface charts as regions of frontogenesis, suggesting that such newly formed fronts are a result rather than a cause of the processes in the upper air. It thus appears that many fronts on the surface weather map are induced by action taking place first in the upper air and later showing up at the ground. This, obviously, means that a frontogenetical wind field (see Chap. V) develops aloft and gradually extends downward.

The above ideas are illustrated in Fig. 178. The light, broken lines labelled z, $z + 1$, etc., are contour lines of an isentropic surface. H indicates regions where the isentropic surface is high, and L regions where it is low. Figure 178a represents the normal topography, and Fig. 178b shows a type of topography that is associated with frontogenesis within the warm air subsequent to the appearance of the trough in the contour lines. The latter case is presumably associated with

frictionally driven anticyclonic eddies which we shall treat in more detail later on.

Finally, we may use the upper-air wind observations as entered directly for the observed heights of the isentropic surface over aerological sounding stations as a guide to the configuration of contour lines. In cases where the pressure distribution aloft is largely determined by the distribution of temperature, the winds blow nearly parallel to the contour lines so that domes or ridges are generally to the left of the current flow.

140. Isentropic Flow Patterns.—An inspection of the distribution of moisture along an isentropic surface covering a sufficiently large area immediately brings to light the fact that there are regions of high and of low moisture concentration. If the network of aerological stations were sufficiently dense, it would be possible to draw mechanically a series of lines, each denoting a given mixing ratio. In this manner, one could locate sources of moisture, or regions of injection of moist tongues, and the regions from which dry air is supplied. Moreover, these currents could be followed in a continuous fashion from day to day as they travel along the isentropic surfaces. Unfortunately, the distribution of aerological stations in any part of the world is much too sparse to permit such a mechanical delineation of moist and dry currents; for this reason, it becomes necessary to develop models and indirect clues by means of which characteristic "flow patterns" may be drawn that approach the real solution.

The topic of the source of our moist and dry currents is reserved for a later section of this chapter. For the present, we shall treat the fundamental flow patterns that thus far have established themselves in the daily isentropic analyses. Once these models are recognized on the daily isentropic chart, the analysis of the moisture lines becomes appreciably simplified.

The patterns of the large-scale motions in the atmosphere appear to be controlled in large part by the rotation of the earth. If we consider a fluid chain of particles located in and moving with an isentropic surface, it follows from Bjerknes' circulation theorem that the total absolute circulation of this chain remains constant as it moves from latitude to latitude. The absolute circulation C_a is equal to the sum of the circulation of the fluid chain relative to the earth, C_r, and the absolute circulation obtained by the chain if it momentarily were fixed to the earth, C_ω; or

$$C_a = C_r + C_\omega$$

Positive values of C_a and C_r indicate circulation with cyclonic sense, negative values that with anticyclonic sense. It can be shown that C_ω is given by

$$C_\omega = 2\omega\Sigma$$

where Σ is the area enclosed by the projection of the fluid chain on the equatorial plane. Thus, if an originally stationary isentropic fluid chain moves northward without change of the horizontal area it encloses, its equatorial projection increases; since $(C_r + 2\omega\Sigma)$ shall remain constant, C_r must decrease; hence, the chain will gain an increasing amount of anticyclonic circulation which adds to the circulation originally possessed by the chain. Similarly, a southward-moving system tends to develop a cyclonic circulation. Cyclonic circulation normally expresses itself as a cyclonic curvature of flow, anticyclonic circulation as an anticyclonic curvature of flow. Thus, the polar currents of cold dry air coming out of the north are generally cyclonically curved, whereas the warm, moist flows from a southerly direction have anticyclonic curvatures. These large-scale flows are the fast-moving streams and generally dominate the flow patterns observed on the daily isentropic charts. The axes of such streams may be delineated on the isentropic charts as curved lines along which the wind velocities are a maximum. Once these current axes are determined, they serve as a framework for isentropic flow patterns.

Once an air mass is set in motion, certain adjustments of the pressure field within and surrounding the current must take place more or less as they do in the case of the wake stream, investigated by Tollmien [85]. Thus, if momentum is injected into a region where no horizontal pressure gradients previously exist, Rossby [65] has shown that there will be a banking of the current so that pressure rises along the right edge of the stream and falls along the left edge. This effect is due to the action of an initially unbalanced Coriolis force which attempts to create a new pressure distribution in order to balance the motion. There is thus a tendency for a mutual adjustment of pressure and velocity distributions. These adjustments are affected whenever atmospheric flow becomes out of balance with its pressure gradient.

The results of Rossby's theory that are of immediate practical value in isentropic analysis are as follows:

1. Fast-moving streams tend to suffer a "banking" process so that a ridge of pressure to the right (in the northern hemisphere) and a trough to the left of the stream tend to build up.

2. The action of lateral shearing stresses operating on a current in which the velocity varies (as in Fig. 177) produces supergradient winds along the boundaries and thereby causes air to be flung across the isobars from lower to higher pressure, and this tends to build up higher pressure along the right edge of the stream.

3. The shear zones on either side of fast-moving currents are dynamically unstable, as shown by Pekeris [51], and tend to break the current into eddies having the vorticity of the original current profile. Thus,

anticyclonic eddies are formed to the right of fast-moving streams, cyclonic eddies to the left.

The development of an eddy affects the moisture distribution and creates a distinct pattern of moisture lines along an isentropic surface. In Fig. 179a, for example, we have a zonal distribution of moisture in an isentropic surface in middle latitudes. The isentropic surface itself is higher to the north and tilts southward, so that it may be 5000 m. above sea level in the north and only 2000 m. high in the south. Let us now superimpose upon this zonal state a velocity field as indicated by the
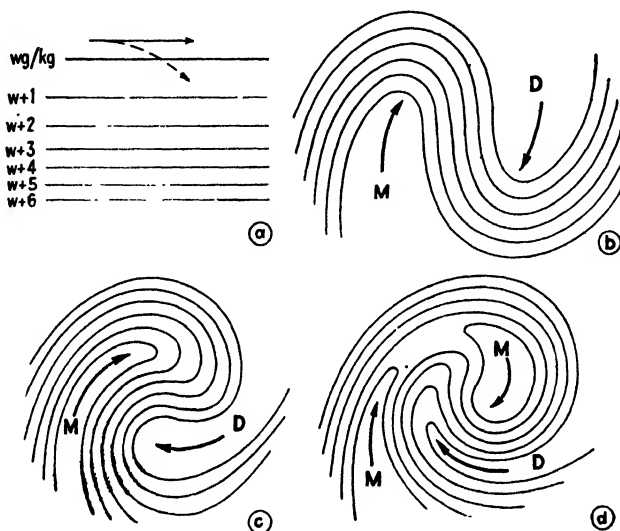
FIG. 179.—Successive stages in the development of an anticyclonic eddy as revealed by the moisture lines.

lower half of Fig. 177. Then air to the south is accelerated through lateral shear, air is piled up to the right of the accelerated stream, and the motion takes on a circulatory pattern indicated by the broken arrow. Since the moisture is carried along by the air and the motion is adiabatic, successive patterns of moisture lines indicated in Figs. 179b to d are soon developed.

Once the moist tongue of an eddy is sketched in an isentropic surface, it is possible, with the help of the cross sections, to apply tests for the existence of the tongue in the specific area chosen. The basis for this test lies in the empirical fact that significant moist tongues spread out aloft, and, if a moist tongue is present on an isentropic surface *between* aerological stations that are not more than 400 to 600 km. apart, it generally shows up in the cross section as an inversion of mixing ratio (or at least a minimum of vertical gradient of moisture) at one or both of the stations. If there are no inversions of moisture above the chosen

isentropic surface at either of the stations in the cross section and if a moist tongue is assumed to be between stations, the tongue must be drawn as a narrow vertical filament of moist air—a highly improbable condition, and certainly one that is rarely observed. This test is perhaps more clearly illustrated by imagining an isentropic chart, say for $\theta = 310°$, where a moist tongue has been entered between two stations; in the axis of this moist tongue, a mixing ratio of 7 grams/kg. has been indicated. Applying the cross-section test, we see that, if the section is of the type shown in the Fig. 180a, the moist tongue is real, while in Fig. 180b it would be highly improbable, for here the moisture lines are arbitrarily drawn.
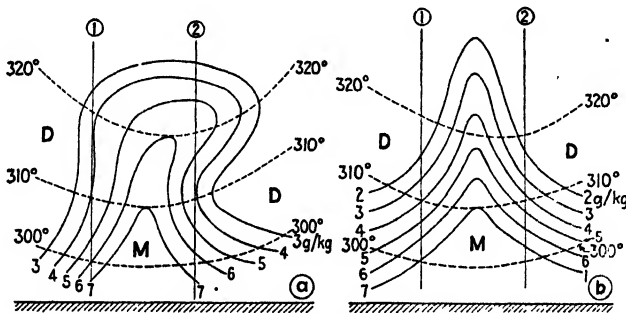
Fig. 180.—Illustrating the cross-section test for moist tongues. *a*, moist tongue probable; *b*, moist tongue highly improbable and solution to be abandoned in favor of another, more logical one.

If the eddies remained stationary and developed in a regular fashion, it would be simple to follow the moist and dry tongues around them. Their life history, however, varies from eddy to eddy and is closely allied with the energy of the current or currents originally responsible for their development. Once the source of energy of the mother current diminishes, the convergence necessary to maintain the eddy fails and the circulation weakens, finally dissipating or merging into some other circulation. Thus, the stability of any particular eddy may, to some extent, be deduced from the distribution of velocity around its center, as shown by Namias [44]. Stable eddies will have well-developed circulations with wind velocities increasing radially outward from the center in a nearly symmetrical fashion. Such eddies will tend to rotate as solids. Once the mother currents weaken, the symmetry of the velocity profile tends to vanish and the eddy gradually dissipates. Also, for this reason, the moisture lines may sometimes indicate an eddy pattern that is the result of some already decayed circulation.

By assuming that the smaller anticyclonic eddies are frictionally driven, it is possible to deduce from the distribution of velocity around their centers the general direction of migration. Suppose we have an

eddy with a velocity distribution as indicated in Fig. 181. This eddy obviously derives its energy from the westerly and northwesterly current; and it may be assumed that air motion, being supergradient, has a small component toward the center. In the southeastern quadrant of the eddy, there is a region where the symmetry is impaired so that there appears to be a region of wind divergence. The converging air piling up into the center of the eddy will naturally follow into the divergent region, and the eddy will follow a path indicated in Fig. 181. Applying this rule in the general case, we may say that frictionally driven anticyclonic eddies tend to move into the region in which the tangential winds about them are lightest. This direction is normally in the direc-
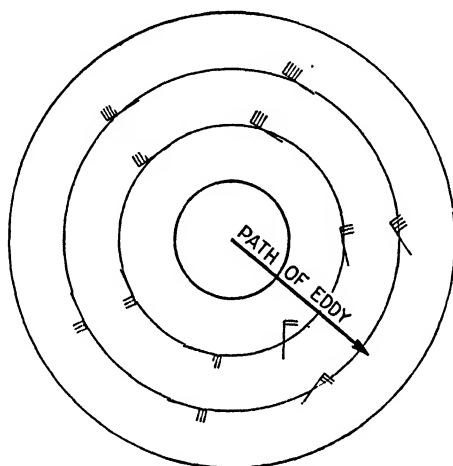
Fig. 181.—Relation of direction of movement of anticyclonic eddies to distribution of wind velocity.

tion of the mother current. It should be emphasized, however, that this rule applies chiefly in the developing stages of the eddy and when it is characterized by asymmetry in the velocity distribution. The use of the above rules for determining the movement and stability of anticyclonic eddies on the isentropic chart will do much to assist in the analysis of the flow patterns and in making forecasts of the movement of moist and dry tongues.

To the left of fast-moving streams, a zone of cyclonic wind shear exists, which tends to develop cyclonic eddies. When cyclonic eddies are sharply defined, they are generally associated with occluding or occluded cyclones. The dominating current in such cases is not the warm moist air coming from the south, but rather the cold dry air streaming into the eddy cyclonically from the north. The structure of the cyclonic flow pattern normally observed in occluding cyclones is shown diagrammatically in Fig. 182. The flow pattern is indicated

by the moisture lines, and the arrows represent the instantaneous flow of dry (*D*) and moist (*M*) currents relative to the movement of the cyclone. In the model, it is observed that two systems are struggling for supremacy: an anticyclonic moist current *M*, to the right, and a cyclonic dry current *D*, to the left. The moist current, having come up from the south, tends to acquire anticyclonic curvature indicated by the direction-flow arrow to the upper right. This part of the pattern may thus be considered as the normal type of anticyclonic eddy observed in tropical currents moving northward. Where the polar air intrudes
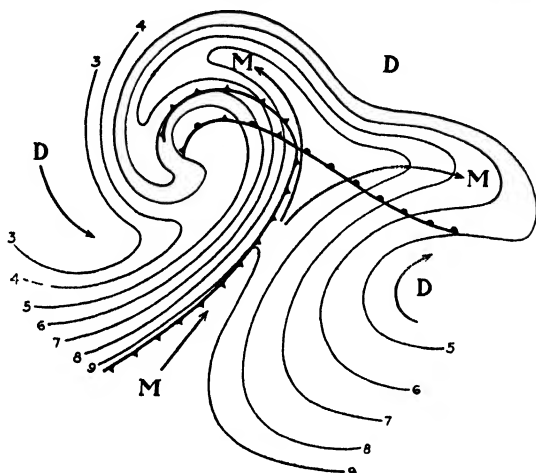
Fig. 182.—Fronts indicated at the surface and schematic flow pattern around an occluded cyclone as shown by the moisture lines in an isentropic surface in mid-air.

into the system from the north, it develops cyclonic vorticity in order to counterbalance the decreasing cyclonic vorticity of the earth's rotation. Each current attempts to impart the vorticity to its surroundings, and this is accomplished through isentropic shearing stresses. Thus, a branch of the moist flow is diverted from the mother current into the cyclonic flow. At some point, there is branching of the moist flow, and this point appears to be situated in the vicinity of the occlusion point on the surface weather map. These moisture patterns agree with the flow pattern around occluding cyclones as was described in Pars. 130 and 135.

If this branching is due chiefly to lateral shearing stresses, we may arrive at some valuable rules by assuming[1] that, in the region of branching, *real horizontal divergence* as well as divergence of the streamlines is occurring. Thus, if the flow pattern is maintained through a fairly deep layer of the atmosphere, the surface pressure falls in the region below the branching. This effect is, of course, superimposed upon the pressure

[1] See Namias [45].

changes due to density advection, as was explained in Par. 133. If the region of divergence is situated some distance from the center of the surface cyclone, a secondary cyclone may form near the peak of the warm sector at the ground (see Par. 134).

The effects of the branching upon the pressure distribution at the surface may be roughly estimated by the strength of the interacting currents. Thus, a weak anticyclonic eddy will generally yield to an invading strong cyclonic flow of polar air, and, in this case, no secondary will result, whereas two strong currents of different vorticity will invariably cause large pressure falls and lead to deepening and possibly to cyclogenesis.
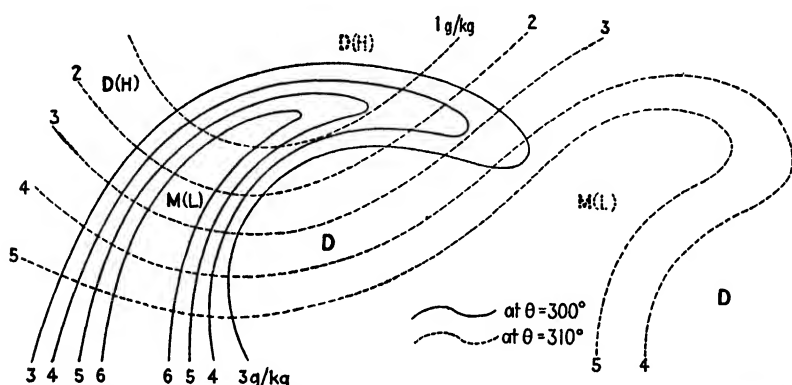
Fig. 183.—Flow patterns at different isentropic surfaces which lead to increasing instability.

141. The Displacement of Flow Patterns with Height.—Thus far we have concerned ourselves with flow patterns observed in one isentropic surface. Experience has shown[1] that there is a relatively small difference in the flow pattern from one isentropic sheet to another. This, however, does not hold true if we choose an isentropic surface which is so low that it comes under the influence of the surface friction. The slight displacement of flow pattern with elevation, which occurs above the friction layer, conforms usually with the displacement with elevation of cyclonic and anticyclonic centers (see Chap. VII). It should be noted, however, that there are exceptions and that these are frequently associated with radical changes in the weather situation.[2] The most important exception, perhaps, is when an anticyclonic eddy is present below a cyclonic eddy. This case is represented schematically in Fig. 183, where the solid lines represent the flow pattern at some isentropic surface and the broken lines show the flow pattern along an isentropic surface 10° higher in potential temperature. The domes of the isentropic surfaces are

[1] SIMMERS [74].
[2] NAMIAS [46].

indicated by H and the troughs by L. With such a vertical distribution of flow patterns, it is clear that, while the lower layers over a region are becoming progressively warmer and moister, the higher layers are becoming colder and drier. The advection thus leads to two processes in which the potential energy of the air column is increased: (1) Where the lower layers are becoming warmer and the upper layers are becoming colder, the lapse rate is made steeper. (2) Since the lower layers are becoming richer in moisture while the upper layers are becoming drier, the energy due to convective instability is increasing. This combination of effects makes it easier for frontal activity to produce precipitation and in general adds to the supply of energy available for cyclogenesis. It also facilitates the outbreak of local showers due to diurnal heating (Chap. II).
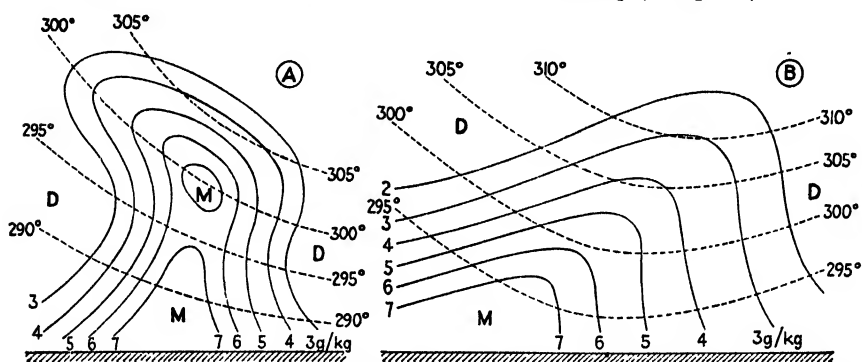
FIG. 184.—*A*, conservative cross section indicating that choice of isentropic surface will not materially affect location of major flow patterns; *B* cross section indicating that flow patterns change appreciably.

A quick test for the conservatism of any particular isentropic flow pattern with height is afforded by the cross sections. Thus, in Fig. 184*A* we have the conservative case in which it makes little difference in the flow pattern what isentropic surface is chosen for analysis; Fig. 184*B* shows the case in which the flow pattern at a surface $\theta = 305°$ would differ appreciably from that on the surface $\theta = 295°$. In the latter case, it is necessary to construct isentropic charts for both these surfaces to obtain a more complete picture of the atmospheric flow patterns.

142. The Representation of Gradient Flow in Isentropic Surfaces.— The principal reason for the use of isentropic charts is that they afford a means of determining atmospheric motion independent of assumptions regarding the existence of gradient flow. Nevertheless, it is frequently desirable to know the gradient flow, and it appears that the mutual adjustment of velocity and pressure distribution takes place in such a fashion that most of the time cross-isobar components of the wind are small compared with the gradient flow.

A highly satisfactory method of representing gradient flow along isentropic surfaces has been suggested by Montgomery [42]. His development leads to the expression for the stream function of the gradient wind in an isentropic surface

$$\psi = c_p T + \Phi$$

where c_p is the specific heat of air at constant pressure, T is the absolute air temperature at the isentropic surface, and Φ the geopotential. Using meter-ton-second units, Φ is expressed in dynamic decimeters, and the value of the constant C_p is approximately 1000.

If lines for equal values of this function (ψ) are drawn on an isentropic chart, they form streamlines and serve a purpose similar to isobars on a constant-level chart. In regions where pilot-balloon wind data are lacking, these isentropic streamlines are quite helpful. Moreover, by comparing the patterns of streamlines from day to day and noting the changes of the ψ values, it is possible to get a better idea of the future trajectory of dry and moist tongues of the isentropic chart. A chart showing the streamlines in an isentropic surface is shown together with the examples in Chap. XI.
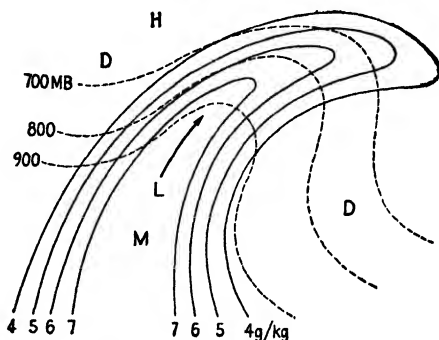
Fig. 185.—Illustrating probable upslope motion of a moist current as deduced from the relation of moisture lines to contour lines.

143. The Relation of Isentropic Flow Patterns to Precipitation.— Since one of the necessary conditions for the formation of precipitation is the presence of sufficient moisture content, it is not surprising that there is generally found some relation between moist tongues and precipitation areas. In winter, when the stratification is relatively stable over the continents, most of the precipitation over continental areas is caused by frontal action. The isentropic chart frequently indicates regions of ascent or descent of air through the relative configurations of the moisture lines with respect to the contour lines. A frequent type of flow pattern is shown in Fig. 185, where a moist tongue ascends the isentropic surface.

It should be mentioned that the configuration of moisture and contour lines shown in Fig. 185 does not always indicate upslope motion; for the shape of these lines is the result of long development, and the upslope motion may have ceased by the time when the synoptic picture was obtained.

Another indication of upslope motion along isentropic surfaces is obtained from the wind observations. If there are sizable wind com-

ponents normal to the contour lines and if the contour patterns are uniquely defined by observations from a dense network of soundings, then it is *probable* that the air is ascending or descending the isentropic slope in the direction of the wind. However, when the contour lines themselves are displaced with the same speed as the wind component normal to them, the wind components normal to the contour lines are not indicative of up- or downslope motion. If there is any doubt as to whether there is upslope or downslope motion, the observed mixing ratios should be compared with the saturation mixing ratios (or the pressure should be compared with the condensation pressure) in order to find out how much lifting is necessary in order to make the air satu-
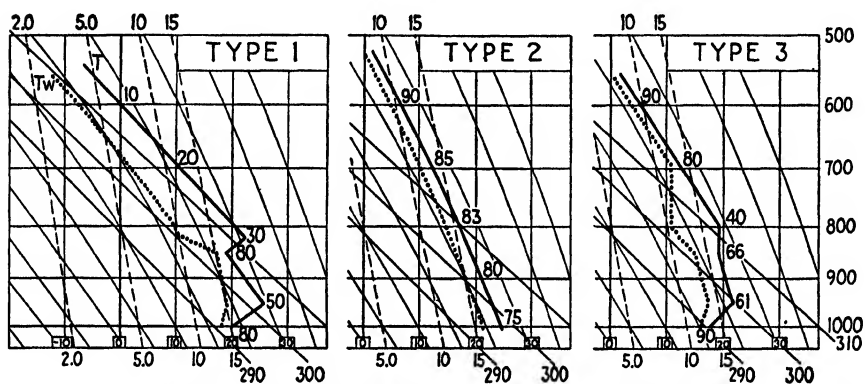
Fig. 186.—Characteristic vertical distributions of temperature and moisture observed over continental United States in summer. Numerals plotted along the ascent curves indicate relative humidity.

rated. In addition, consecutive maps should be compared in order to determine whether or not the air is approaching saturation. A study of the cloud systems and areas of precipitation will give additional information to this end.

In the warmer seasons, much of the precipitation in continental areas is nonfrontal in character. This precipitation is chiefly of the convective type and occurs as local showers and thundershowers. In Chap. II, we discussed the detailed use of energy diagrams for forecasting these showers. However, the use of energy diagrams becomes even more effective when one takes into consideration not only the state represented by the energy diagram at the time of the sounding but also the probable changes with time caused by the advection of moist and dry tongues at various levels. The isentropic analysis offers by far the most satisfactory method of doing this.

We shall first discuss a few of the characteristic vertical distributions of temperature and moisture normally observed over continental United States in summer. The first type (shown in Fig. 186) has an extensive

dry layer overlying a relatively moist stratum of about 2 km. thickness. The transition zone between the lower moist and the overlying dry air is normally a very stable layer, often a marked temperature inversion. The second type has no discontinuities in temperature and moisture content. Furthermore, the air column is not far from saturation. Type 3 represents a transition between the types 1 and 2, and here there is a 2-km. layer of moist air next to the surface, with dry air sandwiched in between this stratum and another layer of high moisture content aloft. As in type 1, there is a stable layer between the dry and moist air, although less stable; and, as in type 2, the lapse rate aloft is fairly uniform and normally slightly steeper than the saturated adiabatic, whereas in type 1 it is almost equal to the dry-adiabatic.

Type 1 usually gives negative areas below and positive areas above for convective impulses from below. Normally, such impulses (even at the time of maximum temperature) are insufficient to frustrate the negative area and cause overturning of the whole air column. Type 2 normally gives large amounts of available energy for upward impulses that occur at the time of maximum temperature. This type represents conditional instability of the real latent type which may easily become realized during the warmer part of the day. Type 3 is very stable for convective impulses near the surface, and normally only negative areas will be observed.

From the above remarks, it might be supposed that showers and convective thunderstorms rarely occur with types 1 and 3 but are common with type 2. Although this simple rule would have considerable success in its application to forecasting, it would fail in certain cases. Before we discuss these cases, it is of interest to comment on such vertical distributions of temperature and moisture as are represented in Fig. 186. In summer, the normal temperature distribution over a large part of the United States is almost barotropic, and the main concentration of solenoids appears to be found along the northern border of the continent.[1] Consequently, strong westerlies are observed over this portion, and we may look upon the zonal distribution of velocity as being similar to that pictured in the lower half of Fig. 177. South of such a westerly current, anticyclonic eddies form which create distinct patterns of moisture. This phenomenon occurs so frequently over certain areas of the United States that mean isentropic charts constructed for a month, season, or group of the same seasons of different years reveal the eddies through the moisture lines.[2] The normal flow pattern shows that dry air from the north curls anticyclonically southward while moist air from the south converges in a spiral fashion together with the dry air into the

[1] See Par. 145 for a more detailed picture of the normal state.
[2] For example, see Fig 189.

anticyclonic eddy. The axis of the dry tongue normally runs through the Mississippi Valley, and the moist tongue generally makes its appearance over north Mexico and then curves eastward.

Comparing this pattern with the normal pressure field observed at the surface,[1] we see that, although the flow of air in the surface layers over eastern United States is uniformly from the south and southwest, there are regions where the current system is reversed aloft. Thus, although the lowest layers of air are generally characterized by considerable homogeneity, there are sections where this moist and warm air,
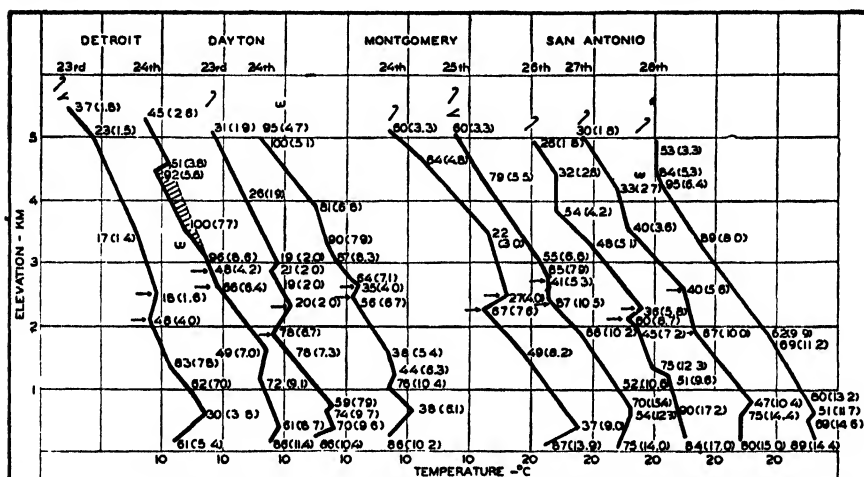
FIG. 187.—Destruction of dry type of stable zones (shown by arrows) after the advection of a moist tongue aloft. These soundings were made from June 23 to 28, 1937. Numbers to the right of the soundings are the relative and (in parentheses) specific humidities. Clouds are indicated by international symbols.

normally of tropical maritime origin, is overrun by drier air coming from the north. Moving southward, the dry air subsides, so that by the time it reaches the core of the anticyclonic eddy it has become warmer and drier than air anywhere in its vicinity. This type of air mass was discussed in Par. 83.

Soundings of type 1 may generally be explained on the above basis. The stable transition zones between the moist and overlying dry air are maintained in part by continued subsidence. These stable zones exist for long stretches of time during the summer season; and when they are especially tenacious, periods of drought result. They are frequently destroyed, however, after the advection of a moist air current aloft. Figure 187 shows some typical examples of cases in which dry stable layers (marked by arrows) were destroyed through advection of moist air aloft. Experience shows that soundings of type 1 will be transformed

[1] See Fig. 81.

into type 3 through advection of moist tongues aloft. Through turbulent redistribution of heat and moisture and through radiative exchange of heat, soundings of type 3 may be transformed into type 2.

Although summer showers and thunderstorms occur most frequently when the soundings are of type 2, they also occur when the soundings are of type 3. Thunderstorms associated with soundings of type 3 occur frequently in the western part of the United States to the east of the Rocky Mountains, and they have a marked tendency to occur in the night. Since the lower portion of the atmosphere is then pronouncedly stable, it is evident that these thunderstorms cannot be due to convection starting from the earth's surface. Since the upper layers are convectively unstable, thunderstorms can be released through lifting, as was explained in Chap. II. This lifting may be due to frontal action, and it may also be due to katabatic winds which develop in the night on the eastern slope of the mountain range. As suggested by Namias [47], it is plausible that nocturnal radiation from the upper cloud surfaces may contribute to the release of precipitation.

The problem of forecasting summer showers therefore depends not only upon the stratification existing aloft in the early morning when soundings are made, or entirely upon the changes brought about by diurnal heating (see Chap. II), but also upon the advection of moist and dry tongues aloft. The best method of estimating these advective changes lies in the isentropic analysis. In this manner, we are able to detect in advance the likelihood of soundings of any of the above types being transformed into other types through advection.

When reliable isentropic charts are at hand, together with the corresponding cross sections, it is possible to obtain information of forecasting value that is not easily obtained from other charts. The problem of shower and thunderstorm forecasting, therefore, revolves chiefly about the determination of the lapse rate and the source and availability of moisture. Tongues of dry and moist air, as shown by the isentropic charts, may be identified from day to day by means of these charts. In summer, it is found almost invariably that thunderstorm activity and showers are associated with the moist tongues, while the dry tongues are free of convective precipitation. Furthermore, by making use of cross sections, one is able to form an idea of the representativeness of the chosen isentropic chart. Sources of moisture indicated within the frictional layer may be found to be shallow and not representative of conditions in higher isentropic surfaces. The presence or invasion of dry air aloft would then counteract the possibility of showers and thunderstorms. Thus, though an energy diagram may offer indications of possibilities for shower activity, one should use the isentropic chart to take into account any likely changes. Suppose, for example, that an

energy diagram indicates large positive areas and that moist air extends to high levels—both indications of thunderstorm activity during the day. If a tongue of dry air is displacing the moist air at upper levels, the probability of thunderstorms is greatly lessened. Then again, the horizontal extent of the source of moisture must be considered. A narrow jet of moist air will suffer lateral mixing with the dry air flanking it on both sides, and this desiccating process will act against thunderstorm formation. The showers, if they occur at all, will then be restricted to the very central portion of the moist tongue (along its horizontal axis), where the moisture is least affected by the admixture of dry air. On the other hand, extensive regions or broad tongues of moisture may remain comparatively unaltered by lateral mixing and thus provide ideal conditions for continued thunderstorm activity.

FIG. 188.—Illustrating the influence of nonadiabatic cooling on the elevation of an isentropic surface.

144. The Processes Which Tend to Disrupt the Continuity of Isentropic Analysis.—From the standpoint of following the same sheet of air from day to day, the ideal method of representation would be one in which nonadiabatic as well as adiabatic influences were taken into consideration. With such a method, one could construct charts along substantial sheets—*i.e.*, sheets that contain the same air particles from day to day. By following these identical sheets and describing the motion of elements with respect to such sheets, one would use the Lagrangian method of attack of describing the changes in the atmosphere. Although at present it is not possible to chart exactly substantial surfaces, there is much evidence to indicate that isentropic surfaces do not depart appreciably from substantial surfaces. Thus, the isentropic method of analysis is essentially a Lagrangian method. In a study of subsidence, Namias [48] has shown that the potential temperatures at the bases and at the tops of subsidence inversions remain fairly constant from day to day. Thus, if isentropic surfaces are used in such cases, it is reasonably certain that we are dealing with the same sheet of air particles from day to day. Moreover, it is frequently observed that sandwiched layers of dry and moist air remain within the same isentropic sheets for several days. From these observations, it appears that, as a first approximation, we may consider isentropic surfaces as substantial surfaces.

Nevertheless, there are always at work nonadiabatic processes that tend to destroy the conservatism of isentropic surfaces and to raise or lower the isentropic surfaces relative to the substantial surfaces and that also tend to transport moisture across the isentropic surfaces. These nonadiabatic processes are mainly due to: (1) radiation, (2) evaporation and condensation, and (3) convection. Although the influences of these processes may be appreciable over long intervals of time, they are usually insufficient for disrupting the fundamental isentropic flow patterns from one day to the next.

The influence of radiative cooling is illustrated in Fig. 188. As cooling proceeds, the temperature distribution changes from *A* to *B* to *C*. The substantial surfaces do not change elevation; but since the temperature decreases, the height of any given isentropic surface increases from day to day. Since the normal moisture distribution is one in which mixing ratio decreases with elevation, the mixing ratio observed in a given isentropic surface decreases with time. Since the rate of radiational cooling in the free atmosphere is small compared with the adiabatic cooling, it does not destroy the essential character of the flow pattern. This slow rate of free-air cooling is indicated by the cooling curves computed by Möller [43], which suggest that the maximum temperature change resulting from the radiative unbalance in the atmosphere hardly exceeds 1.5°C. per day, which with normal lapse rate corresponds to a vertical displacement of the isentropic surface of about 300 m. in one day. Nevertheless, it is at times necessary to introduce this factor to explain changes in moisture content or height of the isentropic surface that cannot satisfactorily be explained by advection or other causes. Where the isentropic surface is not far from snow-covered mountains, cooling by radiation and eddy transfer of heat must frequently be considered.

Opposite effects are observed when there is nonadiabatic heating. Then a substantial surface has its potential temperature raised so that the isentropic surface is lowered; and since the specific humidity normally decreases with elevation, there appears to be an increase in moisture within the affected area of the isentropic chart. This type of nonadiabatic modification is significant when the isentropic surface is near the ground. The influence is greatest in continental areas during the summer season. It is also important in mountainous country during all seasons.

Let us consider next the nonadiabatic effects produced by evaporation and condensation. Since condensation liberates and evaporation consumes heat, it becomes important to know whether these processes occur above, within, or below the isentropic sheet under discussion.

If the chosen isentropic surface lies above the region where condensation occurs, its characteristics will not be materially affected.

An example is afforded by the instability snow showers of polar continental air masses of winter. These showers are generally formed in a shallow layer of air next to the earth's surface—a layer that is far below the representative isentropic surfaces which are chosen so as not to intersect the ground even in tropical air. In this case, isentropic surfaces are practically substantial surfaces.

If condensation and precipitation set in within the chosen isentropic sheet, latent heat is liberated and the potential temperature of the substantial surface is raised. The isentropic surface is then found at lower levels, and, since the specific humidity normally increases downward, the specific humidity in the isentropic surface increases. This increase might erroneously be interpreted as being due to advection from a neighboring source of moisture.

When precipitation falls through an isentropic sheet that is not saturated with moisture, evaporation will cool the air while the specific humidity increases. This lowers the potential temperature of the substantial surface and raises the isentropic surface. If the moisture content decreases with elevation, the mixing ratio at the chosen isentropic surface decreases in proportion to the humidity gradient. On the other hand, if the moisture content increases with elevation (as it often does along well-defined frontal surfaces), the mixing ratio will increase. The increase in moisture with elevation is usually so slight that, though the isentropic surface rises, little change in the pattern of moisture results.

Probably the most significant process at work in causing isentropic surfaces to depart from substantial surfaces is convection, for convective currents are highly effective in transporting moisture to higher levels. If it were not for the replenishment of moisture by convective currents, the moist tongues that are not associated with upglide motion along frontal surfaces would soon be dissipated through lateral mixing with the dry air flanking them.

In the discussion of the influence of convection on the moisture patterns in the isentropic chart, it is convenient to distinguish between widespread convection within unstable air masses and convection associated with fronts. Convection that occurs along fronts (notably cold fronts) is usually restricted to a narrow zone that coincides with a moist tongue on the isentropic chart. Although these convective currents transport moisture to higher levels, water is also precipitated from the frontal cloud system. The convection that occurs along such fronts merely replenishes the moisture content of the moist tongue; it does not disrupt the continuity of the isentropic analysis. This also applies to purely local convection ("pin-point convection"). The matter may, however, be different in cases of widespread convection. The convective transfer of moisture may then, at the beginning of the process, change

the moisture pattern aloft. This is particularly the case in polar continental air when it moves over an ocean, for the convection currents will then transport much moisture to high levels. The convection that occurs in unstable polar continental air moving over land in winter does not usually reach up to the representative isentropic surface; it therefore does not appreciably influence the moisture pattern aloft.

From the above, it follows that the occurrence of convective as well as frontal precipitation is closely related to the moist tongues and that
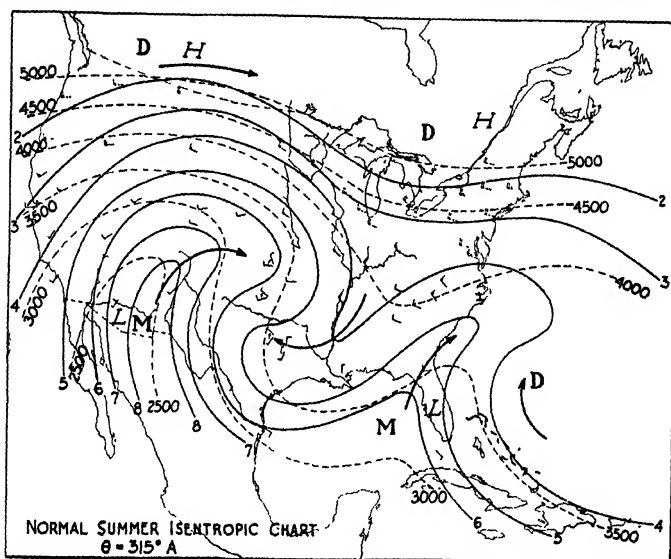
Fig. 189.—The normal flow pattern over United States in summer. This chart is based upon aerological data for summer months from July, 1934, through August, 1938. It was constructed by averaging values interpolated at 5-degree intersections of longitude and latitude from analysed monthly mean isentropic charts. The winds are normal resultant upper-air winds.

the isentropic charts afford the best means for analyzing the processes in the free atmosphere.

145. The Mean State of the Atmosphere as Revealed by Isentropic Charts.—If the daily aerological soundings during a given month are averaged for various stations, we may construct isentropic charts and cross sections representing the mean state of the atmosphere for that month. The mean air flow may be obtained by computing the resultant winds from pilot-balloon observations. Similarly, it is possible to construct mean seasonal isentropic charts and, if data were available, normal charts. An example is shown in Fig. 189. The outstanding feature of the normal summer pattern is the existence of two well-defined anticyclonic cells—one centered over western Texas, the other some-

where off the southeastern coastal states. Some light on the question of the formation of these eddies is furnished by north-south atmospheric cross sections, a typical one for the summer season being reproduced in Fig. 190. This section brings out the well-known fact that, over North America, the principal summertime polar front is generally found in the vicinity of the Canadian border (see Par. 113). Most of the time, the United States is south of this front and is within what appears as a thermally homogeneous air mass. In spite of the zonal homogeneity of temperature and the consequent lack of solenoids to generate kinetic energy, there is observed a prevailing eastward flow of the tropical air.
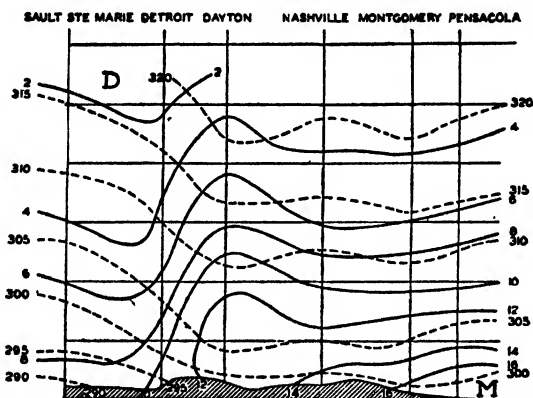
FIG. 190.—North-south vertical cross section for August, 1936, showing the distribution of potential temperature (broken lines) and specific humidity (full lines).

According to Rossby [67], the eastward current in the homogeneous air is maintained by frictional stresses from the much stronger westerly current to the north, and this energy is continually being dissipated in the form of eddies further to the south. If such eddies are maintained in more or less fixed locations over a sufficiently long period of time, the mean chart will display an eddy pattern in the moisture lines and in upper-air winds. The mean isentropic charts for individual summer months invariably reveal such eddies, and most of the time there are observed two anticyclonic cells placed about as they are in Fig. 189.

In all the mean summer isentropic charts studied, there has been a moist tongue projecting from north Mexico and recurving toward the northeast and east. The region covered by this tongue has a maximum of precipitation in summer. It has been suggested by Wexler [87] that this preferred site for the anticyclonic eddy is largely due to topography and results from the field of solenoids to the north as well as from the field of solenoids established between the warm Rocky Mountain region and the colder Pacific region.

The point of injection of the moist tongue of the eastern eddy is normally over Florida, where there is a maximum summer rainfall and a high frequency of thunderstorms.

Although there is a similarity of mean monthly isentropic charts for different summer months and from year to year, it should not be inferred that the moisture patterns are always the same. Considerable deviations from the mean state are always associated with considerable anomalies in rainfall and temperature.[1] Thus, during the month of August, 1936, when one of the most severe droughts and heat waves occurred in the midwest, the mean monthly pattern showed only one very extensive anticyclonic eddy covering the entire country rather than the normal double cellular pattern.

In winter, when the mid-latitude solenoid field is situated farther to the south, the mean isentropic charts do not generally display any outstanding eddies. Simultaneously, the daily charts show pronounced eddies with moist and dry tongues. The individual eddies then move rapidly, without preferring any particular site. Although the above refers to the conditions over the North American continent, there can be little doubt that the principles outlined here apply in a general way throughout the world.

[1] See WEXLER and NAMIAS [88].

CHAPTER IX

FORECASTING OF DISPLACEMENT OF PRESSURE SYSTEMS, FRONTS, AND AIR MASSES

The application of the methods of analysis described in previous chapters gives a fairly complete picture of the physical state of the atmosphere. The physical analysis naturally forms the basis for rational forecasting, but the step from the completed physical analysis to the forecast is perhaps the most difficult one on the windy path from syllogism to ergo. The aim of this chapter will be to develop methods by means of which the movement of cyclones, anticyclones, troughs, wedges, cols, fronts, and air masses can be computed or estimated. Throughout will be an attempt to express the forecasting formulae and rules in terms of pressure only, for atmospheric pressure can be observed with greater accuracy than any other meteorological element. Moreover, atmospheric pressure is the only element that is entirely representative.

The content of this chapter is summarized from the author's papers [55, 58] cited in the references to the literature. The reader is referred to these papers for a more detailed discussion of the theory on which the forecasting principles are based.

146. The Field of Pressure.—The distribution of atmospheric pressure p in a level surface (*e.g.*, a weather map) may be expressed by

$$(1) \qquad\qquad p = p(x,y,t)$$

The analytical form of this function is not known; but when isobars are drawn correctly, the weather map furnishes a graphical picture of the pressure function at a given instant $t = t_0$. A succession of such maps will show how the pressure distribution changes with time. The problem will therefore be to extrapolate the future pressure distribution. A complete solution of this problem offers both theoretical and practical difficulties. However, in most cases, it is possible to compute the future pressure changes at a few points where the solution of the problem is simple. When a few such "fixes" have been obtained, the forecaster will be able to visualize the pressure distribution between these points.

On account of the complicated structure of the hydrodynamic equations, it is, at the present moment, not possible to obtain the future pressure distribution with satisfactory accuracy through integration of these

equations. On the other hand, geometric and kinematic methods have yielded results that are more easily applied to the weather maps.

The method that will be described in the following paragraphs consists in computing the displacement of certain curves and points in the pressure field which can be identified from one map to another; when this is done, the pressure variation on these moving curves or points is computed. The method, therefore, consists in computing the movement and the deepening of the pressure systems that move across the chart. In order to develop this method, it is necessary to introduce mathematical characteristics for the curves and points in the pressure field which can be identified during their motion across the chart.

1. *Isobars.*—The simplest of such identifiable curves is the isobar. At a given moment $t = t_0$, the isobar is defined by

$$(2) \qquad\qquad p(x,y,t_0) = \text{constant}$$

and it can be identified from one map to another by means of the constant (*e.g.*, $p = 1010$ mb.). To be quite accurate, Eq. (2) defines an isobar only when the pressure gradient differs from zero (*i.e.*, $\nabla p \gtrless 0$).

2. *Isallobars.*—The distribution of barometric changes per unit time may be expressed by

$$(3) \qquad\qquad \frac{\partial p}{\partial t} = b(x,y,t)$$

At any given moment $t = t_0$,

$$(4) \qquad\qquad \frac{\partial p}{\partial t} = b(x,y,t_0) = \text{constant}$$

defines an isallobar provided that the isallobaric gradient differs from zero [*i.e.*, $(\nabla \, \partial p/\partial t) \gtrless 0$]. Each isallobar may be identified from one map to the next by means of the constant pressure variation that it represents (*e.g.*, $b = +3$ mb.).

3. *Fronts.*—Any front can be identified by means of the general and special frontal characteristics described in Chap. VI. However, for the discussion in this chapter, it suffices to use the dynamic boundary condition (see Par. 96) which states that the pressure must be continuous at the front. It was shown in Par. 119 (see also Fig. 132) that the following condition defines a front,

$$(5) \qquad\qquad p - p' = 0$$

provided that

$$(6) \qquad\qquad \frac{\partial p}{\partial x} - \frac{\partial p'}{\partial x} > 0$$

A front that moves across the chart may therefore be identified by means of Eq. (5).

4. *Trough Lines.*—A trough line may be defined as a line in the pressure field along which the isobars are symmetrical and curved cyclonically (see Fig. 191*A*). Choosing the *x*-axis normal to the trough line, we see that the following condition characterizes a trough line,

(7)
$$\frac{\partial p}{\partial x} = 0$$

and that

(8)
$$\frac{\partial^2 p}{\partial x^2} > 0$$

5. *Wedge Lines.*—A wedge line is defined as a line in the pressure field along which the isobars are symmetrical and curved anticyclonically (see Fig. 191*B*). Choosing the *x*-axis normal to the wedge line, we obtain

(9)
$$\frac{\partial p}{\partial x} = 0$$

and

(10)
$$\frac{\partial^2 p}{\partial x^2} < 0$$
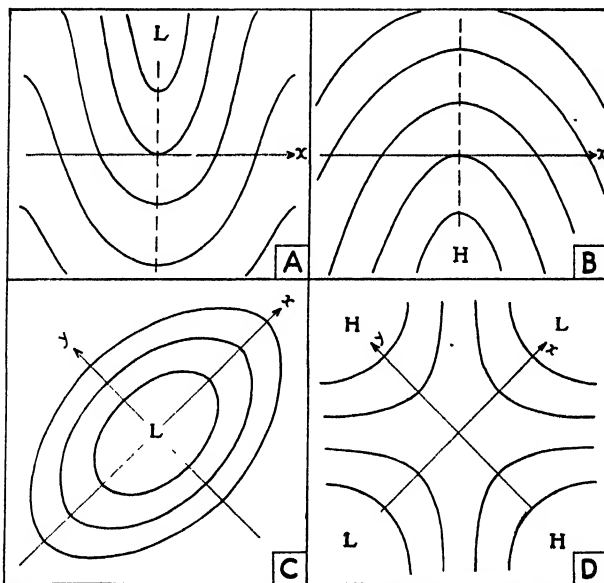
FIG. 191.—Illustrating the definition of trough lines, wedge lines, pressure centers, and cols.

6. *Cyclonic Centers.*—A cyclonic center may be defined as a point in which the pressure is a minimum relative to the surroundings. In general, it is possible to draw two symmetry lines through the cyclonic center. If the isobars around the center are circular, any line through

the center will be a symmetry line. If the isobars are oblong, we may draw one symmetry line where the isobars have a maximum of curvature and another where the isobars have a minimum of curvature (see Fig. 191C). Each of these symmetry lines corresponds to the definition of a trough line. The cyclonic center may, therefore, in general be defined as the point of intersection between two trough lines. Choosing the x-axis along the one and the y-axis along the other symmetry line, we obtain for the center

$$(11) \qquad \frac{\partial p}{\partial x} = \frac{\partial p}{\partial y} = 0$$

and

$$(12) \qquad \frac{\partial^2 p}{\partial x^2} > 0 \qquad \text{and} \qquad \frac{\partial^2 p}{\partial y^2} > 0$$

7. *Anticyclonic Centers.*—In a similar manner, an anticyclonic center may be defined as the point of intersection between two wedge lines (*i.e.*, the lines of approximate symmetry). Choosing as above the coordinate axes along the symmetry lines, we obtain

$$(13) \qquad \frac{\partial p}{\partial x} = \frac{\partial p}{\partial y} = 0$$

and

$$(14) \qquad \frac{\partial^2 p}{\partial x^2} < 0 \qquad \text{and} \qquad \frac{\partial^2 p}{\partial y^2} < 0$$

8. *Cols.*—In order to obtain a convenient characteristic for a col, we choose the coordinate axes as shown in Fig. 191D. The col may then be defined as the point of intersection between a trough line and a wedge line. Consequently, in the col,

$$(15) \qquad \frac{\partial p}{\partial x} = \frac{\partial p}{\partial y} = 0$$

and

$$(16) \qquad \frac{\partial^2 p}{\partial x^2} < 0 \qquad \text{and} \qquad \frac{\partial^2 p}{\partial y^2} > 0$$

9. *Summary of Characteristics.*—From the above discussion, it follows that the pressure field contains a number of lines or points which can be identified from one map to another. The pressure characteristics that hold for such lines or points are summarized in Table 57. It will be seen that the fundamental conditions which characterize these lines or

TABLE 57.—DEFINITIONS OF IDENTIFIABLE LINES AND POINTS IN THE PRESSURE FIELD

Line	Fundamental conditions	Auxiliary conditions	
Isobar....................	$p = $ constant	$\nabla p \gtrless 0$	
Isallobar.................	$\frac{\partial p}{\partial t} = $ constant	$\nabla \frac{\partial p}{\partial t} \gtrless 0$	
Front.....................	$p - p' = 0$	$\frac{\partial p}{\partial x} - \frac{\partial p'}{\partial x} > 0$	
Trough line...............	$\frac{\partial p}{\partial x} = 0$	$\frac{\partial^2 p}{\partial x^2} > 0$	
Wedge line................	$\frac{\partial p}{\partial x} = 0$	$\frac{\partial^2 p}{\partial x^2} < 0$	
Center of low.............	$\frac{\partial p}{\partial x} = \frac{\partial p}{\partial y} = 0$	$\frac{\partial^2 p}{\partial x^2} > 0$	$\frac{\partial^2 p}{\partial y^2} > 0$
Center of high............	$\frac{\partial p}{\partial x} = \frac{\partial p}{\partial y} = 0$	$\frac{\partial^2 p}{\partial x^2} < 0$	$\frac{\partial^2 p}{\partial y^2} < 0$
Col.......................	$\frac{\partial p}{\partial x} = \frac{\partial p}{\partial y} = 0$	$\frac{\partial^2 p}{\partial x^2} < 0$	$\frac{\partial^2 p}{\partial y^2} > 0$

points state that the pressure itself or some derivation of the pressure function remains constant while the curve or point moves across the chart.
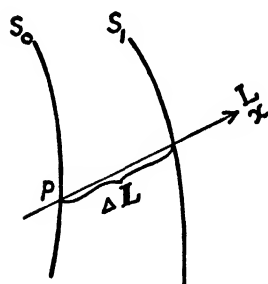
FIG. 192.—Illustrating the definition of the velocity of a curve.

147. Definition of Velocity and Acceleration of a Curve.—Let S_0 in Fig. 192 represent the position of a curve at the instant t_0, and let S_1 denote its position at the instant $t_0 + \Delta t$. We consider the curve element at the point P. Choose an arbitrary axis L through this point so that L is positive in the direction from S_0 to S_1. Let ΔL denote the displacement of the curve along the axis L during the time interval Δt. The velocity of the curve along the axis L may then be defined as

$$c = \lim_{\Delta t \to 0} \left(\frac{\Delta L}{\Delta t} \right)$$

The acceleration of the velocity along the axis L may then be defined as

$$A = \frac{dc}{dt}$$

The velocity and the acceleration of the curve element along the axis L is identical to the velocity and the acceleration that an imaginary particle would obtain if it were forced to remain on the curve S and on the axis L.

Choosing our x-axis along the line L, we obtain

$$c = \lim_{\Delta t \to 0} \left(\frac{\Delta x}{\Delta t}\right)$$

and

(1)
$$A = \frac{dc}{dt} = \frac{\partial c}{\partial t} + c \frac{\partial c}{\partial x}$$

In many cases, it is convenient to choose the axis perpendicular to the curve S. In other cases, however, it is convenient to choose the axis in an arbitrary direction. The reasons for this will become evident when we discuss specific cases.

148. Choice of Systems of Coordinates.—In order to obtain analytical expressions for the velocities and accelerations as defined above, it is convenient to consider the pressure variations in two systems of coordinates: one that is fixed to the map, and one that moves with the pressure system. Let

$$p = p(x,y,t)$$

represent the distribution of pressure. Differentiating with respect to time, we obtain in the fixed system of coordinates

(1)
$$\frac{dp}{dt} = \frac{\partial p}{\partial t} + v \cdot \nabla p$$

where dp/dt is the pressure variation on a moving air parcel, v is the velocity of this parcel relative to the fixed system of coordinates (*i.e.*, the wind velocity), and $-\nabla p$ is the horizontal pressure gradient. Differentiating in the same way, we obtain in the moving system of coordinates

(2)
$$\frac{dp}{dt} = \frac{\delta p}{\delta t} + v' \cdot \nabla p$$

The quantities dp/dt and ∇p must be identical in both systems since they are independent of the choice of coordinate systems. $\delta p/\delta t$ denotes the pressure variation per unit time in the system of coordinates that moves with the pressure system. This term then indicates the deepening $[(\delta p/\delta t) < 0]$ or the filling $[(\delta p/\delta t) > 0]$ of the pressure system. Finally, v' indicates the velocity of the air relative to the moving pressure system.

From Eqs. (1) and (2), we obtain

(3)
$$\frac{\delta p}{\delta t} = \frac{\partial p}{\partial t} + c \cdot \nabla p$$

where $c = v - v'$ is the velocity with which the pressure system moves across the chart. The quantities $\partial p/\partial t$ and ∇p may be obtained from

the isallobars and isobars, respectively. Equation (3) then contains two unknown quantities, *viz.*, the velocity and the deepening of the pressure system. It also shows that the barometric tendency consists of two parts, *viz.*:

1. One that depends on the movement of the pressure system, or the *convective term* represented by $c \cdot \nabla p$.

2. One that depends on the deepening or filling of the pressure systems, or the *individual term* represented by $\delta p / \delta t$. This term represents the internal changes in structure of the pressure systems.

We may therefore write

(4)
$$\dot{b}_0 = b_d - b_m$$

where b_0 stands for the observed barometric tendency, b_d for the deepening (or filling), and b_m for the barometric changes caused by the movement of the pressure system. The principal problem for the analyst will therefore be to separate the observed barometric tendency into the components b_d and b_m.

It is of interest to note that Eq. (3) holds for any variable. We may therefore write symbolically

(5)
$$\frac{\delta}{\delta t} = \frac{\partial}{\partial t} + c \cdot \nabla$$

or, when we choose the x-axis along the vector c,

(6)
$$\frac{\delta}{\delta t} = \frac{\partial}{\partial t} + c \frac{\partial}{\partial x}$$

This operation may be applied to p or any function of p. Applying it to such functions of p as remain constant during the movement of the pressure systems, we obtain

$$\frac{\delta}{\delta t} = 0$$

and the velocity of the pressure system is then obtained from

$$\frac{\partial}{\partial t} + c \frac{\partial}{\partial x} = 0$$

When c is thus found, the operator (5) may be applied to p as shown in Eq. (3). As c is then known, the deepening term may be computed. The problem of separating the observed tendency into a deepening term and a convective term is then solved. We shall therefore first deduce formulae for the velocity of pressure systems and afterwards discuss the analysis of deepening and filling.

149. Velocity Formulae.—It was shown in Par. 146 that there are certain curves in the pressure distribution along which either the pressure

function or some derivative of it remains constant while the curves move relative to the chart.   In a system of coordinates that moves with these curves, the following conditions hold:

$$(1) \qquad \frac{\delta}{\delta t} = \frac{\delta^2}{\delta t^2} = \cdots = 0$$

Applying now the operator defined by Eq. *148*(6) to the fundamental characteristics listed in Table 57 (Par. 146) and making use of the first of the above equations, we obtain the following formulae for the velocity of the various curves in the pressure field:

(2) Isobar: $\qquad\qquad c = -\dfrac{\partial p/\partial t}{\partial p/\partial x}$

(3) Isallobar: $\qquad\quad c = -\dfrac{\partial^2 p/\partial t^2}{\partial^2 p/\partial x\,\partial t}$

(4) Front: $\qquad c = -\dfrac{(\partial p/\partial t) - (\partial p'/\partial t)}{(\partial p/\partial x) - (\partial p'/\partial x)}$

where letters with indices refer to the rear of the front.

In applying the above formulae, the x-axis may be chosen in any convenient direction and not necessarily normal to the line in question.

(5) Trough or wedge line: $c = -\dfrac{\partial^2 p/(\partial x\,\partial t)}{\partial^2 p/\partial x^2}$

The formulae for the velocity of a wedge line is identical to that of a trough line; but $\partial^2 p/\partial x^2$ is positive on the trough line, and negative on the wedge line.   It is important to note that the definition of these lines involves that the x-axis should be chosen normal to the trough or the wedge line.

A cyclonic center was defined as the point of intersection between two trough lines (see Fig. 191*C*); and an anticyclonic center was defined as the point of intersection between two wedge lines.   We choose the x-axis along one trough line and the y-axis along the other.   Theoretically, it is immaterial whether or not the two trough lines are at right angles and whether they are straight or curved lines.   The trough line which coincides with the y-axis will then have a velocity c_x along the x-axis, and that which coincides with the x-axis will have a velocity c_y along the y-axis.   The same applies to an anticlonic center when the term "wedge line" is substituted for the term "trough line."   The pressure center, therefore, has the velocity components c_x and c_y along the coordinate axis.

A col in the pressure distribution is determined by the intersection between a trough line and a wedge line.   The col (see Fig. 191*D*) will

therefore have a velocity component c_x along the trough line and the velocity component c_y along the wedge line.

Each of the velocity components mentioned above is in principle expressed by formula (5) which holds both for troughs and wedges. We may therefore write

(6) Cyclonic and anticy-
clonic centers and cols: $\quad c_x = -\dfrac{\partial^2 p/(\partial x\, \partial t)}{\partial^2 p/\partial x^2}, \quad c_y = -\dfrac{\partial^2 p/(\partial y \partial t)}{\partial^2 p/\partial y^2}$

The practical application of these formulae will be discussed later.

150. Acceleration Formulae.—Expressions for the acceleration of identifiable curves in the pressure field can be obtained most easily by substituting the above expressions for the velocity of such curves into Eq. *147*(1). It is then important to remember that

(1) $$\frac{\partial^3 p}{\partial x^3} = \frac{\partial^3 p}{\partial y^3} = 0$$

whenever the pressure field is symmetrical with respect to the coordinate axes. This is the case along trough and wedge lines and also along the symmetry axes in centers of highs and lows and in cols. From Eq. *147*(1) and the formulae in Par. 149, we then obtain the following expressions for the acceleration of the significant lines:

(2) Isobar: $A = -\dfrac{(\partial^2 p/\partial t^2) + 2c\,(\partial^2 p/\partial x\, \partial t) + c^2(\partial^2 p/\partial x^2)}{\partial p/\partial x}$

An expression for the acceleration of isallobars is easily deduced; but as it contains terms that cannot be evaluated from the weather charts, it will not be reproduced here.

(3) Front:

$$A = -\frac{\dfrac{\partial^2 p}{\partial t^2} - \dfrac{\partial^2 p'}{\partial t^2} + 2c\left(\dfrac{\partial^2 p}{\partial x\, \partial t} - \dfrac{\partial^2 p'}{\partial x\, \partial t}\right) + c^2\left(\dfrac{\partial^2 p}{\partial x^2} - \dfrac{\partial^2 p'}{\partial x^2}\right)}{\dfrac{\partial p}{\partial x} - \dfrac{\partial p'}{\partial x}}$$

On applying the formulae (2) and (3), the x-axis may be chosen in any convenient direction, and not necessarily normal to the isobar or the front.

(4) Trough or
wedge line: $\quad A = -\dfrac{(\partial^3 p/\partial x\, \partial t^2) + 2c\,(\partial^3 p/\partial x^2\, \partial t)}{\partial^2 p/\partial x^2}$

This formula is simpler than those above because the term $\partial^3 p/\partial x^3$ vanishes on account of the symmetry in the pressure distribution along trough and wedge lines. The formula holds both for troughs and wedges;

but $(\partial^2 p/\partial x^2) > 0$ for troughs, and $(\partial^2 p/\partial x^2) < 0$ for wedges. It is important to note that the definition of trough and wedge lines involves that the x-axis should be chosen normal to these lines.

For reasons indicated in the previous paragraph, it is readily seen that formula (4) holds in principle also for cyclonic and anticyclonic centers and for cols. This gives

(5) Cyclonic and anticyclonic centers and cols:
$$A_x = -\frac{(\partial^3 p/\partial x\,\partial t^2) + 2c_x(\partial^3 p/\partial x^2\,\partial t)}{\partial^2 p/\partial x^2}$$
$$A_y = -\frac{(\partial^3 p/\partial y\,\partial t^2) + 2c_y(\partial^3 p/\partial y^2\,\partial t)}{\partial^2 p/\partial y^2}$$

Although the practical applications of these formulae will be discussed later, it is appropriate to remark that the acceleration formulae are difficult to apply numerically to the weather maps. They are, however, useful for a qualitative discussion and for an understanding of when the acceleration term is and is not important.

When the velocity and the acceleration have been evaluated from the weather maps, the displacement S can be computed from the formula

(6) $$S = ct + \tfrac{1}{2}At^2$$

In most cases, it will be necessary to compute the displacement by means of the velocity only, a rough estimate of the influence of the acceleration term being used.

151. The Notations.—For the practical application of the above formulae, it is essential to be thoroughly familiar with the meanings of the symbols that appear in them. In order to demonstrate the meanings, we shall consider the distribution of pressure and pressure tendencies in the vicinity of a trough of low pressure as shown in Fig. 194A.

The term $\partial p/\partial x$ denotes the increase in pressure per unit length along the x-axis. The values of pressure along the x-axis are plotted on cross-section paper in Fig. 194B. The curve p represents the "pressure profile" along the x-axis. $\partial p/\partial x$ then expresses the slope of the pressure profile. It will be seen that the slope vanishes at the trough line where the profile has a maximum of curvature. This curvature is said to be cyclonic, because it resembles a profile through a cyclonic center. Similarly, $\partial p/\partial y$ represents the slope of the pressure profile along the y-axis.

The term $(\partial^2 p/\partial x^2)$ expresses the change in slope of the pressure profile per unit length along the x-axis. Therefore, the greater the curvature of the profile, the larger is $\partial^2 p/\partial x^2$. Moreover, $(\partial^2 p/\partial x^2) > 0$ in troughs and centers of low pressure, and $(\partial^2 p/\partial x^2) < 0$ in wedges and centers of high pressure.. The term $\partial^2 p/\partial y^2$ has the same meaning with regard to the y-axis.

The curvature of the pressure profile in Fig. 194*B* is expressed by

$$\sigma = \frac{\partial^2 p/\partial x^2}{[1 + (\partial p/\partial x)^2]^{3/2}}$$

On the trough line and also on wedge lines and in centers of high and low pressure, $\partial p/\partial x = 0$, so that

$$\sigma = \frac{\partial^2 p}{\partial x^2}$$

Therefore, $\partial^2 p/\partial x^2$ and $\partial^2 p/\partial y^2$ express the curvature of the pressure profiles in the vicinity of pressure centers and trough and wedge lines, cyclonic curvature being positive and anticyclonic curvature being negative.

The term $\partial^2 p/\partial x \, \partial t$ expresses the increase in barometric tendency ($\partial p/\partial t$) per unit length along the x-axis, and $\partial^2 p/\partial y \, \partial t$ has a similar meaning along the y-axis. Therefore, the terms $-(\partial^2 p/\partial x \, \partial t)$ and $-(\partial^2 p/\partial y \, \partial t)$ express the x- and y-components of the isallobaric gradient. The distribution of barometric tendency along the x-axis is plotted in Fig. 194*C*. $\partial^2 p/\partial x \, \partial t$ then denotes the slope of the tendency profile along the x-axis. It will be seen that the tendency profile has an inflection point near the trough line where the slope has a maximum. To the right, the tendency profile has a cyclonic (positive) curvature, and to the left the curvature is anticyclonic (negative).

The term $\partial^3 p/\partial x^2 \, \partial t$ denotes the curvature of the tendency profile along the x-axis as $\partial^2 p/\partial x^2$ expresses the curvature of the pressure profile along the same axis. Likewise, $\partial^3 p/\partial y^2 \, \partial t$ expresses the curvature of the tendency profile along the y-axis.

The term $\partial^2 p/\partial t^2$ expresses the change in barometric tendency per unit time. If a profile were drawn showing the distribution of $\partial^2 p/\partial t^2$ along the x-axis, $\partial^3 p/(\partial x \, \partial t^2)$ would express the slope of this profile.

152. Selection of Points.—The above formulae were deduced without any simplifying assumptions; they are therefore exact and hold in all cases for the instantaneous conditions. However, in applying these formulae to weather charts, several obstacles are encountered that tend to render the computations inaccurate. The art of applying the above formulae does not lie in the mathematical operations but in the choice of points on the map where the conditions are such that the inaccuracy is reduced to a minimum.

In the first place, the formulae for velocities and accelerations contain differentials of pressure and pressure variations. True space differentials cannot be obtained from the weather charts because of the large distance between neighboring stations and because of the inaccuracy in observations and analysis. Nor can we obtain true time differentials because

of the large intervals between consecutive weather charts. The smallest time unit that can be used in connection with weather maps is 3 hr., for the reported barometric tendency is defined as the variation in pressure during the 3 hr. preceding the observation.

In applying the formulae to weather charts, it will, therefore, be necessary to substitute finite differences for differentials, and it is chiefly this operation that may introduce serious errors in the computed results unless special precautions are taken to render such errors ineffective. The analyst must therefore make sure that the formulae are used only in cases in which it is permissible to substitute finite differences for differentials.

Furthermore, even the most careful analysis may contain errors. The formulae should therefore be used only in those areas where the analysis is particularly reliable and where it is permissible to replace differentials by finite differences. Before any computation is made, the analysis in the vicinity of the chosen point should be subjected to a meticulous inspection in order to remove errors.

Although the formulae will give the *instantaneous* values of velocity and acceleration, errors may result when we extrapolate the future position over a large interval of time. In the first approximation, we may neglect the acceleration. The displacement S is then

$$S = ct$$

With acceleration, we obtain

$$S = ct + \tfrac{1}{2}At^2$$

which, theoretically, is a better approximation to the true displacement. Suppose that the computed velocity and acceleration contain the errors Δc and ΔA, respectively. Then

$$S = c_0 t + \tfrac{1}{2}A_0 t^2 + \Delta ct + \tfrac{1}{2}\Delta A t^2$$

where subscript zero indicates the correct values of c and A. As time increases, the error in the accelerational term may become larger than the error due to the inaccuracy in the computed velocity. It will be shown later that the velocity is easily evaluated from the weather maps, though in most cases it is difficult to obtain accurate values for the acceleration. In view of this, the analyst should choose for computation points in the pressure field at which the acceleration is a minimum. The accelerational term may then be neglected. In certain cases, the axis along which the displacement is computed may be chosen arbitrarily. In such cases, the axis should be chosen in the direction in which the acceleration is a minimum.

Summing up, we may say that the formulae should be applied only in cases where simultaneously:

1. The analysis is reliable and simple.

2. The conditions are such that differentials may be replaced by suitable finite differences.

3. The acceleration is a minimum.

How these principles are applied will be demonstrated in the following paragraphs which deal with specific cases.

153. The Movement of Isobars.—The velocity of an isobar along an arbitrary axis is given by Eq. *149*(2), *viz.*:

$$(1) \qquad\qquad c = -\frac{\partial p/\partial t}{\partial p/\partial x}$$

and the acceleration is expressed by

$$(2) \qquad A = -\frac{(\partial^2 p/\partial t^2) + 2c(\partial^2 p/\partial x\,\partial t) + c^2(\partial^2 p/\partial x^2)}{\partial p/\partial x}$$

The terms in the numerator of Eq. (2) are usually small. The acceleration will therefore be small when $\partial p/\partial x$ is large. It is convenient to choose the x-axis normal to the isobar and positive in the direction of increasing pressure. $\partial p/\partial x$ then expresses the magnitude of the horizontal pressure gradient. As some of the terms in Eq. (2) cannot be obtained from the weather charts, the displacement of the isobars can be computed with satisfactory results from Eq. (1) only when the acceleration is negligible. In regions where the pressure gradient has a maximum (*i.e.*, where the isobars are most crowded), $\partial^2 p/\partial x^2 = 0$ and the last term in the numerator vanishes. Where the isallobars are normal to the isobars and also where the barometric tendency has a maximum (*i.e.*, in the isallobaric centers), $\partial^2 p/(\partial x\,\partial t) = 0$. It follows then from Eq. *149*(3) that $\partial^2 p/\partial t^2 = 0$; for otherwise the velocity of the isallobar would be infinite, which is not possible. The three terms in the numerator of Eq. (2) above will then vanish if the isallobaric centers coincide with regions of maximum pressure gradient.

The isallobaric center will usually be found in advance and in the rear of moving cyclones and anticyclones where the pressure gradient is largest. Therefore, *the movement of the isobars may be computed from Eq.* (1) *with reasonable accuracy in the regions occupied by the isallobaric maxima and minima when the pressure gradient is moderate or large.*

Let b denote the barometric tendency expressed in millibars. If isobars are drawn for each fifth millibar, we may put

$$\frac{\partial p}{\partial x} = \frac{5}{H}$$

where H is the distance between the two neighboring isobars. The velocity of the isobars is then

(3)
$$c = -\frac{b \cdot H}{5}$$

Since b indicates the change in pressure in 3 hr., it follows that the point of the isobar which we consider will move the distance $-(b \cdot H/5)$ in 3 hr. If we use H as the unit of length, the isobar will move $-(b/5)$ length units in 3 hr. (*i.e.*, in one tendency interval), and it will move the distance $-(b/5)n$ length units in n tendency intervals.

Experience shows that accurate results can be obtained from formula (3) only when the analysis is particularly reliable. The values for b should be interpolated from the smoothed isallobars, and the values for H should be determined from smoothed isobars. Values for b in the
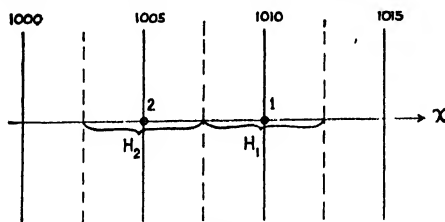
Fig. 193.

rear of and close to fronts are too inaccurate for such computations. Even under the most favorable circumstances, formula (3) will yield satisfactory results only within comparatively short intervals of time; extrapolations of the movement of isobars over periods greater than four tendency intervals (*i.e.*, 12 hr.) are usually inaccurate.

Formula (3) is often useful for determining whether the winds are increasing or decreasing, or changing in direction. Let indices 1 and 2 denote points on two neighboring isobars as shown in Fig. 193. Then the velocities of the points 1 and 2 along the x-axis are $c_1 = -(b_1 H_1/5)$ and $c_2 = -(b_2 H_2/5)$, respectively. The difference between the velocities is

$$c_1 - c_2 = -\tfrac{1}{5}(b_1 H_1 - b_2 H_2)$$

The pressure gradient therefore increases when $b_1 H_1 > b_2 H_2$, and it decreases when $b_1 H_1 < b_2 H_2$. Applying this to regions where the isobars are equidistant (*i.e.*, $H_1 = H_2$), we obtain the following rule: *The pressure gradient and the wind increase when the isallobaric gradient has a component along the pressure gradient and decrease when the isallobaric gradient has a component in the opposite direction.*

In a similar manner, it is readily seen that the component of the isallobaric gradient along the isobars will tend to make the isobars (and the

wind) rotate; whether the rotation is clockwise or counterclockwise is readily seen in each particular case.

The application of formula (3) is particularly simple in warm sectors when the isobars are straight and equidistant. As will be shown in Par. 170, the formula may then be used for determining the rate of development of the cyclone.

154. The Movement of Troughs and Wedges.—The velocity of an arbitrary point on a trough or a wedge line along an axis normal to the trough or wedge line is given by Eq. *149*(5), *viz.*,

$$(1) \qquad c = -\frac{\partial^2 p/(\partial x\,\partial t)}{\partial^2 p/\partial x^2}$$

and the acceleration is expressed by Eq. *150*(4), *viz.*,

$$(2) \quad A = \\ -\frac{(\partial^3 p/\partial x\,\partial t^2) + 2c(\partial^3 p/\partial x^2\,\partial t)}{\partial^2 p/\partial x^2}$$

The terms in the numerator of Eq. (2) are usually small, whereas $\partial^2 p/\partial x^2$ may vary within wide limits. It follows then that the acceleration will be small when $\partial^2 p/\partial x^2$ is large. In such cases, the displacement of a trough or a wedge line may be computed from formula (1), the displacement during n tendency intervals being equal to nc.

The term $\partial^2 p/\partial x^2$ expresses the curvature of the pressure profile along the x-axis, which is normal to the trough or the wedge line. It follows then that the acceleration will be small when this profile has a large curvature. As a large curvature means a pronounced trough or wedge, it follows that formula (1) may be applied to pronounced troughs and wedges. When the trough (or wedge) is weak, neither formula (1) nor (2) will give satisfactory results.

FIG. 194.—*A*, isobars (full lines) and isallobars (broken lines) in the vicinity of a trough of low pressure; *B*, pressure profile along the *x*-axis; *C*, tendency profile along the *x*-axis.

1. *Evaluation of c.*—The procedure will be the same for troughs and wedges. We consider a trough shown in Fig. 194*A*. In the first
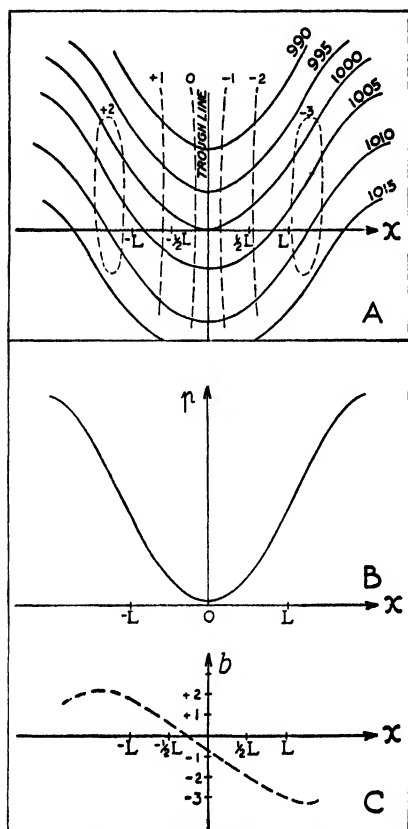
place, formulae (1) and (2) contain differentials which must be replaced by finite differences. The term $\partial^2 p/\partial x\,\partial t$ is represented graphically by the slope of the tendency curve in Fig. 194C. Choose four points on the x-axis with the coordinates L, $\frac{1}{2}L$, $-\frac{1}{2}L$, and $-L$. According to the rules of numerical differentiation,[1] we may write as a first approximation

$$(3) \qquad \frac{\partial^2 p}{\partial x\,\partial t} = \frac{\partial b}{\partial x} = \frac{b^{(\frac{1}{2}L)} - b^{(-\frac{1}{2}L)}}{L}$$

where $b^{(\frac{1}{2}L)}$ and $b^{(-\frac{1}{2}L)}$ denote the barometric tendencies in the points $\frac{1}{2}L$ and $-\frac{1}{2}L$, respectively.

The term $\partial^2 p/\partial x^2$ expresses the curvature (or the variation of the slope) of the pressure profile in the vicinity of the trough line. In a similar manner, we obtain as a first approximation

$$(4) \qquad \begin{aligned} \frac{\partial^2 p}{\partial x^2} &= \frac{1}{L}\left(\frac{p^{(L)} - p^{(0)}}{L} - \frac{p^{(0)} - p^{(-L)}}{L}\right) \\ &= \frac{p^{(L)} - 2p^{(0)} + p^{(-L)}}{L^2} \end{aligned}$$

where $p^{(0)}$ indicates the pressure in the point $x = 0$. This substituted in the formula for the velocity gives

$$(5) \qquad c = -L\,\frac{b^{(\frac{1}{2}L)} - b^{(-\frac{1}{2}L)}}{p^{(L)} - 2p^{(0)} + p^{(-L)}}$$

Since the barometric tendency b indicates the variation in pressure during 3 hr., we may choose 3 hr. as the most convenient unit of time. In a similar manner, we may choose the distance L as a unit of length. The above formulae then reduce to

$$(6) \qquad \frac{\partial^2 p}{(\partial x\,\partial t)} = b^{(\frac{1}{2})} - b^{(-\frac{1}{2})}$$

$$(7) \qquad \frac{\partial^2 p}{\partial x^2} = p^{(1)} - 2p^{(0)} + p^{(-1)}$$

$$(8) \qquad c = -\frac{b^{(\frac{1}{2})} - b^{(-\frac{1}{2})}}{p^{(1)} - 2p^{(0)} + p^{(-1)}}$$

Applying formula (8) to Fig. 194, we obtain $c = 0.18$ length units (L) per 3 hr. During eight tendency intervals, the displacement would be 1.4 length units.

2. *Choice of Length Unit.*—It should be borne in mind that the accuracy of formula (6) depends largely on the choice of length unit. It is readily seen from Fig. 194 that if the length unit L is chosen too large, considerable errors may result. On the other hand, if the length unit

<hr>

[1] RUNGE-KÖNIG, "Nümerisches Rechnen," Berlin, 1924.

is too small, the errors in the analysis will carry more weight. *The length unit should be chosen so large that the errors in the analysis are suppressed; but, on the other hand, it must not be so large that the formulae (6) and (7) fail to give approximate values for the slope of the tendency profile and the curvature of the pressure profile, respectively.*

In order to demonstrate the influence of the errors in the analysis, we return to formula (3). Let subscript t indicate the true value of the barometric tendency. We may then write

$$b^{(\frac{1}{2}L)} = b_t^{(\frac{1}{2}L)} \pm \epsilon_1 \quad \text{and} \quad b^{(-\frac{1}{2}L)} = b_t^{(-\frac{1}{2}L)} \pm \epsilon_2$$

where ϵ_1 and ϵ_2 denote the errors. This substituted into formula (3) gives

$$\frac{\partial^2 p}{\partial x\, \partial t} = \frac{b_t^{(\frac{1}{2}L)} - b_t^{(-\frac{1}{2}L)}}{L} \pm \frac{\epsilon_1 + \epsilon_2}{L}$$

As the errors are independent of the choice of length unit L, it is readily seen that their influence on the computed velocity decreases with increasing L. It will be seen from Fig. 194C that the difference in barometric tendency between the points $\frac{1}{2}L$ and $-\frac{1}{2}L$ increases with increasing L so that, when the tendency profile is not appreciably curved, the errors in observed barometric tendencies and errors in drawing isallobars are effectively suppressed when L is large. However, if L be chosen so large that the points $\frac{1}{2}L$ and $-\frac{1}{2}L$ come within the isallobaric maximum or minimum, or outside these regions, it will be seen from Fig. 194C that the difference $[b^{(\frac{1}{2}L)} - b^{(-\frac{1}{2}L)}]$ fails to render reasonable approximation to the true value of the slope of the tendency profile.

In choosing appropriate length units, we must also consider formula (4). It is readily seen that a length unit which is sufficiently large to suppress the errors in the tendencies will suffice to suppress the errors in the isobars, for the influence of contingent errors in the pressures is inversely proportional to L^2. Moreover, the atmospheric pressure is usually observed with greater accuracy than the barometric tendency. The isobars can therefore be drawn with greater accuracy than the isallobars.

Furthermore, the length unit must be chosen so that formula (4) will render a reasonable approximation to the true curvature of the pressure profile. Experience shows that the length unit may be chosen so large that the points 1 and -1 approach the inflection points in the pressure profile (Fig. 194B).

In Figs. 194B and C, it is of interest to note that the largest length unit which may satisfy one profile may be too large for the other profile. In such cases, *the largest length unit that satisfies both profiles should be chosen.*

The appropriate choice of length unit is shown in Fig. 194. The most accurate computation can be made when the profiles of pressure and tendency are drawn. However, with experience, it will be quite easy to choose the right length unit without drawing such profiles. The length unit may then be chosen by inspecting the isobars and the isallobars on the map (see Fig. 194A). Computations should be made only when the isallobars are fairly evenly spaced in the vicinity of the trough line, and the length unit should be chosen somewhat shorter than the distance between the points on the x-axis that have the largest (positive or negative) barometric tendencies.

When the trough or the wedge is very narrow, the length unit will be small and formula (6) will be inaccurate. In such cases, formula (6) may be replaced by

$$(9) \qquad \frac{\partial^2 p}{\partial x \, \partial t} = \tfrac{1}{2}[b^{(1)} - b^{(-1)}]$$

The advantage of doing this is that the errors in b will be more effectively suppressed.

3. *Acceleration.*—Whereas the velocity of a trough or a wedge is easily evaluated from the weather charts, considerable difficulties are encountered in the way of evaluating the acceleration. The term $\partial^3 p/(\partial x \, \partial t^2)$ in Eq. (2) can be obtained from the isallobars only when consecutive maps at short intervals are available. Let Δb denote the change in barometric tendency at a station. Proceeding in the same way as above, we obtain the following approximate formulae:

$$(10) \qquad \frac{\partial^3 p}{\partial x \, \partial t^2} = \Delta b^{(\frac{1}{2})} - \Delta b^{(-\frac{1}{2})}$$

$$(11) \qquad \frac{\partial^3 p}{\partial x^2 \, \partial t} = b^{(1)} - 2b^{(0)} + b^{(-1)}$$

Formula (10) expresses the slope of the profile of the changes in barometric tendency, and formula (11) expresses the curvature of the tendency profile in the vicinity of the trough line. Usually the term $\partial^3 p/(\partial x \, \partial t^2)$ cannot be evaluated with sufficient accuracy from the weather maps. It will therefore usually not be possible to compute the acceleration. However, it will often be possible to estimate the sign and the approximate magnitude of the acceleration. As the movement of troughs and wedges depends on the movement of neighboring cyclones and anticyclones, the further discussion of the accelerational influence will be deferred to later sections.

155. The Movement of Pressure Centers and Cols.—The velocity of a pressure center is expressed by Eq. *149*(6), and the acceleration is expressed by Eq. *150*(5). These equations are identical with those

expressing the velocity and acceleration of trough and wedge lines, the only difference being that, in the case of pressure centers, there are two coordinate axes and the velocity and acceleration each have a component along each of the coordinate axes. If the isobars around the center are circular, any line through the center will be a symmetry line, and any two such lines may be chosen as coordinate axes. If the isobars are oblong, we may choose the x-axis along the longest and the y-axis along the shortest symmetry axis (see Fig. 191C). The coordinate axis may be curved or straight lines.

After having drawn the symmetry axes on the map, the next step is to choose the appropriate length unit. The principles on which the
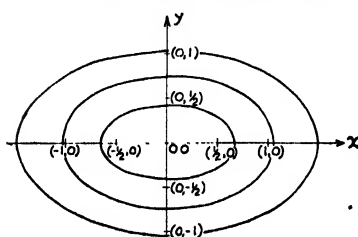
Fig. 195.

choice should be based are exactly the same as those which apply to troughs and wedges, and the procedure is exactly as described under (2) in Par. 154. When the length unit has been chosen, mark the points on the axes whose coordinates are (1,0), ($\frac{1}{2}$,0), (0,0), ($-\frac{1}{2}$,0), (-1,0), (0,1), (0,$\frac{1}{2}$), (0,$-\frac{1}{2}$) and (0,-1) as shown in Fig. 195. As was explained in Par. 154, the differentials entering into Eqs. *149*(6) and *150*(5) may be replaced by finite differences by means of the following formulae:

$$
(1)\begin{cases}
\dfrac{\partial^2 p}{\partial x\, \partial t} = b^{(\frac{1}{2},0)} - b^{(-\frac{1}{2},0)} \quad \text{or} \quad = \tfrac{1}{2}[b^{(1,0)} - b^{(-1,0)}] \\[2mm]
\dfrac{\partial^2 p}{\partial y\, \partial t} = b^{(0,\frac{1}{2})} - b^{(0,-\frac{1}{2})} \quad \text{or} \quad = \tfrac{1}{2}[b^{(0,1)} - b^{(0,-1)}] \\[2mm]
\dfrac{\partial^2 p}{\partial x^2} = p^{(1,0)} - 2p^{(0,0)} + p^{(-1,0)} \\[2mm]
\dfrac{\partial^2 p}{\partial y^2} = p^{(0,1)} - 2p^{(0,0)} + p^{(0,-1)} \\[2mm]
\dfrac{\partial^3 p}{\partial x^2\, \partial t} = b^{(1,0)} - 2b^{(0,0)} + b^{(-1,0)} \\[2mm]
\dfrac{\partial^3 p}{\partial y^2\, \partial t} = b^{(0,1)} - 2b^{(0,0)} + b^{(0,-1)} \\[2mm]
\dfrac{\partial^3 p}{\partial x\, \partial t^2} = \Delta b^{(\frac{1}{2},0)} - \Delta b^{(-\frac{1}{2},0)} \quad \text{or} \quad = \tfrac{1}{2}[\Delta b^{(1,0)} - \Delta b^{(-1,0)}] \\[2mm]
\dfrac{\partial^3 p}{\partial y\, \partial t^2} = \Delta b^{(0,\frac{1}{2})} - \Delta b^{(0,-\frac{1}{2})} \quad \text{or} \quad = \tfrac{1}{2}[\Delta b^{(0,1)} - \Delta b^{(0,-1)}]
\end{cases}
$$

where the alternate formulae are to be used when the length unit is small, as was explained in Par. 154.

Substituting in formula *149*(6), we obtain for the velocity components of the pressure center

$$(2) \qquad c_x = -\frac{b^{(\frac{1}{2},0)} - b^{(-\frac{1}{2},0)}}{p^{(1,0)} - 2p^{(0,0)} + p^{(-1,0)}}$$

$$(3) \qquad c_y = -\frac{b^{(0,\frac{1}{2})} - b^{(0,-\frac{1}{2})}}{p^{(0,1)} - 2p^{(0,0)} + p^{(0,-1)}}$$

As was explained in the previous paragraph, it is frequently impossible to evaluate numerically the acceleration from the data of weather charts. This is mainly due to the fact that it is difficult to obtain accurate values for the quantities $\partial^3 p/\partial x\, \partial t^2$ and $\partial^3 p/\partial y\, \partial t^2$. The movement of pressure centers will therefore have to be computed from the velocity formulae, which express the displacement in terms of the chosen length unit with 3 hr. as the unit of time. The displacement of the center along the coordinate axes during n tendency intervals will then be

$$nc_x \qquad \text{and} \qquad nc_y$$

respectively. Usually, these formulae will not yield satisfactory results for more than eight tendency intervals (*i.e.*, 24 hr.). Although it is difficult to obtain numerical expressions for the acceleration, it is frequently possible, through indirect methods, to determine the sign and the approximate value of the accelerational influence.

It should be noted that the above formulae for the velocity and acceleration apply without restriction to anticyclonic centers, cols, and wedges. *In the cases of cyclonic centers and troughs of low pressure, the formulae hold only when the coordinate axes do not intersect well-defined fronts.* When the coordinate axes intersect well marked fronts, $\partial p/\partial t$, $\partial p/\partial x$, and $\partial p/\partial y$ are discontinuous and the above formulae are invalid. In these cases, the formula pertaining to fronts [Eqs. *149*(4) and *150*(3)] should be used. The practical application of these formulae will be discussed later.

156. Forecasting Rules Concerning the Movement of Troughs and Wedges.—Under favorable circumstances, the above formulae may be applied and the displacements during six or eight tendency intervals computed directly from the data of the weather charts. In many cases, however, it will be found that strict numerical application is not possible. In such cases, the above formulae may be used in a *qualitative* way in order to determine the direction and the approximate speed of the movement. We shall therefore discuss the above formulae with a view to obtaining qualitative forecasting rules. These rules, which are entirely based on the distribution of pressure and pressure tendencies, will be supplemented by other forecasting rules derived from the study of the wind distribution and the movement of fronts.

Since $\partial^2 p/\partial x^2$ is positive in troughs and negative on wedges, it follows directly from Eq. *149*(5) that:

Rule 1.   *Troughs move in the direction of the isallobaric gradient (i.e., from rising toward falling pressure), and wedges move in the opposite direction.*

The speed of the movement is directly proportional to $\partial^2 p/(\partial x\,\partial t)$ and inversely proportional to $\partial^2 p/\partial x^2$.   Since $\partial^2 p/(\partial x\,\partial t)$ expresses the slope of the tendency profile and $\partial^2 p/\partial x^2$ the curvature of the pressure profile (see Fig. 194), we obtain the following rule:

Rule 2.   *The speed of a trough or a wedge is directly proportional to the difference in tendency between the front and the rear of the trough (or wedge) and inversely proportional to the curvature of the pressure profile.*

It was shown in Par. 91 that the isallobaric gradient is proportional to the deviation of the actual wind from the geostrophic wind [Eq. *91*(7)].   In middle and high latitudes where the geostrophic balance is predominant, the isallobaric gradient will not attain excessive values. On the other hand, the curvature of the pressure profile along the x-axis may vary within wide limits.   From this, the following rule results:

Rule 3.   *Troughs and wedges whose pressure profiles have great curvature will move slowly, whereas troughs and wedges whose pressure profiles are slightly curved will move with a speed that varies within wide limits and depends greatly on the isallobaric gradient.*

A large curvature of the pressure profile means that the isobars are crowded in advance and in the rear of the trough or the wedge.   Such troughs or wedges will therefore have a small or moderate speed, but "flat" troughs or wedges *may* move quickly.

From Eq. *150*(4), it follows that the acceleration of a trough or a wedge line is inversely proportional to the curvature of the pressure profile.   Since the quantities in the numerator of this formula are very small, we obtain the following rule:

Rule 4.   *Troughs and wedges whose pressure profiles are greatly curved move with a fairly constant speed, whereas "flat" troughs or wedges may be greatly accelerated or retarded in their movement.*   This is the same as saying that pronounced pressure troughs and wedges have a more steady speed than indistinct troughs or wedges.   Therefore, it is easier to forecast the displacement of a well-developed trough (or wedge) than an indistinct one.   Again, it should be emphasized that the velocity of troughs and wedges depends on both the isallobaric gradient and the curvature of the pressure profile, and the one factor should be weighed against the other in estimating the speed.

Returning again to Eq. *150*(4), we may introduce the expression

$$c' = -\frac{\partial^3 p/(\partial x\,\partial t^2)}{\partial^3 p/(\partial x^2\,\partial t)}$$

Just as Eq. *149*(5) expresses the velocity of the pressure system, the above formula expresses the velocity of the isallobaric system. Substituting c' into Eq. *150*(4), we obtain for the acceleration of a trough or a wedge

$$A = \frac{c' - 2c}{\partial^2 p/\partial x^2} \cdot \frac{\partial^3 p}{\partial x^2\, \partial t}$$

We can always choose the x-axis in such a way that c is positive. Since the isallobaric system and the pressure system must have *approximately* the same velocities (the isallobaric system could not move with a speed that is twice as large as that of the pressure system), it follows that $(c' - 2c)$ must be negative. Since $\partial^2 p/\partial x^2$ is positive for troughs and
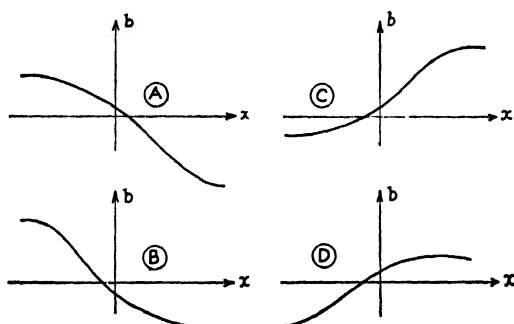
Fig. 196.—Showing the curvature of the tendency profile. *A*, when the trough is accelerated; *B*, when a trough is retarded; *C*, when a wedge is accelerated; *D*, when a wedge is retarded.

negative for wedges, it follows that the sign of the acceleration depends uniquely on $\partial^3 p/(\partial x^2\, \partial t)$, or the curvature of the tendency profile along the x-axis in the vicinity of the trough or the wedge line. From this we obtain the following rule:

Rule 5. A trough is accelerated when the tendency profile is curved as shown in Fig. 196A, and it is retarded when the tendency profile is as shown in Fig. 196B. A wedge is accelerated when the tendency profile is as shown in Fig. 196C, and it is retarded when the tendency profile is curved as shown in Fig. 196D.

This rule refers to the curvature in the immediate vicinity of the trough or wedge line. Furthermore, the rule holds only when the velocity of the trough or wedge is moderate or large. If the velocity were small enough, it is conceivable that $c' > 2c$. On account of the difficulty in the way of obtaining correct values for the curvature of the tendency profile in the vicinity of the trough or the wedge lines, rule 5 should be applied only in cases when the said curvature is appreciable and when the analysis is reliable; when these requirements are satisfied, the rule will give valuable results.

In applying the formulae in Par. 149 or the above qualitative rules, it must be ascertained that the displacement thus determined for one pressure system agrees with the simultaneous displacement of the neighboring systems. Thus, the estimated displacement of a trough must agree logically with the displacement of neighboring wedges. If the application of the above formulae and rules to several pressure systems gives conflicting results, the situation should be reexamined. Some comments on this will be found in Par. 173.

157. Forecasting Rules Concerning Pressure Centers.—The velocity components of a pressure center along the symmetry axes are expressed by Eq. *149*(6), *viz.*,

$$(1) \qquad c_x = -\frac{\partial^2 p/(\partial x\,\partial t)}{\partial^2 p/\partial x^2}, \qquad c_y = -\frac{\partial^2 p/(\partial y\,\partial t)}{\partial^2 p/\partial y^2}$$

and the components of the acceleration are given by Eq. *150*(5), *viz.*,

$$(2) \qquad A_x = -\frac{(\partial^3 p/\partial x\,\partial t^2) + 2c_x(\partial^3 p/\partial x^2\,\partial t)}{\partial^2 p/\partial x^2}$$

$$A_y = -\frac{(\partial^3 p/\partial y\,\partial t^2) + 2c_y(\partial^3 p/\partial y^2\,\partial t)}{\partial^2 p/\partial y^2}$$

If the isobars are circular, or nearly so, the coordinate axes may be chosen arbitrarily. It is then most convenient to choose the x-axis along the isallobaric gradient. Equations (1) then reduce to

$$c_x = -\frac{\partial^2 p/(\partial x\,\partial t)}{\partial^2 p/\partial x^2}, \qquad c_y = 0$$

or, in vector form,

$$(3) \qquad c = \frac{-I}{\partial^2 p/\partial x^2}$$

where $-I$ is the isallobaric gradient. Since $\partial^2 p/\partial x^2$ (the curvature of the pressure profile) is positive in cyclonic centers and negative in anticyclonic centers, we obtain:

Rule 6. Circular (or nearly circular) cyclonic centers move in the direction of the isallobaric gradient, whereas anticyclonic centers move in the opposite direction. The speed is directly proportional to the isallobaric gradient and inversely proportional to the curvature of the pressure profile.

It was shown in Par. 91 that the deviation of the wind from the geostrophic wind [Eq. *91*(7)] is directly proportional to the isallobaric gradient. From this and from the above rule, we obtain the well-known Guilbert rule:

Rule 7. A cyclonic center moves toward the area of undernormal winds, whereas an anticyclonic center moves toward the area of overnormal winds.

For reasons explained in Par. 156, we obtain for cyclonic and anti-cyclonic centers the following rule which corresponds to rule 2 for troughs and wedges.

Rule 8. *Cyclonic and anticyclonic centers whose pressure profiles have great curvature will move slowly. When the pressure profiles are slightly curved, the speed may vary within wide limits, depending on the magnitude of the isallobaric gradient.*

A·large curvature of the pressure profiles means that the isobars around the center are crowded. Such centers will therefore have a small or moderate speed, whereas "flat" centers *may* move with great speed. In each particular case, the speed must be computed or estimated by the aid of the isallobaric gradient and the curvature of the pressure profile.
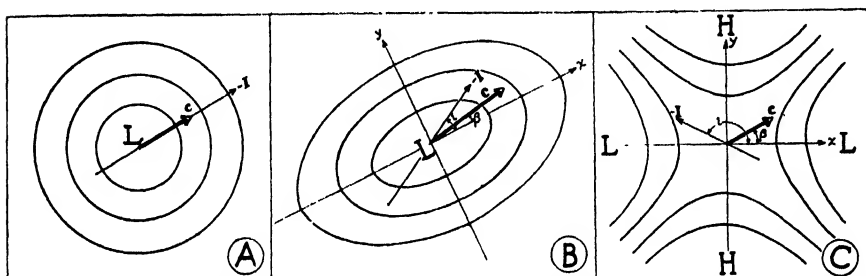
FIG. 197.—Showing the direction of movement of circular (*A*) and oblong (*B*) cyclonic centers and cols (*C*). Anticyclonic centers move in a direction opposite to that of cyclonic centers.

If the isobars around the pressure center are oblong, the above rules are modified. We shall first consider the direction of the movement of the center. Choosing the *x*-axis along the longest symmetry axis (see Fig. 197) and letting β denote the angle between the *x*-axis and the direction in which the center moves, we obtain

$$\tan \beta = \frac{c_y}{c_x} = \frac{-(\partial^2 p/\partial y\, \partial t)}{-(\partial^2 p/\partial x\, \partial t)} \cdot \frac{\partial^2 p/\partial x^2}{\partial^2 p/\partial y^2}$$

or

(4) $$\tan \beta = \tan i \cdot \frac{\partial^2 p/\partial x^2}{\partial^2 p/\partial y^2} = \tan i \cdot \frac{\text{curvature of the } x\text{-profile}}{\text{curvature of the } y\text{-profile}}$$

where i denotes the angle between the *x*-axis and the isallobaric gradient. If the isobars are circular or nearly so, $\partial^2 p/\partial x^2 = \partial^2 p/\partial y^2$, and rule 6 is confirmed. If the isobars are oblong, the curvature of the pressure profile along the *x*-axis is less than that of the pressure profile along the *y*-axis. It follows then that $\tan \beta < \tan i$. Since the curvature of the pressure profile is positive in cyclonic centers and negative in anti-cyclonic centers, we obtain the following rule:

Rule 9.   *The velocity of an elongated cyclonic center lies between the longest symmetry axis and the isallobaric gradient through the center, and the nearer to the longest symmetry axis the more elongated the isobars are. Elongated anticyclonic centers move in the same manner but in the opposite direction.*

Let us consider the extreme case in which the isobars are so elongated that $\partial^2 p / \partial x^2$ is negligible in comparison with $\partial^2 p / \partial y^2$. Equation (4) then shows that β approaches zero when $\partial^2 p / \partial x^2$ approaches zero. From this we obtain:

Rule 10.   *Very oblong centers generally move along the longest symmetry axis or very close to it.*

There is, however, an exception to this rule: When $\partial^2 p / \partial x \, \partial t$ approaches zero, $\tan i$ increases indefinitely, and the effect of the elongation of the isobars decreases with increasing i. Rule 10 should therefore not be used in the rare cases in which the angle between the longest symmetry axis and the isallobaric gradient is very large.

Equations (1) and (4) apply also to cols. Choosing the coordinate axis as shown in Fig. 197, Eq. (4) expresses the angle between the x-axis and the direction in which the col moves. It is important to note that $(\partial^2 p / \partial x^2) < 0$ and $(\partial^2 p / \partial y^2) > 0$ in the col. If the col is symmetrical (as shown in Fig. 197), we may put $(\partial^2 p / \partial x^2) = -(\partial^2 p / \partial y^2)$, and Eq. (4) reduces to

$$\tan \beta = - \tan i$$

which may be expressed in the following rule:

Rule 11.   *A col moves in a direction that, in respect to the y-axis, is symmetrical with the isallobaric gradient.*

Figure 197 illustrates the content of the rules 6, 9, and 11. When the isobars around cyclonic and anticyclonic centers are oblong, we obtain from Eq. *149*(6)

$$c = \frac{-I_x}{\partial^2 p / \partial x^2} \, i + \frac{-I_y}{\partial^2 p / \partial y^2} \, j$$

wnere $-I_x$ and $-I_y$ are the components of the isallobaric gradient along the x- and y-axis, respectively, and i and j are unit vectors along the x- and y-axis. Since the x-axis is chosen along the longest symmetry axis, it follows that $|\partial^2 p / \partial x^2| < |\partial^2 p / \partial y^2|$. This shows that the y-component has less influence on the velocity than the x-component of the isallobaric gradient has. This will tend to make the center move faster along the longest symmetry axis than normal to this axis. When the isobars are elongated, rule 6 holds for each of the velocity components along the coordinate axes.

In many cases, the axes of approximate symmetry are not at right angles to one another. In such cases, the velocity components c_x and

c_y may be computed as shown in Par. 155. However, when the angle between the coordinate axes differs from 90°, the resultant velocity is *not* the vector sum of the components. The method of determining the resultant velocity of the center is shown in Fig. 198. Let oa and ob denote the x- and y-components of the velocity c. Draw a line through a perpendicular to the x-axis and a line through b perpendicular to the y-axis. Let d denote the point of intersection. The vector c from o to d is then the velocity of the center that corresponds to the components c_x and c_y.

Returning now to Eq. (2), we may discuss in a qualitative manner the acceleration of pressure centers. As the terms in the numerators of Eq. (2) are always small whereas $\partial^2 p/\partial x^2$ and $\partial^2 p/\partial y^2$ may vary within limits, we obtain the following rules:

Rule 12. *Circular or nearly circular centers whose pressure profiles have large curvature are little accelerated. Such centers, which may be accelerated in any direction, frequently have curved paths. Flat pressure centers may have considerable acceleration.* It is therefore easier to predict the movement of a pronounced center than that of a weak one.

FIG. 198.—Showing the relation between the velocity components, c_x, and c_y, when the coordinate system is not rectangular.

Rule 13. *Oblong pressure centers are not much accelerated in the direction of the shortest symmetry axis. Such centers usually have straight paths.*

If we proceed as was indicated in Par. 156, it is readily seen that the sign of the acceleration of pressure centers depends on the curvature of the tendency profiles. For pressure centers, we obtain the following rule, which corresponds to rule 5 for troughs and wedges:

Rule 14. *A cyclonic center is accelerated along the x- or y-axis when the curvature of the tendency profile along the x- or y-axis is as shown in Fig. 196A, and it is retarded along the x- or y-axis when the tendency profile along the x- or y-axis is as shown in Fig. 196B. An anticyclonic center is accelerated along the x- or y-axis when the tendency profile along the x- or y-axis is as shown in Fig. 196C, and it is retarded along the x- or y-axis when the tendency profile along the x- or y-axis is as shown in Fig. 196D.*

As in the case of troughs or wedges, this rule should not be applied unless the curvature of the profiles is considerable and the velocity of the center is moderate or large.

Again it should be emphasized that the displacement of a center, either computed from the formulae in Par. 155 or estimated by means of the above rules, must not conflict with the simultaneous displacement of neighboring pressure systems.

158. The Movement of Fronts.—The velocity of an element of a front along an arbitrary x-axis is given by Eq. *149*(4), *viz.*,

$$(1) \qquad c = -\frac{(\partial p/\partial t - (\partial p'/\partial t)}{(\partial p/\partial x) - (\partial p'/\partial x)}$$

where p and p' denote the pressure immediately in advance of and in the rear of the front element, respectively. The acceleration of an element of a front is expressed by Eq. *150*(3). As it is not possible to obtain correct values for the terms $(\partial^2 p/\partial t^2)$ and $(\partial^2 p'/\partial t^2)$ from the data of the weather charts, it is difficult to make use of the acceleration formula. A detailed discussion of the acceleration of various types of fronts will be found in a paper by Petterssen [55] to which the reader is
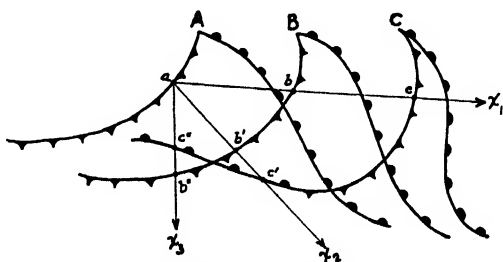
Fig. 199.—Showing how the acceleration varies with the choice of axis. A minimum of acceleration is obtained along the axis x_1 which is parallel to the direction in which the cyclone moves.

referred. For practical purposes, it is advisable to compute or estimate the velocity of fronts by aid of Eq. (1), *choosing the x-axis in such a way that the acceleration is reduced to a minimum.* How this is done is shown in Fig. 199. Let A, B, and C indicate three consecutive positions of the fronts of a warm sector cyclone. We choose an arbitrary point a on the cold front. The x-axis through a may be chosen in any direction. To demonstrate how the acceleration varies with the choice of axis, we choose the three axes x_1, x_2, and x_3 as indicated in the diagram. The axis x_1 is chosen *in the direction in which the wave cyclone moves*. It will be seen that the speed of the front along the axis x_1 is almost constant, which indicates that the acceleration of the front along the axis x_1 is small or negligible.

Let us consider next the displacement of the front along the axis x_3, which is perpendicular to the direction in which the cyclone center moves. During the first time interval, the front moves from a to b''; during the next interval, it moves retrogressively from b'' to c''. It follows then that the acceleration of the front must be very large in the direction of the axis x_3.

We consider next the intermediate case, or the movement along the axis x_2. The front moves first from a to b' and then from b' to c'. The

acceleration along the axis x_2 is greater than that along the axis x_1 but smaller than that along x_3. It is readily seen that *a minimum of acceleration occurs along the axis which is parallel to the general movement of the cyclone to which the fronts belong.* Furthermore, since frontal cyclones move mainly in the direction of the isobars in the warm sector, it is most convenient *to choose the x-axis along the warm sector isobars.*

Before Eq. (1) is applied, the analyst should find out (1) which is the most favorable point on the front for computation, and (2) in which direction the acceleration is a minimum.

FIG. 200.

The first question is readily answered: The most favorable point should be sought on the front within regions where (1) the isobars are more or less straight and equidistant, (2) where the isallobars are accurately drawn. In such regions, it will be easy to replace the differentials in Eq. (1) by finite differences.
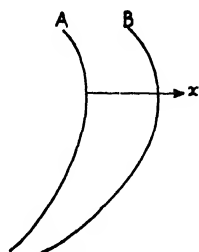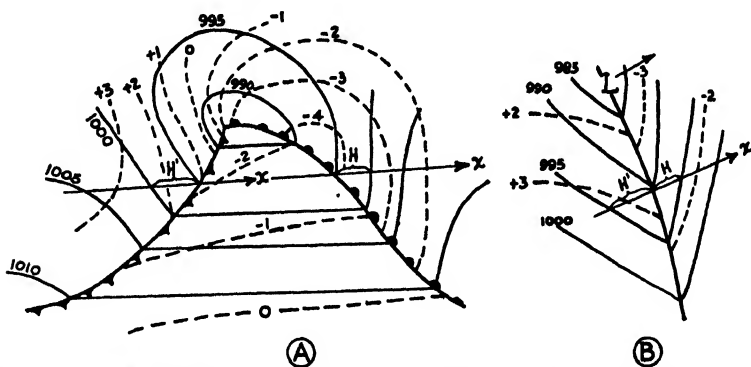
FIG. 201.—*A*, showing how to compute the velocity of a warm and a cold front; *B*, showing how to apply Eq. (1) to other fronts. Full lines are isobars. Broken lines are isallobars.

The second question was discussed above. However, when the front is occluded or when the front in question does not belong to a regular wave cyclone, the rule of choosing the x-axis along the warm-sector isobars does not apply. In such cases, the position of the front on the previous map should be compared with its position on the present map as shown in Fig. 200. Where the isochrones *A* and *B* are parallel, the x-axis may be chosen normal to the front. In most cases, it is easy to find the most favorable direction by studying the wind field in the rear and in advance of the front.

The next step is to apply Eq. (1). Figure 201*A* shows how this is done in connection with warm-sector cyclones, and Fig. 201*B* shows how to compute the velocity in other cases. Since the x-axis in Fig. 201*A*

is drawn along the warm-sector isobars, we obtain for the warm front

$$\frac{\partial p'}{\partial x} = 0, \qquad \frac{\partial p}{\partial x} = \frac{5}{H}, \qquad \frac{\partial p}{\partial t} = -4.2, \qquad \frac{\partial p'}{\partial t} = -1.5$$

The values for $\partial p'/\partial t$ and $\partial p/\partial t$ should be interpolated from the isallobars. Substituting this in Eq. (1), we obtain

$$c = -\frac{-4.2 + 1.5}{5} H = \frac{2.7}{5} H = 0.5H$$

which means that the front will move the distance $0.5H$ in one tendency interval, or $4H$ in eight tendency intervals (*i.e.*, 24 hr.). It is of interest to note that the more crowded the isobars are in advance of the front, the smaller is H, and, other conditions being equal, the smaller is the velocity of the front. Furthermore, it is important to note that a large tendency in advance of the front is not the deciding factor. If, in the above case, the tendency in the rear of the warm front were $+1.5$ instead of -1.5, the front would move $1.1H$ in 3 hr. The velocity is proportional to the *difference* in tendency between the front and the rear of the element that we consider and to the distance between the isobars ahead of the front. It is therefore of utmost importance that the isobars and isallobars be drawn with meticulous care.

Proceeding in the same way, we find for the cold front

$$\frac{\partial p}{\partial x} = 0, \qquad \frac{\partial p'}{\partial x} = -\frac{5}{H'}, \qquad \frac{\partial p}{\partial t} = -2.2, \qquad \frac{\partial p'}{\partial t} = 1.2$$

This gives

$$c = \frac{3.4}{5} H' = 0.7H'$$

This shows that the cold front is moving quicker than the warm front: the warm sector occludes.

In the above example, we have chosen the x-axes through the warm front and the cold front along the same warm-sector isobar. In practice, one should choose the most favorable point on each of the fronts. Usually, the two axes would then not coincide.

In Fig. 201B, the x-axis is not chosen along an isobar. We then obtain

$$\frac{\partial p}{\partial x} = \frac{5}{H}, \qquad \frac{\partial p'}{\partial x} = -\frac{5}{H'}, \qquad \frac{\partial p}{\partial t} = -2.5, \qquad \frac{\partial p'}{\partial t} = 2.7$$

This gives

$$c = -\frac{-2.5 - 2.7}{(5/H) + (5/H')} = \frac{5.2}{5} \frac{HH'}{H + H'}$$

Since in this particular case $H' = 1.4H$, we obtain for the velocity $c = 0.6H$.

159. The Geostrophic-wind Method.—Since a frontal surface is a boundary between adjacent air masses, the movement of the front must be determined by the movement of the air masses. If there were no vertical velocity in the air, the front would move in a direction normal to itself with a speed that is equal to the wind component normal to the front. However, as was shown in Par. 121, the air glides up or down the frontal surface. For this reason, the speed of the front may differ slightly from the speed of the wind. Moreover, since the wind observations are inaccurate and nonrepresentative, the speed of the fronts cannot be obtained with sufficient accuracy from the wind observations. We shall therefore return to the relations between the wind and the pressure distribution as given in Chap. IV in order to obtain expressions for the velocity of fronts.

It was shown in Par. 96 that the kinematic boundary condition can be written in the form

$$(1) \qquad\qquad (v - v') \cdot n = 0$$

where the vectors v and v' denote the velocity of the wind (including vertical component) in the cold and in the warm air, respectively, and n is a unit vector normal to the frontal surface and pointing from the cold toward the warm mass. The above equation states that the velocity components normal to the *frontal surface* must be equal at both sides of the surface. This is the same as saying that the motion must be such that no fissure develops at the frontal surface. It was shown in Par. 120 that the wind must be discontinuous at a frontal surface. This in connection with Eq. (1) shows that the velocity of each of the air masses relative to the frontal surface must be parallel to the frontal surface. Let v_r and v_r' denote these relative velocities. Then,

$$(2) \qquad\qquad v_r \cdot n = 0 \qquad \text{and} \qquad v_r' \cdot n = 0$$

We choose a system of coordinates with the x-axis normal to the front, the y-axis tangential to the front, and the z-axis vertical. Let α, β, γ represent the direction cosines of n. Since the y-axis is tangential to the front, $\beta = 0$. Equation (1) then reduces to

$$(3) \qquad\qquad (v_x - v_x')\alpha + (v_z - v_z')\gamma = 0$$

or, when $\tan \theta_d$ denotes the inclination of the frontal surface,

$$(4) \qquad\qquad v_z - v_z' = (v_x - v_x') \tan \theta_d$$

Let v_f denote the velocity of the front along the x-axis which now is normal to the front. Equations (2) then reduce to

(5a) $$v_x - v_f = v_z \cotan \theta_d$$

(5b) $$v_x' - v_f = v_z' \cotan \theta_d$$

These equations show that $v_x = v_x' = v_f$, when the vertical velocities vanish. In such cases, the front would move with the speed of the velocity component of the wind normal to the front. Examining a large number of distinct fronts, Petterssen [55] found that the vertical velocities at anemometer level were of noticeable magnitude. In Eq. (4), we let indices denote the conditions in the warm air. Now, at warm fronts, $\tan \theta_d > 0$. Then $\Delta v_x = v_x' - v_x$ indicates how much faster the warm air moves normal to the front than the cold air moves in the same direction. At cold fronts, $\tan \theta_d < 0$, and $\Delta v_x = v_x - v_x'$ indicates how much faster the cold air moves normal to the front than the warm air moves in the same direction. The upglide velocity of the warm air relative to the cold air will therefore, both at warm and cold fronts, be proportional to Δv_x. If the inclination of the fronts were $\frac{1}{100}$, the relative vertical velocity would be as many centimeters per second as Δv_x is meters per second. The results of the examination of 62 cases of well-marked fronts in Norway are shown in Table 58. It will be seen that the warm

TABLE 58

Δv_x, m./sec.	Percentage frequency	Mean amount of precipitation, mm.
−4– 0	10	—
0– 4	37	5
4– 8	32	7
8–12	16	8
12–16	5	9

air ascends with a considerable velocity relative to the cold air. Most frequently, Δv_x is about 3 to 6 m./sec., which corresponds to a vertical velocity of about as many centimeters per second. The fact that the amount of precipitation increases with Δv_x seems to indicate that the vertical velocity is not negligible.

It was shown in Par. 121 that the warm air has an upward component along all fronts in the lower atmosphere. Along warm fronts and cold fronts of type A, the cold air also ascends, whereas, along cold fronts of type B (Fig. 139), the cold air has a downward component. If the vertical velocity and the inclination of the frontal surface were known, the velocity of the front could be obtained from Eq. (5). However, as these quantities are not known, we can obtain only approximate results.

We consider first the conditions in the rear of a warm front. Since $v_z' > 0$ and $\cotan \theta_d > 0$, it follows from Eq. (5b) that the warm front

moves along the x-axis (*i.e.*, normal to the front) with a speed which is less than the x-component of the wind in the warm air. Therefore $v_x' > v_f$, and *the difference between the wind velocity and the velocity of the front is proportional to the rate of ascent of the warm air.*

We consider next the conditions in advance of the warm front. Since cotan $\theta_d > 0$ and $v_z > 0$ under the warm front surface (see Par. 121), we obtain the same result as above; but as $v_z' > v_z$, it follows that the speed of the front is closer to v_z than to v_x'.

In the rear of a cold front, Eq. (5a) applies. Since cotan $\theta_d < 0$, we obtain for cold fronts of type A (see par. 121) $v_f > v_x$, whereas, for cold fronts of type B, $v_z < 0$ and therefore $v_f < v_x$. In advance of cold fronts, Eq. (5b) holds. Since $v_z' > 0$ at all cold fronts near the earth's surface and since cotan $\theta_d < 0$, we obtain for both types: $v_f > v_x'$.

The results of the above discussion are summarized in the table below.

TABLE 59.—RELATION BETWEEN THE VELOCITY OF FRONTS (NORMAL TO THE FRONT) AND THE WIND COMPONENTS NORMAL TO THE FRONT

Warm fronts	Cold fronts	
	Type A	Type B
$v_f < v_x$ $v_f < v_x'$	$v_f > v_x$ $v_f > v_x'$	$v_f < v_x$ $v_f > v_x'$

Figure 202 shows diagrammatically the pressure distribution along a cold front extending from the cyclone center toward the col. In the northern part, the front would be of type B, whereas the southwestern portion would be of type A with a region of transition in between. The southwestern portion of the cold front would then have a tendency to move with a speed that is greater than the wind component normal to the front.

The above results apply at any level. However, in the immediate vicinity of the earth's surface, the fronts are much disturbed by the effect of friction. On account of the rapid increase in wind velocity with

FIG. 202.—Showing the pressure distribution along cold fronts of types A and B.

elevation near the earth's surface, a warm-front surface would be deformed as shown in Fig. 203. The frontal surface would approach the horizontal close to the earth's surface if there were no mixing between the cold and the warm air. On account of mixing, the shallow surface layer of cold air is continuously destroyed, and the frontal surface will have a tendency

to prolong itself downward as indicated by the broken line in Fig. 203. Similar results also hold for cold fronts, but the cold air would overrun the warm air close to the earth's surface, and effective mixing would result. It follows then that the front near the earth's surface moves with a speed that depends mostly on the undisturbed wind at the top of
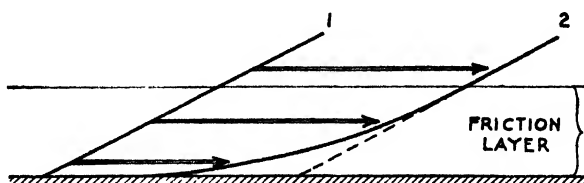
FIG. 203.

and above the friction layer. At this level, the wind is close to the geostrophic wind if the isobars are straight or nearly so and is close to the gradient wind if the isobars have a considerable curvature. We may therefore substitute the geostrophic wind (or the gradient wind) for the actual wind in the above equations. From Table 59, we obtain the following results:

Warm fronts	Cold fronts	
	Type A	Type B
$v_f < \frac{1}{2}(v_x + v_x')$	$v_f > \frac{1}{2}(v_x + v_x')$	$v_f \approx \frac{1}{2}(v_x + v_x')$

Substituting the geostrophic wind normal to the front for the mean wind within the frontal zone [*i.e.*, $\frac{1}{2}(v_x + v_x')$], we see that warm fronts move with a speed which is less than the geostrophic wind and that cold fronts of type A move with a speed which is greater than the geostrophic wind, whereas cold fronts of type B move with a speed which is approximately equal to the geostrophic wind.

The difference between the geostrophic wind and the speed of the front varies considerably from one case to another according to the vertical velocity and the inclination of the front. In the foregoing discussion the retarding influence of friction has not been taken into account. The influence of friction would tend to cause the fronts to move somewhat slower than indicated above. Experience has shown that the following rules will give a first approximation to the speed of the fronts:

Rule 15. *Warm fronts move with a speed that is* 60 *to* 80 *per cent of the geostrophic wind.*

Rule 16. *Cold fronts of type B move with a speed that is* 70 *to* 90 *per cent of the geostrophic wind.* Occasionally, the speed may exceed 90 per cent.

Rule 17.   *Cold fronts of type A move with a speed of about* 100 *per cent of the geostrophic wind.*   In many cases, the front moves faster.   This occurs when the geostrophic wind component normal to the front is slight.   It is often observed that the cold tongues between two cyclones move a considerable distance southward without much geostrophic-wind component normal to the front.

The above rules should be regarded as first approximations only. The stronger the geostrophic wind, the more accurate are the rules. When the geostrophic wind is less than 4 Beaufort, the rules may be inaccurate; but, in such cases, the speed of the front is, of course, small. Furthermore, these rules do not hold in tropical and subtropical latitudes where the geostrophic control is less rigid.   Corrections of the above rules may be applied according to the rate of change in the pressure distribution.   We shall return to this question in Par. 170.

The above rules are most easily applied by using the geostrophic-wind scale (Fig. 102) as explained in Par. 95.   In the above rules, no allowance is made for the curvature of the path.   This may be done as indicated on the geostrophic-wind scale.   However, in most cases, it is preferable to use the scale in such points on fronts where the isobars are sufficiently straight to make the curvature of the path negligible.

When the velocity of the fronts has been computed as shown in Par. 159 or estimated by means of the above rules, the speed of the cyclonic center may be inferred from the speed of the fronts.   It will be seen from Fig. 156 that, in all normal cases, the following rule holds:

Rule 18.   *A cyclonic center moves with approximately the same speed as the warm front and somewhat slower than the cold front.*   The difference between the speed of the cold front and the speed of the center depends on the rate at which the cyclone occludes.   The more unstable the wave is, the greater is the rate at which the cold front overtakes the warm front.   It will be shown in Par. 171 that the rate of occlusion depends on the rate of deepening of the cyclonic center.   If the cyclone is occluded, the center will move with a speed that is slightly less than the speed of the front.

160. The Velocity of Wave Cyclones.—The formulae for the velocity of cyclonic centers discussed in Par. 155 hold only when the coordinate axes do not intersect fronts along which there are marked discontinuities in the pressure gradient and the barometric tendency.   In such cases, it is possible to choose at least one of the coordinate axes so that it does not intersect the front or fronts.   The component of the velocity along this axis may then be computed.

We consider a wave cyclone as shown in Fig. 204.   Choosing the x-axis as indicated and applying formula *155*(2), we obtain the component of the velocity along the x-axis.   The y-axis would intersect the front,

and Eq. *155*(3) would not hold since the tendency distribution is discontinuous at the front. However, as a warm-sector cyclone moves mainly in the direction of the warm sector with a slight component toward the north, it follows that the velocity of the center along the y-axis must be very small when the axes are chosen as shown in Fig. 204.
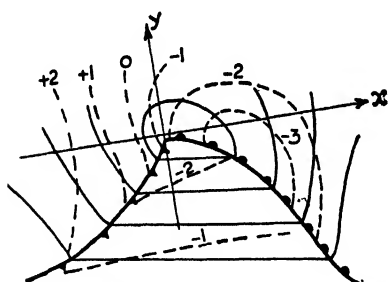
Fig. 204.—Showing how to choose the coordinate axis in warm-sector cyclones.

If the x-axis thus chosen is perpendicular to the isallobars in the cold air, the center will move along the x-axis.

161. Application of the Trough Formula to Weak Fronts.—The formula for the velocity of fronts [*i.e.*, Eq. *158*(1)] will not yield satisfactory results when the tendency discontinuity along the front is indistinct. This is due to the fact that the velocity is proportional to the difference in tendency; and when this difference is slight, even slight errors will influence the computation. In such cases, the trough formula may be used if the tendency profile along the x-axis has a favorable shape.
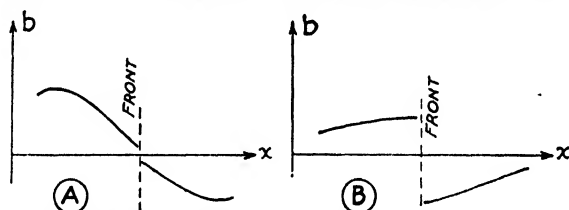
Fig. 205.—*A*, front with slight tendency discontinuity; *B*, front with large tendency discontinuity. In the case *A* the trough formula will apply.

Figure 205 shows two types of tendency profiles through fronts. In case *A*, the tendency curve slopes in the same direction in advance and in the rear of the front, and there is a slight discontinuity in the tendency at the front. This slight discontinuity may be smoothed, and the trough formula (which holds in the case of continuity) may be applied. In case *B*, there is a marked discontinuity in the tendency at the front, and the slope of the tendency curve changes abruptly at the front. In such cases, the trough formula does not hold, but the front formula [Eq. *158*(1)] will give satisfactory results.

162. The Path Method.—So far we have described two methods by means of which we may determine the velocity of fronts and cyclones, *viz.*: (1) the *tendency method* by means of which we can compute or estimate the velocities from the isallobars and isobars, and (2) the *geostrophic-wind method* which applies directly to the movement of fronts and

indirectly (through rule 18) to cyclonic centers. We shall now describe a third and very simple method, *viz., the path method*, which should always be used to supplement the other methods. This method is particularly useful when observations are too scanty for reliable computations to be made.

Let points 1, 2, 3, and 4 in Fig. 206*a* represent four consecutive positions of a pressure center at equal time intervals. These positions show that the center *has* moved with constant speed and direction. From this, we cannot *sans phrase* assume that the center will continue
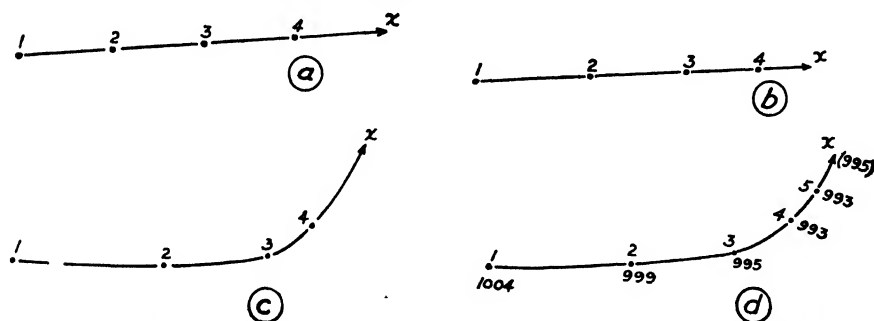
Fig. 206.—Illustrating the path method. The points 1, 2, 3, and 4 indicate consecutive positions of a center, and *x* indicates the probable position on the next map.

to move with constant speed and direction. From what has been said in the previous paragraphs, we know that the speed of a center depends on the slope of the tendency profile and the curvature of the pressure profile. Now, after the path has been drawn on the map as indicated in Fig. 206*a*, we may compare the present map with the preceding map; and if the conditions (pressure and tendency) around the center have not changed appreciably from the previous to the present map, we may safely assume that the center will continue to move with a constant speed and direction. On the next map, the center would then be somewhere near the position *x*.

In a similar manner, Fig. 206*b* shows a case where the center has moved on a straight path with decreasing speed. Again, it would be erroneous to assume that the center would move on with decreasing speed unless the changes in the pressure and tendency distribution around the center from the preceding to the present map indicate that the speed is likely to decrease. But if such changes are observed, it may be assumed that the center will continue to move with a decreasing speed. Its position on the next map would then be somewhere near the point marked *x*.

Figure 206*c* shows a case where the center has moved on a curved path with decreasing speed. If the maps that correspond to the positions 3 and 4 show that the isallobaric gradient has increased from map 3

to map 4 without a corresponding increase in the curvature of the pressure profiles, we should have to assume that the speed of the center would increase again. Allowing for an appropriate increase in speed, the position on the next map is indicated by x.

Figure 206d is much the same as Fig. 206c; but, in addition, the pressure in the center is indicated next to the position marks. It will be seen that the center deepens with decreasing intensity. If we were to forecast its position and pressure at the next map, we should not merely perform a freehand extrapolation but should also ascertain whether or not the changes in the pressure and tendency distribution around
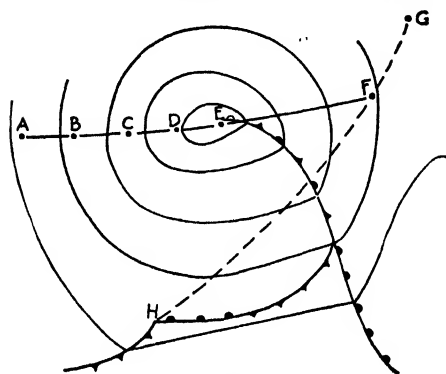
Fig. 207.

the center between the last two maps are such that a freehand extrapolation was justifiable.

In short, the path method involves two operations: (1) *a freehand extrapolation of the path*, and (2) *an adjustment based on a comparison between the present chart and the preceding one.*

This method of extrapolation may be applied safely as long as no larger pressure system "blocks the path." Thus, for example, the prolonged path of a cyclonic center must not run into a stationary or quasi-stationary anticyclone, notably the stationary anticyclones over cold continents in winter. When the path points toward such anticyclones, it will usually be found that the speed of the cyclone center decreases and the path curves northward. *The path continues to curve northward until it becomes parallel to the isobars around the quasi-stationary high.* The speed of the center will be smallest where the curvature of the path is largest. Therefore, the speed will usually increase when the center resumes a more or less straight path (*cf.* Fig. 206c).

What has been said above of cyclonic centers applies in a general way also to anticyclonic centers.

A few comments on the correct way of identifying cyclonic centers may be of interest. As long as the cyclone is an isolated system, the center may be defined as the place where the pressure is a minimum. However, when a secondary forms in the vicinity of an already existing center, it may happen that the secondary gains relative to the primary center. To take an example, we consider Fig. 207 where the primary center has moved from A to E. In the meantime, a wave forms at the point H and travels along the path HFG. At H, the wave is not associated with a pressure center in the usual meaning of the word; but,

as it develops, it acquires its own pressure minimum, while the primary occluded center tends to fill up. At F, the two centers merge, and the resultant low moves from F to G. The path HFG is altogether logical and one that is easy to extrapolate. On the other hand, if the attention is directed to the point where the pressure at any instant is lowest, the path of the center would be AFG, with a discontinuity in the direction at F. In this case, the path from F to G could be extrapolated from the history of the wave prior to its arrival at F, whereas an extrapolation of the path AF would render misleading results.

The path method is applicable also to troughs, wedges, and fronts. The successive positions of the trough, wedge line, or front are then marked on the map, and the future movement is extrapolated as described above for cyclonic centers.

163. The Area of Uncertainty and Timing of the Arrival.—Whatever method of extrapolation is used, the predicted positions of fronts, cyclones, etc., will be more or less inaccurate. Therefore, the future position of any pressure system should be determined by means of as many methods as possible. If we use the tendency method, the geostrophic-wind method, and the path method for determining the future position of a front and if all three methods give approximately the same result, then we should be justified in believing that the prediction would hold with great accuracy. However, if the results obtained by means of one method differ from those obtained by other methods, the analysis and the prediction should be reexamined in order to find the probable cause of the discrepancy. This procedure often divulges details and possibilities that have been overlooked.

In dealing with systems whose structure is simple and resembles the normal models, and when the network is sufficiently dense to allow a detailed analysis, the predictions will usually be fairly accurate. In other cases, it is wise to reckon with a certain inaccuracy in the extrapolated positions. To take a concrete example, say that the position of a front has been extrapolated 24 hr. ahead and, if it is a simple and easy case, the position may be accurate within ±100 km. Suppose now that the speed of the front is 15 km./hr. It would then take the front about 13 hr. to pass through the zone of uncertainty. Suppose next that the speed of the front is 60 km./hr. The front would then pass through the zone in about 3 hr., which would be an accurate forecast over 24 hr. Therefore, *the greater the speed, the more accurately can the time of arrival be forecast.* From this, it follows that when a front, or any pressure system, moves with great speed, the forecaster is justified in timing the arrival with comparatively great accuracy, whereas, when the speed is small, there is very meager justification for an accurate timing. The forecaster should have this in mind when wording the

forecast. Those forecasters who take advantage of the rapidly moving systems in wording the forecasts accurately can afford to use vague phrases when the speed is so low that accurate timing is impossible.

164. Symptoms of Wave Formation.—Cyclone waves form most frequently on stationary fronts or slowly moving cold fronts. When the front is stationary, it follows from Eq. *149*(4) that $\partial p/\partial t = \partial p'/\partial t$,
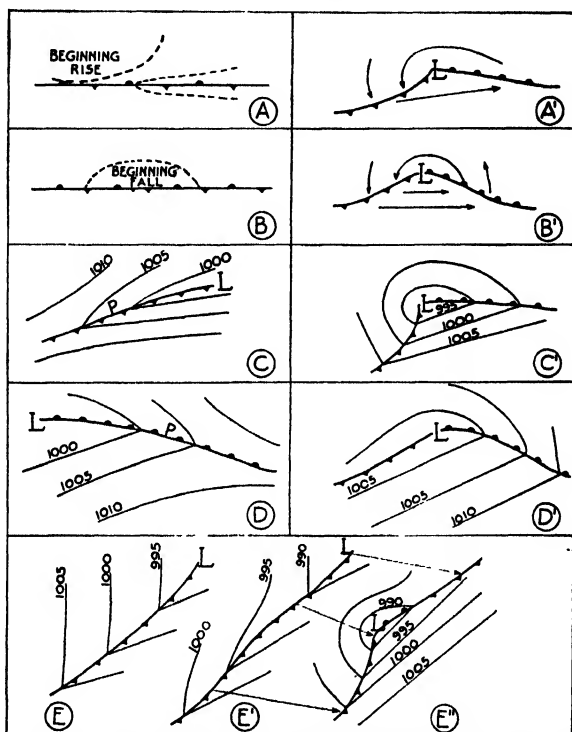
Fig. 208.—Showing some of the symptoms of wave formation and the types of waves that result.

which means that the barometric tendency must be the same at both sides of the front. The isallobars are then continuous through the front. When the front is stationary, $c = 0$ and Eq. *150*(3) reduces to

$$(1) \qquad A = -\frac{(\partial^2 p/\partial t^2) - (\partial^2 p'/\partial t^2)}{(\partial p/\partial x) - (\partial p'/\partial x)}$$

The quantities in the numerator cannot be obtained with sufficient accuracy from the weather charts; it is therefore not possible to compute whether a stationary front is accelerated one way or the other, but a few qualitative results may be obtained from the above formula.

We choose the x-axis normal to the front with the positive direction from the warm toward the cold air. The most frequent indication

of the formation of a wave on a stationary front is a beginning rise in pressure within the cold air as shown in Fig. 208A. This means that part of the front will be accelerated southward. After some time, the position of the front will be as shown in Fig. 208A'. Such waves have an asymmetrical flow pattern, the current in the rear being stronger than that in advance of the wave; they develop and occlude rapidly.

Another less frequent symptom of wave formation on stationary fronts is a beginning fall in the cold air as shown in Fig. 208B. The front will then be accelerated northward within the region of the fall. After some time, the position of the front will be as shown in Fig. 208B'. The wave obtains a rather symmetrical flow pattern. Such waves usually develop and occlude slowly. The reason waves of type A develop and occlude more rapidly than do waves of type B may be sought in the fact that, on account of the asymmetry in the flow of type A, the cold front will move more rapidly than the warm front, whereas the fronts in waves of type B will move with approximately the same speed.

Waves are often observed forming on slowly moving fronts. A frequent case is shown in Fig. 208C. It will be seen that the geostrophic wind normal to the front has a maximum in the region P. This part of the front will then move more rapidly than the portions to the left and to the right of this region. The front would then obtain a wavelike shape; and, after some time, the situation would be as shown in Fig. 208C'. This development is identical with type A discussed above (i.e., rapid development and occlusion).

Occasionally, wave disturbances are observed on slowly moving warm fronts when the pressure distribution is as shown in Fig. 208D. As explained above, the warm front at the point P will move more rapidly than the adjoining portions of the front, and a wavelike disturbance results as shown in Fig. 208D'. In such cases, the development of the wave into a cyclone is slow, and appreciable deepening usually occurs only when the current in the rear of the forming center has increased and obtained a component normal to the cold front.

It is sometimes observed that wave disturbances develop on cold fronts which move with a moderate speed. The development is then as shown in Figs. 208E, E', and E''. The first indication is a decrease in the pressure gradient normal to the front as shown in Fig. 208E'. As the front moves on, part of it becomes retarded relative to the adjoining portions of it, and a wave disturbance gradually develops. This development can easily be detected from the distribution of barometric tendencies. Waves that form in this way resemble type A; they develop and occlude rapidly. Many of the so-called "secondaries" form on such cold fronts in the lower portion of the rear of developed cyclones. Wave formations of the types C and E occur frequently when a cold

front passes a mountain range (see Fig. 147). The center then usually forms at the southern end of the range. Regions noted for high frequency of this type of wave formation are the southern part of the Appalachian Mountains and the southern part of the Scandinavian range. In the latter region, a special type of cyclogenesis (the Skagerrak type) occurs; this will be discussed in Chap. X, where the problem of cyclogenesis through deepening and filling will be discussed.

In connection with the above diagrams, it should be mentioned that indications of wave formations may also be found in the wind circulation. Slight cyclonic circulation may often be detected in the winds before a corresponding deformation of the isobars occurs. This is due to the fact that accelerated and retarded winds deviate from the geostrophic wind.

Returning to the formula for the acceleration of a stationary front, a few comments may be made on the conditions that, as far as the
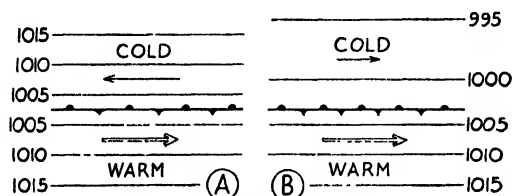
FIG. 209.

pressure field is concerned, are favorable for wave formation on stationary fronts. We consider the two cases shown in Fig. 209. The pressure gradient in the warm air [*i.e.*, $\partial p'/\partial x$] is the same in both cases; moreover, in case A, $\partial p/\partial x = -\partial p'/\partial x$ whereas, in case B, $\partial p/\partial x = \frac{1}{2}(\partial p'/\partial x)$. This means that in the case A the front is situated between two opposite currents of equal strength, whereas, in case B, the front is between two currents of the same direction, the cold air having less speed than the warm air. From Eq. (1), it will be seen that the denominator in case A is four times larger than in case B. Now, the stationary front will be accelerated as soon as $\partial^2 p/\partial t^2$ begins to differ from $\partial^2 p'/\partial t^2$. But since $(\partial p/\partial x) - (\partial p'/\partial x)$ is four times greater in case A than in case B, it will be seen that a larger acceleration of the front will result when the isobars are as shown in Fig. 209B than when they are as shown in Fig. 209A. This seems to show that a stationary front situated between two currents of the same direction is more easily accelerated than is a stationary front between two currents of opposite direction. That this is so was found empirically by Bergeron and Swoboda [5] and also by J. Bjerknes [11] long before the above formula was known.

The above discussion does not explain the processes that lead to wave formation; it merely furnishes a number of simple symptoms by

means of which the complicated processes that lead to the formation of cyclone waves can be recognized from the data of the weather maps. A number of other symptoms will be discussed in Chap. X.

165. Further Remarks on Frontogenesis.—It was shown in Par. 120 that cyclonic wind shear is a general characteristic of all fronts. To the extent that the pressure gradient is balanced by the Coriolis force the quantity $(\partial p/\partial x) - (\partial p'/\partial x)$ expresses the shear at the front. Indices refer to the warm air, and the x-axis is normal to the front. In the discussion in this paragraph, it is convenient to choose the positive direction of the x-axis from the warm toward the cold mass. Then, the velocity of warm fronts is positive, whereas the velocity of cold fronts is negative. With this choice of positive direction, the inclination of both the warm- and the cold-front surfaces is positive. This particular choice of positive direction is a mere convention and does not encroach on the generality of the results.

The inclination of a frontal surface is expressed by Eq. *117*(6), *viz.*:

$$\tan \theta_d = \frac{1}{g(\rho - \rho')}\left(\frac{\partial p}{\partial x} - \frac{\partial p'}{\partial x}\right)$$

Since the inclination always is small, $\tan \theta_d$ varies within narrow limits. On the other hand, since $(\rho - \rho')$ increases when there is frontogenesis (see Chap. V), it follows that $[(\partial p/\partial x) - (\partial p'/\partial x)]$ must increase or decrease as the density discontinuity increases or decreases.[1] Since it is easy to evaluate $[(\partial p/\partial x) - (\partial p'/\partial x)]$ from the isobars, its variation with time is the most convenient indication of frontogenesis. The fact that $[(\partial p/\partial x) - (\partial p'/\partial x)]$ varies in proportion to $(\rho - \rho')$ indicates that *frontogenesis results in concentration of cyclonic vorticity at the front.*

We shall now consider the variation of $(\partial p/\partial x) - (\partial p'/\partial x)$ in a system of coordinates that moves with the front and whose x-axis is normal to the front. Applying the operator defined by Eq. *148*(3), we may write

(1) $$\frac{\delta}{\delta t}\left(\frac{\partial p}{\partial x} - \frac{\partial p'}{\partial x}\right) = \frac{\partial^2 p}{\partial x\,\partial t} - \frac{\partial^2 p'}{\partial x\,\partial t} + c\left(\frac{\partial^2 p}{\partial x^2} - \frac{\partial^2 p'}{\partial x^2}\right)$$

Since the term on the left-hand side is expressive of the intensity of frontogenesis, it will be seen that frontogenesis at a preexisting front depends on two factors, *viz.*: (1) the difference in the x-components of the isallobaric gradients in advance and in the rear of the front, and (2) the curvature of the pressure profiles along the x-axis. The last term

---

[1] The variation in $(\partial p/\partial x) - (\partial p'/\partial x)$ is strictly proportional to the variation in $\rho - \rho'$ only when θ_d remains constant. As shown by Petterssen [55], the variation with time in $\tan \theta_d$ is so small that it may be disregarded in comparison to the variation in $(\rho - \rho')$ when frontogenesis is active.

in Eq. (1) depends also on the speed of the front, so that the curvature term increases with increasing speed.

We shall now consider a few simple types of fronts.

Case 1.   *Stationary Fronts.*—In this case, $c = 0$, and frontogenesis depends entirely on the components of the isallobaric gradients normal to the front.   Let $F > 0$ denote frontogenesis and $F < 0$ frontolysis. From Eq. (1), we obtain for stationary fronts $F > 0$ when the x-components of the isallobaric gradients are as shown by any of the pairs of
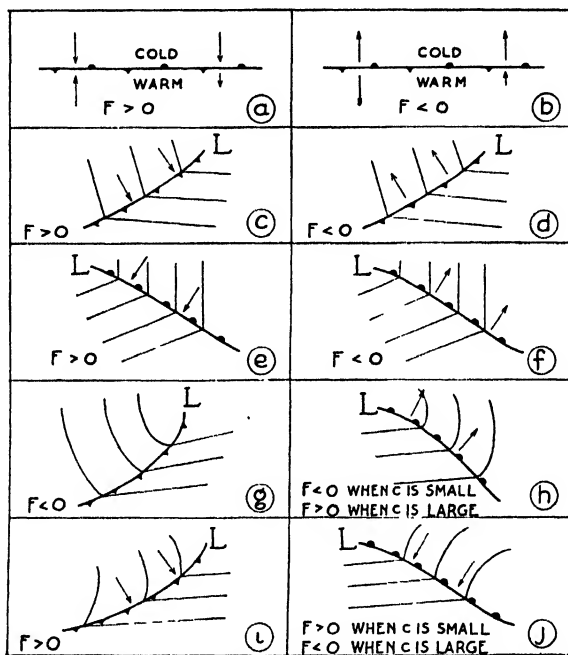
Fig. 210.—Showing types of frontogenetical ($F > 0$) and frontolytical ($F < 0$) fronts. Arrows indicate the component of the isallobaric gradient normal to the front.

arrows shown in Fig. 210a, and $F < 0$ when these components are as indicated by any of the pairs of arrows in Fig. 210b.

Case 2.   *The Isobars Close to the Front Are almost Straight and Equidistant.*—In this case, $\partial^2 p/\partial x^2 = \partial^2 p'/\partial x^2 = 0$.   Since the barometric tendency in the vicinity of fronts is mainly due to advection of cold or warm air masses, the barometric tendency and the isallobaric gradients will be small in the warm air and large in the cold air.   Moreover, the isallobaric gradient in the warm sector is almost parallel to the front so that its component normal to the front is negligible.   We may therefore neglect $\partial^2 p'/\partial x \, \partial t$.   Substituting this into Eq. (1), we obtain the results shown in Fig. 210c.   When isobars are drawn correctly, it will be found that, in most cases, their curvature vanishes close to the front.   The

case discussed here is therefore one that occurs frequently. A simple inspection of the isallobars in the cold air will then furnish valuable symptoms of the intensity of the processes that tend to increase or decrease the frontal discontinuity.

Appreciable curvature of the isobars occurs only in the cold air. In such cases, the last term in Eq. (1) may become predominant when the speed of the front is large.

Case 3. The Isobars in the Rear of a Cold Front are Curved Cyclonically (Fig. 210g).—This is the type of cold front that moves with great speed. The curvature term in Eq. (1) is therefore important. Usually, the components of the isallobaric gradients normal to such fronts are small. Furthermore, $\partial^2 p'/\partial x^2 = 0$ and $\partial^2 p/\partial x^2 > 0$. Since the x-axis is chosen from the warm toward the cold air, c is negative. The last term in Eq. (1) is therefore large and negative, whereas the first term on the right-hand side is small (positive or negative). From Eq. (1), it follows that such cold fronts are exposed to frontolysis. This kind of cold front was discussed in Pars. 121 and 159 where it was referred to as a cold front of type B. Such fronts are characterized by slight temperature discontinuity, slight wind shear, high speed, or considerable acceleration[1] and frontolysis.

Case 4. The Isobars in Advance of a Warm Front are Curved Cyclonically (Fig. 210h).—In such cases, the isallobaric center is found at some distance in advance of the front. Therefore $\partial^2 p/\partial x\,\partial t < 0$, $\partial^2 p/\partial x^2 > 0$, and $\partial^2 p'/\partial x^2 = 0$; and since $\partial^2 p'/\partial x\,\partial t$ is small, it follows that such fronts are exposed to frontolysis when c is small and are exposed to frontogenesis when c is large.

Case 5. The Isobars in the Rear of a Cold Front are Curved Anti-cyclonically (Fig. 210i).—This type of cold front was discovered in Par. 121 where it was referred to as a cold front of type A. Such cold fronts invariably have an isallobaric gradient in their rear directed toward the front. Hence, $\partial^2 p/\partial x\,\partial t > 0$. Furthermore, $c < 0$, $\partial^2 p/\partial x^2 < 0$,

$$\partial^2 p'/\partial x^2 = 0;$$

and since $\partial^2 p'/\partial x\,\partial t$ is small, we obtain from Eq. (1) $F > 0$ unconditionally. *This type of cold front is therefore always exposed to frontogenesis.*

Case 6. The Isobars in Advance of a Warm Front Are Curved Anti-cyclonically (Fig. 210j).—Such warm fronts invariably have an isallobaric gradient in the cold air directed toward the front. Therefore $(\partial^2 p/\partial x\,\partial t) > 0$. Since $c > 0$, $\partial^2 p'/\partial x^2 = 0$ and $\partial^2 p/\partial x^2 < 0$; and since $\partial^2 p/\partial x\,\partial t$ is small (positive or negative), we obtain from Eq. (1) $F > 0$ when c is small and $F < 0$ when c is large.

[1] PETTERSSEN [55].

Summing up, we may say that cold fronts as shown in Fig. 210*g* are always exposed to frontolysis and those of the type shown in Fig. 210*i* are always exposed to frontogenesis. No type of warm front is unconditionally frontogenetical or frontolytical; but since such warm fronts as are shown in Fig. 210*h* usually have a considerable speed, they will be exposed to frontogenesis. Warm fronts of the type shown in Fig. 210*j* may be exposed to frontogenesis in the early stage of wave development when the front velocity is small and will be exposed to frontolysis in the later stages when the speed increases.
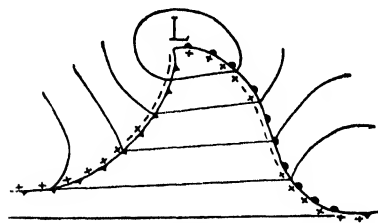
FIG. 211.—Showing the distribution of frontogenesis (+) and frontolysis (−) along the fronts in a young wave cyclone.

Applying the above rules to the fronts in a young cyclone, we obtain the normal picture shown in Fig. 211. It will be seen that the upper portion of the warm front is exposed to frontogenesis and the upper portion of the cold front is exposed to frontolysis. In the southern portion of the cyclone, the conditions are reversed. The occluded front that results from the development of a wave cyclone may therefore be quite distinct.

It is of interest to note that the cold front in the lower portion of Fig. 211 is always exposed to frontogenesis. Furthermore, since this part of the cold front is retarded, it will tend to become quasi-stationary, and eventually a wave may form on it. *The retardation and the reinforcement of this part of the cold front tend to link together the various members of the series of cyclones.* It is therefore important for the analyst to study in great detail the conditions along the part of the cold front that tends to become quasi-stationary. Such fronts are particularly susceptible to the formation of new waves.

The above principles are illustrated in Fig. 212, where a warm front remained almost stationary over France for 48 hr. With such isallobars, there would be converging winds toward the front, and the temperature discontinuity would increase. The mean air temperature being taken within a zone of 100 km. width at either side of the front, it was found that the mean temperature discontinuity on the map shown in Fig. 212 was 1.9°C. During the following 42 hr., the discontinuity increased steadily from 1.9 to 8.5°C.

It should be emphasized that the frontogenetical processes are always counteracted by frontolysis due to mixing. As was explained in Chap. VIII, mixing across the front increases with increasing angle between the frontal surface and the isentropic surfaces in its vicinity. It is therefore well not to expect noticeable frontogenesis unless the

kinematic conditions indicate a considerable degree of frontogenesis; and even when this is the case, real frontogenesis will result only when the frontal surface does not deviate too much from an isentropic surface.

In addition to the above rules, the principles outlined in Chap. V should be used to determine whether there is frontogenesis or not.
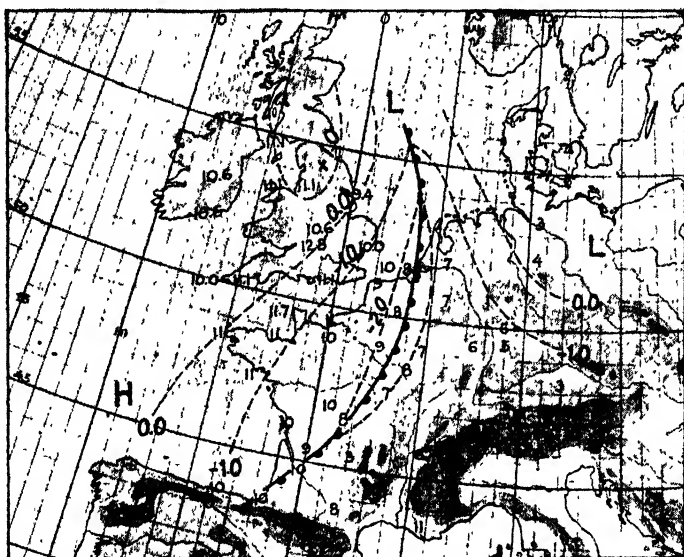
FIG. 212.—Showing an example of frontogenesis through isallobaric winds. Broken lines indicate isallobars; small numerals, air temperature.

166. Isallobaric Gradients and Vertical Velocity along Frontal Surfaces.—It was shown in Par. 91 that, when the curvature of the trajectories of the air motion is not too large, the following equation gives a good approximation to the actual wind at the top of the friction layer

$$(1) \qquad\qquad v = v_{g_s} - \frac{\alpha}{\lambda^2} I$$

In the vicinity of fronts, where the isallobaric gradient (*i.e.,* $-I$) may be considerable, the wind will have a component normal to the isallobars in the direction from high to low values of the barometric tendencies. As was explained in Par. 100, this wind component may result in appreciable convergence or divergence, which, again, results in vertical velocities that may give rise to condensation and precipitation.

The above equation furnishes a simple means for estimation of the amount of vertical velocity along frontal surfaces. We need then consider only the wind components normal to the front. We let indices refer to the warm air, and we choose the x-axis normal to the front from the warm toward the cold mass. For simplicity, we write G_x for the

x-component of the geostrophic wind. From Eq. (1), we obtain for the cold and the warm mass, respectively

$$(2) \qquad v_x = G_x + \frac{\alpha}{\lambda^2}(-I_x) \qquad \text{and} \qquad v_x' = G_x' + \frac{\alpha'}{\lambda^2}(-I_x')$$

where $-I_x$ and $-I_x'$ are the isallobaric gradients normal to the front. As the isobars are continuous at the front, it follows that $\partial p/\partial y = \partial p'/\partial y$. From this, it follows that $G_x = G_x'$, except for a small difference which is due to a slight difference in density. We consider first a warm front. From the above equations, we obtain for the rate at which the warm air moves faster than the cold air in the direction normal to the front

$$v_x' - v_x = \frac{\alpha'}{\lambda^2}(-I_x') - \frac{\alpha}{\lambda^2}(-I_x)$$

Since the density discontinuity is small compared with the discontinuity in the isallobaric gradients, we may put $\alpha' = \alpha$. This gives

$$v_x' - v_x = \frac{\alpha}{\lambda^2}[(-I_x') - (-I_x)]$$
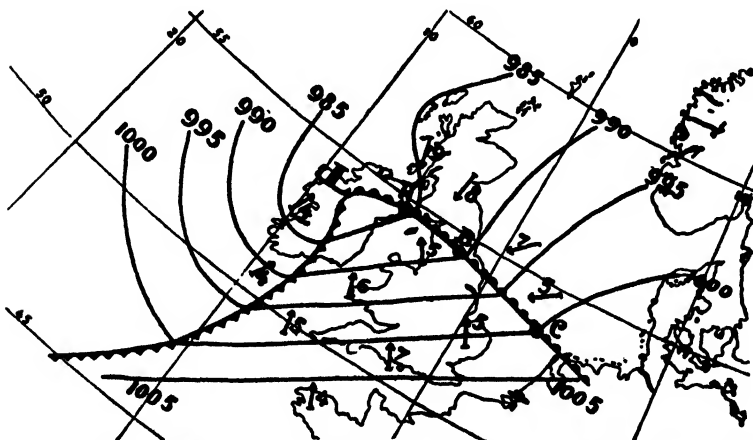
FIG. 213.—Fronts and isobars in a young cyclone wave Jan. 23, 1926, 7 A.M. The arrows indicate the isallobaric wind components computed from Eq. (1).

As was shown in Par. 159, the vertical velocity along the frontal surface must be proportional to the wind discontinuity, it must therefore also be proportional to the discontinuity in the isallobaric gradients at the front.

The application of the above to weather charts is best illustrated by the example shown in Fig. 213. Since the isallobaric gradients in the southern part of the warm sector are fairly uniform, there can be but slight convergence and therefore only slight ascending velocity. The stations Andover and Holyhead, which are situated in this region,

observed rain intensities of 0.1 mm./hr., which corresponds to slight drizzle.

At the peak of the warm sector, the barometric tendency increased to a maximum, and the isallobaric gradient decreased to zero. There must therefore be a strong convergence in the warm air at the peak of the warm sector. Eskdalemuir observed a rain intensity of 5.4 mm./hr. while the peak of the warm sector passed.

It will be seen from Fig. 213 that the isallobaric gradients in the cold air have a marked convergence toward the warm front. It follows from Eq. (1) and Fig. 213 that the cold air immediately in advance of the warm front will move in the direction normal to the front with a speed which is less than the geostrophic-wind component in this direction, whereas the warm air in the rear of the warm front will move with a speed which is closer to the geostrophic wind. Thus, the warm air, which moves faster than the cold air, will ascend along the warm-front surface (see also Par. 159). The convergence toward the warm front is strongest in the northern part. The rain intensities (in millimeters per hour) during the passage of the warm front were as follows: Andover, 2.0; Holyhead, 1.8; and Eskdalemuir, 7.5, which shows that the rain intensities were roughly proportional to the convergence toward the front.[1]

It will be seen from Fig. 213 that the convergence of the isallobaric winds is much smaller at the cold front than at the warm front. Consequently, one should expect slighter rain intensities during the passage of the cold front. The rain intensities observed during the cold-front passage were: Eskdalemuir, 0.2; Holyhead, 1.0; and Andover, 1.5. It is of interest to note that the rain intensities increase along the cold front from the north toward the south. This is quite the normal case along cold fronts of type *B* referred to in Pars. 122 and 159.

The rain intensity along fronts does not depend only on the amount of convergence and upglide motion. It depends also on the slope of the frontal surface, the moisture content, and the stability of the warm air. Thus, when the warm air is convectively unstable, the upglide motion will release convective currents which will cause convective precipitation in addition to that caused by the frontal upglide motion. This was discussed in Pars. 46 and 55.

---

[1] For a more detailed discussion see Petterssen [55].

CHAPTER X

DEEPENING AND FILLING

In the previous chapter, we discussed the various factors that influence the velocity of propagation of the various types of pressure system, and a number of formulae and forecasting rules were deduced. The aim of this chapter will be to discuss the deepening and filling of these pressure systems, or, in other words, their change in intensity while they move across the charts. The physical and dynamic processes that cause deepening and filling were discussed in Chap. VII. In this chapter, we shall concern ourselves only with the symptoms of these processes that the weather charts reveal and shall give a number of formulae and rules by means of which the deepening and filling of pressure systems may be forecast.

167. Definition.—A cyclone center is said to *deepen* when the pressure in the center decreases while it moves across the chart. If the pressure in the center rises, the center is said to *fill*. The same also applies to troughs of low pressure. It is convenient, but perhaps not quite so logical, to use the same expressions about anticyclonic centers and wedges of high pressure. A clear picture of the meaning of the terms deepening and filling is obtained by imagining a number of ships evenly distributed around a pressure center, sailing with exactly the speed of the center, and having courses parallel to the path of the center. If these ships were furnished with barographs, they would record pressure variations entirely due to the deepening or the filling of the pressure system. If, on the other hand, a number of islands were distributed around the center, barographs mounted on these islands (fixed stations) would record pressure variations that express the result of the movement of the center as well as its deepening. Barometric tendencies observed at fixed stations consist, therefore, of two parts, *viz.*: (1) the pressure variation due to the movement of the pressure system, and (2) the pressure variations due to the deepening **or** filling of the pressure system. For analysis and forecasting, it is important to decide what is due to deepening and what is due to movement.

We consider the pressure function (see Par. 146) in a system of coordinates that moves with the pressure system in question. Then, as was shown in Par. 148,

(1)
$$\frac{\delta p}{\delta t} = \frac{\partial p}{\partial t} + c \cdot \nabla p$$

where $\delta p/\delta t$ is the pressure variation per unit time in the moving system, $\partial p/\partial t$ the pressure variation per unit time in the fixed system of coordinates, c (vector) the velocity of the pressure system, and $-\nabla p$ the horizontal pressure gradient at the point which we consider. The term $\delta p/\delta t$ expresses the rate at which the pressure system deepens $[\delta p/\delta t < 0]$ or fills $[(\delta p/\delta t) > 0]$ at the point where the barometric tendency is $\partial p/\partial t$ and the pressure gradient is $-\nabla p$. We shall refer to the term $\delta p/\delta t$ as the *deepening* (or filling) *intensity*.

Differentiating Eq. (1) with respect to time in the moving system of coordinates, we obtain an expression for the *deepening acceleration* (*i.e.,* $\delta^2 p/\delta t^2$). Since the equation for the deepening acceleration contains terms that cannot be evaluated from the weather charts, it will not be discussed here.[1]

It will be seen from Eq. (1) that the deepening term depends on the barometric tendency (or the *local pressure variation* $\partial p/\partial t$) and on the *convective term* (*i.e.,* $c \cdot \nabla p$). Although the first of these terms is readily obtained from the isallobars, the latter is more involved and can be computed only when the velocity of the pressure system has been computed. Computations of the convective term are usually inaccurate. It is therefore advisable to evaluate the deepening term in points or areas or along lines in the pressure field *where the convective term vanishes*. Outside these areas, an estimation of the sign and the approximate magnitude will suffice.

168. Interpretation and Evaluation of the Convective Term.—In order to become familiar with the distribution of the convective term, we shall consider a number of types of pressure system as shown in Fig. 214. Since the pressure gradient (*i.e.,* $-\nabla p$) is normal to the isobars, inversely proportional to the distance between neighboring isobars, and points from high to low values of pressure, the vector ∇p (*i.e.,* the ascendant) will be equal to the pressure gradient, but it will point in the opposite direction.

We consider first a cyclonic center with circular concentric isobars as shown in Fig. 214*A*. The convective term (*i.e.,* $c \cdot \nabla p$) will have a maximum *positive* value in advance of the center where the vector ∇p coincides with the velocity c. The term decreases as the angle between c and ∇p increases; it vanishes along a line through the center normal to the direction in which the center moves (*i.e.,* normal to c). To the left of this line (*i.e.,* in the rear half of the pressure system) the convective term is negative, since the angle between c and ∇p then is greater than $\pm 90°$. The term obtains a maximum negative value in the rear of the center where ∇p is due opposite to c. Furthermore, it will be seen from

---

[1] For a more detailed discussion, see Petterssen [55].

Eq. *167*(1) that the convective term vanishes in the center where $\nabla p = 0$. It also vanishes everywhere when the center is stationary (*i.e.*, $c = 0$).

We consider next Fig. 214*B*. Since a wave cyclone moves mainly in the direction of the warm-sector isobars, it will be seen that the convective term vanishes in the warm sector, for ∇p is perpendicular to c. In advance of the warm front, the term is positive; in the rear of the cold front, it is negative. Since the pressure distribution in Fig. 124*B* is symmetrical, the convective term is symmetrical except for the sign.

Comparing Fig. 214*B* and *C* it will be seen that the convective term in the rear of Fig. 214*C* is negative and much larger than in the rear of Fig. 214*B*. This is due to the fact that, in Fig. 214*C*, the vector ∇p is large and directed along the direction of velocity, whereas, in case *B*, it is small and has an unfavorable angle with the direction of the velocity. In both Fig. 214*B* and Fig. 214*C*, the convective term vanishes throughout the warm sector and also along a line north of the center normal to the direction in which the center moves.

Figure 214*D* shows a case with diverging warm-sector isobars. It will be seen that the convective term in this case is small and positive in the northern part of the warm sector, whereas it is negative in the southern part.

A discussion similar to that above will show that the convective term is positive in advance of and negative in the rear of troughs and vanishes on the trough line where ∇p and c are perpendicular to one another. On wedges, the conditions are the same as in troughs, but with the sign of the convective term reversed. In anticyclonic systems, the convective term is negative in advance and positive in the rear of the center, and it vanishes in the center and where the isobars are parallel to the path of the center.

Since the pressure usually falls in advance of moving cyclones and troughs and rises in advance of moving anticyclones and wedges, it
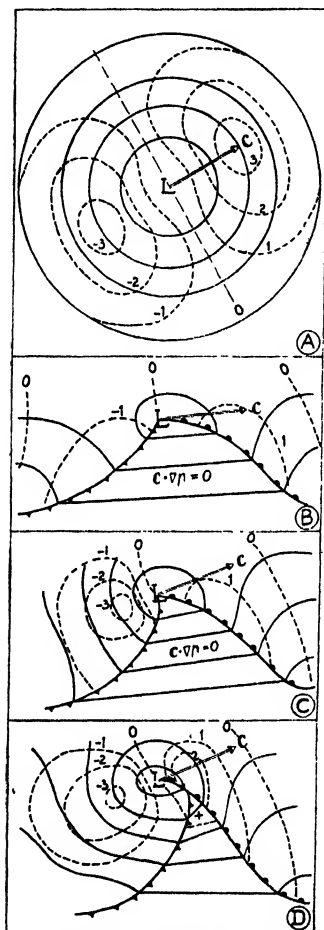
Fig. 214.—Showing the distribution of the convective term. The arrow c indicates the velocity of the pressure center. Broken lines indicate equal values of the convective term.

will be seen from the foregoing discussion that the convective term usually is positive where the barometric tendency is negative, and vice versa, so that the deepening comes out as the balance between the local pressure variation and the convective term. For the analysis of deepening, filling, cyclogenesis, etc., it is exceedingly important to obtain a clear picture of how the convective term varies with the pressure distribution and the velocity of the pressure system in question.

If the barometric tendencies were entirely due to advection, there would be no deepening or filling, and $\delta p/\delta t = 0$. The convective term would then everywhere balance the local pressure variation. Therefore, *the difference between the local pressure variation $\partial p/\partial t$ and the convection term $c \cdot \nabla p$ expresses the amount of pressure variation that is caused by divergence and convergence in the air column. The term $\delta p/\delta t$, therefore, indicates the intensity of the dynamic processes that cause deepening or filling of the pressure systems.* These processes were discussed in Pars. 100, 132 and 133.

169. Deepening and Filling of Pressure Centers, Troughs, and Wedges.—From the discussion in the previous paragraph, it follows that the convective term vanishes where the isobars are parallel to the direction in which the pressure system moves and also where the pressure gradient vanishes. It follows then from Eq. *167*(1) that, in these areas,

$$\delta p/\delta t = \partial p/\partial t$$

and the deepening intensity is then simply equal to the observed barometric tendency. Applying this to the various types of pressure system, we obtain the following forecasting rules:

Rule 19.   *A cyclonic center deepens (or fills) with a speed that is equal to the barometric tendency in the center. The same also applies to anticyclonic centers.*

Rule 20.   *A cyclonic center deepens when the zero isallobar is in the rear of the center, and it fills when the zero isallobar is in advance of the center. Anticyclonic centers obey the reverse rule.*

Rule 21.   *The deepening (or filling) in regions where the isobars are parallel to the path of the center is equal to the barometric tendency.*

By means of the above rules, valuable results can be obtained by simple inspection of the isobars and isallobars. As an example, we consider Fig. 215A. It will be seen that the zero isallobar is in the rear of the center; there is therefore deepening in the center. However, north of the point a and south of the point b, the barometric tendency is positive. According to rule 21, there is filling north of the point a and south of the point b. This obviously means that the center will deepen in its central portion and fill in the outskirts: the pressure gradient and the wind circulation around the center will therefore increase.

If the zero isallobar in Fig. 215A were curved toward the left instead of the right, the center would also deepen, but the deepening would then be a minimum in the center, and the pressure gradient and the wind circulation would be decreasing. In a similar manner, the deepening or filling in the center and along the line normal to the path can be obtained for anticyclonic centers. *An examination of the isallobars in the zone through the center and normal to the path will then show not only whether there is deepening or filling but also whether the deepening or filling results in increasing or decreasing circulation.*
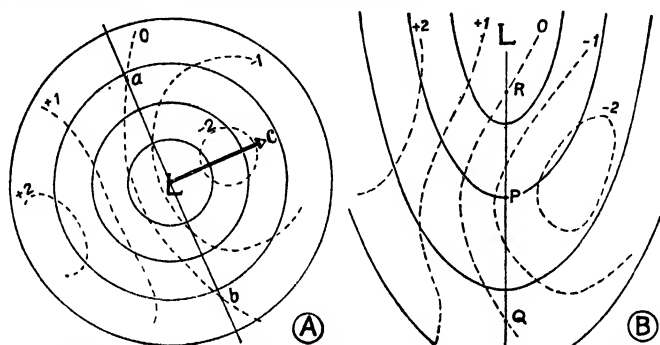
FIG. 215.—Showing how to apply rules 19–21 to pressure centers and troughs.

Since by definition the velocity of a trough or a wedge (see Fig. 191) is normal to the trough or wedge lines, it follows that the convective term vanishes on trough and wedge lines. We therefore obtain the following rules which are analogous to the rules for pressure centers:

Rule 22. *A pressure trough deepens (or fills) with a speed that is equal to the barometric tendency on the trough line. The same applies also to wedges.*

Rule 23. *A pressure trough deepens when the zero isallobar is in the rear of the trough line, and it fills when the zero isallobar is in advance of the trough line. Wedges of high pressure obey the reverse rule.*

The application of these rules is illustrated in Fig. 215B. The deepening has a maximum in the vicinity of P, and there is filling in the trough south of Q and north of R. If the process continues, a cyclonic center will form near P, while the trough as a whole moves in the direction from rising to falling barometer. In a similar manner, the rules may be applied to wedges of high pressure.

The above rules apply to points and lines in the pressure field where the convective term vanishes. In other points, the deepening intensity can be evaluated only if the velocity of the pressure system is known. As was shown in the last chapter, the velocity may be computed from the isobars and isallobars or estimated by means of the forecasting rules. Since computation of the convective term in·several points involves a

considerable amount of labor, it is desirable to obtain an idea of the amount of deepening and filling around the center without computing the convective term. A useful expression for the deepening of a pressure system may be obtained from Eq. *167*(1). We consider the area enclosed by two closed isobars. Let $d\sigma$ denote an element of this area. Multiplying the deepening equation by $d\sigma$ and integrating over an area enclosed by two closed isobars, we obtain[1]

$$\int c \cdot \nabla p \, d\sigma = c \cdot \int \nabla p \, d\sigma = 0$$

which means that the integral of the convective term vanishes over an area enclosed by two closed isobars. Since this must hold for every such area, it is readily seen that the above equation holds for the area enclosed by any closed isobar. From the deepening equation, we then obtain

$$\int \frac{\delta p}{\delta t} \, d\sigma = \int \frac{\partial p}{\partial t} \, d\sigma$$

for any area σ enclosed by a closed isobar. This may be expressed in the following rule:

Rule 24. *A pressure center as a whole deepens when the planimetric value of the barometric tendency is negative within a closed isobar, and it fills when the planimetric value of the barometric tendency is positive.*

This rule, which applies to cyclonic centers as well as to anticyclonic centers, may be applied also to zones limited by two closed isobars. By applying it to several such zones, an idea of the distribution of the deepening around the center is readily obtained. The planimetric value of the barometric tendency need not, of course, be measured; it usually suffices to estimate it from the isallobars. Rule 24 is particularly useful because it can be applied without knowing the speed of the center and the direction in which it moves. It is well to note that rules 19 to 21 can be applied without knowing the speed of the center; it suffices to know the direction in which it is moving. Methods for determining this direction were described in Chap. IX.

170. Deepening and Filling of Warm-sector Cyclones.—In considering the deepening of warm-sector cyclones, it is most convenient to choose a system of coordinates that moves with the front. The x-axis should then be chosen along the warm-sector isobar as shown in Fig. 201*A*. The velocity of the front is then along the x-axis. In the warm sector, the pressure gradient is perpendicular to the direction of the velocity. The convective term, therefore, vanishes in the warm sector, and we obtain:

[1] See PETTERSSEN [55].

Rule 25. *The deepening intensity in any point in the warm sector is equal to the barometric tendency in the point in question.*

The application of this rule may be illustrated by means of Fig. 201A. In the peak of the warm sector, the barometric tendency is about −2 mb. Consequently the center will deepen 2 mb. in 3 hr. In the middle part of the warm sector, the tendency is about −1 mb., and farther to the south it is zero. Rule 25 applied gives the result that the deepening is greatest near the center and decreases southward, and this means that the pressure gradient and the wind in the warm sector will increase. The same result is obtained by applying the formula for the velocity of the isobars to the warm-sector isobars (see Par. 153). It will then be seen that the isobars in the northern part of the warm sector move southward more quickly than do the isobars in the southern part of the warm sector. This leads to crowding of the isobars and increasing of the wind.

We may next apply rule 21 to the region north of the center in Fig. 201A. It will then be seen that the deepening is greatest near the center and decreases northward. The pressure gradient and the easterly wind north of the center will therefore increase. Not only does the distribution of the deepening around the center indicate that the pressure decreases in the center; it also indicates that the center is increasing in strength (*i.e.*, *cyclogenesis*). If the deepening were less in the center than farther away from it, there would be decreasing winds and *cyclolysis*. Some other symptoms of cyclogenesis and cyclolysis will be described in Par. 172.

It was mentioned in Par. 134 that a maximum of deepening sometimes occurs at the peak of the warm sector in partly occluded cyclones. If the maximum is pronounced, it may lead to the development of a new center at the peak of the warm sector while the primary occluded center fills up. Such developments can easily be detected long before the secondary center forms. The classical type of such development is the Skagerrak cyclone first discussed by J. Bjerknes and H. Solberg [9]. A statistical investigation by the author showed that such developments took place only when the isobars in the warm sector diverge as shown in Fig. 214d. In the northern part of the warm sector, the convective term is positive and counteracts the barometric tendency, whereas in the southern portion, the barometric tendency and the convective term are both negative, which results in a large deepening intensity.

Normally, the deepening intensity varies with time. In order to extrapolate the amount of deepening during the forecasting period, it would be necessary to know the deepening intensity as well as the deepening acceleration at the initial moment. As was mentioned in Par. 167, it is in general impossible to obtain the deepening acceleration from the data of the weather charts. However, as has been shown by

Petterssen [55], the deepening acceleration in the warm sector is negligible, which means that the deepening intensity remains constant as long as there is a warm sector at the ground. The deepening may be computed with great accuracy from the barometric tendencies through the use of rule 25. This rule has been substantiated by statistical evidence[1] which shows that accurate results can be obtained for the deepening of warm-sector cyclones during 24 hr. even when the deepening is excessively large. Statistical investigations also show that the deepening intensity continues tó remain constant for some time after the cyclone has commenced to occlude but that, as the occlusion process continues, the deepening intensity decreases and eventually filling sets in. The process is, however, not a symmetrical one: the deepening of a cyclone in its early stages of development is always more intense than the filling in the later stages. Thus, though cyclones in extreme cases may deepen at the rate of 3 to 4 mb. in 3 hr., it is rarely observed that the filling amounts to more than 1.5 mb. in 3 hr. The above may be expressed in the following rule:

Rule 26.—Warm-sector cyclones deepen at the rate indicated by the tendency in the peak of the warm sector. This rate remains almost constant until 6 to 12 hr. after occlusion sets in; the deepening then decreases and changes gradually into a slow filling.

It was mentioned above that the deepening may result in increasing pressure gradient in the warm sector. This would normally mean that the geostrophic wind normal to the front would increase on account of the deepening. A typical example is shown in Fig. 201A. If the deepening is appreciable, rules 15 to 18 (Par. 159) would give too small displacements of the fronts and the center. In such cases, one should use the maximum values for the displacements indicated in these rules. If the distribution of deepening or filling is such that the pressure gradient decreases, one should use the lower limits for the displacements. If there is no appreciable deepening or filling, the mean values would apply.

171. Relation between Deepening and Occlusion of Warm-sector Cyclones.—Let c_c and c_w denote the velocity of the cold and the warm front, respectively. Choosing the x-axis along the warm-sector isobars and letting indices 1 and 2 denote the air in advance and in the rear of the warm front and indices 3 and 4 the air in advance and in the rear of the cold front (see Fig. 216), we obtain from Eq. *149(4)*

$$(1) \quad c_c = -\frac{(\partial p_3/\partial t) - (\partial p_4/\partial t)}{(\partial p_3/\partial x) - (\partial p_4/\partial x)}, \quad c_w = -\frac{(\partial p_1/\partial t) - (\partial p_2/\partial t)}{(\partial p_1/\partial x) - (\partial p_2/\partial x)}$$

Since the x-axis is chosen along the warm-sector isobar

$$\frac{\partial p_2}{\partial x} = \frac{\partial p_3}{\partial x} = 0.$$

PETTERSSEN [55].

Let $c_0 = c_c - c_w$ denote the rate at which the cold front overtakes the warm front. c_0 may then be called the *occluding velocity*. From the above equations, we obtain

$$(2) \qquad c_0 = \frac{(\partial p_3/\partial t) - (\partial p_4/\partial t)}{\partial p_4/\partial x} + \frac{(\partial p_1/\partial t) - (\partial p_2/\partial t)}{\partial p_1/\partial x}$$

When the wave cyclone is symmetrical, or nearly so, we may put

$$\frac{\partial p_1}{\partial x} = -\frac{\partial p_4}{\partial x} = \frac{5}{H},$$
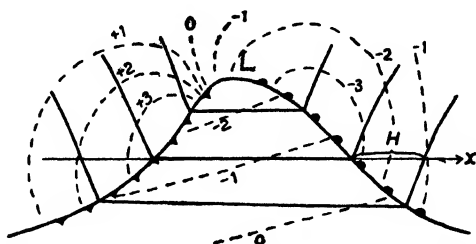
Fig. 216.—Showing how to evaluate the rate of occlusion.

where H has the meaning shown in Fig. 216. If we $\partial p/\partial t = b =$ the barometric tendency, Eq. (2) reduces to

$$c_0 = \frac{b_1 - b_2 - b_3 + b_4}{5} H$$

Since the barometric tendency is negative in advance ($b_1 < 0$) and positive in the rear of the wave cyclone ($b_4 > 0$), b_1 and b_4 will tend to cancel one another. If the tendency distribution also is symmetrical, we obtain

$$c_0 = -\frac{b_2 + b_3}{5} H$$

Putting $\frac{1}{2}(b_2 + b_3) = b_w =$ the warm-sector tendency on the x-axis in the middle of the warm sector (see Fig. 216), we obtain

$$c_0 = -\frac{2}{5} b_w H$$

The rate at the which the warm sector occludes is therefore directly proportional to the warm-sector tendency. According to rule 25, the warm-sector tendency is also indicative of the rate at which the wave cyclone deepens. From this, we obtain the following rule:

Rule 27. Symmetrical warm-sector cyclones deepen and occlude at a rate that is directly proportional to the warm-sector tendency.

Experience shows that this rule holds with reasonable approximation, also, when the wave is not symmetrical.

It was shown in Chap. VII that the cyclone waves are unstable and that the rate of development and occlusion is directly proportional to the degree of instability. From this and from rule 27, we obtain:

Rule 28. *The warm-sector tendency expresses the degree of instability of the wave.*

From the above, it follows that *deepening and occlusion are but two aspects of the same phenomenon, viz., the instability of the cyclone wave.*

The tendencies observed in the peak of warm sectors vary from case to case within the limits of -0.5 to -3.5 mb. It is convenient to use the following scale for indicating the rate of deepening:

Slight deepening........................ b less than -1.0
Moderate deepening..................... b between -1.0 and -2.0
Rapid deepening........................ b between -2.0 and -3.0
Excessive deepening.................... b in excess of -3.0

172. Cyclogenesis and Anticyclogenesis.—In Par. 164, we discussed a number of the symptoms which indicate that cyclone waves will form. Whenever any of these symptoms are present, the analyst should study the isallobars in great detail in order to investigate the distribution of the deepening intensity. If the isallobars show that there is deepening in the areas where there are indications of wave formation, this may be taken as a sign that cyclogenesis is already under way.

Deepening alone is not sufficient evidence of increasing cyclonic circulation or of decreasing anticyclonic circulation. Whether the deepening or filling results in the formation or increasing of cyclonic or anticyclonic circulation depends on the horizontal distribution of the deepening term. For example, it happens sometimes that a cyclonic center fills up while the cyclonic circulation around it increases. This occurs when the filling is more intense in the outskirts of the cyclone than in its center. Conversely, a deepening cyclonic center will decrease its cyclonic circulation when the deepening is less intense in the center than in the environment.

In this paragraph, we shall discuss the criteria for increasing and decreasing circulation around cyclonic and anticyclonic centers. We say that we have *cyclogenesis when the circulation around a cyclonic center increases and cyclolysis when the circulation decreases.* In a similar manner, we may speak of *anticyclogenesis* and *anticyclolysis*.

From what was said above, it follows that cyclogenesis, cyclolysis, etc., depend on the horizontal distribution of the deepening term $\delta p/\delta t$. We shall therefore first study its horizontal variation, or the quantity $\nabla(\delta p/\delta t)$. From Eq. *167*(1), we obtain

$$(1) \qquad \nabla \frac{\delta p}{\delta t} = \nabla \frac{\partial p}{\partial t} + \nabla(\mathbf{c} \cdot \nabla p) = \nabla \frac{\partial p}{\partial t} + \nabla \left(c_x \frac{\partial p}{\partial x} + c_y \frac{\partial p}{\partial y} \right)$$

We substitute for c_x and c_y from Eq. *149*(6) and note that

$$\frac{\partial p}{\partial x} = \frac{\partial p}{\partial y} = \frac{\partial^2 p}{\partial x \, \partial y} = 0$$

in the pressure center.   This gives

$$\nabla \left(c_x \frac{\partial p}{\partial x} + c_y \frac{\partial p}{\partial y} \right) = -\nabla \frac{\partial p}{\partial t}$$

and Eq. (1) reduces to

(2) $$\nabla \frac{\delta p}{\delta t} = 0$$

in the center.   This means that *the deepening (or filling) has a numerical maximum or minimum in the pressure center.*   Thus, there is cyclogenesis when the deepening has a maximum, or the filling a minimum, in the cyclonic center; and there is cyclolysis when there is a minimum of deepening or a maximum of filling in the cyclonic center.   Similar rules hold for anticyclonic centers.

Cyclogenesis then means that the isobars around a cyclonic center become more crowded, and cyclolysis means that they become less crowded.   That is, cyclogenesis results in increasing curvature of the pressure profiles through the center (compare Par. 151), and cyclolysis results in decreasing curvature of these profiles.   It was shown in Par. 151 that $\partial^2 p / \partial x^2$ and $\partial^2 p / \partial y^2$ express the curvatures of the pressure profiles along the x- and y-axis, respectively.   Therefore, when there is cyclogenesis, $\partial^2 p / \partial x^2$ and $\partial^2 p / \partial y^2$ must increase with time in a system of coordinates that moves with the pressure center.   Applying the operator defined by Eq. *148*(3), we obtain

$$\frac{\delta}{\delta t} \left(\frac{\partial^2 p}{\partial x^2} \right) = \frac{\partial}{\partial t} \left(\frac{\partial^2 p}{\partial x^2} \right) + c \cdot \nabla \frac{\partial^2 p}{\partial x^2} = \frac{\partial^3 p}{\partial x^2 \, \partial t} + c_x \frac{\partial^3 p}{\partial x^3} + c_y \frac{\partial^3 p}{\partial x^2 \, \partial y}$$

and a similar equation for the conditions along the y-axis.   Since the coordinate axes are axes of symmetry (see Par. 146),

$$\frac{\partial^3 p}{\partial x^3} = \frac{\partial^3 p}{\partial x^2 \, \partial y} = 0$$

and therefore

$$\frac{\delta}{\delta t} \left(\frac{\partial^2 p}{\partial x^2} \right) = \frac{\partial^3 p}{\partial x^2 \, \partial t}$$

for the profile along the x-axis.   Along the y-axis, the following relation holds:

$$\frac{\delta}{\delta t} \left(\frac{\partial^2 p}{\partial y^2} \right) = \frac{\partial^3 p}{\partial y^2 \, \partial t}$$

It was shown in Par. 151 that $\partial^3 p / (\partial x^2 \, \partial t)$ expresses the curvature of the

tendency profile along the x-axis, and $\partial^3 p/(\partial y^2\,\partial t)$ the curvature of the tendency profile along the y-axis. Furthermore, since $(\partial^2 p/\partial x^2) > 0$ and $(\partial^2 p/\partial y^2) > 0$ in cyclonic centers, whereas they are negative in anticyclonic centers, we obtain the following rules:

Rule 29. *A cyclonic center increases in strength (cyclogenesis) when the tendency profiles are curved cyclonically, and it decreases in strength (cyclolysis) when the tendency profiles are curved anticyclonically.*

Rule 30. *An anticyclonic center increases in strength when the tendency profiles are curved anticyclonically and decreases in strength when the tendency profiles are curved cyclonically.*

Comparing these rules with rule 14 and Fig. 196, we obtain the following rule:

Rule 31. *Cyclonic centers that are exposed to cyclogenesis are usually retarded, and cyclonic centers exposed to cyclolysis are usually accelerated.* A similar rule holds for anticyclonic centers.

Although the rules 29 and 30 hold without exception, rule 14 may fail when the speed of the center is small (see Par. 151). As it is difficult to evaluate $\partial^3 p/(\partial x^2\,\partial t)$ and $\partial^3 p/(\partial y^2\,\partial t)$ accurately from the weather maps, the above rules should be used only when the curvature of the tendency profiles is so large that it may be regarded as certain that it is not appreciably influenced by the errors in the analysis.

The above rules for cyclonic and anticyclonic centers hold also for troughs and wedges, respectively. Thus, a trough increases in intensity when the tendency profile is curved cyclonically (see Fig. 196), and it decreases in intensity when the tendency profile is curved anticyclonically.

173. Adjustment of Displacements and Estimation of Accelerations.— In determining the displacement of pressure systems, it should be ascertained that the computed or estimated displacement of each individual system agrees logically with the simultaneous displacements of adjacent systems. The difficulty in the way of obtaining accurate displacements lies in the fact that it is not possible to determine the acceleration accurately. Therefore, for example, when the movement of two neighboring pressure systems during 24 hr. is extrapolated from the velocities only, it may be found that the forecast movements of the two systems conflict. In such cases, the conflict may be due to three causes:

1. The forecast displacement of one or both systems is erroneously determined or due to errors in the analysis. Therefore, whenever the forecast displacements of neighboring pressure systems clash, the analysis and the determination of the velocities should be reexamined.

2. One or both pressure systems may be accelerated or retarded. Therefore, one should try to apply the rules pertaining to the acceleration of pressure systems in order to find out whether or not the apparent clash may be due to accelerations that have not been taken into account.

3. One or the other of the pressure systems may be in the process of deepening or filling so that it will loose its identity during the forecasting period. Therefore, whenever the forecast displacements of neighboring pressure systems do not harmonize, one should examine the distribution of deepening or filling.

The above rules, which apply to all kinds of pressure systems and fronts, are illustrated in Fig. 217. Suppose that the movement during 24 hr. of the front and the preceding wedge has been determined as shown by the arrows. It is then evident that the frontal trough cannot approach
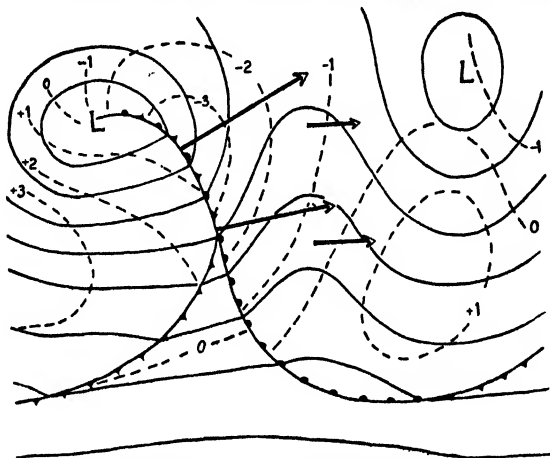
Fig. 217.—Showing a case of rapid movement of the front and disappearance of the preceding wedge through deepening.

the wedge to the extent shown by the arrows while both the frontal trough and the wedge retain their identity. The three possibilities mentioned above should be considered. In the case shown in Fig. 217, it follows from rule 23 that the wedge is "deepening" since the zero isallobar is in advance of the wedge line. The wedge will therefore tend to disappear, and the frontal trough will not be hindered in its motion by the slow motion of the wedge.

On the other hand, if the zero isallobar were near the wedge line, the wedge would retain its identity. The question then arises whether the front will be retarded or the wedge will be accelerated. In order to answer this question, we should try to determine the displacement of the eastern center. If the displacement of the eastern center is comparable with that of the wedge, it is certain that the movement of the front must be retarded. We should then study the curvature of the tendency profile (rule 14) through the western center in order to find additional evidence of retardation.

We suppose again that the zero isallobar was close to the wedge line instead of in advance of it as it is in Fig. 217. The wedge would

then retain its identity. If it now were found that the displacement of the eastern center was considerably larger than that of the wedge, the logical conclusion would be either that the wedge would be accelerated or else that its displacement had been erroneously determined.

Apart from the above tests, the forecast displacements should be compared with the past displacements as described in Par. 162. In this way, it is usually possible to detect appreciable accelerations and to avoid erroneous forecasts of the travel of pressure systems.

In connection with the forecasting of the displacement of cyclones, it should be mentioned that it is frequently advantageous to watch the condition in the region of the col preceding the cyclonic center. Three types of col are shown in Fig. 218. Comparing these with Fig. 113, it will be seen that in case *A* there is no vorticity, whereas type *B* has
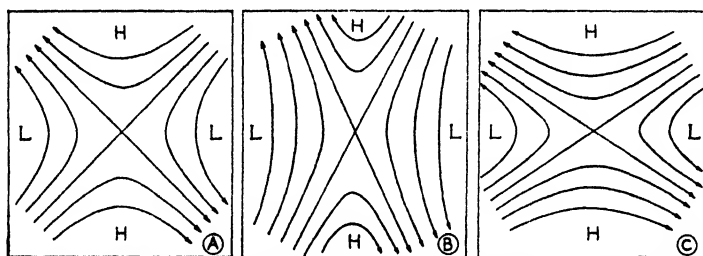
Fig. 218.—Three types of cols: *A*, without vorticity; *B*, anticyclonic vorticity; *C*, cyclonic vorticity.

anticyclonic and type *C* cyclonic vorticity. Experience shows that the type of col which has cyclonic vorticity affords much less "resistance" to advancing cyclones than does a col with anticyclonic vorticity. *A cyclone approaching a col with anticyclonic vorticity will usually slow down.*

Each of the types of col will tend to concentrate isotherms along the axis of outflow, as was explained in Chap. V. But since vorticity is a quasi-conservative property, cols of type *C* will tend to accumulate cyclonic vorticity along the axis of outflow, whereas cols of type *B* will tend to accumulate anticyclonic vorticity along this axis. *Cols of type C, therefore, represent a "potential cyclogenesis."* The forecasting rules of deepening and filling hold also for cols, and, by means of these rules, it is possible to obtain an idea of their future development.

174. Cyclone Tracks and Centers of Action.—From the discussion in Chaps. V and VII, it follows that the extratropical cyclones usually originate on the polar front near the cols between the quasi-permanent anticyclonic systems. The young waves travel along the front; and, in their later (occluded) stages of development, the cyclonic whirls travel northeastward toward the region occupied by the quasi-stationary subpolar cyclone. The forecaster should therefore bear in mind the

importance of studying the changes in position and intensity of the sub-polar central cyclone as well as the slow changes in the quasi-permanent anticyclones.   The paths of the individual cyclones are largely deter-mined by the circulations around these large centers of action.

Figure 219 shows diagrammatically the conditions that prevail in winter over the oceans in the northern hemisphere.   For example, over the Atlantic Ocean, the zone of frontogenesis is found between the cold anticyclone over the North American continent and the warm sub-tropical high.   Waves that form on the front will travel toward the east and northeast, developing as described in Par. 130 and having a
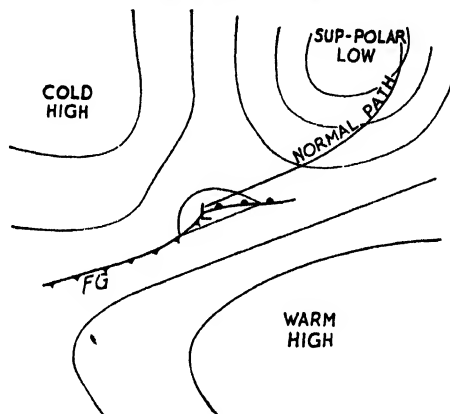
FIG. 219.—Showing the normal path of a cyclone relative to the large centers of action.

speed and course that are mainly determined by the general circulation between the Atlantic high and the Icelandic low.   The future path of the wave cyclone indicated in Fig. 219 can be forecast most accurately when the conditions in the eastern part of the Atlantic Ocean and in western Europe are known.   While the wave moves toward the north-east, the Icelandic low may change its position, and this will influence the path of the wave.   Now, the position and intensity of the Icelandic low depend on the Siberian high and the arctic high which, in turn, depend on the Aleutian low, and so on.   It is therefore necessary to have, at least once a day, a weather map of the entire northern hemisphere so that the changes in the principal centers of action and the interaction between them can be studied.   The slow and gradual changes in the position and intensity of these systems can best be studied by preparing mean-pressure charts covering periods of about 5 days.

CHAPTER XI

THE TECHNIQUE OF ANALYSIS AND FORECASTING

The aim of the analysis is to obtain a reliable diagnosis of the physical, dynamic, and kinematic state of the atmosphere at regular intervals. The general principles of analysis were described in Chaps. I to VIII. The results of the analysis furnish the basis for the prognostication, the general principles of which were described in Chaps. IX and X. The aim of this chapter will be to summarize the general principles and to demonstrate their application to actual forecasting.

175. The Observations.—Simultaneous or quasi-simultaneous observations of the state of the atmosphere are made at a large number of meteorological stations on land and also in some selected ships. These observations are transcribed into coded messages, collected in national centers, and disseminated by the aid of radio or other means of telecommunication for national or international use. In view of the fact that weather maps for an entire hemisphere, or a large portion thereof, are necessary for weather prediction, the weather services in most countries adhere to the regulations laid down by the International Meteorological Organization, which maintains a permanent secretariat in Lausanne, Switzerland.

The regulations laid down by the International Meteorological Organization (abbreviated l' O.M.I.) are primarily concerned with the codes for weather reports, definitions of the significant weather phenomena to be reported, station indices, and timetables for international exchange of reports. As the codes, timetables, etc., are subjected to changes from time to time, they will not be included in this book. All questions concerning weather reports for synoptic purposes are handled by l' O.M.I. through the Commission for Synoptic Weather Information, and all information concerning meteorological broadcasts is contained in Publication 9 of the Secretariat of l' O.M.I.

Complete weather reports from land stations contain the following information[1]: Index number of station (III), barometric pressure (PPP), barometric tendency (app), temperature (TT), relative humidity (U) or dew point (T_sT_s), amount of precipitation (RR), wind direction (DD), wind force (F), form of low clouds (C_L), form of medium clouds (C_M), form of high clouds (C_H), height of base of low clouds (h), amount of

---

[1] The code symbols are indicated in parentheses.

low clouds (N_h), total amount of cloudiness (N), visibility (V), weather at the hour of observation (ww), and past weather (W). The ship reports do not normally contain the items U or T_sT_s, RR, h, and N_h. They contain in addition, however, the position of the ship, the hour of observation in Greenwich time (GG), the difference between air temperature and sea-surface temperature (T_d), the course (d_s) and the speed (v_s) of the ship, and description (K) and direction (D_h) of swell.

It will be noticed that most of the above elements indicate the actual state of affairs at the moment of observation without indication of changes with time. Only two elements, *viz.*, wind velocity and barometric tendency, are essentially change elements. These two elements, therefore, have a direct forecasting significance, whereas the other elements can be used only for analyzing purposes. However, when weather maps are drawn at frequent intervals, it is possible to obtain information about time variations. The difference between two consecutive weather maps will give the *local* variations with respect to time. As the weather depends mainly on such entities as fronts, cyclones, and air masses and as these entities move across the chart, it is obvious that the problem of weather analysis will be to make out the *individual* changes of the entities that determine the weather.

The problem of weather analysis and forecasting may therefore be divided into three partial problems, *viz.*:

1. Analysis of the state of the atmosphere at a given moment.

2. Determination of the displacements of fronts, cyclones, air masses, etc., within the forecasting period.

3. Determination of the changes in the above entities during their travel across the chart.

Before we proceed to discuss the weather reports from this point of view, it will be necessary to discuss some elementary concepts of weather-chart analysis.

176. Symbols.—In order to facilitate the analysis of the vast mass of data that is available from a large area, it has been found convenient to plot the reports on maps of suitable projection and scale. Such maps have been recommended by l' O.M.I. [38]. In order to facilitate the analysis further, the reports are plotted partly as numerals and partly as symbols, on the principle that instrumental observations are plotted as numerals which indicate the corrected readings (reduced to standard levels when necessary), whereas noninstrumental observations (such as clouds and weather) are plotted in symbols. A system of convenient symbols has been adopted for international use by l' O.M.I. The basic symbols of this system are shown in Fig. 220.

The station to which the report refers is indicated by a small circle on the map. The amount of cloudiness is indicated by proportional

filling of the circle. The cloud symbols are made to indicate the characteristic features of the cloud forms that they represent. Thus, clouds of the cumulus family are represented by dome-shaped symbols, stratiform clouds by horizontal strokes, undulated clouds by an undulated curve, frontal clouds by a horizontal stroke indicating their stratiform structure and a sloping stroke resembling the inclination of frontal surfaces, and cirrus by feathery strokes.
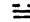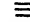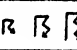
CLOUDS	WEATHER	
CIRRUS	∞ HAZE	❜ DRIZZLE
	= MIST	• RAIN
CIRRO-STRATUS	≡ LOW FOG	✳ SNOW
	≡ FOG	✵ SLEET
ᚖ ALTO-CUMULUS	ᛡ ᛡ ᛡ SHOWER RAIN, SNOW, SLEET	
ALTO-STRATUS	R ᚱ ᚱ THUNDERSTORM LIGHT, MODERATE, SEVERE	
ᚢ STRATO-CUMULUS OR STRATUS	**CLOUDINESS**	
--- LOW RAGGED CLOUDS	○ ◔ ◑ ◑ ◕ ● ● ● ●	
◠ CUMULUS HUMILIS	THE CIRCLES ARE FILLED IN PROPORTION TO THE AMOUNT OF CLOUDS	
△ CUMULUS CONGESTUS		
⧊ CUMULO-NIMBUS	⊗ SKY NOT DISCERNIBLE	
WIND DIRECTION AND FORCE		
NW FORCE 5	NE FORCE 7	SE FORCE 3	SW FORCE 4

Fig. 220.—International symbols for use on weather charts.

The principal weather symbols are composed of horizontal strokes for fog, commas for drizzle, dots for rain, stars for snow, etc. The intensity and the continuous character of precipitation are indicated as follows: Two equal symbols side by side indicate *"continuous;"* two equal symbols, one above the other, indicate *"increased intensity;"* two unequal symbols, one above the other, indicate *"coexistence"* of the weather phenomena that the symbols represent. Thus, for example, one rain symbol alone means light and intermittent rain; two rain symbols side by side mean light continuous rain; two rain symbols, one above the other, mean intermittent rain of medium intensity, and three rain symbols arranged in a triangle mean continuous rain of medium intensity; three rain symbols above one another indicate heavy intermittent rain; and four symbols arranged as ∴ indicate heavy and continuous rain. The same principle applies to the symbols for drizzle, snow, and sleet. If

the precipitation is of a showery character (instability), a triangle with the apex downward is added to the precipitation symbol.

The wind direction is indicated by an arrow "flying with the wind" and ending on the station circle (see Fig. 220). The wind force is indicated by "feathers" so that each whole feather represents two points of the Beaufort scale of wind force, and each half "feather" represents one point.

Symbols are also used to indicate the characteristic of the barograph trace (see Fig. 221).
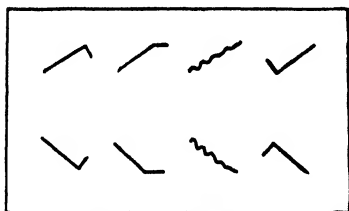
Fig. 221.—Each symbol represents the principal trend of the barograph trace during the last 3 hr. No symbol is used for steady rise or steady fall.
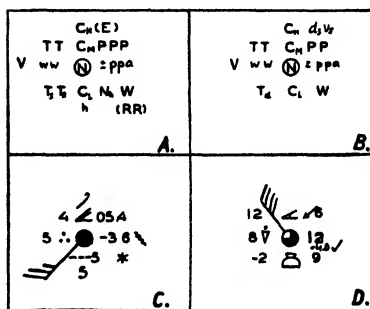
Fig. 222.—International plotting model. *A*, for land stations; *B*, for ships; *C*, example of plotted message from land station; *D*, example of plotted message from ship.

In order to facilitate the interpretation of the charts, a plotting model has been recommended by l' O.M.I. This is shown in Fig. 222*A* for land stations and Fig. 222*B* for ships. Figs. 222*C* and *D* show examples of complete reports plotted around a land station and a ship station, respectively.
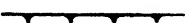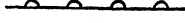
In addition to the symbols mentioned above, the symbols for the results of the analysis have been recommended by l' O.M.I. for international use as shown in Table 60.

In addition to the symbols shown in Table 60, the following symbols will be used to indicate the results of analysis and forecasting:

Double arrows   Computed or estimated displacements of pressure systems, fronts, etc.

Single arrows   Estimated direction of displacements.

I   Increasing pressure in a system of coordinates that moves with the pressure system (*i.e., filling*).

D   Decreasing pressure in a system of coordinates that moves with the pressure system (*i.e., deepening*).

—*FG*—   Frontogenesis

—*FL*—   Frontolysis

CG	Formation or increasing of cyclonic circulation (*i.e.,* *cyclogenesis*).
CL	Decreasing cyclonic circulation (*i.e.,* *cyclolysis*).
AG	Formation or increasing of anticyclonic circulation (*i.e.,* *anticyclogenesis*).
AL	Decreasing anticyclonic circulation.

TABLE 60.—INTERNATIONAL SYMBOLS FOR RESULTS OF ANALYSIS

Phenomenon	On working charts	On printed charts	Direction of motion of fronts
Cold front at the ground....	Continuous blue line		↓
Cold front above the ground.	Broken blue line		↓
Warm front at the ground...	Continuous red line		↑
Warm front above the ground	Broken red line		↑
Occluded front at the ground.	Continuous purple line		↑
Occluded front above the ground.................	Broken purple line		↑
Quasi-stationary front.......	Red-and-blue line		No motion
Areas of fog...............	Continuous yellow area	Distributed fog symbols	—
Areas of tropical air........	Continuous red area	Dotted area	—
Areas of continuous precipitation.	Continuous green area	Hatched area	—

177. Drawing of Isobars.—Throughout the history of weather forecasting, it has been recognized that the distribution of atmospheric pressure is profoundly related to the weather phenomena and the changes in the weather situation. The early methods of weather forecasting were almost entirely based on studies of isobaric pictures (isobar geometry). The improvements in the forecasting technique inaugurated by the

Norwegian meteorologists (frontal analysis, air-mass analysis), Rossby and collaborators (isentropic analysis), and others have not rendered superfluous the analysis of the pressure field. In fact, in order to benefit fully from the advanced methods of analysis, it is necessary to carry out a meticulous analysis of the fields of pressure and pressure changes. That this is so is evident from the discussion in Chaps. IX and X of the forecasting of the movement and development of fronts, cyclones, etc.

Atmospheric pressure is the element that can be observed with greatest accuracy; and as it represents the weight of the air column above the barometer, it is entirely representative. However, the pressure observations may be in error; and as the number of pressure observations often are insufficient, the problem will be for the analyst to eliminate the errors and to connect the observations from scattered stations into a reliable picture. The purpose of the isobaric analysis is, therefore, to draw the *representative* isobars, or the isobars that would result if the barometric observations were perfect, if there were no local errors in reduction to standard level (*e.g.*, mean sea level) and if the observations were strictly synchronous.

The errors that occur in the coded weather reports are: (1) personal or accidental errors of observations, (2) errors of reduction to sea level, (3) errors caused by the observation being made too early or too late relative to the standard hour of observation, (4) errors of coding, transmission, decoding, or plotting.

1. *Personal errors* or errors of accident are difficult to detect when the errors are small. Most frequently such errors amount to 1, 5, or 10 mb. and are due to erroneous reading of the scale. If there is reason to suspect that a pressure report is in error, one should compare the pressure change from the preceding to the present map at the station in question with the simultaneous variations at neighboring stations. Moreover, it should be ascertained that the change is plausible as compared with the barometric tendency. Large errors can always be eliminated in this way. Remaining will be small accidental errors. The irregularities in the isobars that are caused by such errors should show no systematic arrangement. Since *simple isobars are much more probable than complicated isobars*, one should always smooth out irregularities that do not show any systematic arrangement.

2. *Errors of reduction* to sea level affect only stations whose altitude is considerable. The errors increase with the departure of the air temperature from the mean value used for reduction purposes. These errors will usually cause systematic irregularities in the isobars. Reliable pressure reports usually cannot be expected from stations the altitude of which is in excess of 500 m. Errors due to reduction can often be

eliminated to a certain extent by drawing the isobars by means of the reports from the low land stations, the stations of high altitudes being neglected. However, if there is an extensive plateau, this method is not applicable. It is then preferable to reduce the readings not to sea level, but to some convenient level approximately at the mean elevation of the plateau.

3. *Time Errors.*—If the observations are not made exactly at the standard hour of observations, there will be an error in the reported pressure referred to the standard hour of observation. Let b denote the barometric tendency and Δt the error in time. As b is reported as barometric variation in 3 hr. (180 min.), the error in the pressure observation will be $(b/180) \Delta t$, when Δt is expressed in minutes. If, for example, the barometric tendency is ± 5 mb. and the observer reads the barometer 20 min. too early or too late, there will be an error of ± 0.6 mb. in the pressure observation as referred to the hour of observation. The error in reported pressure decreases with the barometric tendency and is negligible if the tendency is less than 1 or 2 mb. When the tendency is large, even small time errors will be noticeable in the reported pressures. Such errors should not show any systematic arrangement on the map and may be eliminated by smoothing of the isobars. There is therefore more reason for smoothing the isobars when the barometric tendencies are large than when they are small.

4. *Errors due to coding, transmission, decoding, and plotting* are entirely accidental and may be eliminated as described in Par. 1.

Although errors in the reported pressure are comparatively rare at land stations, they are comparatively frequent in reports from ships. This is due partly to the circumstance that many ships have barometers of poor quality and partly to the difficulties in obtaining accurate readings when the sea is rough. Furthermore, experience shows that many apparent errors in the pressure distribution at sea are due to errors in the reported position of the ship. The errors in position are usually 5 or 10° latitude or longitude. Such errors can easily be checked by moving the ship on the map to a position which differs 5 or 10° in longitude or latitude from the reported position and in which the reported pressure, temperature, wind and weather agree with neighboring observations.

In trying to neutralize the errors mentioned above, it is useful to bear in mind the following principles:

a. *In representing the large-scale movement of the air, simple isobars are much more probable than complicated isobars.* It is true that the isobars of the turbulent motion may possibly show many ripples and irregularities; but in all air currents which are of such extent and duration that the deviating force regulates the motion, there is a decided tendency to create simple isobars without much local variation in the pressure

gradient. Whenever the geostrophic control is predominant, strong air currents will have smooth isobars. However, in indifferent pressure fields where the wind velocity is slight, the isobars may be irregular. Normally, isobars are drawn for every fifth millibar (*e.g.*, 995, 100, 1005, etc.); but when the pressure distribution is indifferent, isobars should be drawn for every millibar. If the isobars thus drawn show a systematic arrangement of the irregularities like a center of low, a center of high, a trough, or a wedge, one should regard the irregularity as real. In warm summer situations with indifferent pressure distributions, showers, and thunderstorms occur preferably in indistinct troughs or areas of low pressure, particularly when an isallobaric minimum coincides with these systems. Such irregularities in the pressure field occur frequently where a front has dissolved or is dissolving.

   b. The isobars should have such direction and mutual distance that they agree approximately with the geostrophic-wind scale. This applies in high and middle latitudes when the wind force is 4 Beaufort or more. The use of the geostrophic-wind scale for spacing of the isobars was described in Par. 95. At sea, where pressure observations are scanty and of poor quality and the frictional influence on the wind is a minimum, the geostrophic-wind scale will usually give excellent results. Over land, where the frictional influence complicates the relation between pressure gradient and wind, the pressure observations are usually both numerous and of good quality, so that the isobars can be drawn without rigorous use of the wind relation.

   c. The isobars in the vicinity of fronts should be drawn so as to bring out the frontal discontinuity in the horizontal pressure gradient. Correct isobars should always be V-shaped at the front with the point of the V pointing toward high pressure. The reason for this was explained in Par. 119, and the isobars in the vicinity of fronts should be as shown in Fig. 132. If there were no kink in the isobars at fronts, there would be no shearing motion; but the existence of shearing motion is one of the fundamental properties of fronts. Moreover, it follows from Eq. *158*(1) that, if there were no kinks in the isobar, the velocity of the front would be either indeterminate or infinite, which is inconsistent. Although it is wrong not to draw kinks in the isobars at fronts, it is equally wrong to exaggerate the kinks. The reason meticulous accuracy in the drawing of isobars in the vicinity of fronts is required is that it is possible to compute the velocity of the fronts when the exact distribution of pressure is known.

   d. The isobars should be drawn first in those areas where the analysis is simplest.

   e. The isobars should be drawn so as to agree logically with the previous map. Over oceans, where observations are scanty, it is important to

apply this principle.   Thus, if one map shows a young deepening cyclone, the next map should be drawn on the assumption that the cyclone has moved a reasonable distance and deepened; the deepening would then create new isobars around the center, and the isobars would become more crowded.   The skilled analyst will, in such cases, not hesitate to take this development into account in drawing the isobars, even when direct observations are missing from the area in question.

178. Examples of Drawing of Isobars.—The application of the principles outlined in Chaps. IV, VI, and VII and summarized in Par. 177 are illustrated in the following examples:

1. *Smoothing.*—Figure 223a shows isobars that have been drawn strictly according to reported pressures.   Let us imagine that the isobars
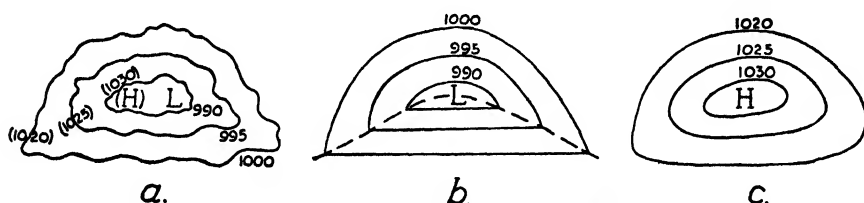
FIG. 223.—Smoothing of isobars.

in Fig. 223a run either around a center of low pressure (*i.e.*, isobars 990, 995, and 1000) or around a center of high pressure (*i.e.*, isobars 1020, 1025, and 1030).   The small wavelike irregularities do not show any systematic arrangement; they should therefore be eliminated by smoothing.   Two troughlike or wedgelike irregularities then remain, one to the right of the center and the other in the lower left part of the figure. As these irregularities are systematically arranged and depend on more than one station, they should be regarded as real.   Figure 223b shows the smoothed isobars around the cyclonic center.   It will be seen at once that these isobars have a marked resemblance to the isobars around a young wave cyclone.   Whether or not there is a front in the pressure trough must be decided by applying the frontal characteristics described in Chap. VI.   If it is evident that there is no front, the isobars should be drawn without kinks.

We imagine next that the isobars in Fig. 223a belong to a center of high pressure.   The smoothed isobars would then be as shown in Fig. 223c.   No kinks should be drawn there, for the kinks would then point from high to low pressure, which is impossible.

2. *Isobars and Wind.*—Figure 224 shows some simple examples of how to utilize the wind reports in drawing the isobars.   The isobars are placed (1) so that the angle between the wind direction and the isobar is correct, (2) so that the pressure gradient agrees with the wind

force (see Par. 95), and (3) so that the distance from the stations to the nearest isobars agrees with reported pressure and the pressure gradient. Moreover, when the wind is strong it may be assumed that it is representative for a comparatively large area around the station in question.   One

may therefore draw several isobars on the basis of one observation only.   In this way, a reliable pressure distribution may be obtained at sea where observations are scanty.

3. *Isobars and Fronts.*—Figure 225 shows two ship observations plotted on a map.   The observations of clouds, weather, and temperature indicate that there is a warm front between the two ships. The problem is to draw the correct isobars and to find the position of the front.   As the

FIG. 224.—The isobars should be drawn so as to fit with the pressure and the direction and force of the winds.

isobars in a warm sector usually are almost straight lines, the best we can do when we have only one observation at our disposal is to use the wind scale (Fig. 102), space the isobars in the warm air as indicated by the scale, and draw the isobars as straight lines.   The isobars in the cold air in advance of the low-pressure center are usually curved, but the curvature normally decreases toward the warm front.   With only one station at our disposal, the best we can do is to draw the isobars in principal agreement with a model of a normal cyclone.   The 990 isobar must go through the easternmost ship. Using the wind scale, we can at least draw three isobars in the vicinity of the easternmost ship.   Next, prolong the isobars in the warm air as straight lines and those in the cold air as slightly curved lines.   The intersection (kinks) will then mark the position of the

FIG. 225.—Example showing how to draw isobars in the vicinity of a front and to find the position of the front.

front.   If the front in Fig. 225 were placed farther to the east, there would have to be an abnormal curvature of the isobars in the warm sector.   If, on the other hand, the front were placed farther to the west, the curvature of the isobars in the cold air would have to increase toward the front, which is not the normal occurrence.   The student is invited to vary the position of the front in Fig. 225 and to draw the isobars that would then result.   It will then be found that very

little latitude is allowed in placing the front if the isobars are correctly drawn. It is important to note that the front should be drawn as a smooth curve. The reason for this is that waves shorter than about 500 km. would be stable waves whose amplitudes are infinitely small (see Par. 129). Fronts with small waves of appreciable amplitudes are therefore not possible.

Figure 226 shows further examples of how to locate fronts by drawing the isobars consistently. In all five cases, the wind direction and force are the same; and, in addition, the pressures are the same at the two southernmost stations. The only difference among the five cases is that the pressure at the northernmost station increases from one case to the next. The figure shows how the isobars should be drawn in order to give a consistent picture. It will be noticed that in case *a* the front must be placed close to the northernmost station. As the pressure at this station increases, the front must be moved farther to the south, and its orientation must be changed so as to run almost east-west in case *d*. In each of the five cases, it will be found that the position of the front can be determined with considerable accuracy by drawing the isobars consistently.

As the front always must be situated in the pressure trough, a rough rule to follow is that it must also be situated nearest the station which has the lowest pressure. The above examples show that this rule holds to a certain extent; but they also show that the position of the front is likewise determined by the direction and the force of the wind.

Fig. 226.—Examples showing how to draw isobars in the vicinity of fronts, and how to find the position of the front.

In drawing isobars over a large area, it is advisable first to draw isobars in those regions where the analysis is simple. As there is no particular difficulty in drawing isobars over land areas where observations

are numerous, one should first draw isobars over land and then prolong them over the adjacent oceans. At sea, it is easiest to draw isobars where observations are most numerous. Other conditions being equal, it is easier to draw isobars in areas where the winds are strong than in those areas where they are weak. For this reason, the last isobars to be drawn over ocean areas should be those which are close to centers of
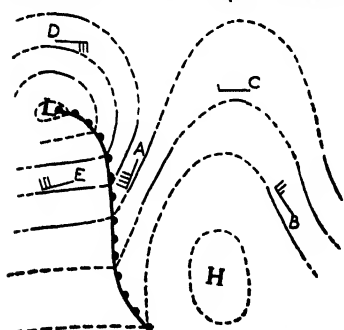
FIG. 227.—Drawing of isobars over a large area. Full lines indicate the isobars which should be drawn first. Broken lines indicate the isobars which result from connecting up the different areas.

lows and highs and those in the vicinity of cols. The application of these rules is illustrated in Fig. 227. Commencing in the areas where the wind is strongest, we obtain isobars as shown by the full lines. In the vicinity of station C, the wind force is so slight that the relation between wind and pressure gradient is unreliable. The most reliable spacing of the isobars can be made in the vicinity of the stations A, B, E, and D. Connecting the isobars from the different areas, we obtain the stippled lines. Around the pressure center L, a sufficient number of isobars should be drawn so as to obtain an even variation of the pressure gradient in approaching the center.

179. Drawing of Isallobars.—The term "barometric tendency" or "tendency" denotes the change in atmospheric pressure that has taken place at a station during the 3 hr. preceding the observation. Curves on the weather map through points of equal tendency are called *isallobars*. The isallobars together with the isobars furnish the bases for computation or estimation of the movement and development of pressure systems. It is therefore important to draw the isallobars correctly.

The tendencies are usually read off an aneroid barograph; this instrument is less accurate than the mercurial barometer which is used for observing atmospheric pressure. The barometric tendencies are therefore less accurate than are the reported pressures. It is thus necessary to smooth the isallobars in order to eliminate errors.

The barometric tendency indicates the *mean* slope of the barograph trace averaged over the 3 hr. preceding the observation. Let $p = p(t)$ represent the pressure as a function of time at a fixed station. Developing in a Taylor series, we obtain

$$p = p_0 + \frac{\partial p}{\partial t} t + \frac{1}{2} \frac{\partial^2 p}{\partial t^2} t^2 + \cdots$$

where p_0 stands for the pressure at the hour of observation. Thus, if the pressure at a future, or past, instant were to be computed, it would be

necessary to know the *instantaneous* slope of the barogram.   However, since the barograph trace contains many irregularities of short duration, the instantaneous slope would not be representative.   For this reason, it has been found practical to report the slope of the barograph trace as the pressure variation per 3 hr.

This method of reporting pressure changes is adequate when the curvature of the barograph trace is small.   However, when the curvature is large or when there is a significant kink in the trace, the barometric tendency does not indicate the representative slope of the barogram. Such conditions occur in the rear of marked fronts and in the rear of intense troughs and cyclones.   In drawing isallobars in such regions,
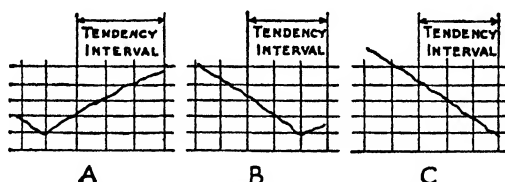
Fig. 228.—Representative and nonrepresentative tendencies in the vicinity of fronts.

the analyst should try to obtain isallobars that indicate the representative slope of the barograph trace.

Suppose that three stations *A*, *B*, and *C* are situated on a straight line and that a front moves in the direction from *A* to *B*.   The front passed the station *A* 4 hr. prior to the observation, it passed the station *B*, say 1 hr. before the observation was made, and it has not passed the station *C*.   The barograph trace at the three stations would then be in principle as shown in Fig. 228.   The barometric tendency reported by the stations *A* and *C* would thus be representative, whereas the tendency reported by the station *B* would be nonrepresentative.   The reported tendency shows a fall, which is the average change over 3 hr., whereas the actual state is a steady rise.   From this, it follows that (1) the barometric tendencies in advance of fronts are representative; (2) the barometric tendencies at stations within the zone which the front has passed during the last 3 hr. are nonrepresentative, and the more so the closer the station is to the front; (3) the barometric tendency in the rear of the front outside the zone passed within the 3 hr. preceding the observation is representative.

The actual error in case 2 is proportional to the sharpness of the frontal pressure trough and to the speed of the front.   These errors can be eliminated by drawing the isallobars as shown in Fig. 229.   The tendencies in advance of the front are representative, and the isallobars are drawn to conform with the observations.   The same is true, also, of the tendencies to the left of the line *AB*; but, in the zone between

this line and the front, the tendencies are nonrepresentative, the error increasing toward the front.   To neutralize these errors, we draw the isallobars in the area to the left of the line *A B* and prolong these isallobars toward the front.   It will then be seen that a discontinuity in the baro-
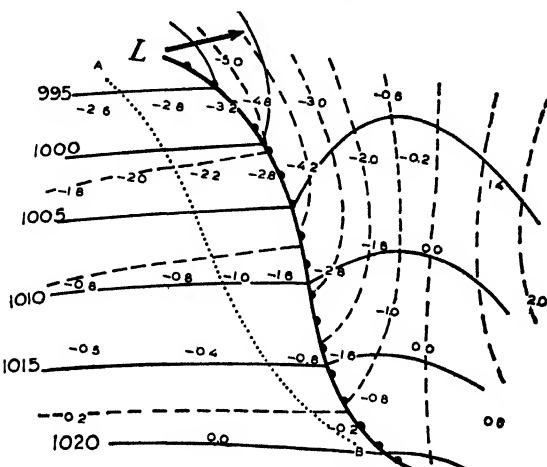
Fig. 229.—Full lines are isobars, broken lines isallobars corrected for the effect of the passage of the front.   Line *AB* indicates the position of the warm front 3 hr. prior to the observation.

metric tendency is revealed as a result of the analysis.   It was shown in Par. 119 that this discontinuity is one of the general frontal characteristics.   The method of obtaining the representative tendencies shown in Fig. 229 is applicable also to cold fronts; but conditions are then more complicated, for the isallobars in the rear of the cold front are more complicated than they are in the rear of a warm front.
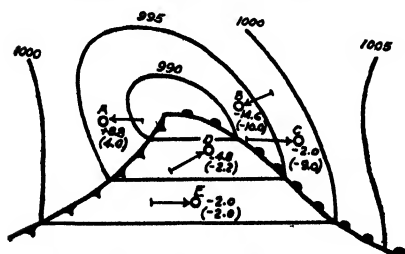
Fig. 230.—Showing how to correct barometric tendencies observed in ships. Numerals without parentheses indicate reported tendencies.   Numerals in parentheses indicate corrected tendencies.

When a cyclonic center passes a station within the 3 hr. preceding the observation, the tendencies will be nonrepresentative.   This effect, which is appreciable only in the immediate rear of the center, can be eliminated by drawing the isallobars outside this area and extrapolating them through the area affected by the passage.

The barometric tendencies reported from ships are nonrepresentative unless the ship moves along the isobars.   When the isobars have been drawn, the effect of the movement of the ship may be corrected for as shown in Fig. 230.   Use the scale *FG* in Fig. 102 as explained in Par.

95, and mark the distance made good by the ship in the 3 hr. preceding the observation.   These distances are shown by arrows in Fig. 230. The pressure differences between the ends of these arrows, interpolated from the isobars, represent the correction that should be applied to the reported tendencies.   When these corrections have been applied, isallobars may be drawn over ocean areas.

180. The Technique of Analysis.—It should be borne in mind that the analysis of fronts and air masses is a three-dimensional problem which involves the knowledge of the conditions in the free atmosphere as well as at the earth's surface.   When a sufficient number of aerological ascents is available from a sufficiently large area, the analysis is greatly facilitated. In most parts of the world, it is possible to draw four surface-weather maps per day, whereas aerological ascents are available only once daily from a few stations within restricted areas.   It will therefore be necessary in general to base the analysis on the data contained in the surface-weather map, using aerological observations as auxiliary aids.   The analysis of the stability and instability conditions of the air masses was discussed in detail in Chaps. II and III.   When a sufficient number of ascents is available, maps should be prepared to show the state of the free atmosphere.   The technique of preparing and analyzing such maps was described in Chap. VIII.   On account of the paucity of aerological observations, upper-air maps can usually be analyzed satisfactorily only in connection with analyzed surface-weather maps.   We shall, therefore, describe here the procedure that should be followed in the analysis of surface weather maps, independently of the analysis of upper-air data.

When aerological ascents are not available or when the number of such ascents is insufficient for obtaining a complete picture of the state of the free atmosphere, the analyst should try to obtain a qualitative picture of the state of the free atmosphere by means of the observations made at the earth's surface.   *Bergeron* calls this method *indirect aerological analysis.*

The method of indirect aerological analysis consists in utilizing those of the surface observations which depend on the state of the free atmosphere.   In the first place, the observations of clouds and hydrometeors are important because they are entirely representative and depend on the state of the free atmosphere.   The forms of clouds and hydrometeors reported by the observers should be referred by the analyst to the genetical classification described in Pars. 21, 23, and 122.   When this is done, the clouds and hydrometeors will indicate the presence of stable and unstable air masses, inversions and fronts.

1. **The first step** in the analysis is, therefore, to examine the forms of clouds and hydrometeors and to indicate the fronts and the stable

and unstable air masses.   This preliminary survey can, of course, give only a rough picture of the distribution of air masses and fronts, which need extension as well as correction as the analysis proceeds.   It is therefore advisable to indicate the fronts in soft pencil so as to facilitate necessary corrections.

It is a basic principle in all analysis that one map must follow logically from the preceding maps.   That is, the air masses present on the current map must be identified with the masses present on the preceding map, and the displacement of these masses from one map to the next must agree with the prevailing winds.   In a similar manner, either the fronts on the current map must be identified with the fronts on the preceding maps, or they must result from a frontogenetical process as described in Chap. V (see also Par. 165).   Moreover, the displacement of the fronts from one map to the next must be in agreement with the prevailing winds.   This principle, which is called *the principle of historical sequence*, is of basic importance, and most errors in the analysis are due to neglect of this principle.

2. The second step in the analysis will usually consist in identification of the fronts and air masses, the previous chart (or charts) being used and the principle of historical sequence applied.   Frequently, when the fronts are indistinct or when they are not accompanied by significant cloud systems or areas of precipitation, the procedure may be reversed: Use the previous map, and extrapolate the positions of the fronts on the current map, letting the fronts move with the speed of the wind; examine next the clouds and hydrometeors in the vicinity of the extrapolated positions in order to find the actual position of the fronts.   It may then happen that a front, or part of a front, is so indistinct that it cannot be discovered in this way.   In such cases, the extrapolated position should be marked on the map and subjected to detailed study when isobars and isallobars are drawn.   It may also happen that the preliminary survey of the clouds and hydrometeors shows indications of fronts that were not present on the previous map.   Such fronts may have formed through frontogenesis, or they may have been overlooked on the previous map.   The previous map should then be reanalyzed in order to decide whether or not a front has been overlooked.   If not, it will be a problem to explain the frontogenesis.   This problem must be left to the later stages of the analysis.

3. The third step in the analysis will usually be to draw the isobars. It is better not to draw each individually throughout the map, but to draw first the isobars within one air mass and then the isobars within the next air mass, and so on.   In other words, they should be drawn "from front to front," and while doing this the analyst should study in detail the weather conditions within each air mass.   When the isobars

within one air mass have been completed, the analyst should have obtained a mental picture of the properties of that mass.

In drawing isobars in the vicinity of fronts, the analyst should ascertain that the general frontal characteristics (see Par. 124) are satisfied at the fronts. Furthermore, the exact position of the front should be found as explained in Par. 178. In difficult cases, preliminary isobars should be drawn in light pencil; when this has been done, the final isobars should be drawn, the principles outlined in Pars. 177 and 178 being used.

4. THE FOURTH STEP in the analysis will usually consist of a detailed examination of the air masses. This study is important not only for the understanding of the weather phenomena that occur within the air masses, but also for the understanding of the structure of the frontal surfaces. This detailed study of the air masses should aim at clarifying the following points.

a. The Type of Air Mass.—The present and the preceding charts should be used in order to study the life history of the air masses. On the basis of this study, the air masses should be referred to the geographical (source) classification and the influence classification described in Par. 73, the principles outlined in Chaps. II and III being applied.

b. Heating and Cooling.—After completion of the study of the clouds and hydrometeors, it should be decided whether the air is heated or cooled from below, the deciding factors being whether the air moves toward warmer or colder regions, or whether the diurnal heating or cooling is appreciable. The principles of this analysis were outlined in Chaps. I to III.

c. Subsidence.—Whenever an air mass is heated from below, it will develop toward instability unless subsidence in the free atmosphere counteracts the instabilizing influence of the heating from below. Subsidence in the lower atmosphere is usually connected with divergence in the horizontal motion (see Chaps. IV and VII). Conditions are particularly favorable for subsidence under cold-front surfaces, in anticyclones, in wedges of high pressure, and in regions of isallobaric maxima. Such areas should be examined carefully in order to detect evidence of subsiding motion. The effect of subsidence on air that is heated from below is to produce an inversion in mid-air (see Par. 54). The convective clouds will then flatten out in their upper portion. All convective clouds, except cumulus congestus and cumulo-nimbus, are characteristic of instability in the lower atmosphere with temperature inversion or subsidence in the air above the unstable layer. Some frequent types of development of air masses that are heated from below were described in Par. 75.

5. The fifth step in the analysis will usually be to examine in all possible detail the conditions along the fronts. This examination should aim at ascertaining the exact location of the front, the type of front, the extent of the cloud systems and the areas of precipitation, and whether or not the front is exposed to frontogenesis.

In studying the exact position of the front, the general and special front characteristics (see Par. 124) should be used, and the results thus obtained should be compared with the previous maps in order to ascertain that there is logical agreement between them. The extent and the nature of the cloud system should be noted and referred to one of the types of front described in Par. 124. This analysis will furnish information as to the distribution of vertical velocity in the air masses close to the front. On the basis of this study and by comparing the present map with the previous maps, the fronts should be referred to the classification described in Par. 121. When this analysis is completed, the fronts and the areas of precipitation, fog, tropical air, etc., should be indicated with the symbols shown in Par. 176.

6. The sixth step.—Although the barometric tendencies should be used in order to locate fronts (see Pars. 119 and 179), it is convenient to leave the actual drawing of the isallobars till the fronts and isobars have been drawn in a final form. The isallobars should then be drawn as broken lines, following the principles outlined in Par. 179.

7. The seventh step in the analysis is to examine the regions where the wind distribution is favorable for frontogenesis. The principles of analysis of frontogenesis and frontolysis were outlined in Chap. V, and further remarks will be found in Par. 165. In the regions where the kinematic conditions are favorable for frontogenesis, the representative large-scale temperature distribution should be studied in order to ascertain that the orientation of the isotherms is favorable and the temperature gradient is sufficient for frontogenesis to develop.

8. The eighth step.—During the entire analysis, frequent comparisons should be made between the present and the preceding charts in order to ascertain that the principle of historical sequence is satisfied. If any discrepancy is found between the present and the preceding map, it is clear that at least one of them must be in error. The two maps should then be examined in detail, the most probable solution should be chosen, and the maps should be adjusted accordingly.

If aerological ascents are available, the analysis of the surface map should be compared with the analysis of the upper-air data (see Chaps. II and VIII) and both analyses should be adjusted so as to render a consistent picture. This comparison between the surface map and the upper-air data should be made throughout the analysis of the surface map.

The weather maps prepared as described above furnish the basis for weather forecasts. But before the forecasts can be issued, it will be necessary to analyze the pressure field in greater detail in order to determine the velocity of propagation and the rate of change of intensity of such phenomena as cyclones, anticyclones, troughs, wedges, cols, and fronts. These problems were discussed in Chaps. IX and X.

181. Examples Illustrating the Technique of Analysis.—Figure 231 shows a highly simplified weather map. In this particular case, the difficulty in the way of obtaining a satisfactory analysis lies in the fact that the reporting stations are widely scattered. However, by following the program outlined in the foregoing paragraph and doing the analysis stepwise in the logical sequence, it is quite easy to obtain a correct analysis.

Step 1.—By studying the forms of clouds, it will be seen that the southeastern and eastern portions of the map are occupied by a stable air mass, whereas the northwestern portion is occupied by an unstable mass. The prevailing winds seem also to indicate the presence of two air masses of widely different life history. The hydrometeors confirm this: there are instability showers north of the British Isles and fog or drizzle over the North Sea. In addition, there is evidence of a frontal rain area from the Shetland Isles, across England down to the west of the English Channel. The two air masses are therefore separated by a distinct front. Although the position of this front may be sketched on the maps, its character and exact position will have to be determined in greater detail as the analysis proceeds.

Step 2.—The time has now come to compare the present map with the preceding one (which is not reproduced here). The suggested front should be identified with the front on the preceding map, and it should be ascertained that its displacement from the preceding to the present map is in agreement with the principle of historical sequence.

Step 3.—Draw preliminary isobars, following the rules described in Par. 177. First draw the isobars in the air mass that has the strongest winds. Apply the rules for locating the position of the fronts (Par. 178). In addition, the barometric tendencies and the characteristics of the barograph traces should be used in order to find out approximately when the front passed the stations in the rear of the front. If there are no kinks in the barograph trace, the front must have passed more than 3 hr. before the hour of observation; if there are frontal kinks with large positive tendencies, the front will have passed early in the tendency interval; and if there are frontal kinks with negative tendencies, the front is likely to have passed in the late part of the tendency interval. This, and the drawing of the isobars, will do much to assist in finding the exact position of the front.
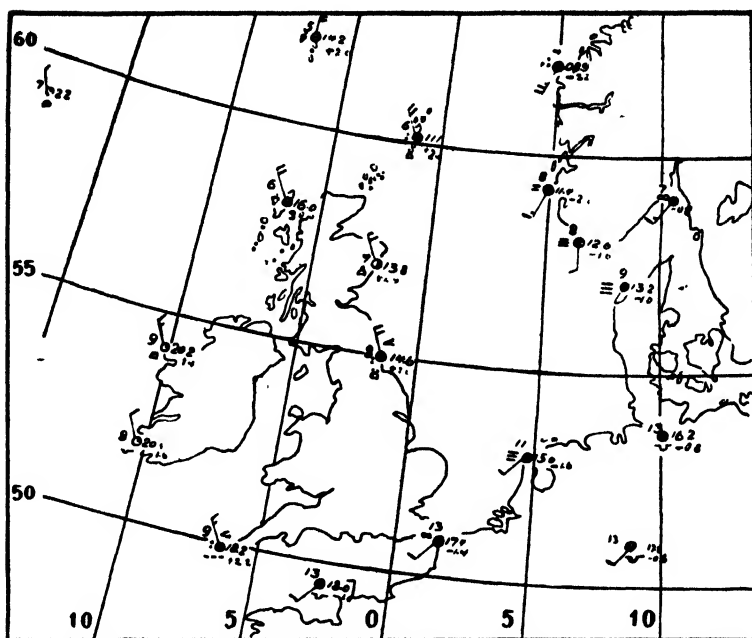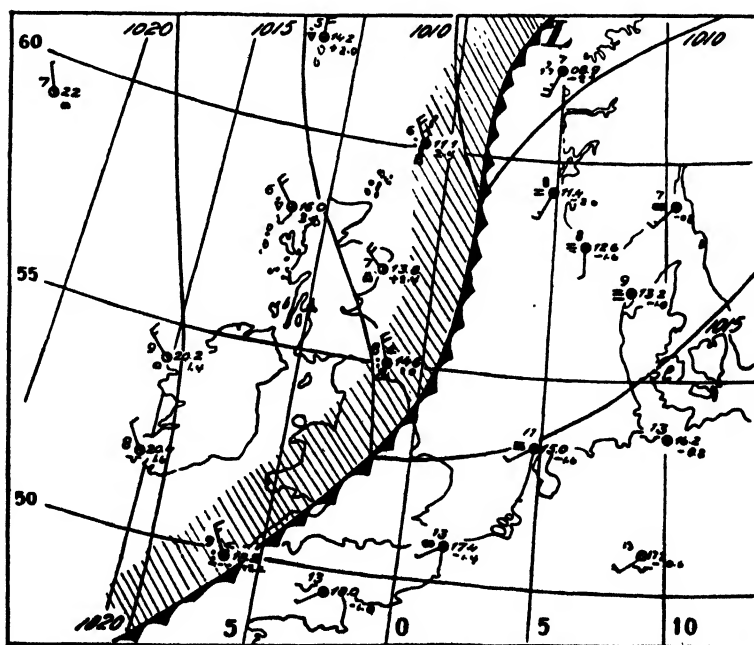
FIG. 231.—*A*, simplified weather chart for exercise; *B*, correct analysis.

Step 4.—When the isobars have been drawn, a clearer picture of the life history of the air masses will be obtained. Comparison with the previous map (or maps) should now be made in order (1) to identify the air masses and (2) to ascertain whether the air masses are developing toward increased or decreased stability. In the present case, which is a simple one, it is evident that the air in the rear of the front is of polar origin, whereas the other mass most probably is of tropical origin.

The warm mass streams slowly northward and will be cooled from below. Furthermore, since, the wind speed is low, there will not be much vertical mixing, and the mass is likely to preserve the temperature inversion at the ground that is suggested by the numerous fog observations.

The unstable polar air streams southward and will therefore be heated from below; this will tend to increase the lapse rate, and convective clouds and showers may result. However, the absence of showers and towering cumulus in the western portion of the map seems to suggest that the heating from below is counteracted by subsidence, with the result that not much change in lapse rate will result. The fact that the stations on the west coast of Ireland report strato-cumulus indicates that subsidence is quite active in the western portion of the map.

Step 5.—The properties of the front should now be examined. From the life history of the air masses, the distribution of wind, and temperature, it is evident that the front is a cold front. The warm mass is exceedingly stable and the numerous observations of fog together with light winds are unmistakable evidence of a ground inversion in the warm air. The surface temperatures in the warm air are therefore nonrepresentative. Since the temperature difference at the front is 2 to 4°C. at the ground, it follows that the temperature difference at the front must be considerably greater above the ground inversion. As far as temperature is concerned, the front is a pronounced one. This conclusion may be verified by means of aerological ascents in the British Isles.

The distribution of clouds and hydrometeors along the front seems to suggest that it is a cold front of type *A* (see Par. 122).

Step 6.—Draw isallobars in both air masses.

Step 7.—It is now easy to determine whether or not the front is exposed to frontogenesis. The convergence of the winds toward the front seems to suggest that the front is exposed to frontogenesis. On the other hand, the isallobaric gradients (see Par. 165) do not seem to suggest frontogenesis at the front. The reason the converging winds do not cause frontogenesis is evident: since the temperature distribution within each of the air masses is uniform, the winds will not transport isotherms toward the front. It may therefore be concluded that the front has already reached its maximum intensity. From the distribution

of winds and temperature, it is evident that there is no region of fronto-
genesis within each of the air masses.

Step 8.—Apply the test of historical sequence, and, if necessary
revise the analyses.
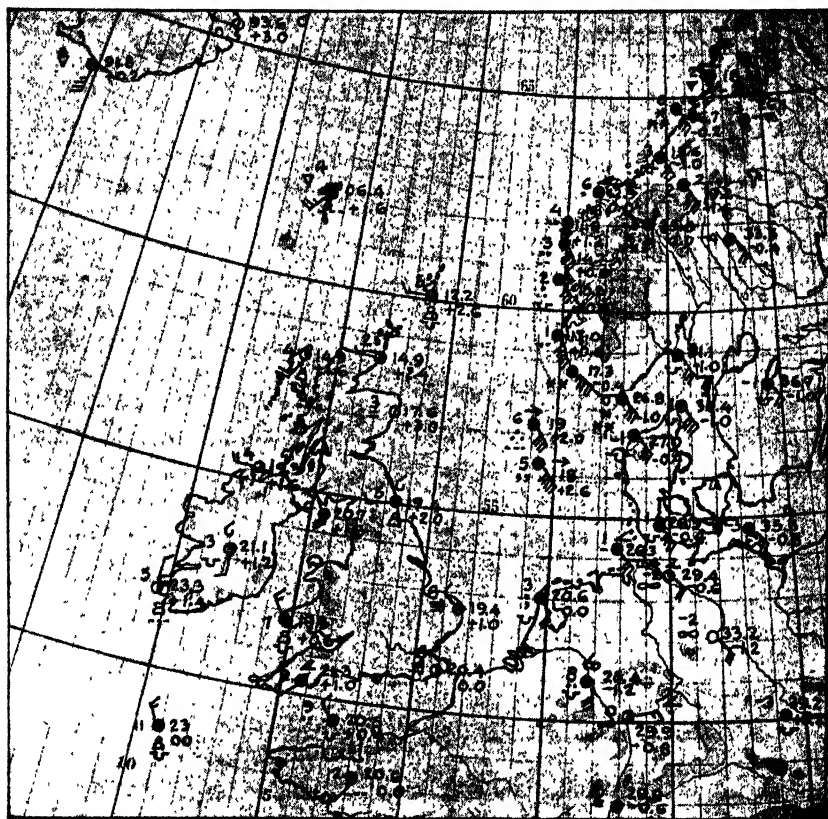
Fig. 232*A*.—Simplified weather map, Jan. 13, 1937, 6 p.m., G.M.T.

Figure 232 shows a highly interesting and instructive example of an
apparently intricate situation which, subjected to a rational analysis,
becomes very simple. This example, which is offered as an exercise for
the student, should be analyzed as described above. In addition, study
of the distribution of the isallobars is recommended, in order to find
whether the wind normal to the front will increase or decrease.

To guide the student in the analysis, it may be stated that the front
over the North Sea must be essentially a warm front; this is suggested
by the area of precipitation and the clouds. However, the warm air
in the rear of the front is definitely not of tropical origin; for its tempera-
tures are too low (*cf.* Fig. 93), and it shows indications of instability.
The front is, therefore, most likely a warm front type occlusion.

182. The Technique of Forecasting.—It should be emphasized at the outset that there is no distinct line between the process of analysis and the process of prognostication.   Almost every step in the analysis consists in considering the physical properties in relation to space and time.
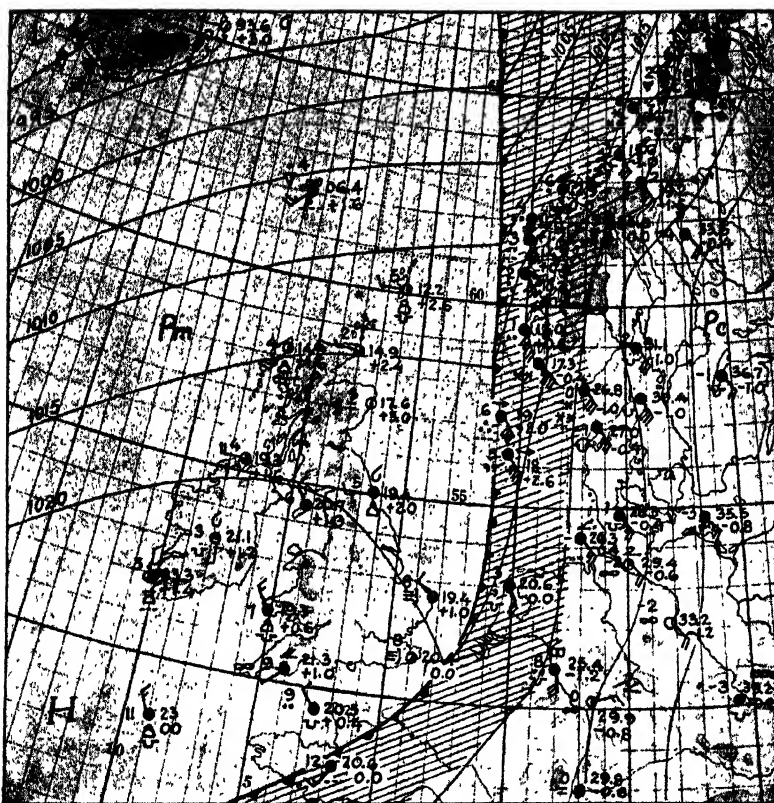
Fig. 232*B*.—Correct analysis of map, Fig. 232*A*.

The analysis, therefore, leads directly to a more or less vague conception of what will happen in the future.

On the other hand, it is convenient to distinguish between the process of analysis and the process of prognostication, the distinction being that the results of the analysis divulge the state of the atmosphere at a given instant, whereas the results of the prognostication essentially concern the future state, including displacements and developments of the entities that the analysis has revealed.

On account of the inadequacy of the observations and the shortcomings of our methods of analysis and prognostication, any forecast of future conditions is admittedly a hypothesis that, at least in parts, is based on assumptions.   However, *the art of analysis and forecasting is*

to assume as little as possible and, as far as possible, to base the forecasts on conclusions drawn from actual observations. To attain this, it is necessary to apply as many mutually independent methods as possible so as to obtain checks on the results derived.

The forecasting of the future weather conditions is not a unique problem; it resolves itself into a number of partial problems that can be solved individually. It will then be found that certain of these partial problems can be attacked only after other problems have been solved. It is therefore important that the partial problems be attacked in the right sequence. Starting from a series of maps analyzed as shown in the previous paragraphs, the forecast may be approached in several steps, each dealing with the solution of one of the partial problems. These steps may be described in brief as follows:

1. The first step.—The displacements of the pressure systems, fronts, etc., should be determined first. Usually it will be possible to determine the displacements during 24 hr., but in uncertain or complicated cases it is advisable to evaluate the displacements for 18 or 12 hr. only. It is always better to obtain an accurate determination of the displacements during a short interval of time than an inaccurate determination during a long interval of time. A determination of the future position is always useful even when the time interval is short. From such a determination, one is in a better position to visualize the possible displacement during the entire forecasting period than when no such determination of displacements is made.

The displacements should be determined numerically by the formulae given in Chap. IX when the analysis is complete and the situation is sufficiently simple. In other cases, the qualitative forecasting rules should be applied. Whenever possible, the displacements should be determined by the three methods described in Chap. IX; *viz.*, the *tendency method*, the *geostrophic-wind method*, and the *path method*. These methods are largely independent of one another. If the application of these methods gives conflicting results, reliance should be placed on the results obtained by the method or methods best adapted to circumstances. Thus, when the isobars and isallobars are well determined and form simple patterns, the tendency method is likely to give more accurate results than the path method and the geostrophic-wind method. Conversely, when the isobars and isallobars are uncertain or complicated, the tendency method will usually be the most inaccurate one.

2. The second step.—After having determined the displacements in a preliminary fashion, the deepening or filling of the various pressure systems should be examined as described in Chap. X. In doing this, it is important to bear in mind that the significant feature to be determined is the *distribution* of deepening and filling, for on it depends the

increase or decrease in the winds.   The deepening (or filling) and its distribution should be determined numerically when the conditions are favorable (*i.e.*, accurate and simple isobars and isallobars); otherwise, the qualitative rules should be used.

3. THE THIRD STEP.—From the examination of the distribution of deepening and filling, evidence of increase or decrease in the intensity of preexisting systems (cyclones, anticyclones, troughs, wedges, fronts, etc.) will be found.   In addition, evidence of the formation of new systems will be found.   The third step in the forecasting procedure is therefore to determine whether or not new systems will form and what influence they will have on the weather situation.   This examination should aim at predicting frontogenesis (see Chap. V and Par. 165), cyclogenesis, or anticyclogenesis (see Chap. X).   It is of particular importance to examine the conditions along fronts where symptoms of wave formation (see Par. 164) are present.

The formation of a new system (*e.g.*, cyclone wave) will usually exert a considerable influence on the neighboring systems; this should be considered.

4. THE FOURTH STEP.—The deepening and filling of existing pressure systems and the formation of new systems may influence the displacements determined as described above.   The next step is therefore to readjust the preliminary determined displacements as explained in Par. 173.   In doing this, it should be ascertained that the displacements of each individual system harmonize with the simultaneous displacement of neighboring pressure systems (see Par. 173).   This examination will lead to a rough estimate of the acceleration of the pressure systems.

5. THE FIFTH STEP.—We should now try to determine the position and the properties of the air mass (or masses) that is going to pass over the forecasting district during the forecasting period.   This is, of course, a direct consequence of the travel of fronts and air masses.   The properties of this air mass (or masses) should be examined in great detail.   A detailed analysis of the clouds, hydrometeors, the ascent curves (adiabatic charts), the moisture patterns aloft (isentropic charts), stream charts, or pressure charts aloft will reveal the physical and kinematic conditions of the air mass in question.

6. THE SIXTH STEP.—An estimate should next be made of the changes in the physical properties of the air mass (or masses) that will occur by the time it arrives within the forecasting district.   The possibilities for heating or cooling, depletion or supply of moisture, subsidence, etc., should be considered.

7. THE SEVENTH STEP.—The modifications caused by local influences should next be considered—*e.g.*, the influences of mountain ranges, valleys, lakes, and land and sea breezes and other coastal effects.

8. THE EIGHTH STEP.—When the foregoing points have been completed, it is well to reexamine the weather charts in order to ascertain whether any phenomenon or alternative has been overlooked. In other words, the analyst should ask himself the question: What can upset the forecast?

9. THE NINTH STEP.—The final point to consider is the wording of the forecast. The forecast should be as clear and unambiguous as possible, and it should express not only the weather conditions but also the degree of certainty of the prediction. For example, it may be quite certain that rain will occur, but somewhat uncertain whether the rain area will arrive in the morning or in the evening. In another case, it may be certain that a front will pass about noon, but not certain whether or not the front will cause precipitation while it passes. The forecasts should contain some indication of the certainty of the prediction, both as far as weather phenomena and the time of occurrence are concerned. Some general principles concerning the timing of the arrival were discussed in Par. 163.

In conclusion, it should be mentioned that much useful knowledge can be obtained from a critical reexamination of the unsuccessful forecasts.

In the following paragraphs, we shall try to apply the above principles to a few weather situations.

183. Example of Ocean Analysis.—In order to demonstrate the application of the principles of analysis and forecasting to ocean areas where observations are scanty, we turn to the weather situation for Feb. 12 to 14, 1937, over the North Atlantic. The maps (Figs. 233 to 237) are highly simplified so as to allow sufficient reduction. During this period the large-scale weather situation is characterized by:

1. A large cold anticyclone over Siberia, Russia, and Scandinavia.
2. A large anticyclone between Spain and Bermuda.
3. A cold continental anticyclone over the North American continent.

Comparison with Fig. 80 will show that these anticyclones are in their normal positions; they constitute the normal wheels in the general circulation.

The cold air from the Arctic and north Canada (*i.e.*, *A* and *Pc* air) streams southward and meets with the tropical maritime air from the Atlantic subtropical anticyclone along an extensive and pronounced polar front which is approximately in its normal position (*cf.* Fig. 124). A number of cyclone waves form along the polar front and move eastward, while they develop in the normal manner (see Par. 130).

Figure 233 shows the situation Feb. 12, 1 P.M. G.M.T. We shall first examine briefly the properties of the various air masses. In Newfoundland, the air temperature is about −13°C. Since the winds are strong and the air is heated from below, the reported temperatures

Fig. 233 – Weather map, Feb. 12, 1907, 1 p.m. G.M.T.

Fig. 234 – Weather map, Feb. 12, 1907, 6 p.m. G.M.T.

Fig. 235.—Weather map, Feb. 13, 1937, 7 A.M. G.M.T. The position of the center is indicated at 12-hr. intervals. The isallobars at sea are corrected for the movement of the ships.
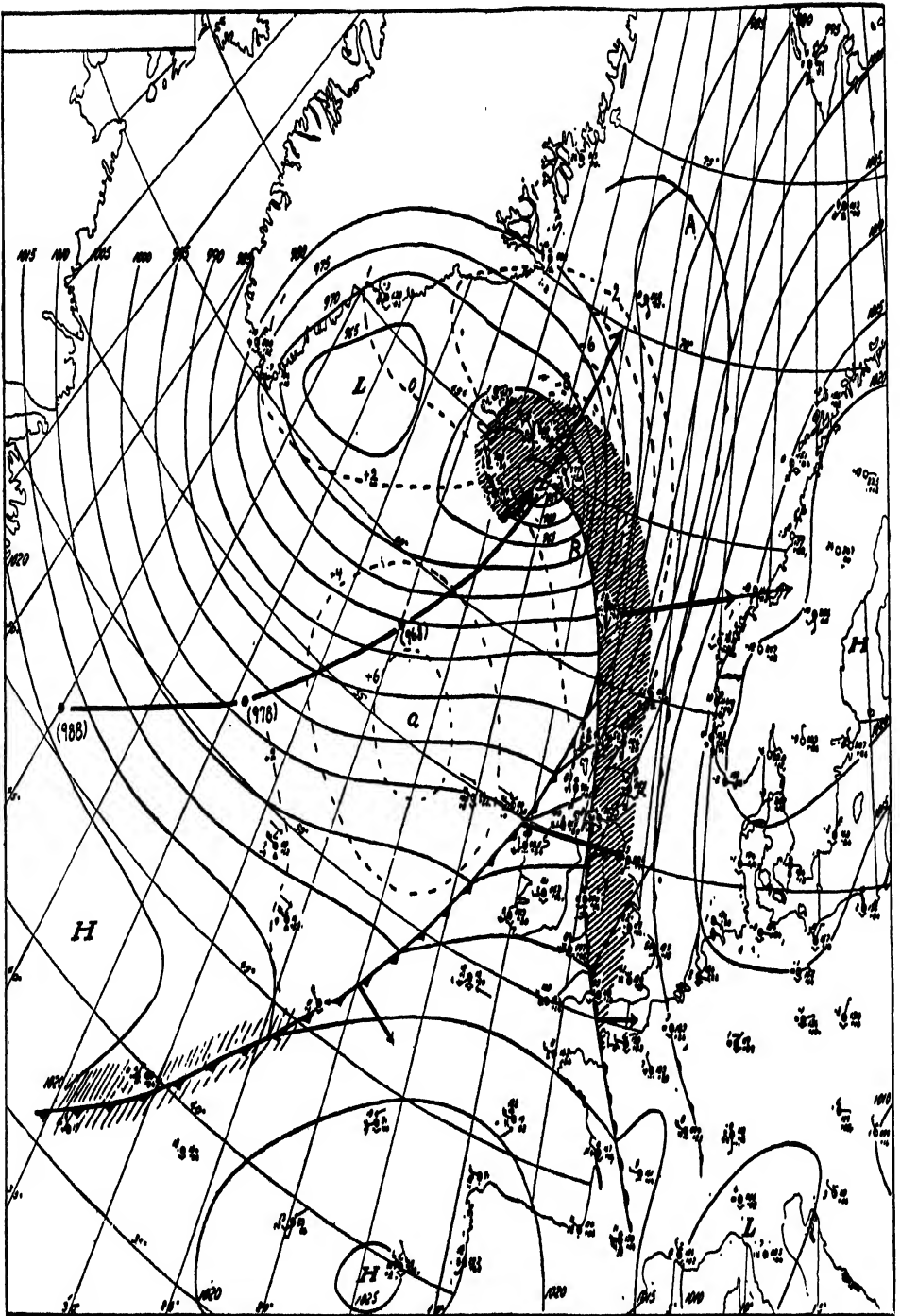
Fig. 236.—Weather map, Feb. 13, 1937, 6 P.M. G.M.T.
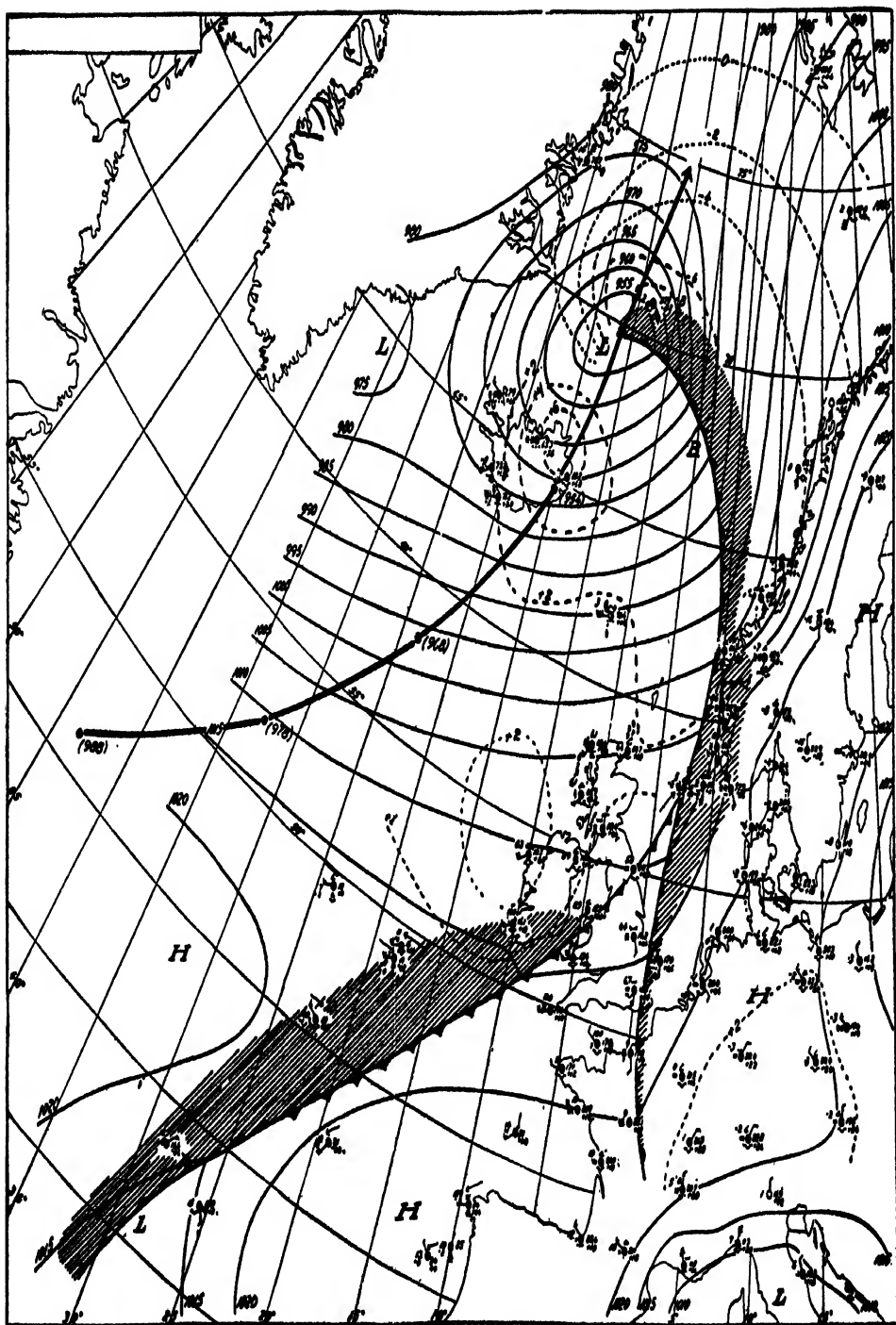
Fig. 237.—Weather map, Feb. 14, 1937, 7 A.M. G.M.T.

8. The eighth step.—When the foregoing points have been completed, it is well to reexamine the weather charts in order to ascertain whether any phenomenon or alternative has been overlooked. In other words, the analyst should ask himself the question: What can upset the forecast?

9. The ninth step.—The final point to consider is the wording of the forecast. The forecast should be as clear and unambiguous as possible, and it should express not only the weather conditions but also the degree of certainty of the prediction. For example, it may be quite certain that rain will occur, but somewhat uncertain whether the rain area will arrive in the morning or in the evening. In another case, it may be certain that a front will pass about noon, but not certain whether or not the front will cause precipitation while it passes. The forecasts should contain some indication of the certainty of the prediction, both as far as weather phenomena and the time of occurrence are concerned. Some general principles concerning the timing of the arrival were discussed in Par. 163.

In conclusion, it should be mentioned that much useful knowledge can be obtained from a critical reexamination of the unsuccessful forecasts.

In the following paragraphs, we shall try to apply the above principles to a few weather situations.

183. Example of Ocean Analysis.—In order to demonstrate the application of the principles of analysis and forecasting to ocean areas where observations are scanty, we turn to the weather situation for Feb. 12 to 14, 1937, over the North Atlantic. The maps (Figs. 233 to 237) are highly simplified so as to allow sufficient reduction. During this period the large-scale weather situation is characterized by:

1. A large cold anticyclone over Siberia, Russia, and Scandinavia.
2. A large anticyclone between Spain and Bermuda.
3. A cold continental anticyclone over the North American continent.

Comparison with Fig. 80 will show that these anticyclones are in their normal positions; they constitute the normal wheels in the general circulation.

The cold air from the Arctic and north Canada (*i.e.*, *A* and *Pc* air) streams southward and meets with the tropical maritime air from the Atlantic subtropical anticyclone along an extensive and pronounced polar front which is approximately in its normal position (*cf.* Fig. 124). A number of cyclone waves form along the polar front and move eastward, while they develop in the normal manner (see Par. 130).

Figure 233 shows the situation Feb. 12, 1 p.m. G.M.T. We shall first examine briefly the properties of the various air masses. In Newfoundland, the air temperature is about −13°C. Since the winds are strong and the air is heated from below, the reported temperatures

are altogether representative. By passing from Newfoundland to the ship indicated by *a*, the air temperature has increased to +1°C., but the air is still considerably colder than the sea surface.

The ships *b*, *c*, and *d* report air temperatures varying from 15 to 19°C., and the temperature of the air is about 1°C. higher than the temperature of the sea surface. This indicates that the air is of warm (subtropical) origin and that it is cooled from below. Normally, this would cause inversions to form (see Par. 54) in the lower layers; but since the winds are very strong, the vertical mixing is sufficiently intense to hinder the formation of appreciable inversions. As a result, none of the ships in this region reports stratus, fog, or drizzle.

The polar air that streams toward Florida is headed rapidly over the warm Gulf Stream. In spite of this, none of the ships in this area reports showers or squalls. This may be due to anticyclonic subsidence which, as far as stability is concerned, counteracts the heating from below. The transformation of the *Pc* air in the region between Bermuda and the coast is apparently of type 1, whereas the transformation of the *Pc* air that streams toward the middle and eastern part of the North Atlantic is of type 2 (*cf.* Par. 75).

Comparison between the reported temperatures in Fig. 233 and the mean air-mass temperature in midwinter (Figs. 93 to 95) will show that the tropical air has temperatures close to the normal, whereas the polar air is unusually cold. The front between the two air masses is very pronounced. In spite of the scarcity of ship reports, the position of the front may be located with great accuracy by drawing the isobars as described in Pars. 177 and 178.[1] It will be seen that the temperature difference along the front varies considerably; it is greatest in the rear of the cyclone *B* where the polar air has had a minimum of travel over warmer water. In the eastern part of the Atlantic, the temperature difference along the front is considerably smaller. This is due to the fact that the polar air has traveled a long while over the ocean. However, as the maritime air proceeds eastward and meets with the cold air over the European continent, the front will increase in intensity.

We shall now apply the forecasting methods and rules to Fig. 233 in order to obtain an idea of the future wind and weather conditions in west Europe and the eastern part of the North Atlantic Ocean.

The first question of interest is: Will the wedge of high pressure over Scandinavia move, or will it continue to remain stationary?

Choose an *x*-axis normal to the wedge line across Scandinavia. It will then be seen that $\partial^2 p/\partial x^2$ is large and $\partial^2 p/(\partial x\,\partial t)$ is approximately

---

[1] Students who are interested in practicing rational analysis should copy the observations from Fig. 233 on blank maps and perform their own analysis using Fig. 233 for comparison.

zero. It follows then from Eq. *154*(1) or rules 1 to 3 that the wedge will remain stationary.

Furthermore, it will be seen that the tendencies on the wedge line are positive. According to rule 23, the wedge will then increase. The tendencies are, however, slight. The correct conclusion is, therefore, that the wedge is stationary, with a slight tendency to increase.

In this case, the reason we examine the behavior of the wedge first is not that the wedge is of primary importance but because it is good policy to start with the problems that can be solved most easily before we approach the more difficult ones.

Let us next examine the probable movement of the front A. A mere inspection of the isobars reveals a comparatively strong geostrophic wind component normal to the front. The front and the frontal trough will therefore move eastward. But since the wedge over Scandinavia shows a slight tendency to spread westward rather than to yield to the approaching front, it should be regarded as certain that the front will slow down as it approaches southwest Norway.

The path of the cyclone center at east Greenland shows that the center has moved with decreasing speed. Applying now the path method (Par. 162) and noting that the barometric tendency at south Greenland is negative, we see that the isallobaric gradient between south Greenland and Jan Mayen is very slight. Since the curvature of the pressure profile in this direction is very large, it follows from rule 9 that the center is now almost stationary.

Knowing that the wedge over Scandinavia and the cyclone center at east Greenland will remain stationary, we try to obtain more specific information of the movement of the front A.

We correct the barometric tendencies observed at sea for the movement of the ships as described in Par. 179 and draw isallobars between the center B and the front A. On account of the scarcity of observations, we obtain only a rough idea of the distribution of the barometric tendencies; but it will, nevertheless, be seen that the front has a considerable speed eastward. The velocity can be obtained from Eq. *158*(1), but the computed result is likely to be inaccurate. In this particular case, it is far better to apply the geostrophic-wind method (Par. 159). Since the front at A is a warm-front type occlusion, we may apply rule 15. With normal speed, the front would be displaced eastward during the coming 18 hr. as shown by the thin arrows in Fig. 233. However, as the front necessarily must be retarded, we should reckon with a considerable decrease in the speed, particularly during the late part of the period. The appropriate position of the front next morning (7 P.M. G.M.T.) is indicated by the heavy arrows.

Further evidence of the retardation of the front can be obtained from the isallobars. It will be seen that the barometer rises at south Iceland and falls rapidly in advance of the wave cyclone B. This will cause the isobars between A and B to rotate toward a north-south direction; the geostrophic wind normal to the front will decrease, and the speed of the front A, also. As the point A moves eastward, the storm and the area of precipitation in advance of it will arrive in the North Sea next day; but since the anticyclone over Scandinavia persists, neither of them will reach the west coast of Norway.

We consider next the wave cyclone B. In the first place, the open warm sector and the great temperature contrast indicate a large source of energy and a rapid development. From rules 25 and 26, it follows that a wave cyclone deepens and occludes at a rate which is indicated by the warm-sector tendencies. The ship d reports $+0.4$; but, correcting for the movement of the ship, we obtain a barometric tendency of about -3 mb., which, according to Par. 171, indicates a rapid deepening.

Since the barometric tendencies around the center B are not known with satisfactory accuracy, we cannot compute the velocity of the center by means of Eq. *157*(1). On the other hand, we may use the path method (Par. 162). The heavy line in the rear of the center indicates the distance traversed in 6 hr. The arrow indicates the probable movement during the coming 18 hr. The direction of this movement agrees with the rule that warm-sector cyclones move parallel to the warm-sector isobars. Moreover, such cyclones move parallel to the isobars around the subtropical anticyclone.

The above extrapolation can be checked by using the geostrophic-wind method and applying rules 15 to 18 (Par. 159) to the cold and the warm front. The results thus obtained agree with what was found by means of the path method.

The weather situation on Feb. 12, 6 P.M. G.M.T., is shown in Fig. 234. The student is advised to analyze this map independently and to try to forecast the displacements and developments by means of the method and rules given in Chaps. IX and X.

The weather situation on Feb. 13, 7 A.M., is shown in Fig. 235. It will be seen that the centers and fronts have moved as predicted. The wind component normal to the front A has decreased and is still decreasing. The front A is becoming stationary across the North Sea, but it still moves toward the northeast over the Norwegian Sea.

The center B has deepened from about 983 to about 968 mb. in 18 hr., which agrees well with the previous estimate of 3 mb./3 hr. It will be seen that the center B is beginning to occlude and that its path is slightly curved northward. As the center proceeds eastward, its

path will tend to become parallel to the isobars around the quasi-stationary anticyclone over the continent.

We shall now try to forecast the movement and development of the center southwest of Iceland. Since the tendencies at sea are not known with sufficient accuracy, we can use only the path method and the geostrophic-wind method.

We consider first the point B on the warm front. Use the geostrophic-wind scale, and determine the displacement during 12 hr. of the point B normal to the warm front. With 100 per cent displacement, the front would move toward the position x in 12 hr. Using rule 15 (Par. 159), we find that the warm front will move to the point y in 12 hr. Using next rule 16, we find that the cold front (which is of type B) will move approximately to the same position in 12 hr. We now apply rule 18 and find that the center will move to the southeastern part of Iceland. This displacement is almost parallel to the warm-sector isobars, and the predicted path is allowed to continue to curve northward so as to become parallel to the isobars around the quasi-stationary anticyclone.

Applying now the path method, we find exactly the same displacement; we may therefore assume that the determination of the speed of the center is reliable.

Along the position marks in Fig. 235 is plotted the pressure in the center at 12-hr. intervals. It will be seen that the center has deepened with a speed of about 10 mb. in 12 hr. Applying rule 26 (Par. 170), we find that the pressure in the center is likely to be about 958 mb. 12 hr. later. It will be seen from Fig. 236 that the center deepened slightly more.

Figure 236 shows the situation the same evening. It will be seen that the front A has remained almost stationary and that the sky on the west coast of Norway is still cloudless. The front is dissolving, as can be seen from the fact that the pressure trough along it decreases. That this indicates frontolysis was explained in Par. 165.

So far we have seen that the westward extension of the continental anticyclone over Scandinavia caused the front A to become stationary off the coast. The cautious forecaster will therefore keep watching this anticyclone for symptoms which might indicate that it will yield to the invasion of Atlantic air. The first symptoms of this appear in Fig. 235. The pressure rise over north Germany increases, and slight falls occur along the coast of north Norway. This is more pronounced in Fig. 236. There is a definite isallobaric gradient across the wedge line, and the wedge will commence to move toward the south. As, simultaneously, the pressure falls in advance of the center B, the isobars and the winds will rotate from a southerly to southwesterly direction. The fronts and the rain area will then reach the Scandinavian Peninsula. As the

front *A* is dissolving, the problem is what will happen to the center *B* and its fronts.

From the path of the center *B*, we see that the center has moved with a constant speed along a slightly curved path. At first sight, it might seem logical to assume that the path would continue to curve northward. However, as the anticyclone over Scandinavia moves southward, the path will become parallel to the isobars between the center *B* and the anticyclonic ridge. *The northward curvature of the path will then cease.*

It might also seem plausible to assume that the speed of the center *B* would remain constant. However, since the curvature of the pressure profile through the center in Fig. 236 has increased considerably and is more than twice as large as on the previous map, it follows from rule 6 that the speed is likely to decrease. On the other hand, the isallobaric gradient through the center has increased too, which would tend to maintain the speed. We should therefore reckon with only a slight retardation of the movement. The appropriate displacement in 12 hr. is indicated by the arrow in Fig. 236. It will be seen that the predicted path is almost perpendicular to the isallobars through the center, in accordance with Eq. *157*(4) and rule 9.

Since it is now more than 12 hr. since the center commenced to occlude, it follows from rule 26 that the rate of deepening will decrease, and the center will soon attain its minimum pressure. An inspection of the isallobars within the area enclosed by the 965 isobar will show that the planimetric value of the tendencies is negative. This, according to rule 24, indicates that the center is still deepening. We can, therefore, conclude that the center is still deepening at a decreasing rate.

We determine next the movement of the front in the vicinity of the Faeroe Isles. If the front moved with the geostrophic wind, it would in 12 hr. traverse the distance indicated by the thin arrow. Since the front is a warm front type occlusion, we may use rule 15 (Par. 159). We then obtain the 12-hr. displacement shown by the heavy arrow. The front *B* will then have caught up with the front *A*.

In the same manner, the movement of various points on the front is determined, and the future position of the center and the fronts is obtained. In extrapolating the movement of the southern portions of the fronts, it should be taken into account that a ridge of high pressure is building up between the southern part of Sweden and Spain. As the fronts approach this ridge, they will be retarded as they tend to become almost parallel to the isobars.

Figure 236 shows some features of interest for the forecasting of winds. The barometric tendency at the Faeroe Isles is −4.6, whereas the tendencies on the west coast of Norway are almost zero. Applying

the principle in Par. 153, we find that the pressure gradient and the winds along the west coast will increase.

We consider next the conditions northwest of Ireland. The pressure tendency in the vicinity of the point a is $+6$ mb., and it decreases in all directions. To the south of a, the pressure gradient decreases rapidly; as a result, the geostrophic wind normal to the front will decrease, and the fronts will move more slowly. As the cyclone center at Iceland moves northeastward, the isallobaric center in its rear will move in the same direction, and a general decrease in the westerlies will result.

Figure 237 shows the situation the following morning. It will be seen that the development is in agreement with the predictions. The student is advised to try to predict the future movement of the pressure systems. It is most convenient to determine the movement of the cyclone center first, then the movement of the ridge of high pressure over Sweden and central Europe. When this has been done, the movement of the occluded front should be determined.

The western portion of the cold front is approaching the quasi-stationary state. In the extreme west, it has changed its movement and become a warm front. That this is so is shown by the fact that the barometric tendency is negative north of the front, but positive south of it. From what was said in Par. 164, it is evident that a new wave is about to form near the Azores.

The cold front to the south of Ireland is of type A (see Par. 122). In spite of the slight geostrophic-wind component normal to it, it will move toward the southeast (compare Par. 159) and overtake the warm front over France.

During the period preceding the map shown in Fig. 237, warm air from the Bermuda region has moved toward the northeast and arrived in western Europe. Meanwhile, the air has been cooled from below; it has become saturated and excessively stable, as is indicated by the weather observations within the warm sector in Fig. 237. As this air moves farther to the east, it will come over still colder ground, and stratus, fog and drizzle will prevail.

The air in the rear of the front originated from northern Canada. This air mass has traveled rapidly toward warmer regions and developed an unstable or indifferent stratification. Showers, squalls, and other convective weather phenomena are therefore reported throughout this mass. However, when the air in the rear of the front enters the continent of Europe, it will be warmer than the underlying surface. It will then develop a stable stratification and gradually become transformed into a polar continental mass.

A branch of the polar air in the southwestern portion of Fig. 237 moves toward the southwest on the equatorial side of the polar high.

This air will gradually develop into a tropical maritime mass. As the high north of the western part of the polar front (Fig. 237) moves eastward, a new col will develop between this high and the continental high over North America. Between these anticyclones, a frontogenetical wind field will exist which will create a new front, and this, in time, will create new waves.

184. Examples of Displacements and Deepening.—In the previous paragraph, we discussed some examples from the North Atlantic Ocean. In these cases, the observations were so scanty that none of the forecasting formulae could be used in a quantitative manner. We shall now turn to some examples from the European continent in order to show how the forecasting formulae can be used in a more direct manner.

Figure 238 shows the weather situation Feb. 15, 1938, 7 A.M. G.M.T. In order to allow for a sufficient reduction, very few of the observations on which the analysis is based are plotted on the maps. Throughout the period, an anticyclone was situated over the British Isles. The lower strata of this anticyclone consist of polar air. The eastern part of the anticyclone is considerably colder than the western part. It follows then from the equation of static equilibrium (see Par. 47) that the pressure will decrease more rapidly along the vertical in the eastern part of the anticyclone than in the western part. This implies that there is a northerly current in the free air across the wedge to the east of the anticyclonic center. This air is of maritime origin and therefore potentially warmer than the cold air in the lower layers of the anticyclone. To the west of the anticyclone, there is a narrow stream of transitional maritime tropical air from the Azores to Iceland. To the north, there is an extensive front that separates the warm air from the cold arctic air.

A series of waves have developed on this front. The warm westerly current in the free air north of the anticyclone will, during its eastward movement, diverge with one branch over the Baltic toward Germany and another branch toward the east or northeast into the cyclonic system. The above conclusions are brought out by the analysis of upper-air charts. These maps are not reproduced here. What we are here concerned with describing is the determination of the movement and the development of the fronts and pressure systems on the surface maps.

We begin by computing the movement of the wedge across the Baltic, using Eq. *154*(1). The appropriate length unit is indicated on the map, and the computed displacement in 24 hr. is indicated on the map by a double arrow. We consider next the movement of the anticyclone over Scotland. Since the barometric tendencies are uniform in all directions, it follows from Eqs. *155*(2) and (3) that the center is stationary. Moreover, since the barometric tendencies are zero in the anticyclonic center and also along the wedge line to the east, it follows from rules 19,
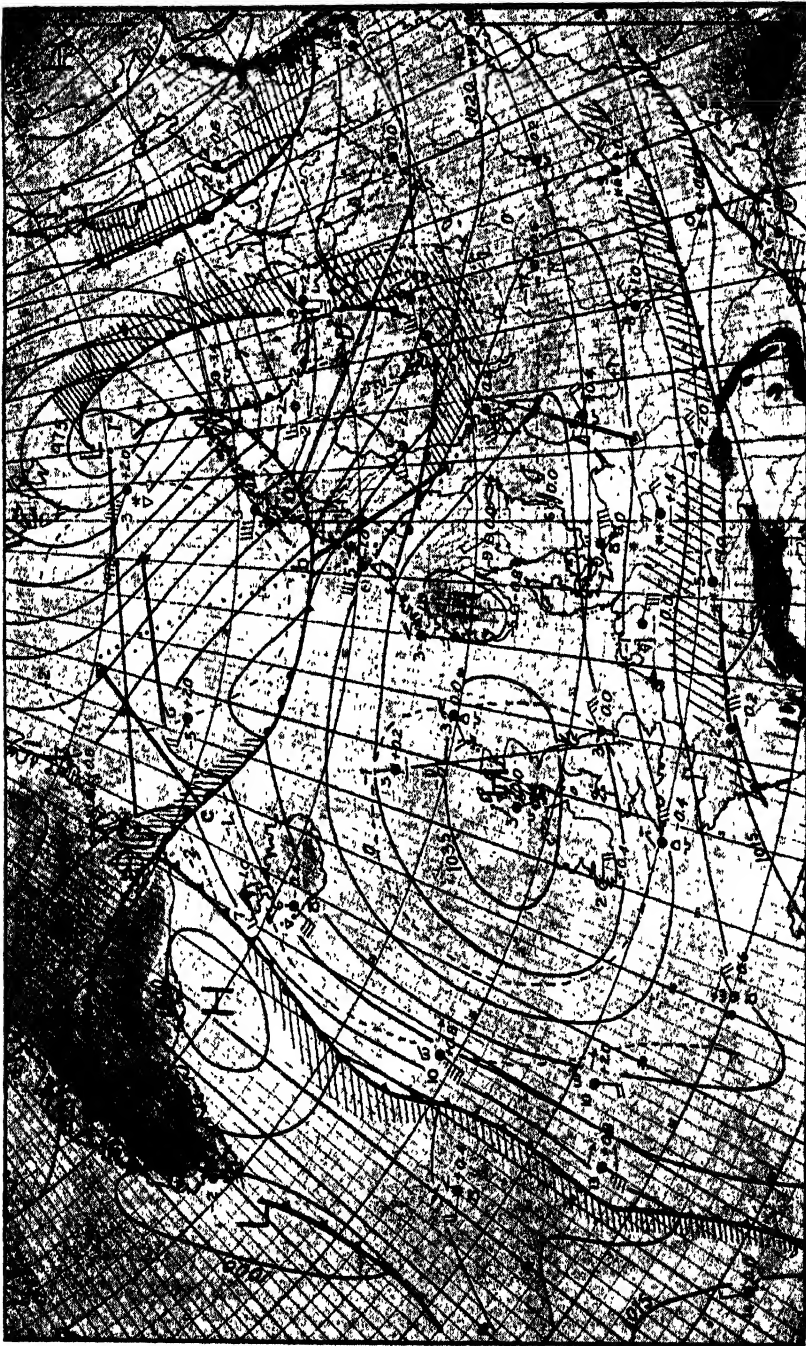
Fig. 238.—Weather situation, Feb. 15, 1938, 7 a.m. G.M.T.

20, 22, and 26 that there is no deepening or filling in the anticyclonic center and on the wedge line. The same also applies to the local anticyclonic center over southern Norway. The above computations show, therefore, that the high-pressure area over Scotland and southern Norway will remain stationary, while the wedge farther to the east will move southward, as shown by the arrow.

The plotting of tendency profiles along axes normal to the wedge line will show that there is no marked curvature in the vicinity of the wedge line. The same also applies to tendency profiles through the anticyclonic center. It follows then from rules 5 and 14 that neither the anticyclone nor the wedge line is accelerated.

The above results may be regarded as certain, and the following predictions, which are more intricate, should be made to agree with the above results.

We consider next the cyclonic center in the extreme north. Its path is shown on the map with position marks at 12-hr. intervals. It will be seen that a center is strongly retarded in its eastward movement. Moreover, in the first 12-hr. interval, the center deepened 16 mb., whereas in the last 12-hr. interval it deepened only about 8 mb. The strong retardation of the eastward movement and the deepening indicate that the center is approaching a stationary state. On account of the lack of observations in the extreme north, it is not possible to extrapolate the future movement and development directly. We shall therefore turn to the neighboring systems; and when their behavior has been forecast, we shall return to the pressure center in the extreme north.

The barometric tendencies to the west of the high over northern Siberia are slightly positive. This shows that this high is not giving way to the advancing cyclone. This seems to indicate, also that the cyclone center must be strongly retarded.

We consider next the movement of the cold front at the point indicated by the letter *a*. Since the pressure trough at the front is indistinct, Eq. *158*(1) will give inaccurate results. However, since the geostrophic wind is very strong, we may apply with confidence the geostrophic-wind method. Using rule 16, we find the 24-hr. displacement shown by the arrow. Proceeding in the same way, we find the 24-hr. displacement of the point *b* and also the displacement of point *c* on the warm front north of Iceland, the latter displacement being determined by means of rule 15. The dotted line then indicates the displacement during 24 hr. of the portion of the frontal system under consideration.

Before we go any further, it will be necessary to consider the deepening of the warm sector over the Bay of Bothnia. Choose an *x*-axis along the arrow through the point *a*, and consider the movement of the cold and the warm front along this axis. According to rule 25, the deepening

intensity at any point on this axis is equal to the barometric tendency. It will then be seen that there is a maximum of deepening in the region indicated by *D*. Since the barometric tendency in this region is approximately -2 mb., the deepening is approximately 2 mb./3 hr., or about 16 mb. in 24 hr. According to rule 26, this deepening is likely to persist until some time after the warm sector has occluded. Since the warm sector is very wide, the deepening is likely to last 24 hr. It was pointed out earlier that the anticyclone in the northeast corner of the map is not yielding to the advancing cyclone. Furthermore, since the cyclone center is occluded and is deepening at a rapidly decreasing rate, it is reasonable to assume that filling will set in as the center approaches the stationary high farther to the east. Through the combined effect of filling in the center and deepening in the eastern part of the warm sector, a pronounced trough of low pressure will form along the occluded front. With this distribution of deepening and filling, an isallobaric gradient will be established which tends to cause the occluded center to move toward the southeast.

Let us now consider the movement of the front at the point *d*. Using the geostrophic-wind scale and rule 15, we obtain a large 24-hr. displacement of the point *d*. But since the anti-cyclone to the east is stationary and the cyclone center is going to move toward the southeast, we must reckon with a considerable retardation of the eastward movement of the front at *d*. Taking this into account, we see that the double arrow through the point *d* indicates the probable movement during 24 hr. A further proof of the fact that the front at the point *d* is retarded can be obtained in the following manner: Since there is considerable deepening in the region *D* while the center fills, the geostrophic-wind component normal to the front at *d* must decrease, and this would mean that the eastward movement of the front is retarded.

It remains now to discuss the behavior of the wedge to the northeast of Iceland. As the warm front north of Iceland moves toward the northeast, the preceding wedge must also move with approximately the same speed as indicated by the arrow. Furthermore, since the zero isallobar is in the rear of the wedge, it follows from rule 22 that the wedge will increase in intensity while it moves eastward.

The tendencies in Iceland indicate that the warm sector is deepening very slowly. According to rule 26, we should not expect much development in the warm sector while it moves toward the northeast.

We have now obtained a fairly accurate picture of the pressure distribution and the positions of the various fronts 24 hr. in advance. From the above displacements, the time of arrival of any of the fronts and air masses involved can be obtained and the forecasts worked out accordingly. In doing this, it is important to bear in mind that the
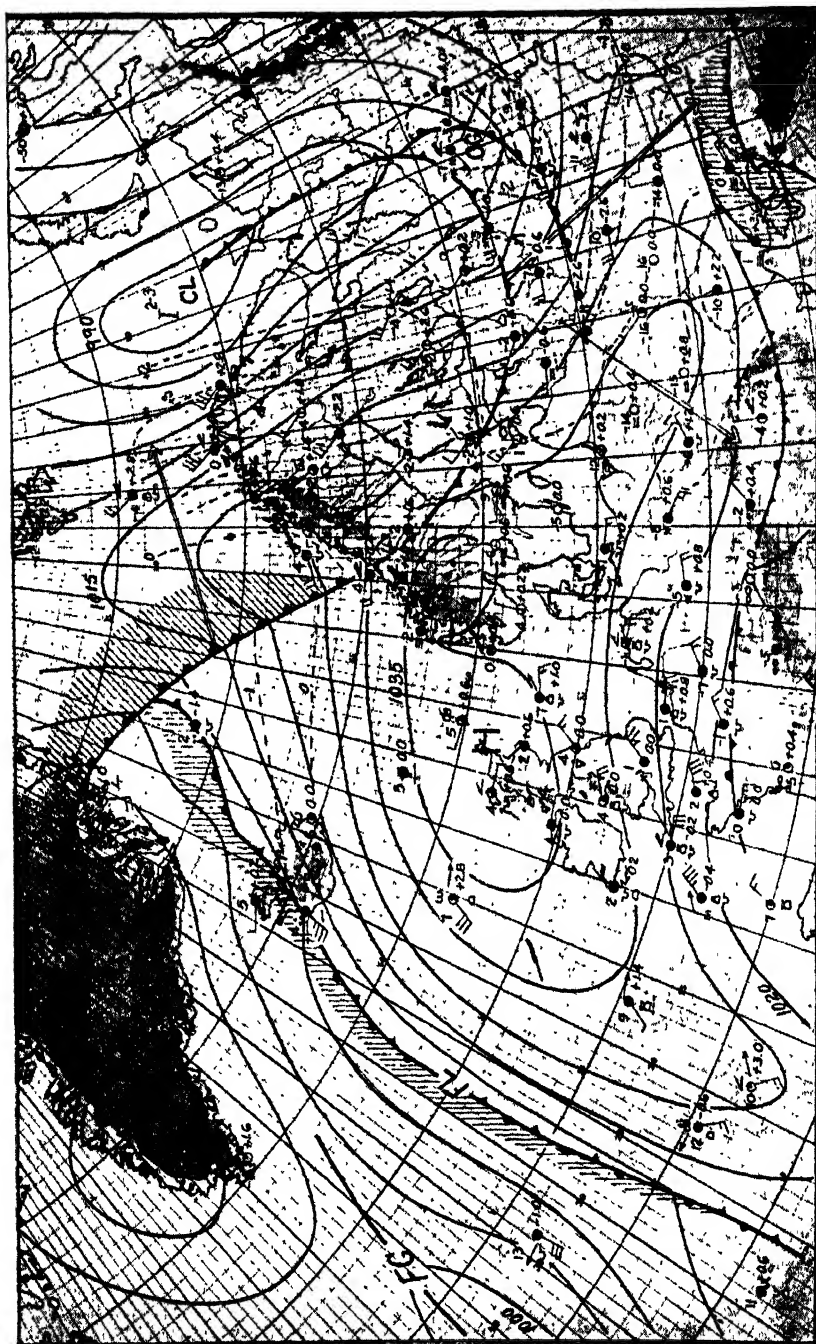
FIG. 239.—Weather map, Feb. 16, 1938, 7 A.M. G.M.T.
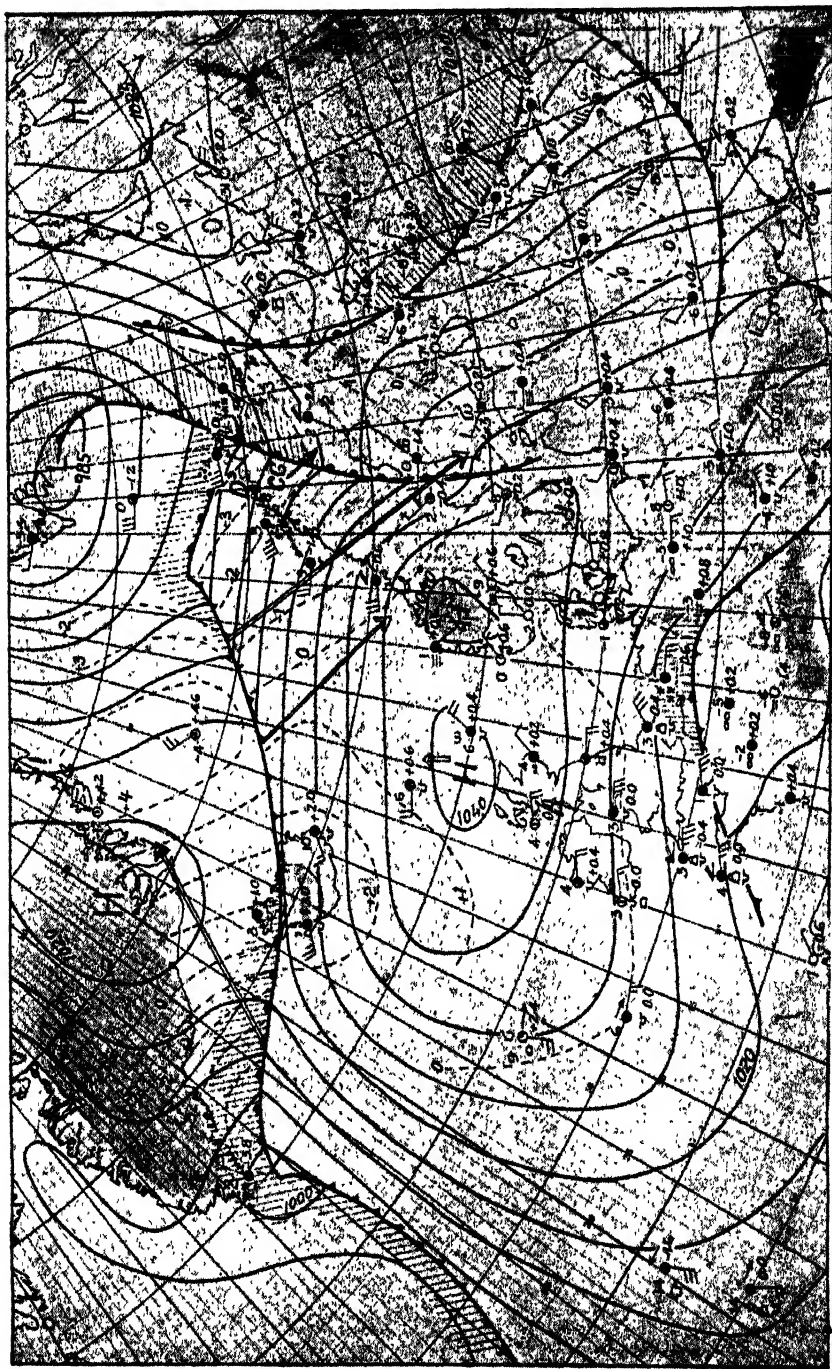
Fig. 240.—Weather map, Feb. 17, 1938, 7 a.m. G.M.T.

FIG. 241.—Weather map, Feb. 18, 1938, 7 A.M. G.M.T.

arrival of a front or a pressure system can be timed with great accuracy when the speed is high, whereas no great accuracy can be obtained when the speed is low.   The reason for this was explained in Par. 163.   Apart from the displacements, deepenings, and fillings, the forecast will depend on the changes that occur in the physical properties of the air masses during the forecasting period.

Figure 239 shows the weather situation 24 hr. after the period of the preceding map.   It will be seen that the extrapolations are in all essentials correct.[1]   Finally, Figs. 240 and 241 show the weather situation 24 and 48 hr. after the time of the map shown in Fig. 239.   The displacements and developments have been determined 24 hr. in advance, as shown by arrows and symbols on the maps.   The student is advised to determine the displacements and developments independently by means of the methods described above, using the results indicated in the maps as means of verification.

185. Example of Three-dimensional Analysis.—We shall now turn to a very complicated weather situation and analyze it in all three dimensions.   In addition, we shall, as far as possible, compute the displacements and developments during the coming 24 hr.

Figure 242 shows the surface map Dec. 12, 1939, 7.30 A.M. E.S.T. The salient features of the weather situation are as follows: A young wave cyclone has formed on the Atlantic polar front off the east coast of North America, and an extensive ridge of high pressure of polar continental air is situated over the coastal states.   Over western Canada, the polar continental air forms a pronounced wedge of high pressure which is separated from a mass of transitional polar maritime (Pacific) air farther to the south.   Maritime tropical air from the Gulf of Mexico streams slowly northward, forming a warm sector between a weak warm front and a pronounced cold front.   It will be seen that maritime tropical air is very uniform, with temperatures ranging from 65 to 60°F. and dew-point temperatures ranging from 65 to 58°F.   The discontinuity in temperature and dew point is very pronounced along the cold front and less distinct along the warm front.   From the peak of the warm sector, an occluded front extends northward into the cyclone center over central Canada.   A cold front in the rear of the cyclone center separates the fresh polar continental air from the transitional air farther to the south. In the extreme west, this front changes into a warm front.

It is of interest to note that precipitation occurs in the vicinity of the cyclone center over Canada and that no precipitation occurs in connection with the fronts that extend southward from this center.

---

[1] The above extrapolations are not the results of after-analyses; they are copied from the actual working maps of Vervarslinga på Vestlandet, Bergen, Norway.
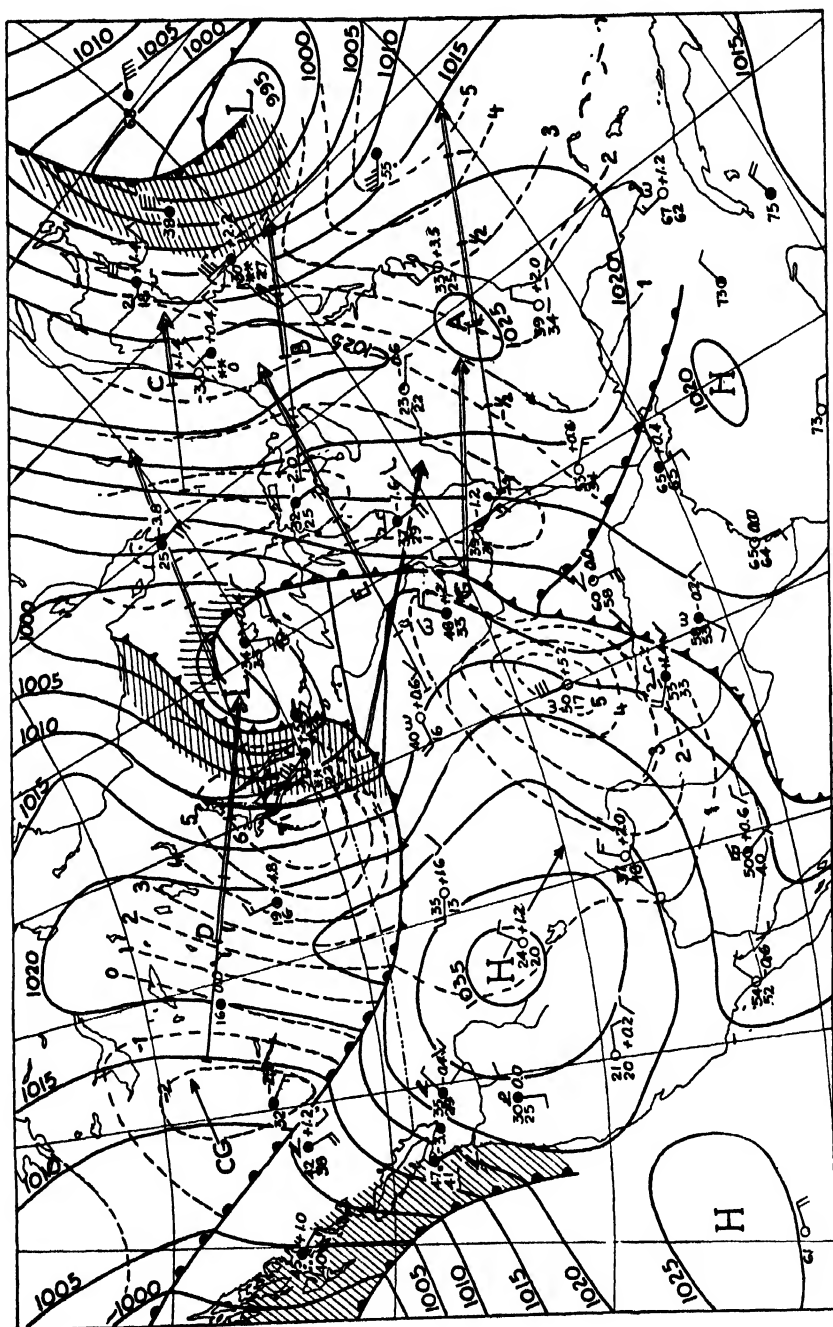
FIG. 242.—Surface weather map, Dec. 12, 1939, 7.30 A.M. E.S.T.
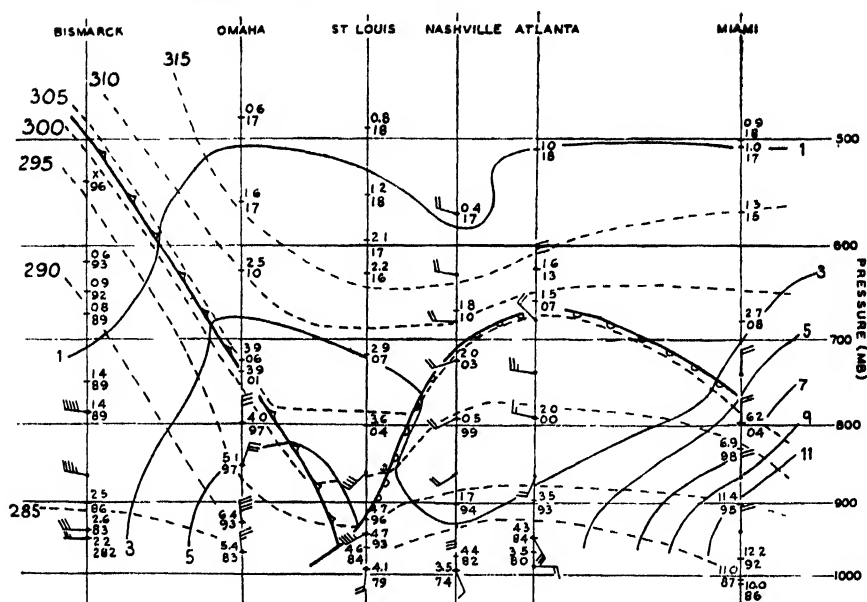
FIG. 243.—Vertical cross section from Miami to Bismarck. Upper numeral at each point on vertical lines indicates specific humidity; lower numeral indicates the two last digits of potential temperature (°A); full lines indicate specific humidity, and broken lines indicate potential temperature. Wind direction and force are indicated by arrows, the direction of which refers to the base line of the cross section.
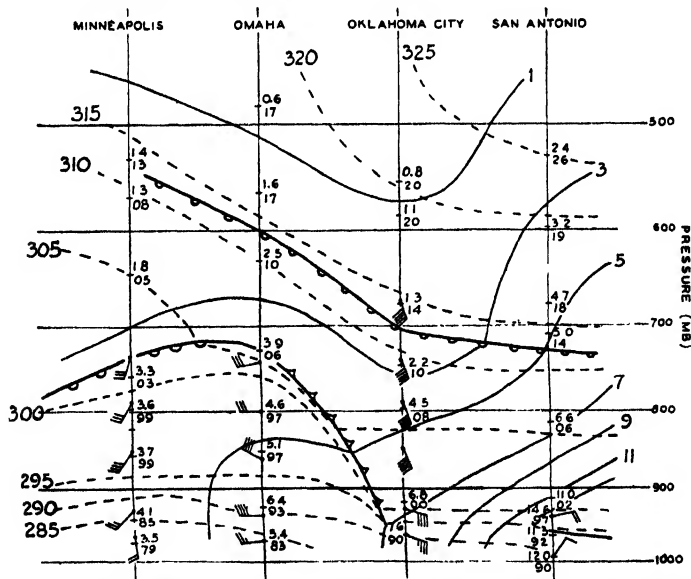
FIG. 244.—Vertical cross section from San Antonio to Minneapolis. Symbols as in Fig. 243.

This is surprising, since the tropical air in the warm sector is very moist, the temperatures being close to the dew points.

The vertical structure of the fronts and air masses involved is shown in three vertical cross sections (Figs. 243 to 245). It will be seen from these cross sections that the tropical air is moist only in the lower layers and that it is relatively dry aloft. Moreover, it will be seen from the cross section from Miami to Bismarck that the cold front in the southwest portion of the map is very distinct, its inclination is large, it reaches to
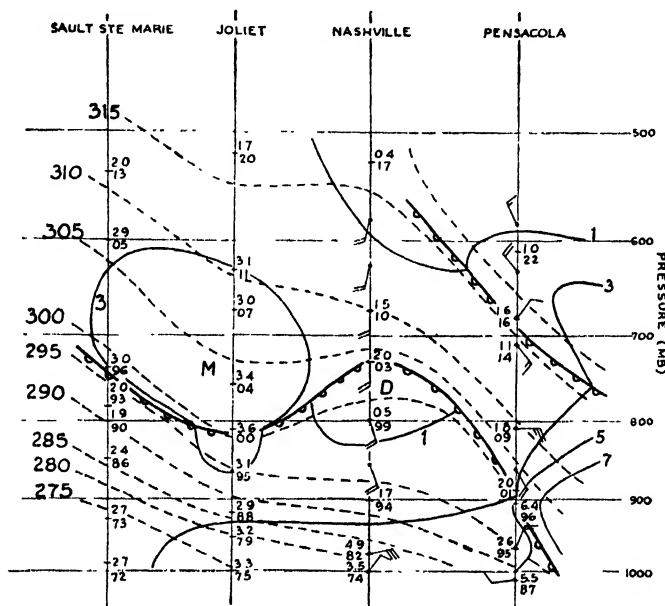
FIG. 245.—Vertical cross section from Pensacola to Sault Ste. Marie. Symbols as in Fig. 243.

great altitudes, and it coincides with an isentropic surface, except in the friction layer where several isentropic surfaces intersect the frontal surface. The warm front, on the other hand, is rather indistinct, and several isentropic surfaces intersect it. It was explained in Chap. VIII that lateral mixing occurs mainly along isentropic surfaces. The cold front in Fig. 243 will therefore not be much influenced by mixing, whereas the warm front will be appreciably affected. From this, we may conclude that the warm-front surface will dissolve, whereas the cold front will be maintained.

Figure 246 shows the physical conditions of the air in the isentropic surface $\theta = 299°A$. It will be seen that a moist region is present over Texas and north Mexico. From this region, two moist tongues project northward, with one branch along the Rocky Mountains and another
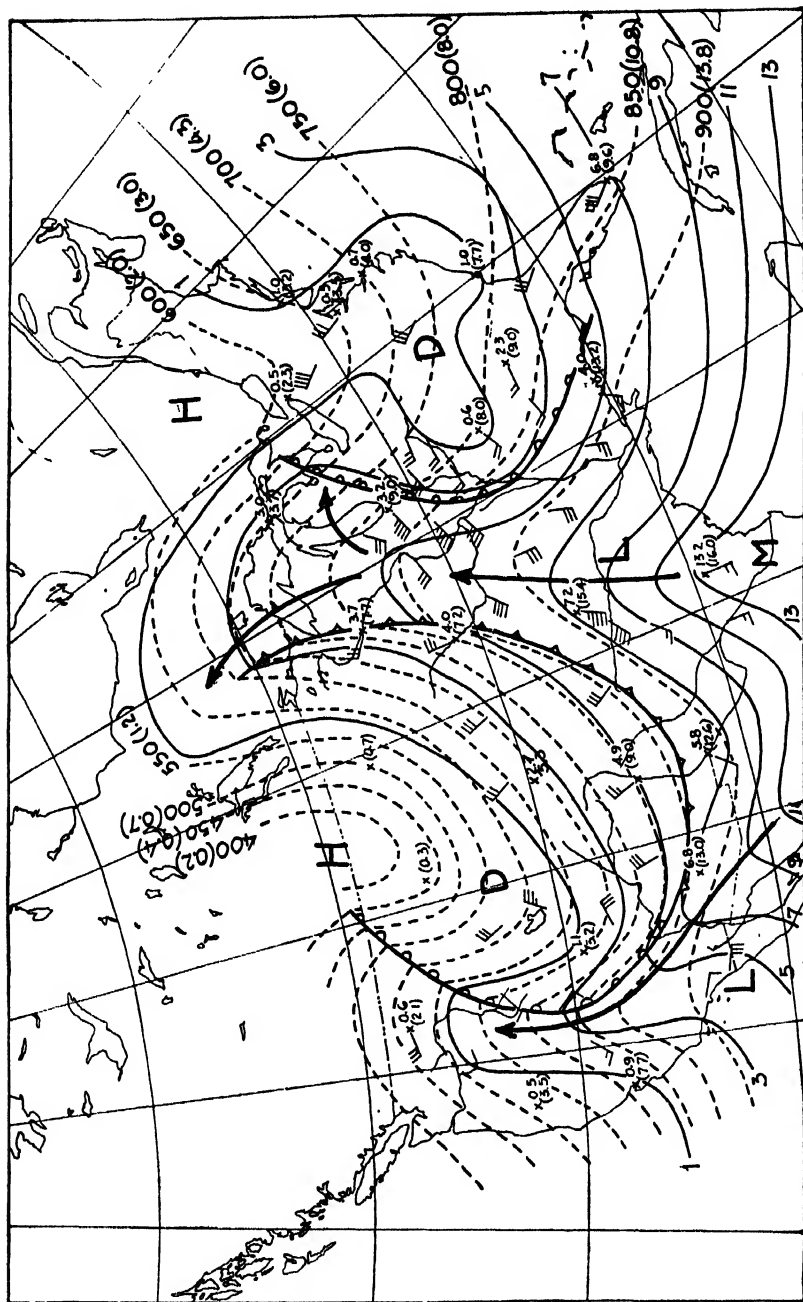
Fig. 246.—Isentropic chart (θ = 299°A), Dec. 12, 1939, 1:30 A.M. E.S.T.   Full lines indicate specific humidity; broken lines indicate atmospheric pressure (mb.) in the isentropic surface.   Numerals in parentheses indicate the saturation specific humidity at the pressure indicated by the broken lines.   *H*, domes; and *L*, troughs in the isentropic surface; *M* and *D*, moist and dry regions, respectively.
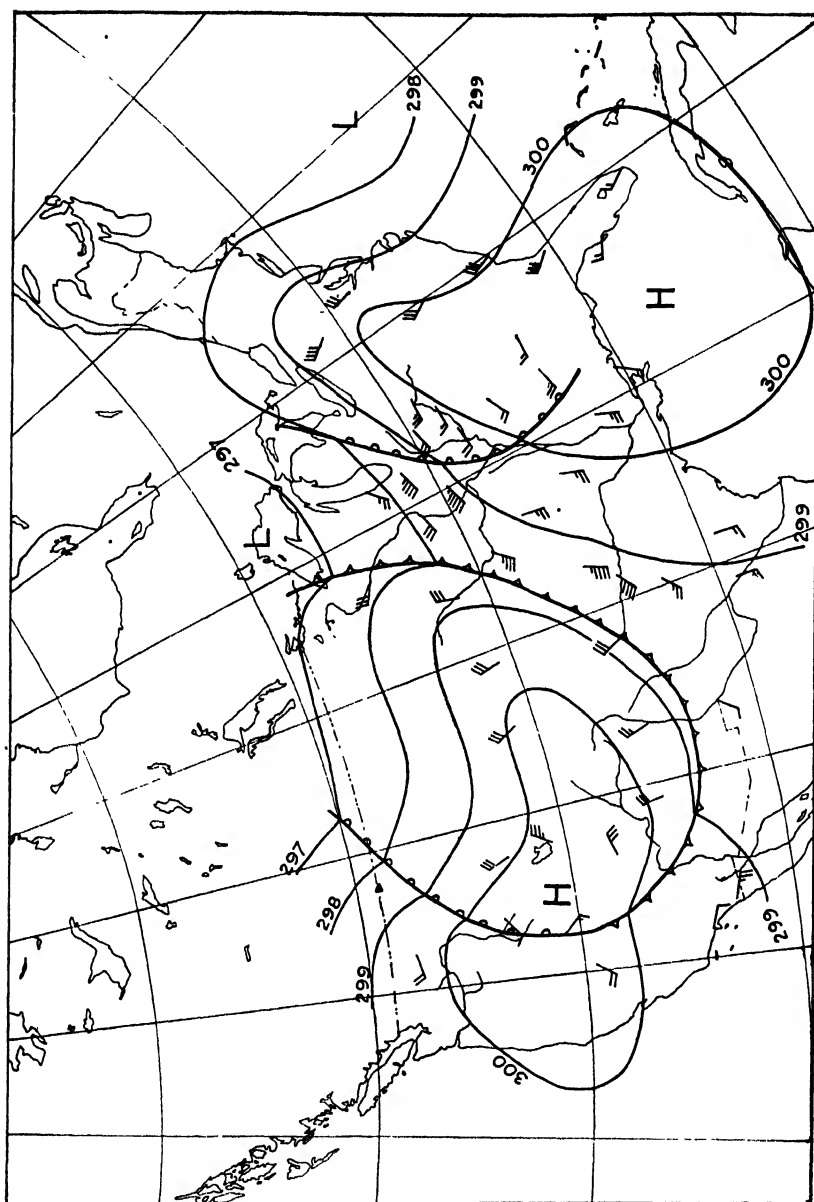
FIG. 247.—Showing the distribution of the stream function in the isentropic surface $\theta = 299°$ A.   Arrows indicate pilot balloon winds.

branch along the occluded front extending northward to the cyclone center over Canada. Within the warm sector, the isentropic surface is practically horizontal, and the air motion is mainly along the contour lines of the isentropic surface. Only in the extreme north has the warm-sector air a component up the slope of the isentropic surface. This explains why precipitation occurs along the occluded front only in the extreme north.

In the regions occupied by the high-pressure areas on the surface map, the flow in the isentropic surface has a downslope direction. In these regions, we find extensive dry tongues in the isentropic map. It will also be noted that the moist tongues coincide with the troughs and that the dry tongues coincide with the domes in the isentropic surface.

Figure 247 shows the distribution of the stream function in the isentropic surface computed as described in Par. 142, and Fig. 248 shows the distribution of pressure, temperature, specific humidity, and winds in the level 3 km. above sea level.

Seeing how the moist and dry tongues and the flow pattern aloft are closely related to the pressure distribution, air masses, and the fronts at the ground, we return to the surface weather map (Fig. 242) in order to find out how the pressure systems and fronts will move during the coming 24 hr. As usual, we begin by computing the displacement of the pressure systems whose structures are simplest. It is then natural first to compute the displacement of the ridge of high pressure along the east coast of the United States. We choose three axes normal to the wedge line through the points *A*, *B*, and *C*. The appropriate length units are indicated on the map (Fig. 242), and the computed 24-hr. displacements are indicated by the arrows. It will be seen that the wedge moves more rapidly in the south than in the north.

We next compute the movement of the wedge of high pressure over western Canada. The length unit and the 24-hr. displacement are shown on the map. The wedge is moving rapidly toward the east-south-east, and this seems to indicate that the cyclonic center will move with a considerable speed.

We may now attack the more difficult problem, *viz.*, to compute the displacement of the cyclone center and the fronts. Since the pressure distribution around the center and along the occluded front is rather irregular, it is difficult to find suitable points for computation. As explained in Par. 160, we may compute the movement of the cyclone center along an axis that does not intersect the front. The appropriate choice of axis and the computed 24-hr. displacement are indicated on the map.

We consider next the pressure and tendency distribution in the vicinity of the point *E* on the occluded front. It is obviously difficult
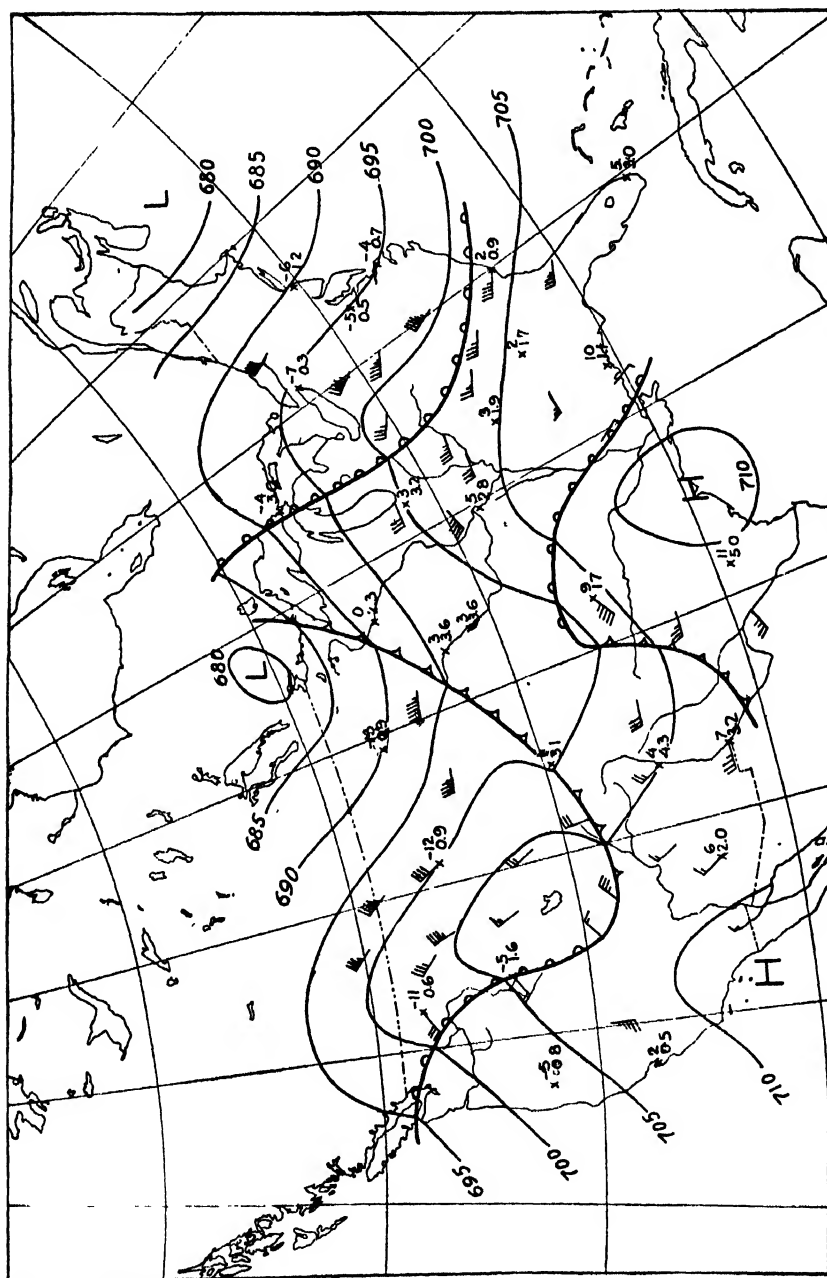
Fig. 248.—Weather map for the 3-km. level.

to apply the formula for the velocity of a front.   On the other hand, it follows from what was said in Par. 161 that the trough formula may be used, since the tendency discontinuity at the front is very slight.   Choosing an axis through the point E, as shown on the map, we obtain the 24-hr. displacement as shown by the arrow.

To the south of the point E, the distribution of pressure and tendency is so complicated that no reliable computation is possible.

We consider next the point F on the cold front to the southwest of the cyclone center.   Since the geostrophic wind across the front is strong, we may determine the velocity of the front by means of the geostrophic-wind method (see Par. 159).   The 24-hr. displacement of the point F is indicated by the arrow.

The anticyclone north of Salt Lake will move toward the southeast in the direction of the isallobaric gradient; but since the tendency distribution around the center is highly irregular, it is not possible to compute its displacement.

After having determined the displacements as shown above, we should:

1. Compare the computed displacements with the displacements from the previous to the present map.

2. Compare the computed displacements of the neighboring pressure systems in order to ascertain that there is reasonable agreement between them.

An inspection of the map will show that the computed displacements are in good harmony with one another; and since they also agree logically with previous displacements,[1] we may take it for granted that the various pressure systems will move approximately as computed.

We consider now the point G on the occluded front.   Since we are not able to compute its displacement, we may try to determine it indirectly from the simultaneous displacements of the neighboring systems. Assuming that the trough will move approximately with the speed of the preceding wedge, we obtain the displacement indicated by the arrow through G.   With this displacement, the cold front to the northwest would tend to overtake the occluded front which, in this case, is a logical development.

An inspection of the tendency profiles along the various axes will show that there are no appreciable accelerations (see Par. 156).   Furthermore, the tendency distribution shows that the cyclone center over Canada and the trough to the south of it are filling up slowly; but the changes are so slight that they are not likely to influence the computed displacements materially.   A slight deepening is likely to occur over western Canada in the region indicated by CG, since there is a maximum

[1] Not indicated on the map.
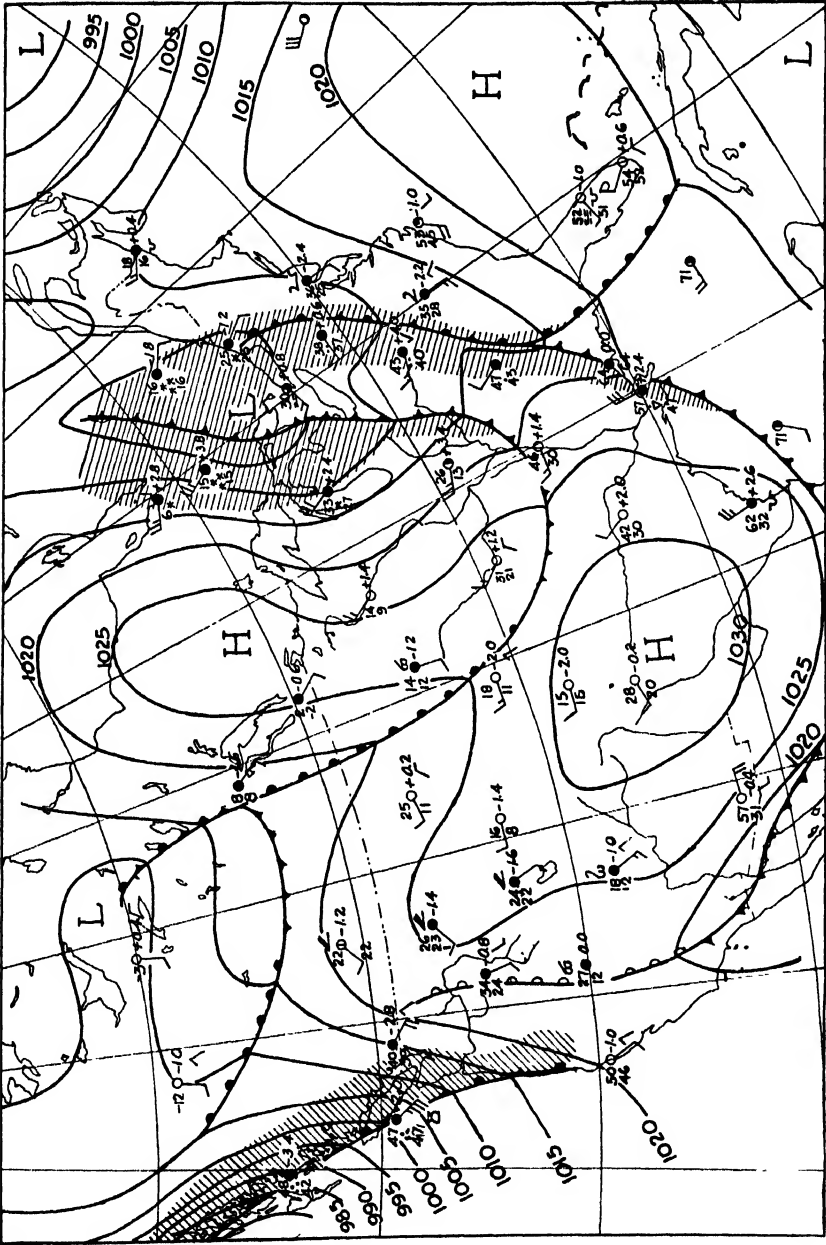
Fig. 249.—Surface weather map, Dec. 13, 1939, 7.30 A.M. E.S.T.

of barometric fall in the comparatively flat pressure distribution. This development, too, is presumably of but slight intensity. Since there are no appreciable deepenings or fillings, the computed displacements need not be adjusted as explained in Par. 173.

It was mentioned at the beginning of this paragraph that no precipitation occurred along the occluded front or along the warm and the cold front farther to the south. The question now arises: Will these fronts remain dry or will precipitation develop along them during the forecasting period? In order to answer this question, we return to the isentropic chart (Fig. 246) and the stream-function chart (Fig. 247). It appears from these charts that moist air from the Gulf of Mexico will stream northward into the trough along the occluded front, causing a general increase in moisture. Furthermore, as the occlusion process continues, the warm air will ascend and precipitation is likely to occur. If there were not a pronounced supply of moisture to the south, the front would probably remain dry; but, with the present distribution of moisture and air flow within the warm air, precipitation will soon develop. A forecast based on the surface map alone would, in spite of the accurate computations of displacements, perhaps have failed to indicate the development of an area of precipitation along the entire front.

Figure 249 shows the situation 24 hr. later. It will be seen that the fronts and the pressure systems have moved in good agreement with the computations and that an extensive area of precipitation has developed along the front.

In addition to the above analysis of the state of the free atmosphere, the individual ascent curves should be analyzed by means of adiabatic charts in order to determine the stability conditions of the various air masses, through the methods described in Chap. II.

Although the above example admittedly is a highly complicated one, it will be seen that a detailed three-dimensional analysis and a methodical determination of displacements and developments will yield satisfactory results.

REFERENCES TO LITERATURE

1. BERGERON, T.: Über die dreidimensional verknüpfende Wetteranalyse, *Geof. Pub.*, Vol. V, No. 6, Oslo, 1928.
2. BERGERON, T.: On the Physics of Clouds, *Memo. Met. Assoc., Intern. Union for Geodesy and Geophysics*, Lisbon, 1933.
3. BERGERON, T.: Description on Hydrometers, *Intern. Meteor. Organization*, 1937.
4. BERGERON, T.: Richtlinien einer dynamischen Klimatologie, *Met. Zeitschr.*, 1930.
5. BERGERON, T., and SWOBODA, G.: Wellen und Wirbel an einer quasistationären Grenzflache über Europa, *Veröff. Geophys. Inst. Leipzig*, Bd. 3, 1924.
6. BLATON, J.: Zur Kinematik nichtstationärer Luftströmungen, *Bull. Soc. Geophys. Varsovie*, 1938.
7. BLEEKER, W.: On the Conservatism of the Equivalent Potential and the Wetbulb Potential Temperature, *Quart. Jour. Roy. Met. Soc.*, Vol. 65, 1939.
8. BJERKNES, J : Saturated Ascent of Air through a Dry-adiabatically Descending Environment, *Quart. Jour. Roy. Met. Soc.*, Vol. 64, 1938.
9. BJERKNES, J.: On the Structure of Moving Cyclones, *Geof. Pub.*, Vol. I, No. 2, Oslo, 1918.
10. BJERKNES, J.: Exploration de quelques perturbations atmosphérique à l'aide de sondages rapprochés dans le temps, *Geof. Pub.*, Vol. IX, No. 9, Oslo, 1932.
11. BJERKNES, J.: Practical Examples of Polar-Front Analysis, *Geophys. Mem.* No. 50, London, 1930.
12. BJERKNES, J.: Theorie der Aussertropischen Zyklonenbildung, *Met. Zeitschr.*, 1937.
13. BJERKNES, J.: La Circulation atmosphérique dans les latitudes soustropicales, *Scientia*, 1935.
14. BJERKNES, J., and SOLBERG, H.: Life Cycle of Cyclones and the Polar Front Theory of Atmospheric Circulation, *Geof. Pub.*, Vol. LII, No. 1, Oslo, 1922.
15. BJERKNES, J., and PALMEN, E.: Investigations of Selected European Cyclones by Means of Serial Ascents, *Geof. Pub.*, Vol. XII, No. 2, Oslo, 1937.
16. BJERKNES, V., BJERKNES, J., SOLBERG, H., and BERGERON, T.: "Physikalische Hydronamik," Berlin, 1933.
17. BJERKNES, V.: Application of Line Integral Theorems to Hydrodynamics of Terrestrial and Cosmic Vortices, *Astrophysica Norvegica*, Vol. II, 1937.
18. BJERKNES, V.: Über die Bildung von Cirkulationsbewegungen, *Videnskabsselskabets Skrifter*, Oslo, 1898.
19. BRUNT, D.: "Physical and Dynamical Meteorology," Cambridge University Press, 1934.
20. BRUNT, D., and DOUGLAS, C. K. M.: On the Modification of the Strophic Balance, *Mem. Roy. Soc.*, Vol. 3, No. 22.
21. BYERS, H. R.: On the Thermodynamic Interpretation of Isentropic Charts, *Monthly Weather Rev.*, 1938.
22. CLAPP, P. F.: The Causes and the Forecasting of Fogs at Cheyenne, *Bull. Am. Met. Soc.*, 1938.
23. DEFANT, A.: Die Veränderung der allgemeinen Zirkulation der Atmosphäre in den gemässigten Breiten der Erde, *Weiner Sitzungsber.*, Vol. 121.

24. EKMAN, V. W.: Studien zur Dynamik der Meresströmungen, *Beitr. Geophys.*, Vol. 36, p. 385, 1932.
25. EMDEN, R.: Über Strahlungsgleichgewicht und atmosphärische Strahlung, *Sitzungsber. K. Bayerischen Akad. Wiss.*, Math.-Phys. Klasse, 1913.
26. FINDEISEN, W.: Die Kolloidmeteorologische Vorgänge bei der Neiderschlagsbildung, *Met. Zeitschr.*, 1938.
27. GODSKE, C. L.: Zur Theorie der Bildung aussertropischer Zyklonen, *Met. Zeitschr.*, 1936.
28. GOLD, E.: Barometric Gradient and Wind Force, No. 190, *Met. Office*, London.
29. GOLD, E.: Fronts and Occlusions, *Quart. Jour. Roy. Met. Soc.*, Vol. 61, 1935.
30. GRIMMINGER, G.: The Intensity of Lateral Mixing in the Atmosphere as Determined from Isentropic Charts, *Trans. Am. Geophys. Union*, 1938.
31. HAURWITZ, B.: On the Vertical Wind Distribution in Anticyclones, Extratropical and Tropical Cyclones under the Influence of Eddy Viscosity, *Gerlands Beitr. Geophys.*, Vol. 47, 1936.
32. HESSELBERG, TH., and SVERDRUP, H. U.: Die Reibung in der Atmosphäre, *Veröff. Geophys. Inst. Leipzig*, 1915.
33. HUANG, H. C.: Aerological Soundings by Kite Flights at Peiping, China (not published).
34. International Atlas of Clouds and States of Sky, *Office Nat. Met.*, Paris, 1932.
35. International Meteorological Organization, Conference of Directors, Warsaw, 1935.
36. International Meteorological Organization, "Über Aerologische Diagrammpapiere," Berlin, 1938.
37. International Meteorological Organization, Resolutions Adopted at Salzburg, 1937.
38. Commission on Projection for Meteorological Maps, *Intern. Met. Organization*, Pub. 39, 1939.
39. JEFFREYS, H.: On the Dynamics of Wind, *Quart. Jour. Roy. Met. Soc.*, Vol. 48, 1922.
40. KÖPPEN, W.: "Die Klimate der Erde," Berlin, 1924.
41. MARGULES, M.: Über die Energie der Stürme, *Jahrbuch k. k. Zentr. Met. Geodyn.*, Vienna, 1903.
42. MONTGOMERY, R. B.: A Suggested Method for Representing Gradient Flow in Isentropic Surfaces, *Bull. Am. Met. Soc.*, Vol. 18, 1937.
43. MÖLLER, F.: Die Wärmequellen in der freien Atmosphäre, *Met. Zeitschr.*, Vol. 52, p. 408, 1935.
44. NAMIAS, J.: Forecasting Significance of Anticyclonic Eddies on Isentropic Surfaces, *Trans. Am. Geophys. Union*, 1938.
45. NAMIAS, J.: The Use of Isentropic Analysis in Short Term Forecasting, *Jour. Aeronautical Sciences*, Vol. 6, No. 7, 1939.
46. NAMIAS, J.: Two Important Factors Controlling Winter-time Precipitation in the Southeastern United States, *Trans. Am. Geophys. Union*, 1939.
47. NAMIAS, J.: Thunderstorm Forecasting with the Aid of Isentropic Charts, *Bull. Am. Met. Soc.*, Vol. 19, No. 1, 1938.
48. NAMIAS, J.: Subsidence within the Atmosphere, *Harvard Meteor. Studies*, No. 2, 1934.
49. NORMAND, C. W. B.: On Instability from Water Vapour, *Quart. Jour. Roy. Met. Soc.*, Vol. 64, No. 273, January, 1938.
50. PARR, A. E.: On the Probable Relationship between the Vertical Stability and Lateral Mixing Processes, *Jour. du Conseil*, Vol. XI, No. 3, 1936.
51. PEKERIS, C. L.: Wave-perturbations in a Homogeneous Current, *Trans. Am. Geophys. Union*, 1938.

52. PETTERSSEN, S.: Contributions to the Theory of Convection, *Geof. Pub.*, Vol. XII, Oslo, 1939.

53. PETTERSSEN, S.: Some Aspects of Formation and Dissipation of Fog, *Geof. Pub.*, Vol. XII, Oslo, 1939.

54. PETTERSSEN, S.: On the Causes and the Forecasting of the California Fog, *Bull. Am. Met. Soc.*, 1938.

55. PETTERSSEN, S.: Kinematical and Dynamical Properties of the Field of Pressure with Application to Weather Forecasting, *Geof. Pub.*, Vol. X, Oslo, 1933.

56. PETTERSSEN, S.: Contribution to the Theory of Frontogenesis, *Geof. Pub.*, Vol. XI, Oslo, 1936.

57. PETTERSSEN, S.: Frontogenesis and Fronts in the Atlantic Area, *Mem. Met. Assoc., Intern. Union for Geodesy and Geophysics*, Edinburgh, 1936.

58. PETTERSSEN, S.: Practical Rules for Prognosticating the Movement and the Development of Pressure Centers, *Mem. Met. Assoc., Intern. Union for Geodesy and Geophysics*, Lisbon, 1933.

59. REED, T. R.: The North American High Level Anticyclone, *Monthly Weather Rev.*, Vol. 61, 1933.

60. REFSDAL, A.: Das Aerogramm, Ein neues Diagrammpapier fur Aerologische Berechnungen, *Met. Zeitschr.*, 1935.

61. REFSDAL, A.: Aerologische Diagrammpapiere, *Geof. Pub.*, Vol. XI, Oslo, 1937.

62. ROBITSCH, M.: Die Verwertung der durch aerologische Versuche gewonnenen Feuchtigkeitsdaten zur Diagnose der jeweiligen atmospharischen Zustände, *Die Arbeiten des Preussischen Aeronautischen Observatoriums bei Lindenberg*, Bd. XVI, *Wiss. Abh.*, Heft C, Braunschweig, 1928.

63. ROSSBY, C.-G.: Thermodynamics Applied to Air Mass Analysis, *Papers in Physical Oceanog. Met.*, Vol. I, No. 3, 1932.

64. ROSSBY, C.-G.: Dynamics of Steady Ocean Currents in the Light of Experimental Fluid Mechanics, *Papers in Oceanog., Met.*, Vol. V., No. 1, 1936.

65. ROSSBY, C.-G.: On the Mutual Adjustment of Pressure and Velocity Distributions in Certain Simple Current Systems, I and II, *Sears Foundation: Jour. Marine Research*, Vol. I, Nos. 1 and 3, 1937 and 1938.

66. ROSSBY, C.-G.: Note on Shearing Stresses Caused by Large-scale Lateral Mixing, *Proceedings of the Fifth International Congress of Applied Mechanics*, 1938.

67. ROSSBY, C.-G.: On the Maintenance of the Westerlies South of the Polar Front, Part IA of Fluid Mechanics Applied to the Study of Atmospheric Circulations, *Papers in Physical Oceanog.*, Vol. VII, No. 1, 1938.

67a. ROSSBY, C.-G.: Relation between Variations in the Intensity of the Zonal Circulation of the Atmosphere and the Displacements of the Semi-permanent Centers of Action, *Sears Foundation: Jour. Marine Research*, Vol. II, No. 1, 1939.

68. ROSSBY, C.-G., and *collaborators*, Aerological Evidence of Large-scale Mixing in the Atmosphere, *Trans. Am. Geophys. Union*, 1937.

69. ROSSBY, C.-G., and *collaborators*, Isentropic Analysis, *Bull. Am. Met. Soc.*, Vol. 18, 1937.

70. SANDSTRÖM, J. W., Dynamic Meteorology and Hydrography, Vol. II (by V. Bjerknes and J. W. Sandström), Washington, D. C., 1910.

71. SCHINZE, G. Die praktische Wetteranalyse, *Archiv deut. Seewarte*, Bd. 52, 1932.

72. SCHAMAUSS, A. and WIGAND, A.: "Die Atmosphäre als Kolloid," Braunschweig, 1929.

73. SHAW, SIR NAPIER: "Manual of Meteorology," Vol. 3, Cambridge University Press, 1933.

73a. SHAW, SIR NAPIER: "Manual of Meteorology," Vol. 2, Cambridge University Press, 1933.

74. SIMMERS, R. G.: Isentropic Analysis of a Case of Anticyclogenesis. Part IC of Fluid Mechanics Applied to the Study of Atmospheric Circulations, *Papers in Physical Oceanog. Met.*, Vol. VII, No. 1, 1938.

75. SIMPSON, G. C.: The Mechanism of Thunderstorms, *Proc. Roy. Soc.*, Ser. A, Vol. 114, London, 1927.

76. SIMPSON, G. C., and SCRASE, F. J.: The Distribution of Electricity in Thunderstorms, *Proc. Roy. Soc.*, Ser. A, Vol. 161, London, 1937.

77. SIMPSON, G. C.: The South West Monsoon, *Quart. Jour. Roy. Met. Soc.*, Vol. 47, 1921.

78. STONE, R. G.: *Bull. Am. Met. Soc.*, 1938.

79. STUVE, S.: Potentielle and Pseudopotentielle Temperature, "*Beitr. Physik der Freien Atmosphäre*," Bd. XIII. Heft 3, 1927.

80. SVERDRUP, H. U.: The Ablation on Isachsen's Plateau on the Fourteenth of July Glacier in Relation to Radiation and Meteorological Conditions, Scientific Results of the Norwegian-Swedish Spitsbergen Expedition 1934, Part IV, *Geograf. Ann.*, Stockholm, 1935.

81. SVERDRUP, H. U.: "North Polar Expedition with the 'Maud,' 1918–1925," Vol. 2, Part 1, 1933.

82. SVERDRUP, H. U.: Zur Bedeutung der Isallobarkarten, *Ann. J. Hydrogr. Mar. Met.*, Hamburg, 1917.

83. TAYLOR, G. I.: The Formation of Fog and Mist, *Quart. Jour. Roy. Met. Soc.*, Vol. 43, 1917.

84. THORADE, H.: Über die Kalifornische Meeresströmungen. *Ann. Hydr. Mar. Met.*, Bd. 37, 1909.

85. TOLLMIEN, W.: Berechnung turbulenter Ausbrietungsvorgänge, *Zeits. Angew. Math. Mech.*, Band 6, 1926.

86. WEXLER, H.: Cooling in the Lower Atmosphere and the Structure of Polar Continental Air, *Monthly Weather Rev.*, Vol. 64, No. 4, 1936.

87. WEXLER, H.: Observed Transverse Circulations in the Atmosphere and Their Climatological Implications, 1939. (As yet unpublished.)

88. WEXLER, H. and NAMIAS, J.: Mean Monthly Isentropic Charts and Their Relation to Departures of Summer Rainfall, *Trans. Geophys. Union*, 1938.

89. WILLETT, H. C.: American Air Mass Properties. *Papers in Physical Oceanog. Met.*, Vol. II, No. 2, 1934.

INDEX OF NAMES

495

INDEX OF SUBJECTS

INDEX OF STATIONS